COFFEE BOOK
On
ANIMAL MODELS IN NEURODEGENERATIVE DISORDERS



Neuroscience Research Lab
Department of Neurology,
PGIMER Chandigarh, India

Foreword

Dear Reader,



I am delighted to present the book "Animal models in Neurodegenerative Disorders", a compilation of articles that were published from Neuroscience Research Laboratory (NRL). NRL, since its inception is committed to continuously advance the knowledge in field of neurodegenerative disorders such as Alzheimer disease, AMD, retinal ischemia, DMD and ALS.

The research in NRL can be broadly divided into two divisions. One is based on clinical samples collected from patients suffering from diseases which are studied for biomarker discovery to serve as a tool for early prognosis of disease. The second division involves use of lab animals to mimic the neurodegenerative disorders and then use these animal models to better understand the pathophysiology of these diseases at cellular and molecular levels as well as to test various treatment strategies to prevent disease progression. These two divisions work closely together, in sync, generating useful scientific data and are two arms that hold the lab high enough to make a mark in this competing scientific world.

Scientific writing and academic publishing in form of research articles/reviews is an important part of scientific communications that makes data generated at one end available to wider community on which other researchers can build on new developments. Research on bench is half part of picture, the other half being its writing and presentation to the world. Over the years, the Lab has contributed significantly to enhancing the knowledge in the field through evidence-based data generation and its peer-reviewed publications. These are assets of lab which has led to recognition of lab at national and international level. Each article is a harvest of the seed of conceptual idea sown and nourished by research efforts for long time of 4 to 5 years.

This book is a result of hard work and dedication of many people associated with the lab in past 20 years. This lab stands on the foundation of knowledge that PI (Dr. Akshay Anand) gain during his own postdoctoral phase and you can find the publications in this book when he himself was a postdoc and in his very young phase of learning. The reader can appreciate that how the research field diversifies in the lab from that period to current time by still holding strong to its roots.

Although with growing technology almost every article can be accessed in few clicks within seconds from various repositories available online. However, this compilation eases the accessibility and saves from the hassle of looking for an individual article and sometimes from paid access restrictions of certain articles imposed by journals.

I am confident that NRL will continue to grow and accomplish its research goals by motivating young scientists to dive deep into the field making a positive difference in the scientific community and society as a whole.

Shweta Modgil,
Alumni, Neuroscience Research Lab.

Contents

SL No.	Title	Page No
1.	Effect of retinal injury induced by laser photocoagulation on visuospatial memory in mouse model	1-6
2.	Transplantation efficacy of human ciliary epithelium cells from fetal eye and Lin-ve stem cells from umbilical cord blood in the murine retinal degeneration model of laser injury	7-18
3.	Electrophysiological assessment of retinal functions by ERG in ischemia/ reperfusion (I/R) allium cepa pre-treated mice	19-29
4.	Allium cepa exerts neuroprotective effect on retinal gangling cells of pterygopalatine artery (PPA) ligated mice	30-35
5.	Alpha lipoic acid attenuates the long-term effects of lead exposure in retinal ischemic injury mouse model	36-46
6.	Early life Pb exposure and its effect on later life retinal degeneration	47-58
7.	Modeling transient retinal ischemia in mouse by ligation of pterygopalatine artery	59-62
8.	Effect of human umbilical cord blood derived lineage negative stem cells transplanted in amyloid-β induced cognitive impaired mice	63-76
9.	Cytoskeleton dynamics in the retina	77-90
10.	Does DcR1 (TNF-related apoptosis-inducing-ligand Receptor 3) have any role in human AMD pathogenesis?	91-95
11.	Preclinical non-human models to combat dementia	96-101
12.	Preclinical models to investigate retinal ischemia: advances and drawbacks	102-107
13.	Animal models of retinal ischemia	108-129
14.	Analysis of homing potential of marrow-derived mononuclear cells in an experimentally-induced brain stroke mouse model	130-135
15.	Neuroprotective effect of *Bacopa monniera* on ischemia induced brain injury	136-141
16.	Antiamnesic effect of *B. monniera* on L-NNA induced amnesia involves calmodulin	142-151
17.	Scopolamine induced amnesia is reversed by *Bacopa monniera* through participation of kinase-CREB pathway	152-160
18.	*Bacopa monniera* alleviates N_{ω}-Nitro-$_{L}$-Arginine-induced but not MK-801-induced amnesia: a mouse morris water maze study	161-167
19.	*Bacopa monniera* ameliorates amnesic effects of diazepam qualifying behavioral-molecular partitioning	168-176
20.	Sustained inhibition of brotizolam induced anterograde amnesia by norharmane and retrograde amnesia by l-glutamic acid in mice	177-185
21.	Mouse models of visual deficits	186
22.	An animal model of age-related macular degeneration in senescent Ccl-2- or Ccr-2-deficient mice	187-194

23.	Macrophage depletion inhibits experimental choroidal neo-vascularization	195-202
24.	Targeted disruption of the CD18 or ICAM-1 gene inhibits experimental choroidal neovascularization	203-209
25.	Sustained inhibition of corneal neovascularization by genetic ablation of CCR5	210-213

Published online: 2021-06-25

Effect of Retinal Injury Induced by Laser Photocoagulation on Visuospatial Memory in Mouse Model

Priya Mehra[1,2] Parul Bali[3] Jagtar Singh[1] Pradip Kumar Saha[4] Akshay Anand[2]

[1]Department of Biotechnology, Panjab University, Chandigarh, India
[2]Neuroscience Research Lab, Department of Neurology, Postgraduate Institute of Medical Education and Research, Chandigarh, India
[3]Department of Biological Science, IISER - Indian Institute of Science Education and Research, Mohali, India
[4]Department of Obstetrics and Gynecology, Postgraduate Institute of Medical Education and Research, Chandigarh, India

Address for correspondence Parul Bali, PhD, Department of Biological Science, IISER - Indian Institute of Science Education and Research, Mohali 140306, Punjab, India (e-mail: parul28bali@gmail.com);

Akshay Anand, PhD, Neuroscience Research Lab, Department of Neurology, Postgraduate Institute of Medical Education and Research, Chandigarh 160012, India (e-mail: akshay1anand@rediffmail.com).

J Neurosci Rural Pract 2021;12:586–591.

Abstract

Visual pathway reveals the connection between neuronal activity of the brain and eye. The neural networks of brain amplify the retinal signals resulting in the formation of visual image. The laser injury in the retina may affect the visual pathway and may lead to disruption of neuronal signals/activity. Therefore, we aimed to study the effect of retinal injury induced by laser on cognitive abilities in laser-induced mouse model. We have established laser model to understand the relation between retina and brain by disrupting retinal pigment epithelial (RPE) layer and evaluate the effect of laser-induced retinal injury on visuospatial memory. Age- and sex-matched C57BL/6J male mice were taken for conducting the experiments. The laser model was established by using laser photocoagulator to disrupt the RPE layer of the retina. After defined irradiation of laser onto mouse retina, the fundus fluorescein angiography was performed to confirm the laser spots. The visuospatial and short-term memory was performed using neurobehavioral test, that is, Morris water maze (MWM), and passive avoidance, respectively. In MWM experiment, results showed that escape latency time, which was taken by healthy and laser-injured mice was comparable. This was further validated by another neurobehavioral analysis, that is, passive avoidance that showed nonsignificant difference between these two groups using independent *t*-test. Visuospatial memory may not be affected by retinal injury induced by laser photocoagulation. It may depend on the power of the laser and duration of the laser. The severe injury in the retina such as optic nerve damage may cause dysfunctioning of visual pathway.

Keywords
- visual impairment
- laser photocoagulation
- retinal degeneration
- cognition
- memory

published online
June 25, 2021

DOI https://doi.org/10.1055/s-0041-1730747
ISSN 0976-3147

© 2021. Association for Helping Neurosurgical Sick People.
This is an open access article published by Thieme under the terms of the Creative Commons Attribution-NonDerivative-NonCommercial-License, permitting copying and reproduction so long as the original work is given appropriate credit. Contents may not be used for commercial purposes, or adapted, remixed, transformed or built upon. (https://creativecommons.org/licenses/by-nc-nd/4.0/).

Thieme Medical and Scientific Publishers Pvt. Ltd. A-12, 2nd Floor, Sector 2, Noida-201301 UP, India

Introduction

Several eye disorders such as age-related macular degeneration (AMD), diabetic retinopathy, glaucoma, retinal vein occlusion, retinal ischemia, and retinal pigmentosa have retinal degeneration as a main symptom. It is considered as one of the major causes of blindness.

Visual impairment affects retina, optic nerve, and different parts of brain such as thalamus, optic chiasma, optic radiation, occipital lobes, and visual cortex. According to the World Health Organization, globally 285 million people are visual impaired, out of which 39 million are blind and majority of people are above 50 years of age or more,[1] whereas 123.7 million people are with refractive errors, 6.9 million with glaucoma, 65.2 million with cataract, 3 million with diabetic retinopathy, and 11 million with AMD, and it is expected to double in next 10 years.[2] In developing countries, leading causes of visual impairment are AMD, glaucoma, and diabetic retinopathy.

However, the prevalence of visual impairment is expected to increase twofold by 2050.[3,4] Moreover, there is a close relationship between visual impairment and cognitive decline as both are neurodegenerative disorders and are related to aging.[5,6] The study showed the relation between macular degeneration and Alzheimer's disease (AD) in older age group resulting in poor reading ability, distorted blurred faces due to lack of sensory stimulus, and brain stimulus activity.[7] It was studied that visual performance has significant effect on memory deterioration.[8] A study reported correlation of memory and learning with vision in 1,000 cataract-operated patients and found significant improvement in memory task and learning.[9] Therefore, such results show that memory and learning are significantly associated with vision.

Various research have shown the association of visual performance with cognition function.[6,7] The dysregulations of blood retinal barriers has implicated age-related cognitive decline.[10] In neurological disorders, disruption of retinal blood barrier leads to cognitive decline as signaling get disrupted.[11] Laser model has been used to study the visuospatial memory by either disrupting retinal layers or optic nerve that transmits signal from retina to brain where visual image formation occur known as visual perception.[12] The primary site of injury using laser photocoagulation is retina. There are two methods by which retina get disrupted by laser, that is, one by targeting the Bruch's membrane that is an innermost layer of the choroid below retinal pigment epithelial (RPE) layer. The proliferation of choroidal vessels takes place that penetrate RPE through Bruch's membrane and leakage of lipids and blood from these new fragile blood vessels under the retina and sometimes between the retinal layers also occurs. This process is known as choroidal neovascularization.[13] Second method is by directly targeting the RPE that absorb laser beam, which gets converted into thermal energy leading to denaturation of cellular proteins.[14] The retinal injury model can be validated by visualizing damaged retina through fundus fluorescein angiography (FFA), optical coherence tomography, and electroretinogram. In our study, we have established the laser model and tried to investigate that whether the retinal injury affects visuospatial memory.

Some studies have shown that visual impairment leads to visual cortex damage. It has shown that neuronal cells in the retina as well as its thickness also get affected in AD.[15,16] The retina shares various functions with central nervous system, transmission of signal leads to visual perception, cognition, image formation, and spatial memory. Therefore, keeping in mind this doubted or unconfirmed relation between visual problems and visuospatial memory or cognitive learning, this laser-induced retinal injury model was established. This model was used to study the effects of laser on visuospatial memory or cognitive abilities via retinal degeneration using standardized parameters such as 100-µm size of the laser.

Methods

All the experiments were performed under good laboratory practice guidelines. All the protocols were approved by the study director and quality assurance personnel.

Study Design

In this study, 6 to 8 weeks C57BL/6J male mice were used. Animals were fed on standard diet and RO drinking water was available *ad libitum*. Animals were maintained in a 12-hour light/dark cycle. Utmost care was taken while performing experiments. All the experiments were conducted in accordance with Institutional Animal Ethical Committee (105/IAEC/720).

Laser Photocoagulation

Mice were anesthetized with the mixture of ketamine and xylazine in the ratio 1:10 intraperitoneally in to mice and their pupil was dilated with 1% tropicamide and phenylephrine. A slit lamp connected with laser photocoagulator (IRIDEX) with 532 nm argon green laser wavelength was used. Eight laser shots were given to both eyes. The laser shots were given around optic disc in each eye with coverslips as a contact lens. The size of laser spots was 100 µm; duration of exposure to laser pulse was 100 milliseconds; power of the laser was 200 mW. These all parameters were already standardized in our laboratory.[17] The mice whiskers were trimmed and eyes were kept moist and clean with sterile saline. After that, mice were placed on slit lamp laser system. The fundus was observed using coverslip with one drop of hydroxypropyl methylcellulose. Once the site got visualized, eight laser shots were given to each eye in circular fashion around the optic disc.

Fundus Fluorescein Angiography

To validate the laser model, FFA was done after 24 hours of laser injury. The animals were anesthetized and pupil was dilated. The mice received tail vein injection of 0.2 µL of fluorescein dye diluted in 1 mL normal saline. Immediately

after injecting, fundus was focused. The vascular leakage and size of laser lesion was determined by using Heidelberg Engineering software. The laser-induced leakage validated the establishment of laser model.

Neurobehavioral Analysis

Rotarod

The rotarod consists of circular rod rotating at constant speed to measure muscular strength, motor coordination of mice. After 1 month of laser injury, neurobehavioral assessment was done. The mice were kept on rotating rod at constant speed of 15 rpm for 180 seconds. The mice were allowed to rotate on rotarod for 3 minutes to maintain the balance and to avoid falling. The time taken by the mice to fall from rotating rod was recorded. The trial was done for three times daily followed by Morris water maze (MWM).

Morris Water Maze

MWM was performed to measure the spatial memory of the mice. After laser injury, the mice underwent neurobehavioral analysis. It was 7 days protocol, first 6 days were acquisition days and the seventh day was retrieval day. Before MWM, mice were screened for swimming ability by rotarod experimentation. MWM consists of circular tank filled with water with equally divided four quadrants named Q1, Q2, Q3, and Q4. A circular white platform was submerged 1 cm below the water surface kept in Q1 quadrant. The visual cues were placed on the walls and pool side. The background of water was colored white to identify and track the darker mice against bright background in ANY-maze software. The complete protocol was recorded and tracked by using ANY-maze video software connected with webcam. The water temperature was maintained between 21 and 24°C. Four trials were done every day and each trial was for 120 seconds. ANY-maze software measures various parameters such as escape latency time of the mice, mean speed from platform to different quadrant, time spent by mice in each quadrant, distance traveled by mice from each quadrant to platform, and mean distance from the platform.

Passive Avoidance

Passive avoidance is the learning task used to measure short-term memory. The instrument divided into two equal parts named light chamber and dark chamber with a gate between two. This protocol was performed for 3 days for 10 minutes. On first day, mice were allowed to explore both chambers freely. On second day (acquisition day) mice were kept in the light chamber and gate was opened after 30 seconds and then time was recorded when mice entered the dark chamber. In dark chamber, the mice received mild foot shock of 20 mW and after that mice were removed immediately from the box. On third day (test day), the time spent by mice in light chamber was recorded to avoid foot shock in dark.

Enucleation of Eye

Mice were euthanized by overdose of ketamine: xylazine combination. The eyes were enucleated and stored at 80°C for further experiments.

Results

Retinal Assessment

FFA: The fundus imaging was done after 24 hours of laser injury. The vascular leakage at the injury site showing laser lesions in eight laser group. The images were captured by Heidelberg Engineering software as shown in ►**Fig. 1**.

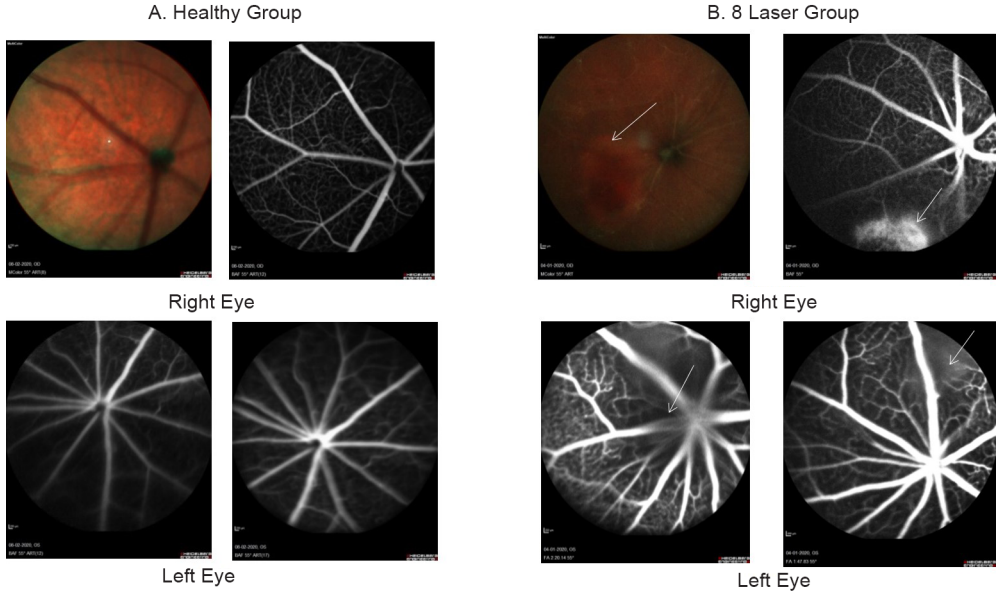


Fig. 1 Fundus fluorescein angiography shown fundus image of the eye. (**A**) The healthy control group shows no leakage of fluorescein dye in left and right eyes. (**B**) Although in eight laser group, the white arrows show leakage at injury site in both right and left eyes of laser group after 24 hours of laser injury.

 © 2021. Association for Helping Neurosurgical Sick People.

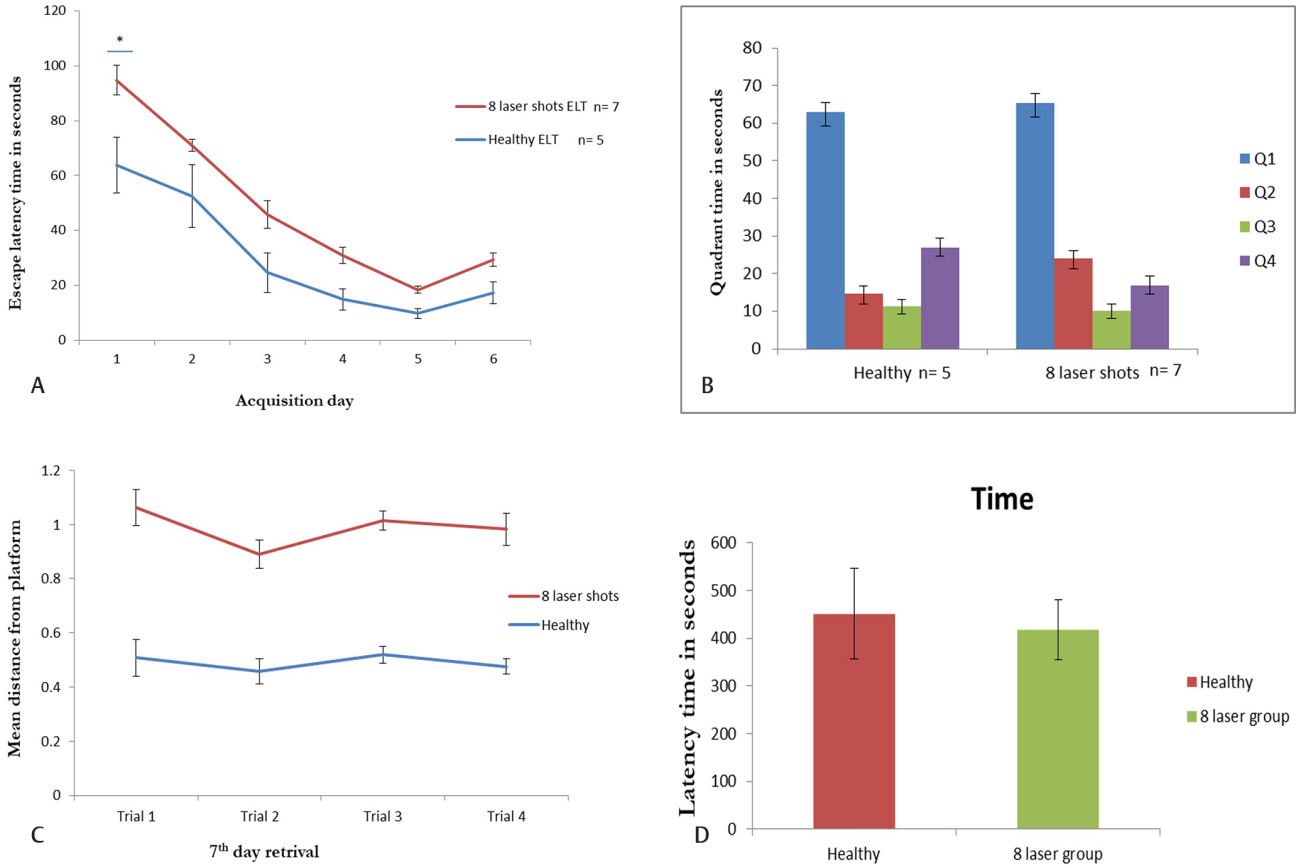


Fig. 2 The MWM analysis showing learning in mice. (**A**) The day-wise escape latency time during acquisition days of mice in healthy control (*N* = 5) and eight laser injury (*N* = 7). The ELT was found to be more in mice with eight laser group at day 1 as compared with the healthy control group. (**B**) *Quadrant time*: The time spent by mice in MWM quadrants Q1, Q2, Q3, and Q4 on retrieval day (seventh day). (**C**) The search error measured as mean distance from hidden platform traveled was less in healthy group as compared with laser group but nonsignificant. (**D**) Passive avoidance found more latency in eight laser group as compared with healthy group. The trial lasts for maximum 10 minutes. ELT, escape latency time; MWM, Morris water maze.

Neurobehavioral Assessment

Morris water maze: Before MWM, the mice were undergone rotarod experiment to determine the swimming ability. All mice were found to be swim well, and their motor coordination and muscular strength was strong. After three trials of 3 minutes, mice had undergone MWM experiment. ANY-maze software was attached to webcam to track the mice. It was found significant reduction in the swimming path on day 1 in healthy group as compared with laser group (►**Fig. 2A**). However, all mice were learned to reach the platform but were nonsignificantly. ►**Fig. 2B** depicts that the mice spent time mice in each quadrant at seventh day of the experiment. It was found that mice spent more time in Q1 quadrant where the hidden platform was placed but nonsignificantly, whereas, mice spent maximum time in Q2 and Q4 quadrants significantly (►**Fig. 2B**). The mean distance from platform was found to be nonsignificant in both groups (►**Fig. 2C**).

Passive Avoidance

After MWM, to confirm the learning and memory ability, the mice were subjected to passive avoidance in which time spent by mice in the light chamber to avoid shock was noted. We found that mice had learned and remain in the light chamber maximum time for 10 minutes on day 3 in both healthy control and laser group (►**Fig. 2D**).

Statistical Analysis

IBM SPSS version 22 was used for the statistical analysis, whereas baseline values were checked for normalcy and baseline group comparisons were done by using independent samples *t*-test.

Discussion

Visual system is the process in which signals get transmitted, processed, and interpreted by axonal retinal ganglion cells and primary cortex in brain to form visual perception. The neuronal cells in the retina extend axons from retinal ganglion cells to optic nerve to brain mainly in primary cortex to form image. Brain is able to remember entire series of images formed by retina when we move eye results in spatial memory. Since the image produced by eye is directly correlated with the brain[18] as the electrical signal get transmitted from retinal photoreceptors cells to brain through optic nerve which is responsible for visual perception, thus impairment

in the visual function will affect the brain function and understanding directly. Understanding the mechanism of visual and cognitive function will provide evidence to understand the disease with another important perspective. This invokes the need to study the effects of visual impairment on brain function and to study the effect of the treatment used for vision repair on the brain function.

In retinal degenerations such as retinitis pigmentosa and AMD, diabetic retinopathy begins with loss of photoreceptor, impaired macula and later on results in loss of inner retinal neurons, but significant numbers of bipolar and ganglion cells remain for many years that can be reversed by electrical stimulation of the retina or the optic nerve.[19]

In our study, we observed that laser-induced retinal injury do not affects the learning and memory. In spatial memory test, laser-injured mice showed learning and memorizing at the retrieval day when the hidden platform was removed. This test was validated by fear-motivated test in which laser-injured as well as healthy mice spent maximum time in light chamber to avoid foot shock. Some of the studies have shown that learning and visual memory may not be correlated. Yancopoulos (2016) used anti-VEGF treatment to abolish clinical neovascularization; however, investigations to examine its association with cognitive improvement have been lacking. While they found significant results in the treatment of angiogenic eye disorders, they did not report the impact on neurobehavioral.[13,20] Prusky et al examined the role of visual acuity in animal model and found that the mice with reduced visual acuity were found to be deficit in place of learning and do not differ their learning ability in MWM.[21] Similarly, Storchi et al demonstrated that innate behavior has various advantages in vision test mainly by determining the visual capabilities with intact visual function in mice model and in retinal degeneration.[22]

Hence, we studied the association between laser-induced retinal injury and memory in mice model. Many studies have shown that the neuronal and retinal degeneration are correlated with each other. Neuronal cell death results in cognitive and visual impairment. Also, neurodegeneration affects retina. In neurological disorders such as AD and Parkinson's disease, retinal thickness reduced in mild cognition impairment as compared with healthy control group.[23,24] Although various studies from our group have independently analyzed the role of risk and genetic factors in onset of neurodegeneration, we had not examined the association between two clinical situations, that is, vision loss and cognitive deficit.[25-43] However, there are studies that have shown the correlation between visual impairment and cognition in the population and found significant association between them.[44-46]

Oktem et al found significant correlation between retinal thickness and mild cognition in AD patients as compared with control group.[47] However, our results have shown that visuospatial memory is independent of retinal injury induced by laser photocoagulation.

Limitations of the Study

The molecular analysis such as reverse transcription polymerase chain reaction, immunohistochemical staining to check the expression of different neuronal marker and apoptotic marker is yet to be done. The samples were stored at –80°C for further experimentation.

Conclusion

Visuospatial memory may not affect by retinal injury induced by laser photocoagulation. It may depend on the power of the laser and duration of the laser. The severe injury in the retina such as optic nerve damage may cause dysfunctioning of visual pathway.

Ethical Approval

The ethical approval was taken by Institute Animal Ethical committee. The ethical approval number is 105/IAEC/720.

Funding

None.

Conflict of Interest

None declared.

Acknowledgment

The authors acknowledge Mr. Arun Kapil from the Department of Opthalmology, PGIMER, for Fundus Fluorescein Fngiography FFA imaging.

References

1 World Health Organization, Blindness and Vision Impairment Prevention. World Health Organization; 2020. Available at: https://www.who.int/news-room/fact-sheets/detail/blindness-and-visual-impairment
2 World Health Organization, Blindness and Vision Impairment. World Health Organization; 2020. Available at: https://www.who.int/blindness/Vision2020_report.pdf
3 Flaxman SR, Bourne RR, Resnikoff S, et al. Vision Loss Expert Group of the Global Burden of Disease Study. Global causes of blindness and distance vision impairment 1990-2020: a systematic review and meta-analysis. Lancet Glob Health 2017;5(12):e1221–e1234
4 Stevens GA, White RA, Flaxman SR, et al. Vision Loss Expert Group. Global prevalence of vision impairment and blindness: magnitude and temporal trends, 1990-2010. Ophthalmology 2013;120(12):2377–2384
5 Uhlmann RF, Larson EB, Koepsell TD, Rees TS, Duckert LG. Visual impairment and cognitive dysfunction in Alzheimer's disease. J Gen Intern Med 1991;6(2):126–132
6 Salthouse TA, Hancock HE, Meinz EJ, Hambrick DZ. Interrelations of age, visual acuity, and cognitive functioning. J Gerontol B Psychol Sci Soc Sci 1996;51(6):317–330
7 Klaver CC, Ott A, Hofman A, Assink JJ, Breteler MM, de Jong PT. Is age-related maculopathy associated with Alzheimer's disease? The Rotterdam study. Am J Epidemiol 1999;150(9):963–968
8 Anstey KJ, Luszcz MA, Sanchez L. Two-year decline in vision but not hearing is associated with memory decline in very old adults in a population-based sample. Gerontology 2001;47(5):289–293

9 Fagerström R. Correlations of memory and learning with vision in aged patients before and after a cataract operation. Psychol Rep 1992;71(3 Pt 1):675–686
10 Park MH, Lee JY, Park KH, et al. Vascular and neurogenic rejuvenation in aging mice by modulation of ASM. Neuron 2018;100(1):167–182.e9
11 Venkat P, Chopp M, Chen J. Blood–brain barrier disruption, vascular impairment, and ischemia/reperfusion damage in diabetic stroke. J Am Heart Assoc 2017;6(6):e005819
12 Birtel J, Harmening WM, Krohne TU. Holz FG, Charbel Issa P, Herrmann P. Retinal injury following laser pointer exposure: a systematic review and case series. Dtsch Arztebl Int 2017;114(49):831–837
13 Ambati J, Fowler BJ. Mechanisms of age-related macular degeneration. Neuron 2012;75(1):26–39
14 Glickman RD. Phototoxicity to the retina: mechanisms of damage. Int J Toxicol 2002;21(6):473–490
15 Armstrong RA. Visual field defects in Alzheimer's disease patients may reflect differential pathology in the primary visual cortex. Optom Vis Sci 1996;73(11):677–682
16 Parisi V, Restuccia R, Fattapposta F, Mina C, Bucci MG, Pierelli F. Morphological and functional retinal impairment in Alzheimer's disease patients. Clin Neurophysiol 2001;112(10):1860–1867
17 Bammidi S, Bali P, Kalra J, Anand A. Transplantation efficacy of human ciliary epithelium cells from fetal eye and Lin -ve stem cells from umbilical cord blood in the murine retinal degeneration model of laser injury. Cell Transplant 2020;29:963689720946031
18 Quigley HA, Sanchez RM, Dunkelberger GR, L'Hernault NL, Baginski TA. Chronic glaucoma selectively damages large optic nerve fibers. Invest Ophthalmol Vis Sci 1987 28(6):913–920
19 Loewenstein JI, Montezuma SR, Rizzo JF II. Outer retinal degeneration: an electronic retinal prosthesis as a treatment strategy. Arch Ophthalmol 2004;122(4):587–596
20 Yancopoulos GD. Use of a VEGF antagonist to treat angiogenic eye disorders. Google Patents. 2016
21 Prusky GT, West PW, Douglas RM. Reduced visual acuity impairs place but not cued learning in the Morris water task. Behav Brain Res 2000;116(2):135–140
22 Storchi R, Rodgers J, Gracey M, et al. Measuring vision using innate behaviours in mice with intact and impaired retina function. Sci Rep 2019 9(1):10396
23 Akar G, Gozke E, Agirman Y, Kurna SA. Retinal nerve fiber layer thickness in cases with mild cognitive impairment and Alzheimer-type dementia. Biomed Res 2014;25(4):597–602
24 Oktem EO, Derle E, Kibaroglu S, Oktem C, Akkoyun I, Can U. The relationship between the degree of cognitive impairment and retinal nerve fiber layer thickness. Neurol Sci 2015;36(7):1141–1146
25 Anand A, Banik A, Thakur K, Masters CL. The animal models of dementia and Alzheimer's disease for pre-clinical testing and clinical translation. Curr Alzheimer Res 2012;9(9):1010–1029
26 Anand A, Gupta PK, Sharma NK, Prabhakar S. Soluble VEGFR1 (sVEGFR1) as a novel marker of amyotrophic lateral sclerosis (ALS) in the North Indian ALS patients. Eur J Neurol 2012;19(5):788–792
27 Anand A, Saraf MK, Prabhakar S. Sustained inhibition of brotizolam induced anterograde amnesia by norharmane and retrograde amnesia by L-glutamic acid in mice. Behav Brain Res 2007;182(1):12–20
28 Anand A, Saraf MK, Prabhakar S. Antiamnesic effect of B. monniera on L-NNA induced amnesia involves calmodulin. Neurochem Res 2010;35(8):1172–1181
29 Anand A, Sharma NK, Gupta A, et al. Single nucleotide polymorphisms in MCP-1 and its receptor are associated with the risk of age related macular degeneration. PLoS One 2012;7(11):e49905
30 Anand A, Thakur K, Gupta PK. ALS and oxidative stress: the neurovascular scenario. Oxid Med Cell Longev 2013;2013:635831
31 Anand A, Tyagi R, Mohanty M, Goyal M, Silva KR, Wijekoon N. Dystrophin induced cognitive impairment: mechanisms, models and therapeutic strategies. Ann Neurosci 2015;22(2):108–118
32 Banik A, Brown RE, Bamburg J, et al. Translation of pre-clinical studies into successful clinical trials for Alzheimer's disease: what are the roadblocks and how can they be overcome? J Alzheimers Dis 2015;47(4):815–843
33 English D, Sharma NK, Sharma K, Anand A. Neural stem cells-trends and advances. J Cell Biochem 2013;114(4):764–772
34 Goyal K, Koul V, Singh Y, Anand A. Targeted drug delivery to central nervous system (CNS) for the treatment of neurodegenerative disorders: trends and advances. Cent Nerv Syst Agents Med Chem 2014;14(1):43–59
35 Gupta PK, Prabhakar S, Abburi C, Sharma NK, Anand A. Vascular endothelial growth factor-A and chemokine ligand (CCL2) genes are upregulated in peripheral blood mononuclear cells in Indian amyotrophic lateral sclerosis patients. J Neuroinflammation 2011;8(1):114
36 Sharma NK, Gupta A, Prabhakar S, Singh R, Sharma S, Anand A. Single nucleotide polymorphism and serum levels of VEGFR2 are associated with age related macular degeneration. Curr Neurovasc Res 2012;9(4):256–265
37 Mathur D, Goyal K, Koul V, Anand A. The molecular links of re-emerging therapy: a review of evidence of Brahmi (*Bacopa monniera*) Front Pharmacol 2016;7:44
38 Sharma K, Sharma NK, Anand A. Why AMD is a disease of ageing and not of development: mechanisms and insights. Front Aging Neurosci 2014;6:151
39 Sharma NK, Gupta A, Prabhakar S, Singh R, Bhatt AK, Anand A. CC chemokine receptor-3 as new target for age-related macular degeneration. Gene 2013;523(1):106–111
40 Sharma NK, Gupta A, Prabhakar S, et al. Association between CFH Y402H polymorphism and age related macular degeneration in North Indian cohort. PLoS One 2013;8(7):e70193
41 Sharma NK, Prabhakar S, Gupta A, et al. New biomarker for neovascular age-related macular degeneration: eotaxin-2. DNA Cell Biol 2012;31(11):1618–1627
42 Singh T, Prabhakar S, Gupta A, Anand A. Recruitment of stem cells into the injured retina after laser injury. Stem Cells Dev 2012;21(3):448–454
43 Vinish M, Prabhakar S, Khullar M, Verma I, Anand A. Genetic screening reveals high frequency of PARK2 mutations and reduced Parkin expression conferring risk for Parkinsonism in North West India. J Neurol Neurosurg Psychiatry 2010;81(2):166–170
44 Spierer O, Fischer N, Barak A, Belkin M. Correlation between vision and cognitive function in the elderly: a cross-sectional study. Medicine (Baltimore) 2016;95(3):e2423
45 Lim ZW, Chee ML, Soh ZD, et al. Association between visual impairment and decline in cognitive function in a multiethnic Asian population. JAMA Netw Open 2020;3(4):e203560
46 de Kok DS, Teh RO, Pillai A, et al. What is the relationship between visual impairment and cognitive function in octogenarians? N Z Med J 2017;130(1460) :33–47
47 Pena MCS, Sobreira EST, Souza CP, Oliveira GN, Tumas V, do Vale FAC. Visuospatial cognitive tests for the evaluation of patients with Parkinson's disease. Dement Neuropsychol 2008;2(3):201–205

Check for updates

Original Article

Cell Transplantation
Volume 29: 1–12
© The Author(s) 2020
Article reuse guidelines:
sagepub.com/journals-permissions
DOI: 10.1177/0963689720946031
journals.sagepub.com/home/cll
SAGE

Transplantation Efficacy of Human Ciliary Epithelium Cells from Fetal Eye and Lin-ve Stem Cells from Umbilical Cord Blood in the Murine Retinal Degeneration Model of Laser Injury

Sridhar Bammidi[1,*], Parul Bali[1,2,*], Jaswinder Kalra[3], and Akshay Anand[1]

Abstract

A number of degenerative conditions affecting the neural retina including age-related macular degeneration have no successful treatment, resulting in partial or complete vision loss. There are a number of stem cell replacement strategies for recovery of retinal damage using cells from variable sources. However, literature is still deficit in the comparison of efficacy of types of stem cells. The purpose of the study was to compare the therapeutic efficacy of undifferentiated cells, i.e., lineage negative stem cells (Lin-ve SC) with differentiated neurosphere derived from ciliary epithelium (CE) cells on retinal markers associated with laser-induced retinal injury. Laser-induced photocoagulation was carried out to disrupt Bruch's membrane and retinal pigmented epithelium in C57BL/6 mouse model. Lineage negative cells were isolated from human umbilical cord blood, whereas neurospheres were derived from CE of post-aborted human eyeballs. The cells were then transplanted into subretinal space to study their effect on injury. Markers of neurotropic factors, retina, apoptosis, and proliferation were analyzed after injury and transplantation. mRNA expression was also analyzed by real-time polymerase chain reaction at 1 week, and 3-month immunohistochemistry was evaluated at 1-week time point. CE cell transplantation showed enhanced differentiation of rods and retinal glial cells. However, Lin-ve cells exerted paracrine-dependent modulation of neurotrophic factors, which is possibly mediated by antiapoptotic and proliferative effects. In conclusion, CE transplantation showed superior regenerative outcome in comparison to Lin-ve SC for rescue of artificially injured rodent retinal cells. It is imperative that this source for transplantation may be extensively studied in various doses and additional retinal degeneration models for prospective clinical applications.

Keywords

subretinal, laser injury, lineage negative stem cells, ciliary epithelium cells, umbilical cord blood, retinal degeneration

Introduction

Degenerative conditions of the retina, viz. retinitis pigmentosa, age-related macular degeneration, diabetic retinopathy, glaucoma, etc., do not have any successful treatment to reverse the vision loss. Their widespread use in industrial, medical, and military fields has caused severe vision loss in a number of individuals[1]. Laser injuries are also a part of severe retinal damage, as a result of occupational eye injuries[2].

Cell-based therapies may provide treatment avenues for injuries as well as degenerative disorders by using

[1] Neuroscience Research Lab, Department of Neurology, Post Graduate Institute of Medical Education and Research, Chandigarh, India
[2] Department of Biophysics, Post Graduate Institute of Medical Education and Research, Chandigarh, India
[3] Department of Obstetrics and Gynaecology, Post Graduate Institute of Medical Education and Research, Chandigarh, India
* Both the authors contributed equally and are co-first authors of this article.

Submitted: January 15, 2020. Revised: May 16, 2020. Accepted: July 9, 2020.

Corresponding Author:
Akshay Anand, PhD, Neuroscience Research Lab, Department of Neurology, Post Graduate Institute of Medical Education and Research, Chandigarh 160012, India.
Email: akshay1anand@rediffmail.com

Creative Commons Non Commercial CC BY-NC: This article is distributed under the terms of the Creative Commons Attribution-NonCommercial 4.0 License (https://creativecommons.org/licenses/by-nc/4.0/) which permits non-commercial use, reproduction and distribution of the work without further permission provided the original work is attributed as specified on the SAGE and Open Access pages (https://us.sagepub.com/en-us/nam/open-access-at-sage).

reproducible laser injury models. Current ongoing stem cell work findings have also raised hopes of individuals suffering from such untreatable disorders[3–5]. Stem cells from different sources such as neural stem cells, retinal progenitors, hematopoietic, mesenchymal, embryonic, and induced pluripotent stem cells (iPSCs) have been studied for their differentiation potential into neuronal, retinal as well as glial cell lineages[3,6,7]. Stem cell therapies for targeting such chronic diseases may provide effective solutions. However, the field suffers from lack of comparative analysis of the various types of stem cells even though there is overemphasis on iPSCs[8] and embryonic stem cells[9] without any comparative studies between the two and/or other types of stem cells.

Recent studies show that stem cell transplantation at the site of neural injury or neuronal niche may facilitate differentiation into neurons, resulting in functional improvements in animal models[10,11]. Although the use of stem cells derived from umbilical cord blood (UCB) has been employed with several injury/disease models involving the central nervous system, it is limited as compared to the burgeoning number of cord banks being set up in the Asian countries[12]. The study tested the effect of UCB-derived stem cells in laser-induced injury in rabbit trabecular meshwork[13]. Similarly, the efficacy of transplantation of ciliary epithelium (CE) cells has not been adequately investigated let alone compared with other cell types despite repeated failure to regenerate the damaged or diseased retina. However, several groups have identified and continued with studies of transplantation of CE stem cells in retinal injury models[14,15].

In our previous study, we characterized human umbilical cord blood (hUCB)-derived lineage negative stem cells (Lin-ve SC) on the basis of morphology and cell surface marker expression[16]. We identified these cells under scanning electron microscopy and reported homogenous morphology, i.e., size, shape, and structure as compared to lineage positive and mononucleated cells. Lin-ve SC showed significantly increased expression of hematopoietic stem cells expression, i.e., CD117 and CD34, which ameliorated amyloid-induced memory loss upon transplantation in mouse model. The presence of CD34+ and CD117+ in Lin-ve SC showed 99% positive expression of CD45 marker[17]. These cells exerted neurotrophic factors mediated paracrine effects causing anti-apoptotic activity and amyloid clearance by the activation of astrocytes[18,19].

As lasers have been used for creating the models of retinal degeneration in fish, rodents, and primates[20,21], we established a modified animal model, injuring the Bruch's membrane and the surrounding retinal pigment epithelium (without causing choroidal neovascularization). CE cell–derived neurospheres were cultured under in vitro conditions using recombinant fibroblast growth factor (rhFGF) and recombinant epidermal growth factor (rhEGF), which showed increased size and number on sixth day of culture[22]. These neurospheres were dissociated and transplanted in the subretinal space of mice after laser injury. This resulted in marked increase in neurotrophic marker expression.

This study describes the comparative efficacy of differentiated human fetal CE-derived neurospheres and undifferentiated Lin-ve hUCB-derived stem cells, in the subretinal space of laser-induced retinal injury mouse model. We wanted to understand which source provides effective outcomes. Our results showed that the transplantation of CE cells presumably differentiated it into rods and retinal ganglion cells (RGCs) after migration from subretinal space. However, Lin-ve SC rescued the retinal damage by inducing neurotrophic factors, which may exert antiapoptotic and proliferation activity. Hence, we conclude that differentiated (CE cells) cells can be a superior source for cell transplantation therapy in comparison to undifferentiated (Lin-ve SC) cells after laser injury.

Materials and Methods

Animals

C57BL/6 J syngeneic mice ($N = 3$ per group) of 6- to 8-week-old male were used in the study after the approval from Institutional Animal Ethics Committee (IAEC), Post Graduate Institute of Medical Education and Research, Chandigarh, India [71(69)/IAEC/423]. Animals were kept in animal house facility in a 12-h light/dark cycle (LD 12:12). Mice were fed with standard chow diet and access them freely to clean drinking water.

Laser-Induced Retinal Injury in Mouse Model

The laser-induced retinal injury was established using Argon green laser (532 nm, Iris Medical, USA). The C57 mouse was anesthetized with xylazine hydrochloride (10 mg/kg) (Sigma-Aldrich, St. Louis, MO, USA) and ketamine hydrochloride (100 mg/kg) (Nirlife, Sachana, Gujarat, India) in 1:10 ratio. Mice were kept over heating pad to prevent cold cataract. The local anesthesia, i.e., lignocaine solution, was given to the cornea and 1% tropicamide solution (Akums Drugs and Pharmaceuticals Ltd, Haridwar, Uttarakhand, India) applied for pupil dilation. The fundus shots were obtained through slit lamp by placing the anesthetized mice in front of laser photo-coagulator (IRIDEX, Mountain View, CA, USA). Eight even laser spots in circular fashion were subjected around optic disk in both the eyes. The standardized parameters used in laser photocoagulation were spot size of 100 μm, power of 200 mW, and duration of pulse of 100 ms. Sham control group was operated for subretinal injection without injecting any liquid/vehicle.

Isolation of Lin-ve Stem Cells from hUCB for Subretinal Transplantation

Human UCB samples were obtained after the approval from Institutional Committee for Stem Cell Research and Therapy (IC-SCRT: Approval No. PGI-ICSCRT-53-2014/1469), Post Graduate Institute of Medical Education and Research, Chandigarh-India. Pregnant women of age 20–35 years and

≥28 weeks of gestation period were included in the study. UCB was taken from the umbilical cords of newborns after filling proper informed consent, in the presence of an independent witness. The collected UCB was layered over histopaque solution (Sigma-Aldrich) for enrichment of MNCs using density gradient centrifugation. These MNCs were then subjected to magnetic associated cell sorter (MACS) (Miltenyi Biotech, Bergisch Gladbach, Germany) for the isolation of Lin-ve SC using human Lin-ve isolation kit (Miltenyi Biotech). The kit works on the basis of biological affinity of biotin and streptavidin. The primary antibody cocktail consisted of biotinylated monoclonal antibodies, which include CD123, CD235a (Glycophorin A), CD56, CD19, CD16, CD15, CD14, CD11b, CD3, and CD2.

MNCs were suspended in MACS-BSA buffer and 10 µl of biotin antibody cocktail was added per 107 cells. These were incubated for 15–20 min at 4–8°C and tapped/gently agitated regularly. The cells were then incubated with the second solution, i.e., streptavidin coated magnetic microbeads. Twenty microliters of these microbeads per 107 cells was added and incubated again with gentle tapping for 20–30 min at 4–8°C. The cells were then diluted with 1–2 ml of the buffer, mixed well, and washed twice at 1,500 rpm for 5 min at 4°C. Supernatant was completely pipetted out. Up to 10^8 cells were suspended in 500 µl of freshly made PBS/MACS-BSA buffer. The cells were then subjected to magnetic separation. The magnetic separation unit along with magnetic separation column was kept in a laminar hood and the column was washed with appropriate amount of buffer solution twice. This was shifted to a fresh collection tube, and the cell suspension was passed through the column at a very slow and steady rate, taking care that there are no air spaces/bubbles inside the column. One milliliter of the buffer was then passed through the column twice to completely elute the cells of interest. Turbid white suspension was obtained as flow through.

Ciliary Epithelial Isolation and Culture

Human fetal eye globes were obtained from abortus after legal termination of pregnancy up to 20 weeks of gestation in accordance to ethical guidelines approved by IC-SCRT (Approval no. PGI-ICSCRT-53-2014/1469). The samples were collected from the terminations at the MTP-OT, SLR, and the Emergency-OT, PGIMER, Chandigarh.

Appropriate informed consents were obtained for every donor, on a prescribed consent form, and all the detailed procedures and objectives related to sample collection were explained to them. All the donors were screened and the following conditions were noted before collection of eye samples:

Inclusion Criteria. The samples were obtained of mid-trimester and up to 20 weeks of fetal abortions. This was on suggestion from the experts at both Department of Obstetrics and Gynecology and the Institutional Committee on Stem Cell Research (IC-SCR), PGIMER, Chandigarh.

Exclusion Criteria.

- Hepatitis virus B and C
- Human immunodeficiency virus
- Samples bearing congenital abnormalities
- Any malformation of fetus effecting head
- Evidence of chorioamnionitis (fever, foul smell liquor)
- Intrauterine fetal death

The fetal eyes were carefully enucleated immediately after abortion and transported in an ice cold sterile Hanks' Balanced Salt Solution (HBSS) (Gibco, Grand Island, NY, USA). The surgical procedure was performed under stereozoom microscope (Leica EZ4, Leica Microsystems, Wetzlar, Germany) in order to isolate CE. Eye was held with forceps and a cut at the anterior edge of pars plana was made in order to carefully get the strip of ocular tissue containing CE. Ciliary rings were isolated and washed with sterile HBSS without taking nonpigmented epithelium, retinal pigmented epithelium (RPE), iris as well as retina. CE was dissociated first mechanically using blade and trypsinized using 4–5 ml of 0.25% trypsin (Gibco, Life Technologies, Burlington, ONT, Canada) with ethylenediaminetetraacetic acid at 37°C for 20–30 min. The action of trypsin was further neutralized with advanced Dulbecco's modified Eagle's medium/F12 (Gibco). The unwanted debris was removed by 0.70 µm cell strainer (BD Biosciences, Discovery Labware, Durham, NC, USA) and then centrifuged at 800G for 10 min. The number of pigmented cells was estimated with hemocytometer (Hausser Scientific, Horsham, PA, USA) and also with automatic cell counter (Millipore, Darmstadt, Germany). Finally, 3,000 cells/well were cultured in 96-well plate using retinal culture medium containing advanced DMEM/F12 (Gibco), 2 mM L-glutamine (Gibco, Paisley, Scotland, UK), N2 supplement (Gibco, Life Technologies), 100 U penicillin–streptomycin (Gibco), and fungizone (Gibco, Paisley, Scotland, UK). The cells were provided with proliferative growth factors, i.e., rhEGF (20 ng/ml; R&D Systems, Minneapolis, MN, USA) and rhFGF basic (20 ng/ml; R&D Systems). The size, shape, and structure of culture neurospheres were estimated using Image J software. The sixth day CE cultured neurospheres were harvested for subretinal transplantation in laser injured retina of mouse.

Transplantation of hCE-Derived Neurospheres and hUCB Lin-ve Stem Cells

We labeled our transplanted cells with fluorescent dye–carboxyfluorescein succinimidyl ester (CFDA-SE) (Sigma-Aldrich) in order to track the Lin-ve SC population and the CE-derived neurospheres after transplantation. For CFDA

Table 1. List of Antibodies Used in Immunohistochemical Experiments Real-Time PCR.

Antibody		Make	Dilution
Primary antibodies			
1.	Rhodopsin	Santa Cruz Biotechnology, USA	1:100
2.	Thy1	Santa Cruz Biotechnology, USA	1:100
3.	BDNF	Santa Cruz Biotechnology, USA	1:100
4.	CNTF	Santa Cruz Biotechnology, USA	1:100
Secondary antibodies			
1.	Cy3 conjugated Donkey α Rabbit	Jackson Immunoresearch, USA	1:200
2.	Cy3 conjugated Donkey α Mouse	Jackson Immunoresearch, USA	1:200
3.	Cy3 conjugated Donkey α Rabbit	Jackson Immunoresearch, USA	1:200
4.	Cy3 conjugated Donkey α Rabbit	Jackson Immunoresearch, USA	1:200

BDNF: brain-derived neurotrophic factor; CNTF: ciliary neurotrophic factor; PCR: polymerase chain reaction.

staining, cells were counted and 50,000 were suspended in 1 µl of PBS, then transplanted after 24 h of injury through transcorneal subretinal route. The endpoint analysis was carried out at 1 week and 3 months after transplantation. The subretinal injection in mice was performed under surgical microscope after giving anesthesia. The prick was made at the cornea–scleral junction with beveled 31G insulin needle and pressure was released without injuring the cornea. A microsyringe (EXMIRE, Fuji, Shizouka, Japan) of 33G was introduced through the pricked area and moved behind the lens and moved till it touched the retina without exerting pressure on it. One milliliter suspension of 50,000 cells was injected carefully and bleb formation was observed. This served as a marker for successful subretinal delivery.

Immunohistochemistry

The eye balls were enucleated after sacrifice and frozen at −80°C and cryosectioned (Leica Cryostat, Buffalo Grove, IL, USA). Immunohistochemistry was performed to analyze the protein expression changes in the retinal layers viz. rhodopsin (Santa Cruz Biotechnology, Dallas, TX, USA), Thy1 (Santa Cruz Biotechnology), brain-derived neurotrophic factor (BDNF; Santa Cruz Biotechnology), and ciliary neurotrophic factor (CNTF; Santa Cruz Biotechnology). The sections were fixed using HistoChoice (Sigma-Aldrich) and then incubated with primary antibody (1:100 dilution) at 4°C overnight. Next day, the sections were kept in Cy3 labeled secondary antibody solution (1:200 dilution) (Jackson Immunoresearch, West Grove, PA, USA) for half an hour and nuclei were counterstained with 4′,6-diamidino-2-phenylindole (Sigma-Aldrich) (1:1,000 dilution) (Table 1). The sections were subsequently imaged under a confocal microscope to analyze the protein expression.

Real-Time Polymerase Chain Reaction

Relative fold change in the expression of the mRNA levels was detected using real-time polymerase chain reaction (PCR). The RNA was isolated from the dissected retinae of the enucleated eye balls, and converted to cDNA libraries, using standard kit protocols (Qiagen, Velno, The Netherlands and Thermo Fisher Scientific, Waltham, MA, USA). Real-time PCR was performed using primers for rhodopsin (Eurofins, Bangalore, India), Thy1 (Eurofins), BDNF (Sigma-Aldrich, New Delhi, India), CNTF (Sigma-Aldrich, New Delhi, India), BCl2 (Eurofins), and Ki67 (Eurofins). β-Actin (Sigma-Aldrich, New Delhi, India) was used for an endogenous housekeeping control (Table 2). Expression levels were quantified and analyzed using StepOne, Applied Biosystems real-time PCR software (Thermo Fisher Scientific).

Statistical Analysis

Data were analyzed by calculating mean ± standard error of the mean, and normality of data was analyzed using 1-KS sampling test. The data were analyzed by one-way analysis of variance (ANOVA) followed by LSD and Scheffe and Dunnett's test for post hoc analysis. Statistical analysis of results was analyzed using 16.0 version of SPSS. $*P \leq 0.05$, $**P \leq 0.01$, and $***P \leq 0.001$ were considered as statistically significant.

Results

CE Cell Transplantation Enhances the Formation of Rod Cells

We used laser-induced retinal injury mouse model without causing CNV. For this, we targeted eight shots in a circular pattern around the optic disc. These shots were focused at the Bruch's membrane, which resulted in the damage to RPE and caused the breach of blood retinal barrier. We validated this model using fundus fluorescein angiography showing leakage in the retinal blood vessels as well as electroretinogram that showed changes in the wave pattern[22]. RPE plays crucial role in providing nutrients to the retina and phagocytosis of photoreceptor's outer segment for its renewal[23]. Therefore, we wanted to analyze the rhodopsin expression, a pigment that makes up rod photoreceptors. The immunohistochemistry for its expression showed significant reduction

Table 2. List of Genes Analyzed and Their Primer Sequences Used for Real-Time PCR.

Sl no.	Gene	Primer sequence	
1.	Rho (mouse)	Forward	5′-CAGTACTCGGAATGCAGCAA-3′
		Reverse	5′-CAGTCTTCAGGGGCTCTGTC-3′
2.	Thy1 (mouse)	Forward	5′-ATTCAGGCCTGCCGGGGTAC-3′
		Reverse	5′-AGTTCTTTCGTGAGCATGGA-3′
3.	BDNF (mouse)	Forward	5′-GCCCTTCGGAGTTTAATCAG-3′
		Reverse	5′-TACACTTGCACACACACGCT-3′
4.	CNTF (mouse)	Forward	5′-GCGAGCGAGTCGAGTGGTTGTCTG-3′
		Reverse	5′-TTAGCTTTCGGCCACCAGAGTGGAGAATTC-3′
5.	Ki67 (mouse)	Forward	5′-CAGTACTCGGAATGCAGCAA-3′
		Reverse	5′-CAGTCTTCAGGGGCTCTGTC-3′
6.	Bcl-2 (mouse)	Forward	5′-GCCCTTCGGAGTTTAATCAG-3′
		Reverse	5′-TACACTTGCACACACACGCT-3′

BDNF: brain-derived neurotrophic factor; CNTF: ciliary neurotrophic factor; PCR: polymerase chain reaction.

in rhodopsin levels in mice injured with laser, in comparison to the control mice. We then transplanted two types of cells, i.e., sixth day dissociated neurospheres differentiated from CE cells or undifferentiated Lin-ve SC derived from human UCB. The protein expression of rhodopsin at 1 week was found to be significantly higher in the retina transplanted with CE differentiated cells in comparison to the group transplanted with Lin-ve SC (Fig. 1A, B). The mRNA expression of rhodopsin was also estimated at 1 week and 3 months after transplantation. We found increased expression of rhodopsin in CE cells transplanted group as compared to Lin-ve SC transplanted group (Fig. 1C).

Differentiated CE Neurospheres Increase the Retinal Ganglion Cells (RGCs) of Retina

RGCs are a type of neurons present on the inner layer of retina. They transmit the visual stimulus at photoreceptor layer by engaging two types of neurons, i.e., bipolar and amacrine cells[24]. As rhodopsin was found to be significantly altered by laser-induced injury therefore, we wanted to analyze the effect of injury as well as transplantation of Lin-ve SC on RGCs. We found reduction of Thy1 protein expression after laser-induced retinal injury. However, transplantation of CE cells induced the upregulation of Thy1 expression (in comparison to control and laser injured mice) evident from quantitative analysis of immunohistochemical staining carried out at 1 week after transplantation (Fig. 2A, B). The mRNA expression of Thy1 showed significant increase after Lin-ve SC transplantation at 1 week, but this expression was abolished significantly when analyzed at 3 months after transplantation (Fig. 2C).

Neurotrophic Modulation by Paracrine Effects Exerted by Undifferentiated hUCB Lin-ve SC Transplantation

The existing literature of stem cell transplantation suggests that these cells either differentiate or aid integration in the host tissues, while others argue that stem cells act by providing neuroprotection mediated by the release of paracrine factors[25]. In the light of paracrine effects, we analyzed the expression levels of BDNF as well as CNTF in all the groups. We report that BDNF levels were upregulated more by transplantation of undifferentiated Lin-ve SC as compared to differentiated CE cells, when analyzed at 1 week (Fig. 3A, B). The mRNA expression of BDNF was concomitantly found increased after Lin-ve SC transplantation (in comparison to laser injured mice at 1 week). However, this effect was again diminished when analyzed at a longer time duration, i.e., 3 months (Fig. 3C).

CNTF is a ciliary neurotrophic factor and regarded as a survival factor for various neuronal types[26]. We estimated CNTF by immunohistochemistry, using confocal microscopy (Fig. 4A). By quantitative analysis (by Image J software), we found significant CNTF expression in laser injured mice. CNTF protein expression was also found upregulated in mice transplanted with CE cells in comparison to Lin-ve SC transplanted mice (Fig. 4B). The mRNA expression of CNTF, analyzed by real-time PCR, showed significant increase in Lin-ve SC transplanted mice in comparison to all other groups at 1-week after transplantation. However, this expression was diminished after 3 months of transplantation (Fig. 4C).

hUCB Lin-ve SC Transplantation Enhances Antiapoptotic and Proliferative Activity in Laser Injured Retina

The stem cells are reported to exert paracrine effects by releasing neurotrophic factors upon transplantation. These neurotrophic factors act as a ligand and initiate cell signaling pathways. BDNF acts as a ligand for TrkB receptor and activates CREB transcriptional factor, further promoting cell survival and maintenance of neuronal cells[27]. Likewise, CNTF is known to initiate Jak-STAT pathway and provides antiapoptotic and proliferative effect[28]. Bcl2, a well-known antiapoptotic marker, acts as a downstream molecule of CNTF initiated pathway. We found significant upregulation

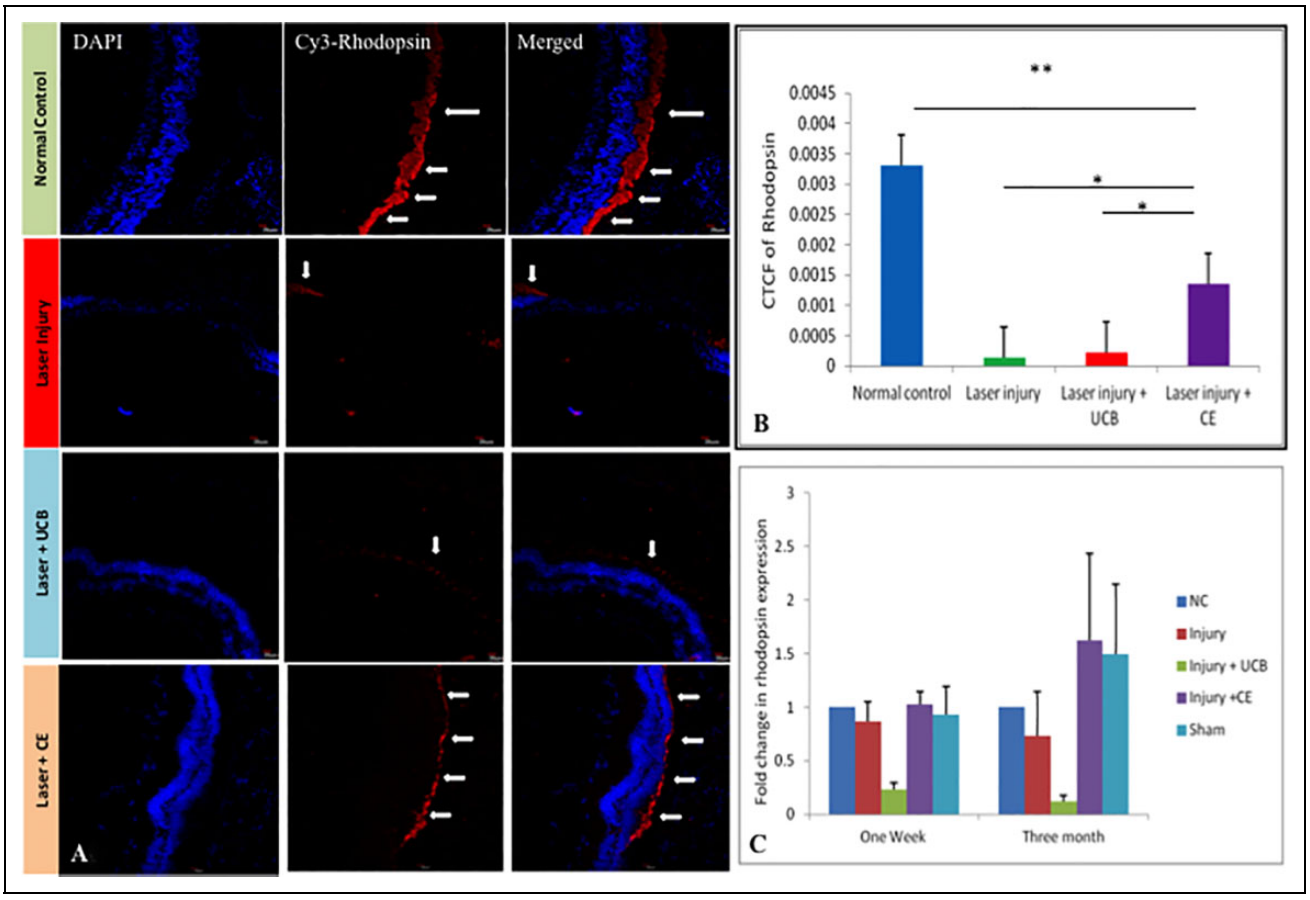


Figure 1. Differentiated CE cells transplantation enhances rod cells expression. (A) Immunohistochemistry of rhodopsin showing Cy3 (red fluorescence marked by arrows) expression bound to primary antibody at 20× visualized under confocal microscope in normal control, laser injured retina mice, laser injured transplanted with Lin-ve SC mice, and laser injured transplanted with CE cells mice. (B) Quantitative protein expression of rhodopsin at 1-week time point measured by corrected total cell fluorescence of immunohistochemistry images using Image J software. (C) mRNA expression of rhodopsin in all four groups was analyzed using real-time PCR at 1 week and 3 months after transplantation. Statistical analysis was performed using one-way ANOVA test for immunohistochemistry and real-time PCR results. This was followed by post-hoc analysis using LSD, Scheffe, and Dunnett's test. *$P \leq 0.05$ and **$P \leq 0.01$ were regarded as statistically significant. ANOVA: analysis of variance; CE: ciliary epithelium; Lin-ve SC: lineage negative stem cells; PCR: polymerase chain reaction.

of Bcl2 mRNA expression after Lin-ve SC transplantation in laser injured mice in comparison to all the groups of 1 week and 3 months after transplantation. However, Bcl2 expression remained unaffected at 3 months after cells transplantation (Fig. 5A).

As proliferation markers are routinely analyzed in stem cell therapies, Ki67, a nuclear antigen of proliferation[29], was found highly upregulated upon transplantation of hUCB-derived Lin-ve SC (as compared to other groups at 1 week after transplantation). However, Ki67 expression was unaltered in all the groups at 3 months after transplantation (Fig. 5B).

Discussion

The series of degenerative changes in retina are due to diseased state with certain injuries resulting in irreversible damage. The currently used drugs have potential for symptomatic relief without halting the disease progression. Our data provide the comparative outcomes of transplantation of differentiated versus undifferentiated cells by utilizing a reproducible model of laser injured mouse retina. We wanted to examine the role of candidate markers of retinal repair and proliferation by transplantation of stem cells isolated from different origins. For that purpose, human eye from abortus fetuses was used to harvest the CE sourced stem cells. Second, we purified the Lin-ve SC from hUCB, a richly harvested source of undifferentiated stem cells.

Retina is an accessible and well-studied part of central nervous system. The retinal cellular structures have been studied in detail[30,31]. The existing studies provide evidence of the existence of stem cells in rodent retina. CE is one of the sources of stem cells shown as a rich source of cells with tremendous differentiation potential[15]. It has also been shown to possess the capacity to differentiate into specific retinal cell lineages for better

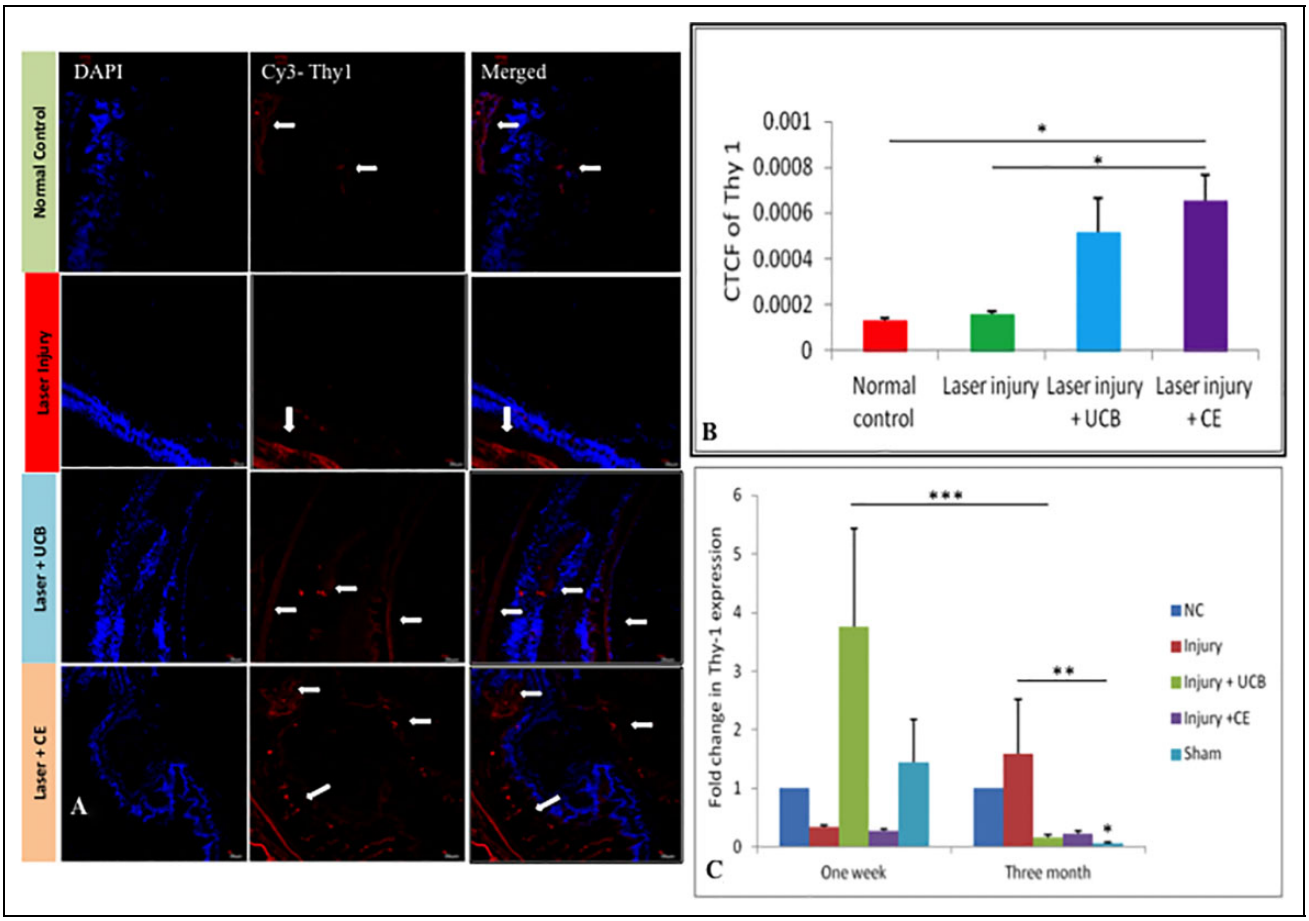


Figure 2. Differentiated CE cell transplantation enhances expression of retinal ganglion cells. (A) Immunohistochemistry of Thy1 showing Cy3 (red fluorescence marked by arrows) expression bound to primary antibody at 20× visualized under confocal microscope in normal control mice, laser injured retina mice, laser injured transplanted with Lin-ve SC mice, and laser injured transplanted with CE cells mice. (B) Quantitative protein expression of Thy1 at 1 week after transplantation was measured by corrected total cell fluorescence of immunohistochemistry images using Image J software (C). mRNA expression of Thy1 in all four groups was analyzed using real-time PCR at 1 week as well as 3 months after transplantation. Statistical analysis was performed using one-way ANOVA test for immunohistochemistry and real-time PCR results. This was followed by post hoc analysis using LSD, Scheffe, and Dunnett's test. $^{*}P \leq 0.05$, $^{**}P \leq 0.01$, and $^{***}P \leq 0.001$ were regarded as statistically significant. ANOVA: analysis of variance; CE: ciliary epithelium; Lin-ve SC: lineage negative stem cells; PCR: polymerase chain reaction.

integration into host tissue because of a similar niche. The pigmented CE has been shown to result in BrdU incorporation when provided with mitogens in vivo along with increase in cyclin D1 and Ki67 expression[32]. These cells, when stimulated with growth factors, rhEGF and bFGF, have been shown to form self-renewing colonies expressing retinal progenitor marker, i.e., Chx10[33]. Therefore, we used neurospheres that were differentiated from CE cells from human fetal eyes to examine how the stem cell markers are altered in laser-induced retinal injury in comparison to other cell types. We subretinally transplanted sixth day dissociated neurospheres into the laser-induced injury in retina of the mouse model. A significant expression of rhodopsin and Thy1 was reported in the mice retina after 1 week of transplantation (Figs. 1, 2). These data suggest that CE cells are involved in the rescue of retinal injury by activating the progenitor cells residing in the retina, which aid their differentiation into rods and RGCs. In comparison, CE cells are better positioned in the repair by activating the retinal markers and exerting neurotrophic effects superior to Lin-ve SC.

It has been shown that mesenchymal stem cells derived from hUCB exert neuroprotective effects by secreting several trophic factors including TGFbeta-1, NT-3, BDNF, and CNTF. These stem cells showed repair and regeneration of damaged neurons when transplanted in rat optic tract model[34]. Further, studies have shown transplantation of these cells intravenously in a neonatal hypoxic ischemia induced injury rat model could recover motor abilities mediated by neurotrophic factors, i.e., GDNF, BDNF, and NGF[35]. Endogenous cells secrete these neurotrophic factors mediated by paracrine effectors of transplanted cells. These

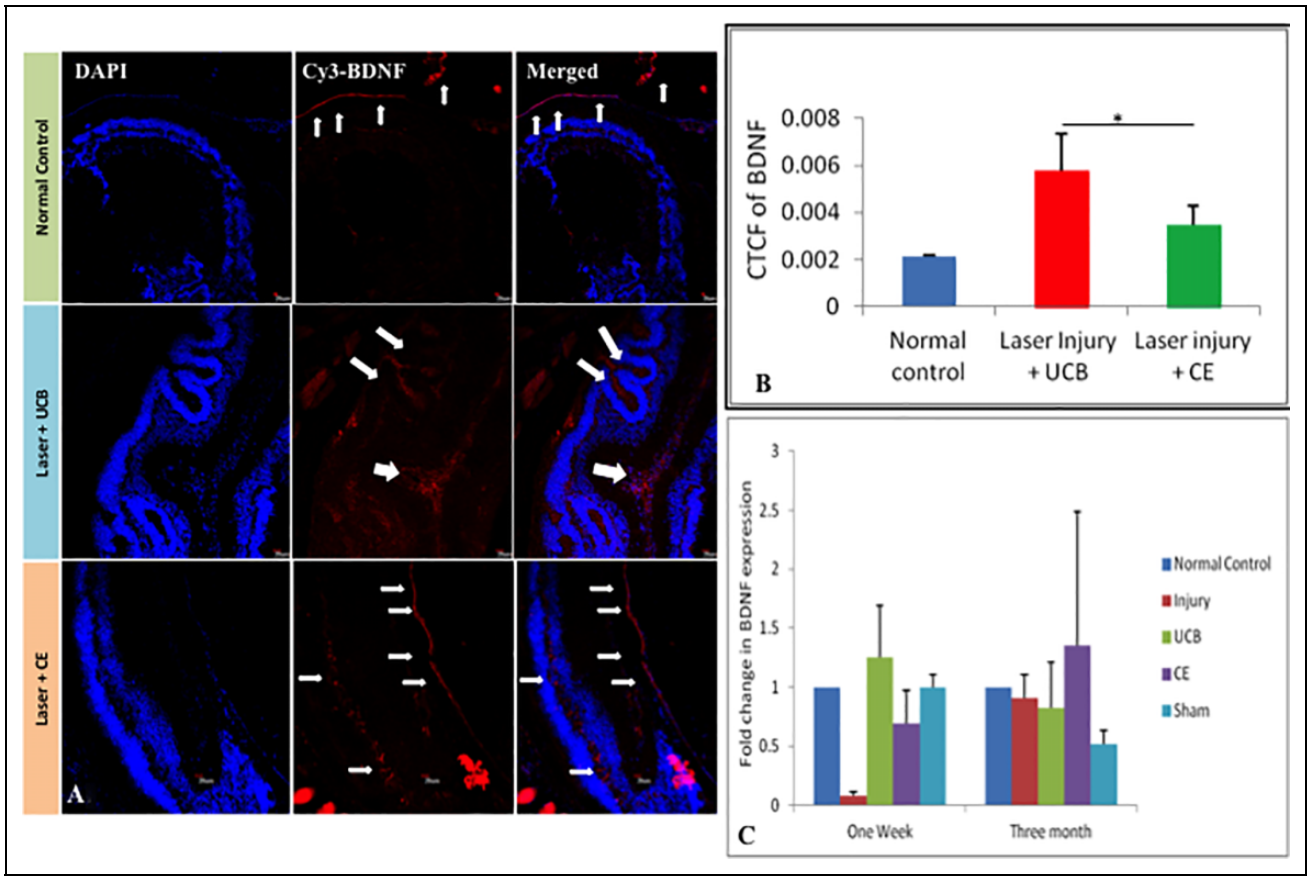


Figure 3. Neurotrophic factor modulation by the Lin-ve SC transplantation. (A) Immunohistochemistry of BDNF showing Cy3 (red fluorescence marked by arrows) expression bound to primary antibody at 20× visualized under confocal microscope in normal control, laser injured mice transplanted with Lin-ve SC, and laser injured mice transplanted with CE cells. (B) Quantitative protein expression of BDNF at 1-week time point measured by corrected total cell fluorescence of immunohistochemistry images using Image J software. (C) mRNA expression of BDNF in all four groups was analyzed using real-time PCR at 1-week as well as 3-month time point. Statistical analysis was performed using one-way ANOVA test for immunohistochemistry and real-time PCR results. This was followed by post hoc analysis using LSD, Scheffe, and Dunnett's test. *$P \leq 0.05$ was regarded as statistically significant. ANOVA: analysis of variance; BDNF: brain-derived neurotrophic factor; CE: ciliary epithelium; Lin-ve SC: lineage negative stem cells; PCR: polymerase chain reaction.

trophic factors generally play an active role in neuronal development and survival by promoting proliferation, regeneration, and maturation of neurons[32]. The administration of trophic factors, e.g., CNTF, BDNF, and NT-4 has resulted in prevention of ON-injury-induced RGC death[36]. Other studies have described the effect of trophic factor administration (CNTF, BDNF, or PEDF) via intravitreal route on prevention of phototoxic-induced degeneration of photoreceptors cells[37]. Hence, such studies provide the necessary basis of studying the levels of these paracrine factors in transplantation studies. Our results that there is upregulation of BDNF after Lin-ve SC transplantation are consistent with other studies (Fig. 3).

Our results showed that there was significant enhancement in the expression of CNTF in the Lin-ve SC transplanted retina (when compared to the laser injured and CE cells transplanted group). CNTF is known to regulate via JAK/STAT pathway[28]. Bcl2 comprises the downstream effector molecule[38] and hence the upregulation of Bcl2 and CNTF mRNA (Figs. 4C, 5A). However, immunohistochemistry shows the shoot in the level of neurotropic factors in injured group, which are maintained sustainably by the CE injected group while there is not the similar sustenance in the UCB injected group. The dichotomy of CNTF mRNA and protein expression can be ascribed to post-translational differences in both the experimental and intervention groups. This can be further examined by using specific inhibitors of CNTF.

Ki67 is the universal molecule for investigating proliferation. It was found to have increased expression upon Lin-ve SC transplantation (Fig. 5B). The activity of the enhanced endogenous proliferation needs further elaboration. Therefore, our results unanimously reveal that hUCB-derived Lin-ve SC, when transplanted at the site of retinal injury, induce expression of neurotrophic factors, which may exert neuroprotective effect mediated by the antiapoptotic and

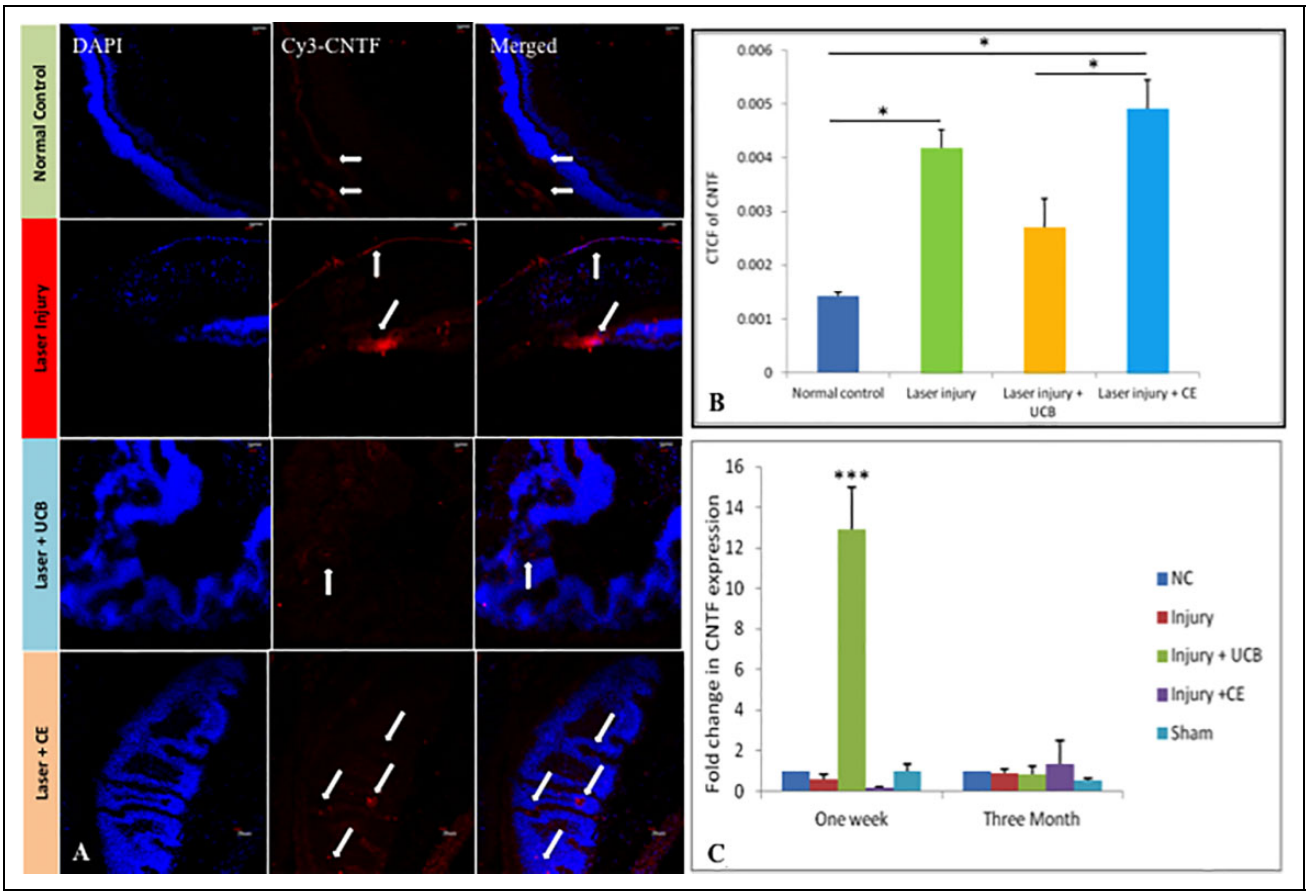


Figure 4. CE cell transplantation upregulated ciliary neurotrophic factor in the laser injured retina. (A) Immunohistochemistry of CNTF showing Cy3 (red fluorescence marked by arrows) expression bound to primary antibody at 20× visualized under confocal microscope in normal control, laser injured mice, laser injured mice transplanted with Lin-ve SC, and laser injured mice transplanted with CE cells. (B) Quantitative protein expression of CNTF at 1-week time after transplantation measured by corrected total cell fluorescence of immunohistochemistry images using Image J software. (C) mRNA expression of CNTF in all four groups was analyzed using real-time PCR at 1 week as well as 3 months after transplantation. Statistical analysis was performed using one-way ANOVA for immunohistochemistry and real-time PCR results. This was followed by post hoc analysis using LSD, Scheffe, and Dunnett's test. *$P \leq 0.05$, **$P \leq 0.01$, and ***$P \leq 0.001$ were regarded as statistically significant. ANOVA: analysis of variance; CE: ciliary epithelium; CNTF: ciliary neurotrophic factor; Lin-ve SC: lineage negative stem cells; PCR: polymerase chain reaction.

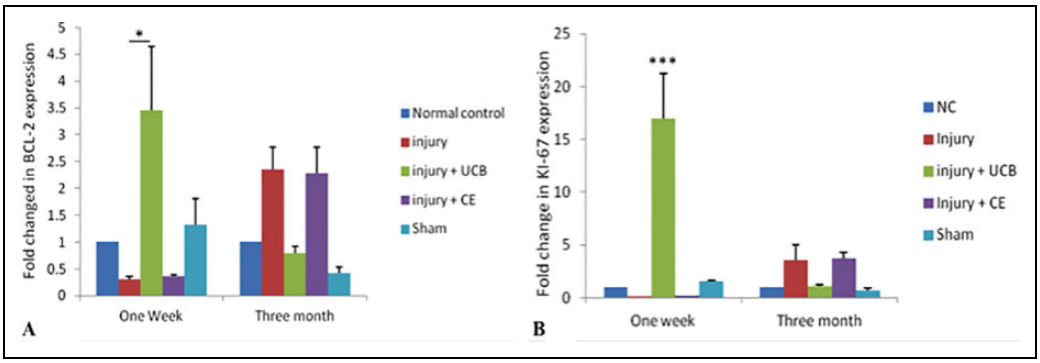


Figure 5. Antiapoptotic and proliferative activity enhanced by Lin-ve SC transplantation in laser injured retina. (A, B) mRNA expression of antiapoptotic marker Bcl2 and proliferative marker, i.e., Ki67 in all four groups was analyzed using real-time PCR at 1 week as well as 3 months after transplantation. Statistical analysis was performed using one-way ANOVA for real-time PCR results. This was followed by post hoc analysis using LSD, Scheffe, and Dunnett's test. *$P \leq 0.05$, **$P \leq 0.01$, and ***$P \leq 0.001$ were regarded as statistically significant. ANOVA: analysis of variance; CE: ciliary epithelium; Lin-ve SC: lineage negative stem cells; PCR: polymerase chain reaction.

proliferative mechanisms. Importantly, our study indicates the need for the multiple doses of Lin-ve SC transplantation instead of single dose as the paracrine effects noted in the study did not last for longer duration investigated.

Briefly, we explain the superior outcomes from transplantation of CE-related stem cells by ascribing it to same niche, i.e., retina providing conducive niche for rescue when compared to undifferentiated Lin-ve SC. In the context of noted paracrine effects, Lin-ve SC provide comparable outcomes but mediated by antiapoptotic and proliferative mechanisms. However, as Lin-ve SC effects lasted for a few weeks, it is suggested to examine the associated pathway at extended time frame using multiple doses of Lin-ve SC. Such studies will be helpful in utilizing the cord blood stored in the banks and for developing therapies for untreatable disorders of the retina. The main limitation of the study is that we were not able to perform immunohistochemistry of BDNF due to limited availability of eye samples.

Conclusion

The transplantation of CE cells showed superior outcomes than the undifferentiated Line-ve UCB-derived SC when tested in retinal injury mouse model. Based on the retinal marker analysis, we hypothesize that while the CE cells aid the formation of rods and ganglion cell layer, the Lin-ve SC transplantation promotes antiapoptotic and proliferative activity by neurotrophic modulation. We could not test the therapeutic outcome on the neuroprotective or paracrine effects from transplantation of multiple doses of Lin-ve SC or those at extended time points as the study was limited for a few weeks. Also, we have neither tested the per se effect of the transplantation of prominent markers on retinal repair nor evaluated the physiological changes. Hence, this study provides the rationale for more comprehensive analysis of the different sources of stem cells and their transplantation effects for extended duration. It is pertinent to note that clinical trial recently used RPE cells differentiated from autologous iPSCs and resulted in successful transplantation[39,40]. Our study thus provides preliminary data for future clinical application of the stem cell therapy for treating several retinal injuries.

Data Availability

All raw data are available with the first author of this manuscript.

Ethical Approval

Ethical approval for animals was obtained from Institutional Animal Ethics Committee (IAEC), Post Graduate Institute of Medical Education and Research, Chandigarh, India [71(69)/IAEC/423]. Human UCB samples were obtained after the approval from Institutional Committee for Stem Cell Research and Therapy, Post Graduate Institute of Medical Education and Research, Chandigarh, India (IC-SCRT: Approval No. PGI-ICSCRT-53-2014/1469).

Statement of Human and Animal Rights

All the experimental procedures were conducted in accordance with Committee for the Purpose of Control and Supervision of Experiments on Animals (CPSEA) guidelines.

Statement of Informed Consent

The samples were obtained after filling the proper informed consent forms by participants after explaining the complete protocol.

Declaration of Conflicting Interests

The author(s) declared no potential conflicts of interest with respect to the research, authorship, and/or publication of this article.

Funding

The author(s) disclosed receipt of the following financial support for the research, authorship, and/or publication of this article: Funding was obtained from Department of Science and Technology, Science and Engineering Research Board, India (EMR/2016/000190) and Department of Biotechnology, India.

ORCID iD

Akshay Anand https://orcid.org/0000-0001-9003-3532

References

1. Dietrich KC. Aircrew and handheld laser exposure. Aerosp Med Hum Perform. 2017;88(11):1040–1042.
2. Sliney DH. Risks of occupational exposure to optical radiation. Med Lav. 2006;97(2):215–220.
3. Orlacchio A, Bernardi G, Orlacchio A, Martino S. Stem cells: an overview of the current status of therapies for central and peripheral nervous system diseases. Curr Med Chem. 2010;17(7):595–608.
4. Hill AJ, Zwart I, Tam HH, Chan J, Navarrete C, Jen LS, Navarrete R. Human umbilical cord blood-derived mesenchymal stem cells do not differentiate into neural cell types or integrate into the retina after intravitreal grafting in neonatal rats. Stem Cells Dev. 2009;18(3):399–409.
5. Muthaian R, Minhas G, Anand A. Pathophysiology of stroke and stroke-induced retinal ischemia: emerging role of stem cells. J Cell Physiol. 2012;227(3):1269–1279.
6. Qiu XC, Jin H, Zhang RY, Ding Y, Zeng X, Lai BQ, Ling EA, Wu JL, Zeng YS. Donor mesenchymal stem cell-derived neural-like cells transdifferentiate into myelin-forming cells and promote axon regeneration in rat spinal cord transection. Stem Cell Res Ther. 2015;6(1):105.
7. Byun JS, Lee CO, Oh M, Cha D, Kim WK, Oh KJ, Bae KH, Lee SC, Han BS. Rapid differentiation of astrocytes from human embryonic stem cells. Neurosci Lett. 2019;716:134681.
8. Rowland TJ, Buchholz DE, Clegg DO. Pluripotent human stem cells for the treatment of retinal disease. J Cell Physiol. 2012;227(2):457–466.
9. Karamali F, Esfahani MN, Hajian M, Ejeian F, Satarian L, Baharvand H. Hepatocyte growth factor promotes the proliferation of human embryonic stem cell derived retinal pigment epithelial cells. J Cell Physiol. 2019;234(4):4256–4266.

10. Wang X, Zhao Y, Wang X. Umbilical cord blood cells regulate the differentiation of endogenous neural stem cells in hypoxic ischemic neonatal rats via the hedgehog signaling pathway. Brain Res. 2014;1560:18–26.
11. Wang XL, Zhao YS, Hu MY, Sun YQ, Chen YX, Bi XH. Umbilical cord blood cells regulate endogenous neural stem cell proliferation via hedgehog signaling in hypoxic ischemic neonatal rats. Brain Res. 2013;1518:26–35.
12. Pandey D, Kaur S, Kamath A. Banking Umbilical Cord Blood (UCB) stem cells: awareness, attitude and expectations of potential donors from one of the largest potential repository (India). PLoS One. 2016;11(5):e0155782.
13. Sihota R, Sen S, Mohanty S, Ahmad M, Ravi A, Gupta V, Bhatla N. Effect of intracameral human cord blood-derived stem cells on lasered rabbit trabecular meshwork. Int ophthalmol. 2019;39(12):2757–2766.
14. Coles BL, Angenieux B, Inoue T, Del Rio-Tsonis K, Spence JR, McInnes RR, Arsenijevic Y, van der Kooy D. Facile isolation and the characterization of human retinal stem cells. Proc Natl Acad Sci U S A. 2004;101(44):15772–15777.
15. Xu H, Sta Iglesia DD, Kielczewski JL, Valenta DF, Pease ME, Zack DJ, Quigley HA. Characteristics of progenitor cells derived from adult ciliary body in mouse, rat, and human eyes. Invest Ophthalmol Vis Sci. 2007;48(4):1674–1682.
16. Bali P, Bammidi S, Banik A, Nehru B, Anand A. CD34 and CD117 stemness of lineage-negative cells reverses memory loss induced by amyloid beta in mouse model. Front Behav Neurosci. 2018;12:222.
17. Banik A, Prabhakar S, Kalra J, Anand A. An enriched population of CD45, CD34 and CD117 stem cells in human umbilical cord blood for potential therapeutic regenerative strategies. Curr Neurovasc Res. 2014;11(4):312–320.
18. Bali P, Banik A, Nehru B, Anand A. Neurotrophic factors mediated activation of astrocytes ameliorate memory loss by amyloid clearance after transplantation of lineage negative stem cells. Mol Neurobiol. 2019;56(12):8420–8434.
19. Kim DH, Lim H, Lee D, Choi SJ, Oh W, Yang YS, Oh JS, Hwang HH, Jeon HB. Thrombospondin-1 secreted by human umbilical cord blood-derived mesenchymal stem cells rescues neurons from synaptic dysfunction in Alzheimer's disease model. Sci Rep. 2018;8(1):354.
20. Goody RJ, Hu W, Shafiee A, Struharik M, Bartels S, López FJ, Lawrence MS. Optimization of laser-induced choroidal neovascularization in African green monkeys. Exp Eye Res. 2011; 92(6):464–472.
21. Ail D, Perron M. Retinal degeneration and regeneration—lessons from fishes and amphibians. Curr Pathobiol Rep. 2017; 5(1):67–78.
22. Bammidi S, Modgil S, Kalra J, Anand A. Human fetal pigmented ciliary epithelium stem cells have regenerative capacity in the murine retinal degeneration model of laser injury. Curr Neurovasc Res. 2019;16(3):187–193.
23. Boulton M, Dayhaw-Barker P. The role of the retinal pigment epithelium: topographical variation and ageing changes. Eye (Lond). 2001;15(Pt 3):384–389.
24. Belenky MA, Smeraski CA, Provencio I, Sollars PJ, Pickard GE. Melanopsin retinal ganglion cells receive bipolar and amacrine cell synapses. J Comp Neurol. 2003;460(3):380–393.
25. Bali P, Lahiri DK, Banik A, Nehru B, Anand A. Potential for stem cells therapy in alzheimer's disease: do neurotrophic factors play critical role? Curr Alzheimer Res. 2017;14(2): 208–220.
26. Ip NY, Li Y, Van de Stadt I, Panayotatos N, Alderson R, Lindsay R. Ciliary neurotrophic factor enhances neuronal survival in embryonic rat hippocampal cultures. J Neurosci. 1991; 11(10):3124–3134.
27. Finkbeiner S. CREB couples neurotrophin signals to survival messages. Neuron. 2000;25(1):11–14.
28. Peterson WM, Wang Q, Tzekova R, Wiegand SJ. Ciliary neurotrophic factor and stress stimuli activate the Jak-STAT pathway in retinal neurons and glia. J Neurosci. 2000;20(11): 4081–4090.
29. Zhang X, Barile G, Chang S, Hays A, Pachydaki S, Schiff W, Sparrow J. Apoptosis and cell proliferation in proliferative retinal disorders: PCNA, Ki-67, caspase-3, and PARP expression. Curr Eye Res. 2005;30(5):395–403.
30. Kidd M. Electron microscopy of the inner plexiform layer of the retina in the cat and the pigeon. J Anat. 1962;96(Pt 2): 179–187.
31. Cowan WM, Powell TP. Centrifugal fibres to the retina in the pigeon. Nature. 1962;194:487.
32. Heo JH, Yoon JA, Ahn EK, Kim H, Urm SH, Oak CO, Yu BC, Lee SJ. Intraperitoneal administration of adipose tissue-derived stem cells for the rescue of retinal degeneration in a mouse model via indigenous CNTF up-regulation by IL-6. J Tissue Eng Regen Med. 2018;12(3):e1370–e1382.
33. Ahmad I, Tang L, Pham H. Identification of neural progenitors in the adult mammalian eye. Biochem Biophys Res Commun. 2000;270(2):517–521.
34. Zwart I, Hill AJ, Al-Allaf F, Shah M, Girdlestone J, Sanusi AB, Mehmet H, Navarrete R, Navarrete C, Jen L-S. Umbilical cord blood mesenchymal stromal cells are neuroprotective and promote regeneration in a rat optic tract model. Exp Neurol. 2009; 216(2):439–448.
35. Yasuhara T, Hara K, Maki M, Xu L, Yu G, Ali M, Masuda T, Yu S, Bae E, Hayashi T. Mannitol facilitates neurotrophic factor up-regulation and behavioural recovery in neonatal hypoxic-ischaemic rats with human umbilical cord blood grafts. J Cell Mol Med. 2010;14(4):914–921.
36. Spalding K, Cui Q, Harvey A. Retinal ganglion cell neurotrophin receptor levels and trophic requirements following target ablation in the neonatal rat. Neuroscience. 2005;131(2): 387–395.
37. Ortín-Martínez A, Valiente-Soriano FJ, García-Ayuso D, Alarcón-Martínez L, Jiménez-López M, Bernal-Garro JM, Nieto-López L, Nadal-Nicolás FM, Villegas-Pérez MP, Wheeler LA. A novel in vivo model of focal light emitting diode-induced cone-photoreceptor phototoxicity: neuroprotection afforded by brimonidine, BDNF, PEDF or bFGF. PLoS One. 2014;9(12):e113798.

38. Sepulveda P, Encabo A, Carbonell-Uberos F, Minana M. BCL-2 expression is mainly regulated by JAK/STAT3 pathway in human CD34+ hematopoietic cells. Cell Death Differ. 2007; 14(2):378–380.
39. Takag S, Mandai M, Gocho K, Hirami Y, Yamamoto M, Fujihara M, Sugita S, Kurimoto Y, Takahash M. Evaluation of transplanted autologous induced pluripotent stem cell-derived retinal pigment epithelium in exudative age-related macular degeneration. Ophthalmol Retina. 2019; 3(10):850–859.
40. Parolini B, Di Salvatore A, Finzi A. Autologous choroidal RPE patch transplantation in hemorrhagic age-related macular degeneration. In: Hattenbach LO, editors. Management of Macular Hemorrhage. Cham: Springer; 2018. p. 83–92.

Electrophysiological assessment of retinal functions by ERG in Ischemia/Reperfusion (I/R) *Allium cepa* pre-treated mice

Saurabh Kumar, Richa Shri, Sushmita Kaushik, Varinder Singh, Akshay Anand*

Neuroscience Research Lab, Department of Neurology, Post Graduate Institute of Medical Education and Research (PGIMER), Chandigarh, India.

KEY WORDS

Allium cepa
pretreatment
ERG
PPA
Retina

ABSTRACT

Retinal disorders are the one of the most challenging and complex degenerative diseases that need to be addressed because of rapid increase in the number of affected individuals. Most of the available treatments strategies are inadequate to exert permanent solution to the patients. Therefore, as an alternative approach we wanted to test the efficacy of *Allium cepa* (*A. cepa*) in an Ischemia/Reperfusion (I/R) mouse model. We orally administered the aqueous extract of *A. cepa* at different dosages 100 mg/kg, 200 mg/kg, 300 mg/kg 24 hrs prior to the surgery. Electroretinogram (ERG) analysis was carried out at 7 day, 21 day, and 28 day after the surgery. ERG recording depicted that *A. cepa* administration is able to increase the implicit time but not at the statistically significant level for which larger sample size and deeper analysis is required.

doi: 10.38205/imcr.010118

*Corresponding author

Akshay Anand, PhD
Neuroscience Research Lab
Department of Neurology
Post Graduate Institute of Medical Education and Research (PGIMER), Chandigarh, India
Contact no: +91-9914209090
E-mail: akshay1anand@rediffmail.com

Introduction

Repeated failure in treating different neurodegenerative diseases have left no option for the researchers to think about the alternative approaches. Fruits and vegetables are the excellent alternative source to treat such disorders (1). Different studies suggest the potential role of fruits and vegetables in reducing the risk of degenerative diseases (2, 3). Flavonoids, a polyphenolic secondary metabolite are known to have antioxidant, anti-inflammatory, and anti-microbial properties. These flavonoids have been used in different *in vitro* and *in vivo* models and several studies suggests its protective role in degenerative diseases (4, 5).

Eye related disorders are most common degenerative disorders and have very limited scope of permanent cure. However, to overcome this, various traditional approaches like herbal remedy and homeopathy have been employed by ophthalmologist (6). Scientific studies have reported preventive role of onion on different eye related disorders like; Cataract (7, 8), Age-related Macular Degeneration (AMD) (9).

Onion bulbs (*Allium cepa L.*) are the rich source of flavonoid, especially in quercetin. Different groups have elucidated the potential biological activity of *A. cepa* as neuroprotective, antioxidant, antiallergic, and anti-inflammatory (5, 10, 11). Published literature explains that onion extract (OE) lowers the total cholesterol content in rabbits (12) and in rats (13) fed with high cholesterol diet. Protective role of ethanolic extract of *A. cepa* was found in case of cognition impairments in streptozotocin induced rat diabetes model (14). The neuroprotective effect of flavonoid is known to exert by two processes: First, by interacting with lipid kinase thereby leading to the inhibition of the apoptosis. Second, by benefiting the vascular system (15).

Retinal ischemia which is a leading cause of blindness, results due to insufficient supply of blood to the retina and is known to be associated with several eye related disorders like glaucoma, diabetic retinopathy, and optic retinopathy (16). There have not been many studies on neuroprotective role of onion in rescuing the retinal ganglion cell death resulting due to retinal ischemia. Therefore, in the present study we have investigated the efficacy of aqueous extract of *Allium cepa* in rescuing the retinal functions depicted by electroretinogram (ERG) analysis. Ischemia/Reperfusion (I/R) induced retina injured mouse model was used to alter the retinal functions thereby affecting the vision.

ERG is a non-invasive technique used to depict the retinal functions. The ability of ERG to detect and isolate various signals from a different set of retinal neurons makes it a important tool for electrophysiological measures and this can be achieved by controlling/changing the stimulus, light intensity or adaptation, and parameters for data processing (17). Data acquisition in the form of wave pattern is a means to represent and distinguish different retinal cells activity. The wave pattern generally starts in the following pattern: "a-wave" is the first negative deflection and represents the primary retinal neurons (photoreceptors: rods and cones); "b-wave" is the

positive peak which represents the bipolar cells (17); c-wave originates from retinal pigment epithelium (RPE) cells; oscillatory potentials (OP) originates from inner retina/amacrine cells (18). We used scotopic ERG (dark-adapted mice) for this purpose.

Methods

Animals

A C-57BL/6J male 8- to 10-week old mouse was used for the experimentation purpose. The weight of the mice ranges from 25 g–30 g. Ethical approval was obtained from animal ethical committee (IAEC) of Post Graduate Institute of Medical Education & Research (PGIMER), Chandigarh, India. The animals were kept in the sterile cages and temperature and humidity controlled facility of PGIMER animal house with no restriction to food and water. A 12 hr light/dark cycle was followed. The animals were divided into 4 groups **(Figure 1)**.

Experimental groups

The complete experiment was carried according to the GLP guidelines at Neuroscience Research Laboratory (19, 20). The *A. cepa* extract preparation is detailed in our previous publication (21). Different dosages of *A. cepa* (100 mg/kg, 200 mg/kg, 300 mg/kg) was administered 24 hours prior to the surgery. Animals were divided into 4 different groups: group 1 (Injury alone), group 2 (Injury + 100 mg/kg *A. cepa* pretreatment), group 3 (Injury + 200 mg/kg *A. cepa* pretreatment), and group 4 (Injury + 300 mg/kg *A. cepa* pretreatment).

Surgery

Combination of Xylazine (50 mg/ml) / Ketamine (1:4 ratio) was used to anesthetize the mice. Intraperitoneal injection (IP) was administrated. Approximately 1.5 cm incision was made around the neck region. Initially, the CCA was exposed by retracting the muscles. The bifurcation was exposed and ECA was

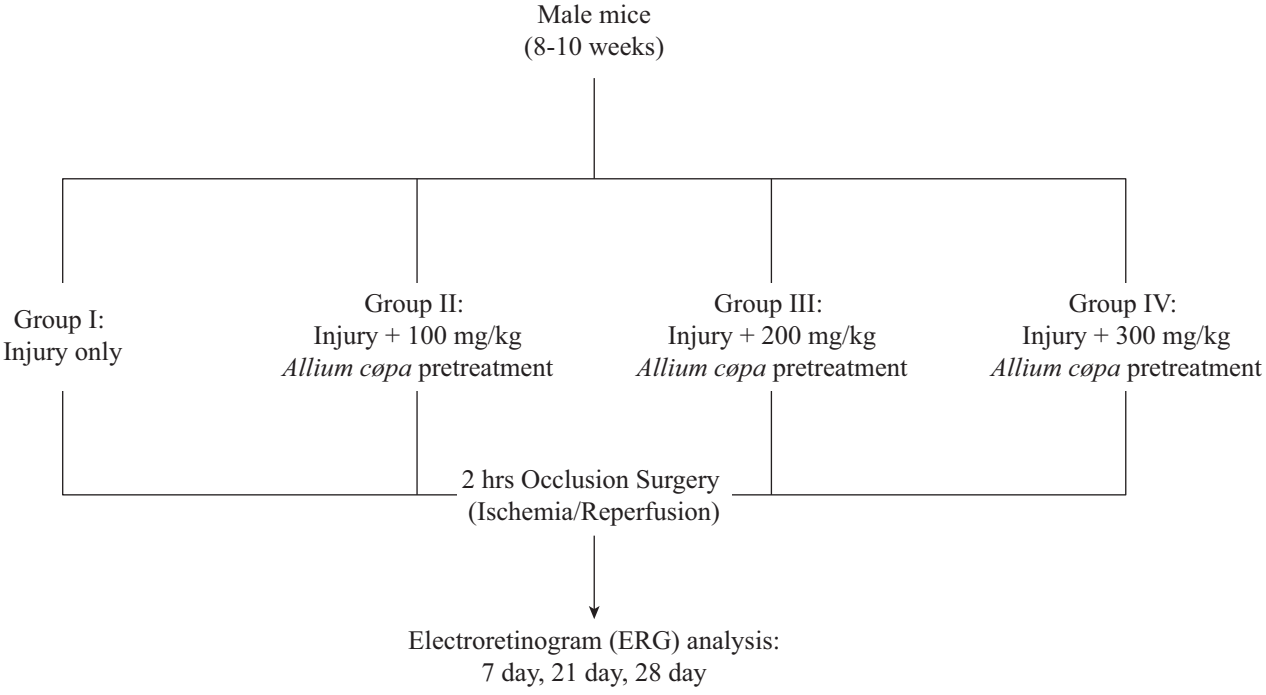


Fig. 1: Representation of the study design.

ligated with a fine suture. Further, the bifurcation of ICA was traced down and PPA was ligated with a 7.0 mm ethicon suture. The ligation was maintained for 2 hrs after that the ligated sutures were removed and mice was allowed to reperfuse (7 day, 21 day, and 28 day) under the sterile condition. The surgery was carried out under the Leica Stereozoom microscope.

Electroretinography recordings

Scotopic electroretinography (ERG) was performed to evaluate the function of retina caused due to 2 hrs of ischemia. The experiment was carried out using iWork ERG instrument (Dover, USA). The ERG data was recorded and evaluated using Labscribe software. ERG was done for all the 4 groups. This experiment was performed once the 24 hrs dark adaptation completed. Anesthesia was administrated intraperitoneally and the animals were kept on heating pad. Tropicamide and methylcellulose eye drops were used to dilate the pupils. Ground electrode was placed on tail, negative electrode in between the ears, and positive electrode was connected to the cornea (19). The readings were taken with flashes of light.

Right eye represents the 'test eye' whereas the left eye was taken as the 'control eye'. Later on, the amplitudes of different wave were measured.

Results

Table 1 represents the implicit time and amplitude of both a- and b- waves depicted by ERG. Scotopic ERG was performed on 24 hrs dark adapted mice. We recorded four important parameters, i.e. implicit time to a-wave, implicit time to b-wave, amplitude of a-wave, and amplitude of b-wave. At 7 day, the implicit time to a-wave was found to be 45 ± 5.78 for Injury alone, 35 ± 8.01 for 100 mg/kg pretreated, 44.85 ± 2.86 for 200 mg/kg pretreated, and 45.45 ± 1.72 for 300 mg/kg pretreated group. We found that at 21 day the mean implicit time to a wave was highest 43.55 ± 1.72 for 200 mg/kg, whereas for injury alone it was 42.25 ± 4.51, for 100 mg/kg group it was 42.27 ± 1.62 and for 300 mg/kg it was 36.95 ± 6.75. With the increase in time points the we observed that at 28 day the implicit time to a wave also increased i.e. 51.13 ± 3.12, 43.33 ± 0.85, 44.33 ± 1.84, 46.2 ± 0.76 for injury alone, 100 mg/kg, 200 mg/kg, and 300 mg/kg, respectively. Positive wave i.e. the b-wave implicit time was found to be 88.27 ± 9.26 for injury alone at 7 day, whereas for 21 day it was 77.25 ± 7.67, and for 28 day it recorded 102.27 ± 5.72. For *A. cepa* pretreatment group's implicit time to b wave at 7 day was 88.8 ± 7.17 for 100 mg/kg, 90.8 ± 2.19 for 200 mg/kg and 92.3 ± 1.45

Table 1: Electroretinogram (ERG) analysis for Injury alone, and *A. cepa* pretreated groups (100 mg/kg, 200 mg/kg, 300 mg/kg) at different time points (7 day, 21 day, 28 day) (A). a-wave implicit time; b-wave implicit time (B). a-wave amplitude; b-wave amplitude. The data is represented as mean ± SE. For Injury alone group sample size was (7 day (n = 3); 21 day (n = 4); 28 day (n = 3)); for 100 mg/kg pretreated group (7 day (n = 4); 21 day (n = 3); 28 day (n = 3)); for 200 mg/kg pretreated group (7 day (n = 4); 21 day (n = 4); 28 day (n = 3)); for 300 mg/kg pretreated group (7 day (n = 4); 21 day (n = 4); 28 day (n = 4)).

A.	Implicit Time a (Time in ms ± SE)				Implicit Time b (Time in ms ± SE)			
Time/Groups	**Injury**	**100 mg/kg**	**200 mg/kg**	**300 mg/kg**	**Injury**	**100 mg/kg**	**200 mg/kg**	**300 mg/kg**
7 day	45 ± 5.78	35 ± 8.01	44.85 ± 2.86	45.45 ± 1.72	88.27 ± 9.26	88.8 ± 7.17	90.8 ± 2.19	92.3 ± 1.46
21 day	42.25 ± 4.51	42.27 ± 1.62	43.55 ± 1.72	36.95 ± 6.75	77.25 ± 7.67	87.2 ± 8.25	86.4 ± 3.89	88.3 ± 8.09
28 day	51.13 ± 3.12	43.33 ± 0.85	44.33 ± 1.84	46.2 ± 0.76	102.27 ± 5.72	79 ± 4.06	82 ± 4.56	89.6 ± 5.09

B.	Amplitude a (Time in ms ± SE)				Amplitude b (Time in ms ± SE)			
Time/Groups	**Injury**	**100 mg/kg**	**200 mg/kg**	**300 mg/kg**	**Injury**	**100 mg/kg**	**200 mg/kg**	**300 mg/kg**
7 day	−0.198 ± 0.031	−0.192 ± 0.045	−0.339 ± 0.071	−0.595 ± 0.013	0.0163 ± 0.016	0.021 ± 0.03	0.007 ± 0.02	0.086 ± 0.007
21 day	−0.1025 ± 0.048	−0.363 ± 0.05	−0.205 ± 0.031	−0.407 ± 0.024	0.0295 ± 0.024	0.0673 ± 0.026	0.0617 ± 0.012	0.078 ± 0.020
28 day	−0.124 ± 0.017	−0.188 ± 0.026	−0.302 ± 0.029	−0.356 ± 0.062	0.004 ± 0.038	0.0163 ± 0.006	0.1076 ± 0.035	0.074 ± 0.044

for 300 mg/kg. At 21 day we found slight decrease in the implicit time to b-wave i.e. 87.2 ± 8.25 (100 mg/kg), 86.4 ± 3.89 (200 mg/kg), 88.3 ± 8.09 (300 mg/kg). Similar trends where observed for 28 day where mean implicit time to b-wave was recorded as follows: 79 ± 4.06, 82 ± 4.56, and 89.6 ± 5.09 for 100 mg/kg, 200 mg/kg, 300 mg/kg respectively.

Further, the amplitude for both the waves was recorded. The amplitude of a-wave for injury alone was −0.198 ± 0.031 (7 day), −0.1025 ± 0.048 (21 day), −0.124 ± 0.017 (28 day); for 100 mg/kg pretreatment group it was -0.192 ± 0.045 (7 day), −0.363 ± 0.05 (21 day), −0.188 ± 0.026 (28 day); for 200 mg/kg pretreatment group it was −0.339 ± 0.071 (7 day), −0.205 ± 0.031 (21 day), −0.302 ± 0.029 (28 day); and for 300 mg/kg pretreatment group it −0.595 ± 0.013 (7 day), −0.407 ± 0.024 (21 day), −0.356 ± 0.062 (28 day). Similarly, the mean amplitude of b-wave was as follows: 0.0163 ± 0.016, 0.0295 ± 0.024, 0.004 ± 0.038 for injury alone group; 0.021 ± 0.03, 0.0673 ± 0.026, 0.0163 ± 0.006 for 100 mg/kg group; 0.007 ± 0.02, 0.0617 ± 0.012, 0.1076 ± 0.035 for 200 mg/kg group; 0.086 ± 0.007, 0.078 ± 0.020, 0.074 ± 0.044 for 300 mg/kg *A. cepa* pretreated group at 7, 21, and 28 day time points respectively. The details of significance level have been incorporated in the supplementary file (Supplementary Table 1).

Discussion

Retinal ischemia is a serious complication associated with glaucoma, diabetic retinopathy, and optic retinopathy (16). The associated condition may lead to blindness if appropriate and adequate treatments are not given on time. We have established a retinal ischemia mouse model by ligating two important arteries i.e. ophthalmic artery (PPA) and ECA (20). It's a 2 hr occlusion model followed by reperfusion for 3 different time points: 7, 21, and 28-day. Because of the repeated failure (24) and side effects (25) of the available commercial drugs, we wanted to test the alternative approach of testing

A. cepa (onion) as the pretreatment strategy to explore if it is able to improve the vision or not. Apart from its many biological benefits in the form of antioxidant, anti-inflammatory, and neuroprotective activity (as shown by previous studies) its common availability makes it an important biological product to be tested for its efficacy (5, 10, 11). For this, 3 different concentrations of aqueous extract of commonly used red onion was tested i.e. 100 mg/kg, 200 mg/kg and 300 mg/kg. The functional efficacy of *A. cepa* in the form of retinal wave analysis is very important in retinal degeneration cases and to the best of our knowledge it has not been previously reported in such models. According to standardized protocols the ERG recordings are depicted by three important factors- the instrument setup, intensity of the light stimulus, and animal state (26).

ERG recording depicted that implicit time to a-wave decreased in all the *A. cepa* administered groups except for slight increase in 300 mg/kg in comparison to the Injury alone group for 7-day, however, this decrease was not statistically significant. Similarly, the implicit time to b-wave for both 21-day and 28-day increased throughout the *A. cepa* administered groups in comparison to the injury alone group. However, for 28-day, the implicit time to b-wave was highest for injury alone group followed by 300 mg/kg. From this, it can be said that A.cepa administration is able to increase the implicit time but not at the statistically significant level for which larger sample size and deeper analysis is required. Delay in implicit time a-wave have previously been reported in diseased cases (27). Similarly, reduction in a-wave amplitude has also been reported in certain cases. Mixed results were obtained in case of both amplitude a- and b- wave. Amplitude a-wave was recorded to be decreased in most of the *A. cepa* administered groups with respect to the injury alone group. Further, b-wave amplitude was highest at 7 day for 100 mg/kg; at 21 day for 300 mg/kg, and at 28 day for 200 mg/kg. So, from this data it can be concluded that *A. cepa* may able to improve the retinal functions depicted by ERG analysis.

Limitations of the study

Though we have tried to minimise the limitation, factors such as intensity of light stimulus, temperature/humidity, anesthesia, ocular environment, adaptive state, and other technical difficulties affecting the ERG recordings cannot be ruled out. Large sample size and more group like: Injury+ PBS/solvent comparison is needed.

Acknowledgments

Authors would like to acknowledge the Ministry of AYUSH, Govt. of India for providing the funding (Z.28015/106/2014-HP-C(EMR)-AYUSH-A).

Authors Contribution

SK: Experimentation, data analysis, original writing
AA: Conceptualization, editing of the manuscript, securing funding.
RS: Co-conceptualization
SK: Co-conceptualization
VS: Experimentation

Ethical statement

All experiments were performed after getting the approval from Institutional Animal Ethical Committee (IAEC) via approval no: 67/IAEC/390R.

Conflicts of interests

The authors declare that they have no conflict of interest.

Source of funding

Thanks to ministry of AYUSH file No. (Z.28015/106/2014-HPC (EMR)-AYUSH-A) Government of India

Received Date: 10-02-20; Revised Date: 12-02-20

Accepted Date: 26-02-20

References

1. Essa MM, Akbar M, Guillemin G. The Benefits of Natural Products for Neurodegenerative Diseases: Springer; 2016.
2. Sofi F, Dinu MR. Nutrition and prevention of chronic-degenerative diseases. Agriculture and agricultural science procedia. 2016;8: 713–7.
3. Jiang X, Huang J, Song D, Deng R, Wei J, Zhang Z. Increased Consumption of Fruit and Vegetables Is Related to a Reduced Risk of Cognitive Impairment and Dementia: Meta-Analysis. Frontiers in aging neuroscience. 2017;9:18.
4. Sarchielli E, Morelli A, Guarnieri G, Iorizzi M, Sgambati E. Neuroprotective effects of quercetin 4'-O-β-d-diglucoside on human striatal precursor cells in nutrient deprivation condition. Acta histochemica. 2018;120(2):122–8.
5. Shri R, Bora KS. Neuroprotective effect of methanolic extracts of *Allium cepa* on ischemia and reperfusion-induced cerebral injury. Fitoterapia. 2008;79(2):86–96.
6. Nejabat M, Salehi A, Noorani Azad P, Ashraf MJ. Effects of onion juice on the normal flora of eyelids and conjunctiva in an animal model. Jundishapur journal of microbiology. 2014;7(5):e9678–e.
7. Javadzadeh A, Ghorbanihaghjo A, Bonyadi S, Rashidi MR, Mesgari M, Rashtchizadeh N, et al. Preventive effect of onion juice on selenite-induced experimental cataract. Indian journal of ophthalmology. 2009;57(3):185.
8. Stefek M, Karasu C. Eye lens in aging and diabetes: effect of quercetin. Rejuvenation research. 2011;14(5):525–34.
9. Agte V, Tarwadi K. The importance of nutrition in the prevention of ocular disease with special reference to cataract. Ophthalmic research. 2010;44(3):166–72.
10. Sato A, Zhang T, Yonekura L, Tamura H. Antiallergic activities of eleven onions (*Allium cepa*) were attributed to quercetin 4'-glucoside using QuEChERS method and Pearson's correlation coefficient. Journal of Functional Foods. 2015;14:581–9.
11. Singh T, Goel RK. Neuroprotective effect of *Allium cepa* L. in aluminium chloride induced neurotoxicity. Neurotoxicology. 2015;49:1–7.
12. Movahedian A, Sadeghi H, Ghannadi A, Gharavi M, Azarpajooh S. Hypolipidemic activity of Allium porrum L. in cholesterol-fed rabbits. Journal of medicinal food. 2006;9(1):98–101.
13. Kumari K, Augusti K. Lipid lowering effect of S-methyl cysteine sulfoxide from *Allium cepa* Linn in high cholesterol diet fed rats. Journal of ethnopharmacology. 2007;109(3):367–71.

14. Tamtaji OR, Hosseinzadeh H, Talaei SA, Behnam M, Firoozeh SMT, Taghizadeh M, et al. Protective Effects of Red Onion (*Allium cepa*) Ethanolic Extract on Learning and Memory Impairments in Animal Models of Diabetes. Galen Medical Journal. 2017;6(3): 249–57.
15. Vauzour D, Vafeiadou K, Rodriguez-Mateos A, Rendeiro C, Spencer JPE. The neuroprotective potential of flavonoids: a multiplicity of effects. Genes & nutrition. 2008;3(3-4):115–26.
16. Minhas G, Morishita R, Anand A. Preclinical models to investigate retinal ischemia: advances and drawbacks. Frontiers in neurology. 2012;3:75.
17. Tomiyama Y, Fujita K, Nishiguchi KM, Tokashiki N, Daigaku R, Tabata K, et al. Measurement of electroretinograms and visually evoked potentials in awake moving mice. PloS one. 2016;11(6).
18. Hema L. Ramkumar KDE, Koushik Tripathy, Peter A. Karth, Usha Rajapuram Kumar, and Vinay A. Shah. Electroretinogram: EyeWiki; [updated 15 November 2019. Available from: https://eyewiki.aao.org/Electroretinogram.
19. Neuroscience Research Lab DoN, Post Graduate Institute of Medical Education and Research, Chandigarh. Redefining Quality Standards in Basic Research Investigations by Broadening the Purview of GLP: Quality Council of India.
20. Bammidi S, Sharma K, Tyagi R, Sharma NK, Anand A. Eye Genetics: The Road Ahead to Quality Standards. Advances in Vision Research, Volume I: Springer; 2017. p. 473–80.
21. Kumar S, Modgil S, Bammidi S, Minhas G, Shri R, Kaushik S, et al. *Allium cepa* exerts neuroprotective effect on retinal ganglion cells of pterygopalatine artery (PPA) ligated mice. J Ayurveda Integr Med. 2020.
22. Modgil S, Cameotra SS, Sharma VL, Anand A. Early Life Pb Exposure and its Effect on Later Life Retinal Degeneration. Journal of cellular biochemistry. 2017.
23. Minhas G, Prabhakar S, Morishita R, Shimamura M, Bansal R, Anand A. Transplantation of lineage-negative stem cells in pterygopalatine artery ligation induced retinal ischemia–reperfusion injury in mice. Molecular and cellular biochemistry. 2017;429(1–2):123–36.
24. Kumar S, Modgil S, Bammidi S, Minhas G, Shri R, Kaushik S, et al. *Allium cepa* exerts neuroprotective effect on retinal ganglion cells of pterygopalatine artery (PPA) ligated mice. Journal of Ayurveda and Integrative Medicine. 2020.
25. Farkouh A, Frigo P, Czejka M. Systemic side effects of eye drops: a pharmacokinetic perspective. Clinical Ophthalmology (Auckland, NZ). 2016;10:2433.
26. Brandli A, Stone J. Using the electroretinogram to assess function in the rodent retina and the protective effects of remote limb ischemic preconditioning. JoVE (Journal of Visualized Experiments). 2015(100):e52658.
27. Hancock HA, Kraft TW. Oscillatory potential analysis and ERGs of normal and diabetic rats. Investigative ophthalmology & visual science. 2004;45(3):1002-8.

Supplementary Table 1

POST HOC TESTS

1. IMPLICIT TIME A-WAVE

Multiple Comparisons

1.1. Dependent Variable: Implicit Time A-Wave: 7 Day

7 Day	(I) Group	(J) Group	Mean Difference (I-J)	Std. Error	Sig.	95% Confidence Interval	
						Lower Bound	Upper Bound
Scheffe	Injury	Hundred	10.0000	7.6475	.646	−15.089	35.089
		Two Hundred	.1500	7.6475	1.000	−24.939	25.239
		Three Hundred	−.4500	7.6475	1.000	−25.539	24.639
	Hundred	Injury	−10.0000	7.6475	.646	−35.089	15.089
		Two Hundred	−9.8500	7.0803	.602	−33.077	13.377
		Three Hundred	−10.4500	7.0803	.557	−33.677	12.777
	Two Hundred	Injury	−.1500	7.6475	1.000	−25.239	24.939
		Hundred	9.8500	7.0803	.602	−13.377	33.077
		Three Hundred	−.6000	7.0803	1.000	−23.827	22.627
	Three Hundred	Injury	.4500	7.6475	1.000	−24.639	25.539
		Hundred	10.4500	7.0803	.557	−12.777	33.677
		Two Hundred	.6000	7.0803	1.000	−22.627	23.827
Dunnett t (2-sided)[a]	Injury	Three Hundred	−.4500	7.6475	1.000	−21.281	20.381
	Hundred	Three Hundred	−10.4500	7.0803	.364	−29.735	8.835
	Two Hundred	Three Hundred	−.6000	7.0803	1.000	−19.885	18.685

1.2. Dependent Variable: Implicit Time A-Wave: 21 Day

21 Day	(I) Group2	(J) Group 2	Mean Difference (I-J)	Std. Error	Sig.	95% Confidence Interval	
						Lower Bound	Upper Bound
Scheffe	Injury	Hundred	−.01667	6.68074	1.000	−21.9335	21.9001
		Two Hundred	−1.30000	6.18516	.997	−21.5910	18.9910
		Three Hundred	5.30000	6.18516	.863	−14.9910	25.5910
	Hundred	Injury	.01667	6.68074	1.000	−21.9001	21.9335
		Two Hundred	−1.28333	6.68074	.998	−23.2001	20.6335
		Three Hundred	5.31667	6.68074	.887	−16.6001	27.2335
	Two Hundred	Injury	1.30000	6.18516	.997	−18.9910	21.5910
		Hundred	1.28333	6.68074	.998	−20.6335	23.2001
		Three Hundred	6.60000	6.18516	.770	−13.6910	26.8910
	Three Hundred	Injury	−5.30000	6.18516	.863	−25.5910	14.9910
		Hundred	−5.31667	6.68074	.887	−27.2335	16.6001
		Two Hundred	−6.60000	6.18516	.770	−26.8910	13.6910
Dunnett t (2-sided)[a]	Injury	Three Hundred	5.30000	6.18516	.736	−11.5473	22.1473
	Hundred	Three Hundred	5.31667	6.68074	.774	−12.8805	23.5138
	Two Hundred	Three Hundred	6.60000	6.18516	.601	−10.2473	23.4473

1.3. Dependent Variable: Implicit Time A-Wave: 28 Day

28 Day	(I) Group3	(J) Group 3	Mean Difference (I-J)	Std. Error	Sig.	95% Confidence Interval	
						Lower Bound	Upper Bound
Scheffe	Injury	Hundred	7.80000	2.58314	.085	–.9932	16.5932
		Two Hundred	6.80000	2.58314	.145	–1.9932	15.5932
		Three Hundred	4.93333	2.41630	.308	–3.2919	13.1586
	Hundred	Injury	–7.80000	2.58314	.085	–16.5932	.9932
		Two Hundred	–1.00000	2.58314	.984	–9.7932	7.7932
		Three Hundred	–2.86667	2.41630	.711	–11.0919	5.3586
	Two Hundred	Injury	–6.80000	2.58314	.145	–15.5932	1.9932
		Hundred	1.00000	2.58314	.984	–7.7932	9.7932
		Three Hundred	–1.86667	2.41630	.895	–10.0919	6.3586
	Three Hundred	Injury	–4.93333	2.41630	.308	–13.1586	3.2919
		Hundred	2.86667	2.41630	.711	–5.3586	11.0919
		Two Hundred	1.86667	2.41630	.895	–6.3586	10.0919
Dunnett t (2–sided)[a]	Injury	Three Hundred	4.93333	2.41630	.171	–1.9099	11.7766
	Hundred	Three Hundred	–2.86667	2.41630	.540	–9.7099	3.9766
	Two Hundred	Three Hundred	–1.86667	2.41630	.796	–8.7099	4.9766

2. IMPLICIT TIME B-WAVE

2.1. Dependent Variable: Implicit Time B-Wave: 7 Day

7 Day	(I) Group1	(J) Group 1	Mean Difference (I-J)	Std. Error	Sig.	95% Confidence Interval	
						Lower Bound	Upper Bound
Scheffe	Injury	Hundred	–.53333	8.02095	1.000	–26.8468	25.7802
		Two Hundred	–2.53333	8.02095	.991	–28.8468	23.7802
		Three Hundred	–4.03333	8.02095	.967	–30.3468	22.2802
	Hundred	Injury	.53333	8.02095	1.000	–25.7802	26.8468
		Two Hundred	–2.00000	7.42596	.995	–26.3616	22.3616
		Three Hundred	–3.50000	7.42596	.973	–27.8616	20.8616
	Two Hundred	Injury	2.53333	8.02095	.991	–23.7802	28.8468
		Hundred	2.00000	7.42596	.995	–22.3616	26.3616
		Three Hundred	–1.50000	7.42596	.998	–25.8616	22.8616
	Three Hundred	Injury	4.03333	8.02095	.967	–22.2802	30.3468
		Hundred	3.50000	7.42596	.973	–20.8616	27.8616
		Two Hundred	1.50000	7.42596	.998	–22.8616	25.8616
Dunnett t 2-sided)[a]	Injury	Three Hundred	–4.03333	8.02095	.924	–25.8810	17.8143
	Hundred	Three Hundred	–3.50000	7.42596	.936	–23.7270	16.7270
	Two Hundred	Three Hundred	–1.50000	7.42596	.994	–21.7270	18.7270

2.2. Dependent Variable: Implicit Time B-Wave: 21 Day

21 Day	(I) Group2	(J) Group 2	Mean Difference (I-J)	Std. Error	Sig.	95% Confidence Interval	
						Upper Bound	Lower Bound
Scheffe	Injury	Hundred	−9.95000	10.50654	.826	−44.4177	24.5177
		Two Hundred	−9.15000	9.72716	.828	−41.0609	22.7609
		Three Hundred	−11.05000	9.72716	.736	−42.9609	20.8609
	Hundred	Injury	9.95000	10.50654	.826	−24.5177	44.4177
		Two Hundred	.80000	10.50654	1.000	−33.6677	35.2677
		Three Hundred	−1.10000	10.50654	1.000	−35.5677	33.3677
	Two Hundred	Injury	9.15000	9.72716	.828	−22.7609	41.0609
		Hundred	−.80000	10.50654	1.000	−35.2677	33.6677
		Three Hundred	−1.90000	9.72716	.998	−33.8109	30.0109
	Three Hundred	Injury	11.05000	9.72716	.736	−20.8609	42.9609
		Hundred	1.10000	10.50654	1.000	−33.3677	35.5677
		Two Hundred	1.90000	9.72716	.998	−30.0109	33.8109
Dunnett t (2-sided)[a]	Injury	Three Hundred	−11.05000	9.72716	.557	−37.5451	15.4451
	Hundred	Three Hundred	−1.10000	10.50654	.999	−29.7180	27.5180
	Two Hundred	Three Hundred	−1.90000	9.72716	.995	−28.3951	24.5951

2.3. Dependent Variable: Implicit Time B-Wave: 28 Day

28 Day	(I) Group3	(J) Group 3	Mean Difference (I-J)	Std. Error	Sig.	95% Confidence Interval	
						Upper Bound	Lower Bound
Scheffe	Injury	Hundred	23.26667	7.36009	.070	−1.7875	48.3209
		Two Hundred	20.26667	7.36009	.123	−4.7875	45.3209
		Three Hundred	12.66667	6.88473	.388	−10.7694	36.1027
	Hundred	Injury	−23.26667	7.36009	.070	−48.3209	1.7875
		Two Hundred	−3.00000	7.36009	.982	−28.0542	22.0542
		Three Hundred	−10.60000	6.88473	.529	−34.0361	12.8361
	Two Hundred	Injury	−20.26667	7.36009	.123	−45.3209	4.7875
		Hundred	3.00000	7.36009	.982	−22.0542	28.0542
		Three Hundred	−7.60000	6.88473	.752	−31.0361	15.8361
	Three Hundred	Injury	−12.66667	6.88473	.388	−36.1027	10.7694
		Hundred	10.60000	6.88473	.529	−12.8361	34.0361
		Two Hundred	7.60000	6.88473	.752	−15.8361	31.0361
Dunnett t (2-sided)[a]	Injury	Three Hundred	12.66667	6.88473	.230	−6.8318	32.1651
	Hundred	Three Hundred	−10.60000	6.88473	.349	−30.0984	8.8984
	Two Hundred	Three Hundred	−7.60000	6.88473	.591	−27.0984	11.8984

3. AMPLITUDE a-WAVE

3.1. Dependent Variable: Amplitude a-Wave: 7 Day

7 Day	(I) Group 1	(J) Group 1	Mean Difference (I-J)	Std. Error	Sig.	95% Confidence Interval	
						Lower Bound	Upper Bound
Scheffe	Injury	Hundred	–.0062500	.0701467	1.000	–.236373	.223873
		Two Hundred	.1410000	.0701467	.310	–.089123	.371123
		Three Hundred	.3965000*	.0701467	.001	.166377	.626623
	Hundred	Injury	.0062500	.0701467	1.000	–.223873	.236373
		Two Hundred	.1472500	.0649432	.222	–.065802	.360302
		Three Hundred	.4027500*	.0649432	.001	.189698	.615802
	Two Hundred	Injury	–.1410000	.0701467	.310	–.371123	.089123
		Hundred	–.1472500	.0649432	.222	–.360302	.065802
		Three Hundred	.2555000*	.0649432	.018	.042448	.468552
	Three Hundred	Injury	–.3965000*	.0701467	.001	–.626623	–.166377
		Hundred	–.4027500*	.0649432	.001	–.615802	–.189698
		Two Hundred	–.2555000*	.0649432	.018	–.468552	–.042448
Dunnett t (2-sided)[b]	Injury	Three Hundred	.3965000*	.0701467	.000	.205433	.587567
	Hundred	Three Hundred	.4027500*	.0649432	.000	.225856	.579644
	Two Hundred	Three Hundred	.2555000*	.0649432	.006	.078606	.432394

*. The mean difference is significant at the 0.05 level.

3.2. Dependent Variable: Amplitude a-Wave: 21 Day

21 Day	(I) Group 2	(J) Group 2	Mean Difference (I-J)	Std. Error	Sig.	95% Confidence Interval	
						Lower Bound	Upper Bound
Scheffe	Injury	Hundred	.2615000*	.0570859	.007	.074224	.448776
		Two Hundred	.1032500	.0528513	.332	–.070134	.276634
		Three Hundred	.3055000*	.0528513	.001	.132116	.478884
	Hundred	Injury	-.2615000*	.0570859	.007	–.448776	–.074224
		Two Hundred	-.1582500	.0570859	.108	–.345526	.029026
		Three Hundred	.0440000	.0570859	.896	–.143276	.231276
	Two Hundred	Injury	-.1032500	.0528513	.332	–.276634	.070134
		Hundred	.1582500	.0570859	.108	–.029026	.345526
		Three Hundred	.2022500*	.0528513	.021	.028866	.375634
	Three Hundred	Injury	-.3055000*	.0528513	.001	–.478884	–.132116
		Hundred	-.0440000	.0570859	.896	–.231276	.143276
		Two Hundred	-.2022500*	.0528513	.021	–.375634	–.028866
Dunnett t (2-sided)[b]	Injury	Three Hundred	.3055000*	.0528513	.000	.161542	.449458
	Hundred	Three Hundred	.0440000	.0570859	.789	–.111492	.199492
	Two Hundred	Three Hundred	.2022500*	.0528513	.007	.058292	.346208

*. The mean difference is significant at the 0.05 level.

3.3. Dependent Variable: Amplitude a-Wave: 28 Day

28 Day	(I) Group3	(J) Group 3	Mean Difference (I-J)	Std. Error	Sig.	95% Confidence Interval	
						Lower Bound	Upper Bound
Scheffe	Injury	Hundred	.0640000	.0637237	.800	–.152920	.280920
		Two Hundred	.1776667	.0637237	.117	–.039253	.394586
		Three Hundred	.2315000*	.0596081	.026	.028590	.434410
	Hundred	Injury	–.0640000	.0637237	.800	–.280920	.152920
		Two Hundred	.1136667	.0637237	.413	–.103253	.330586
		Three Hundred	.1675000	.0596081	.114	–.035410	.370410
	Two Hundred	Injury	–.1776667	.0637237	.117	–.394586	.039253
		Hundred	–.1136667	.0637237	.413	–.330586	.103253
		Three Hundred	.0538333	.0596081	.844	–.149076	.256743
	Three Hundred	Injury	–.2315000*	.0596081	.026	–.434410	–.028590
		Hundred	–.1675000	.0596081	.114	–.370410	.035410
		Two Hundred	–.0538333	.0596081	.844	–.256743	.149076
Dunnett t (2-sided)[b]	Injury	Three Hundred	.2315000*	.0596081	.010	.062682	.400318
	Hundred	Three Hundred	.1675000	.0596081	.052	–.001318	.336318
	Two Hundred	Three Hundred	.0538333	.0596081	.717	–.114985	.222651

*. The mean difference is significant at the 0.05 level.

4. AMPLITUDE b-WAVE

4.1. Dependent Variable: Amplitude b-Wave: 7 Day

7 Day	(I) Group1	(J) Group 1	Mean Difference (I-J)	Std. Error	Sig.	95% Confidence Interval	
						Lower Bound	Upper Bound
Scheffe	Injury	Hundred	–.0046667	.0343660	.999	–.117407	.108074
		Two Hundred	.0093333	.0343660	.994	–.103407	.122074
		Three Hundred	–.0696667	.0343660	.303	–.182407	.043074
	Hundred	Injury	.0046667	.0343660	.999	–.108074	.117407
		Two Hundred	.0140000	.0318167	.978	–.090378	.118378
		Three Hundred	–.0650000	.0318167	.297	–.169378	.039378
	Two Hundred	Injury	–.0093333	.0343660	.994	–.122074	.103407
		Hundred	–.0140000	.0318167	.978	–.118378	.090378
		Three Hundred	–.0790000	.0318167	.165	–.183378	.025378
	Three Hundred	Injury	.0696667	.0343660	.303	–.043074	.182407
		Hundred	.0650000	.0318167	.297	–.039378	.169378
		Two Hundred	.0790000	.0318167	.165	–.025378	.183378
Dunnett t (2-sided)[a]	Injury	Three Hundred	–.0696667	.0343660	.160	–.163274	.023940
	Hundred	Three Hundred	–.0650000	.0318167	.156	–.151663	.021663
	Two Hundred	Three Hundred	–.0790000	.0318167	.075	–.165663	.007663

4.2. Dependent Variable: Amplitude b-Wave: 21 Day

21 Day	(I) Group 2	(J) Group 2	Mean Difference (I-J)	Std. Error	Sig.	95% Confidence Interval	
						Lower Bound	Upper Bound
Scheffe	Injury	Hundred	–.0378333	.0306341	.685	–.138331	.062665
		Two Hundred	–.0322500	.0283616	.735	–.125293	.060793
		Three Hundred	–.0485000	.0283616	.439	–.141543	.044543
	Hundred	Injury	.0378333	.0306341	.685	–.062665	.138331
		Two Hundred	.0055833	.0306341	.998	–.094915	.106081
		Three Hundred	–.0106667	.0306341	.989	–.111165	.089831
	Two Hundred	Injury	.0322500	.0283616	.735	–.060793	.125293
		Hundred	–.0055833	.0306341	.998	–.106081	.094915
		Three Hundred	–.0162500	.0283616	.953	–.109293	.076793
	Three Hundred	Injury	.0485000	.0283616	.439	–.044543	.141543
		Hundred	.0106667	.0306341	.989	–.089831	.111165
		Two Hundred	.0162500	.0283616	.953	–.076793	.109293
Dunnett t (2-sided)[a]	Injury	Three Hundred	–.0485000	.0283616	.261	–.125752	.028752
	Hundred	Three Hundred	–.0106667	.0306341	.972	–.094109	.072775
	Two Hundred	Three Hundred	-.0162500	.0283616	.894	–.093502	.061002

4.3. Dependent Variable: Amplitude b-Wave: 28 Day

28 Day	(I) Group 3	(J) Group 3	Mean Difference (I-J)	Std. Error	Sig.	95% Confidence Interval	
						Lower Bound	Upper Bound
Scheffe	Injury	Hundred	–.0123333	.0541912	.997	–.196804	.172137
		Two Hundred	–.1036667	.0541912	.358	–.288137	.080804
		Three Hundred	–.0700000	.0506913	.611	–.242556	.102556
	Hundred	Injury	.0123333	.0541912	.997	–.172137	.196804
		Two Hundred	–.0913333	.0541912	.458	–.275804	.093137
		Three Hundred	–.0576667	.0506913	.736	–.230223	.114890
	Two Hundred	Injury	.1036667	.0541912	.358	–.080804	.288137
		Hundred	.0913333	.0541912	.458	–.093137	.275804
		Three Hundred	.0336667	.0506913	.929	–.138890	.206223
	Three Hundred	Injury	.0700000	.0506913	.611	–.102556	.242556
		Hundred	.0576667	.0506913	.736	–.114890	.230223
		Two Hundred	–.0336667	.0506913	.929	–.206223	.138890
Dunnett t (2-sided)[a]	Injury	Three Hundred	–.0700000	.0506913	.429	–.213564	.073564
	Hundred	Three Hundred	–.0576667	.0506913	.570	–.201231	.085898
	Two Hundred	Three Hundred	.0336667	.0506913	.855	–.109898	.177231

[a] Dunnett t-tests treat one group as a control, and compare all other groups against it.

Journal of Ayurveda and Integrative Medicine xxx (xxxx) xxx

Contents lists available at ScienceDirect

Journal of Ayurveda and Integrative Medicine

journal homepage: http://elsevier.com/locate/jaim

Original Research Article (Experimental)

Allium cepa exerts neuroprotective effect on retinal ganglion cells of pterygopalatine artery (PPA) ligated mice

Saurabh Kumar [a], Shweta Modgil [a], Sridhar Bammidi [a], Gillipsie Minhas [a], Richa Shri [b], Sushmita Kaushik [c], Akshay Anand [a, *], Varinder Singh [b]

[a] *Neuroscience Research Lab, Department of Neurology, Postgraduate Institute of Medical Education and Research (PGIMER), Chandigarh, 160012, India*
[b] *Department of Pharmaceutical Sciences and Drug Research, Punjabi University, Patiala, 147002, India*
[c] *Advanced Eye Centre, Postgraduate Institute of Medical Education and Research (PGIMER), Chandigarh, 160012, India*

ARTICLE INFO

Article history:
Received 17 November 2018
Received in revised form
24 July 2019
Accepted 16 August 2019
Available online xxx

Keywords:
Allium cepa
Neuroprotection
Ischemia/reperfusion
Retinal ischemia

ABSTRACT

Background: Repeated failure to rescue the damaged retinal ganglion cells (RGCs) by various drugs has warranted the need to screen common herbal compounds available in the form of various eye formulations for their efficacy.
Objective: We aimed to investigate the neuroprotective effect of pretreatment with aqueous extract of *A. cepa* in Ischemia/Reperfusion (I/R) induced retinal injury.
Methods: Ischemia was induced for 2 h by pterygopalatine artery (PPA) ligation in C57BL/6J mice, followed by reperfusion. The neuroprotective role of oral pretreatment with aqueous extract of *A. cepa* (300 mg/kg) was analyzed with respect to control and injury only group at 7, 14, and 28 day after the surgery for expression of different genes in the retina by Real-Time PCR.
Results: Molecular analysis at different time points showed increased expression of BCl-2, GDNF, GFAP, and Brn3b in the retina at 14 and 28 day after *A. cepa* treatment in comparison to the injury alone group. However, at shorter time point (7th day), the expression of these genes was pronounced in the injury only group in comparison to the injury and pretreated group.
Conclusion: Pretreatment with aqueous extract of *A. cepa* may protect from the neuronal damage in I/R-induced retinal injury in mice by altering the expression of neurotrophic factor.
© 2019 The Authors. Published by Elsevier B.V. on behalf of Institute of Transdisciplinary Health Sciences and Technology and World Ayurveda Foundation. This is an open access article under the CC BY-NC-ND license (http://creativecommons.org/licenses/by-nc-nd/4.0/).

1. Introduction

Retinal ischemia, one of the leading causes of sight impairment or blindness, is associated with grave retinal ailments like ischemic optic neuropathy (ION), rubeotic glaucoma, and diabetic retinopathy [1–4]. In general, ischemia occurs because of the blockage in the arteries, which could lead to serious complications like stroke or heart attack. Stenosis or occlusion of carotid artery can lead to ocular ischemic syndrome (OIS) [5,6]. One of the most common type of OIS is Amaurosis fugax, which is retinal ischemia resulting into transient blindness [7]. In case of ION, there is inadequate blood supply to the optic nerve, causing loss of retinal ganglion cells (RGCs) [8].

Previous studies suggest that retinal ischemia/reperfusion (I/R) models imitate various medical conditions like retinal vascular occlusion and acute glaucoma [9]. Glaucoma is one of the devastating neurodegenerative disorder [10] affecting millions of people worldwide. According to Liang et al. the total number of people affected in 2013 was 64.3 million and is expected to be 76.0 million by 2020 [11]. The prevalence of glaucoma in India is about 11.9 million [12] and by 2020, India will be the second most affected nation with glaucoma. Thus, it is imperative for researchers to revisit the prognostic and therapeutic strategies to rescue the damaged retinal ganglion cells affected by the disease. The approved drugs like Timolol and Letanoprost have been shown to cause toxic effects and have failed to repair the damaged RGCs [13,14]. Timolol has been used for glaucoma treatment for more than 30 years, however, even its topical administration may have

* Corresponding author. Neuroscience Research Lab, Department of Neurology, Postgraduate Institute of Medical Education and Research (PGIMER), Chandigarh,160012, India.
E-mail address: akshay1anand@rediffmail.com (A. Anand).
Peer review under responsibility of Transdisciplinary University, Bangalore.

https://doi.org/10.1016/j.jaim.2019.08.002
0975-9476/© 2019 The Authors. Published by Elsevier B.V. on behalf of Institute of Transdisciplinary Health Sciences and Technology and World Ayurveda Foundation. This is an open access article under the CC BY-NC-ND license (http://creativecommons.org/licenses/by-nc-nd/4.0/).

Please cite this article as: Kumar S et al., *Allium cepa* exerts neuroprotective effect on retinal ganglion cells of pterygopalatine artery (PPA) ligated mice, J Ayurveda Integr Med, https://doi.org/10.1016/j.jaim.2019.08.002

adverse effects [15]. In view of this, the conventional treatment approach is inadequate [16], and awaits alternative interventions. Various herbal extracts have been used as therapeutics since several years. It may not be out of context to state that 70% of the Indian population and almost 90% of the African population is dependent on traditional medicine, whether or not preclinically tested. 90% of Chinese general hospitals reportedly have units for traditional medicine, where *Ginkgo biloba, Allium sativum,* and *Panax ginseng* are the most common and top-prescribed herbal products, yet the evidence-based approach is still lacking. *Allium cepa (A. cepa)* is one of the commonly used botanical product in our routine diet, because of its broad mechanism of action (as antioxidant, antidiabetic, anticancer, antiatherogenic), and has even been tested for its therapeutic efficacy on damage induced by nicotine [17]. It is also a rich source of organosulphur elements like thiosulphimates and cepaenes, and flavanols like quercetin, kaempferol, and myricetin [18]. The antioxidant role of quercetin and its derivatives present in *A. cepa* are well known [19]. It has been shown that quercetin also helps in prevention of other eye disorders like age-related macular degeneration (AMD) and cataract [20]. While the methanolic extracts of *A. cepa* are believed to exert neuroprotective effects on brain I/R injury [21].

Over the time different animal models have been used to validate therapies and to develop understanding of the disease pathogenesis. The ischemic models include both chemical induced (cobalt chloride), as well as surgical models (middle cerebral artery occlusion (MCAO), common carotid artery (CCA) occlusion, or pterygopalatine artery (PPA) ligation) [22]. PPA ligation model has been used to screen drugs for retinal ischemia. The novel model was first used to induce retinal ischemia by occluding External carotid artery (ECA) and pterygopalatine artery by a group of researchers from Japan and France [3,23]. Studies suggest that ligation of both PPA and ECA induces histological damage and deficits in the retina, without affecting the mice brain [3]. Our previous reports have shown that PPA ligation can be used to study transient ischemia in mice [1,22]. Hideaki Hara and Takashi Ishibashi, patented astaxanthin, showing retinal protective action in the above said PPA ligation model.

Therefore, in this study, we analyzed the mRNA expression of Glial Fibrillary Acidic Protein (GFAP), B-cell lymphoma 2 (BCl-2), Glial Cell Derived Neurotrophic Factor (GDNF), and Brn3b in *A. cepa* pretreated mice subjected to PPA ligation-induced I/R injury and indicate a neuroprotective role for *A. cepa* in preservation of RGCs.

2. Methodology

2.1. Preparation of A. cepa extract

A. cepa aqueous extract was prepared at Department of Pharmaceutical Sciences and Drug Research, Punjabi University, Patiala, India. Initially, the red onion bulbs and outer scales (500 g) were chopped in boiling water (1100 ml) followed by sonication for 30 min, placed in shaking incubator at 100 rpm (37 °C) for 24 h, filtered, and concentrated under reduced pressure. The yield was calculated with respect to dry weight (9.78% w/w). The dried extract was tested for toxicity according to the OECD guidelines.

2.2. Animals

All the experiments were performed on C57BL/6J male mice (8–10 weeks, 25 g–30 g) as per Institutional Animal Ethical Committee (IAEC) approval **(67/IAEC/390R)**. The animals were given free access to feed and water while exercising control over humidity and temperature in the animal house. The animals were housed under 12 h light/dark cycle. The animals were divided into three groups: Normal Control, Injury only, and Injury and 300 mg/kg *A. cepa* pretreatment. Details of groups are provided in Fig. 1. The mice were allowed to reperfuse for 7-days, 14-days, and 28-days, after which the animals were sacrificed and end point analysis were done.

2.3. Administration of A. cepa

Fresh aqueous extract of *A. cepa* (300 mg/kg) was administered by oral gavage 24 h prior to the surgery.

2.4. Surgery

The animals were anaesthetized intraperitoneally with Xylazine (50 mg/ml)/Ketamine (50 mg/ml). The I/R retinal injury was induced as described earlier [1,2,22]. Briefly, mice were fixed in a supine position and approximately 1.5 cm midline incision was made under a stereozoom microscope (Leica S6D microscope + EC3 Camera). The muscles were retracted and the right CCA was exposed. The bifurcation was traced and the ECA was ligated with a suture (Ethicon; 7.0). Upon ligation of ECA, bifurcation of internal carotid artery (ICA) was traced and PPA was ligated with the suture (Ethicon; 7.0). Ischemic condition was maintained for 2 h. After 2 h, the ligated sutures were removed and the blood circulation was allowed to reperfuse. After 7, 14, and 28 days of reperfusion, the animals were sacrificed, and the ipsilateral eyes were enucleated and stored for retina isolation.

2.5. RT-PCR

The expression of different cell markers (GDNF, BCl-2, Brn3b, and GFAP) was analyzed through real-time PCR (Applied Biosystems). RNA was isolated from retina using Qiagen RNeasy Mini kit and quantified using a UV spectrophotometer (Beckman–Coulter DU730 UV/Vis Spectrophotometer). Using cDNA synthesis kit (Verso Thermo Fisher Scientific), total RNA was converted into cDNA (as per the manufacturer's protocol). The cDNA was stored at −20 °C for further analysis and 20 ng was later used as a template against specific primers (Sigma and Eurofins, Genomics) (Table 1) for amplification using the Sybr Green master mix (Applied Biosystems) as per the following protocol: initial denaturation at 95 °C for 10 min; 35 cycles of denaturation (95 °C for 1 min), annealing (63 °C for 1 min) and extension (72 °C for 1 min); and final extension at 72 °C for 1 min (35 cycles). The beta actin was used as the house-keeping gene.

2.6. Statistical analysis

Normality of the data was analyzed by Kolmogorov–Smirnov test (K–S test). One sample t-test was applied for comparison of means (M±SD) with normative values. For comparison of two different groups, independent t-test was applied. All the statistical tests were two-sided and performed at a significance level of $p < .05$. The analysis was conducted using IBM SPSS Statistics Software (Version 22.0).

3. Results

3.1. A. cepa increases Brn3b expression

Brn3b mRNA expression analyzed by real time PCR was found to be downregulated with time after the I/R injury (Group II) ($p = .076$, .015, .087 for 7, 14, and 28 day, respectively). However, *A. cepa* pretreatment group (Group III) showed an increased expression with time ($p < .001$, $p = .074$, .003 for 7, 14, and 28 day, respectively) (Fig. 2).

Please cite this article as: Kumar S et al., *Allium cepa* exerts neuroprotective effect on retinal ganglion cells of pterygopalatine artery (PPA) ligated mice, J Ayurveda Integr Med, https://doi.org/10.1016/j.jaim.2019.08.002

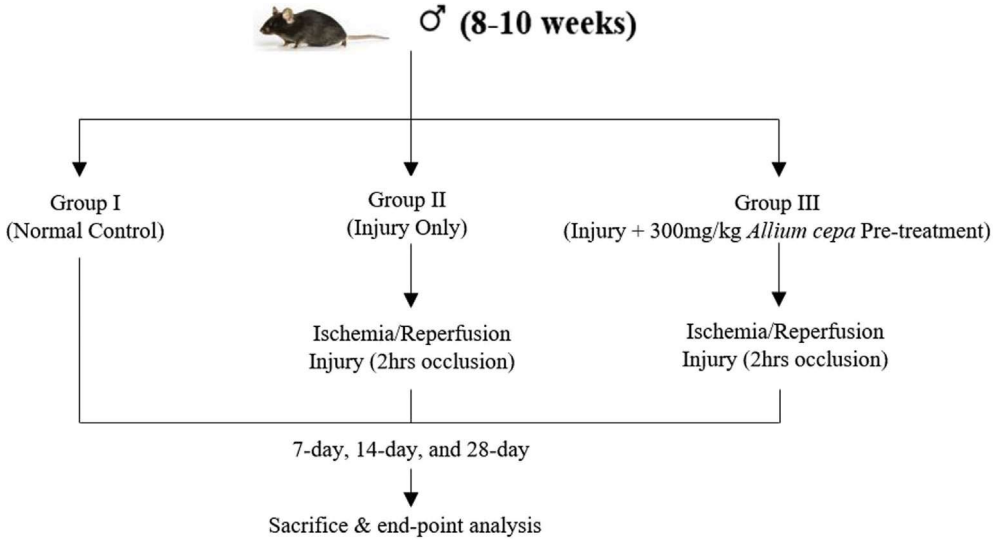


Fig. 1. Schematic representation of the experimental plan.

Table 1
Primer sequence for different marker genes used in real-time PCR.

Target Gene	Primer Sequence (5′→3′)
Brn3b	F: GCAGTCTCCACTTGGTGCTTACTC
(Sigma)	R: TTCCCCCTACAAACAAACCTCC
BCl-2	F: GCCCTTCGGAGTTTAATCAG
(Eurofins Genomics)	R: TACACTTGCACACACACGCT
GFAP	F: ACAGACTTTCTCCAACCTCCAG
(Sigma)	R: CCTTCTGACACGGATTTGGT
GDNF	F: TGGGCTATGAAACCAAGGAG
(Sigma)	R: CAACATGCCTGGCCTACTTT
B-actin	F: AGCCATGTACGTAGCCATCC
(Sigma)	R: CTCTCAGCTGTGGTGGTGAA

3.2. *A. cepa induces BCl-2 expression*

Molecular analysis (RT-PCR) of *A. cepa* pretreated mice retina revealed alteration in mRNA expression of BCl-2 at all the time points analyzed, with an increasing trend in expression with days after reperfusion.

We found statistically significant expression in both injury only ($p < .001$, $p = .010$, and .039) and *A. cepa* pretreated group ($p < .001$, $p = .030$, .002) at 7, 14, and 28 day as compared to the normal control (Fig. 3).

3.3. *Upregulated GFAP expression in both injury and A. cepa pretreated group*

In comparison to the normal control, GFAP was found to be upregulated when analyzed by real time PCR at 14 and 28 day ($p = .002$, .013 and .004, <.001 for injury only and injury + pretreatment group, respectively) (see Fig. 4).

3.4. *Increased expression of GDNF in A. cepa pretreatment*

mRNA expression of GDNF was analyzed in the *A. Cepa* treated mice and was found to be upregulated at various time points. The expression was highly significant in both injury only ($p = .004$, .026 at 7 and 14 day, respectively) and injury + pretreatment group ($p < .001$, $p = .021$, .003 at 7, 14, and 28 day, respectively) with respect to the normal control group (Table 2) (see Fig. 5).

4. Discussion

Retinal ischemia, a clinical condition associated with many vision impairing diseases, can lead to RGC damage, and hence, necessitates the need to investigate treatment approaches. PPA ligation-induced retinal ischemia model has been used to test different therapeutic strategies. The model is characterized by increased GFAP expression, thinning of retinal vasculature, and decreased retinal thickness [1,2]. We have previously reported a decrease in the inner plexiform layer (IPL) thickness as well as an increase in GFAP levels after the I/R surgery in mice [2]. In the current study, we analyzed the differential mRNA expression of genes upon oral administration of *A. cepa* using Real-Time PCR. The blood retinal barrier (BRB) in the eye acts as a physical deterrent for drug delivery as well as harmful substances. Retinal capillaries contain tight junctions, which makes their permeability poor for even smaller substances like sodium [24]. However, fenestrated capillaries present in the choroid are highly permeable to molecules with low molecular weight. *A. cepa* contains quercetin as an active component. Different *in vitro* and *in vivo* studies suggest that quercetin is able to cross the BRB or Blood brain barrier [25], thereby, reducing the cell apoptosis [26,27]. In our study, comparison between injury and pretreated group revealed that most of the genes like BCl-2, GDNF, and Brn3b show an upregulation at 7 day in the injury group, and *A. cepa* treatment failed to exert any significant effect at 7 day. It may be hypothesized that at 7-day time point, the elevated expression could be due to an immediate protective effect induced by the I/R injury. However, it is interesting to note that at the later time points (14 and 28 day), *A. cepa* pretreatment group showed significantly increased expression (p value at 14 day- BCl-2: .030; GDNF: .021; GFAP: < .001, and at 28 day- BCl-2: .002; GDNF: .003; GFAP: <.001).

RGCs express certain specific markers like Thy1, and Brn3b, which are used as a marker for RGC injury [28]. Brn3b is a major transcription factor that belongs to mammalian POU family. It is a key regulatory marker of RGCs and is known to play an important role in RGC development and survival [29]. BCl-2 and Brn3b are neuroprotective in their action, as there is a binding locus for Brn3b present at the upstream site of BCl-2 [29]. A study by Buckingham et al. suggests that the injury decreases the number of cells expressing these markers [30]. However, the reduced Brn3b expression could indicate either loss of RGCs or decrease in the

Please cite this article as: Kumar S et al., *Allium cepa* exerts neuroprotective effect on retinal ganglion cells of pterygopalatine artery (PPA) ligated mice, J Ayurveda Integr Med, https://doi.org/10.1016/j.jaim.2019.08.002

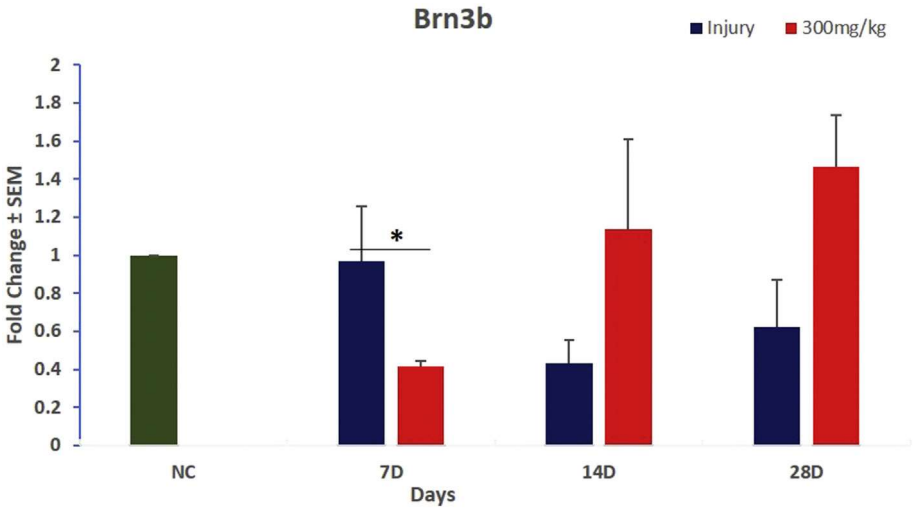


Fig. 2. Fold change in the gene expression of Brn3b for injury and 300 mg/kg A. *cepa* group estimated through Real Time PCR analysis for 7-day, 14-day, and 28-day after PPA surgery in ipsilateral eye. The values were normalized against the endogenous control (β-Actin) (n = 3). The data was found to be significant at $P \leq .05$ (* = **.022**).

Table 2
Real-Time PCR data mean, S.D + S.E, P-Value for BCl-2, Brn3b, GFAP, and GDNF genes at different time points (7-day, 14-day, and 28-day). The values were normalized against absolute controls. The P-values are indicated with respect to the normal control. The data was found to be statistically significant at $P \leq .05$

Genes	Time Points	Injury Only (Group II)			Injury + 300 mg/kg pretreatment (Group III)		
		Mean	SD+S.E	P-Value	Mean	SD+S.E.	P-value
BCl-2	7D	.418115	.0911550 + .0372139	<.001	.198191	.0463812 + .0189350	<.001
	14D	.291388	.1748523 + .0713831	.010	.333727	.2721050 + .1110864	.030
	28D	.478668	.2726384 + .136319	.039	.671248	.2729234 + .1114205	.002
Brn3b	7D	.971327	.4919620 + .28403	.076	.415720	.0679446 + .02774	<.001
	14D	.432939	.2897533 + .11829	.015	1.135345	1.055326 + .47196	.074
	28D	.621289	.4941992 + .2471	.087	1.465695	.6634392 + .27085	.003
GFAP	7D	1.47267	.19378 + .13702	.059	2.290373	.55309 + .27655	.004
	14D	.26484	.11359 + .04637	.002	2.267443	.33967 + .13867	<.001
	28D	3.48528	1.29944 + .64972	.013	3.728287	.71831 + .32124	<.001
GDNF	7D	2.01358	.9668 + .3947	.004	1.056857	.117665 + .0480	<.001
	14D	.22600	.177815 + .0726	.026	3.740277	2.743927 + 1.12020	.021
	28D	3.71870	6.292648 + 3.6331	.414	3.812304	.903641 + .45182	.003

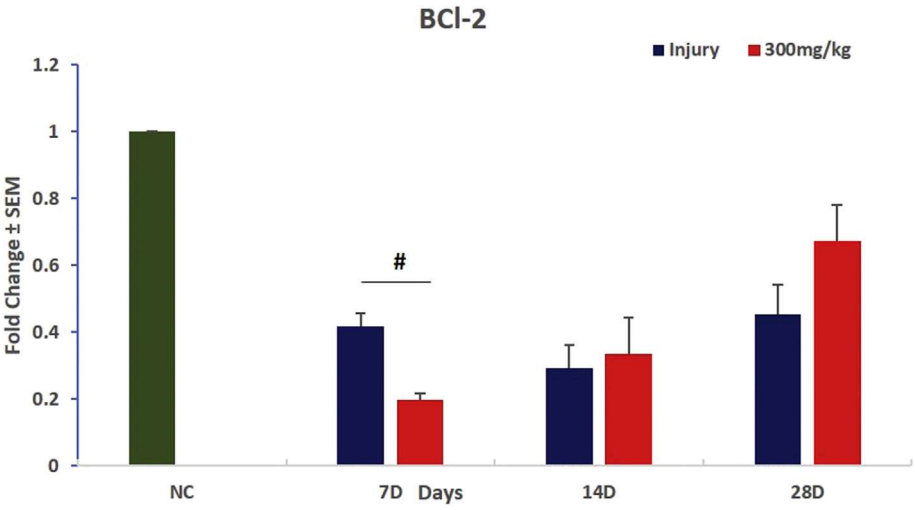


Fig. 3. Fold change in the BCl-2 mRNA expression for injury and 300 mg/kg A. *cepa* group estimated through Real Time PCR analysis at 7, 14, and 28 day after PPA surgery in ipsilateral eye. The values were normalized against the endogenous control (β-Actin) (n = 3). The data was found to be significant at $P \leq .05$ (# = **<.001**).

Please cite this article as: Kumar S et al., *Allium cepa* exerts neuroprotective effect on retinal ganglion cells of pterygopalatine artery (PPA) ligated mice, J Ayurveda Integr Med, https://doi.org/10.1016/j.jaim.2019.08.002

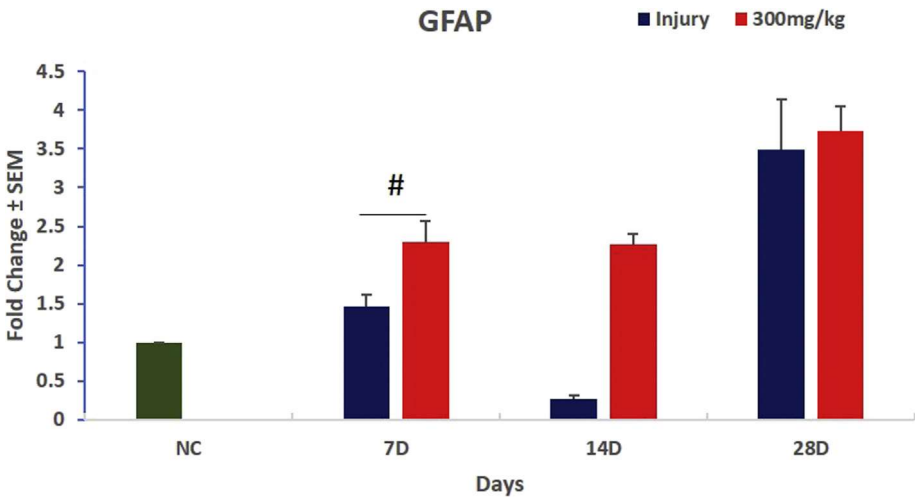


Fig. 4. Fold change in the gene expression of GFAP (Glial Fibrillary Acidic protein) for injury and 300 mg/kg A. *cepa* group estimated through Real Time PCR analysis for 7-day, 14-day, and 28-day after PPA surgery in ipsilateral eye. The values were normalized against the endogenous control (β-Actin) (n = 3). The data was found to be significant at $P \leq .05$ (# = ≤**.001**).

optic nerve fibers [31]. In our study, the expression of Brn3b declined after the injury and we observed a reduced expression at day 14 and day 28. And after the *A. cepa* pretreatment, we found that at a later time point i.e., 14 and 28 day, there was significant increase in the expression of Brn3b.

Next, we investigated the role of *A. cepa* pretreatment on the cell apoptosis during retinal I/R injury. BCl-2, an anti-apoptotic gene critical for the regulation of programmed cell death [32], is known as an essential controller of photoreceptors (rods, cones) and RGCs death in degenerated retinas [33]. In the current study, there was a significant reduction in the expression of BCl-2 at 7 day in both injury and pretreatment groups as compared to the control. There was a trend of increase in BCl-2 expression in treatment group analyzed at 14th and 28th-day post treatment, as compared to respective injury groups, though the difference was not significant. Further study with different doses and time points is needed to understand the BCl-2 temporal expression profile.

GFAP, a class III intermediate filament protein mainly expressed in astrocytes, is known to play an important role during CNS development. It has been reported that astrocytes are activated post retinal injury, evident from the studies showing an increase in expression of GFAP [2,34,35]. Muller cells and RGCs are the two types of cells that express GFAP in retina. We report a similar pattern in our studies, where after I/R injury, the expression of GFAP was found to be elevated at 7-day ($p = .059$) and 28-day ($p = .013$) post treatment. However, in *A. cepa* treated group there was increased expression of GFAP at 7 day ($p \leq .001$) in comparison to the injury group. According to Lewis et al., the expression of intermediate filaments and Muller cells differs on the basis of detachment or reattachment of retina [35]. This indicates a differential expression (and an important role) of GFAP in both injury and pretreatment group.

Neurotrophic factors are known to enhance the cell survival mechanisms and hence, exert neuroprotective effect towards injury and degeneration. GDNF is a neurotrophic factor that has been shown to promote the survival of RGCs when introduced in different retinal injury rat models [36–39]. The effect of aqueous extract of *A. cepa* on the expression of GDNF was examined in I/R injury and it was found that the expression at 7 day was similar to that of normal control while it increased in the injury group, as it is

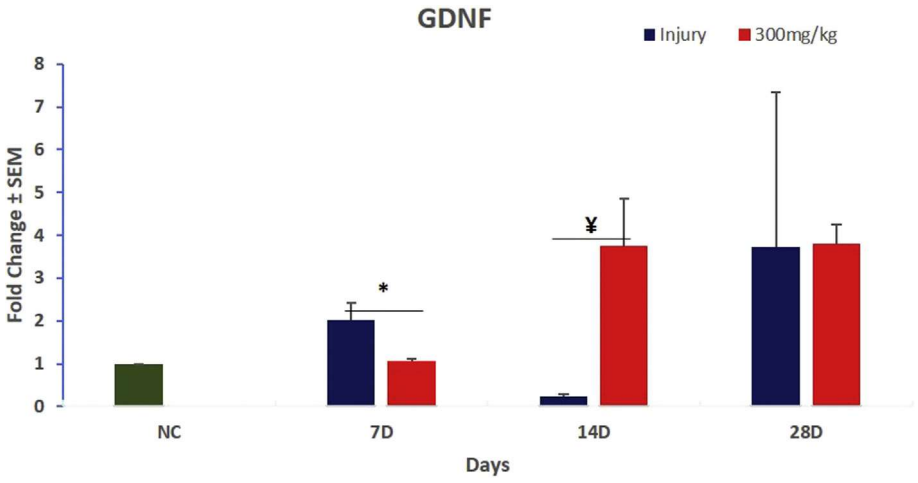


Fig. 5. Fold change in the gene expression of Glia derived Neurotrophic factor (GDNF) for injury and 300 mg/kg A. *cepa* group estimated through Real Time PCR analysis for 7-day, 14-day, and 28-day after PPA surgery in ipsilateral eye. The values were normalized against the endogenous control (β-Actin) (n = 3). The data was found to be significant at $P \leq .05$ (* = **.037**, ¥ = **.011**).

Please cite this article as: Kumar S et al., *Allium cepa* exerts neuroprotective effect on retinal ganglion cells of pterygopalatine artery (PPA) ligated mice, J Ayurveda Integr Med, https://doi.org/10.1016/j.jaim.2019.08.002

known that an injury or degeneration can initiate protective strategies to prevent further damage. However, the expression was augmented at 14 day and 28 day with the *A. cepa* treatment. This data suggests that *A. cepa* extract is associated with the increase in the GDNF expression at later time points, which will further promote cell survival. The increased expression in response to *A. cepa* pretreatment at later time points suggests its potential role in recovery from I/R injury.

5. Conclusion

The current study explores the neuroprotective role of an herbal extract (*A. cepa*) in rescuing the damaged RGCs in I/R induced injury in mouse model of PPA ligation. The study investigated the expression of genes by RT-PCR, however, no dose dependent neuroprotective effect of *A. cepa* was observed. We plan to examine the related apoptotic pathway genes in our future study, which might have a role to play in the neuroprotective effect of *A. cepa*.

Source of funding

Authors would like to acknowledge the Ministry of AYUSH, Govt. of India for providing the funding (Z.28015/106/2014-HPC (EMR)-AYUSH-A) for research work.

Declaration of Competing Interest

The authors declare that they have no conflict of interest.

References

[1] Minhas G, Morishita R, Shimamura M, Bansal R, Anand A. Modeling transient retinal ischemia in mouse by ligation of pterygopalatine artery. Ann Neurosci 2015;22(4):222–5.
[2] Minhas G, Prabhakar S, Morishita R, Shimamura M, Bansal R, Anand A. Transplantation of lineage-negative stem cells in pterygopalatine artery ligation induced retinal ischemia–reperfusion injury in mice. Mol Cell Biochem 2017;429(1–2):123–36.
[3] Ogishima H, Nakamura S, Nakanishi T, Imai S, Kakino M, Ishizuka F, et al. Ligation of the pterygopalatine and external carotid arteries induces ischemic damage in the murine retina. Invest Ophthalmol Vis Sci 2011;52(13):9710–20.
[4] Chung H, Harrisa A, Ciulla T, Kagemann L. Progress in measurement of ocular blood flow and relevance to our understanding of glaucoma and age-related macular degeneration. Prog Retin Eye Res 1999;18(5):669–87.
[5] Terelak-Borys B, Skonieczna K, Grabska-Liberek I. Ocular ischemic syndrome–a systematic review. Med Sci Monit 2012;18(8):RA138–44.
[6] Faries PL, Chaer RA, Patel S, Lin SC, DeRubertis B, Kent KC. Current management of extracranial carotid artery disease. Vasc Endovasc Surg 2006;40(3):165–75.
[7] Slepyan DH, Rankin RM, Stahler C, Gibbons GE. Amaurosis fugax: a clinical comparison. Stroke 1975;6(5):493–6.
[8] Smith C, Vianna J, Chauhan B. Assessing retinal ganglion cell damage. Eye 2017;31(2):209–17.
[9] Sun MH, Pang JH, Chen SL, Han WH, Ho TC, Chen KJ, et al. Retinal protection from acute glaucoma-induced ischemia-reperfusion injury through pharmacologic induction of heme oxygenase-1. Invest Ophthalmol Vis Sci 2010;51(9):4798–808.
[10] Gupta N, Yucel YH. Glaucoma as a neurodegenerative disease. Curr Opin Ophthalmol 2007;18(2):110–4.
[11] Liang YB, Zhang Y, Musch DC, Congdon N. Proposing new indicators for glaucoma healthcare service. Eye Vis 2017;4(1):6.
[12] George R, Vijaya L. Prevalence of glaucoma in India: a review. J Curr Glaucoma Pract 2007;1(2):7–11.
[13] Anand A, Modgil S, Sharma VL, Shri R, Kaushik S. Preserving neural retina through Re-emerging herbal interventions. J Cell Biochem 2014;115(10):1659–68.
[14] Pisella P-J, Debbasch C, Hamard P, Creuzot-Garcher C, Rat P, Brignole F, et al. Conjunctival proinflammatory and proapoptotic effects of latanoprost and preserved and unpreserved timolol: an ex vivo and in vitro study. Invest Ophthalmol Vis Sci 2004;45(5):1360–8.
[15] Volotinen M, Hakkola J, Pelkonen O, Vapaatalo H, Mäenpää JJB, pharmacology c, et al. Metabolism of ophthalmic timolol: new aspects of an old drug. Basic Clin Pharmacol Toxicol 2011;108(5):297–303.
[16] Cheung W, Guo L, Cordeiro MF. Neuroprotection in glaucoma: drug-based approaches. Optom Vis Sci 2008;85(6):406.
[17] Helen A, Krishnakumar K, Vijayammal P, Augusti K. Antioxidant effect of onion oil (Allium cepa. Linn) on the damages induced by nicotine in rats as compared to alpha-tocopherol. Toxicol Lett 2000;116(1–2):61–8.
[18] Hwang IK, Lee CH, Yoo K-Y, Choi JH, Park OK, Lim SS, et al. Neuroprotective effects of onion extract and quercetin against ischemic neuronal damage in the gerbil hippocampus. J Med Food 2009;12(5):990–5.
[19] Ramos FA, Takaishi Y, Shirotori M, Kawaguchi Y, Tsuchiya K, Shibata H, et al. Antibacterial and antioxidant activities of quercetin oxidation products from yellow onion (Allium cepa) skin. J Agric Food Chem 2006;54(10):3551–7.
[20] Agte V, Tarwadi K. The importance of nutrition in the prevention of ocular disease with special reference to cataract. Ophthalmic Res 2010;44(3):166–72.
[21] Shri R, Bora KS. Neuroprotective effect of methanolic extracts of Allium cepa on ischemia and reperfusion-induced cerebral injury. Fitoterapia 2008;79(2):86–96.
[22] Modgil S, Cameotra SS, Sharma VL, Anand A. Early life Pb exposure and its effect on later life retinal degeneration. J Cell Biochem 2017;118(10):3213–24.
[23] Lelong DC, Bieche I, Perez E, Bigot K, Leemput J, Laurendeau I, et al. Novel mouse model of monocular amaurosis fugax. Stroke 2007;38(12):3237–44.
[24] Tornquist P, Alm A, Bill A. Permeability of ocular vessels and transport across the blood-retinal-barrier. Eye (Lond) 1990;4(2):303.
[25] Li Y, Zhou S, Li J, Sun Y, Hasimu H, Liu R, et al. Quercetin protects human brain microvascular endothelial cells from fibrillar β-amyloid1–40-induced toxicity. Acta Pharm Sin B 2015;5(1):47–54.
[26] Arikan S, Ersan I, Karaca T, Kara S, Gencer B, Karaboga I, et al. Quercetin protects the retina by reducing apoptosis due to ischemia-reperfusion injury in a rat model. Arq Bras Oftalmol 2015;78(2):100–4.
[27] Ola MS, Ahmed M, Shams S, Al-Rejaie SS. Neuroprotective effects of quercetin in diabetic rat retina. Saudi J Biol Sci 2017;24(6):1186–94.
[28] Das AV, James J, Rahnenführer J, Thoreson WB, Bhattacharya S, Zhao X, et al. Retinal properties and potential of the adult mammalian ciliary epithelium stem cells. Vision Res 2005;45(13):1653–66.
[29] Phatak NR, Stankowska DL, Krishnamoorthy RR. Bcl-2, Bcl-xL, and p-AKT are involved in neuroprotective effects of transcription factor Brn3b in an ocular hypertension rat model of glaucoma. Mol Vis 2016;22:1048–61.
[30] Buckingham BP, Inman DM, Lambert W, Oglesby E, Calkins DJ, Steele MR, et al. Progressive ganglion cell degeneration precedes neuronal loss in a mouse model of glaucoma. J Neurosci 2008;28(11):2735–44.
[31] Stankowska DL, Minton AZ, Rutledge MA, Mueller BH, Phatak NR, He S, et al. Neuroprotective effects of transcription factor Brn3b in an ocular hypertension rat model of glaucoma. Invest Ophthalmol Vis Sci 2015;56(2):893–907.
[32] Tsujimoto Y. Role of Bcl-2 family proteins in apoptosis: apoptosomes or mitochondria? Genes Cells 1998;3(11):697–707.
[33] Chen J, Flannery JG, LaVail MM, Steinberg RH, Xu J, Simon MI. bcl-2 overexpression reduces apoptotic photoreceptor cell death in three different retinal degenerations. Proc Natl Acad Sci 1996;93(14):7042–7.
[34] Hol EM, Pekny M. Glial fibrillary acidic protein (GFAP) and the astrocyte intermediate filament system in diseases of the central nervous system. Curr Opin Cell Biol 2015;32:121–30.
[35] Lewis GP, Fisher SK. Up-regulation of glial fibrillary acidic protein in response to retinal injury: its potential role in glial remodeling and a comparison to vimentin expression. Int Rev Cytol 2003;230:264–90.
[36] Lawrence JM, Keegan DJ, Muir EM, Coffey PJ, Rogers JH, Wilby MJ, et al. Transplantation of Schwann cell line clones secreting GDNF or BDNF into the retinas of dystrophic Royal College of Surgeons rats. Invest Ophthalmol Vis Sci 2004;45(1):267–74.
[37] Jiang C, Moore MJ, Zhang X, Klassen H, Langer R, Young M. Intravitreal injections of GDNF-loaded biodegradable microspheres are neuroprotective in a rat model of glaucoma. Mol Vis 2007;13:1783–92.
[38] Hauck SM, Kinkl N, Deeg CA, Swiatek-de Lange M, Schöffmann S, Ueffing M. GDNF family ligands trigger indirect neuroprotective signaling in retinal glial cells. Mol Cell Biol 2006;26(7):2746–57.
[39] Koeberle PD, Ball AK. Effects of GDNF on retinal ganglion cell survival following axotomy. Vision Res 1998;38(10):1505–15.

Please cite this article as: Kumar S et al., *Allium cepa* exerts neuroprotective effect on retinal ganglion cells of pterygopalatine artery (PPA) ligated mice, J Ayurveda Integr Med, https://doi.org/10.1016/j.jaim.2019.08.002

Environmental Science and Pollution Research
https://doi.org/10.1007/s11356-019-04700-6

RESEARCH ARTICLE

Alpha lipoic acid attenuates the long-term effects of lead exposure in retinal ischemic injury mouse model

Shweta Modgil[1,2] · Sridhar Bammidi[1] · Avijit Banik[3] · Vijay Lakshmi Sharma[2] · Akshay Anand[1]

Received: 7 June 2018 / Accepted: 25 February 2019
© Springer-Verlag GmbH Germany, part of Springer Nature 2019

Abstract

Lead (Pb) exposure is reported to be unsafe for humans. There have been several studies documenting acute and chronic Pb toxicity on the organ systems. New studies suggest that early-life exposure to such environmental toxins may increase the susceptibility to late-onset degenerative disorders. We aimed to examine the long-term effects of early-life postnatal exposure of Pb on retinal degeneration. Pb exposure (200 ppm) was provided either at postnatal day 1 through lactation (early-life exposure) or at 7th week of age (adulthood exposure) directly through drinking water for 20 days. The Pb-treated mice were followed till 20 weeks of age. At 20th week, ischemia/reperfusion (I/R) injury was induced in these mice by pterygopalatine artery ligation. Further, alpha lipoic acid (ALA) was administered to examine its neuroprotective effects against retinal damage. Histological and molecular analysis revealed that Pb-treated mice had greater retinal damage after I/R injury as compared to untreated or ALA treated mice, suggesting that ALA protects the early-life Pb exposure and its consequent impact on later life. The elevated levels of glial derived neurotrophic factor (GDNF) and ciliary neurotrophic factor (CNTF) and reduced levels of glial fibrillary acidic protein (GFAP) upon ALA pre-treatment suggest that it probably exerts anti-inflammatory effects via upregulation of neurotrophic factors.

Keywords Ischemia/reperfusion · Lead toxicity · Retina · Developmental exposure · Alpha lipoic acid

Introduction

Early-life exposure and its long-term effects on the late-onset disease aetiology have been ignored in health research. Environmental toxins like Pb have been studied for their influence on development of neurodegenerative disorders, but no studies on retinal degeneration have been carried out. Pb exposure to children is common through the use of toys that contain Pb as well as from their habit of wall-licking that contain also contain Pb (Flora et al. 2012; Patrick 2006). There is no prescribed limit for Pb levels that are considered safe for onset of long-term effects as there are very few studies that have examined this relationship longitudinally (Grandjean and Landrigan 2014). As the central nervous system is not fully developed and prone to metal-induced toxicity (London et al. 2013; Lidsky and Schneider 2003) through underdeveloped blood–brain barrier (Foulkes 2000), even low doses of Pb have been shown to exert toxic effects at old age. Although such studies are limited, yet, due to serious health hazard, Center for Disease Control and Prevention (CDC) reduced the admissible lead levels from 10 to 5 μg/dl in children (CDC 2012).

Lead toxicity in retina has also been investigated in the form of limited studies. Fox and coworkers reported that retina is more sensitive to gestational Pb toxicity as compared to the kidney (Fox et al. 1991). They further demonstrated that it induces mitochondrial dysfunction and rods apoptosis by altering cGMP phosphodiesterase activity in the damaged retina (Fox et al. 1998; Fox et al. 2008). Gestational exposure of low Pb also affects retinal function, as reported by electroretinography (Fox et al. 2008). It results in increased RPC proliferation while delaying rod and bipolar cells differentiation (Chaney et al. 2016). Children with

Responsible editor: Philippe Garrigues

✉ Akshay Anand
akshay1anand@rediffmail.com

[1] Neuroscience Research Lab, Department of Neurology, Post Graduate Institute of Medical Education and Research, Chandigarh, India

[2] Department of Zoology, Panjab University, Chandigarh, India

[3] Department of Pharmacology, Emory University School of Medicine, Rollins Research Center, Atlanta, USA

Published online: 03 April 2019

prenatal Pb exposure revealed supernormal ERG (Rothenberg et al. 2002). The increased a- and b-wave amplitudes in supernormal ERG were hypothesised to be associated with increase in rods, decreased dopamine content or low Zn^{2+} concentration in retina (Fox et al. 2008). It has further been documented that Pb exposure through mother's milk may lead to photoreceptor and INL cells necrosis and also increased permeability of blood–retinal barrier (BRB) (Santos-Anderson et al. 1984). Recently, the USA reported a public health crisis (Laidlaw et al. 2016) from elevated blood Pb levels in children above recommended level. This renewed the interest of researchers.

There was general belief that low dose of Pb may not have late-life outcomes; however, recent studies have demonstrated its long-term effects on brain-related pathologies and cognition. Monkeys exposed to low dose of Pb at infantile stage were reported with *tau*-like pathology in adulthood (Wu et al. 2008), supported by similar study on humans which reported cognition deficit in children exposed to low dose of Pb (Lanphear et al. 2005). This led to a complete paradigm shift in research related to Pb toxicity, and it was postulated that even though low dose of Pb does not show any toxicity-related symptoms in short time, it may have long-term consequences leading to neurodegeneration. For example, low dose of Pb was found to increase susceptibility towards Alzheimer-related symptoms; however, its effects on retinal degeneration were never examined. Retina, being the extension of CNS, consists of blood–retinal barrier and thus an ideal tissue of interest for testing the late-life consequences of early-life exposure to Pb. Therefore, we designed a study consisting of two time points of Pb exposure: one at developmental stage postnatal day (PND1–20) and the other at an adult stage (7th week age). We had earlier shown that early-life Pb exposure has mild adverse effects on retinal ischemic susceptibility at a shorter duration of 10 weeks of age (Modgil et al. 2017). We now wanted to examine whether these toxic effects may last up to 20 weeks.

As ischemia is one of the major contributing factors in various retinopathies, transient I/R injury was induced in mice using pterygopalatine artery (PPA) ligation model of retinal degeneration (Minhas et al. 2015; Otsuka et al. 2016). Similar model has been earlier used to screen the effectiveness of potential therapeutic agents against ischemic injury and is thus well established (Ishizuka et al. 2013; Li et al. 2011). Such ischemia-based models lead to cell death due to increased ROS resulting from decreased production of endogenous antioxidants. Alpha-lipoic acid (ALA) is a naturally occurring substance (Golbidi et al. 2011) that has been previously evaluated for its protective role against brain stroke as well as myocardial ischemia (Hall et al. 2010; Volobouéva et al. 2005). This is attributed to its ability to prevent oxidative stress (Deng et al. 2015; Wang et al. 2011).

Results

Lead estimation at 20th week

No difference in the consumption of drinking water or food habits was observed in untreated and Pb-treated mice used in this study. Body weight was found to be similar in pups from all groups during the time of surgery, and no adverse behaviour was noticed in Pb-treated dams or pups. Blood Pb estimation at 20-week age showed no significant difference between untreated and lead-treated groups. Animals from 7W-Pb group showed blood Pb levels of 1.3 ppm + 0.009 (SE) while PND-Pb animals showed blood levels of 1.03 ppm + 0.01(SE) when compared to untreated animals having blood Pb concentration of 1.25 ppm + 0.004 (SE). Thus, at 20-week age, the blood Pb concentration in Pb-treated mice was found to be similar to that of untreated mice. This is attributed to the fact that half-life of Pb in blood is 40 days.

Unchanged retinal thickness Eyes were cryosectioned and retinal sections were stained with haematoxylin–eosin stain. From each group, three animals were used for cryosections as per ethical approval limits. Images were captured under light microscope, and retinal thickness was measured from retinal pigment epithelium (RPE) to ganglion cell layer (GCL). The retinal thickness was found decreased in all groups when compared to normal control. The retinal thickness was in the following order: normal control (NC) > injury only > 7W-Pb + injury > PND-Pb + injury. The retinal thickness in NC group was found to be 263.84 μm ± 6.5 (SE) while in injury only group, it was 259.51 μm ± 4.7 (SE). In lead-treated groups, PND-Pb + injury mice showed greater decrease with retinal thickness of 248.97 μm ± 4.2 (SE) as compared to 7W-Pb + injury group with retinal thickness of 257.40 μm ± 7.7 (SE) (Fig. 1).

Pb-treated mice showed increased retinal apoptosis

Apoptotic cells were examined using terminal deoxynucleotidyl transferase (TdT) dUTP nick-end labelling (TUNEL) assay. Retinal cryosections were stained for apoptotic marker labelled with FITC. Images were captured under confocal microscope, and corrected total cell fluorescence (CTCF) was determined using ImageJ software. More apoptotic cells were found in retinal sections from lead-treated mice (both PND-Pb + injury and 7W-Pb + injury groups) as compared to injury only group (Fig. 2a–d). The fold change in fluorescence intensity of the apoptotic marker was found to be significantly higher in 7W-Pb + injury (1.51-fold) and PND-Pb + injury mice (1.65-fold) as compared to NC. The I/R injury alone showed 0.88-fold fluorescent intensity as compared to NC but this was not significant (Fig. 2e).

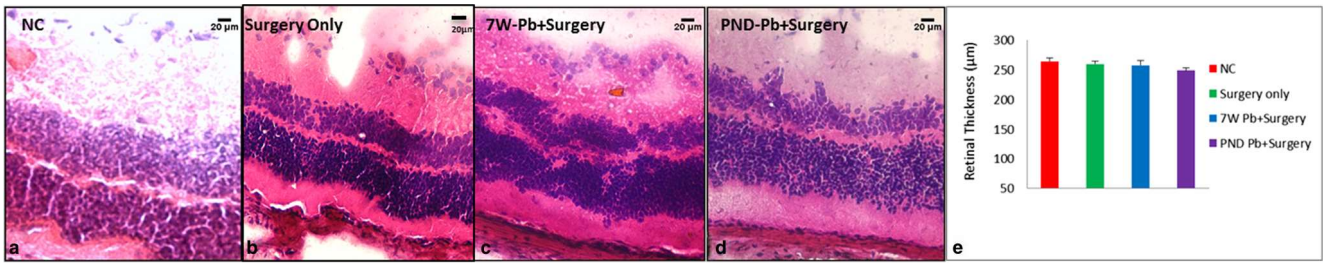


Fig. 1 Representative retinal sections from normal control (**a**), surgery only (**b**), 7th W Pb + surgery (**c**) and PND Pb + surgery (**d**). Quantitative analysis of retinal thickness in various groups (**e**)

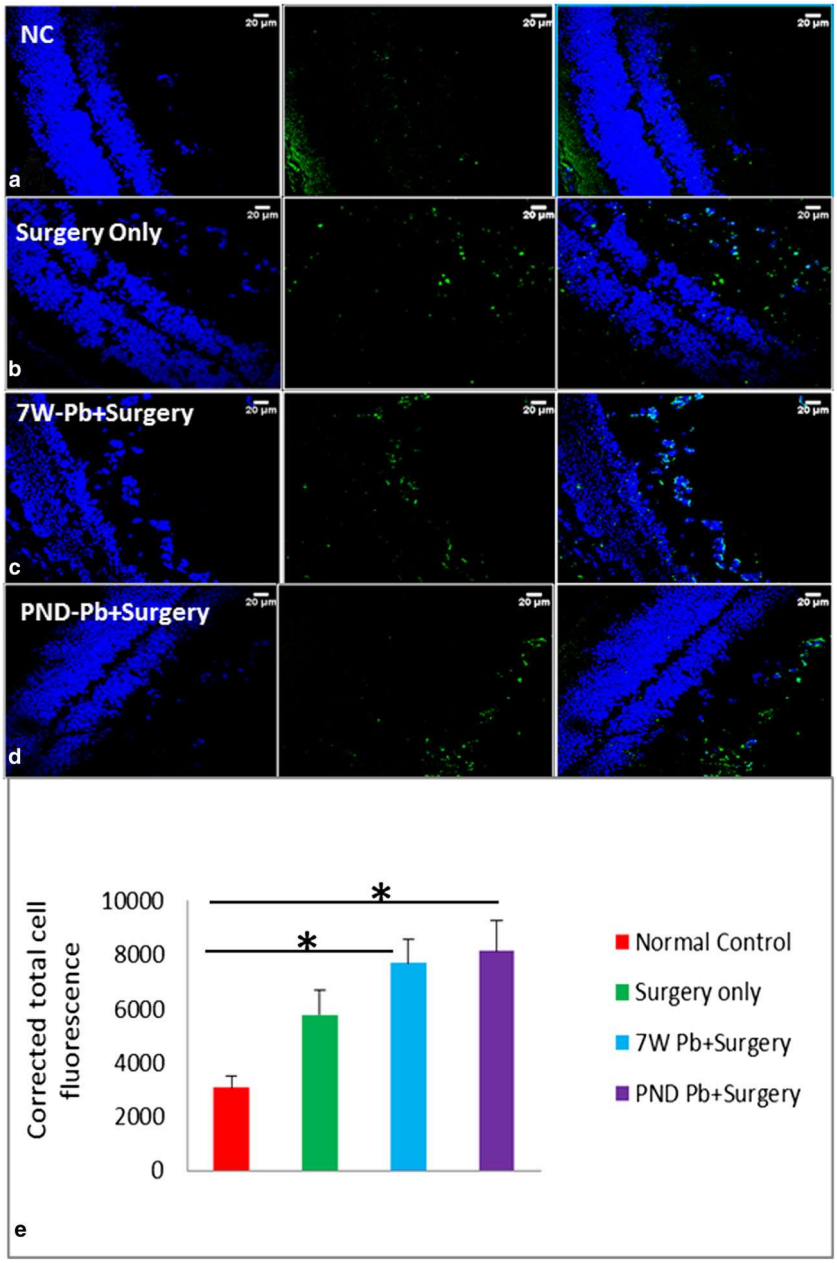


Fig. 2 Representative retinal sections from normal control (**a**), surgery only (**b**), 7th W Pb + surgery (**c**) and PND Pb + surgery (**d**) showing retinal sections stained with DAPI (left), TUNEL-positive cells in green colour (middle) and merged images (right). Quantitative analysis of corrected total cell fluorescence (CTCF) in various groups (**e**)

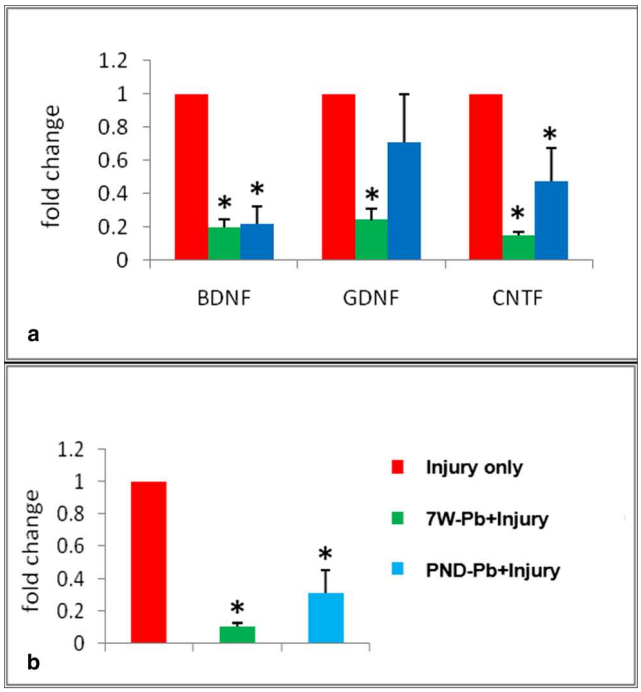


Fig. 3 Fold change in gene expression of various neurotrophin factors BDNF ($p < 0.001$), GDNF ($p < 0.05$), and CNTF ($p < 0.05$) in 7th WPb and PND Pb-exposed groups (**a**). Decreased expression of brn3b in lead-exposed groups ($p = 0.001$) (**b**)

Reduced expression of neurotrophic factors in Pb-treated groups

mRNA neurotrophic factor levels were examined from retina after the surgery in lead-treated and untreated groups using real-time PCR. Brain-derived neurotrophin factor (BDNF), glial derived neurotrophic factor (GDNF) and ciliary neurotrophic factor (CNTF) showed a significant decrease in its expression in Pb-treated groups as compared to the untreated group. BDNF was decreased by a factor of 0.19-fold in 7W-Pb + injury group while PND-Pb + injury group reduced by 0.21-fold as compared to injury only group (Fig. 3a). Likewise, GDNF and CNTF expressions were reduced by 0.24-fold and 0.14-fold respectively in 7W-Pb + injury group. Similarly, PND-Pb + injury group showed reduced expression by 0.7-fold in GDNF and 0.46-fold in CNTF expression (Fig. 3a).

As Brn3b is a marker for retinal ganglion cells, its mRNA expression was expectedly found to be reduced in Pb-treated groups as compared to untreated (injury only) group. A fold change of 0.1 and 0.31 was found in 7W-Pb + injury group and PND-Pb + injury group, respectively when compared to injury only (Fig. 3b).

Reduced BDNF and increased GFAP immunolocalization in Pb-treated retinal sections

BDNF and GFAP protein expressions were determined using immunofluorescence, analysed through confocal microscopy. The retinal sections were labelled with anti-BDNF and anti-GFAP antibodies. The images were further quantified by using ImageJ. The expression of BDNF was found to be decreased in Pb-treated groups and was correlated to the gene expression of BDNF (Fig. 3a). BDNF expression was found predominantly decreased in both 7W-Pb + injury group and PND-Pb + injury group as compared to injury only group (Fig. 4a–c). This was further quantified and found significantly reduced in both the Pb-treated groups (Fig. 4d).

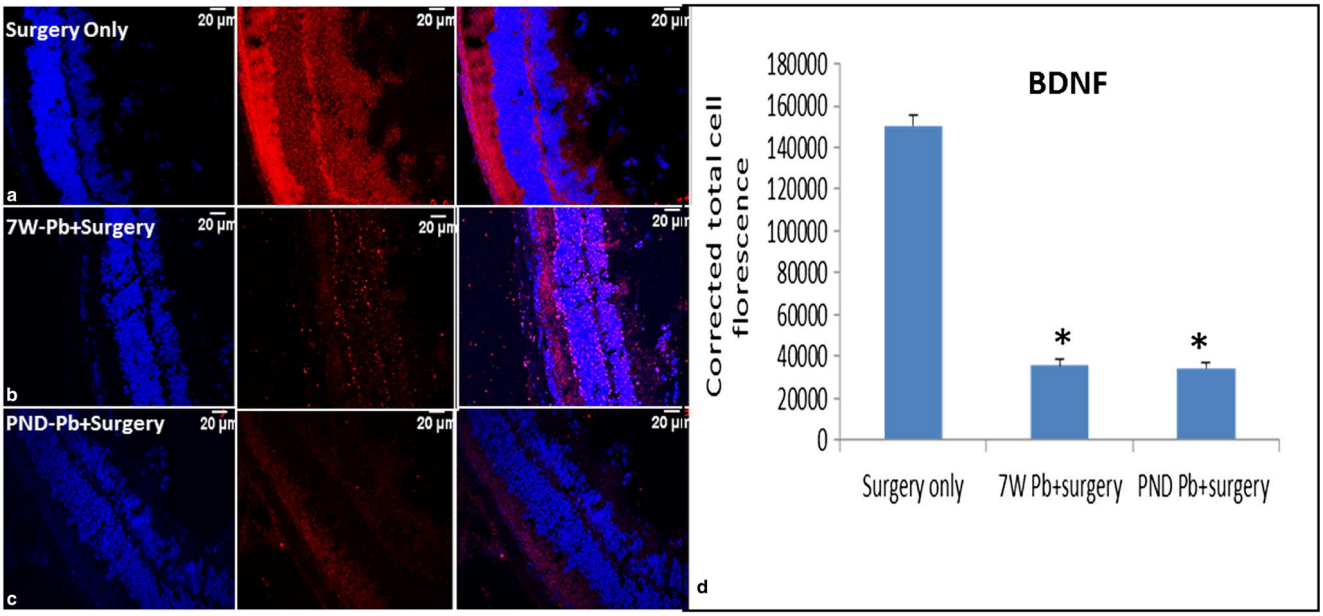


Fig. 4 Expression of BDNF protein in surgery only (**a**), 7th WPb + surgery (**b**) and PND Pb + surgery (**c**). Left panels shows DAPI-stained retinal sections, middle panel shows expression of BDNF and right panel shows merged DAPI and BDNF (**d**). Histogram showing CTCF measurement ($p < 0.004$)

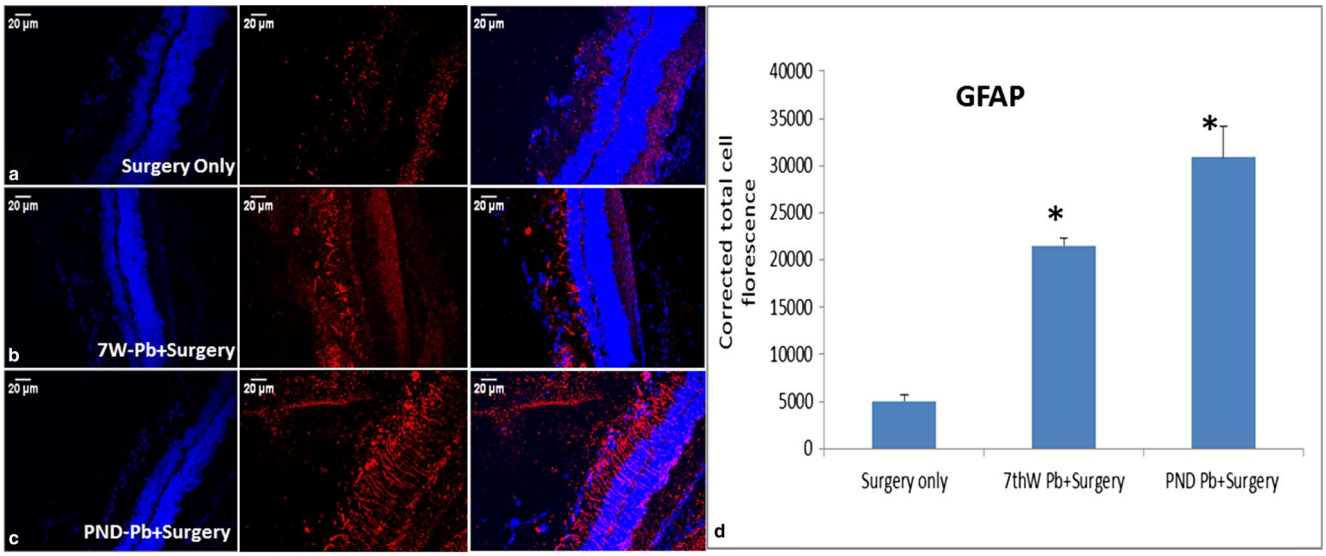


Fig. 5 Expression of GFAP protein in surgery only (**a**), 7th WPb + surgery (**b**) and PND Pb + surgery (**c**). Left panels shows DAPI-stained retinal sections, middle panel shows expression of GFAP and right panel shows merged DAPI and BDNF (**d**). Histogram showing CTCF measurement ($p < 0.002$)

GFAP (glial fibrillary acidic protein) is a marker for inflammation and its expression was also examined using immunofluorescence which showed elevated levels in Pb-treated groups. Both 7W-Pb + injury and PND-Pb + injury groups showed elevated expression of GFAP as compared to injury only group (Fig. 5a–c), which was further found to be significantly higher, analysed by ImageJ quantification (Fig. 5d), since other parameters confirmed that Pb-treated groups showed more damage as compared to the untreated group after I/R injury.

ALA pre-treatment protects Pb/IR injury induced alterations in retinal architecture

Increased ROS leads to tissue injury and cell death and ALA has antioxidant properties. Animals were pre-treated with ALA for 24 h prior to I/R injury in order to examine its neuroprotective effect against retinal damage. Retinal thickness measurements revealed that ALA pre-treatment prevented the alteration in retinal architecture as reported in Pb-treated groups (Fig. 6). The thickness of retina in the ALA pre-treated group was superior as compared to ALA untreated counterpart at 20th week after Pb exposure. The difference between 7W-Pb + injury groups with retinal thickness of 257.4 µm and ALA+7W-Pb + injury group with thickness of 279.1 µm was significant. The ALA + PND-Pb + injury group showed better retinal thickness (288.03 µm) as compared to PND-Pb + injury group (248.9 µm), suggesting ALA has a therapeutic potential to prevent the I/R induced long-term retinal damage in both the Pb-treated mice.

ALA promotes neurotrophic factor expression

Gene expression of neurotrophic factors such as GDNF and CNTF showed significant increase in the ALA pre-treatment groups as compared to groups which do not receive ALA pre-treatment (Fig. 7a, b).

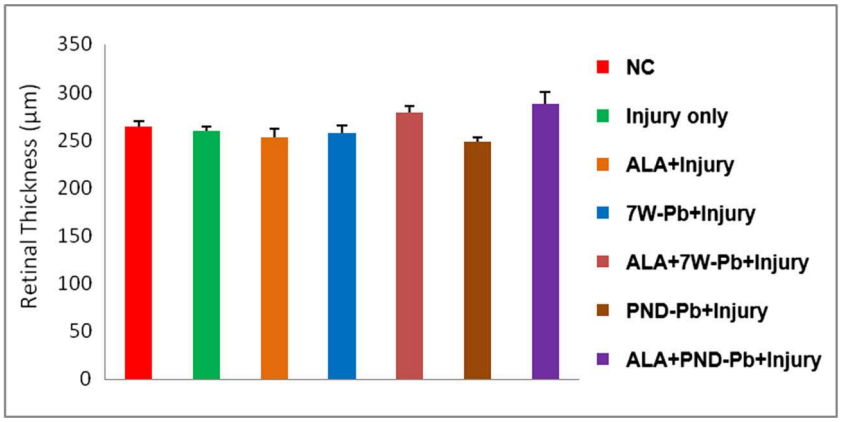


Fig. 6 Histogram showing retinal thickness (µm) in ALA pre-treated and non-treated groups

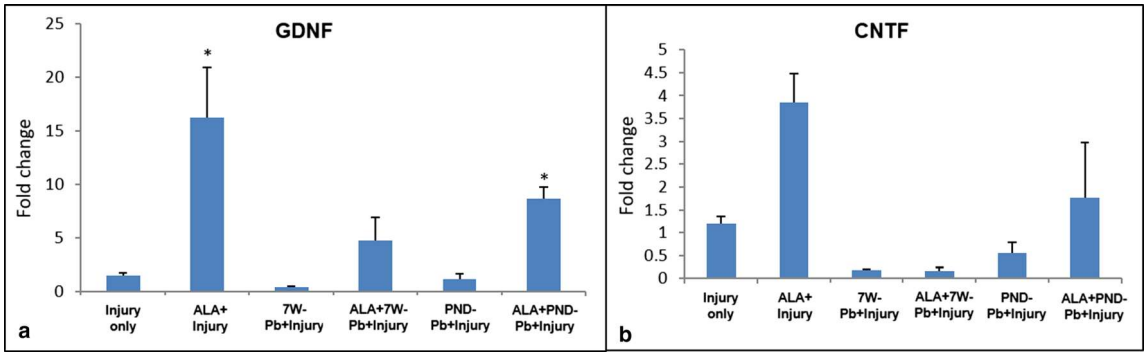


Fig. 7 Fold change in gene expression of various neurotrophin factors GDNF (**a**) and CNTF (**b**). S surgery only group, S + ALA ALA pre-treatment + surgery, 7W 7WPb + surgery, 7W + ALA 7WPb + ALA + surgery, PND PND Pb + surgery, PND + ALA PND Pb + ALA + surgery. $p < 0.001$

ALA exerts anti-inflammatory effects

GFAP expression was found to be increased in Pb-treated groups; its expression was also examined in the ALA-pre-treated groups in order to determine whether ALA treatment ameliorates retinal inflammation. In ALA pre-treated group, the expression of GFAP was downregulated (Fig. 8), suggesting that ALA suppressed inflammation after I/R injury.

Discussion

Acute metal toxicity is well reported with adverse effects ranging from liver disorders, respiratory diseases and cardiovascular disorders to death (Johri et al. 2010; Duruibe et al. 2007). However, longitudinal effects of sub-toxic metal exposure have not been studied extensively. There are some studies reporting early-life exposure and its late-life consequences (Needleman et al. 1990). Environmental toxins have been studied with respect to neurodegeneration and cognitive decline in adults with early-life exposure in childhood (Sethi et al. 2008; Sadiq et al. 2012). I/R injury has been known to result in neuronal cell death. There are various models to induce retinal degeneration such as chemical injury (Jindal et al. 2017), laser photocoagulation (Singh et al. 2011) and intraocular pressure elevation (Hartsock et al. 2016). PPA ligation is another such model to induce ischemia (Ishizuka et al. 2013). Gestational exposure of Pb has shown decreased dopamine content in retina and functional deficit in ERG (Fox et al. 2008, 2011). This study attempted to determine the effect of low-dose lead exposure on severity of retinal damage after ischemia. Pb exposure in early life was found to have late-life adverse effects. Our study revealed that Pb exposure increased the extent of damage caused by ischemia as assessed by reduction of retinal thickness and cell death by TUNEL assay.

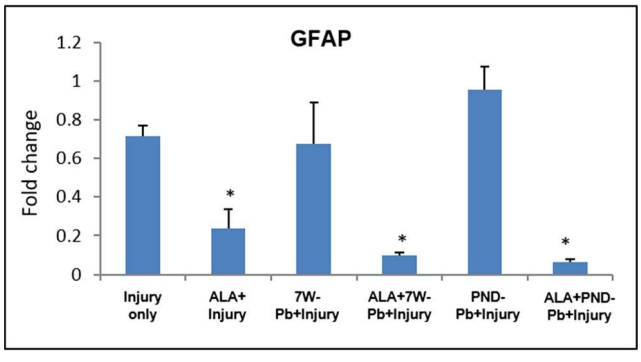


Fig. 8 Fold change in gene expression of GFAP. S surgery only group, S + ALA ALA pre-treatment + surgery, 7W 7WPb + surgery, 7W + ALA 7WPb + ALA + surgery, PND PND Pb + surgery, PND + ALA (PND Pb + ALA + surgery). $p < 0.001$

Earlier, I/R injury in mice has been shown to be correlated with thickness of retina (Ogishima et al. 2011) and Pb toxicity has also been found to damage blood–retinal barrier, thereby further reducing the retinal thickness in adults (Shen et al. 2016). Thus, it can be hypothesised that Pb exposure in early life may exacerbate the effect of I/R injury than late-life Pb exposure. This is why the Pb-treated groups showed reduced retinal thickness. Decreased expression of neurotrophic factors further showed that the toxic effects of Pb in later life may manifest as retinal degeneration. The expression of neurotrophic factors was found to be downregulated in ischemic injury (Guo et al. 2014). Our study showed relative decrease in BDNF, GDNF and CNTF levels in Pb-treated mice retina following PPA surgery, thereby implying that Pb exacerbates the effect of ischemic injury. Increased GFAP expression is associated with inflammation (Abcouwer et al. 2013) and could potentially prime the process of retinal degeneration. Our finding that it was upregulated in Pb-treated retina not only shows the toxic effects of Pb but relatively increased expression of GFAP in PND-Pb + injury group than 7W-Pb + injury group also suggests that early Pb treatment in I/R injury can potentially induce higher inflammation and late-life damage to retina. More experiments with greater sample size are required in order to dissect the role of epigenetic factors that govern retinal susceptibility to early-life Pb treatment. Periodic measurements of Pb could have provided vital information related to the amount of Pb crossing BRB; however, this was possible only for 10 and 20 weeks due to limited access to resources.

Table 1 Comparison on the basis of various parameters between ALA pre-treated and non-treated groups

Parameter	Time of Pb exposure	ALA non-treated	ALA pre-treated
GDNF (fold change w.r.t injury only)	7WPb + injury	0.413	4.729
	PNDPb + injury	1.215	8.62
CNTF (fold change w.r.t injury only)	7WPb + injury	0.172	0.170
	PNDPb + injury	0.544	1.763
GFAP (fold change w.r.t injury only)	7WPb + injury	0.673	0.097
	PNDPb + injury	0.955	0.064
Retinal thickness (μm)	7WPb + injury	248.9	288.03
	PNDPb + injury	257.4	279.1

While increased inflammation and decreased level of neurotrophic factors contribute to the damage caused by Pb-PPA ligation (Li et al. 2012; Carr and Salinthone 2014), ALA prevents the same by likely reducing the microglial activation (Wu et al. 2016; Choi et al. 2015). Although we did not study the mechanism of action, it is attractive to speculate that ALA protected the endogenous secretion of BDNF and CNTF against Pb-induced glial activation. This was corroborated by GFAP levels in the two groups (Table 1).

A probable underlying mechanism of action of ALA-mediated neuroprotection in Pb treated and I/R injured retina has also been proposed (Fig. 9) for simplification. Although BDNF is known to mediate neuroprotection through ERK and PI3 kinase pathway by inhibiting the activity of caspase 3 (Han and Holtzman 2000; Almeida et al. 2005), we did not use inhibitors or estimated caspase levels to dissect this. BDNF expression is known to maintain its level through autocrine signalling, which is further regulated by a positive

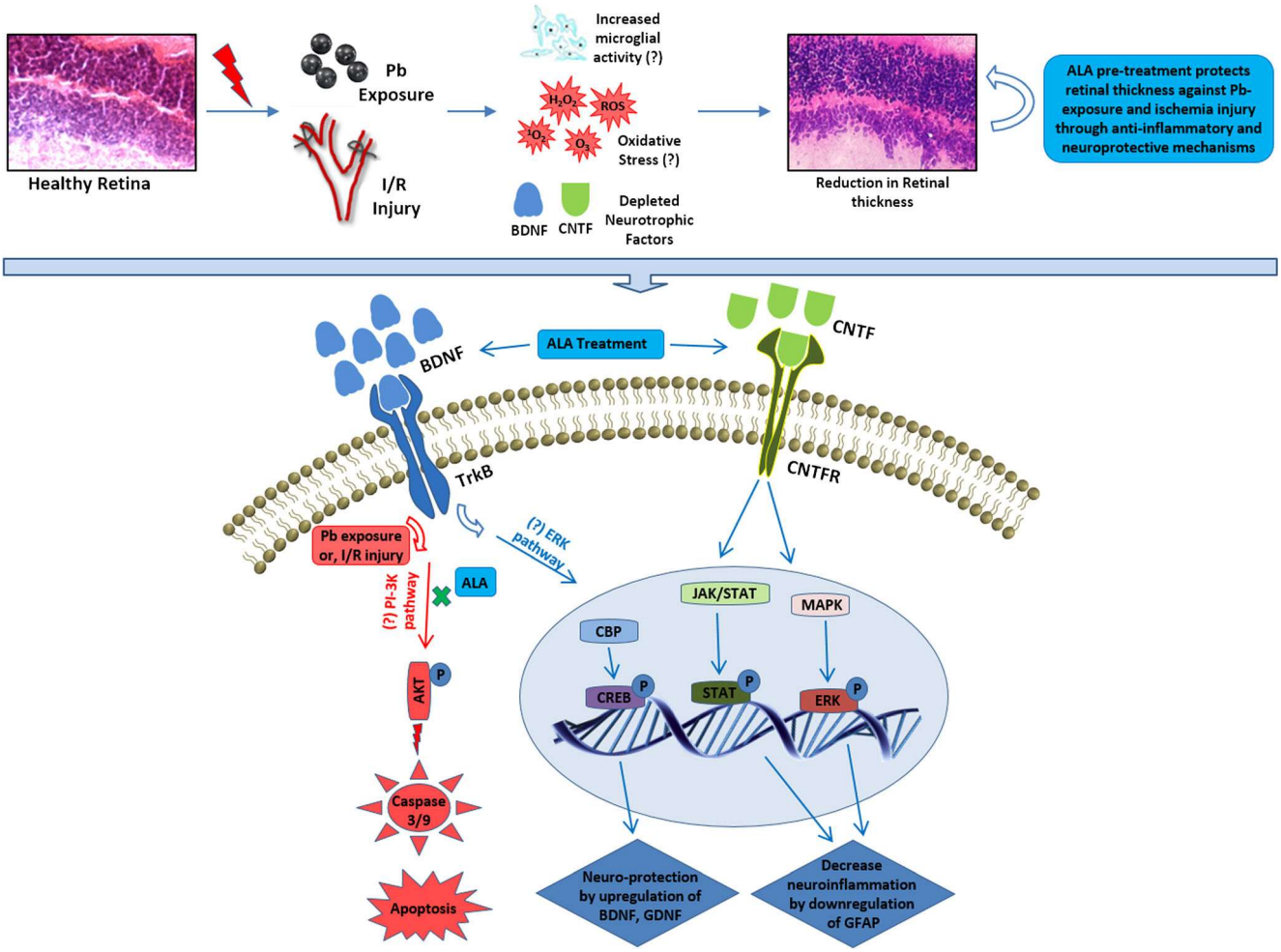


Fig. 9 Flow diagram showing probable underlying mechanism of action of ALA-mediated neuroprotection in Pb treated and I/R injured retina

Table 2 Experimental groups used in the study with details of interventions

Group	Group name	Intervention
1	Normal control (NC)	No intervention till 20th week
2	Injury only	No Pb exposure + ischemia injury at 20th week
3	PND-Pb + injury	Pb exposure (200 ppm through maternal drinking water) at PND 1–20 days + ischemic injury at 20th week
4	7W-Pb + injury	Pb exposure (200 ppm through drinking water) at 7th week for 20 days + ischemic injury at 20th week
5	ALA + injury	24 h early pre-injection of ALA (70 mg/kg IP) + ischemic injury at 20th week
6	ALA + PND-Pb + injury	Pb exposure at PND 1–20 days + 24 h early pre-injection of ALA (70 mg/kg IP) + ischemic injury at 20th week
7	ALA + 7W-Pb + injury	Pb exposure at 7th week for 20 days + 24 h early pre-injection of ALA (70 mg/kg IP) + ischemic injury at 20th week

feedback loop mechanism (Cheng et al. 2011) which is important to meet the requirement during chronic injury. Likewise, CNTF has been known to activate Janus kinase/signal transducer, activator of transcription (Jak-STAT) and ras-mitogen activated protein kinase (ras-MAPK) (Askvig et al. 2013). It exerts anti-inflammatory effects by altering GFAP expression (Fang et al. 2013), but additional experiments are required for the purpose.

Thus, it can be concluded that Pb exposure in early life increases the susceptibility for late-life retinal disorders and the damage caused due to retinal ischemia in later life is enhanced in individuals with early-life Pb exposure. More detailed analysis in the mechanism will help to understand the plausible pathways that are involved in such long-term effects with specific reference to epigenetic regulation of marker molecules involved.

Methods

Animals and study groups All experiments were performed on Swiss albino mice after taking approval of institutional animal ethical committee (IAEC 406). Experiments were performed in accordance with CPCSEA guidelines and animals were taken proper care of during experiments to prevent any discomfort. Animals were placed in Central animal house facility, which is well regulated for temperature and humidity variations. Polypropylene cages with sterile corn cob bedding were used for animals and 12 h dark/light cycle was strictly followed. Gravid Swiss albino mice were issued, and the next day of delivery was considered as postnatal day 1 (PND1). Pups were weaned at PND 21, and both sex (male/female) pups were used for the study. After weaning, pups were segregated into different cages with three pups per cage. All animals were provided with food and water ad libitum throughout the study. There were a total of seven groups included in the study. Details of groups are provided in Table 2, and time point intervention is depicted in the study design flow diagram (Fig. 10).

Lead exposure Early-life treated group received Pb from PND 1–20 days through lactating mothers, provided with 200 ppm lead acetate in drinking water. On PND21, pups were segregated and were kept as such with free access to food and water. On the other hand, adult group was treated to Pb at 7th week of age (200 ppm) directly through drinking water for 20 days and free access to food and water besides this duration of 20 days.

Pre-treatment with ALA Twenty-four hours prior to ischemia/reperfusion (I/R) injury, animals were pre-treated with 70 mg/kg body weight of ALA intraperitoneally.

Surgical intervention At 20th week, ischemia/reperfusion injury was surgically (Stereo Zoom Microscope, Leica) induced in mice by pterygopalatine artery ligation. PPA in mouse bifurcates into ophthalmic artery and supply blood to the retina, and external carotid artery (ECA) is believed to anastomose, further strengthening the blood flow. In this model, PPA along with ECA was ligated to induce ischemia to the retina, as already described (10). In brief, the animals were anaesthetised with xylazine–

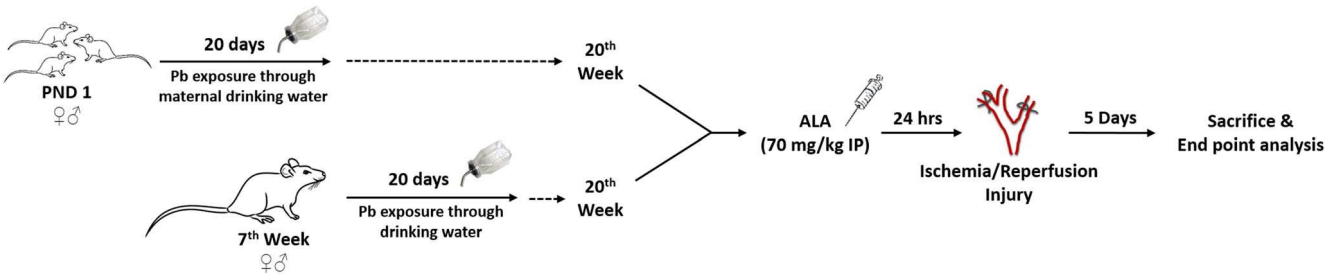


Fig. 10 Study design showing time point interventions in the study

ketamine and kept in supine position. Fur was removed, and incision was made near neck region. Thereafter, muscles were retracted using retractor to expose underlying arteries. Common carotid artery was located, and ECA and ICA (internal carotid artery) bifurcations were tracked. ECA was ligated using (Silk braided, suture 7-0, Ethicon) followed by PPA (Prolene, Suture 6-0, Ethicon). Arteries were kept ligated for 2 h, and tissue was reperfused by removing suture. Animals were allowed to reperfuse for 5 days, after which they were sacrificed. After recovery from anaesthesia, animals were kept in sterilised cages with heating lamp to prevent hypothermia and were monitored till sacrifice.

Histological analysis Immediately after the sacrifice, eyes were enucleated and snap frozen at − 80 °C. For cryosectioning, eyes were fixed in OCT (optimal cutting temperature) media and mounted on cryotome. Six to eight micron thick sections were taken on poly-L-lysine coated slides and were kept at − 20 °C for IHC and TUNEL studies. For histological studies, retinal sections were stained with haematoxylin–eosin stain and images of retina under light microscope were taken. Retinal micrographs were analysed using ImageJ software to measure retinal thickness. Central retina was used for thickness, which is a measure of length from retinal pigment epithelium to ganglion cell layer. Three animals were used per group for thickness measurements, and three sections per animal were taken. The mean of retinal measurements (in μm) from three animals was used for final calculations.

Immunofluorescence Immunohistochemistry analysis was carried out quantify the expression of brain-derived neurotrophic factor (BDNF) (Santa Cruz) and glial fibrillary acidic protein (GFAP) (Santa Cruz). The retinal sections were fixed in acetone for 20 min and, after washing with 1× PBS, blocked with 5% donkey serum for 30 min at room temperature in humidified chamber. Sections were incubated with either anti-BDNF or anti-GFAP primary antibody (1:100 dilution) for overnight at 4 °C. Excess primary antibody was washed, and sections were then incubated with 1:200 diluted cy3 tagged secondary antibody (Jackson ImmunoResearch) for 1 h at room temperature in dark. After washing, sections were counterstained with DAPI and mounted in fluorSave (Millipore) to avoid quenching. Total cell fluorescence was quantitated using ImageJ software. The region of interest (ROI) was selected from each image. Three measurements per section were taken, and ROI was selected such that the whole retinal image was covered in three subsequent measurements and area used remained constant in each image. Integrated density, area of the selected cell, and mean fluorescence of background were measured by selecting these parameters in software. Fluorescence intensity was calculated using formula: Corrected total cell fluorescence (CTCF) = Integrated Density − (Area of selected cell × Mean fluorescence of background readings).

TUNEL assay Terminal deoxynucleotidyl transferase (TdT) dUTP nick-end labelling (TUNEL) assay was performed according to kit's protocol (Millipore, USA). Briefly, retinal sections were fixed (4% paraformaldehyde) and washed in PBS, followed by post-fixation with (2:1) acetic acid:ethanol. After applying equilibrium buffer for 10 s, incubation with Tdt enzyme was carried out for 1 h in humid chamber at 37 °C. Sections were counterstained with DAPI after washing. Finally, excess DAPI was removed by washing, and sections were mounted with FluorSave reagent (Millipore).

Real-time PCR For carrying out molecular analysis, retina was isolated from enucleated eyes and RNA extraction was done according to manufacturer's protocol (Qiagen, USA). RNA was used as a template to synthesise cDNA as per kit protocol (Thermo Scientific, USA). The expression of different genes was determined by subjecting cDNA (100ng) to real time PCR analysis (Applied Biosystems) using specific primers (Sigma USA and Eurofins Genomics). Primer details and reaction protocol are given in Table 3 and Table 4 respectively). The relative fold change expression was analysed, and data was normalised with β-actin expression of each sample.

Statistical analysis All eye samples and RNA samples were blinded to the experimenter to remove any bias. All results were expressed as mean ± S.E.M of three animals per technique. Data was statistically analysed using 16.0 version of SPSS. Data normality was checked using 1-KS sampling.

Table 3 PCR conditions for different genetic markers

Steps	Initial denaturation	Denaturation	Annealing		Extension	Final extension
Temperature	95 °C	95 °C	GFAP	63 °C	72 °C	72 °C
			BDNF	63 °C		
			CNTF	63 °C		
			GDNF	62 °C		
			Brn3b	62 °C		
Duration	10 min	1 min	1 min		1 min	10 min

Table 4 Target genes and their primer sequences used in PCR

Target gene	Target length (bp)	Primer sequence (5′ ➔ 3′)
BDNF	131	F: TGGCTGACACTTTTGAGCAC R: CAAAGGCACTTGACTGCTGA
CNTF	62	F: TTGATTCCACAGGCACAAAA R: CCCTGCCTGACTCAGAGGT
GDNF	142	F: TGGGCTATGAAACCAAGGAG R: CAACATGCCTGGCCTACTTT
Brn3b	149	F: GCAGTCTCCACTTGGTGCTTACTC R: TTCCCCCTACAAACAAACCTCC
GFAP	63	F: ACAGACTTTCTCCAACCTCCAG R: CCTTCTGACACGGATTTGGT
B-actin	228	F: AGCCATGTACGTAGCCATCC R: CTCTCAGCTGTGGTGGTGAA

Normally distributed data was analysed using one-way ANOVA, followed by Scheffe and Dunnett's test for post-hoc analysis. $p < 0.05$ was regarded as statistically significant.

Author contribution AA conceptualised and edited manuscript; SM performed experiments and manuscript writing; SB performed experiments; AB and VS edited the manuscript.

Funding The funding was provided by Council for Scientific and Industrial Research, grant no. 09/135(0666)/2012.

Compliance with ethical standards

Conflict of interest The authors declare that they have no conflict of interest.

References

Abcouwer SF, C-m L, Shanmugam S, Muthusamy A, Barber AJ et al (2013) Minocycline prevents retinal inflammation and vascular permeability following ischemia-reperfusion injury. J Neuroinflammation 10:913

Almeida R, Manadas B, Melo C, Gomes J, Mendes C et al (2005) Neuroprotection by BDNF against glutamate-induced apoptotic cell death is mediated by ERK and PI3-kinase pathways. Cell Death Differ 12:1329–1343

Askvig JM, Lo DY, Sudbeck AW, Behm KE, Leiphon LJ, Watt JA (2013) Inhibition of the Jak-STAT pathway prevents CNTF-mediated survival of axotomized oxytocinergic magnocellular neurons in organotypic cultures of the rat supraoptic nucleus. Exp Neurol 240:75–87

Carr DW, Salinthone S (2014) Lipoic acid, inflammation and diseases of the nervous system. In: Systems biology of free radicals and antioxidants. Springer, p 2349–2368

Chaney SY, Mukherjee S, Giddabasappa A, Rueda EM, Hamilton WR et al (2016) Increased proliferation of late-born retinal progenitor cells by gestational lead exposure delays rod and bipolar cell differentiation. Mol Vis 22:1468

Cheng P-L, Song A-H, Wong Y-H, Wang S, Zhang X, Poo MM (2011) Self-amplifying autocrine actions of BDNF in axon development. Proc Natl Acad Sci 108:18430–18435

Choi K-H, Park M-S, Kim H-S, Kim K-T, Kim H-S, Kim JT, Kim BC, Kim MK, Park JT, Cho KH (2015) Alpha-lipoic acid treatment is neurorestorative and promotes functional recovery after stroke in rats. Mol Brain 8:9

Control and Disease and Prevention (2012) Response to Advisory Committee on Childhood Lead Poisoning Prevention recommendations in "Low level lead exposure harms children: a renewed call of primary prevention". CDC, Atlanta

Deng H, Zuo X, Zhang J, Liu X, Liu L et al (2015) α-Lipoic acid protects against cerebral ischemia/reperfusion induced injury in rats. Mol Med Rep 11:3659–3665

Duruibe J, Ogwuegbu M, Egwurugwu J (2007) Heavy metal pollution and human biotoxic effects. Int J Phys Sci 2:112–118

Fang IM, Yang CM, Yang CH, Chiou SH, Chen MS (2013) Transplantation of induced pluripotent stem cells without C-Myc attenuates retinal ischemia and reperfusion injury in rats. Exp Eye Res 113:49–59

Flora G, Gupta D, Tiwari A (2012) Toxicity of lead: a review with recent updates. Interdiscip Toxicol 5:47–58

Foulkes E (2000) Transport of toxic heavy metals across cell membranes. Proc Soc Exp Biol Med 223:234–240

Fox DA, Rubinstein SD, Hsu P (1991) Developmental lead exposure inhibits adult rat retinal, but not kidney, Na+, K+-ATPase. Toxicol Appl Pharmacol 109:482–493

Fox DA, He L, Poblenz AT, Medrano CJ, Blocker YS et al (1998) Lead-induced alterations in retinal cGMP phosphodiesterase trigger calcium overload, mitochondrial dysfunction and rod photoreceptor apoptosis. Toxicol Lett 102:359–361

Fox DA, Kala SV, Hamilton WR, Johnson JE, O'Callaghan JP (2008) Low-level human equivalent gestational lead exposure produces supernormal scotopic electroretinograms, increased retinal neurogenesis, and decreased retinal dopamine utilization in rats. Environ Health Perspect 116:618–625

Fox DA, Hamilton WR, Johnson JE, Xiao W, Chaney S, Mukherjee S, Miller DB, O'Callaghan JP (2011) Gestational lead exposure selectively decreases retinal dopamine amacrine cells and dopamine content in adult mice. Toxicol Appl Pharmacol 256:258–267

Golbidi S, Badran M, Laher I (2011) Diabetes and alpha lipoic acid. Front Pharmacol 2

Grandjean P, Landrigan PJ (2014) Neurobehavioural effects of developmental toxicity. Lancet Neurol 13:330–338

Guo XJ, Tian XS, Ruan Z, Chen YT, Wu L, Gong Q, Wang W, Zhang HY (2014) Dysregulation of neurotrophic and inflammatory systems accompanied by decreased CREB signaling in ischemic rat retina. Exp Eye Res 125:156–163

Hall ED, Vaishnav RA, Mustafa AG (2010) Antioxidant therapies for traumatic brain injury. Neurotherapeutics 7:51–61

Han BH, Holtzman DM (2000) BDNF protects the neonatal brain from hypoxic-ischemic injury in vivo via the ERK pathway. J Neurosci 20:5775–5781

Hartsock MJ, Cho H, Wu L, Chen W-J, Gong J et al (2016) A mouse model of retinal ischemia-reperfusion injury through elevation of intraocular pressure. JoVE (J Vis Exp) e54065

Ishizuka F, Shimazawa M, Umigai N, Ogishima H, Nakamura S, Tsuruma K, Hara H (2013) Crocetin, a carotenoid derivative, inhibits retinal ischemic damage in mice. Eur J Pharmacol 703:1–10

Jindal N, Banik A, Prabhakar S, Vaiphie K, Anand A (2017) Alteration of neurotrophic factors after transplantation of bone marrow derived Lin-ve stem cell in NMDA-induced mouse model of retinal degeneration. J Cell Biochem 118:1699–1711

Johri N, Jacquillet G, Unwin R (2010) Heavy metal poisoning: the effects of cadmium on the kidney. Biometals 23:783–792

Laidlaw MA, Filippelli GM, Sadler RC, Gonzales CR, Ball AS, Mielke H (2016) Children's blood lead seasonality in flint, Michigan (USA), and soil-sourced lead hazard risks. Int J Environ Res Public Health 13:358

Lanphear BP, Hornung R, Khoury J, Yolton K, Baghurst P, Bellinger DC, Canfield RL, Dietrich KN, Bornschein R, Greene T, Rothenberg SJ, Needleman HL, Schnaas L, Wasserman G, Graziano J, Roberts R (2005) Low-level environmental lead exposure and children's intellectual function: an international pooled analysis. Environ Health Perspect 113:894–899

Li S-Y, Yang D, Yeung C-M, Yu W-Y, Chang RC-C et al (2011) *Lycium barbarum* polysaccharides reduce neuronal damage, blood-retinal barrier disruption and oxidative stress in retinal ischemia/reperfusion injury. PloS One 6:e16380

Li S-Y, Fung FK, Fu ZJ, Wong D, Chan HH et al (2012) Anti-inflammatory effects of lutein in retinal ischemic/hypoxic injury: in vivo and in vitro studies. Invest Ophthalmol Vis Sci 53:5976–5984

Lidsky TI, Schneider JS (2003) Lead neurotoxicity in children: basic mechanisms and clinical correlates. Brain 126:5–19

London A, Benhar I, Schwartz M (2013) The retina as a window to the brain—from eye research to CNS disorders. Nat Rev Neurol 9:44–53

Minhas G, Morishita R, Shimamura M, Bansal R, Anand A (2015) Modeling transient retinal ischemia in mouse by ligation of pterygopalatine artery. Ann Neurosci 22:222

Modgil S, Cameotra SS, Sharma VL, Anand A (2017) Early life Pb exposure and its effect on later life retinal degeneration. J Cell Biochem 118(10):3213–3224

Needleman HL, Schell A, Bellinger D, Leviton A, Allred EN (1990) The long-term effects of exposure to low doses of lead in childhood: an 11-year follow-up report. N Engl J Med 322:83–88

Ogishima H, Nakamura S, Nakanishi T, Imai S, Kakino M, Ishizuka F, Tsuruma K, Shimazawa M, Hara H (2011) Ligation of the pterygopalatine and external carotid arteries induces ischemic damage in the murine retina. Invest Ophthalmol Vis Sci 52:9710–9720

Otsuka T, Shimazawa M, Inoue Y, Nakano Y, Ojino K, Izawa H, Tsuruma K, Ishibashi T, Hara H (2016) Astaxanthin protects against retinal damage: evidence from in vivo and in vitro retinal ischemia and reperfusion models. Curr Eye Res 41:1465–1472

Patrick L (2006) Lead toxicity, a review of the literature. Part I: exposure, evaluation, and treatment. Altern Med Rev 11:2–23

Rothenberg SJ, Schnaas L, Salgado-Valladares M, Casanueva E, Geller AM et al (2002) Increased ERG a- and b-wave amplitudes in 7- to 10-year-old children resulting from prenatal lead exposure. Invest Ophthalmol Vis Sci 43:2036–2044

Sadiq S, Ghazala Z, Chowdhury A, Büsselberg D (2012) Metal toxicity at the synapse: presynaptic, postsynaptic, and long-term effects. J Toxicol

Santos-Anderson RM, Tso MO, Valdes JJ, Annau Z (1984) Chronic lead administration in neonatal rats: electron microscopy of the retina. J Neuropathol Exp Neurol 43:175–187

Sethi P, Jyoti A, Singh R, Hussain E, Sharma D (2008) Aluminium-induced electrophysiological, biochemical and cognitive modifications in the hippocampus of aging rats. Neurotoxicology 29:1069–1079

Shen X-F, Huang P, Fox DA, Lin Y, Zhao Z-H, Wang W, Wang JY, Liu XQ, Chen JY, Luo WJ (2016) Adult lead exposure increases blood-retinal permeability: a risk factor for retinal vascular disease. Neurotoxicology 57:145–152

Singh T, Prabhakar S, Gupta A, Anand A (2011) Recruitment of stem cells into the injured retina after laser injury. Stem Cells Dev 21:448–454

Volobouéva LA, Liu J, Suh JH, Ames BN, Miller SS (2005) (R)-α-lipoic acid protects retinal pigment epithelial cells from oxidative damage. Invest Ophthalmol Vis Sci 46:4302–4310

Wang X, Yu Y, Ji L, Liang X, Zhang T, Hai CX (2011) Alpha-lipoic acid protects against myocardial ischemia/reperfusion injury via multiple target effects. Food Chem Toxicol 49:2750–2757

Wu J, Basha MR, Brock B, Cox DP, Cardozo-Pelaez F, McPherson CA, Harry J, Rice DC, Maloney B, Chen D, Lahiri DK, Zawia NH (2008) Alzheimer's disease (AD)-like pathology in aged monkeys after infantile exposure to environmental metal lead (Pb): evidence for a developmental origin and environmental link for AD. J Neurosci 28:3–9

Wu M-H, Huang C-C, Chio C-C, Tsai K-J, Chang C-P, Lin NK, Lin MT (2016) Inhibition of peripheral TNF-α and downregulation of microglial activation by alpha-lipoic acid and etanercept protect rat brain against ischemic stroke. Mol Neurobiol 53:4961–4971

Publisher's Note Springer Nature remains neutral with regard to jurisdictional claims in published maps and institutional affiliations.

ARTICLE
Journal of Cellular Biochemistry 118:3213–3224 (2017)

Journal of Cellular Biochemistry

Early Life Pb Exposure and its Effect on Later Life Retinal Degeneration

Shweta Modgil,[1,2] Swaranjit S. Cameotra,[3] Vijay L. Sharma,[2] and Akshay Anand[1]*

[1]*Neuroscience Research Lab, Department of Neurology, Post Graduate Institute of Medical Education and Research, Chandigarh, India*

[2]*Department of Zoology, Panjab University, Chandigarh, India*

[3]*Institute of Microbial Technology (IMTECH), Chandigarh, India*

ABSTRACT

The study presents the longitudinal effect of early life lead exposure on retinal ischemia. Swiss albino mice were exposed to lead acetate at two different timepoints viz. postnatal day 1–20 and at 7th week of age. These mice were then followed till 10 week of age and subjected to retinal ischemia. Retinal ischemia was induced using pterygopalatine artery ligation. The effect of prior lead exposure on ischemic insult was determined using various histological and molecular parameters. Although toxic effects of Pb are well reported, but the results in this study showed not much significant effect of early life Pb exposure on later life retinal degeneration. While retinal thickness was decreased in surgery group and 7th week Pb exposed group, PND Pb exposed mice showed retinal thickness comparable to normal control. There was no difference in TUNEL positive cells in Pb exposed group when compared to surgery group. The molecular studies revealed overexpression of BDNF and GFAP in PND Pb exposed mice reflecting more injury and inflammation. The combined results revealed that Pb exposure have mild effect on overall susceptibility to retinal damage in later life. The Pb may exert its toxic effects at longer duration and thus the toxic effects may be mapped at longer timepoints. The study provides a new dimension to the already well known toxic effects of lead which needs to be further explored. J. Cell. Biochem. 118: 3213–3224, 2017. © 2017 Wiley Periodicals, Inc.

KEY WORDS: ISCHEMIA; LEAD EXPOSURE; HORMESIS; RETINAL DEGENERATION; EARLY LIFE

The role of epigenetics in neurodegenerative disorders is being increasingly studied highlighting the significance of early life in disorders of ageing [Fernandez-Teruel et al., 1997; Shonkoff et al., 2012]. Various studies support the notion that early life stress in any form is associated with almost every disease [Pechtel and Pizzagalli, 2011]. On the other hand enriched environment protects from disease onset in later age [Young et al., 1999; Williams et al., 2001]. Many models have been proposed to explain the early life origin of diseases in adulthood [Barker et al., 2002; Modgil et al., 2014]. Central nervous system related diseases are particularly believed to be associated such studies. This could be partly due to the fact that central nervous system is not fully developed in early stages. Blood brain barrier and blood retinal barrier which protects them from any stress are under development in children because of which they are more prone to any environmental related stress [Engel et al., 2011; Calderon-Garcidueñas et al., 2013]. In this context, the heavy metals are believed to readily cross the underdeveloped barrier, resulting in neurological disorders [Zheng et al., 2003]. Heavy metals such as Mercury, Lead, Chromium, Zinc, and Manganese are, therefore, reported to have deleterious effect on living organisms [Jaishankar et al., 2014]. Lead is one of the most abundant heavy metals present in environment and its adverse effects are well reported [Bihaqi and Zawia, 2013; Mason et al., 2014]. Although no levels of Pb are considered safe, the approved blood lead level in blood by center for disease control and prevention in 2012 is below 5 μg/dl in children. Studies have shown that lead exposure during early life result in behavioral alterations as well as cognitive decline in individuals at later stage [Bihaqi et al., 2014a,b; Hanson et al., 2015]. Prospective studies on animal models carried out in this context have also reported the morphological as well as neurobehavioral changes at adult age [Howell et al., 2013; Tomi et al., 2013]. Studies carried out on rodents [Faulk et al., 2013] and macaques have shown that infantile exposure to Pb results in long term effect on brain and lead to tau like pathology in adulthood [Bihaqi et al., 2011, 2014a,b].

Conflicts of interest: None.

Grant sponsor: Council for Scientific and Industrial Research; Grant number: 09/135(0666)/2012.

*Correspondence to: Dr. Akshay Anand, Neuroscience Research Lab, Department of Neurology, Post Graduate Institute of Medical Education and Research, Chandigarh, India. E-mail: akshay1anand@rediffmail.com

Manuscript Received: 23 January 2017; Manuscript Accepted: 1 March 2017

Accepted manuscript online in Wiley Online Library (wileyonlinelibrary.com): 6 March 2017

DOI 10.1002/jcb.25968 • © 2017 Wiley Periodicals, Inc.

However, whether low level of Pb would exacerbate the damage caused by diseases in later life is not well studied in relation to retina. In respect to this, we wanted to study the effect of Pb on retinal injury caused by ischemia. The retinal ischemia models are well studied models to induce retinal degeneration. The ischemic models range from chemical induced ischemia using Cobalt chloride [Lan et al., 2013] to surgical models such as mid cerebral artery (MCA) or Pterygopalatine artery (PPA) occlusion [Allen et al., 2013; Ishizuka et al., 2013]. We have earlier shown that PPA occlusion is good model to induce transient ischemia and retinal degeneration in mice [Minhas et al., 2015]. Thus, Pb exposed mice were subjected to PPA injury, and damage to retina was studied using various histological and molecular parameters.

MATERIALS AND METHODS

STUDY PLAN

The study was carried out after obtaining the Institute Animal ethics committee approval. The gravid females were maintained in polypropylene cages. The Group 1 pups received Pb acetate in water from PND1 (Postnatal day) to PND20 through mother, after which they were given normal water. Group 2 pups received Pb acetate in water at 7th week for 20 days and kept on normal water otherwize. Group 3, that is, control group received normal water throughout experimentation. At 10th week, the animals from all groups were exposed to PPA ligation surgery (2 h occlusion and 5 day reperfusion). After 5th day of surgery, the animals were sacrificed and eyes were enucleated for further experimentation. The timeline of study plan has been represented by Figure 1.

ANIMALS

All experiments were carried out on Swiss Albino mice. Animals were used with permission from Institutional animal ethical committee (IAEC), and proper care and maintenance of animals was rendered during experimental protocol. Animals were kept in polypropylene cages with autoclaved corn husk bedding. Temperature and humidity of animal house was maintained and 12 h light/dark cycle was followed. Animals were provided free access to feed and water all the time except if required otherwize in the protocol.

LEAD ACETATE EXPOSURE

Animals were exposed to lead in the form of lead acetate dissolved in drinking water. A 200 ppm of lead was given for 20 days. In Group 1, the pups received lead through their mother's milk. Dams exposed to Pb during gestation or during lactation have shown to pass the Pb to pups through placenta or milk, respectively. Earlier studies have shown that gestational or postnatal treatment of Pb increases the level of Pb in blood of pups [Fox et al., 1991; Leasure et al., 2008]. The 7th week pups received lead acetate in drinking water directly. Except for treatment period, all animals had access to normal water *ad libitum*.

RETINAL ISCHEMIA MODEL ESTABLISHMENT AND VALIDATION

To induce retinal ischemia in mice, animals were anaesthetized with xylazine-ketamine cocktail. After placing mice on supine position, hair around the neck region was removed and an incision was made.

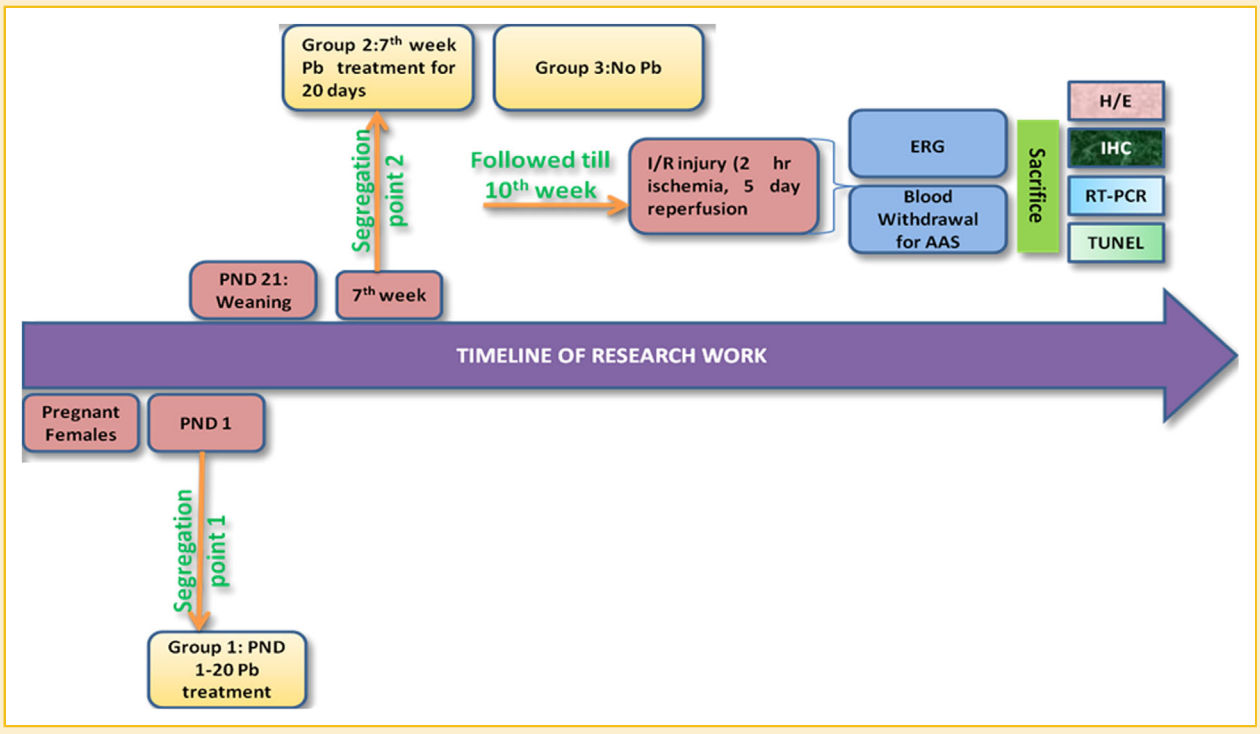


Fig. 1. Timeline of experimental work plan.

Muscles were cleared to expose the common carotid artery (CCA) which runs parallel to vagus nerve. CCA was followed to track down bifurcation of internal carotid artery (ICA) and external carotid artery (ECA). ECA was ligated with suture, and then the PPA was tracked down and ligated. Retinal ischemia was induced for 2 h, after which sutures were removed and the tissue was reperfused for 5 days. Animals were sacrificed after 5 days, eyes enucleated and stored for further processing.

LEAD ESTIMATION USING ATOMIC ABSORPTION SPECTROSCOPY

At the time of sacrifice, blood was drawn intra-cardially from the mice. A 0.5 ml of blood was mixed with HNO_3:H_2O_2 (2:1) and subjected to wet digestion by heating at 60–70°C in a closed vessel until clear solution was obtained. The digested solution was injected to flame atomic absorption spectroscopy to determine lead concentration.

HISTOLOGICAL ANALYSIS

Enucleated eyes were cryo-sectioned and sections were stained with haematoxylin-eosin stain for histological studies. Photographs were taken using light microscope and images were analyzed using Image J software. The retinal thickness was determined by measuring the distance between retinal pigment layer and ganglion cell layer.

IMMUNOFLORESCENCE STUDIES

Immunoflorescence study of various retina related markers was done. Briefly, sections were fixed and then washed with PBS. After serum incubation for ½ h in a humidified chamber, sections were incubated with primary antibody overnight at 4°C. Next day, secondary antibody incubation in a dark and humidified chamber, for 1 h at room temperature, followed by washing the excess stain, was carried out as per standard operating procedure. Finally, the sections were counterstained with DAPI, washed and mounted in flourosave. The sections were photographed using confocal microscopy and images were edited using photoshop, in accordance with publication ethics.

TUNEL

TUNEL assay was performed according to manufacturer's protocol (Apoptag florescein, Millipore, S7110). Briefly, sections were fixed with 1% paraformaldehyde, postfixed with 2:1 (ethanol:acetic acid) and washed with PBS. Tdt buffer was applied to sections for 10 s at room temperature and then incubated with Tdt enzymes for 1 h at 37°C in a humidified chamber. Reaction was stopped with Stop buffer. After washing, anti-digoxigenin conjugate was finally added and slides were incubated for half an hour in dark. DAPI counterstaining was carried out followed by fixation step in Florosave. The images were acquired using confocal microscope.

REAL TIME PCR

RNA isolation was carried out using kits protocol on the isolated retina and RNA quantitation was carried out using UV spectrophotometer. RNA was converted into cDNA using standard protocol as per manufacturers' instructions. The gene expression study was carried out using Real time PCR analysis. The relative gene expression in control and test groups was determined by using RT-PCR whose conditions have been summarized in Table I. All the values were normalized with their respective β-Actin expression. Data was analyzed using SPSS 16.0 by repeated measures ANOVA.

ELECTRORETINOGRAPHY

Electroretinography (ERG) was used for functional analysis. All experiments were performed using ERG instrument from iWorx (Dover) and signals were recorded using Labscribe software. The animals were dark adapted for 24 h and all experiments were carried out in red light. The animals were anaesthetized and placed on a heating pad for thermal regulation. The eyes were dilated using tropicamide and dryness was preventing by moistening the eyes with methylcellulose eye drops. Electrodes were placed, ground electrode on tail, negative electrode between ears, and positive electrode on cornea. The recordings were made with flashes of light. A wave amplitude, b wave amplitude, time to a wave, and time to b wave was analyzed and compared between groups.

STATISTICAL ANALYSIS

Statistical analysis was performed using SPSS 16.0. Data normality test was performed using One-Sample Kolmogorov–Smirnov Test. Parametric data was assessed using independent *t*-test for two groups and analysis of Variance for more than two groups followed by Dunnet post host analysis. Non-parametric test were performed using Mann–Whitney for two groups and Kruskal–Wallis for multiple groups. Data are presented as mean ± SE and $P < 0.05$ was considered as significant.

RESULTS

RETINAL ISCHEMIA INDUCTION AND VALIDATION

PPA is known to give rise to ophthalmic artery in mice and unilateral occlusion of this artery interrupts blood supply to retina leading to monocular amaurosis fugax [Lelong et al., 2007]. Retinal ischemia was induced by surgically ligating arteries (ECA and PPA) supplying blood to tissue (Representative images, Fig. 2). Occlusion of ECA and PPA for 2 h results in reduced blood flow to the eye as depicted in Figure 3c, which shows blood flow measurement by laser Doppler before surgery, during occlusion and after reperfusion. There is a dip in blood flow during the occlusion which returns back to normal after reperfusion. The retinal vessels were thinner in surgical eye as compared to the

TABLE I. Table Showing Real Time PCR Conditions

Steps / Variable		Initial denaturation	Denaturation	Annealing		Extension	Final extension
	Temparature	95°C (10 min)	95°C (1 min)	GFAP	63°C (1min)	72°C (1 min)	72°C (10 min)
				BDNF	63°C		
				HIF1α	61.1°C		
				Thy1	62°C		

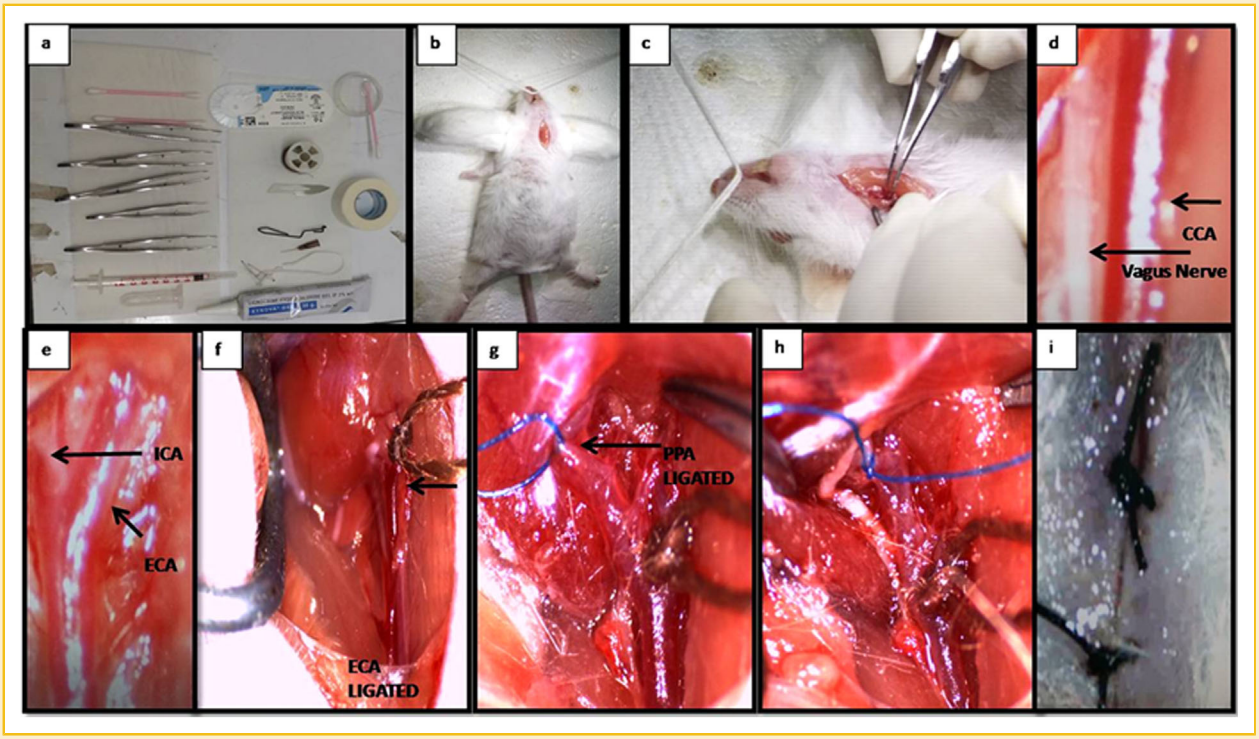


Fig. 2. Representative images of pterygopalatine artery ligation (a); surgical and other requirements for surgery (b); fixing animal in supine position (c); muscle retraction (d); identifying CCA (e); tracking CCA, and locating ECA and ICA (f); ligating CCA (g) and (h) ligating PPA; i) suturing after reperfusion.

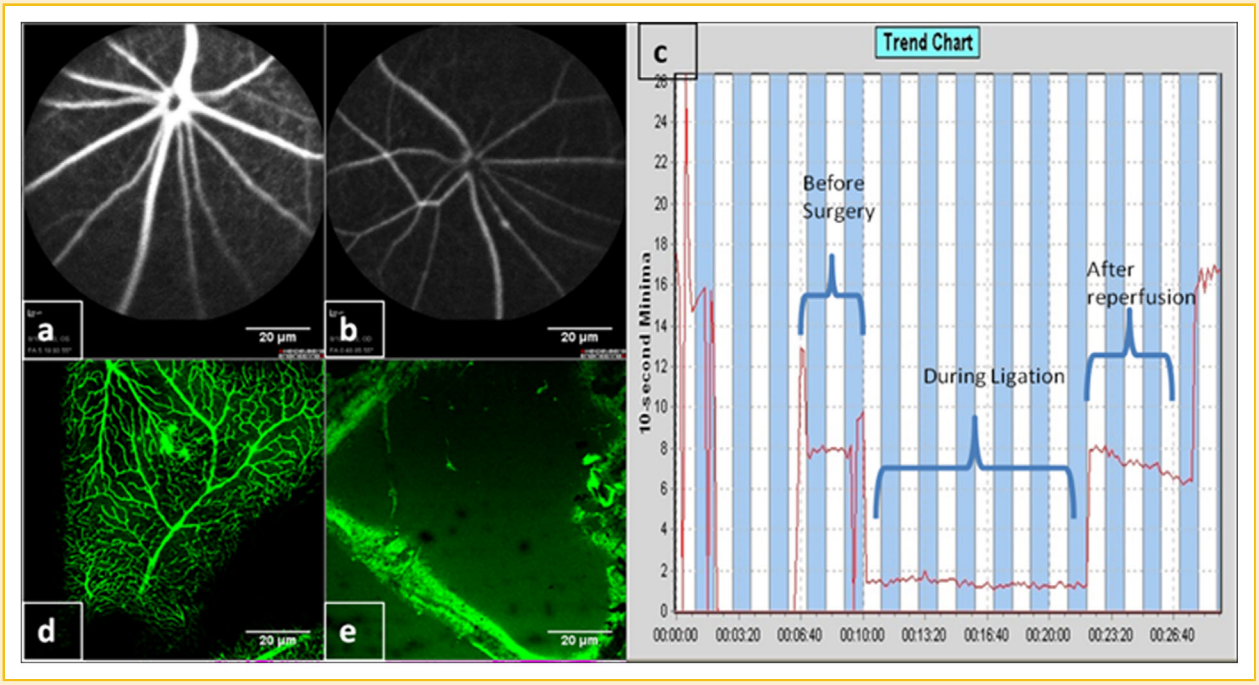


Fig. 3. Fundus florescein Angiography (FFA) of control eye (a) and test eye (b) depicting thinning of arteries in later case. Blood flow measurement by laser Doppler showed decreased blood flow during ligation which return back to normal after reperfusion (c). Confocal microscopy of retinal flatmounts after systemic injection of sodium fluorescein showing retinal microvascular in control (d) and test eye (e).

contralateral eye, as seen in fundus micrographs after fundus florescein imaging (Fig. 3a and b). Retinal microvasculature images of retinal whole mounts supported the above results. No blood supply by central retinal artery, its branches, or choroidal arteries could be seen in retinal flatmounts prepared from the test eye thus ensuring complete ischemia after PPA ligation (Fig. 3d and e).

LEAD ESTIMATION

The animals were treated with lead acetate water (200 ppm) daily for 20 days from PND 1–20 (pups receive lead from mother acquiring the lead acetate water) and another group received the lead treatment at 7th week of age for 20 days. Animals received normal water before and after the experimental time frame for lead treatment. The control group animals received normal water throughout life until sacrifice. All group of animals were followed till 10 week of age and then blood was collected. Blood lead estimation using atomic absorption spectroscopy after 10 week of age showed significant difference of lead concentration between the control group and 7th week lead treated group. However, animals that were treated at early age, that is, PND 1–20 showed comparable lead levels with the control group (Fig. 4). The blood lead levels in control mice was found $0.95 + 0.0131$ ppm (SE), the PND group have blood levels $1.283 + 0.01715$ ppm (SE) while in 7th week group the Pb level was highest among all, that is, $2.55 + 0.037$ ppm (SE). Half life of lead in blood is 35–40 days, therefore, it can be suggested that in postnatal treated group, the time of Pb exposure (PND1-20) and Pb estimation (10 week of age) is more than 2 months and thus blood lead levels may have return back to the normal levels during this time as control group animals. Study carried by Giddabasappa et al. [2011] showed that after gestational exposure of Pb the lead levels were increased immediately after exposure but 20 days after exposure the levels were found to be equivalent to control [Giddabasappa et al., 2011]. However, one of the drawbacks of present study is that if Pb estimation at PND 20 would have been done it would have strengthened the data. The lead treated animals were not reported with any other adverse behavioral or morphological deviations from control group as observed during the experimentation duration.

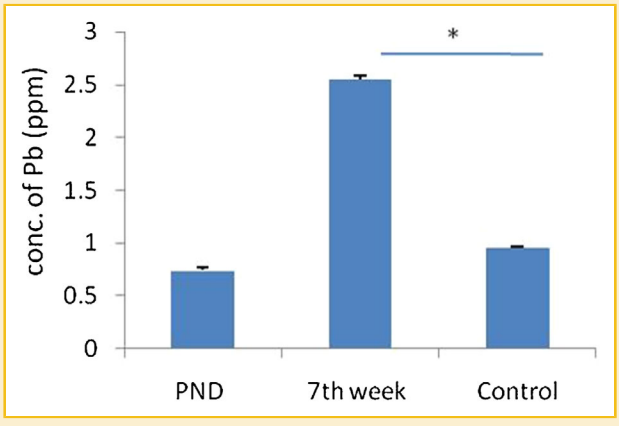


Fig. 4. Lead estimation by atomic absorption spectroscopy showing significant difference between 7th week lead exposed group and control group ($^{*}P < 0.05$). PND lead exposed group did not show any difference from control group.

EFFECT ON RETINAL THICKNESS

The animals were sacrificed; eyes enucleated and whole eye was used for cryosectioning. The images for the whole retina were taken for animals in each group ($n = 3$ per group). The images captured were used to measure total retinal thickness. The thickness of total retina (including all retinal layers viz. retinal pigment epithelium [RPE], outer nuclear layer [ONL], outer plexiform layer [OPL], inner nuclear layer [INL], inner plexiform layer [IPL], and retinal ganglion cell layer [GCL]) was measured using Image J software. The retinal thickness in the 7th week Pb + Surgery group ($220.4713 + 5.199193$ μm) and surgery only ($247.0629 + 7.720382$ μm) group decreased significantly as compared to normal control group ($271.582 + 5.34441$ μm) while retinal thickness of the PND Pb + Surgery group ($267.5516 + 2.364409$ μm) showed no significant difference (Fig. 5a–e). This trend may be attributed to the differential bioavailability of lead at 10th week than 7th week group.

TUNEL ASSAY

Terminal deoxynucleotidyl transferase dUTP nick end labeling (TUNEL) assay was used to determine the retinal cells undergoing apoptosis. The TUNEL positive cells were increased in animals with retinal ischemic injury. Retinal sections from surgery only group showed slight increase in TUNEL positive cells as compared to Pb exposed groups. Although, the number of apoptotic cells were fewer in PND group the difference was not significant compared to non-exposed group (Fig. 6). Pb exposure resulted in marginal decrease in apoptotic cells but it was non-significant which calls for additional cell survival makers which could not be used due to paucity of funds. Thus, as suggested by TUNEL assay it can be said that Pb exposure does not affect the degree of apoptosis after retinal ischemic injury.

GENE EXPRESSION STUDIES OF MARKER GENES (NEUROTROPHIN, INFLAMMATORY, AND HYPOXIA) SHOWED THAT LEAD EXPOSURE AMELIORATES (REDUCED THE DAMAGE CAUSED BY) THE EFFECTS OF ISCHEMIA–REPERFUSION INJURY

To study the effect of lead exposure on damage caused by retinal ischemia, 5 days after reperfusion animals were sacrificed and retina was isolated. RNA was isolated from retina and cDNA synthesis was carried out followed by real time PCR for the associated markers. Brain Derived Neurotrophic Factor (BDNF) belongs to family of neurotrophic factors that helps in survival and maintenance of neurons. Its neuroprotective role in ischemia-reperfusion injury is well documented. In animals exposed to lead at very early age (postnatal group), there was slight increase in endogenous expression of BDNF. The BDNF expression was increased 1.57-fold as compared to Surgery only group whereas

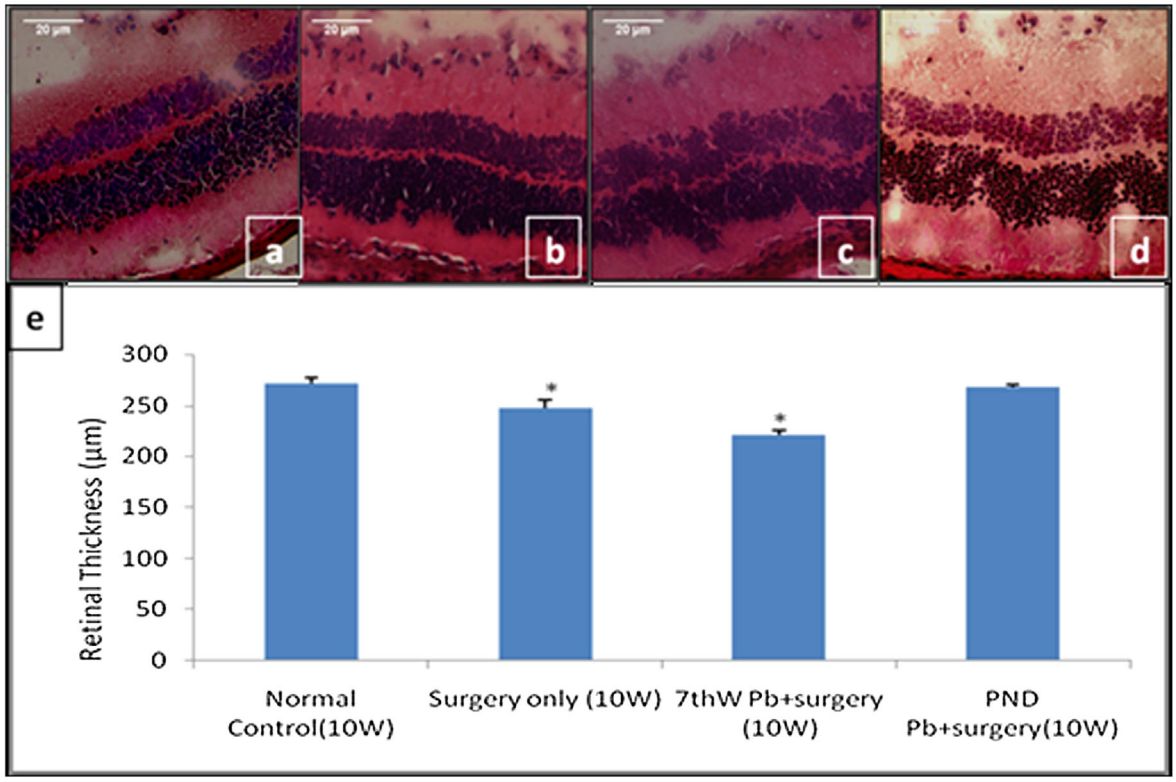


Fig. 5. Retinal thickness (RPE + ONL + IPL + INL + IPL + GCL) of different groups, (a–d) representative images of Control group, no lead + surgery group, 7th week Pb + Surgery group, and PND Pb + surgery group, respectively, (e) quantitative analysis showed significant difference between between control group and 7th week lead exposed group was seen ($^{*}P < 0.05$). There was increase in thickness of PND group however this increase was not significant compared to control group.

there was little increase in 7th week group (1.05-fold), however, the difference was not significant compared to non Pb exposed groups. Hypoxia inducible factor (HIF1α) is associated with adaptive response to ischemia or hypoxic condition. It is well known to have regulatory role in expression of other hypoxia related genes such as erythropoietin, vascular endothelial growth factor (VEGF), glucose transporters, etc. HIF expression has been found to increase after ischemic insult to overcome the effects of hypoxia. Increased HIF is known to in turn increase the expression of regulatory genes to compensate for vascular changes. Decreased expression of this gene in Pb exposed groups indicates that response to cope with ischemic injury has been reduced in these animals. Lead exposed + surgery animals showed decreased expression of HIF1α when compared to surgery only group. The expression of HIF1α was found to be 0.231 in PND group ($P < 0.05$) while 7th week group showed a fold change of 0.523 ($P < 0.05$). Significant difference in expression of HIF suggests less intrinsic response to induced hypoxia. Increased expression of Thy1 in Pb exposed groups may correspond to the increased survival of retinal ganglion cells. Glial Fibrillary acidic protein (GFAP) is marker for glial cell activity against neuronal damage. GFAP expression was found to be upregulated in the PND lead exposed group with 3.02-fold change, 7th week group also showed GFAP upregulation (2.73-fold change) but the difference is not significant (Fig. 7). This upregulation suggests activated microphages which are responsible for endogenous response against ischemia leading to inflammation. Thus, altered expression of molecular markers in lead exposed + surgery groups in relation to surgery only group suggests that lead exposure seems to have marginal adverse effect on second insult, that is, ischemic-reperfusion injury.

FUNCTIONAL EFFECT OF LEAD TREATMENT ON ISCHEMIA SUSCEPTIBILITY

ERG was used to determine functional changes in retina. The perimeters studied to assess functional outcome, that is, implicit time to a wave, Implicit time to a wave, amplitude a wave, and amplitude of b wave. Scotopic ERG, after dark adaptation, showed no significant changes in implicit time for a wave and b wave. (Fig. 8). Implicit time a wave was found to be reduced by 30% in surgery only group while the change in 7 week group was reported to be upto 21%, PND group showed same decrease as surgery only, that is, 30% decrease as compared to the control group. Implicit time b wave was found to be 4.56% decreased in PND group while the decrease in 7 week Pb exposed group and surgery only group was 27.18%, and 6.91%, respectively, as compared to control. As compared to control the amplitude of a wave and amplitude of b wave was reduced by 32.08%, and 46.19% in PND lead exposed

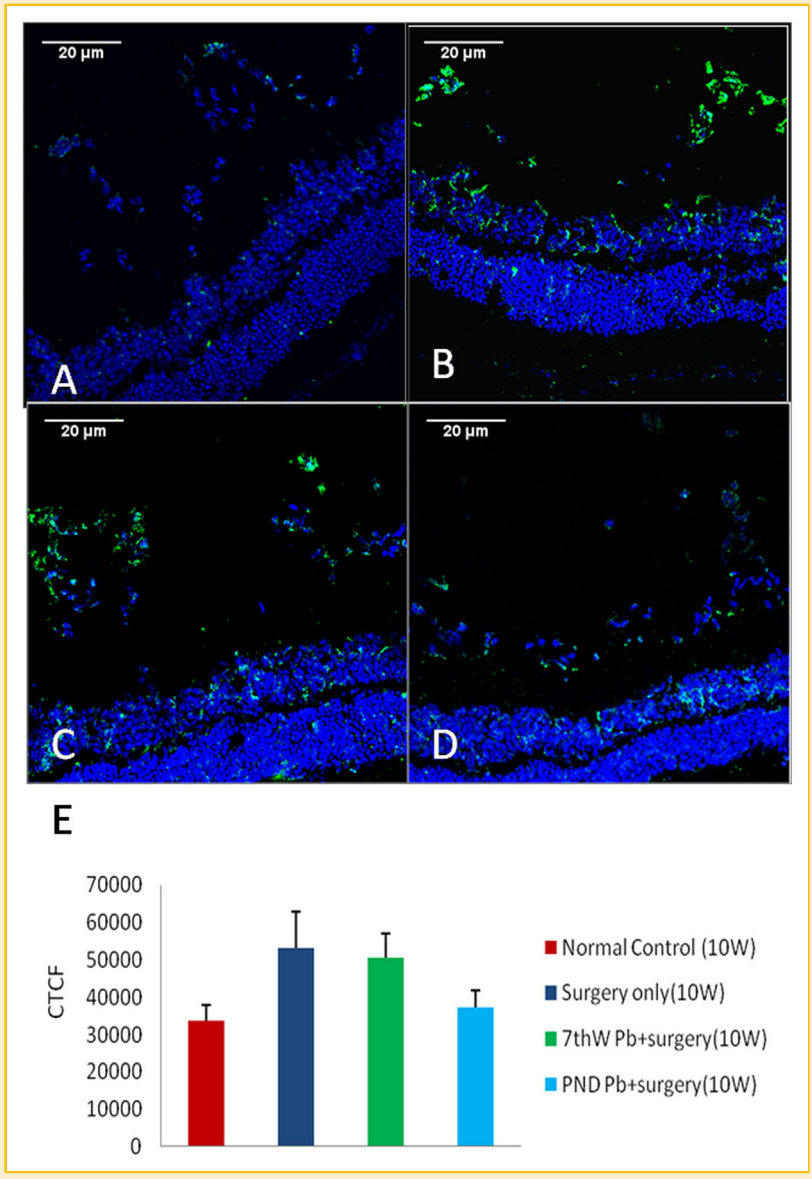


Fig. 6. Retinal sections showing TUNEL positive cells in green. (A) Control group; (B) no lead + surgery group; (C) 7th week Pb exposure + surgery group; (D) PND1–20 Pb exposure + surgery group; (E) quantitative analysis of TUNEL florescence by Image J.

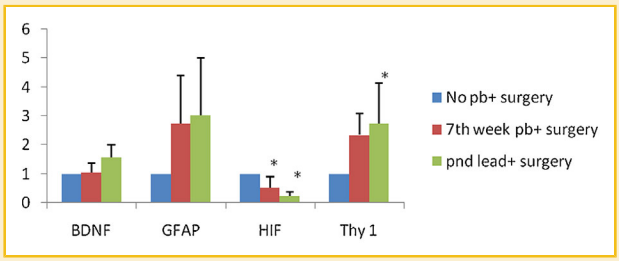


Fig. 7. Real time PCR of marker genes showing fold change in expression of BDNF, GFAP, HIF, and Thy1. $^{*}P < 0.05$

group while the decrease in non exposed group was 51.01% and 73.74%, respectively. The 7th week lead exposed group showed a decrease of 48.18% in a-wave amplitude and 22.21% reduction in b wave amplitude. The result suggests that lead exposed groups have lesser change in retinal function compared to non lead exposed group, however, the difference was not statistically significant.

IMMUNOFLORESCENCE

To confirm the results from real time analysis we carried out immunoflorescence assay for two marker genes, BDNF and GFAP (Fig. 9). The retinal sections were incubated with primary antibody (anti-BDNF, anti-GFAP) and then tagged with florochrome. The results supported the data obtained from real time PCR analysis. The

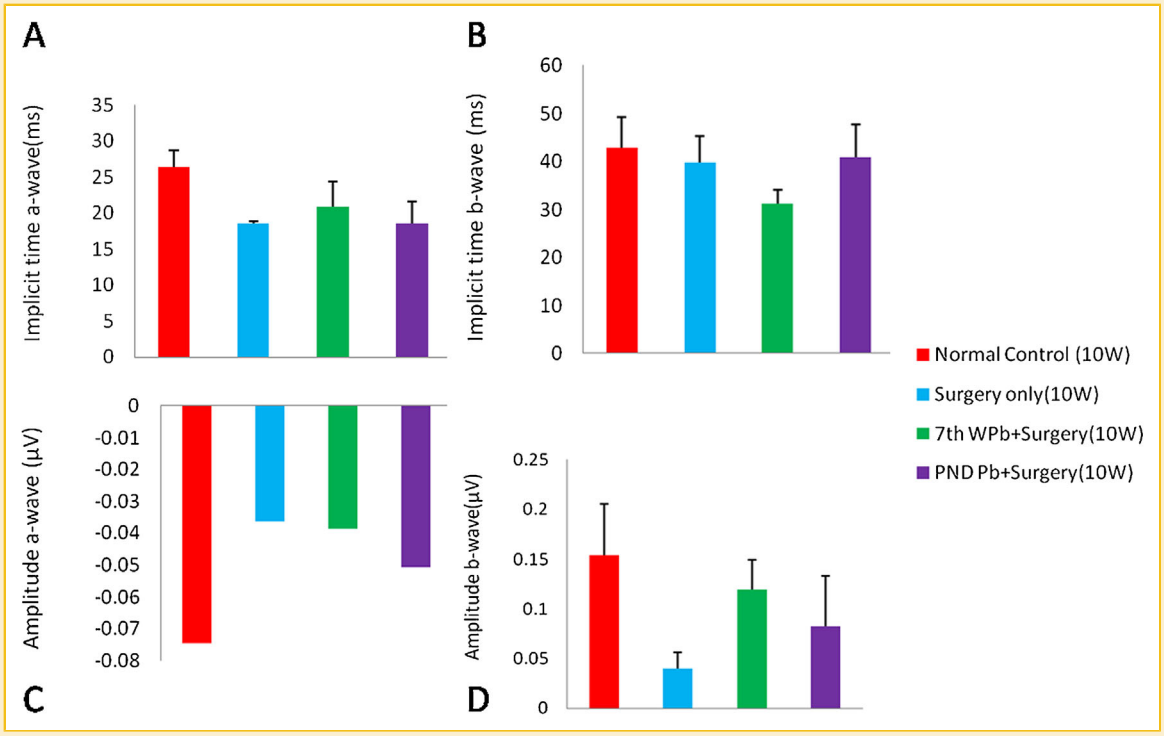


Fig. 8. Functional changes in different groups showing change in (A) implicit time to a wave; (B) implicit time to b wave; (C) amplitude a wave; (D) amplitude of B wave.

GFAP expression was found to be elevated in PND lead exposed group when compared to 7th week lead exposed group and surgery only group. However, quantitative analysis of florescence intensity showed no significant increase in GFAP expression in PND and 7th week group. Likewise, BDNF was expressed more in lead exposed group as compared to control. The levels of BDNF were increased in both PND lead exposed and 7th week lead exposed group (with $P < 0.05$). Although the gene expression using RT-PCR showed elevated BDNF levels in Pb exposed groups but the difference was non-significant unlike IHC data showing significantly altered BDNF levels.

DISCUSSION

Based on past literature related to lead toxicity and epigenetic models such as LEARn [Lahiri and Maloney, 2010] we postulated that early life Pb exposure will affect the later life retinal degeneration by enhancing the damage caused by ischemia. During the entire course of lifetime, the individuals adapt to the environment through different epigenetic changes [Bale et al., 2010]. Early life events are particularly important as they alter the genetics in a way that make individuals more adjusting to the anticipated future environment [Rickard and Lummaa, 2007; van den Heuvel et al., 2013]. There have been lot of work in this field in past one decade yet a concrete theory has not come into existence. There have been studies that early life adverse environment makes individual more susceptible to diseases [Danese et al., 2009; Murgatroyd et al., 2009].

We exposed mice to lead in drinking water at either PND 1–20 or at 7th week age and then subjected them to retinal ischemia at 10 week. ERG is generally employed to access the functional aspect of retina. Decreased a and b wave is a measure of retinal injury [Brandli and Jonathan, 2015]. When lead exposed mice were subjected to ischemia/reperfusion injury by ligation of ECA and PPA arteries it showed reduced damage to retina evidenced by ERG. The a and b wave amplitude in lead exposed mice, as compared to surgery only showed no significant difference from non-exposed groups in term of functional aspect as assessed by ERG. Thus, functional damage to retina by ischemia/reperfusion injury was comparable in Pb exposed versus non-exposed animals.

The main results deduced from study are: (1) Pb exposure in early life does not aggravates apoptosis induced due to I/R injury; (2) there is more survival of RGC cells in Pb exposed mice compared to non exposed; (3) inflammatory response in Pb exposed mice elevated, though not significant, after retinal injury; (4) response to hypoxia was reduced in Pb exposed mice as shown by HIF reduced levels and thus downstream signaling is hampered; and (5) elevated BDNF levels in Pb exposed suggests endogenous stimulation of protective factor to cope up with the damage caused by ischemic/reperfusion injury.

Lead has been shown to exert toxic effects [Gidlow, 2004; Patrick, 2006; Flora et al., 2012] and even low dose of lead in early life has been reported to result in diseased condition in older age [Needleman et al., 1990; Basha et al., 2005; Leasure et al., 2008]. Lead is a widely accepted toxin and its association with various neurological disorders has been well documented [Lyngbye et al., 1988; Grandjean and Landrigan, 2014]. Thus, according to our hypothesis that lead exposure may increase the subsequent retinal damage

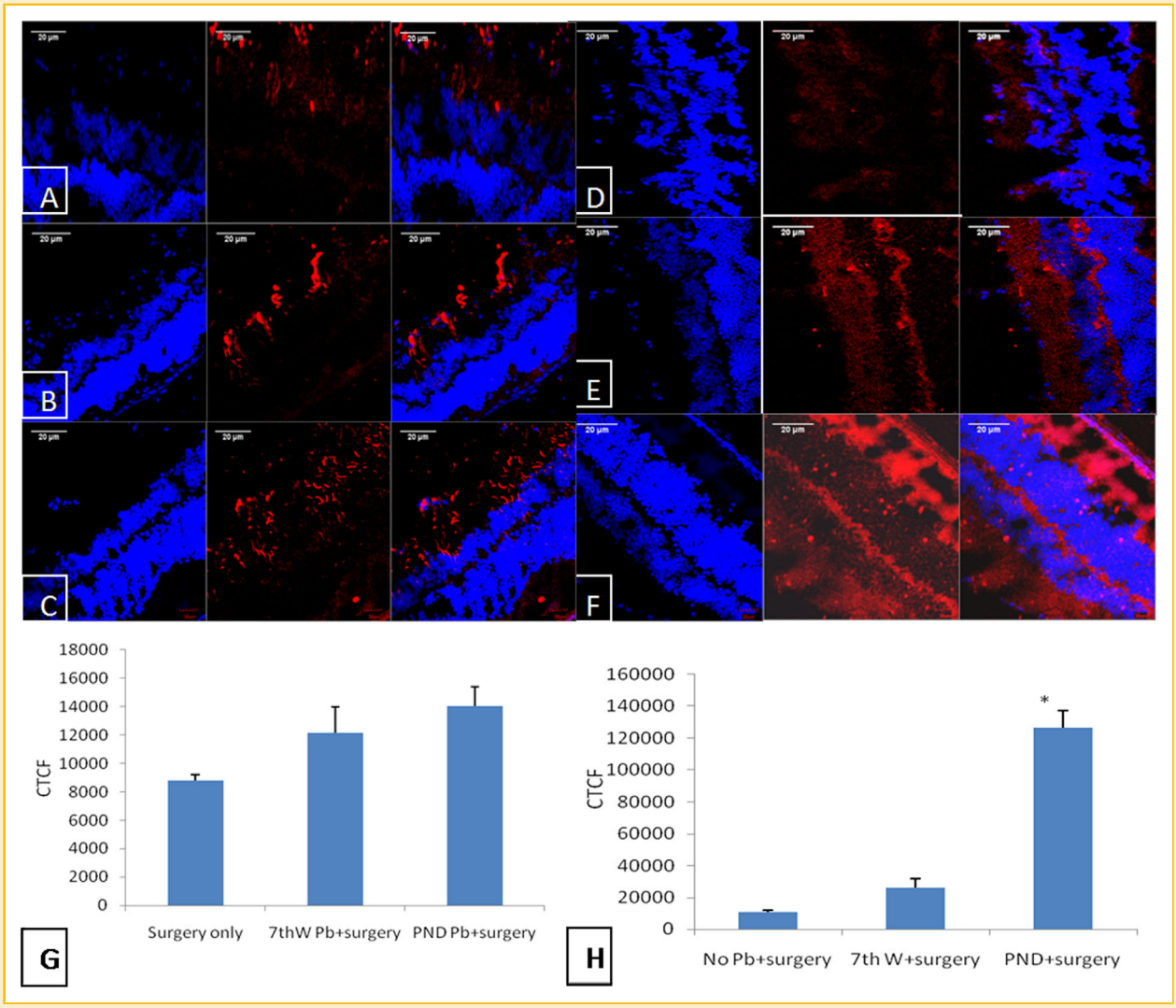


Fig. 9. Immunoflorescence GFAP showing DAPI stained retinal section, GFAP staining and merged images, Panel A (control), Panel B (7th week Pb exposed), Panel C (PND Pb exposed), and BDNF immunostaining and merged panels Panel D (control), Panel E (7th week Pb exposed), Panel F (PND Pb exposed), G shows quantitative analysis of GFAP expression while quantitative analysis of BDNF expression is shown in H $^{*}P < 0.05$, variable.

induced by ischemia, the results showed exacerbated damage in Pb exposed group but any significant adverse effects were not reflected. The 7th week group, however, showed significant decreased retinal thickness and increased levels of neurotrophins (supplementary file). It has been postulated in earlier studies that, depending on early life experience, the body prepares itself for the upcoming events. While many argue that the enriched environment is responsible for positive epigenetic modifications and adverse environment lead to negative modifications others believe, and vice-versa [Raine et al., 2003; Kagitcibasi et al., 2009; Roth et al., 2009; Conti et al., 2012]. Also, Daskalakis postulated that if the future events match the early life exposure then the adaptations proves to be useful in adapting to adverse conditions, however, if inverse occurs and there is mismatch of exposures, the adaptations are deleterious [Daskalakis et al., 2012]. The environmental cues from early life prepare an organism for anticipated adverse events in near future as a result of adaptive response [Shanks et al., 2000; Khan et al., 2004]. Gluckman and Hanson [2004] gave the term predictive adaptive response (PAR) for this phenomenon. Oomen et al. [2010] in their study have reported that mild stress in early life may not be overall unfavorable. However, for such adaptive responses it is believed that there is a critical window period, any positive or negative event reprograms the gene expression of response genes and thus imprints a response for that event.

Even though most of findings including clinical reports indicate that lead exposure may lead to toxicity like optic neuritis, optic atrophy, peripheral and central scotomas, decreased cell volume density and retinal apoptosis, the data interpretation remains persuasive in the context of nature, timing, and dose of lead. This is supported by authors who have shown in their study that mild early life stress results in hippocampal reprogramming which improves later life synaptic

plasticity and increases emotional learning in later life stress conditions [Oomen et al., 2010]. The elevated BDNF levels in the "exposed" animals as compared to non-exposed group, as determined by real time PCR and IHC can thus be suggestive of adaptive response due to Pb exposure. In our lab we have earlier found that stem cells administration in injured retina also lead to BDNF upregulation [Jindal et al., 2016]. BDNF is a well known neurotrophicfactor that is a proven neuroprotective against ischemic/reperfusion injury [Han and Holtzman, 2000]. Authors in this study have shown that neuroprotective effects of BDNF are exhibited by activation of ERK pathway. Further, another study reported the anti-mutagenic and anti-cytotoxic effects of lead acetate conferred by the activation of ERK ½ pathway [Lin et al., 2003]. BDNF overexpression may be a compensatory response to retinal injury conferred by activation of ERK pathway. However, to reach such a conclusion additional experiments by using inhibitors (like U 0126) to block ERK ½ pathway or associated intervention studies need to be carried out. The positive and negative roles of glial activation have been discussed in retinal ischemia/reperfusion injury [Minhas et al., 2015]. The increased glial activity in lead exposed groups can thus be a mark of internal defence mechanism against injury. Elevated GFAP levels particularly in PND Pb group may thus either be explained as internal defence or inflammatory response. Lead has always been studied as a metal toxin that is widely understood as harboring adverse effects on the biological system. However, there are some studies that suggested the non-toxic effects of Pb as well. These studies categorize the toxins into a stimulants (at lower dose) based on the phenomenon of hormesis [Mushak, 2007]. According to hormesis toxins have a U shape dose response, that is, at a lower dose the potential toxins may act opposite to their nature and instead of toxicity they stimulate or exert protective effects [Davis and Svendsgaard, 1990]. The non toxic effects of Pb in this study can be explained by this phenomenon of hormesis, however, the limitation is that a higher dose is lacking as we started with the hypothesis that Pb will exert toxic effects. Contrasting results were reported in another study where exposure of Pb resulted in increased bone mass density as expected from general norms but affect overall bone health [Beier et al., 2016]. Similarly, a study by Barbeito et al. [2010] showed that lead exposure leads to upregulation of VEGF and increase the survival time in amyotrophic lateral sclerosis. Thus, results described here provide an opportunity to argue that the effects of lead exposure can be varied depending on dose and tissue concerned. As shown in present study it can be speculated that early life exposure affects late life induction of retinal ischemia although the data presented involved only a small number of animals with $n = 3$ for each parameter analyzed. Thus, more studies related to long term effects of lead exposure are required to understand the effect of low dose early life lead exposure. A longer time point studies may be warranted as according to LEARn model there is a latency period in the appearance of disease symptoms. The observations from present study help to understand the complexities of Pb exposure and open a new area of research to be explored.

ACKNOWLEDGMENTS

The funding was provided by Council for Scientific and Industrial Research, grant No. 09/135(0666)/2012, and Department of Science and Technology grant No. SR/SO/HS-01/2010.

REFERENCES

Allen R, Sayeed I, Cale H, Morrison K, Choi P, Boatright J, Pardue M, Stein D. 2013. Comparison of retinal and cerebral inflammatory responses after middle cerebral artery occlusion. Invest Ophthalmol Vis Sci 54:104.

Bale TL, Tallie ZB, Alan SB, Jill MG, Thomas RI, Margaret MM, Charles BN. 2010. Early life programming and neurodevelopmental disorders. Biol Psychiatry 68:314–319.

Barbeito AG, Martinez-Palma L, Vargas MR, Pehar M, Mañay N, Beckman JS, Barbeito L, Cassina P. 2010. Lead exposure stimulates VEGF expression in the spinal cord and extends survival in a mouse model of ALS. Neurobiol Dis 37:574–580.

Barker DJ, Eriksson JG, Forsén T, Osmond C. 2002. Fetal origins of adult disease: Strength of effects and biological basis. Int J Epidemiol 31:235–239.

Basha MR, Wei W, Saleh AB, Nathalie B, Hasan KS, Yuan-Wen G, Debomoy KL, Nasser HZ. 2005. The fetal basis of amyloidogenesis: Exposure to lead and latent overexpression of amyloid precursor protein and β-amyloid in the aging brain. J Neurosci 25:823–829.

Beier EE, Holz JD, Sheu TJ, Puzas JE. 2016. Elevated lifetime lead exposure impedes osteoclast activity and produces an increase in bone mass in adolescent mice. Toxicol Sci 149:277–288.

Bihaqi SW, Bahmani A, Adem A, Zawia NH. 2014a. Infantile postnatal exposure to lead (Pb) enhances tau expression in the cerebral cortex of aged mice: Relevance to AD. Neurotoxicology 44:114–120.

Bihaqi SW, Bahmani A, Subaiea GM, Zawia NH. 2014b. Infantile exposure to lead and late-age cognitive decline: Relevance to AD. Alzheimers Dement 10:187–195.

Bihaqi SW, Huang H, Wu J, Zawia NH. 2011. Infant exposure to lead (Pb) and epigenetic modifications in the aging primate brain: Implications for Alzheimer's disease. J Alzheimers Dis 27:819–833.

Bihaqi SW, Zawia NH. 2013. Enhanced taupathy and AD-like pathology in aged primate brains decades after infantile exposure to lead (Pb). Neurotoxicology 39:95–101.

Brandli A, Jonathan S. 2015. Using the electroretinogram to assess function in the rodent retina and the protective effects of remote limb ischemic preconditioning. J Vis Exp 100:e52658–e52658.

Calderon-Garcidueñas L, Serrano-Sierra A, Torres-Jardón R, Zhu H, Yuan Y, Smith D, Delgado-Chávez R, Cross JV, Medina-Cortina H, Kavanaugh M, Guilarte TR. 2013. The impact of environmental metals in young urbanites' brains. Exp Toxicol Pathol 65:503–511.

Conti G, Christopher H, James JH, Matthew FXN, Angela R, Stephen JS. 2012. Primate evidence on the late health effects of early-life adversity. Proc Natl Acad Sci USA 109:8866–8871.

Danese A, Terrie EM, HonaLee H, Barry JM, Guilherme P, Carmine MP, Richie P, Avshalom C. 2009. Adverse childhood experiences and adult risk factors for age-related disease: Depression, inflammation, and clustering of metabolic risk markers. Arch Pediatr Adolesc Med 163: 1135–1143.

Daskalakis NP, Oitzl MS, Schächinger H, Champagne DL, de Kloet ER. 2012. Testing the cumulative stress and mismatch hypotheses of psychopathology in a rat model of early-life adversity. Physiol Behav 5:707–721.

Davis JM, Svendsgaard DJ. 1990. U-Shaped dose-response curves: Their occurrence and implications for risk assessment. J Toxicol Environ Health, Part A Current Issues 30:71–83.

Engel SM, Wetmur J, Chen J, Zhu C, Barr DB, Canfield RL, Wolff MS. 2011. Prenatal exposure to organophosphates, paraoxonase 1, and cognitive development in childhood. Environ Health Perspect 119:1182.

Faulk C, Barks A, Liu K, Goodrich JM, Dolinoy DC. 2013. Early-life lead exposure results in dose-and sex-specific effects on weight and epigenetic gene regulation in weanling mice. Epigenomics 5:487–500.

Fernandez-Teruel A, Escorihuela BC, Gonzalez B, Tobena A. 1997. Neonatal handling and environmental enrichment effects on emotionality, novelty/reward seeking, and age-related cognitive and hippocampal impairments: Focus on the Roman rat lines. Behav Genet 27:513–526.

Flora G, Deepesh G, Archana T. 2012. Toxicity of lead: A review with recent updates. Interdiscip Toxicol 5:47–58.

Fox DA, Rubinstein SD, Hsu P. 1991. Developmental lead exposure inhibits adult rat retinal, but not kidney, Na+, K + −ATPase. Toxicol Appl Pharmacol 109(3):482–493.

Giddabasappa A, Hamilton WR, Chaney S, Xiao W, Johnson JE, Mukherjee S, Fox DA. 2011. Low-level gestational lead exposure increases retinal progenitor cell proliferation and rod photoreceptor and bipolar cell neurogenesis in mice. Environ Health Perspect 119:71–77.

Gidlow DA. 2004. Lead toxicity. Occup Med 54:76–81.

Gluckman PD, Hanson MA. 2004. Development origins of disease paradigm: A mechanistic and evolutionary perspective. Pediatr Res 56:311–317.

Grandjean P, Landrigan PJ. 2014. Neurobehavioural effects of developmental toxicity. Lancet Neurol 2014(13):330–338.

Han BH, Holtzman DM. 2000. BDNF protects the neonatal brain from hypoxic-ischemic injuryin vivo via the ERK pathway. J Neurosci 15: 5775–5781.

Hanson JL, Nacewicz BM, Sutterer MJ, Cayo AA, Schaefer SM, Rudolph KD, Shirtcliff EA, Pollak SD, Davidson RJ. 2015. Behavioral problems after early life stress: Contributions of the hippocampus and amygdala. Biol Psychiatry 77:314–323.

Howell BR, McCormack KM, Grand AP, Sawyer NT, Zhang X, Maestripieri D, Hu X, Sanchez MM. 2013. Brain white matter microstructure alterations in adolescent rhesus monkeys exposed to early life stress: Associations with high cortisol during infancy. Biol Mood Anxiety Disord 3:21.

Ishizuka F, Shimazawa M, Umigai N, Ogishima H, Nakamura S, Tsuruma K, Hara H. 2013. Crocetin, a carotenoid derivative, inhibits retinal ischemic damage in mice. Eur. J. Pharmacol. 703:1–10.

Jaishankar M, Tseten T, Anbalagan N, Mathew BB, Beeregowda KN. 2014. Toxicity, mechanism and health effects of some heavy metals. Interdiscip Toxicol 7:60–72.

Jindal N, Banik A, Prabhakar S, Vaiphie K, Anand A. 2016. Alteration of neurotrophic factors after transplantation of bone marrow derived Lin-Ve stem cell in NMDA induced mouse model of retinal degeneration. J Cell Biochem 9999:1–13.

Kagitcibasi C, Diane S, Sevda B, Nazli B, Zeynep C. 2009. Continuing effects of early enrichment in adult life: The Turkish Early Enrichment Project 22 years later. J Appl Dev Psychol 30:764–779.

Khan I, Vasia D, Mark H, Lucilla P, Paul T. 2004. Predictive adaptive responses to maternal high-fat diet prevent endothelial dysfunction but not hypertension in adult rat offspring. Circulation 110:1097–1102.

Lahiri DK, Maloney B. 2010. The "LEARn" (Latent Early-life Associated Regulation) model integrates environmental risk factors and the developmental basis of Alzheimer's disease, and proposes remedial steps. Exp Gerontol 45:291–296.

Lan A, Xu W, Zhang H, Hua X, Zheng D, Guo R, Shen N, Hu F, Feng J, Liu D. 2013. Inhibition of ROS-activated p38MAPK pathway is involved in the protective effect of H2S against chemical hypoxia-induced inflammation in PC12 cells. Neurochem Res 38:1454–1466.

Leasure JL, Giddabasappa A, Chaney S, Jr Johnson, Lau K, Fox YS. 2008. Low-level human equivalent gestational lead exposure produces sex-specific motor and coordination abnormalities and late-onset obesity in year-old mice. Environ Health Perspect 116(3):355.

Lelong DC, Bieche I, Perez E, Bigot K, Leemput J, Laurendeau I, Vidaud M, Jais JP, Menasche M, Abitbol M. 2007. Novel mouse model of monocular amaurosis fugax. Stroke 38(12):3237–3244.

Lin YW, Chuang SM, Yang JL. 2003. Persistent activation of ERK1/2 by lead acetate increases nucleotide excision repair synthesis and confers anti-cytotoxicity and anti-mutagenicity. Carcinogenesis 24:53–61.

Lyngbye T, Ole NH, Philippe G. 1988. Neurological deficits in children: Medical risk factors and lead exposure. Neurotoxicol Teratol 10:531–537.

Mason LH, Harp JP, Han DY. 2014. Pb neurotoxicity: Neuropsychological effects of lead toxicity. Bio Med Res Int 840547. https://doi.org/10.1155/2014/840547

Minhas G, Morishita R, Shimamura M, Bansal R, Anand A. 2015. Modeling transient retinal ischemia in mouse by ligation of pterygopalatine artery. Ann Neurosci 22:222.

Modgil S, Lahiri DK, Sharma VL, Anand A. 2014. Role of early life exposure and environment on neurodegeneration: Implications on brain disorders. Transl Neurodegener 3:9.

Murgatroyd C, Alexandre VP, Yonghe W, Vincenzo M, Yvonne B, Dieter F, Florian H, Carsten TW, Osborne FA, Dietmar S. 2009. Dy namic DNA methylation programs persistent adverse effects of early-life stress. Nat Neurosci 12:1559–1566.

Mushak P. 2007. Hormesis and its place in nonmonotonic dose-response relationships: Some scientific reality checks. Environ Health Perspect 2007 115:500–506.

Needleman HL, Alan S, David B, Alan L, Elizabeth NA. 1990. The long-term effects of exposure to low doses of lead in childhood: An 11-year follow-up report. N Engl J Med 322:83–88.

Oomen CA, Soeters H, Audureau N, Vermunt L, van Hasselt FN, Manders EM, Joëls M, Lucassen PJ, Krugers H. 2010. Severe early life stress hampers spatial learning and neurogenesis, but improves hippocampal synaptic plasticity and emotional learning under high-stress conditions in adulthood. J Neurosci 30:6635–6645.

Patrick L. 2006. Lead toxicity, a review of the literature. Part I: Exposure, evaluation, and treatment. Altern Med Rev 11:2–23.

Pechtel P, Pizzagalli DA. 2011. Effects of early life stress on cognitive and affective function: An integrated review of human literature. Psychopharmacology (Berl) 214:55–70.

Raine A, Kjetil M, Jianghong L, Peter V, Sarnoff AM. 2003. Effects of environmental enrichment at ages 3–5 years on schizotypal personality and antisocial behavior at ages 17 and 23 years. Am J Psychiatry 160: 1627–1635.

Rickard IJ, Lummaa V. 2007. The predictive adaptive response and metabolic syndrome: Challenges for the hypothesis. Trends Endocrinol Metab 18:94–99.

Roth TL, Farah DL, Adam JF, David S. 2009. Lasting epigenetic influence of early-life adversity on the BDNF gene. Biol Psychiatry 65:760–769.

Shanks N, Richard JW, Paula AP, Michael SH, David SJ, Colin DI, Stafford LL. 2000. Early-life exposure to endotoxin alters hypothalamic-pituitary-adrenal function and predisposition to inflammation. Proc Natl Acad Sci USA 97:5645–5650.

Shonkoff JP, Andrew SG, Benjamin SS, Mary ID, Marian FE, McGuinn Laura, David LW. 2012. The lifelong effects of early childhood adversity and toxic stress. Pediatrics 129:e232–e246.

Tomi M, Zhao Y, Thamotharan S, Shin BC, Devaskar SU. 2013. Early life nutrient restriction impairs blood-brain metabolic profile and neurobehavior predisposing to Alzheimer's disease with aging. Brain Res 1495: 61–75.

van den Heuvel J, Saastamoinen M, Brakefield PM, Kirkwood TB, Zwaan BJ, Shanley DP. 2013. The predictive adaptive response: Modeling the

life-history evolution of the butterfly Bicyclus anynana in seasonal environments. Am Nat 181:E28–E42.

Williams BM, Yuan L, Christopher W, Kacy R, Russell G, Stan AK, John GM. 2001. Environmental enrichment: Effects on spatial memory and hippocampal CREB immunoreactivity. Physiol Behav 73:649–658.

Young D, Patricia AL, Paola L, Michael D, Matthew JD. 1999. Environmental enrichment inhibits spontaneous apoptosis, prevents seizures and is neuroprotective. Nat Med 5:448–453.

Zheng W, Michael A, Jean-Francois G. 2003. Brain barrier systems: A new frontier in metal neurotoxicological research. Toxicol Appl Pharmacol 192:1–11.

SUPPORTING INFORMATION

Additional supporting information may be found in the online version of this article at the publisher's web-site.

Modeling transient retinal ischemia in mouse by ligation of pterygopalatine artery

Gillipsie Minhas[1], Ryuichi Morishita[3], Munehisa Shimamura[3], Reema Bansal[2], Akshay Anand[1*]

[1]Neuroscience Research Lab, Department of Neurology, Postgraduate Institute of Medical Education and Research, Chandigarh, INDIA; [2]Department of Ophthalmology, Postgraduate Institute of Medical Education and Research, India, [3]Department of Clinical Gene Therapy, Graduate School of Medicine, Osaka University, Osaka, Japan

KEY WORDS

Ischemia-reperfusion
Mouse model
Pterygopalatine artery
External carotid artery

Corresponding Author:

Akshay Anand
Tel : +91-9914209090
E-mail : akshay1anand@rediffmail.com

ABSTRACT

Background: Retinal ischemia is a major cause of visual impairment and blindness worldwide. The available therapeutic strategies have limited potential.
Purpose: In order to understand the pathophysiology and validating therapies for retinal ischemia, establishment of reproducible animal models is necessary.
Methods: In the model discussed in this article, the pterygopalatine artery (PPA) is ligated along with the external carotid artery for 3.5 hours and thereafter allowed to reperfuse. Because PPA supplies the blood to the ophthalmic artery, the ligation of this artery causes retinal ischemia.
Results: This article describes the validation of retinal ischemia-reperfusion model in mouse through PPA ligation and its validation through fluorescein fundus angiography (FFA) and immunofluorescence staining for glial fibrillary acidic protein (GFAP), a glial injury marker.
Conclusions: In conclusion this article describes the creation of mouse model of retinal ischemia-reperfusion injury which can be reproduced in a shorter time duration resulting in reduced mortality.
doi : 10.5214/ans.0972.7531.220406



Introduction

Retinal ischemia is a major cause of blindness world-wide and is associated with various disorders such as diabetic retinopathy, glaucoma, stroke, optic neuropathy and other retinopathies.[1] It is caused by obstruction in blood supply to retina decreasing the oxygen and glucose supply. If the blood supply is not restored, the damage becomes permanent leading to cell death and consequent vision loss. The damage caused to the retina can be due to various pathways which result in energy failure, excitotoxicity, ion channels imbalance, free-radical generation.[2] Reperfusion i.e. the restoration of blood flow to the retina leads to more damage to the retina than the ischemia itself. The re-establishment of blood supply to the ischemic retina increases the infiltration of macrophages and also leads to the generation of free-radicals causing more damage.[3]

Small animals, such as rats and mice are attractive models because they have vascular and phylogenetic similarities to humans. Besides, the availability, reproducibility and the relevance to humans are other factors that are important for use of mice for pre-clinical investigations.

Many different approaches have been used in establishment of animal models of retinal ischemia. One approach is through the elevation of intraocular pressure (IOP).[4] In this method the IOP is increased above the systolic pressure. Selles-Navarro et al. quantified the retinal ganglion cells (RGC) survival at different time points in the high IOP model of retinal ischemia.[5] Photocoagulation of blood vessels is another means to cause retinal ischemia.[6] Another model for transient retinal ischemia involves temporary ligation of ophthalmic vessels. Lafuente et al. examined the RGC loss in this model of retinal ischemia by ligating the vessels for varying intervals of time and concluded that the degree of RGC loss depends on the severity of injury caused.[7,8] In the same model, another study showed a significant decrease in the ERG wave amplitude along with the histological changes represented as decrease in inner retinal layer thickness.[9] Another approach includes middle cerebral artery occlusion (MCAO)[10] and chronic bilateral common carotid artery occlusion (BCCAO).[11] Some of these vascular models are based on the obstruction of blood supply to the ophthalmic artery which also receives the blood supply from the pterygopalatine artery (PPA) and the external carotid artery (ECA) in mice. The ligation of PPA along with the external carotid artery thus reduces the blood supply to the retina.[12–14] This information has been successfully exploited to establish mouse model of retinal ischemia.

Thus, this study describes the methodology for creation of mouse model of transient retinal ischemia and its validation through fluorescein fundus angiography and immunofluorescence analysis for glial fibrillary acidic protein (GFAP).

Methods

The experiments were performed on 6 to 8 weeks old C57BL/6J male mice. The mice were anaesthetized using xylazine (50mg/ml) and ketamine (50mg/ml). The right common carotid artery and its branches were exposed after a midline incision (Figure 1). The external carotid artery (ECA) and the pterygopalatine artery (PPA), a branch of internal carotid artery (ICA) were ligated using suture (size 7–0; Ethicon, New Jersey, USA). After 3.5 hours of ligation, the blood supply was restored to allow reperfusion (Supplementary video S1). The changes in the cerebral blood flow were measured using Laser-doppler blood flow-meter (Moor Instruments, UK) by placing the probe in the cortical region on the skull on the ipsilateral side of the brain. The ligation was validated using fluorescein fundus angiography, where sodium fluorescein was injected intravenously after 45 minutes of ligation of PPA and fundus images of right and left eye were

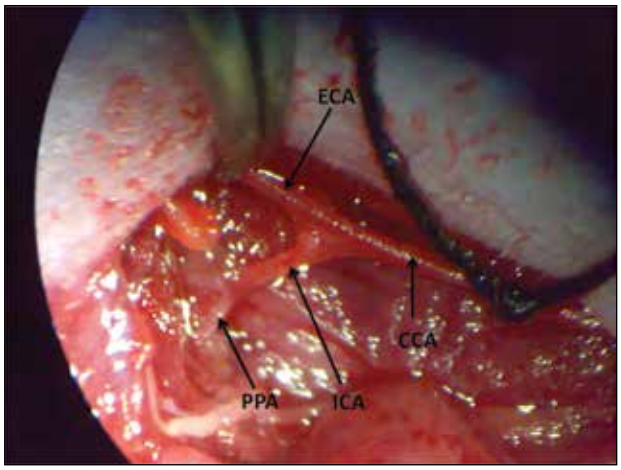


Fig. 1: Screen-shot for the mouse arteries. The figure shows the right common carotid artery and its branches, where CCA- common carotid artery; ECA – external carotid artery; ICA – internal carotid artery; PPA – pterygopalatine artery.

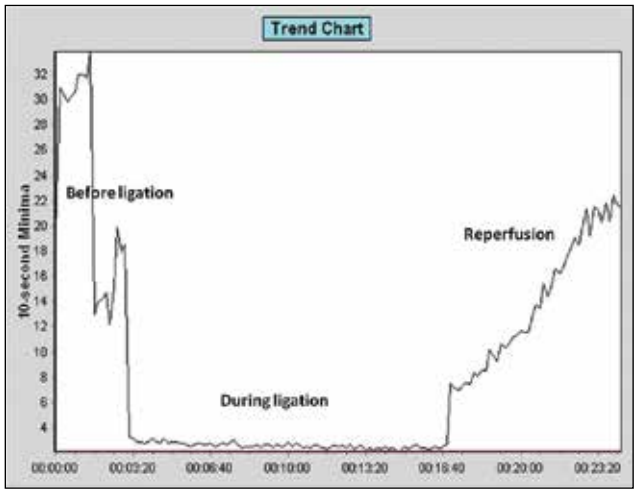


Fig. 2: Blood flow measurement using Laser Doppler. The trend chart from laser doppler blood-flow meter demonstrates the changes in the cerebral blood flow before ligation, during the ECA and PPA ligation and after the ligation is removed for reperfusion.

captured using Spectralis HRA + OCT (Heidelberg Engineering, Heidelberg, Germany).

After 5 days of reperfusion, the mice were sacrificed and the eyes were enucleated. The cryosections were cut and placed on slides. The control and injured sections were blocked in the serum of animal species in which secondary antibody was raised and incubated with primary antibody for glial fibrillary acidic protein (GFAP) overnight at 4^{o}C. After washing with PBS, the sections were incubated with secondary antibody for 1 hour and counterstained with the nuclear stain, DAPI (1:1000, Life Technologies, USA). The sections were mounted with FluorSave reagent (Calbiochem, USA). The slides were observed under an upright fluorescent microscope (BX51, Olympus Corporation, Japan). The primary antibody used for immunofluorescence was GFAP goat polyclonal IgG antibody (1:100, Santa Cruz Biotechnology Inc., USA) and the secondary antibody was Cy3 conjugated donkey anti-goat antibody (1:200, Jackson ImmunoResearch Laboratories Inc., USA). The images were adjusted for contrast using Adobe Photoshop software.

All procedures were carried out following the GLP norms and according to the Standard Operating Procedures (SOP) established in the research facility. The experiments were approved by the Institutional Animal Ethical Committee (53/IAEC/273).

Results

In this study, the changes in blood flow to the brain were examined using laser doppler (n = 3). The laser doppler trend showed a decrease in blood flow during the ligation and was restored after the reperfusion of blood supply (Figure 2). The injury was further validated through fluorescein fundus angiography (FFA), where the fundus of the mouse after ligation was evaluated for fluorescein circulation (n = 4). The fundus photographs after the ligation of the artery showed thinning of the vessels as compared to the contralateral eye (Figure 3).

The mice were sacrificed after 5 days of reperfusion and the validation of retinal ischemia model was done through histological and immunohistochemical analysis of retinal cryo-sections for injury markers such as glial fibrillary acidic protein (GFAP; n = 3).

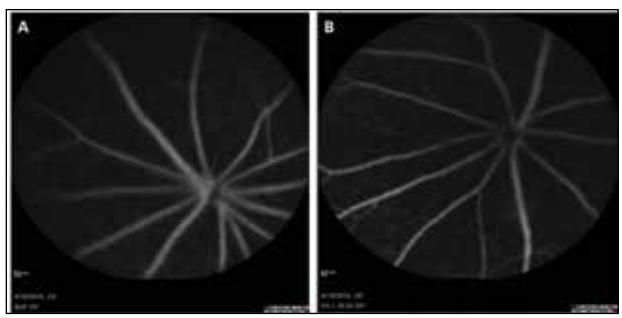


Fig. 3: Fluorescein fundus angiography (FFA) of mouse eye. The figure shows the fundus photographs of mouse eye after PPA ligation. **A.** Left eye is without PPA ligation; B. Right eye is after PPA ligation – which shows thinning of the vessels.

In this model of retinal ischemia, 3.5 hrs of ligation and 5 days of reperfusion was shown to have an increased expression of GFAP (Figure 4).

Discussion

Retinal ischemia can be validated through histological and immunohistochemical analysis of retinal cryosections, quantitation of mRNA expression of injury markers in retina homogenate, blood flow measurements using laser doppler blood flow meter, electroretinography for electrophysiological changes and fluorescein fundus angiography.

The glial fibriallry acidic protein (GFAP) being a glial injury marker is known to be upregulated in response to neuronal injury and/or photoreceptor degeneration.[15–17] Osborne et al. have shown that the decrease in blood supply to retina caused by clamping of both carotid arteries led to increased GFAP expression which could be used as an index of retinal degeneration.[18] GFAP over expression has been reported in rat model of chronic BCCAO[19] as well as in the optic nerve crush model.[20] Eisenfield et al. reported elevated GFAP expression in RCS rats with genetic retinal degeneration.[21]

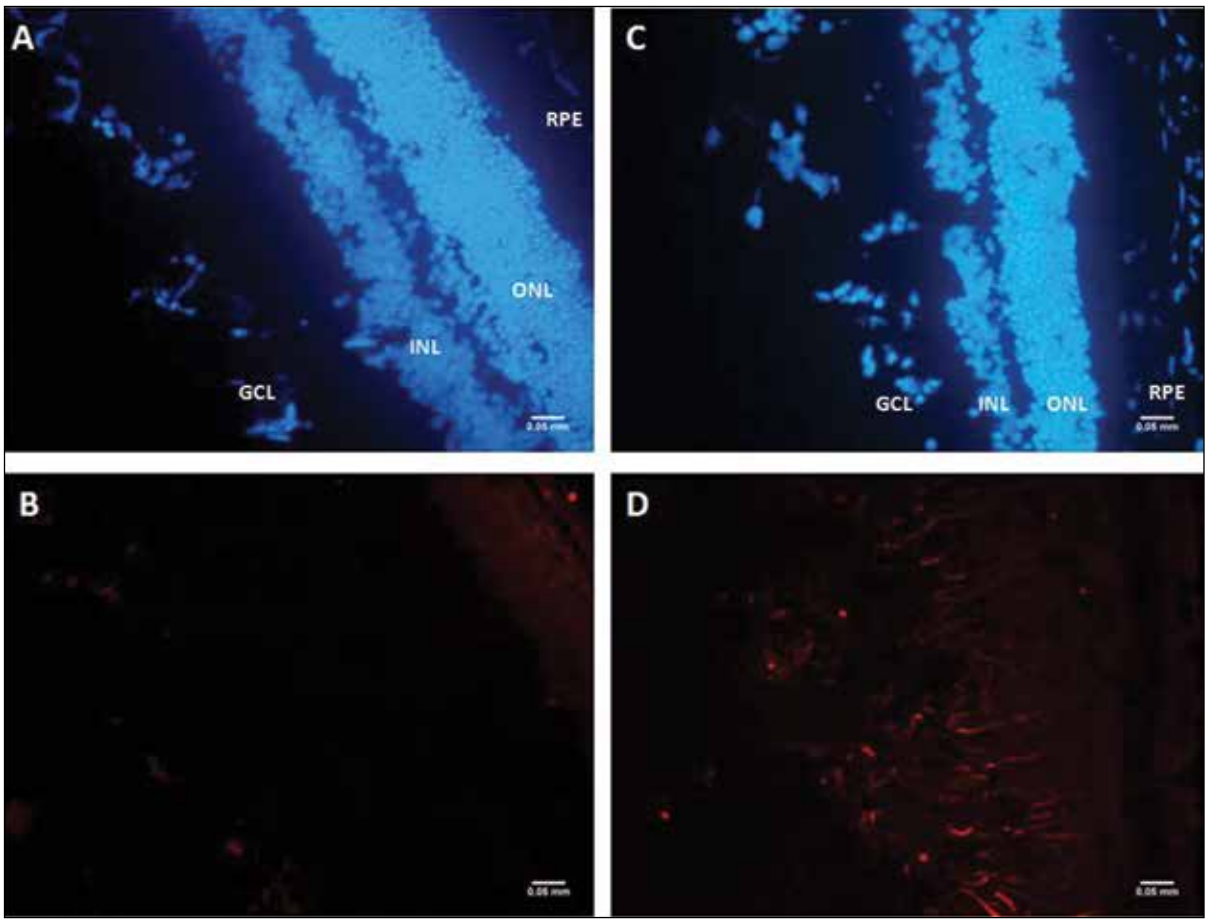


Fig. 4: Immunofluorescence of GFAP expression after PPA ligation. Immunohistochemical staining for glial fibrillary acidic protein (GFAP) in cryosections for control (A-B) and experimental mice (C-D); GFAP is stained with Cy3; blue is DAPI which stains the nuclei *(Scale bar – 50 microns).*

The mouse model of retinal ischemia reported in this article involves the ligation of both the external carotid artery and the pterygopalatine artery for the stipulated time-period. This leads to retinal damage by transient ischemia-reperfusion injury. This model has advantages over the other models that are being used to study retinal ischemia. The model established by elevation of intraocular pressure causes damage to retina through both ischemia and high pressure[22,23] unlike the PPA ligation model which is more specific and well defined. The photocoagulation model, on the contrary, cannot be used to study transient ischemia as the damage caused is permanent. The middle cerebral artery occlusion model leads to both cerebral and retinal ischemia thus enhancing the mortality rate in the experimental animals.[24]

This model can be created in short period of time and has low mortality rate. The few confounders that need to be taken care of include the body temperature, infection, feed and housing conditions. The model can also be modified for the degree of retinal injury caused by changing the duration of ligation as well as reperfusion and can be further used to test new drugs and other therapeutic strategies for retinal ischemia.

Authorship Contributions

Gillipsie Minhas: Performed the surgery **Ryuichi Morishita, Munehisa Shimamura:** Provided training, **Reema Bansal:** Supervised the FFA, **Akshay Anand:** Designed, supervised and provided resources for the study.

Acknowledgements

The authors acknowledge the Department of Science and Technology (F.No. SR/SO/HS-0001/2010), Council of Scientific and Industrial Research, India and Disease Models and Mechanisms Fellowship, London UK.

This article complies with International Committee of Medical Journal editor's uniform requirements for manuscript.

Conflict of interest: None; Funding: None.

Competing Interests: The authors declare no competing interests.

Received Date : 22 February 2015; Revised Date : 14 March 2015;
Accepted Date : 23 March 2015

References

1. Osborne NN, Casson RJ, Wood JP et al. Retinal ischemia: mechanisms of damage and potential therapeutic strategies. Progress in Retinal and Eye Research. 2004; 23(1): 91–147.
2. Bonne C, Muller A, Villain M. Free radicals in retinal ischemia. General Pharmacology. 1998; 30(3): 275–80.
3. Jennings RB, Sommers HM, Smyth GA. Myocardial necrosis induced by temporary occlusion of a coronary artery in the dog. Archives of Pathology. 1960; 70: 68–78.

4. Buchi ER, Suivaizdis I, Fu J. Pressure-induced retinal ischemia in rats: An experimental model for quantitative study. Ophthalmologica. 1991; 203(3): 138–47.
5. Selles-Navarro I, Villegas-Perez MP, Salvador-Silva M et al. Retinal ganglion cell death after different transient periods of pressure-induced ischemia and survival intervals. A quantitative *in vivo* study. Investigative Ophthalmology & Visual Science. 1996; 37(10): 2002–14.
6. Mosinger JL, Olney JW. Photothrombosis-induced ischemic neuronal degeneration in the rat retina. Experimental Neurology. 1989; 105(1): 110–3.
7. Lafuente Lopez-Herrera MP, Mayor-Torroglosa S, Miralles de Imperial J et al. Transient ischemia of the retina results in altered retrograde axoplasmic transport: Neuroprotection with brimonidine. Experimental Neurology. 2002; 178(2): 243–58.
8. Lafuente MP, Villegas-Perez MP, Selles-Navarro I et al. Retinal ganglion cell death after acute retinal ischemia is an ongoing process whose severity and duration depends on the duration of the insult. Neuroscience. 2002; 109(1): 157–68.
9. Mayor-Torroglosa S, De la Villa P, Rodriguez ME et al. Ischemia results 3 months later in altered ERG, degeneration of inner layers, and deafferented tectum: Neuroprotection with brimonidine. Investigative Ophthalmology & Visual Science. 2005; 46(10): 3825–35.
10. Steele EC, Jr., Guo Q, Namura S. Filamentous middle cerebral artery occlusion causes ischemic damage to the retina in mice. Stroke. 2008; 39(7): 2099–104.
11. Block F, Schwarz M, Sontag KH. Retinal ischemia induced by occlusion of both common carotid arteries in rats as demonstrated by electroretinography. Neuroscience Letters. 1992; 144(1–2): 124–6.
12. Lelong DC, Bieche I, Perez E et al. Novel mouse model of monocular amaurosis fugax. Stroke. 2007; 38(12): 3237–44.
13. Ogishima H, Nakamura S, Nakanishi T et al. Ligation of the pterygopalatine and external carotid arteries induces ischemic damage in the murine retina. Investigative Ophthalmology & Visual Science. 2011; 52(13): 9710–20.
14. Ishizuka F, Shimazawa M, Umigai N et al. Crocetin, a carotenoid derivative, inhibits retinal ischemic damage in mice. European Journal of Pharmacology. 2013; 703(1–3): 1–10.
15. Ekstrom P, Sanyal S, Narfstrom K et al. Accumulation of glial fibrillary acidic protein in Muller radial glia during retinal degeneration. Investigative Ophthalmology & Visual Science. 1988; 29(9): 1363–71.
16. Xue LP, Lu J, Cao Q et al. Muller glial cells express nestin coupled with glial fibrillary acidic protein in experimentally induced glaucoma in the rat retina. Neuroscience. 2006; 139(2): 723–32.
17. Xue L, Ding P, Xiao L et al. Nestin is induced by hypoxia and is attenuated by hyperoxia in Muller glial cells in the adult rat retina. International Journal of Experimental Pathology. 2011; 92(6): 377–81.
18. Osborne NN, Safa R, Nash MS. Photoreceptors are preferentially affected in the rat retina following permanent occlusion of the carotid arteries. Vision Research. 1999; 39(24): 3995–4002.
19. Barnett NL, Osborne NN. Prolonged bilateral carotid artery occlusion induces electrophysiological and immunohistochemical changes to the rat retina without causing histological damage. Experimental Eye Research. 1995; 61(1): 83–90.
20. Bignami A, Dahl D. The radial glia of Muller in the rat retina and their response to injury. An immunofluorescence study with antibodies to the glial fibrillary acidic (GFA) protein. Experimental Eye Research. 1979; 28(1): 63–9.
21. Eisenfeld AJ, Bunt-Milam AH, Sarthy PV. Muller cell expression of glial fibrillary acidic protein after genetic and experimental photoreceptor degeneration in the rat retina. Investigative Ophthalmology & Visual Science. 1984; 25(11): 1321–8.
22. Peachey NS, Green DJ, Ripps H. Ocular ischemia and the effects of allopurinol on functional recovery in the retina of the arterially perfused cat eye. Investigative Ophthalmology & Visual Science. 1993; 34(1): 58–65.
23. Marmor MF, Dalal R. Irregular retinal and RPE damage after pressure-induced ischemia in the rabbit. Investigative Ophthalmology & Visual Science. 1993; 34(8): 2570–5.
24. Minhas G, Morishita R, Anand A. Preclinical models to investigate retinal ischemia: advances and drawbacks. Frontiers in Neurology. 2012; 3: 75.

Behavioural Brain Research 291 (2015) 46–59

Contents lists available at ScienceDirect

Behavioural Brain Research

journal homepage: www.elsevier.com/locate/bbr

Research report

Effect of human umbilical cord blood derived lineage negative stem cells transplanted in amyloid-β induced cognitive impaired mice

Avijit Banik[a], Sudesh Prabhakar[a], Jasvinder Kalra[b], Akshay Anand[a,*]

[a] Neuroscience Research Lab, Department of Neurology, Postgraduate Institute of Medical Education and Research, Chandigarh, India
[b] Department of Obstetrics and Gynecology, Postgraduate Institute of Medical Education and Research, Chandigarh, India

HIGHLIGHTS

- Umbilical cord blood derived Lin −ve stem cells alleviate amyloid-β induced behavioral deficits.
- Lin −ve cells showed a time and dose specific spatial memory improvement in mice.
- These cells mediate up-regulation of BDNF and CREB in brain.
- Concomitant downregulation of Fas-L expression were also observed.

ARTICLE INFO

Article history:
Received 6 January 2015
Received in revised form 7 May 2015
Accepted 10 May 2015
Available online 17 May 2015

Keywords:
Alzheimer's disease
Amyloid-β
Umbilical cord blood
Lineage negative
BDNF
CREB

ABSTRACT

Alzheimer's disease (AD) is pathologically characterized by extracellular deposition of insoluble amyloid-β (Aβ) plaques and intracellular tangles made up of phosphorylated tau in brain. Several therapeutic approaches are being carried out in animal AD models for testing their safety and efficacy in altering disease pathology and behavioral deficits. Very few studies have examined the effect of human umbilical cord blood (hUCB) derived stem cells in degenerative disease models despite growing number of cord blood banks worldwide. Here we have examined the therapeutic efficacy of hUCB derived lineage negative (Lin −ve) stem cells in alleviating behavioral and neuropathological deficits in a mouse model of cognitive impairment induced by bilateral intrahippocampal injection of Aβ-42. Lin −ve cells were transplanted at two doses (50,000 and 100,000) at the site of injury and examined at 10 and 60 days post transplantation for rescue of memory deficits. These cells were found to ameliorate cognitive impairment in 50,000—60 days and 100,000—10 days groups whereas, 50,000—10 days and 100,000—60 days groups could not exert any significant improvement. Further, mice showing spatial memory improvement were mediated by up-regulation of BDNF, CREB and also by concomitant down regulation of Fas-L in their brain. The transplanted cells were found in the host tissue and survived up to 60 days without expressing markers of neuronal differentiation or reducing Aβ burden in mouse brain. We suggest that these undifferentiated cells could exert neuroprotective effects either through inhibiting apoptosis and/or trophic effects in the brain.

© 2015 Elsevier B.V. All rights reserved.

1. Introduction

Alzheimer's disease (AD) is one of the most common neurodegenerative diseases of central nervous system (CNS). In 2013 the Alzheimer's association estimated 5.2 million people suffering from AD in USA alone with an alarming rate of diagnosing one case every 68 s. This number is expected to rise to 13.8 million by 2050, with a rate of nearly a million people newly diagnosed for AD each year [1]. In India, the number of people suffering from AD and other dementia is estimated to approximate 3.7 million and this number is expected to double by the year 2030 [2]. With such prevalence, AD is threatening to be epidemic worldwide. The current treatment strategies can only provide symptomatic relieves without altering

Abbreviations: AD, Alzheimer's disease; AP, anterioposterior; Aβ, amyloid-β; BDNF, brain derived neurotrophic factor; CFDA–SE, carboxyfluorescein diacetate–succinimidyl ester; CNS, central nervous system; CREB, cAMP response element binding protein; CTCF, corrected total cell fluorescence; DV, dorsoventral; HSC, hematopoietic stem cell; hUCB, human umbilical cord blood; IAEC, Institute Animals Ethical Committee; IP, intraperitoneal; MACS, magnetic associated cell sorter; ML, mediolateral; MSCs, mesenchymal stem cells; MWM, Morris water maze; NFT, neurofibrilary tangles; PBS, phosphate buffer saline; RO, reverse osmois; RT, room temperature.

* Corresponding author. Tel.: +91 172 2756090; fax: +91 172 2744401.
http://neurologypgi.org.
E-mail address: akshay1anand@rediffmail.com (A. Anand).

http://dx.doi.org/10.1016/j.bbr.2015.05.014
0166-4328/© 2015 Elsevier B.V. All rights reserved.

underlying disease pathologies. The acetylcholinesterase inhibitors and NMDA receptor antagonists are currently approved drugs for AD but none of them are efficient in delaying or halting the disease progression [3].

AD is pathologically characterized by intracellular neurofibrilary tangles (NFT) and extracellular β-amyloid (Aβ) plaques, leading to selective neuronal loss in diseased brain. There is progressive memory loss and cognitive decline as the disease progresses [4]. In AD brain autopsies it is demonstrated that synaptic plasticity and neuronal hypertrophy are imbalanced leading to disease pathology whereas a compensatory mechanism sets in rescue for normal cognitive aging [5]. At present, there are no definitive consensus preventive measures established in management of AD. There are no promising outcome obtained from several AD trials in last two decades leading to explore other causative mechanisms instead of targeting Aβ and tau pathologies alone [6]. The putative role of neuroinflammatory cytokines [7], cytoskeletal associated proteins [8] and exocytic lysosomal enzymes [9] are under extensive investigations to alleviate the pathological burden of the disease.

There have been multiple approaches carried out to establish animal models of AD in preclinical setting [10]. Aβ induced selective neurotoxicity is well demonstrated in experimental rodent models. Tang et al. demonstrated that fibrillar form of Aβ(1–40), when administered in rat hippocampus, formed insoluble aggregates showing Congo red positivity and induced neurotoxicity in the DG and CA3 regions [11]. It is also reported that Aβ induced toxicity downregulates one of the important neurotrophins, such as, brain derived neurotrophic factor (BDNF) and its major regulatory molecule, cAMP response element-binding protein (CREB) in both in-vitro and in-vivo studies [12,13].

Cell based preclinical therapies in AD have been limited owing to the presumption that the pathology in brain is not as well localized as in case of PD or ALS. Hence, the recent developments in early diagnosis and treatment strategies of AD have raised an unparallel requirement to screen a suitable drug, alternative extracts or cell based therapeutics. Stem cell transplantation (SCT) therapy is attracting attention for chronic diseases of ageing especially those that result from a defined and localized deficit not characterized in AD. However, despite the hope held by cord banks, the human umbilical cord blood (hUCB) derived stem cells have not been adequately studied. A limited number of studies with disease models of stroke [14], AD [15] and spinal cord injury [16] have been conducted even though it has been argued that stem cells from hUCB banks can provide a reliable source for replacing damaged neurons and restoring their functional activity [17]. There are potential studies demonstrating therapeutic effects of neural stem cells by offering pathological and functional recovery in AD models. Although there are few studies supporting the neuronal replacements by transplanted stem cells as a therapeutic mechanism but larger number of studies have reported that this neuroprotection offered by transplanted cells are mediated by their neurotrophic effects [18]. It has been reported that neural stem cells (NSCs) derived from embryonic stem cells, when transplanted at the site of neural degeneration, can facilitate neuronal differentiation, leading to functional recovery from motor and cognitive impairments in a mouse model of AD [19]. In another study, transplantation of NSCs derived from postnatal brain in a triple transgenic AD model does not alter underlying Aβ or tau pathology, instead, exerts cognitive improvement mediated by neurotrophins such as BDNF [20]. A recent study also demonstrated the therapeutic effect of NSCs in AD mice by enhanced expression of cognitive related proteins and neurotrophins without altering the Aβ pathology [21].

Although, very few studies have been reported demonstrating the therapeutic role of hUCB derived stem cells in AD. Largely, mesenchymal stem cell (MSCs) population from hUCB has been tested in AD models. Lee et al. has reported that hUCB–MSCs play potential role in reducing Aβ deposition, tau hyperphosphorylation and BACE1 activity through microglial immunomodulation in APP/PS1 mice [22]. Darlington et al. demonstrated the therapeutic effects of hUCB derived mononucleated cells in PS/APP transgenic mice. Multiple low dose infusion of these cells in peripheral circulation between 6 to 12 months of age has led to cognitive improvement in a battery of spatial memory testing paradigm followed by reduced load of Aβ plaques and microgliosis [23]. It is reported that autologous T regulatory cells purified from transgenic AD mice when co-cultured with human umbilical cord derived mesenchymal stem cells in-vitro and transplanted in the systemic circulation in these AD mice, they could exert a protective effect on AD pathology by decreasing microglial activation and levels of systemic inflammatory factors [24]. Above studies reveal that stem cells in hUCB has significant clinical potential but not adequately tested in AD pathology. Hence our study is a timely intervention to evaluate the therapeutic role of hUCB derived lineage negative (Lin −ve) cells in AD treatment.

Lin −ve cells, the purified subset of cells without expressing surface antigens associated with lineage commitment are reported to have unrecognized heterogeneity within the hematopoietic stem cell (HSC) population [25–27] but not adequately studied thereafter. Such primitive population of cells are deprived of any mature hematopoietic markers such as, CD2, CD3, CD14, CD16, CD19, CD24, CD56, CD66b, and CD235a (glycophorin A) [28] and found to be present in only 0.1% population of mono-nucleated cells enriched from hUCB [29] These are also found in peripheral blood and bone marrow cell in a very limited fraction [30,31]. These cells were shown to have the potential to differentiate into granulocyte-macrophage, erythroid and megakaryocytic colony forming units when cultured in-vitro [32]. Unrestricted somatic stem cells from hUCB, when induced with dopaminergic regulatory factor in-vitro, can be differentiated into dopaminergic neurons expressing tyrosin hydroxylase [33]. Limited studies show that Lin −ve cells are capable of integrating and differentiating in different tissues of the host organs when transplanted in the peritoneal cavity of goats [34]. Unfortunately, there are not many in-vivo studies to demonstrate their efficacy in disease models. We had earlier shown that Lin −ve stem cells derived from mouse bone marrow, when transplanted via intravenous route, survived for 8 weeks and repaired the laser induced lesions in mouse retina without undergoing differentiation [27]. Similarly, this study further advances our current knowledge of Lin −ve cells by testing the role of such primitive cells derived from hUCB. We show that these cells have potential to rescue memory loss mediated by pathways relevant to cell survival not necessarily linked to differentiation.

2. Materials and methods

2.1. Animals

All the experiments were conducted in GLP compliant laboratory supported by quality assurance program, using periodically calibrated instruments and molecular biology grade chemicals. Each experimental step was recorded and archived in appropriate formats and samples were coded and stored in dedicated storage locations ensuring back traceability of both data and samples. All animals were obtained from Institute's central animal facility vide Registration No. 47/1999/CPCSEA and all the experiments were carried out by trained animal experimenter following the guidelines approved by the Institute Animals Ethical Committee (Approval no. 46/IAEC/217). Appropriate measures were taken to minimize the pain or discomfort subjected to the animals used in the experiments. Sex (male) and age (4–6 weeks) matched, inbred Swiss albino mice (20–35 g) were used for all the experiments. Mice

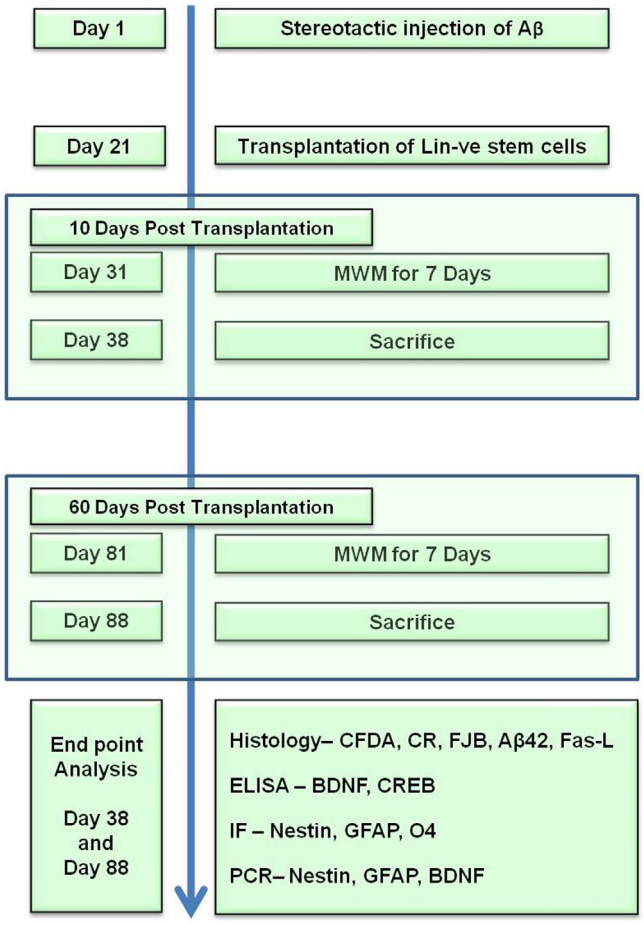


Fig. 1. Day wise plan explaining time course of the treatment and analysis.

were kept in the central animal house with rooms regulated for humidity (45–55%) and temperature (20–23 °C) and kept on a 12 h light/dark cycle. Chow diet (protein 20–24%, fat 4–5%, fiber 4–5%, Ca 1–1.5%, P 0.5% and vitamin supplements 0.5%) and RO drinking water were available ad libitum. Six mice were kept in a transparent polypropene cage (38 cm × 24 cm × 16 cm), using sterilized corn cob as bedding material. The experiments were carried out in between 9 AM and 6 PM in a semi-soundproof working laboratory (Fig. 1).

Before recruiting animals they were tested in Morris water maze (MWM) for their swimming ability. Animals showing normal behavioral pattern, with standard vision and motor activities were included in the study. They were allowed to freely swim in the MWM pool for 3 min to verify their general exploratory behavior to escape from water. The rota rod tests were performed to exclude the animals with irregular muscle coordination. Only those mice which could sustain 3 min of locomotory behavior on rota rod, at a speed of 15 rpm, were included in the study. There were 12 groups formulated for the study and 10 mice were included in each group (Table 1). All the mice underwent stereotactic surgery at two time points, namely Aβ delivery at day 1 and cell transplantation at day 21. PBS was injected in control groups in place of Aβ or cells. All the mice were tested in MWM after either 10 days or 60 days post transplantation of stem cells. Mice were sacrificed post MWM analysis by I.P. injection of an over dose of anesthesia (xylazine–ketamine cocktail) in accordance with the approved guidelines of IAEC and brains were stored at −80 °C for immunohistological, biochemical and molecular analysis (Fig. 2). Measures were taken to minimize the use of animals for experiments. $n = 6–8$ mice were recruited for MWM analysis and further 2 brain samples for each group were used for IHC, ELISA and PCR analysis.

2.2. Intra-hippocampal injection of aggregated Amyloid-β peptide

Hippocampus injury was induced by stereotaxic injection of aggregated form of Amyloid-β (1–42) peptide (Sigma, USA). The peptide was made by dissolving it in 1× phosphate buffered solution (PBS) and incubated at 37 °C overnight for aggregate formation. Mice were anesthetized using xylazine (10 mg/kg)–ketamine (100 mg/kg) cocktail and mounted in a stereotaxic apparatus. Bilateral craniotomies were done for the injection by exposing the skull and drilling the injection points using a 26G needle according to the Bregma scale following the stereotaxic coordinates [35]. Bregma coordinates used for the hippocampal delivery was anterioposterior (AP) 2 mm, mediolateral (ML) ±2 mm and dorsoventral (DV) 2.5 mm. 800 pMol of aggregated form of Aβ solution (Stock conc. 250 μg/ml) in 5 μl of PBS was injected in a controlled rate of 1–2 μl/min using a microinjector. The needle of the microsyringe was kept unmoved for 5 min after the solution was delivered in the hippocampus for and then slowly removed from the brain by unscrewing the stereotaxic arm of the injection [36]. PBS was injected bilaterally for sham-operated groups.

2.3. Enrichment of Lin −ve stem cells for transplantation

Human UCB samples were collected from the umbilical cords of newborns delivered by pregnant women (aged between 20 and 35 years) at gestation period of ≥28 weeks after proper informed consent was taken in accordance with ethical guidelines approved by Institutional Committee on the Stem Cell Research and Therapy (IC-SCRT) (Approval no. IC-SCRT/10/DTM-3272). hUCB samples were processed by density gradient centrifugation, using histopaque (Sigma, USA), for enrichment of mono-nucleated cell population (MNCs). The Lin −ve stem cells were isolated from such MNC population using a magnetic associated cell sorter (MACS) (Miltenyi Biotech, Germany) with human Lin −ve isolation kit (Miltenyi Biotech, Germany). Finally, Lin −ve cells were analyzed using an automated cell counter (Millipore, USA) for their absolute counts and diameters. These cells were labeled with fluorescent CFDA–SE dye (amine-reactive carboxyfluorescein succinimidyl ester) (Invitrogen, USA) for post-transplantation analysis. Briefly, cell pellet was suspended in 1× PBS containing CFDA (10 μM). Cells were incubated at 37 °C for 15 min accompanied with mild shaking. These cells were further suspended in pre-warmed (37 °C) 1× PBS for another 30 min to ensure complete reaction. Finally, theses cells were washed and suspended in 1× PBS for transplantation. The CFDA labeled cells were also validated through flowcytometric analysis to ensure complete staining.

2.4. Flowcytometry analysis of Lin −ve stem cells

The Lin −ve cells isolated from UCB—were characterized by flowcytometry for the presence of stem cell markers. CD45, CD34 and CD117 marker profile was analyzed in all the three populations of UCB viz., MNCs, Lin +ve and Lin −ve cells. Approximately one million cells were suspended in 100 μl FACS or MACS buffer (PBS–BSA–azide solution). FC blocking reagent (20 μl for up to 10^7 cells) (Miltenyi Biotech, USA) was added in each tube and incubated for 30 min at RT. Antibody-conjugated with fluorochrome (Conc: 20 μl/1 × 10^6 cells) (BD Bioscience, India) was added and incubated for 1 h at RT. Further, 1 ml of FACS or MACS buffer (PBS–BSA–azide solution) was added and washed 2 times with the buffer to remove unbound antibodies in the solution. The cells were suspended in 300 μl of buffer and processed in flowcytometer (within 2–6 h of

Table 1
Details of experimental groups.

Group	Stereotaxic injection at day 1	Stereotaxic injection at day 21	Post-trnaplantation analysis at day 31/81
PBS–PBS—10 d	5 μl PBS	5 μl PBS	Day 31: analyzed in MWM after 10 days of second injection
PBS–PBS—60 d	5 μl PBS	5 μl PBS	Day 81: analyzed in MWM after 60 days of second injection
PBS-50,000—10 d	5 μl PBS	50,000 Lin −ve stem cells (5 μl)	Day 31: analyzed in MWM after 10 days of cell transplantation
PBS-50,000—60 d	5 μl PBS	50,000 Lin −ve stem cells (5 μl)	Day 81: analyzed in MWM after 60 days of cell transplantation
PBS-100,000—10 d	5 μl PBS	100,000 Lin −ve stem cells (5 μl)	Day 31: analyzed in MWM after 10 days of cell transplantation
PBS-100,000—60 d	5 μl PBS	100,000 Lin −ve stem cells (5 μl)	Day 81: analyzed in MWM after 60 days of cell transplantation
Aβ-PBS—10 d	800 pM Aβ-42 (5 μl)	5 μl PBS	Day 31: analyzed in MWM after 10 days of second injection
Aβ-PBS—60 d	800 pM Aβ-42 (5 μl)	5 μl PBS	Day 81: analyzed in MWM after 60 days of second injection
Aβ-50,000—10 d	800 pM Aβ-42 (5 μl)	50,000 Lin −ve stem cells (5 μl)	Day 31: analyzed in MWM after 10 days of cell transplantation
Aβ-50,000—60 d	800 pM Aβ-42 (5 μl)	50,000 Lin −ve stem cells (5 μl)	Day 81: analyzed in MWM after 60 days of cell transplantation
Aβ-100,000—10 d	800 pM Aβ-42 (5 μl)	100,000 Lin −ve stem cells (5 μl)	Day 31: analyzed in MWM after 10 days of cell transplantation
Aβ-100,000—60 d	800 pM Aβ-42 (5 μl)	100,000 Lin −ve stem cells (5 μl)	Day 81: analyzed in MWM after 60 days of cell transplantation

antibody labeling). If these were not analyzed immediately, cells were fixed with 300 μl of fixation buffer solution (BD Bioscience, USA) and stored at 4 °C till processed in flowcytometer.

2.5. Transplantation of Lin −ve stem cells at the site of Aβ injection

Cell transplantation was carried out using a stereotaxis apparatus and same protocol as was used for Aβ injection. CFDA–SE labeled Lin −ve stem cells were suspended in PBS in two different cell doses i.e. 50,000 or 100,000 cells and were stereotactically transplanted in the respective mice after 21 days of Aβ injury. The cells were delivered bilaterally at the site of the Aβ lesions in the hippocampus at the speed of 1–2 μl/min with the auto-injector. Vehicle treated groups were given bilateral injection of PBS.

2.6. Evaluation of spatial memory in Morris water maze

The loss of spatial memory following Aβ injection and also the effect of cell transplantation in these animals was tested in MWM. The MWM pool (diameter 2 m, height 45 cm) was filled with water (22–24 °C) and nontoxic black poster color (Camel, India) was added to make it opaque. Seven days protocol was followed for this experiment. Mice were subjected to acquisition trials for first 6 days, followed by retrieval trial on 7th day. Each animal was given 4 trials a day with a resting phase of 20 min in between two trials for individual mouse. The starting position of each mouse was changed from Q1 → Q2 → Q3 → Q4 for 4 trials in a day. The position of the hidden platform (submerged 1 cm below the water level) was kept constant for the entire period of acquisition trials and it was removed from the pool during retrieval trials. All the activities inside the MWM pool were digitally recorded by an automated video tracking system using Anymaze software (Stoelting Co, USA). Escape latency time (ELT) was measured, as an index of acquisition, by estimating the time taken by the mice to reach the hidden platform. The swimming path for all the mice was mapped for each trial comprising of 120 s. If the animals were not able to reach the platform within the stipulated time, they were gently guided to the hidden platform using a wooden stick. On 7th Day (retrieval) the mice were freely allowed to swim for 120 s in the pool and the time spent by each mouse in the target quadrant as well as the path used while exploration was measured as a degree of retrieval of acquired memories.

2.7. Histological studies

8–12 μm coronal brain sections were taken on poly-L-lysine coated glass slides using a Cryotome (Leica, USA) and tissue embedding media (Leica, USA). Sections were stored at −20 °C until further processing for histological and immunofluorescent analysis. Images were analyzed for quantitation of immunefluorescence in ImageJ software by normalizing the background fluorescence from total fluorescence. Images have been edited using Adobe photoshop to enhance visibility in compliance with publishing ethics. Integrated density (INT DEN) for all the images and their respective backgrounds (2–3 randomly chosen areas/image) were measured and their corrected total cell fluorescence (CTCF) were analyzed using the formula: CTCF = [Integrated Density − (Area of selected cell × Mean fluorescence of background readings)].

2.7.1. Congo red staining

Brain sections were stained by Alcoholic Congo red (HiMedia, India) solution for identification of Aβ plaques in the mouse brain. Brain sections were fixed with histochoice fixing solution (Sigma, USA) for 5 min at room temperature (RT) and then washed with water. Sections were then subjected to hydration in 90%, 70% and 50% ethanol, respectively, followed by washing in water. Nuclei were stained with haematoxylin for 3 min at room temperature. Sections were thoroughly washed in water and stained with 1% alcoholic Congo red solution for about 30 min at room temperature. The slides were immersed in 70% alcohol for a few seconds to remove excess stain and then dipped in xylene before mounting them with fluorosave mounting medium (Calbiochem, USA).

2.7.2. Immunofluorescent staining

Fluorescent-tagged antibodies viz., MAP2 (1:50, Santa Cruz, USA) for microtubule proteins in host neurons, Nestin (1:100, Santa Cruz, USA) for neuronal progenitors, GFAP (1:100; Santa Cruz, USA) for astrocytes, O4 (1:50; Sigma USA) for oligodendrocytes, Aβ42 (1:100, Novus Biological, USA) for amyloid plaques and Fas-L (1:100; Chemicon, USA) for apoptotic cells co-stained with DAPI nuclear stain (1:1000; Life Technologies, USA) were used to analyze the histopathological changes in brains upon cell transplantation. The slides were incubated overnight at 4 °C with respective primary antibodies. After removing the solutions from slides they were incubated with respective secondary antibodies (1:200; Jackson, USA) for 1 h at RT. The sections were washed with PBS for 3 times and counter-stained with DAPI for 5 min at RT. The slides were rinsed with PBS for 3 times and mounted with fluorosave mounting medium before examining under the fluorescent microscope.

2.8. Estimation of neurotrophic factors in mouse brain homogenate

Brain homogenates from different groups (were subjected to quantitative expression of neurotrophin such as brain derived neurotrophic factor (BDNF) and its regulatory molecule cAMP-response element binding protein (CREB). Whole brains were homogenized using freshly prepared lysis buffer composed of 1% Triton-X, 10% Glycerol, 150 nM NaCl, 50 nM HEPES buffer, 1 mM EGTA, 1 mM sodium orthovanadate, 1 mM sodium fluoride, 1 mM PMSF, 10 μg/ml aprotinin and 10 μg/ml leupeptin. These factors

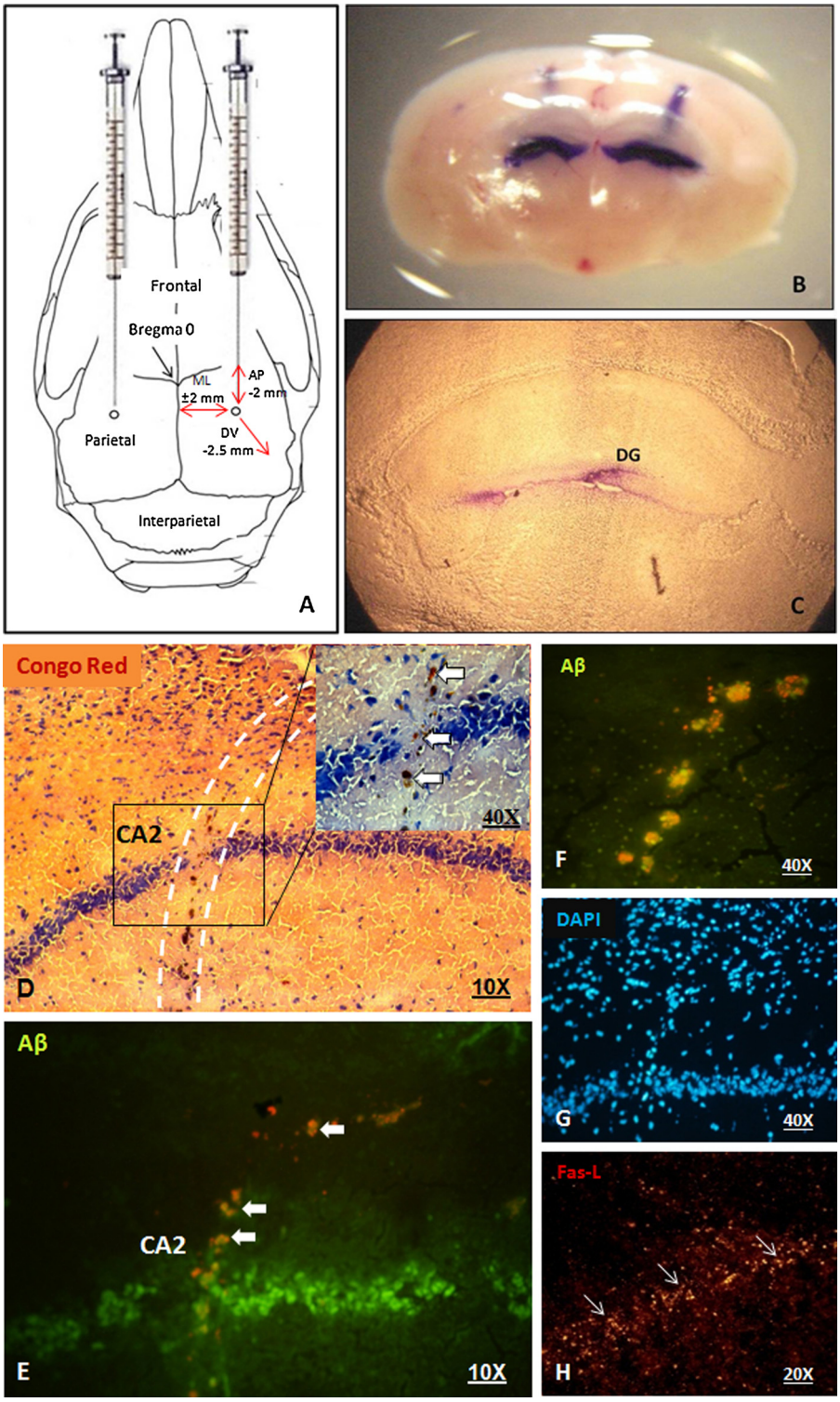


Fig. 2. *Intra-hippocampal micro-injection and AD like pathology in mouse brain.* (A) Coordinates for hippocampus showing site of injections indicated by circle. Arrow indicates Bregma 0. (B) Gross section of mouse brain showing diffused crystal violet dye through-out the hippocampal area with a prominent needle track under dissection microscope. (C) Cryosection of the brain showing the deposition of dye in dentate gyrus (DG) region of the hippocampus. (D) Arrows show appearance of Congo red positive Aβ aggregates in the CA2 region of mouse hippocampus. Dotted line shows deposition of Aβ along the tract of injection. The CA2 layer was also found to be dissociated in this section due to Aβ deposition. (E) Immunofluorescent staining for Aβ42 antibody confirms Aβ42 positive plaques in these sections. (F) Immunofluorescent staining for Aβ42 at higher magnification. (G) Corresponding DAPI image of section F showing CA2 region of hippocampus. (H) Fas-L positive cells were present around the Aβ plaques confirming their neurodegenerative effects in mouse brain.

were estimated by ELISA at 450 nm using protocol prescribed by the manufacturer of ELISA kits (Cusa Biotech, China). All the ELISA values were normalized to their respective total protein values estimated by Bradford method.

2.9. Quantitative real time PCR

Molecular expression of different cell markers and neurotrophic factors were analyzed using quantitative PCR (qPCR) (Applied

Table 2
Primer sequence of target genes for qPCR.

Target gene	Target length (bp)	Primer sequence (5′ → 3′)	Annealing temperature (°C)
BDNF	131	F: TGGCTGACACTTTTGAGCAC R: CAAAGGCACTTGACTGCTGA	59
GFAP	63	F: ACAGACTTTCTCCAACCTCCAG R: CCTTCTGACACGGATTTGGT	63
Nestin	235	F: AACTGGCACACCTCAAGATGT R: TCAAGGGTATTAGGCAAGGGG	63
β-Actin	228	F: AGCCATGTACGTAGCCATCC R: CTCTCAGCTGTGGTGGTGAA	59–63

Table 3
Amplification conditions for qPCR.

Stage	Initial denaturation	Denaturation	Annealing	Extension	Final extension
Temperature (°C)	95	95	59 (BDNF) 63 (GFAP) 63 (Nestin)	72	72
Duration (min)	10	1	1	1	10
Cycles	1	35			1

Biosystem, USA). The expression of BDNF, Nestin and GFAP was estimated according to their relative fold change in mRNA expression as compared to control samples. Total RNA was isolated from the brain tissues by Qiazol RNA extraction kit (Qiagen, USA). cDNA was synthesized from their respective RNA using cDNA synthesis kit (Thermo Scientific, USA) and was subjected to PCR amplification using standard primers. This was normalized to corresponding β-actin expression. The quantitative expression by qPCR confirmed the results obtained from immunofluorescent and biochemical observations. The primer sequence of target genes and PCR details are listed in Tables 2 and 3, respectively.

2.10. Statistical analysis

All the brain and RNA samples were blinded to the experimenter to remove any experimenter bias. All results were expressed as mean ± S.E.M. Data was statistically analyzed using 16.0 version of SPSS. In MWM, the acquisition and retrieval data was analyzed by repeated-measures ANOVA with acquisition days and retrieval trials as a measure of repeated observations. Further, LSD test was used for post-hoc analysis. For ELISA and qPCR observations were measured by repeated measure ANOVA with follow-up comparisons using LSD test. $p < 0.05$ was considered as statistically significant in the results obtained from statistical analysis.

3. Results

3.1. Standardization of Bregma coordinates for intra-hippocampal micro-injection

Crystal violet dye was injected in the hippocampus of mouse brain to standardize the Bregma coordinates for mouse hippocampus. The coordinates for hippocampus were standardized as anterioposterior (AP) 2 mm, mediolateral (ML) ±2 mm and dorsoventral (DV) 2.5 mm (Fig. 2A). The mouse was sacrificed immediately after injection and brain was removed for histological analysis. Gross section of the brain under dissection microscope showed diffuse crystal violet dye throughout the hippocampal region with a prominent needle track (Fig. 2B). Brain was also embedded in tissue freezing medium and 10–15 μm cryosections were obtained. Brain sections examined under microscope showed a streak of dye deposited in the dentate gyrus region of mouse hippocampus (Fig. 2C).

3.2. Deposition of Aβ aggregates in the mouse brain after 21 days of intra-hippocampal injection

Brain sections were stained with 1% alcoholic Congo red dye to identify the Aβ aggregates. Congo red has a high affinity towards insoluble Aβ plaques. The stained sections showed presence of Congo red positive Aβ aggregates in the mouse hippocampus. The deposits appeared brownish red in color and were found to be aggregated along the needle tract of the injection. CA2 layer of the hippocampus was found to be disrupted by Aβ deposition visible by H&E staining (Fig. 2D). Immunofluorescent staining for Aβ42 antibody also confirmed the presence of Aβ aggregates in these sections followed by dissociation of CA2 layers in the hippocampus (Fig. 2E–G). Immunostaining for Fas-L showed presence of apoptotic cells at the site of Aβ injury (Fig. 2H).

3.3. Characterization of Lin −ve stem cells isolated from human UCB

Lin −ve stem cells isolated from hUCB by MACS using Lin −ve isolation kit were characterized by automated cell counter to estimate the absolute number and size of these cells. About 100 μl of cell suspension was loaded into the cell counter using a 60 μm sensor. A histogram was generated by the counter showing distribution of the cells based on their diameter. The average diameter of cells was found to be 8.73 μm with a range of 6–14 μm (Fig. 3A and B). These cells were labeled with CFDA dye in order to track them after 60 days of transplantation. These CFDA labeled cells were found to be 86.7% positive for green fluorescence when analyzed in a flowcytometer (Fig. 3D and E). They were also found to express green fluorescence when observed under the microscope (Fig. 3C). These cells were smaller in size compared to Lin +ve cells (average diameter 11.40) and appear as a separate bunch in FSC/SSC plot in flowcytometer.

MACS enriched Lin −ve cells were characterized by FACS using antibodies for hematopoietic progenitors such as, CD45, CD34 and CD117 antigens. These cells were found to express 38.33% of CD34 and 43.13% of CD117 markers as compared to very low expression (<1%) among MNCs and Lin +ve cells ($p < 0.001$, $F = 16.051$ and

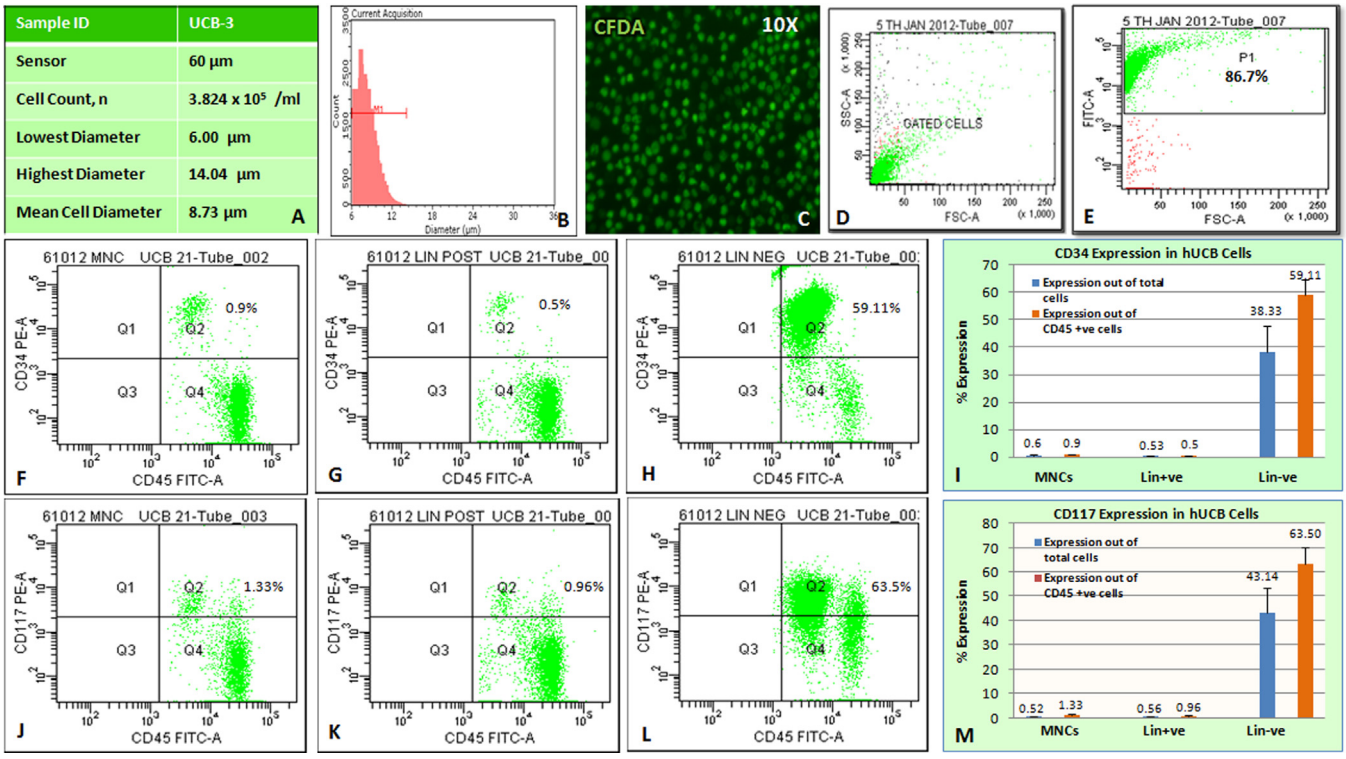


Fig. 3. *Characterization of Lin −ve stem cells from human UCB.* (A) Table showing characteristic features of analyzed Lin −ve cells isolated from hUCB in the automated cell counter showing average diameter of the cells (8.73 µm) and cell count. (B) Histogram showing distribution of cells based on their diameter (µm) varying from 6 to 14 µm. (C) CFDA labeled Lin −ve stem cells showing green fluorescence under the microscope. (D and E) CFDA labeled cells showing 86.7% positivity (P1) for green channel in flowcytometric analysis. Further the UCB samples (were analyzed for CD45, CD34 and Cd117 expression. (F)–(H) Expression of CD34 in CD45 positive cells was found to be (F) 0.9% in MNCs, (G) 0.5% in Lin +ve cells and (H) 59.11% in Lin −ve cells. (I) Comparative expression of CD34 in total gated cells and CD45 positive cells. (J)–(L) Expression of CD117 in CD45 positive cells was found to be (J) 1.33% in MNCs, (K) 0.96% in Lin +ve cells and (L) 63.5% in Lin −ve cells. (M) Comparative expression of CD117 in total gated cells and CD45 positive cells. (For interpretation of the references to color in this figure legend, the reader is referred to the web version of this article.)

df = 2 for CD34 expression; $p < 0.001$, $F = 17.24$ and df = 2 for CD117 expression). The CD34 and CD117 expression was found to be significantly higher (59.11% and 63.5%, respectively) in Lin −ve cells when analyzed in CD45 positive cells ($p < 0.001$, $F = 101.008$ and df = 2 for CD34 expression; $p < 0.001$, $F = 87.189$ and df = 2 for CD117 expression) (Fig. 3F–M).

3.4. Aβ induced cognitive impairment was rescued by Lin −ve stem cell transplantation

After 21 days of Aβ injection the mice were subjected to either Lin −ve stem cell transplantation or vehicle treatment. After 10 days or 60 days post transplantation all the mice were evaluated in MWM for their spatial memory performance. Aβ injured mice showed significant cognitive impairment in both 10 and 60 days groups when compared to PBS injected control groups. There was significant delay in escape latency time (ELT) in acquisition trials from day 1 to 6 in Aβ-PBS—10 d and Aβ-PBS—60 d groups. The average ELT on day 6 for Aβ-PBS—10 d group was 89.44 s when compared to 29.48 s in PBS–PBS—10 d group (Fig. 4A). The ELT on day 6 was found to be 107.18 s in Aβ-PBS—60 d group as compared to 29.10 s noted in PBS–PBS—10 d group (Fig. 4B). These mice, when tested for retrieval on day 7, showed similar pattern of swimming, compared to learned control mice, which spent maximum time in target quadrant in search of the platform (Fig. 4C). The search error index also revealed increased average distance of the mice from the platform zone indicating higher search error due to cognitive impairment in Aβ injured mice (Fig. 4D). The swimming track recorded by the video tracking system showed thigmotactic swimming pattern in these mice even after 6 days of acquisition trials (Fig. 4E).

When Lin −ve stem cells were transplanted in these mice, there was an improvement in spatial memory performance with specific cell dose. Two cell doses i.e. 50,000 or 100,000 cells were transplanted at 10 or 60 days post transplantation and all the mice were evaluated in MWM. Aβ-50,000—60 d group showed best recovery of impaired spatial memory in the mice induced by Aβ delivery. The ELT of these mice was significantly reduced in acquisition trials (50.28 s on day 6) as compared to Aβ-PBS—60 d group (107.18 s on day 6) (Fig. 4B). There was no improvement found in Aβ-50,000—10 d group. In Aβ-100,000—10 d group, mice showed significant recovery from day 1 (89.43 s) to day 6 (53.73 s) but it was not found to be significantly improved when compared to Aβ-PBS—10 d mice (Fig. 4A). The retrieval trials on day 7 revealed that both Aβ-50,000—60 d group and Aβ-100,000—10 d group spent maximum time in target quadrant (Q1) compared to Aβ-PBS—10 d group. There was no significant difference among other cell transplanted groups in term of retrieval index (Fig. 4B). The search error on day 7 was correspondingly found to be significantly reduced in both Aβ-50,000—60 d group and Aβ-100,000—10 d group compared to Aβ injured mice (Fig. 4D) (df = 11; $p < 0.001$, $F = 13.627$ for ELT; $p < 0.001$, $F = 3.679$ for quadrant time; $p < 0.001$, $F = 4.15$ for search error).

3.5. Localization and characterization of transplanted cells in mouse brain

All the mice were sacrificed after completing MWM trials and the brains were analyzed to investigate the fate of transplanted

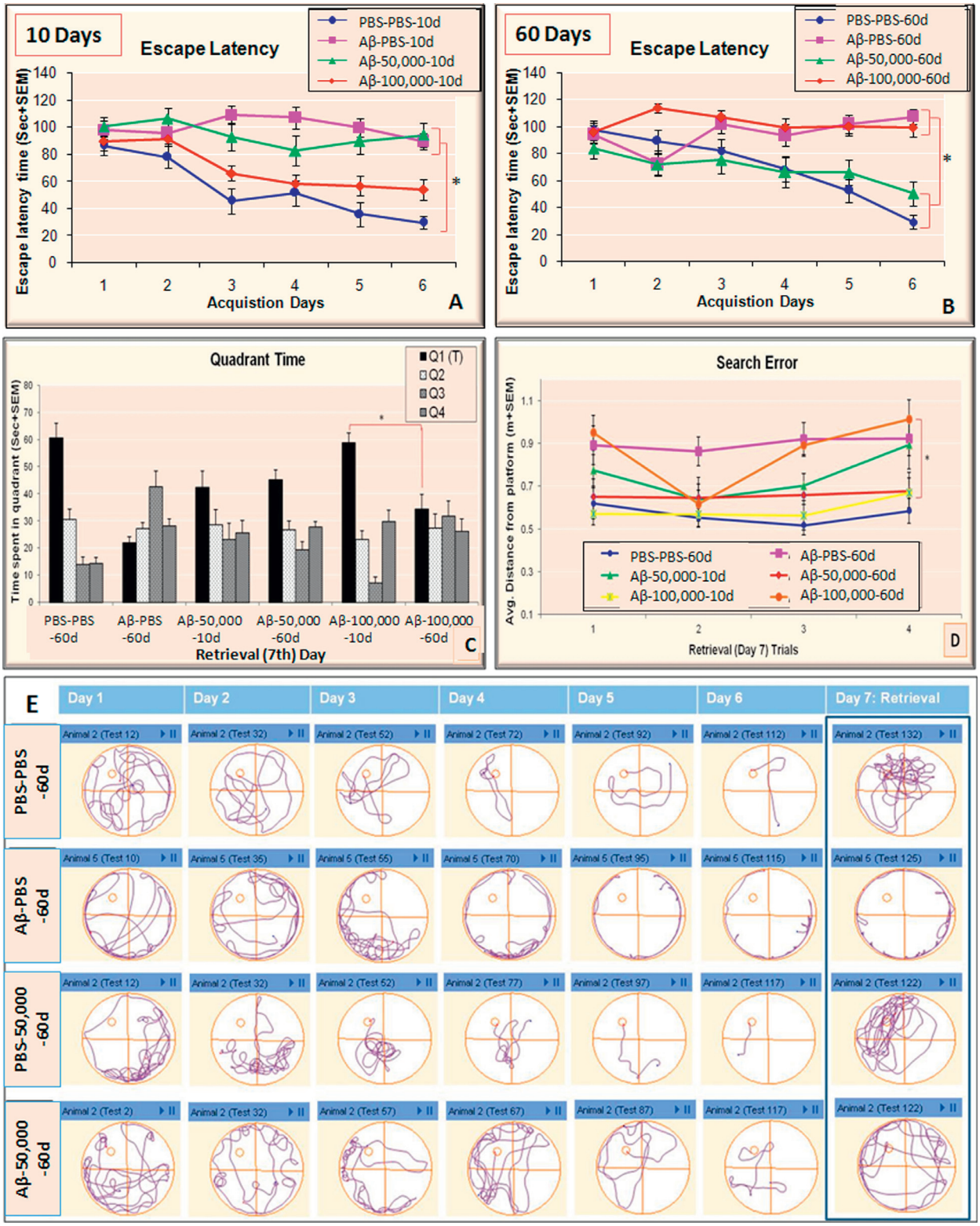


Fig. 4. *Morris water maze analysis of mice with Aβ injury and Lin −ve stem cell transplantation.* (A) Acquisition trials in 10 day group show impaired learning in Aβ-PBS—10 d mice marked by significantly higher escape latency time (ELT) as compared to PBS–PBS—10 d mice. There was no improvement in Aβ-50,000—10 d group. In Aβ-100,000—10 d group, mice showed significant recovery from day 1 to day 6 but it was not significantly improved when compared to Aβ injury alone. (B) Aβ induced cognitive impairment was evident in Aβ-PBS—60 d group. Aβ-50,000—60 d mice showed significant improvement in ELT, whereas there was no improvement shown by Aβ-100,000—60 d group. (C) In retrieval trials time spent in the target quadrant (Q1) was found to be significantly higher in Aβ-100,000—10 d groups. Aβ-50,000—10 d group also spent maximum time in Q1 but it was not significantly higher compared to Aβ injured group. (D) Reduced search error was observed in Aβ-50,000—60 d and Aβ-100,000—10 d, compared to their other cell dose groups showing time and dose dependent recovery of spatial memory. All results expressed as mean ± S.E.M. Data statistically analyzed using SPSS 16.0 by repeated-measures ANOVA with acquisition days as repeated measure. Other comparisons by LSD test. * $p < 0.001$. (E) Representative swimming track plots revealed that Aβ-PBS—60 d mice showed thigmotactic swimming pattern without decreasing their swimming track even after 6 days of acquisition. Length of swimming track was significantly reduced in Aβ-50,000—60 d group from day 1 to day 6. On day 7, when platform was removed, these mice spent maximum time in target quadrant similar to control PBS–PBS—60 d mice, showing the cognitive improvement after 60 days of 50,000 Lin −ve stem cells transplantation.

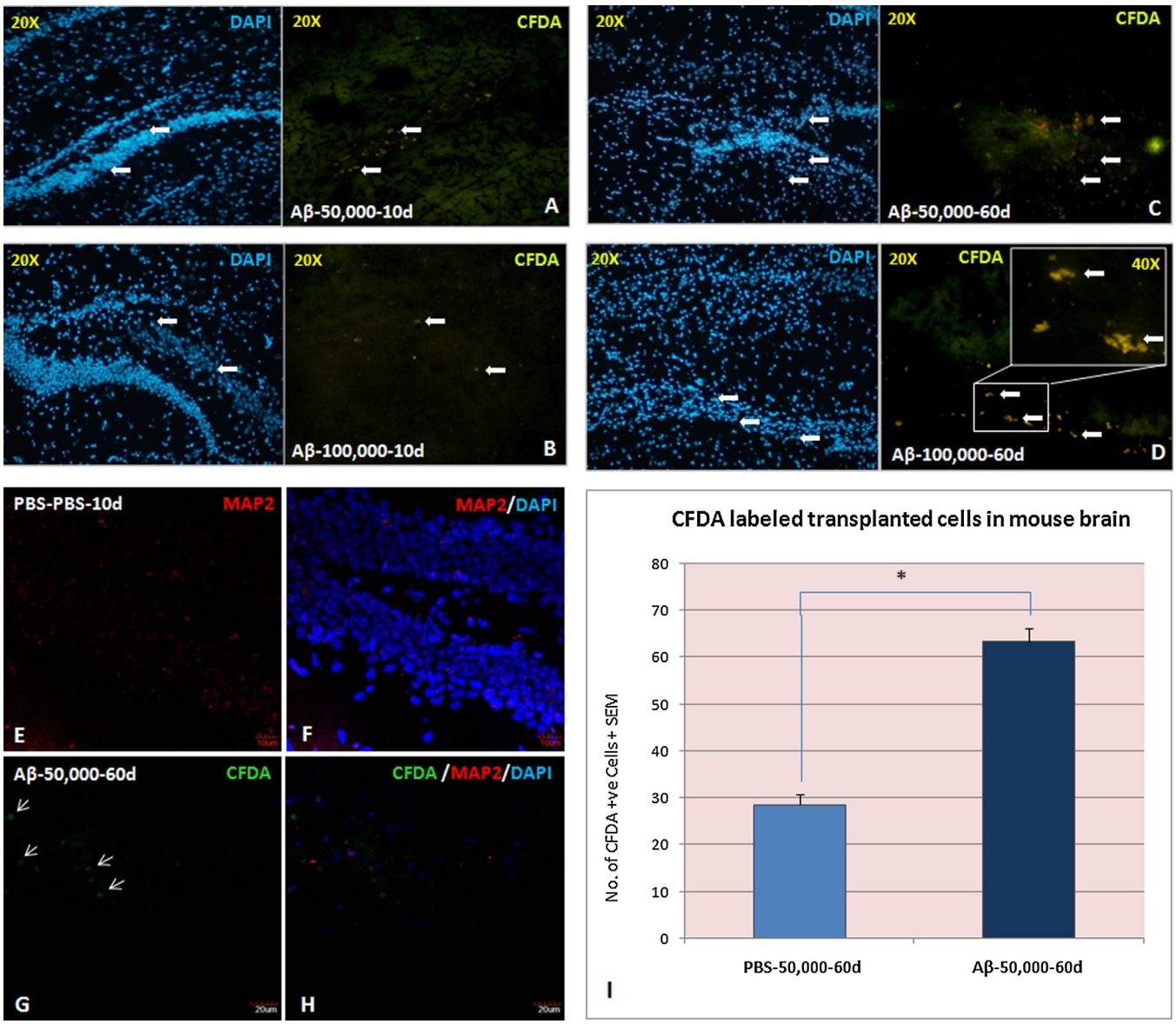


Fig. 5. *CFDA labeled transplanted Lin −ve stem cells in hippocampal sections of different stem cell transplanted groups.* (A) Aβ-50,000—10 d brain section showed presence of CFDA labeled Lin −ve cells in the dentate gyrus (DG) region. B) CFDA +ve cells were also identified in Aβ-100,000—10 d mouse hippocampus. (C) Aβ-50,000—10 d brain showed maximum numbers of CFDA +ve cells in DG layer and they were found to be incorporated along with the host cells. (D) In Aβ-100,000—60 d brain these cells were found to be aggregated in clusters of cells without being incorporated in the host tissue. All the corresponding sections (blue) left to individual group shows DAPI stained nucleuses. (E) MAP2 positive mouse neuronal cells (red) were identified in hippocampal layers in PBS–PBS—10 d (control) brain section. (F) Corresponding merged image with DAPI showing nuclear stain along with MAP2 markers. (G) CFDA +ve transplanted cells (green) were identified in Aβ-50,000—10 d mouse hippocampus. (H) Co-staining of MAP2 positive host neurons (red) and CFDA +ve transplanted cells (green) were identified in the brain section. (I) Quantitative analysis of CFDA +ve transplanted cells in brain sections. All results expressed as mean ± S.E.M. Data statistically analyzed using SPSS 16.0 by *T* test. * $p < 0.001$. (For interpretation of the references to color in this figure legend, the reader is referred to the web version of this article.)

Lin −ve cells and their pattern of distribution in the brain tissue. A significant number of CFDA labeled Lin −ve cells were identified in Aβ-50,000—60 d mouse brains in comparison to PBS-50,000—60 d mice (Fig. 5I). The confocal imaging revealed that these CFDA labeled transplanted cells were found to be co-localized with the host cells (MAP2 +ve) in the layers of hippocampus (Fig. 5G and H). Transplanted cells were found to be aggregated in Aβ-100,000—60 d mouse brains, without being incorporated in the host hippocampus (Fig. 5D). Immunolocalization of different neuronal markers viz., Nestin, GFAP and O4 and their molecular expression analyzed by RT-PCR, in cell transplanted brains revealed that these cells were not differentiated even after 60 days of transplantation (data not shown). The results also showed that a large number of transplanted cells tend to form aggregates in the long term, in a diseased brain.

3.6. Down-regulation of apoptotic marker Fas-L in cell transplanted brain

To analyze the molecular basis of behavioral improvement noted in MWM, the mouse brain sections from different groups were immunostained for Fas-L apoptotic expression. Fas-L expression was found to be down regulated in Aβ-50,000—60 d mouse brain, showing remarkable reversal of attenuated Fas-L when

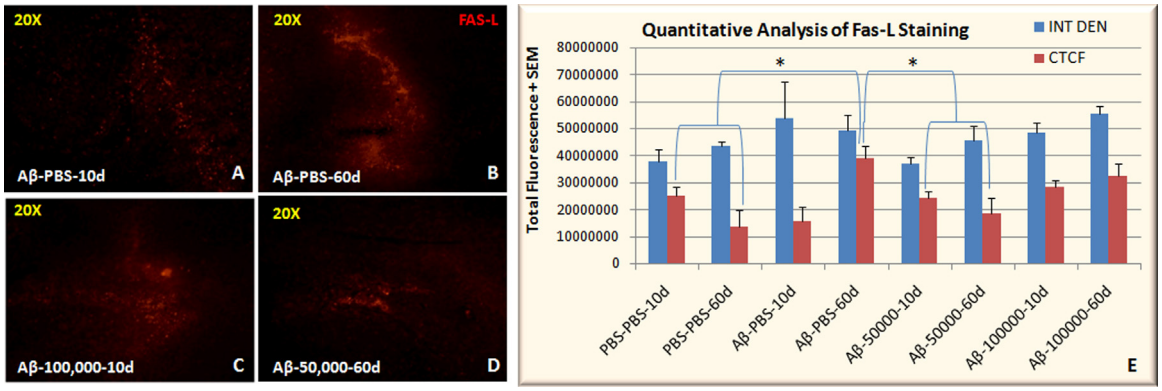


Fig. 6. *Expression of Fas-L in brain sections of representative Aβ injured and stem cell transplanted groups.* (A) Expression of Fas-L in Aβ-PBS—10 d group showing presence of apoptotic cells at the site of injection. (B) Higher Fas-L +ve apoptotic cells were observed in Aβ-PBS—60 d group. (C) This expression was not changed in Aβ-100,000—10 d group. (D) The expression was found to be significantly down-regulated in Aβ-50,000—60 d time point when compared to only Aβ injured mice. (E) Quantitative expression of total cell fluorescence from different groups showing down-regulated Fas-L expression in Aβ-50,000—60 d group. *Y* axis measures mean total fluorescence (INT DEN) and normalized fluorescence (CTCF) from multiple sections. Data was analyzed in ImageJ software using SPSS 16.0 by univariate ANOVA. Follow-up comparisons were made using LSD test. * $p \leq 0.05$, $F = 3.766$ for CTCF. INT DEN: integrated density; CTCF: corrected total cell fluorescence.

compared with Aβ-PBS—60 d brain sections. This expression was found to be relatively higher in Aβ-100,000—10 d group (Fig. 6).

3.7. Up-regulation of CREB and BDNF after transplantation of hUCB Lin −ve cells

Whole brain tissue from all the experimental groups was used for biochemical estimation of CREB and BDNF. The expression was estimated in all the brain homogenates using ELISA kits for CREB and BDNF and all the values were normalized to their corresponding total protein concentrations. The CREB expression was found to be significantly up-regulated in Aβ-50,000—60 d mouse brains as compared to Aβ-100,000—10 d or Aβ-100,000—60 d groups (Fig. 7A). BDNF expression was found to be unaltered in all the brain homogenates among different Aβ injured and cell transplanted groups (Fig. 7B) (df = 11; $p < 0.05$, $F = 3.077$ for CREB; $p = 0.67$, $F = 2.478$ for BDNF). Interestingly, when BDNF expression was analyzed at mRNA level, the molecular analysis showed its up-regulation in the Aβ-50,000—60 d mouse brains when compared to other stem cell transplanted groups (Fig. 7C) (df = 11, $p = 0.623$, $F = 0.831$).

4. Discussion

We have examined the effect of intra-hippocampal delivery of Aβ on mouse neuronal degeneration as evaluated by MWM analysis, immunostaining, molecular and biochemical expression. Transplantation of Lin −ve stem cells in these mice showed significant reversal of impaired spatial memory in a specific cell dose group. Aβ-50,000—60 d group showed best recovery from memory loss as compared to other groups with different cell doses and time intervals. The transplanted cells were found to be co-localized with the host tissue without being differentiated to neuronal lineage and also found to down-regulate the Fas-L mediated neural toxicity induced by Aβ delivery. Further, biochemical and molecular studies revealed that CREB and BDNF were also significantly up-regulated in Aβ-50,000—60 d mouse brains when compared to other cell transplanted groups.

The transgenic models of AD may not always carry the true pathology of disease as the target gene is induced under forceful mutation. Even the transgenic mouse models for AD do not exhibit the most common sporadic nature of the disease, rather represent rarer familial mutations. Overall, no animal model is able to reproduce disease onset, progression, and relapse, reminiscent of human AD. Hence we have chosen the Aβ induced neurotoxicity model which is the most common pathological features in AD. There are several groups demonstrating the toxic effect of different form of Aβ aggregates in mice leading to selective neuronal loss and cognitive impairment [37,38]. de Oliveira et al. have reported localized neuroinflammation, oxidative stress and neuronal loss followed by memory impairment in C57BL/6 mice upon acute intracerebroventricular injection of aggregated form of Aβ-40 peptide in the hippocampus [37].

Cell survival mechanisms are key to understand the pathophysiology for several neurodegenerative diseases. Therefore, we have validated the role of neurotrophins and apoptotic factors in short-term and long-term memories which are mediated by chemical changes inside the cells. These changes in neurons lead to secretion of a series of neurotransmitting factors (like acetyl choline, glutamate or Ca^{2+} etc.) in pre-synaptic spaces. These molecules act as messenger molecules which bind to the post-synaptic receptors of the neurons. Any disruption in neurotransmitter generation at pre synaptic neuron, binding to their receptors at post-synaptic neuron or degeneration of neurons can hamper the signal transmission from target tissue to the CNS or vice versa. Such attenuated signal transmission can retard the cognitive activity of an individual or experimental animal and may depend on BDNF, CREB or Fas-L. Impaired cognitive function being the common hallmark for AD is often ascribed to degeneration of neurons which may be induced by protein aggregates in extra-cellular matrix (ECM) like tau protein, Aβ-amyloid protein or oxidative stress. There are several strategies which have been applied to validate and screen potential therapeutic agents for the treatment of AD targeting disease pathology instead of symptomatic relief alone. In last two decades different cell replacement therapies were extensively tested on animal models in order to attenuate pathophysiological and behavioral burden of AD. Our study demonstrates, for the first time, that Lin −ve stem cells, one of the primitive population found in hUCB, can ameliorate AD related cognitive impairment and Aβ induced neuronal degeneration in a mouse model.

The increased immunoreactivity for Fas-L noted in Aβ injected brains suggests enhanced neuronal cell death accounting for learning deficits. Recently, it has been reported that Aβ induced neuronal apoptosis is mediated by increased ROS production [39]. Postmortem study in AD patients also revealed increased Fas expression and Fas-L immunoreactivity on reactive astrocytes in frontal and hippocampus region, especially in tangle-bearing and non-tangle-bearing neurons [40]. The 50,000 cell dose mediated downregulation of Fas-L after 60 days of transplantation in Aβ

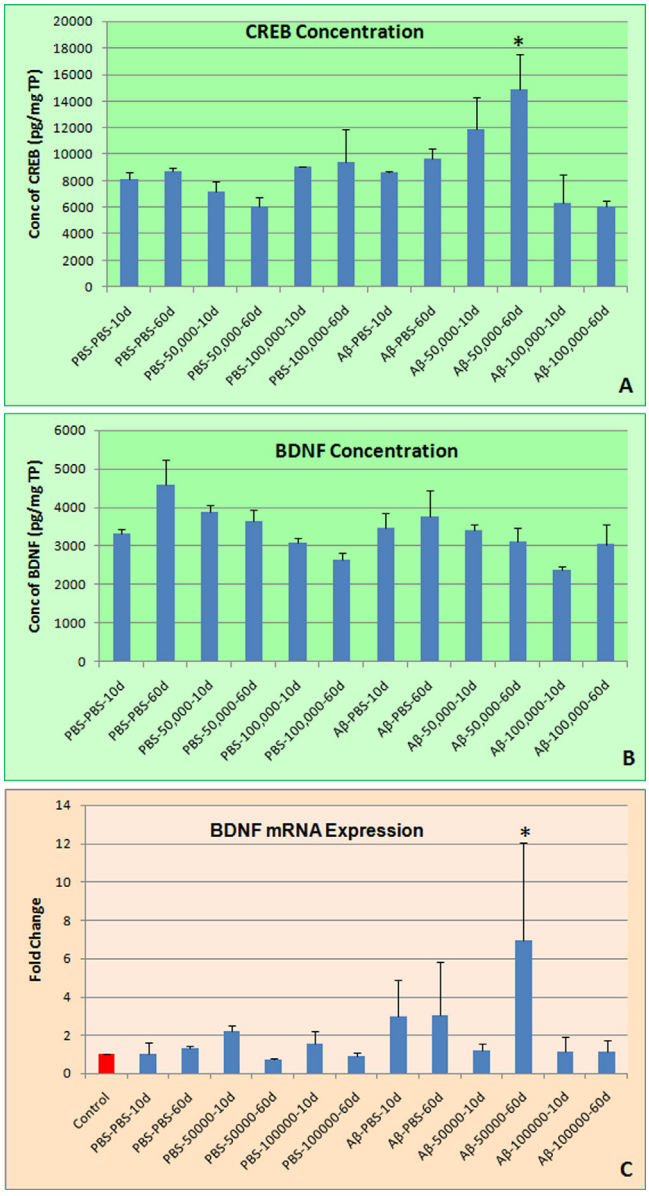


Fig. 7. *Biochemical (A and B) and molecular expression (C) of BDNF and CREB in Aβ injured and stem cell transplanted groups.* (A) CREB level was found to be significantly up-regulated in brain homogenates of Aβ-50,000—60 d group when compared to Aβ-100,000—10 d or Aβ-100,000—60 d groups. $p < 0.05$, $F = 3.077$. (B) No significant difference in BDNF level was found in brain homogenates among different cell dose groups. $p = 0.67$, $F = 2.478$. Absorbance measured in triplicate at 450 nm. All the values were normalized with their respective total protein concentration. (C) Significant increase in fold expression of BDNF mRNA in Aβ-50,000—60 d group was found as compared to other cell dose groups. $p = 0.623$ ($p < 0.05$ between Aβ-50,000—60 d and other Aβ-cell transplanted groups), $F = 0.831$. All the values were normalized with their respective β-actin expression. Data was analyzed using SPSS 16.0 by repeated measures ANOVA. Follow-up comparisons were made using LSD test.

injured brain suggests that these transplanted cells offer neuroprotection to host cells undergoing apoptosis augmenting reversal of cognitive impairment. In a similar study, intra-hippocampal transplantation of bone marrow derived mesenchymal stem cells, when transplanted in Aβ induced AD model, showed cognitive improvement by inhibiting oxidative stress induced apoptosis in mouse hippocampus [41]. In intracerebroventricular transplantation studies it is also evident that needle injury due to stereotaxic injection may induce damage of neuronal cells and also attract the transplanted cells along the needle tract surrounding the site of injury [11]. Therefore, it is pertinent to mention that needle induced cell death should be also considered in pathological outcomes of these cell transplantation studies. Hence we have included two control groups viz., PBS injected and Stem cell injected group in our study without exposing them to Aβ injury. These mice did not show any significant behavioral changes due to needle injury in MWM when compared to absolute healthy control (data compared with control group from our previously published study) [42]. In our study the Aβ load was found to be unaltered in all the stem cell transplanted groups even after 60 days. It is postulated that these transplanted cells do not play a redundant role in cell survival either mediated by alleviation of ROS production or other neuromodulatory mechanisms which are independent of Aβ dissolution. It is possible that sequestration of soluble Aβ results in improved cognitive decline. In this context it is compelling to refer to a study which showed that Aβ immunization in a transgenic AD model led to amelioration of memory deficits without altering the Aβ burden proposing that this must have been mediated by sequestration of soluble forms of Aβ peptides, something we did not examine in this study [43].

The role of CREB, however, remains well documented in the formation of spatial memory and its consolidation into long term memory [44]. It is one of the important cellular transcription factors regulating the expression of several genes like, c-fos, tyrosine hydroxylase, several neuronal peptides and importantly, neurotrophin BDNF which is involved in the mammalian memory mechanisms [45]. These gene expression profiles are activated through CREB, mediated by Ca^{2+}, protein kinase A (PKA) and activation of cAMP [46–48]. Studies show that up-regulation of CREB enhances both short-term and long-term memory in mice [49]. Therefore, enhanced CREB expression in 50,000 cell transplanted group suggests its non redundant role in behavioral improvement confirming it as an important target for cell replacement therapy. The role of BDNF is also well described in AD literature. Several studies have demonstrated the neuroprotective effect of BDNF in Aβ induced neurotoxicity in cultured neurons [50–53]. Enhanced BDNF expression was found to be protective against apoptotic cells in APP/PS1 double transgenic mouse model of AD [54]. Even in the postmortem brains of AD patients, BDNF levels were found to be decreased when compared to the healthy controls [55–58]. From these findings, the therapeutic role of BDNF in rescuing the spatial memory in Aβ injured mice becomes worth further investigation. As CREB is a known factor for regulation of BDNF expression in mammalian brain, it is, therefore, possible that up-regulation of BDNF and CREB activity cooperatively enhances learning and retrieval [59–61].

Our results reveal that Aβ injury alone did not alter the levels of BDNF and CREB in mouse brains but in Aβ-50,000—60 d brains their levels were found to be upregulated when compared to PBS injected control brains. Interestingly, this upregulation in BDNF and CREB was not found in stem cell transplanted brain without Aβ injury (PBS-50,000—10 d and PBS-50,000—60 d groups). Our data illustrates that Aβ injury alone could not exert any effect on the expression level of BDNF and CREB but there could be a possibility that this injury stimulates the transplanted cells in a manner to upregulate BDNF and CREB in cell transplanted brains. Further, these cells could not exert similar effect when transplanted alone in mouse brains without any injury. Hence it is relevant to mention that injury play a critical role to facilitate some paracrine effects induced by the transplanted stem cells in a disease brain. Moreover, it is reported earlier that decreased levels of neurotrophins after traumatic brain injury in rat go back to their normal level (compared to sham control) after 24 h of injury in their cortical neurons [62]. As we estimate the levels of BDNF and CREB after 31 and 81 days of injury, it could be possible that the early effects of Aβ injury on these neurotrophins might have stabilized over time.

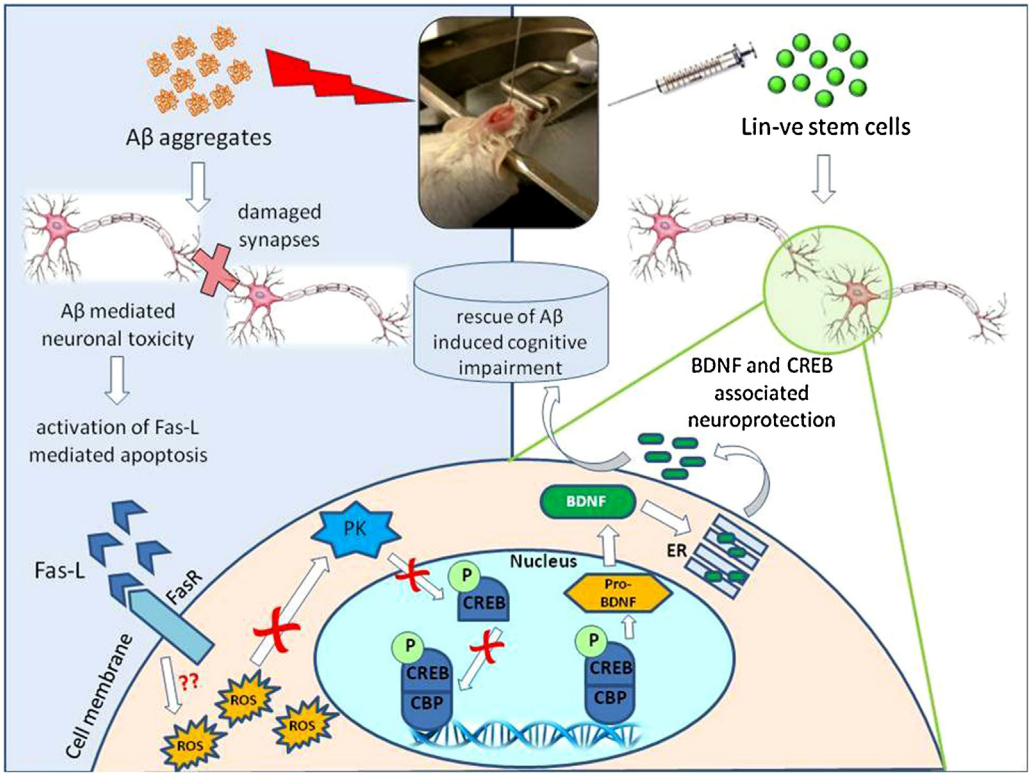


Fig. 8. Proposed mechanism of action in Lin −ve stem cell mediated reversal of Aβ induced neuronal cell death and cognitive impairment.

On the other hand, in water maze task, lower dose of cells (50,000) was ineffective at 10 days but effective at 60 days post-transplantation, whereas this effect was found to be reversed in higher dose (100,000). The inability of 50,000 cells at 10 days and 100,000 cells at 60 days to improve spatial memory could be accounted for unaltered expression of BDNF and CREB levels. Why these doses fail to restore lost memories raises additional research questions which we are unable to explain. However, it can be concluded that the optimal effect of stem cells remain highly dependent on dose and time of transplantation which needs to be carefully factored in planning additional experimental studies. In this respect it is pertinent to cite Darsalia et al. study which showed the effect of number and time of transplanted cells which triggers their survival in stroke induced rat brains. This is mediated by differential cell migration magnitude, neuronal differentiation and cell proliferation in the grafted region. The higher number of transplanted cells did not show greater cell survival or neuronal differentiation [63]. We propose that lower dose of cells could not sufficiently mount a therapeutic effect at an early time point which a higher dose of cells could achieve whereas higher number of transplanted cells possibly form aggregates at later time point which is not the case in lower cell dose. Likewise, higher cell dose at later time point possibly provoke immunomodulatory response, as these cells are derived from human origin, rendering them ineffective in the rescue of Aβ induced neurodegeneration, which the lower dose of cells are protected from.

Regardless of the absence of convincing evidence underlying the mechanisms of rescue of memory deficits, the study unambiguously reveals that Lin −ve stem cells, consisting of endothelial progenitor cells, isolated from hUCB have potential to reverse Aβ induced cognitive impairment through a neuroprotective mechanism mediated by CREB and BDNF (Fig. 8). Furthermore, our study also strengthens the need to explore other sub sets of hUCB besides examining the preclinical effects of cryo-preserved cord blood. Additional approaches may include investigating the effect of other doses, routes and cell type comparisons with other non hUCB cell types with varying severity of injuries. Future studies may focus not only on associated functional molecular links of hippocampal BDNF and CREB, resulting from hUCB transplantation but also the effects of their supplementation on cognitive improvement, using knock out animals and si RNA approach.

Author contributions

Writing and editing of manuscript was done by Avijit Banik and Akshay Anand. Conceptualization of the project was done by Akshay Anand and data acquisition was done by Avijit Banik. UCB samples were taken in cooperation with Jasvinder Kalra and the work was co-supervised by Sudesh Prabhakar.

Conflict of interest statement

The authors declare no competing financial interests and compliance to ICMJE guidelines. The corresponding author declares that he had full access to all the data in the study and takes responsibility for the integrity of the data and the accuracy of the data analysis as well as the decision to submit for publication.

Acknowledgements

We thank the Indian Council for Medical Research, New Delhi, India for funding this project through Senior Research Fellowship program (grant no. 81/6/2009-BMS) and Mr. Sumit Rana for Quality Assurance and blinding of experiments and Prof. Suresh Sharma for conducting statistical analysis.

References

[1] Thies W, Bleiler L. Alzheimer's disease facts and figures. Alzheimers Demen 2013;9:208–45.

[2] ARDSI. The dementia India report. Prevalence, impact, costs and services for dementia. Alzheimer's & Related Disorders Society of India (ARDSI); 2010.
[3] Massoud F, Gauthier S. Update on the pharmacological treatment of Alzheimer's disease. Curr Neuropharmacol 2010;8:69–80.
[4] Tiraboschi P, Hansen LA, Thal LJ, Corey-Bloom J. The importance of neuritic plaques and tangles to the development and evolution of AD. Neurology 2004;62:1984–9.
[5] O'Brien RJ, Resnick SM, Zonderman AB, Ferrucci L, Crain BJ, Pletnikova O, et al. Neuropathologic studies of the Baltimore Longitudinal Study of Aging (BLSA). J Alzheimers Dis 2009;18:665–75.
[6] Herrup K, Carrillo MC, Schenk D, Cacace A, Desanti S, Fremeau R, et al. Beyond amyloid: getting real about nonamyloid targets in Alzheimer's disease. Alzheimers Demen 2013;9, 452.e1- 458.e1.
[7] Sudduth TL, Schmitt FA, Nelson PT, Wilcock DM. Neuroinflammatory phenotype in early Alzheimer's disease. Neurobiol Aging 2013;34:1051–9.
[8] Davis RC, Marsden IT, Maloney MT, Minamide LS, Podlisny M, Selkoe DJ, et al. Amyloid beta dimers/trimers potently induce cofilin-actin rods that are inhibited by maintaining cofilin-phosphorylation. Mol Neurodegener 2011; 6:10.
[9] Annunziata I, Patterson A, Helton D, Hu H, Moshiach S, Gomero E, et al. Lysosomal NEU1 deficiency affects amyloid precursor protein levels and amyloid-beta secretion via deregulated lysosomal exocytosis. Nat Commun 2013;4: 2734.
[10] Anand A, Banik A, Thakur K, Masters CL. The animal models of dementia and Alzheimer's disease for pre-clinical testing and clinical translation. Curr Alzheimer Res 2012;9:1010–29.
[11] Tang J, Xu H, Fan X, Li D, Rancourt D, Zhou G, et al. Embryonic stem cell-derived neural precursor cells improve memory dysfunction in Abeta(1–40) injured rats. Neurosci Res 2008;62:86–96.
[12] Hu Y, Wen Q, Liang W, Kang T, Ren L, Zhang N, et al. Osthole reverses beta-amyloid peptide cytotoxicity on neural cells by enhancing cyclic AMP response element-binding protein phosphorylation. Biol Pharm Bull 2013;36:1950–8.
[13] Prakash A, Kumar A. Role of nuclear receptor on regulation of BDNF and neuroinflammation in hippocampus of beta-amyloid animal model of Alzheimer's disease. Neurotox Res 2014;25:335–47.
[14] Taguchi A, Soma T, Tanaka H, Kanda T, Nishimura H, Yoshikawa H, et al. Administration of CD34+ cells after stroke enhances neurogenesis via angiogenesis in a mouse model. J Clin Invest 2004;114:330–8.
[15] Nikolic WV, Hou H, Town T, Zhu Y, Giunta B, Sanberg CD, et al. Peripherally administered human umbilical cord blood cells reduce parenchymal and vascular beta-amyloid deposits in Alzheimer mice. Stem Cells Dev 2008;17: 423–39.
[16] Kao CH, Chen SH, Chio CC, Lin MT. Human umbilical cord blood-derived CD34+ cells may attenuate spinal cord injury by stimulating vascular endothelial and neurotrophic factors. Shock 2008;29:49–55.
[17] Bjorklund A, Lindvall O. Cell replacement therapies for central nervous system disorders. Nat Neurosci 2000;3:537–44.
[18] Chen WW, Blurton-Jones M. Concise review: can stem cells be used to treat or model Alzheimer's disease? Stem Cells (Dayton, Ohio) 2012;30:2612–8.
[19] Wang Q, Matsumoto Y, Shindo T, Miyake K, Shindo A, Kawanishi M, et al. Neural stem cells transplantation in cortex in a mouse model of Alzheimer's disease. J Med Invest 2006;53:61–9.
[20] Blurton-Jones M, Kitazawa M, Martinez-Coria H, Castello NA, Muller FJ, Loring JF, et al. Neural stem cells improve cognition via BDNF in a transgenic model of Alzheimer disease. Proc Natl Acad Sci USA 2009;106:13594–9.
[21] Zhang W, Wang PJ, Sha HY, Ni J, Li MH, Gu GJ. Neural stem cell transplants improve cognitive function without altering amyloid pathology in an APP/PS1 double transgenic model of Alzheimer's disease. Mol Neurobiol 2014;50:423–37.
[22] Lee HJ, Lee JK, Lee H, Carter JE, Chang JW, Oh W, et al. Human umbilical cord blood-derived mesenchymal stem cells improve neuropathology and cognitive impairment in an Alzheimer's disease mouse model through modulation of neuroinflammation. Neurobiol Aging 2012;33:588–602.
[23] Darlington D, Deng J, Giunta B, Hou H, Sanberg CD, Kuzmin-Nichols N, et al. Multiple low-dose infusions of human umbilical cord blood cells improve cognitive impairments and reduce amyloid-beta-associated neuropathology in Alzheimer mice. Stem Cells Dev 2013;22:412–21.
[24] Yang H, Yang H, Xie Z, Wei L, Bi J. Systemic transplantation of human umbilical cord derived mesenchymal stem cells-educated T regulatory cells improved the impaired cognition in AbetaPPswe/PS1dE9 transgenic mice. PLoS ONE 2013;8:e69129.
[25] Bhatia M, Bonnet D, Murdoch B, Gan OI, Dick JE. A newly discovered class of human hematopoietic cells with SCID-repopulating activity. Nat Med 1998;4:1038–45.
[26] Gallacher L, Murdoch B, Wu DM, Karanu FN, Keeney M, Bhatia M. Isolation and characterization of human CD34(−)Lin(−) and CD34(+)Lin(−) hematopoietic stem cells using cell surface markers AC133 and CD7. Blood 2000;95: 2813–20.
[27] Singh T, Prabhakar S, Gupta A, Anand A. Recruitment of stem cells into the injured retina after laser injury. Stem Cells Dev 2012;21:448–54.
[28] Jaatinen T, Laine J. Isolation of hematopoietic stem cells from human cord blood. Curr Protoc Stem Cell Biol 2007, http://dx.doi.org/10.1002/9780470151808.sc02a02s1 (Chapter 2:Unit 2A).
[29] Forraz N, Pettengell R, McGuckin CP. Characterization of a lineage-negative stem-progenitor cell population optimized for ex vivo expansion and enriched for LTC-IC. Stem Cells (Dayton, Ohio) 2004;22:100–8.
[30] Jawad M, Cole C, Zanker A, Giotopoulos G, Fitch S, Talbot CJ, et al. QTL analyses of lineage-negative mouse bone marrow cells labeled with Sca-1 and c-Kit. Mamm Genome 2008;19:190–8.
[31] Preffer FI, Dombkowski D, Sykes M, Scadden D, Yang YG. Lineage-negative side-population (SP) cells with restricted hematopoietic capacity circulate in normal human adult blood: immunophenotypic and functional characterization. Stem Cells (Dayton, Ohio) 2002;20:417–27.
[32] Rutella S, Bonanno G, Marone M, De Ritis D, Mariotti A, Voso MT, et al. Identification of a novel subpopulation of human cord blood CD34–CD133–CD7–CD45 + lineage-cells capable of lymphoid/NK cell differentiation after in vitro exposure to IL-15. J Immunol 2003;171: 2977–88.
[33] Greschat S, Schira J, Kury P, Rosenbaum C, de Souza Silva MA, Kogler G, et al. Unrestricted somatic stem cells from human umbilical cord blood can be differentiated into neurons with a dopaminergic phenotype. Stem Cells Dev 2008;17:221–32.
[34] Zeng F, Chen MJ, Baldwin DA, Gong ZJ, Yan JB, Qian H, et al. Multiorgan engraftment and differentiation of human cord blood CD34+ Lin-cells in goats assessed by gene expression profiling. Proc Natl Acad Sci USA 2006;103:7801–6.
[35] Franklin K, Paxinos G. The mouse brain in stereotaxic coordinates. 3rd ed. Amsterdam: Elsevier; 2008.
[36] Mazzola C, Micale V, Drago F. Amnesia induced by beta-amyloid fragments is counteracted by cannabinoid CB1 receptor blockade. Eur J Pharmacol 2003;477:219–25.
[37] de Oliveira J, Moreira EL, dos Santos DB, Piermartiri TC, Dutra RC, Pinton S, et al. Increased susceptibility to amyloid-beta-induced neurotoxicity in mice lacking the low-density lipoprotein receptor. J Alzheimers Dis 2014;41: 43–60.
[38] Lee DS, Choi J, Kim SH, Kim S. Ameliorating effects of HX106N, a water-soluble botanical formulation, on Abeta25–35-induced memory impairment and oxidative stress in mice. Biol Pharm Bull 2014;37:954–60.
[39] Bashir M, Parray AA, Baba RA, Bhat HF, Bhat SS, Mushtaq U, et al. beta-Amyloid-evoked apoptotic cell death is mediated through MKK6-p66shc pathway. Neuromolecular Med 2014;16:137–49.
[40] Ferrer I, Puig B, Krupinsk J, Carmona M, Blanco R. Fas and Fas ligand expression in Alzheimer's disease. Acta Neuropathol 2001;102:121–31.
[41] Lee JK, Jin HK, Bae JS. Bone marrow-derived mesenchymal stem cells attenuate amyloid beta-induced memory impairment and apoptosis by inhibiting neuronal cell death. Curr Alzheimer Res 2010;7:540–8.
[42] Banik A, Anand A. Loss of learning in mice when exposed to rat odor: a water maze study. Behav Brain Res 2011;216:466–71.
[43] Dodart JC, Bales KR, Gannon KS, Greene SJ, DeMattos RB, Mathis C, et al. Immunization reverses memory deficits without reducing brain Abeta burden in Alzheimer's disease model. Nat Neurosci 2002;5:452–7.
[44] Silva AJ, Kogan JH, Frankland PW, Kida S. CREB and memory. Annu Rev Neurosci 1998;21:127–48.
[45] Martin SJ, Grimwood PD, Morris RG. Synaptic plasticity and memory: an evaluation of the hypothesis. Annu Rev Neurosci 2000;23:649–711.
[46] Jensen KF, Ohmstede CA, Fisher RS, Sahyoun N. Nuclear and axonal localization of Ca^{2+}/calmodulin-dependent protein kinase type Gr in rat cerebellar cortex. Proc Natl Acad Sci USA 1991;88:2850–3.
[47] Matthews RP, Guthrie CR, Wailes LM, Zhao X, Means AR, McKnight GS. Calcium/calmodulin-dependent protein kinase types II and IV differentially regulate CREB-dependent gene expression. Mol Cell Biol 1994;14: 6107–16.
[48] Nakamura Y, Okuno S, Sato F, Fujisawa H. An immunohistochemical study of Ca^{2+}/calmodulin-dependent protein kinase IV in the rat central nervous system: light and electron microscopic observations. Neuroscience 1995;68:181–94.
[49] Suzuki A, Fukushima H, Mukawa T, Toyoda H, Wu LJ, Zhao MG, et al. Upregulation of CREB-mediated transcription enhances both short- and long-term memory. J Neurosci 2011;31:8786–802 (The Official Journal of the Society for Neuroscience).
[50] Arancibia S, Silhol M, Mouliere F, Meffre J, Hollinger I, Maurice T, et al. Protective effect of BDNF against beta-amyloid induced neurotoxicity in vitro and in vivo in rats. Neurobiol Dis 2008;31:316–26.
[51] Holback S, Adlerz L, Iverfeldt K. Increased processing of APLP2 and APP with concomitant formation of APP intracellular domains in BDNF and retinoic acid-differentiated human neuroblastoma cells. J Neurochem 2005;95: 1059–68.
[52] Kitiyanant N, Kitiyanant Y, Svendsen CN, Thangnipon W. BDNF-, IGF-1- and GDNF-secreting human neural progenitor cells rescue amyloid beta-induced toxicity in cultured rat septal neurons. Neurochem Res 2012;37: 143–52.
[53] Tong L, Balazs R, Thornton PL, Cotman CW. Beta-amyloid peptide at sublethal concentrations downregulates brain-derived neurotrophic factor functions in cultured cortical neurons. J Neurosci 2004;24:6799–809 (The Official Journal of the Society for Neuroscience).
[54] Li N, Liu GT. The novel squamosamide derivative FLZ enhances BDNF/TrkB/CREB signaling and inhibits neuronal apoptosis in APP/PS1 mice. Acta Pharmacol Sin 2010;31:265–72.
[55] Fahnestock M, Garzon D, Holsinger RM, Michalski B. Neurotrophic factors and Alzheimer's disease: are we focusing on the wrong molecule. J Neural Transm Suppl 2002;62:241–52.
[56] Fumagalli F, Racagni G, Riva MA. The expanding role of BDNF: a therapeutic target for Alzheimer's disease. Pharmacogenomics J 2006;6:8–15.

[57] Peng S, Wuu J, Mufson EJ, Fahnestock M. Precursor form of brain-derived neurotrophic factor and mature brain-derived neurotrophic factor are decreased in the pre-clinical stages of Alzheimer's disease. J Neurochem 2005;93:1412–21.
[58] Siegel GJ, Chauhan NB. Neurotrophic factors in Alzheimer's and Parkinson's disease brain. Brain Res Brain Res Rev 2000;33:199–227.
[59] Hu YS, Long N, Pigino G, Brady ST, Lazarov O. Molecular mechanisms of environmental enrichment: impairments in Akt/GSK3beta, neurotrophin-3 and CREB signaling. PLoS ONE 2013;8:e64460.
[60] Lee Y, Kim J, Jang S, Oh S. Administration of phytoceramide enhances memory and upregulates the expression of pCREB and BDNF in hippocampus of mice. Biomol Ther (Seoul) 2013;21:229–33.
[61] Florczynski M. The effects of CREB-mediated BDNF expression on memory- and anxiety-related behaviours in the adult mouse. Toronto, Ontario: Institute of Medical Science, University of Toronto; 2012 (M.Sc. Thesis).
[62] O'Dell DM, Raghupathi R, Crino PB, Eberwine JH, McIntosh TK. Traumatic brain injury alters the molecular fingerprint of TUNEL-positive cortical neurons in vivo: a single-cell analysis. J Neurosci 2000;20:4821–8 (The Official Journal of the Society for Neuroscience).
[63] Darsalia V, Allison SJ, Cusulin C, Monni E, Kuzdas D, Kallur T, et al. Cell number and timing of transplantation determine survival of human neural stem cell grafts in stroke-damaged rat brain. J Cereb Blood Flow Metab 2011;31:235–42.

Critical Reviews™ *in Eukaryotic Gene Expression,* 24(3):255-268 (2014)

Cytoskeleton Dynamics in the Retina

Akshay Anand[1,*,**] Sridhar Bammidi[1,**] & Parul Bali[2]

[1]Department of Neurology, PGIMER, Chandigarh 160012, India; [2]Department of Biophysics, Panjab University, Chandigarh 160014, India

*** Address all correspondence to:** Akshay Anand, Associate Professor**,** Neuroscience Research Lab, Department of Neurology, PGIMER, Chandigarh- 16001; Tel.: +91-991429090; Email: akshay1anand@rediffmail.com.

**Both are first authors with equal contribution.

ABSTRACT: Background: Cytoskeleton is one of the essential forms of protein, important in the existence of both eukaryotic as well as prokaryotic cells. Its transformation plays a vital role in cell division and intracellular transportation by facilitating intracellular vesicular traffic. Among the various tissue types in the body, the neural tissue exhibits the maximum heterogeneity, and hence the role of cytoskeleton at both developmental and functional levels becomes paramount. Cytoskeleton dynamics have been established in the neural physiology, but only at the level of axonal development and growth. Retina has not been adequately studied in the context of cytoskeletal proteins. **Methods:** We reviewed the last 10 years of literature with reference to the development, growth, degeneration, and regeneration of the retina and the role of cytoskeleton in each aspect. We have focused on various changes that the retina undergoes at the cytosolic and cytoskeletal levels in the course of degeneration as well as regeneration. **Findings:** For this review, we compiled research articles pertaining to the role of cytoskeletal and other associated proteins involved in development of retina, which used various animal models. The effect of SNPs in the cytoskeletal proteins and their impact in retinal degeneration is also discussed. **Conclusion:** Studies describing the role of cytoskeleton in the anatomy and physiology of retina and its layers, although they are few, collectively provide an opportunity to understand retinal development in the context of cytoskeleton dynamics.

KEY WORDS: microtubule, intermediate filament, microfilament, cytoskeleton

I. INTRODUCTION

The anatomical, physiological, and functional aspects of life start from a single cell and can be best understood through study at the cellular level. The zygote, from the time of fertilization, undergoes a series of divisions, physiological and structural changes, and a vast array of differentiation and compartmentalization at both inter- and intracellular levels to reach its fate. Furthermore, these cellular mechanisms occur in a series of well-defined and accurate mechanisms of transcription and translation of protein macromolecules that govern physiological and phenotypic expression. The cytosol stores various codes for its behavior and metabolic activities such as migration, translocation, nutrition, phagocytosis, division, differentiation, and signaling. Codes in the form of proteins can express structurally as well as functionally. One of the essential forms of proteins that is of utmost importance in the existence of cell (whether eukaryotic or prokaryotic) is the cytoskeleton. The cytoskeleton forms the scaffold or skeleton at the cellular level in the cytoplasm of the cell. The cytoskeleton participates in a variety of activities of the cell. These involve the structural matrix of the individual cell and also in the cellular movement through cilia,[1] flagella,[2] and lamellipodia.[3] The cytoskeleton and its transformation play vital roles in cell division and intracellular transportation by facilitating intracellular vesicular traffic. The fact that the shape of different cell types is determined by the organization of a network of tubules (eventually termed cytoskeleton) was established by Nikolai Koltsov, in 1903. The term cytoskeleton (French: *cytosquelette*) was first introduced in 1931 by the French embryologist Paul Wintrebert. The association of cytoskeletal proteins with the plasma membrane and its rearrangement has a very interesting and well-elaborated role in cell locomotion,[4] translocation, and defense mechanisms of the

1045-4403/14/$35.00 © 2014 Begell House, Inc. www.begellhouse.com

cell, such as phagocytosis. The cytoskeleton has a well-defined role in spindle formation in cell division[5] and also in pili formation during conjugation of the prokaryotic cell.[6]

In the past two decades, researchers have investigated how the changes in the cell are governed by the changes and modifications in the cytoskeleton. The changes signify the overall reprogramming of the cell while differentiating in the course of tissue- or organ-level compartmentalization.[7] The various subtypes of the cell and the cellular organization, originating from the same germ layer, are largely influenced by their structural pattern, which again is governed by cytoskeletal proteins.[8] There has been increased emphasis on the role of cytoskeleton in the development, growth, and differentiation of the cell and its various types. The cytoskeleton and its ultra-structural complexities constitute not only the gross framework of a cell but also the localization and functioning of its organelles.[9]

There has been a recent re-emergence of emphasis on the concepts of neural cytoskeleton. The study of degeneration in the CNS and the neural niche throughout different organisms has exposed many myths about the nervous system. The dogma that the CNS consists of immutable neurons whose loss is permanent has been disproved by the advances in regeneration studies.[10] The present evidence clearly shows the presence and replacement of neurons in the organism throughout life, at different levels. Among the various tissue types in the body, the neural tissue exhibits the maximum heterogeneity,[11] and hence the role of cytoskeleton at both developmental and functional levels is very important. The polarization of the neuron, consisting of axonal and dendritic development and arrangement has a series of mechanical and biochemical cues in the rearrangement of the various cytoskeletal proteins.[12] The cytoskeleton plays a major role in the formation and disruption of the neural network, and in the formation, viability, and degeneration of the neurons.

The retina, with its well-defined layers, has been established as a good model with which to study the CNS, due to its common ectodermal origin. The neural retina is extensively studied for its nature, structure, function, and physiology and has been manipulated in various ways in studying the disease models.

This review focuses on the cellular arrangement of neural retina and the pattern of different cytoskeletal proteins participating in the development, disease, and regeneration of the retina.

II. COMPOSITION OF THE CYTOSKELETON

Neurocytoskeleton is the protein skeleton distributed throughout the cytoplasm that serves such functions such as providing mechanical strength, cell shape, morphology, locomotion, and transportation of organelle. Eukaryotic cells contain mainly three types of cytoskeleton filaments (microfilament, intermediate filament, and microtubule), which show dynamic behavior by their assembly and disassembly. Microfilaments are polymers of actin-forming bundles and three-dimensional structures. The assembly and disassembly of microfilament is regulated by the various actin-binding proteins. Intermediate filament, mainly type-VI nestin, expresses in dividing neuronal cells during development. Its expression is higher in neuronal stem cells and diminishes in adult neurons. In adulthood, the injury of CNS enhances expression of nestin.

Microtubule is the third component of cytoskeleton that is a polymer of tubulin protein. The neuronal morphology shows a distinct arrangement of microtubules. Axonal transportation requires the assistance of the microtubule-associated proteins kinesin and dynein. Kinesin is a coiled structure with globular head that interacts with microtubules to move toward the plus end while dynein moves toward the minus end. Both kinesin and dynein move opposite each other. Interruption in axonal transport due to mutation in these microtubule-associated proteins is the key player in mediating neuropathological states, as in the cases of Alzheimer's and Parkinson's disease.

On close observation of the micrograph of a cell, a dense disorganized network of filaments can be seen. There is a marked distinction in the regions of cell protrusions or in the junctions of

two adherent cells. These regions have filaments concentrated into bundles. These bundles further spread out into the interiors of cells as a network of filaments. Bundles and networks form the most common arrangements of cytoskeletal filaments in a cell. Bundles and networks structurally differ in the organization of filaments. The filaments are packed closely into arrays in bundles, which are arranged loosely in a crisscross in the case of networks. Networks further show planar (two-dimensional) or net-like arrangements as in nuclear and plasma membrane, and three-dimensional arrangements, which, for example, gives cytosol its gel-like properties. In each of these arrangements, the filaments are held together by various cross-linking proteins.

Actin filaments are responsible for the distinct shape of any cell. The organization of the actin filaments and their associated proteins that connect the microfilaments to the membrane govern the cell morphology. On attachment to a bundle of filaments, the membrane acquires the shape of a microvillus.

III. RETINA AS A MODEL FOR STUDYING THE CENTRAL NERVOUS SYSTEM

As an extension of the central nervous system, the retina, with its well-studied layers, provides a relatively simpler and convenient tool for investigating the complex central nervous system. Relatively, it can be easily manipulated from the outside (unlike brain), making it feasible to test the homing and regenerative potential of various types of stem cells, pharmacological compounds, and neurotropic factors. The common ectodermal origin of retina and brain during embryonic development makes retina an excellent experimental tool for studying the CNS. The similarity in cellular architecture of retina across various species of experimental organisms has further led to a wide range of organisms being used for retina-based investigations.

Mammalian retina is composed of seven distinct layers consisting of different neurons and glia: a ganglion cell layer, amacrine cells, bipolar cells and muller glia in inner nuclear layer that act as inter neurons, rod and cone photoreceptors in the photoreceptor layer (also considered the outer nuclear layer), and the retinal pigment epithelial layer. The axons of ganglion cells traverse through the optic nerve and connect to the visual cortex of the brain. These different and highly diverse cell types arise from the population of retinal progenitor cells, which are a population of quiescent and actively dividing cells. Recent research has sought to elucidate the mechanisms controlling the complex processes of neuronal differentiation from the same source.

IV. NEURONAL/AXONAL DEVELOPMENTAL CASCADE (FIG. 1)

The cytoskeleton plays a very vital role in neuronal development. The polarity of the neural cell is established by the activity and expression of various intermediate and associated proteins. Structurally, neurons have a polarized morphology with two types of processes, i.e., a long and slender axon and several short and tapered dendrites. Neurons are not in the polarized morphology in the course of their development. They are a result of asymmetrical cell division of the neural precursors, which is controlled by cytoskeleton.[13] The present understanding of the role and contribution of cytoskeleton-associated proteins in the cellular mechanisms is not enough. One of the examples that can best substantiate this fact is the structural proteins like tau, a microtubule-binding protein that has been extensively studied in the field of neurodegenerative diseases. Its molecular mechanisms and functions are well elaborated, but the function within the normal or diseased neurons has not yet been elucidated.[14,15] The study of cytoskeleton development in neurons can be best reviewed by examining the dynamics of axonal growth, although the available literature is relatively scarce. Axons, among all cell types, are the longest in mature and full-grown animals. Axons propagate (electrical) messages toward the synaptic connections in the target cells several meters away through the neuronal cell body. The unusual architecture of the axonal shafts is maintained by the bundles of parallel microtubules.

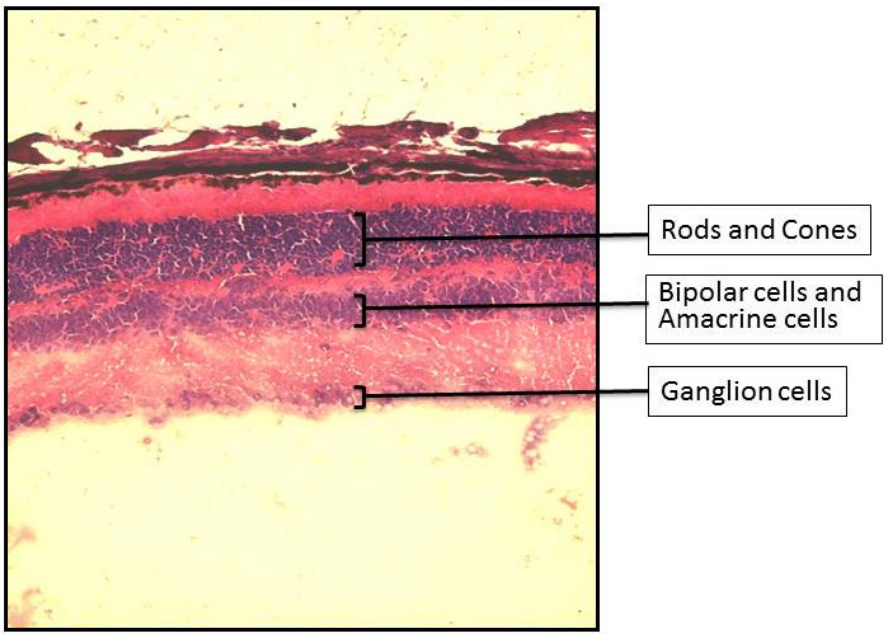


FIG. 1: Hematoxylin & Eosin stain of mouse eye cryosection

This provides support for structural and long-distance transport.[16] Microtubules in axons are not continuous and, unlike most cells, are not attached to the centrosome for their organization.[17] The plus ends of the microtubules mostly point distally.[18–20] Short actin filaments, organized by spectrin (scaffolding protein) into repetitive rings, line the cortex of axon shafts. This linkage to the axonal cell membrane is again brought about by a second set of proteins called ankyrins.[21] Ankyrins are the anchorage and nodal proteins which show robustness in maintaining the axonal integrity as discussed in the mouse model of cerebral hypoperfusion.[22] The specific size and shape (varying diameters) of the different classes of axons are regulated further by a number of intermediate filaments.[23] Axons have a very long span of life, and the dying neurons are a characteristic feature of the ageing brain.[24] Severe disorganization in the axonal microtubule bundles are believed to trigger the axonal loss.[25,26] The structural microtubule-binding proteins such as tau and MAP1B are believed to stabilize the axonal bundles.[27] Moreover, continuous polymerization of microtubules has been reported in mature axons, maintaining the steady turnover of microtubules.[28] The structural plasticity of neurons demonstrated by the shortening and lengthening,[29–31] the branching, the re-growth, and the axonal pruning that occurs for sizing the overgrowth,[32] are all important in the regeneration of the damaged neurons. This regeneration and its associated processes are very important in synapse formation related to learning and memory.[33,34] The formation of small neuritic protrusions on the neuronal cell bodies mark the onset of the formation of axons. The migration of microtubules by pushing beyond the cell body and the removal of barrier function is dynamically assisted by the rearrangement of the cortical actin cytoskeleton[35–37] and the formation of filopodia for extension of microtubules into the membrane.[38,39] In a vertebrate neuron, an axon is formed from the extension of a single neurite out of the many neurites formed on the cell body simultaneously. This selective process is termed neuron polarization, and it involves a signaling cascade of cell polarity factors for targeted and specific localization,[40] which also requires specificity of stabilization of microtubules of the selected neurite.[41,42]

After their establishment, axons follow a stereotype in growth toward their target cell. This process is generated and executed by growth cones at the axon tips. The spatio-temporal pattern of chemical signaling guides the growth cones toward their specific target tissue.[43] These guiding signals have been identified and well elaborated in their mechanism,[44,45] controlling the behavior of growth cone. The morphogenetic movements, such as growth velocity, pausing, turning, retraction or collapse downstream of guidance signaling, are achieved by the particular arrangement of growth cone actin and microtubule cytoskeleton.[46]

The growth cones can be divided into three different zones: the actin-rich peripheral zone; central zone, rich in microtubules; and the transition zone of microtubule and F-actin overlap. The microtubules spread into the peripheral zone starting from the center of the growth cones comprising the axonal tips. The peripheral zone consists of actin-rich membrane protrusions, which include finger-like filopodia and veil-like lamellipodia. Filopodia (containing parallel F-actin bundles) and lamellipodia (containing F-actin lattices), after guidance from the peripheral zone, present their receptors on their surface. The continuous aggregation and assembly of actin filaments at the leading edge constantly changes the shape. These filaments flow back in a reverse orientation, depolymerize, and recycle further in the transition zone. Filopodia then reach into the growth cone and behave as signaling and adhesion sensors.[47–50] The microtubule behavior in guided axon extension is essentially influenced by this series of events. Lamellipodia acts as site of substrate adhesion and myosin-II–driven contraction and force generation.

In another model of growth-cone guidance, the stabilization of the single microtubule in the peripheral zone is triggered by external signals,[51,52] which are further joined by a bulk of microtubules from the center, giving rise to a new axonal segment. The final step in elongation is the relocation of the lamellipodia and filopodia in the axon tip. Microtubules have a crucial role in the implementation of axon extension in this model, while the directionality of the extension is achieved by F-actin. Notably, therefore, the blocking of microtubule dynamics results in the inhibition of axonal growth.[53–55] On the other hand, the inhibition of actin polymerization either by pharmacological or by genetic approaches had no suppression of the axonal growth, *in vitro* or *in vivo*. Such interference showed some aberration in the turning and path-finding dynamics of the growth cone.[56,57–61] In this regard, it is interesting to note that the role of F-actin is not always essential in the directional movement of growth cones. Many signaling mechanisms are targeted to microtubules. Phosphorylation of some signaling molecules, like MTBPs APC1, MAP1B, and/or CLASP, mediated by GSK3 directly regulate the stability of microtubules in growth cones.[62–64]

The generation of neurons and their differentiation followed thereafter is regulated by a number of intrinsic and extrinsic factors. The proteins belonging to the basic helix–loop–helix (bHLH) family like Neurogenin 2 (Ngn2) or Mash (mammalian achaete-scute complex)-1 or Math (mammalian atonal homolog)-1 are some of the pro-neural genes reported in neurogenesis. These mechanisms are all regulated necessarily by an array of distinct signaling molecules like Notch signaling, transforming growth factor (TGF)-β/bone morphogenic protein (BMP) and fibroblast growth factor (FGF). The formation and generation of different types of neuronal types from their progenitors is regulated by regulatory proteins. The cell cycle is switched off to regulate number of cells post neurogenesis.[65] The regulation of cell cycle in this context is extremely important for the development of the nervous system. The patterning of neural tissue is determined by SRY (sex-determining region Y) box, Sox, and the Pax (paired box) family of proteins. Pax6 (a paired-box transcription factor), which is highly conserved among vertebrate development, is responsible for the overall patterning of the embryonic nervous system.[66] It directly regulates the expression of Ngn2 and also upregulates the expression of cell adhesion molecules as well as the cell-cycle inhibitors such as p27.[67] This eventually links together the differentiation and the withdrawal from the cell cycle. Again, the maintenance of

neural cells in the undifferentiated state is brought about by Sox1, Sox2, and Sox3 proteins via suppression of neurogenesis.[68]

Coordination of transcriptional program in the neurogenesis occurs also at the epigenetic level. The overexpression of HDAC4 (histone deacetylase) in granule neurons, shields them from apoptosis without undergoing the PI3K or ERK/MAPK pathways. The phenomenon of neuroprotection is brought about by blocking the abnormal progression of cell cycle by the inhibition of CDK1 (cell cycle kinase).[69]

The overall transcriptional programs and epigenetic regulation is mediated by signal transduction pathways. The signal transduction pathways are further regulated by the events in cell cycle. The essential role of Notch signaling in neurogenesis has been demonstrated both *in vitro*[70] and *in vivo*.[71] It inhibits the neural gene expression laterally, and hence limits the number of differentiating neurons. In vertebrate neurogenesis, the notch and delta signaling are restricted only to some stages in the events of cell cycle.[72]

V. THE GROWTH AND DIFFERENTIATION DYNAMICS

After exit from the cell, the generation of intricate networks of the microtubule in neurons and the extensions has to be brought about by a well-orchestrated differentiation program. This is also brought about by the timed entry and exit of the cell cycle. While studying the mutations in dynactin in a zebrafish model, a premature cell cycle exit and acceleration of neurogenesis was exhibited by the retinal progenitors. The cell signaling also governs cell fate. The defects in trafficking of Notch to the apical region of retinal progenitors has been reported in affecting the early cell fates at the expense of late ones.[73]

Neurons migrate to their functional location from the site of their origin via polarized movement of the cytoskeleton.[74] In the case of neurogenesis in the retina, a specific pattern is followed. During the development of the retina, retinal ganglion cells are the first to differentiate, then cones, followed by horizontal cells. After these, the rod cells and the amacrine cells are formed. The last cells to differentiate are the bipolar cells. Retinal neurons in mammals differentiate before birth.[75–77] Neurogenesis of retinal ganglion cells is determined intrinsically. A number of genes have been identified in this process of neurogenesis.[78] The deletion of Pax6, Barhl2, or Math5 reduces and/or blocks the differentiating RGCs in mice.[79, 81–83]

VI. CYTOSKELETAL PROTEINS IN THE RETINA AT DIFFERENT LEVELS

From the beginning, understanding the cell-fate specifications and mechanisms has remained a challenge in the study of retinal development. The Rho family plays a key role in cytoskeletal arrangements in the RPE in the TGF-β1–induced pathway. It has been demonstrated experimentally that treatment with TGF-β1 induces cytoskeleton reorganization, expression of α-SMA, an increase in the phosphorylation of ERK, Smad, AKT, and activation of Rac1 and RhoA. These mechanisms are inhibited by treatment with Rho inhibitors. TGF-β1 also increases LIMK and cofilin phosphorylation. Based on these observations, it has been well proposed and established that the cytoskeletal actin rearrangement in human RPE is induced by TGF-β1 via the Rho GTPase-dependent pathways modulating LIM kinase and cofilin activity.[84]

The role of cytoskeleton proteins can also be well elaborated in the phagocytosis mechanism of the RPE. The shed photoreceptor outer segments are phagocytosed by the cells of the RPE (retinal pigment epithelium) through a mechanism that involves αv integrins upstream of Rho GTPases and tyrosine kinases. Retinal pigment epithelial cells have the tendency to activate and redistribute Rac1, but they do not do the same with RhoA or Cdc42 during phagocytosis. The particle engulfment, in this case by the RPE, is prevented when dominant-negative Rac1 is overexpressed as well as when Rac1 expression is decreased. It has been further experimentally demonstrated that αvβ5 integrin and its ligand MFG-E8 (milk fat globule EGF factor-8), are required for the activation of

Rac1 during phagocytosis, but they do not involve the receptor tyrosine kinase MerTK. FAK inhibition hinders the tyrosine kinase signaling downstream of αvβ5 toward MerTK. This specific hindrance does not prevent Rac1 activation nor does it prevent the recruitment of F-actin during phagocytosis. Inhibition of Rac1 does not effect FAK or MerTK activation. Therefore, activation/recruitment of MerTK and F-actin via FAK and Rac1, respectively, require MFG-E8–ligated αvβ5 integrin. These pathways have independent activation and are essential for clearance phagocytosis. The major source of endothelin-1 (ET-1) at the blood retinal barrier is the retinal pigment epithelium (RPE). Thrombin can act on the RPE and can probably injure the blood retinal barrier. The activation of protein kinase C and the transient intracellular calcium mobilization brought about by thrombin probably play a minor role in endothelin-1 synthesis in the retinal pigment epithelium.[85]

The outgrowth of the neurites, and eventually the growth cone repulsion, are mediated by a member of the subfamily of cell adhesion molecules, i.e., protein tyrosine phosphatase (RPTP). PTPμ acts as a permissive substrate for the growth of retinal ganglion cell (RGC) neurites while it inhibits the growth of temporal retinal ganglion cells. In temporal neurons, Rac 1 acts as the regulating switch between the permissive and repulsive responses to PTPμ. For the repulsion of temporal neurons, Rac 1 needs to be inhibited. Being an inhibitor for nasal growth, the activity of Cdc42 is essential for both permissive and repulsive responses to PTPμ. However, inhibition of Rac1 activity is the key to PTPμ-dependent repulsion in temporal RGC neurons.[86]

Studies on the activity of actin/cofilin proteins have shown an active role in axonal extension[87–91] and have an implications in the regulation of neurotrophins on filopodial responses.[92,93] A recent study showed that the direct role of actin/cofilin proteins in response to bone morphogenic proteins displays growth-cone guidance in the spinal neurons of *Xenopus laevis.*[94] Another very important member of this group of molecules is the Rho family of GTPases. Of the various molecules amongst the small GTPase related to Rho, Rac1 is involved in the regulation of cytoskeletal dynamics and is critically involved in the development of neuron, axonal growth, and cell survival. Rac1 in its constitutively active form has been shown to promote the growth of axons in inhibitory environments of *in vivo*[95] as well as *in vitro*[96] models. It has been reported to promote survival *in vivo* as well.[97, 98] In studies involving the developing chick retina, NF-M, i.e., mid-size neurofilament[99–101] and a chick-specific MAP (microtubule associated protein), have been extensively studied to identify ganglion cells and ganglion precursor cells.[102] It has been demonstrated that the expression of MAP(RA4) and NF-M proteins in the chick retina is not restricted to ganglion cells alone as otherwise thought and accepted. Rather, it is established that these proteins are expressed transiently in a developmentally regulated manner by all neuronal retinal progenitors.[103] The Lim-kinase (LIMK) proteins essentially regulate the actin cytoskeleton. It is therefore believed that they control many processes, including cell cycling, cell integrity, migration and axonal guidance, during development.[104] The loss of LIMK1 resulted in defects in the neuronal growth cone, dendritic spines, and the organization of actin. These results were demonstrated by the different experiments *in-vitro* and *in-vivo* and resulted in abnormal long-term potentiation of the hippocampus and synaptic changes.[105] Glycogen synthase kinase (GSK3) regulates a large number of transcription factors, including β-catenin, c-Jun, and CREB (cAMP response element-binding protein), to name a few.[106] A study involving the regulation of transcription factors by GSK3β shows the involvement of kinase essentially in the pruning of developmental axon both *in vitro* and *in vivo.*[107] A wide range of cytoskeleton dynamics and several types of purinergic receptors are controlled by extracellular ATP. An intracellular Ca(2+) increase, induced by the ATP, follows cofilin rod formation. Cells that express another variant of cofilin (unphosphorylatable) do not exhibit ATP-induced cofilin rod formation. The formation of cofilin rods is induced by the calcineurin-dependent dephosphorylation of cofilin induced by the influx of Ca(2+)

through P2X receptors. This pathway may essentially elucidate how ATP effects development, degeneration, and injury of a neuron.[108]

VII. ROLE OF CYTOSKELETON IN NEURAL/ NEURONAL DEVELOPMENT IN ANIMAL MODELS

The study of neuronal polarity and synaptogenesis and associated proteins has been studied in *Drosophila, Caenorhabditis elegans, Xenopus*, and zebrafish models. A study of *Drosophila* demonstrated that when Cyfip, a cytoplasmic FMRP-interacting protein, is mutated, it inhibits the filamentous actin (F-actin) to assemble, which is a key regulating aspect of synaptogenesis. The study also proposed that Cyfip inhibits actin assembly as well, regulating the development of synapse as well as endocytosis.[109] Intraflagellar transport (IFT) is essential in developing the ciliated sensory outer segments (OS), which sequester a number of proteins in the vertebrate phototransduction machinery. Rho GTPases are essential regulators of cytoskeletal reorganization in the case of *Drosophila* as well. Cofilin is a protein responsible for the depolymerization of actin, very essential in the process of neurogenesis. It is regulated by the inhibition of LIM kinase and activation of Slingshot phosphatase. During Axon growth, the genetic analysis of the different pathways have revealed convergent and divergent pathways from Rho GTPases to the cytoskeleton achieved by biases in pathway selection.[110] In one of the experiments involving *Drosophila*, neuronal cells *in vitro* demonstrated that the regulation of cellular actin dynamics, the deficiency of pantothenatekinase (PANK), a catalyst that converts pantothenic acid to co-enzyme A, leads to abnormal organization in the F-actin. A reduction in in the activity of PANK up-regulates the phosphorylated form of cofilin, which is a conserved protein responsible for the severing of actin filament.[111]

However, the mechanism of the cytoskeletal proteins and the associated proteins/molecules have been studied in the *C. elegans* model. In a study using *C. elegans*, it was demonstrated that during axonal outgrowth, the Arp2/3 complex regulates the initiation of growth cone filopodia.[112] The axon guidance in *C. elegans* has been shown to be affected by UNC-115/abLIM and UNC-34/Enabled, which are actin modulatory proteins.[113–115] Enabled essentially regulates the formation of filopodia in neurons. It probably acts by blocking the actin-capping activity, resulting in long filament growth in filopodia.[116,117] Some other studies show that Enabled might express the anti-capping independent roles[118] involved in filopodia formation.[119] OSM-3, belonging to the family of homodimeric kinesin 2 motor, has an essential role in a few sensory cilia.[120,121] Kif17, a homologue for the OSM-3 gene in vertebrates, is known to be responsible for the trafficking of dendrites in neurons. Its role in the process of ciliogenesis has not yet been defined. Kif17 is widely expressed in the zebrafish nervous system and retina.[122] Sufficient evidence has proven the role of ADF (actin depolymerizing factor) and cofilin in the regulation of axonal growth and actin dynamics. The expression of ADF/cofilins is high in neuronal growth cones, especially in the areas where there is a high rate of actin disassembly.[123] Furthermore, the overexpression of these proteins in a *Xenopus* model showed a nearly 50% increase in the length of neurites.[124]

VIII. SNPS IN CYTOSKELETON IMPAIRMENT

Various molecules have been studied to acquire deeper mechanistic understanding of retinal degeneration. The mutations and/or deletions or single nucleotide polymorphisms seen in the molecules during disease or degeneration lack proper co-relation with the cytoskeleton. The dynamics of the cytoskeleton plays a critical role in neural-crest cell migration. One important molecules discussed from the beginning of this review is cofilin. The dynamics of cytoskeleton components, especially in neural tube development, is regulated by cofilin. Cofilin is encoded by the gene *Cfl1*, and its polymorphisms have been investigated and established as a risk factor of spina bifida. In a population-based control study in California of non-Hispanic white infants with spina bifida, five SNPs in the gene

enhanced disease risk by greater than two-fold.[125] The regulation of the cytoskeleton is essentially brought about by protein–protein interactions. The interaction of integrin and actin is regulated by the *FLNA* gene. Mutations in the *FLNA* gene result in congenital malformations in craniofacial structures.[126] In one genetic study of two siblings having an unusual set of disease conditions (i.e. optic atrophy, early-onset spastic paraplegia, and neuropathy), one homozygous c.316C>T(p. R106C) variant in the Trk-fused gene (TFG) was the only plausible mutation upon linkage analysis, genome-wide SNP-typing, and exome sequencing. The characterization of this protein did not yield any self-assembly into an oligomeric complex, which is essential for the normal functioning of TFG. The inhibition of TFG alters endoplasmic reticulum (ER) morphology while slowing down its protein secretion. This results in the disruption of peripheral tubules and eventually the ER collapses over the cytoskeleton beneath it. This study highlights the link between the involvement of cytoskeleton through altered ER architecture and neurodegeneration.[127] TUBA8 gene, encodes a variant of α-tubulin with unknown function and it regulates the function of microtubules during the migration of cortical neurons. One study has reported that the mutation of this gene results in generalized polymicrogyria along with optic nerve hypoplasia (PMGOH). This study suggests the role of TUBA8 in the regulation of brain development in mammals.[128] Mutations in PFN1, a gene encoding the actin monomer-binding protein profilin 1, were recently reported in 1–2% of familial amyotrophic lateral sclerosis (ALS) patients. Two rare non-synonymous variants (E117D and E117G) have been identified in sporadic ALS patients.[129] Cerebral PGV (proliferative glomeruloid vasculopathy) is a severe autosomal recessive disorder of brain angiogenesis that results in abnormal thickening and unusually perforated vessels which lead to hydranencephaly. Mutation and deletion in the *FLVCR2* gene, which encodes a 12-transmemberane domain constituting a putative transporter, results in the absence of alpha-smooth muscle actin, suggesting a deficit in pericytes.[130]

IX. CONCLUSION

The field of retinal neural cytoskeletal dynamics in the growth and development of the vertebrate retina needs definition. This review highlights the role of retinal architecture and the involvement of cytoskeletal proteins in the growth and differentiation of the neuronal cells, thus indicating the need for translational research. Therefore, the study of retinal development, growth, and differentiation is likely to contribute significantly in the context of functional retinal repair. The mechanisms underlying differentiation and compartmentalization provide new insights into retinal development. In this regard, regenerative approaches in stem cell transplantation need to integrate such methodologies to account for poor results and irreproducible data.

REFERENCES

1. Burgoyne T, Dixon M, Luther P, Hogg C, Shoemark A. Generation of a three-dimensional ultrastructural model of human respiratory cilia. Am J Respir Cell Mol Biol. 2012;47:800–6.
2. Lin J, Heuser T, Song K, Fu X,Nicastro D. One of the nine doublet microtubules of eukaryotic flagella exhibits unique and partially conserved structures. PLoS One. 2012;10: e46494.
3. Ingerman E, Hsiao JY, Mullins RD. Arp2/3 complex ATP hydrolysis promotes lamellipodial actin network disassembly but is dispensable for assembly. 2013;5:619–33.
4. Samoilov VO, Bigdai EV, Kryzhanovskii EV, Dudich BA, Panov SA, Smirnov DD, Nesterov AS. Respiratory and olfactory cilia molecular machines of locomotor apparatus. Biofizika. 2013;2:269–75.
5. Wang H, Brust-MascherI, Cheerambathur D, Scholey JM. Coupling between microtubule sliding, plus-end growth and spindle length revealed by kinesin-8 depletion. Cytoskeleton. 2010; 11:715–28.
6. Cowles KN, Gitai Z. Surface association and the MreB cytoskeleton regulate pilus production, localization and function in Pseudomonas aeruginosa. Mol Microbiol. 2010;6:1411–26.
7. Chen J, Lippincott-Schwartz J, Liu J. Intracellular spatial localization regulated by the microtubule network. PLoS One. 2012; 4:e34919.
8. Krainer EC, Ouderkirk JL, Miller EW, Miller MR, Mersich AT, Blystone SD. The multiplicity of human formins: Expression patterns in cells and tissues. Cytoskeleton. 2013.
9. Tervaniemi MH, Siitonen HA, Söderhäll C, Minhas G,

Vuola J, Tiala I, Sormunen R, Samuelsson L, Suomela S, Kere J, Elomaa O. Centrosomal localization of the psoriasis candidate gene product, CCHCR1, supports a role in cytoskeletal organization. PLoS One 2012;11:49920.
10. Ma WP, Li YT, Tao HW. Down regulation of cortical inhibition mediates ocular dominance plasticity during the critical period. J Neurosci. 2013;27:11276–80.
11. Liu X, Zhang Z, Ribelayga CP. Heterogeneous expression of the core circadian clock proteins among neuronal cell types in mouse retina. PloS One. 2012;11:50602.
12. Fukata M, Nakagawa M, Kaibuchi K. Roles of Rho-family GTPases in cell polarisation and directional migration. Curr Opin Cell Biol. 2003;5:590–7.
13. Knoblich JA. Mechanisms of asymmetric stem cell division. Cell. 2008;132:583–97.
14. Hirokawa N, Niwa S, Tanaka Y. Molecular motors in neurons: transport mechanisms and roles in brain function, development, and disease. Neuron. 2010;68:610–38.
15. Morris M, Maeda S, Vossel K, Mucke L. The many faces of tau. Neuron. 2011;70:410–26.
16. Twelvetrees A, Hendricks AG, Holzbaur ELF. SnapShot: axonal transport. Cell. 2012;149:950.
17. Kuijpers M, Hoogenraad CC.Centrosomes, microtubules and neuronal development. Mol Cell Neurosci. 2011;4:349–58.
18. Ahmad FJ, Yu W, McNally FJ, Baas PW. An essential role for katanin in severing microtubules in the neuron. J. Cell Biol. 1999;145:305–15.
19. Baas PW, Lin S. Hooks and comets: The story of microtubule polarity orientation in the neuron. Dev. Neurobiol. 2011;71:403–18.
20. Stiess M, Maghelli N, Kapitein LC, Gomis-Rüth S, Wilsch-Bräuninger M, Hoogenraad C C,Tolić-Nørrelykke IM, Bradke F. Axon extension occurs independently of centrosomal microtubule nucleation. Science. 2010;327:704–7.
21. Xu K, Zhong G, Zhuang X. Actin, Spectrin, and associated proteins form a periodic cytoskeletal structure in axons. Science 2013; Reimer MM, McQueen J, Searcy L, Scullion G, Zonta B, Desmazieres A, Holland PR, Smith J, Gliddon C, Wood ER, Herzyk P, Brophy PJ, McCulloch J, Horsburgh K. Rapid disruption of axon-glial integrity in response to mild cerebral hypoperfusion. J Neurosci. 2011;49:18185–94.
22. Perrot R, Eyer J. Neuronal intermediate filaments and neurodegenerative disorders. Brain Res Bull. 2009;80:282–95.
23. Marner L, Nyengaard JR, Tang Y, Pakkenberg B. Marked loss of myelinated nerve fibers in the human brain with age. J Comp Neurol. 2003;462:144–52.
24. Adalbert R, Nogradi A, Babetto E, Janeckova L, Walker SA, Kerschensteiner M, Misgeld T, Coleman MP. Severely dystrophic axons at amyloid plaques remain continuous and connected to viable cell bodies. Brain. 2009;132: 402–16.
25. Fiala JC, Feinberg M, Peters A, Barbas H. Mitochondrial degeneration in dystrophic neurites of senile plaques may lead to extracellular deposition of fine filaments. Brain Struct. Funct. 2007; 212:195–207.
26. Chilton J, Gordon-Weeks P. Role of microtubules and MAPs during neuritogenesis. In Intracellular Mechanisms for Neuritogenesis de Curtis, I Springer. 2007; ed57–88.
27. Kollins KM, Bell RL, Butts M, Withers GS. Dendrites differ from axons in patterns of microtubule stability and polymerization during development. Neural Dev. 2009;4:26.
28. Küppers MB, Letzkus JJ, Lüer K, Technau G, Schmidt H, Prokop A. A new culturing strategy optimises Drosophila primary cell cultures for structural and functional analyses. Dev. Biol. 2004;269:459–78.
29. Lamoureux P, Heidemann SR, Martzke NR, Miller KE. Growth and elongation within and along the axon. Dev. Neurobiol. 2010;70:135–49.
30. Rajagopalan J, Tofangchi A, Saif MT. Drosophila neurons actively regulate axonal tension in vivo. Biophys. J. 2010;99:3208–15.
31. Letourneau PC. Actin in axons: stable scaffolds and dynamic filaments. Results Probl.Cell Differ. 2009;48:265–90.
32. Saxena S, Caroni P. Mechanisms of axon degeneration: from development to disease. Prog. Neurobiol. 2007;83:174–91.
33. Bradke F, Fawcett JW, Spira ME. Assembly of a new growth cone after axotomy: the precursor to axon regeneration. Nat. Rev. Neurosci. 2012;13:183–93.
34. Flynn KC, Hellal F, Neukirchen D, Jacob S, Tahirovic S, Dupraz S, Stern S, Garvalov BK, Gurniak C, Shaw AE, Meyn L, Wedlich-Söldner R, Bamburg JR, Small JV, Witke W, Bradke F. ADF/cofilin-mediated actin retrograde flow directs neurite formation in the developing brain. Neuron 2012;76:1091–107.
35. Neukirchen D, Bradke F. Neuronal polarization and the cytoskeleton. Semin. Cell Dev. Biol. 2011;22:825–33.
36. Saengsawang W, Mitok K, Viesselmann C, Pietila L,Lumbard DC, Corey SJ, Dent EW. The F-BAR protein CIP4 inhibits neurite formation by producing lamellipodial protrusions. Curr. Biol. 2012;22: 494–501.
37. Dent EW, Kwiatkowski AV, Mebane LM, Philippar U, Barzik M, Rubinson DA, Gupton S, Van Veen JE, Furman C, Zhang J, Alberts AS, Mori S, Gertler FB. Filopodia are required for cortical neurite initiation. Nat. Cell Biol. 2007;9:1347–59.
38. Gonçalves-Pimentel C, Gombos R, MihályJ, Sánchez-Soriano N, Prokop A. Dissecting regulatory networks of filopodia formation in a *Drosophila* growth cone model. PLoS One. 2011;6:e18340.
39. Barnes AP, Polleu F. Establishment of axon-dendrite

polarity in developing neurons. Annu. Rev. Neurosci. 2009;32:347–81.
40. Brandt R. Cytoskeletal mechanisms of axon outgrowth and pathfinding. Cell Tissue Res. 1998;292:181–9.
41. Chen S, Chen J, Shi H, Wei M, Castaneda-Castellanos DR, Bultje RS, Pei X, Kriegstein AR, Zhang M, Shi SH. Regulation of microtubule stability and organization by mammalian Par3 in specifying neuronal polarity. Dev. Cell. 2013;24:26–40.
42. Tessier-Lavigne M, Goodman CS. The molecular biology of axon guidance. Science. 1996;274:1123–33.
43. Araújo SJ, Tear G. Axon guidance mechanisms and molecules: lessons from invertebrates. Nat Rev Neurosci. 2003;4:910–22.
44. Huber AB, Kolodkin AL, Ginty DD, Cloutier JF. Signaling at the growth cone: ligand-receptor complexes and the control of axon growth and guidance. Annu Rev Neurosci. 2003;26:509–63.
45. Fan J, Mansfield SG, Redmond T, Gordon-Weeks PR, Raper JA. The organization of F-actin and microtubules in growth cones exposed to a brain-derived collapsing factor. J Cell Biol. 1993;121:867–78.
46. Chien CB, Rosenthal DE, Harris WA, Holt CE. Navigational errors made by growth cones without filopodia in the embryonic *Xenopus* brain. Neuron. 1993;11:237–51.
47. Davenport W, Dou P, Rehder V, Kater SB. A sensory role for neuronal growth cone filopodia. Nature. 1993;361:721–24.
48. Dwivedy A, Gertler FB, Miller J, Holt C E, Lebrand C.Ena/VASP function in retinal axons is required for terminal arborization but not pathway navigation. Development. 2007;134:2137–46.
49. Mattila PK, Lappalainen P. Filopodia: molecular architecture and cellular functions. Nat. Rev Mol Cell Biol. 2008; 9:446–54.
50. Dent EW, Gupton SL, Gertler FB. The growth cone cytoskeleton in axon outgrowth and guidance. Cold Spring Harb Perspect Biol. 2011;3:3.
51. Lowery LA, Van VD. The trip of the tip: understanding the growth cone machinery. Nat. Rev Mol Cell Biol. 2009;10:332–343.
52. Letourneau PC, Ressler AH. Inhibition of neurite initiation and growth by taxol. J Cell Biol. 1984;98:1355–1362.
53. Sánchez SN, Gonçalves PC, Beaven R, Haessler U, Ofner ZL, Ballestrem C, Prokop A. Drosophila growth cones: a genetically tractable platform for the analysis of axonal growth dynamics. Dev. Neurobiol. 2010;70:58–71.
54. Tanaka E, Ho T, Kirschner MW. The role of microtubule dynamics in growth cone motility and axonal growth. J Cell Biol. 1995;128:139–55.
55. Buck KB, Zheng JQ. Growth cone turning induced by direct local modification of microtubule dynamics. J Neurosci. 2002;22:9358–67.
56. Challacombe JF, Snow DM, Letourneau PC. Actin filament bundles are required for microtubule reorientation during growth cone turning to avoid an inhibitory guidance cue. J Cell Sci. 1996;109:2031–40.
57. Chien CB, Rosenthal DE, Harris WA, Holt CE. Navigational errors made by growth cones without filopodia in the embryonic *Xenopus* brain. Neuron. 1993;11:237–51.
58. Kaufmann N, Wills ZP, Van VD. Drosophila Rac1 controls motor axon guidance. Development. 1998;125:453–61.
59. Marsh L, Letourneau PC. Growth of neurites without filopodial or lamellipodial activity in the presence of cytochalasin B. J Cell Biol. 1984;99:2041–7.
60. Hur EM, Saijilafu Lee BD, Kim SJ, Xu WL, Zhou FQ. GSK3 controls axon growth via CLASP-mediated regulation of growth cone microtubules. Genes Dev. 2011;25:1968–81.
61. Lucas FR, Goold RG, Gordon-Weeks PR, Salinas PC. Inhibition of GSK-3beta leading to the loss of phosphorylated MAP-1B is an early event in axonal remodelling induced by WNT-7a or lithium. J Cell Sci. 1998;111:1351–61.
62. Purro SA, Ciani L, Hoyos FM, Stamatakou E, Siomou E, Salinas PC. Wnt regulates axon behavior through changes in microtubule growth directionality: a new role for adenomatous polyposis coli. J Neurosci. 2008;28:8644–54.
63. Maurange C, Cheng L, Gould AP. Temporal transcription factors and their targets schedule the end of neural proliferation in Drosophila. Cell. 2008;133:891–902.
64. Osumi N, Shinohara H, Numayama-Tsuruta K, Maekawa M. Pax6 transcription factor contributes to both embryonic and adult neurogenesis as a multifunctional regulator. Stem Cells 2008;26:1663–72.
65. Sandberg M, Källström M, Muhr J. Sox21 promotes the progression of vertebrate neurogenesis. Nat Neurosci. 2005;8:995–1001.
66. Majdzadeh N, Wang L, Morrison BE, Bassel-Duby R, Olson EN, D'Mello SR. HDAC4 inhibits cell-cycle progression and protects neurons from cell death. Dev Neurobiol. 2008;68:1076–92.
67. Abburi C, Prabhakar S, Kalra J, Huria A, Anand A. Vascular endothelial growth factor (VEGF) induced proliferation of human fetal derived ciliary epithelium stem cells is mediated by jagged-N cadherin pathway. Curr Neurovasc Res. 2013;2:93–102.
68. Hu QD, Ma QH, Gennarini G, Xiao ZC. Cross-talk between F3/contactin and Notch at axoglial interface: a role in oligodendrocyte development. Dev Neurosci. 2006;28:25–33.
69. Cisneros E, Latasa MJ, García-Flores M, Frade JM.Instability of Notch1 and Delta1 mRNAs and reduced Notch activity in vertebrate neuroepithelial cells undergoing S-phase. Mol Cell Neurosci. 2008;37:820–

31.
70. Götz M, Huttner WB. The cell biology of neurogenesis. Nat Rev Mol Cell Biol. 2005;6:777–88.
71. Marin O, Valiente M, Ge X, Tsai LH. Guiding neuronal cell migrations. Cold Spring Harb Perspect Biol. 2010;2:a001834.
72. Altshuler D, Turner D, Cepko C. Specification of cell types in the vertebrate retina, Development of the Visual System (Lam D., Shatz C., eds),1991;pp 37–58 MIT Press Boston
73. Cepko CL, Austin C P, Yang X, Alexiades M, Ezzedine D. Cell fate determination in the vertebrate retina. Proc Natl Acad Sci. 1996;93:589–95.
74. Marquardt T and Gruss P. Generating neuronal diversity in the retina: one for nearly all. Trends Neurosci. 2002;25:32–8.
75. Mu X, Klein WH. Gene regulatory networks and retinal ganglion cell development. Eye, Retina, and Visual System of the Mouse. PNAS. 2008;19:6942–7.
76. Brown NL, Patel S, Brzezinski J, Glaser T. Math5 is required for retinal ganglion cell and optic nerve formation. Development. 2001;128:2497–508.
77. Marquardt T, Ashery PR, Andrejewski N, Scardigli R, Guillemot F, Gruss P. Pax6 is required for the multipotent state of retinal progenitor cells. Cell. 2001;105:43–55.
78. Wang SW, Kim BS, Ding K, Wang H, Sun D, Johnson RL, Klein WH, Gan L. Requirement for math5 in the development of retinal ganglion cells. Genes Dev. 2001;15:24–9.
79. Lee J, Ko M, Joo CK. Rho plays a key role in TGF-beta1-induced cytoskeletal rearrangement in human retinal pigment epithelium. J Cell Physiol. 2008;216:520–6.
80. Narayan S, Prasanna G, Tchedre K, Krishnamoorthy R, Yorio T. Thrombin-induced endothelin-1 synthesis and secretion in retinalpigment epithelial cells is rho kinase dependent. J Ocul Pharmacol Ther. 2010;26:389–97.
81. Major DL, Brady-Kalnay SM.Rho GTPases regulate PTPmu-mediated nasal neurite outgrowth and temporal repulsion of retinal ganglion cell neurons. Mol Cell Neurosci2007;34:453–67.
82. Bamburg JR, Bray DJ. Distribution and cellular localization of actin depolymerizing factor. Cell Biol. 1987;105:2817–25.
83. Birkenfeld J, Betz H, Roth D. Inhibition of neurite extension by overexpression of individual domains of LIM kinase 1. J Neurochem. 2001;78:924–7.
84. Kuhn TB, Meberg PJ, Brown MD, Bernstein BW, Minamide LS, Jensen JR, Okada K, Soda EA, Bamburg JR. Regulating actin dynamics in neuronal growth cones by ADF/cofilin and rho family GTPases. J Neurobiol. 2000;44:126–44.
85. Meberg PJ, Bamburg JR. Increase in neurite outgrowth mediated by overexpression of actin depolymerizing factor. J Neurosci. 2000;20:2459–69.
86. Meberg PJ, Ono S, Minamide LS, Takahashi M, Bamburg JR. Actin depolymerizing factor and cofilin phosphorylation dynamics: response to signals that regulate neurite extension. Cell Motil Cytoskeleton. 1998;39:172–90.
87. Chen TJ, Gehler S, Shaw AE, Bamburg, JR, Letourneau PC. Cdc42 participates in the regulation of ADF/cofilin and retinal growth cone filopodia by brain derived neurotrophic factor. J Neurobiol. 2006;66:103–14.
88. Gehler S, Shaw AE, Sarmiere PD, Bamburg JR, Letourneau PC. Brain-derived neurotrophic factor regulation of retinal growth cone filopodial dynamics is mediated through actin depolymerizing factor/cofilin. J Neurosci. 2004;24:10741–9.
89. Wen Z, Han L, Bamburg JR, Shim S, Ming GL, Zheng JQ. BMP gradients steer nerve growth cones by a balancing act of LIM kinase and slingshot phosphatase on DF/cofilin. J Cell Biol. 2007;178:107–19.
90. Jain A, McKeon RJ, Brady-Kalnay SM, Bellamkonda RV. Sustained delivery of activated Rho GTPases and BDNF promotes axon growth in CSPG-rich regions following spinal cord injury. PLoS One. 2011;6:e16135.
91. Jain A, Brady-Kalnay SM, Bellamkonda RV. Modulation of Rho GTPase activity alleviates chondroitin sulfate proteoglycan-dependent inhibition of neurite extension. J Neurosci Res. 2004;77:299–307.
92. Linseman DA, Laessig T, Meintzer MK, McClure M, Barth H, Aktories K, Heidenreich KA. An essential role for Rac/Cdc42 GTPases in cerebellar granule neuron survival. J Biol Chem. 2001;276:39123–31.
93. Le SS, Loucks FA, Udo H, Richardson-Burns S, Phelps RA, Bouchard RJ, Barth H, Aktories K, Tyler KL, Kandel ER, Heidenreich KA, Linseman DA. Inhibition of RacGTPase triggers a c-Jun- and Bim-dependent mitochondrial apoptotic cascade in cerebellar granule neurons. J Neurochem. 2005;94:1025–39.
94. Bennett GS, DiLullo C. Expression of a neurofilament protein by the precursors of a subpopulation of ventral spinal cord neurons. Dev Biol. 1985;1:94–106.
95. Grant P, Pant HC. Neurofilament protein synthesis and phosphorylation. J Neurocytol. 2000;29:843–72.
96. Grant P, Sharma P, Pant HC. Cyclin-dependent protein kinase 5 (Cdk5) and the regulation of neurofilament metabolism. Eur J Biochem. 2001;6:1534–46.
97. Poulain FE, Sobel A. The microtubule network and neuronal morphogenesis: dynamic and coordinated orchestration through multiple players. Mol Cell Neurosci. 2010;1:15–32.
98. Gutierrez C, McNally M, Canto-Soler MV. Cytoskeleton proteins previously considered exclusive to ganglion cells are transiently expressed by all retinal neuronal precursors. BMC Developmental Biology. 2011;11:46.
99. Lindström NO, Neves C, McIntosh R, Miedzybrodzka Z, Vargesson N, Collinson JM. Tissue specific characterisation of Lim-kinase 1 expression during mouse embryo-

genesis. Gene Expr Patterns. 2011;11:221–32.
100. Meng Y, Zhang Y, Tregoubov V, Janus C, Cruz L, Jackson M, Lu WY, MacDonald JF, Wang JY, Falls DL, Jia Z. Abnormal spine morphology and enhanced LTP in LIMK-1 knockout mice. Neuron 2002;35:121–33.
101. Hur EM, Zhou FQ. GSK3 signalling in neural development. Nat Rev Neurosci. 2010;11:539–51.
102. Chen M, Maloney JA, Kallop DY, Atwal JK, Tam S J, Baer K, Kissel H, Kaminker JS, Lewcock JW, Weimer RM, Watts RJ. Spatially coordinated kinase signaling regulates local axon degeneration. J Neurosci. 2012;39:13439–53.
103. Homma S, Shimada T, Hikake T, Yaginuma H. Expression pattern of LRR and Ig domain-containing protein (LRRIG protein) in the early mouse embryo. Gene Expr Patterns. 2009;9:1–26.
104. Zhao L, Wang D, Wang Q, Rodal AA, and Zhang YQ. Drosophila cyfip regulates synaptic development and endocytosis by suppressing filamentous actin assembly. PLoS Genet. 2013;4.
105. Ng J, Luo L. Rho GTPases regulate axon growth through convergent and divergent signaling pathways. Neuron. 2004;5:779–93.
106. Siudeja K, Grzeschik NA, Rana A, de Jong J, Sibon C. Cofilin/Twinstar phosphorylation levels increase in response to impaired coenzyme a metabolism. PLoSOne 2012;8:e43145.
107. Norris AD, Dyer JO, Lundquist EA. The Arp2/3 complex, UNC-115/abLIM, and UNC-34/Enabled regulate axon guidance and growth cone filopodia formation in *Caenorhabditis elegans*. Neural Dev. 2009;4:38.
108. Struckhoff EC, Lundquist EA. The actin-binding protein UNC-115 is an effector of Rac signaling during axon pathfinding in *C. elegans*. Development. 2003;130:693–704.
109. Shakir MA, Gill JS, Lundquist EA. Interactions of UNC-34 Enabled with RacGTPases and the NIK kinase MIG-15 in *Caenorhabditis elegans* axon pathfinding and neuronal migration. Genetics. 2006;172:893–913.
110. Withee J, Galligan B, Hawkins N, Garriga G. Caenorhabditis elegans WASP and Ena/VASP proteins play compensatory roles in morphogenesis and neuronal cell migration. Genetics. 2004;167:1165–76.
111. Lebrand C, Dent EW, Strasser GA, Lanier LM, Krause M, Svitkina TM, Borisy GG, Gertler FB. Critical role of Ena/VASP proteins for filopodia formation in neurons and in function downstream of netrin-1. Neuron. 2004;42:37–49.
112. Barzik M, Kotova TI, Higgs HN, Hazelwood L, Hanein D, Gertler FB, Schafer DA. Ena/VASP proteins enhance actin polymerization in the presence of barbed end capping proteins. J Biol Chem. 2005;280:28653–62.
113. Bear JE, Gertler FB. Ena/VASP: towards resolving a pointed controversy at the barbed end. J Cell Sci. 2009;122:1947–53.
114. Applewhite DA, Barzik M, Kojima S, Svitkina TM, Gertler FB, Borisy GG. Ena/VASP proteins have an anticapping independent function in filopodia formation. Mol Biol Cell. 2007;18:2579–91.
115. Ans JE, Snow JJ, Gunnarson AL, Ou G, Stahlberg H, McDonald KL, Scholey JM. Functional modulation of IFT kinesins extends the sensory repertoire of ciliated neurons in Caenorhabditis elegans. J Cell Biol. 2006;172:663–9.
116. Snow JJ, Ou G, Gunnarson AL, Walker MR, Zhou HM, Brust MI, Scholey JM. Two anterograde intraflagellar transport motors cooperate to build sensory cilia on *C. elegans* neurons. Nat Cell Biol. 2004;6:1109–1113.
117. Insinna C, Pathak N, Perkins B, Drummond I, Besharse JC. The homodimeric kinesin, Kif17, is essential for vertebrate photoreceptor sensory outer segment development. Dev Biol. 2008;1:160–70.
118. Yoon BC, Zivraj KH, Strochlic L, Holt CE. 14-3-3 Proteins regulate retinal axon growth by modulating ADF/Cofilin activity. Dev Neurobiol. 2012;4:600–14.
119. Gurniak CB, Perlas E, Witke W. The actin depolymerizing factor n-cofilin is essential for neural tube morphogenesis and neural crest cell migration. Dev Biol. 2005;1:231–41.
120. Huiping Z, James OEE, Chen M, Gary MS, Edward JL, Richard HF. Association between CFL1 gene polymorphisms and spina bifida risk in a California population. BMC Medical Genetics. 2007;8:12.
121. Robertson SP, Twigg SR, Sutherland-Smith AJ, Biancalana V, Gorlin RJ, Horn D, Kenwrick SJ, Kim CA, Morava E, Newbury-Ecob R, Orstavik KH, Quarrell OW, Schwartz CE, Shears DJ, Suri M, Kendrick-Jones J, Wilkie AO. Localized mutations in the gene encoding the cytoskeletal protein filaminA cause diverse malformations in humans. Nature Genetics. 2003;4:487–91.
122. Beetz C, Johnson A, Schuh AL, Thakur S, Varga RE, Fothergill T, Hertel N, Bomba-Warczak E, Thiele H, Nürnberg G, Altmüller J, Saxena R, Chapman ER, Dent EW, Nürnberg P, Audhya A. Inhibition of TFG function causes hereditary axon degeneration by impairing endoplasmic reticulum structure. 2013;13:5091–6.
123. Abdollahi MR, Morrison E, Sirey T, Molnar Z, Hayward BE, Carr IM, Springell K, Woods CG, Ahmed M, Hattingh L, Corry P, Pilz DT, Stoodley N, Crow Y, Taylor GR, Bonthron DT, Sheridan E. Mutation of the variant a-tubulin TUBA8 results in polymicrogyria with optic nerve hypoplasia. Am J Human Genetics. 2009;85:737–44.
124. Shu Y, Jennifer AF, Kelly LW, Sadaf TW, Roger P, Garth AN, Ian PB. Mutation analysis and immunopathological studies of PFN1 in familial and sporadic amyotrophic lateral sclerosis. 2013;9: 2235:e7–10.
125. Thomas S, Encha-Razavi F, Devisme L, Etchevers H,

Bessieres-Grattagliano B, Goudefroye G, Elkhartoufi N, Pateau E, Ichkou A, Bonnière M, Marcorelle P, Parent P, Manouvrier S, Holder M, Laquerrière A, Loeuillet L, Roume J, Martinovic J, Mougou-Zerelli S, Gonzales M, Meyer V, Wessner M, Feysot CB, Nitschke P, Leticee N, Munnich A, Lyonnet S, Wookey P, Gyapay G, Foliguet B, Vekemans M, Attié-Bitach T. High-throughput sequencing of a 4.1 Mb linkage interval reveals FLVCR2 deletions and mutations in lethal cerebral vasculopathy. Human Mutation. 2010;10:1134–41.

SCIENTIFIC REPORTS



OPEN

SUBJECT AREAS:
MOLECULAR BIOLOGY
PROGNOSTIC MARKERS

Received
2 December 2013

Accepted
22 January 2014

Published
18 February 2014

Correspondence and requests for materials should be addressed to A.A. (akshay1anand@rediffmail.com)

* These authors contributed equally to this work.

Does DcR1 (TNF-related apoptosis-inducing-ligand Receptor 3) have any role in human AMD pathogenesis?

Akshay Anand[1]*, Neel K. Sharma[1]*, Ramandeep Singh[2]*, Amod Gupta[2], Sudesh Prabhakar[1], Neeru Jindal[2], Arvind K. Bhatt[3], Suresh K. Sharma[4] & Pawan K. Gupta[1]

[1]Neuroscience Researh Lab, Department of Neurology, Post Graduate Institute of Medical Education and Research (PGIMER), Chandigarh, India, [2]Department of Ophthalmology, Post Graduate Institute of Medical Education and Research (PGIMER), Chandigarh, India, [3]Department of Biotechnology, Himachal Pradesh University, Shimla, India, [4]Department of Statistics, Panjab University, Chandigarh, India.

It has been postulated that there is a link between age related degenerative diseases and cancer. The TNF-related apoptosis-inducing ligand (TRAIL) has been shown to selectively kill tumor cells by binding to pro-apoptotic and anti-apoptotic receptors. Our aim was to study the levels of anti-apoptotic receptor (DcR1) in age related macular degeneration (AMD) and controls. AMD patients (115) were classified into two groups: Dry and Wet AMD. Wet AMDs were further classified into occult, predominant classic and minimal classic. 61 healthy individuals were recruited as normal controls. After normalization with total protein, DcR1 levels were analyzed by ELISA. Mann Whitney U-statistic was used for analysis of DcR1 ELISA results. We have observed DcR1 levels in serum sample which were significantly lower in AMD patients as compared to controls ($p = 0.001$). On the other hand, we did not find difference in DcR1 levels between wet and dry AMD. The present study defines the plausible role of DcR1 in AMD pathology signifying a new therapeutic target for AMD.

Age is the most important risk factor for neurodegenerative disorders including age-related macular degeneration (AMD)[1]. It is a leading cause of irreversible vision loss in elderly in both the developed as well as developing world. The disease is broadly classified according to the severity of disease. It has been reported that about two million individuals are affected with AMD in United Kingdom[2] and statistics on AMD in India show frequency varies from 2.7% early AMD to 0.6% late AMD in South India to 4.7% in North India[3]. The major hallmark characteristic of early AMD is the presence of drusen. Drusen are tiny accumulations of extracellular material which accumulate between the retinal pigment epithelium and Bruch's membrane of the eye. The drusen consists of lipoproteins (especially Lipoprotein E), complement system components (Complement factor H, complement factor B and complement factor C etc.), apolipoproteins (apolipoproteins B48 and B100), clusterin and some exosome molecules [CD63 (Cluster of Differentiation 68), LAMP2 (Lysosome-associated membrane protein 2), and CD81(Cluster of Differentiation 81) etc)[4]. There are two types of AMD i.e. Dry AMD and Wet AMD. Dry AMD is marked by drusen or depigmentation caused by products of the photoreceptors and retinal pigment epithelium (RPE). Wet AMD is caused due to the growth of abnormal blood vessels below the retina and RPE, which results in subretinal bleeding and consequent scar formation occluding vision. This may affect any one or both of the eyes. Patients with dry AMD may progress into wet AMD. Several genetic and environmental factors have already been associated with AMD. Among the genetic factors, the genes which are involved in cell apoptosis and its regulation have not been much investigated in AMD. However, apoptosis plays a major role in pathology of AMD[5]. In this study, we measured the expression level of DcR1 in serum of AMD patients. Previously, many genetic studies have confirmed the role of various genes in AMD by use of whole blood from AMD patients of similar sample size[6–9]. The disease progression is characterized by impairment of regulatory processes like apoptosis, chronic inflammation, increase in cell numbers, invasiveness etc. Moreover, there are some common risk factors and underlying molecules for AMD and cancer like smoking, complementary factor H (CFH) with inflammation being main mediator in the progression of diseases

91

Table 1 | Demographic characteristics of Controls and AMD patients

Variables	AMD	Controls
Total	115	61
Wet AMD	84	----
Dry AMD	31	----
Sporadic Cases	105	----
Familial Cases	10	----
Duration of disease¥	23 ± 2.6 (M)	----
Smokers	50	11
Non Smokers	65	44
Alcoholic	37	17
Non-alcoholic	78	38
Vegetarian	61	31
Non-vegetarian	54	24
Age	64.97 ± 7.1	60.38 ± 13.2
Heart Disease	16	----
No Heart Disease	60	55
Male	75	40
Female	40	21

Demographic and clinical details of subjects. Age, Age of onset; M, Months; ¥ Duration of disease is the interval between appearance of first symptom of AMD and collection of sample. Values are mean ± SD.

pathology[10]. TNF-related apoptosis-inducing ligand (TRAIL) acts as antitumor agent, which induces apoptosis in cancer cells. TRAIL is a cytokine and can bind with four receptors i.e. Death receptor 4 (DR4) and Death receptor 5 (DR5) (pro-apoptotic) and with anti-apoptotic (DcRs), Death receptor 1 (DcR1) and Death receptor 2 (DcR2)[11]. By binding with DR4 or DR5 receptors TRAIL can induce apoptosis by caspase-8 dependent manner which further activates the effector caspases like caspases-3, 6,7 etc. DcR1 is a GPI-anchored member of the tumor necrosis factor receptor (TNFR) super family which is also known as CD263, TRID and TRAIL-R3. It is not expressed in all tumors. It includes a transmembrane domain and an extracellular TRAIL binding domain. It does not contain a functional death domain. It acts as TRAIL decoy receptor by reducing the apoptosis. The TRAIL's binding to DcR1 or DcR2 stimulate the NFk-β leading to activation of transcription genes antagonizing apoptotic mechanisms or promoting inflammation. Decoy receptors after binding to TRAIL inhibit the TRAIL-induced apoptosis by inhibiting binding to proapoptotic receptors i.e. DR4 and DR5.

In this study, we hypothesized that the lower levels of DcR1 in serum of AMD patients may provide an environment conducive for degenerative processes. TRAIL binding and therefore, DcR1 mediated anti-apoptotic process may not be active which may lead to photoreceptor degeneration leading to AMD.

Results

Summary statistics of main variables has been reported in Table 1. The serum concentration of DcR1 is shown in Table 2. DcR1 serum levels were skewed therefore, Kruskal-Wallis test was applied for statistical comparison. The serum concentration of DcR1 was found to be lower in AMD cases as compared to controls (Table 2, Figure 1A, $p = 0.0001$). Difference was not significant between serum concentration of DcR1 in dry and wet AMD (Table 2, Figure 1B, $p = 0.093$). The levels of dry and wet AMD were significantly lower as compared to normal controls (Figure 1B, $p = 0.001$ & 0.0001 respectively). To estimate the predictive value of DcR1, serum levels of DcR1 were again segregated into minimal classic, predominant classic and occult AMD. No significant difference was found between the wet AMD subgroups (Table 2). While adjusting the risk factors to AMD an independent analysis was carried out. Important risk factors like smoking, alcohol, food habits, diabetes and heart diseases were analyzed to examine their association with DcR1. However, no significant difference observed between AMD smokers versus AMD never smokers, alcohol consumers versus never alcohol consumers, vegetarian versus non vegetarian, diabetic versus non diabetic, AMD with heart disease versus AMD without heart disease and Male versus female (Table 2). When multivariate analysis was carried out with adjustment for age, smoking, alcohol, food habits, diabetes and heart disease, we found significant difference between AMD and controls (OR = 11.181, $p = 0.001$).

The association between levels of DcR1 in AMD and age have been computed using Chi square ($\chi^2 = 3.929$, $p = 0.141$), which shows that there is no significant association between age and DcR1 levels. However, the association between severity of AMD and levels of DcR1 was significant ($\chi^2 = 5.982$, $p = 0.014$). The prediction equation for AMD, by considering DcR1 levels as independent variable, shows that 74.4% of the cases have been correctly classified with

Table 2 | Comparison of serum DcR1 levels between control, AMD and their subtypes along with odds ratio (adjusted for covariates)

		Mann Whitney Statistic	Unadjusted p value	Multivariate analysis adjusted for, age smoking, alcohol, food habits, diabetes and heart disease		
Subjects	Mean Rank	Z -Value	p-value	Odd Ratio	CI (95%)	p- value
AMD	48.12	5.762	0.0001*	11.181	2.67–46.7	0.001
Control	86.32					
Dry	41.85					
Wet	33.29	1.681	0.093	0.296	0.049–1.790	0.182
Minimal Classic	17.00					
Predominant Classic	12.11	0.867	0.386	*	*	*
Occult	20.05	0.611	0.541	*	*	*
Alcoholic	38.38					
Non Alcoholic	35.56	0.538	0.591	0.286	0.021–3.892	0.347
Smokers	37.40					
Non Smokers	35.86	0.308	0.758	0.457	0.053–3.962	0.477
Vegetarian	38.19					
Non Vegetarian	34.71	0.704	0.481	0.964	0.165–5.638	0.968
Heart Disease	28.00					
No heart Disease	25.57	0.445	0.671	0.529	0.044–6.309	0.614
Diabetic	33.62					
No Diabetes	35.93	0.370	0.711	1.727	0.246–12.136	0.583
Male	37.09					
Female	35.52	0.308	0.758	0.182	0.011–2.99	0.233

*Odds ratio can not be computed (with reference category as minimal classic) because of the constant values.

92

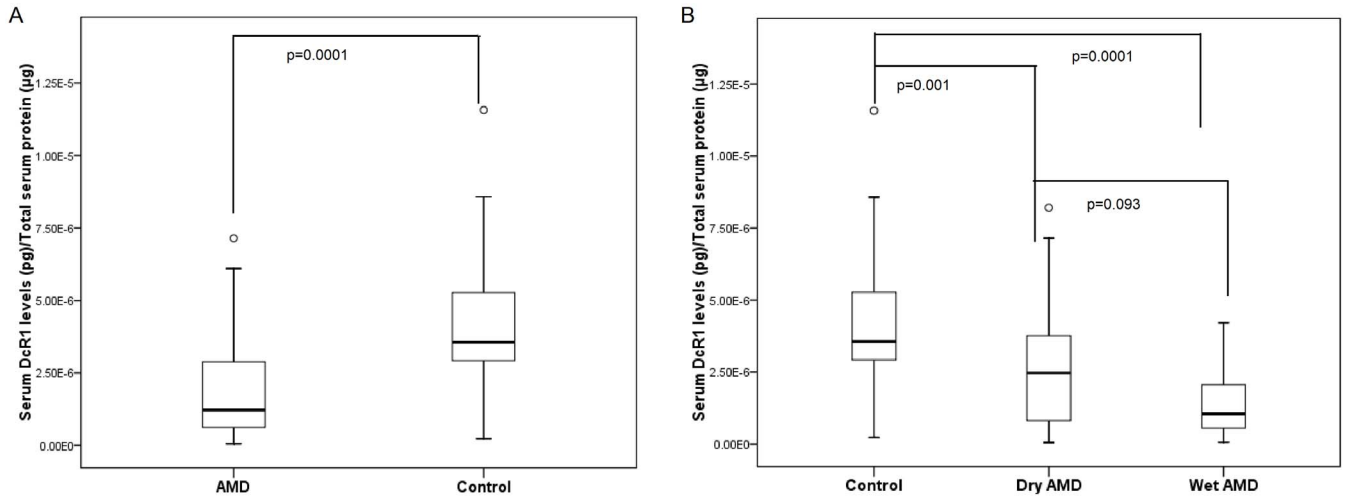


Figure 1 | (A) Serum levels of DcR1 in AMD and controls. (B) Serum levels of DcR1 in dry, wet and normal controls. pg, picogram; µg, microgram.

model authenticity of 74.4% and close confidence intervals for ROC curve. The area under ROC was 0.75 (p = .0001) with standard error of 0.044 and confidence interval of 0.660–0.834 (Figure 2).

Discussion

In a number of diseases, apoptosis plays a major role in development of disease pathology like AMD and retinitis pigmentosa. AMD causes a gradual loss of central vision due to the death of photoreceptors in the retina especially in central part of retina called the macula. The study was performed to determine whether the difference in the levels of serum DcR1 are associated with AMD. We showed that the DcR1 expression decreased significantly in patients of AMD as compared to controls irrespective of other environmental factors that indicates the noon redundant role of DcR1 mediated processes independent of these factors. Additionally, we also did not find the considerable difference in serum DcR1 levels in between dry AMD and wet AMD indicating apoptosis as a common phenomenon in both types of AMD.

In pathological processes of many degenerative diseases, apoptosis and necrosis play an important role. Histochemical and ultrastructural analysis shows that during AMD, RPE cells overlying drusen degenerate because of necrosis[12]. Initiation of necrosis in cells results in morphological modifications, membrane rupture which may lead to release of cytoplasmic contents from the cell. Necrotic material from these cells is believed to activate the complement, inducing inflammation in local tissue. Krabb et al has also shown that histones, which are released during necrosis, also constitute drusen[13] leading to RPE atrophy which further results in geographic atrophy. There are several studies which have simultaneously implicated the role of apoptotic processes in degeneration of photoreceptors, retinal pigment epithelium (RPE) and inner nuclear layer (INL) in AMD[14]. It has already been reported that reduced expression of DcR1 was associated with sensitivity to TRAIL in many cell lines of cancers[15]. In carcinomas, it has also been examined that lack of expression of the DcRs may provide them extra susceptibility to apoptosis induced by TRAIL[16].

However, apoptotic action mediated by TRAIL has been shown to be exerted by participation of p53 thus exacerbating anti-tumor activity by down regulating the DcR1 expression in colon cancer[17]. Moreover, it has been found to be overexpressed in the p53 mutated cell line. Recently, Ambati et al have also examined the role of p53 in retinal angiogenesis and have found disruption of p53 transcriptional network can abolish the anti-angiogenic activity of Nutlin3 (drugs commonly used in cancer). Even though the group did not show any relation with DcR1 or DcR2 receptors the role of DcR1 in apoptotic process could be examined in the context of p53 processes[18]. Several mouse models for retinal degeneration have been established by genetic manipulations in several retinal related genes and also created by light injury of retinal layers in which apoptosis contributes towards photoreceptor cell death[19–21]. Human retinitis pigmentosa, serous retinal detachment and pathologic myopia are characterized by similar pathologic photoreceptor apoptosis[22,23]. In glaucoma retinal ganglion cells also undergo apoptosis[24]. Additionally, it was also shown that the number of TUNEL-positive cells in the retinal pigment epithelium, choroid, outer nuclear layer, and inner nuclear layer are significantly more in AMD eyes as compared to control eyes, signifying that these cells may possibly die by apoptosis[12]. Therefore, these studies have revealed that main cause of photoreceptor death in retinal and other diseases presumably regulated by TRAIL signaling. Due to low levels of DcR1, TRAIL has increased affinity to bind with TRAILR1 or TRAILR2 which results in receptor oligomerization and initiation of apoptosis. Enhanced

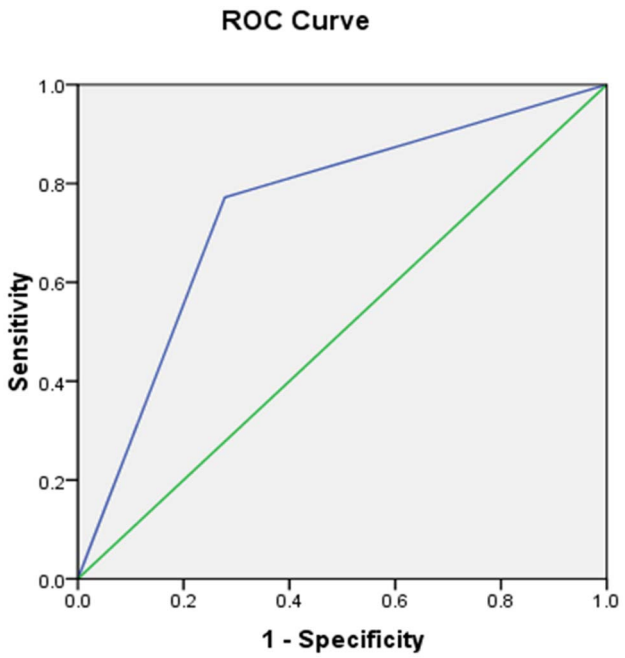


Figure 2 | **Receiver operating characteristic (ROC) obtained from binary logistic regression model which generates significant predictors of AMD.** Area under the curve is reported to be 75%.

93

apoptosis can result in tissue degeneration, a feature of AMD, while reduced apoptosis results in accumulation of immune cells. Therefore, cellular protection protocols engage a delicate balance in pro- apoptotic and anti-apoptotic factors. Apoptosis involves two major signaling pathways: the extrinsic death pathway and intrinsic death pathway. Extrinsic pathway is initiated through apoptotic signal transduction cascades mediated by members of TNFR while intrinsic death pathway is mediated by pro-apoptotic and anti-apoptotic Bcl2 family proteins at the mitochondria[25].

We did not find any difference in the levels of DcR1 for dry and wet AMD and the difference was not found to be significant for wet AMD subtypes. However, after categorizing DcR1 levels (below and above median) the association with severity of AMD was found to be significant but it was not significant with age. While analyzing the other risk factors to AMD, no association of DcR1 levels was observed. Death of photoreceptor cells is the main cause in the pathogenesis of AMD. We have attempted to predict AMD based on DcR1 levels (below and above median) using logistic regression, which showed 74.4% model predictivity and AUC is 0.75. The moderate value of AUC may be used to diagnose AMD patients with very less standard error. TNF-related apoptosis inducing ligand stimulates apoptosis and DcR1 is believed to act as dominant-negative receptor for TNF-related apoptosis sensitising ligand. Due to low levels of DcR1, the levels of TNF-related apoptosis inducing ligand may be enhanced resulting in apoptosis mediated AMD. The present study highlights that the lower levels of DcR1 may be associated with AMD however additional mechanistic studies can shed more light on the putative mechanism.

Conclusion

Conclusively, this study substantiates the role of apoptosis mediated by DcR1 receptor. A bigger study is imperative. An effective method of neuroprotection based on targeting of DcR1 could potentially supplement the current treatment strategies for this disorder.

Methods

Study population. A signed informed consent was taken from each participant. Individuals with AMD were recruited from advanced eye centre, PGIMER, Chandigarh, India. We included 176 cases which contained 115 AMD samples (75 male and 40 females) and 61 normal healthy controls (40 male and 21 females) after obtaining a signed informed consent as per inclusion exclusion criteria. The unrelated attendants like spouses who accompanied AMD patients to Eye clinic were recruited as controls. The samples were collected at the same site using same procedure by the same individual. Ethical clearance was taken from the Ethics Committee of the Institute vide letter No Micro/10/1411.

Inclusion and exclusion criteria. Inclusion criteria included the age of 50 years or older with the diagnosis of age related macular degeneration defined by choroidal neovascularization and/or dry AMD with at least five drusen in one eye. The controls were of 50 years or older without drusen and without any AMD diagnostic criteria. Exclusion criteria excluded the retinal diseases in the outer retinal layers and/or photoreceptors (other than AMD) like central serous retinopathy, high myopia, diabetic retinopathy, retinal dystrophies, uveitis, vein occlusion and other problems that precluded satisfactory stereo fundus photography. These situations contain occluded pupils due to ocular diseases like cataracts, opacities and synechiae[9].

Diagnosis of AMD. A retina consultant examined the patients for best corrected visual acuity (BCVA), intraocular pressure, slit lamp biomicroscopy (SLB) of anterior and posterior segment with 90D lens and indirect ophthalmoscopy for peripheral fundus examination. All patients underwent fluorescein fundus-angiography (FFA) and optical coherence-tomography (OCT). AMD diagnosis was based on ophthalmoscopic and FFA findings[10].

Demographic profile. The demographic detail was taken by a trained interviewer after getting signed consent form using a risk factor questionnaire[9]. The detail (age, sex, race, cigarette smoking, food habit, alcohol intake, diabetes and heart diseases) was self reported by participants. Smokers were districted as those having smoked at least three cigarettes per day or 54-boxes for at least 6 contiguous months and were separated further into never smokers and smokers. Non-vegetarian patients were distincted as those consuming meat, chicken,or fish for at least 6 contiguous months and alcohol consumer patients were defined as those having rum, whiskey, wine or homemade alcohol for at least 6 contiguous months. Heart diseases were determined based on the participant's answers to whether a physician had ever told them about this finding and whether they had ever taken medicine for this situation[10].

Serum separation. Blood samples were collected from all individuals for carrying out ELISA. About 4.0 ml of blood was collected in a serum separator tube (BD Biosciences, USA) and was left for 30 minutes at room temperature to allow it to clot and after centrifugation at 3000-rpm for 30 minutes, serum was separated. The samples were labeled, coded and stored to study the levels by established procedures described below.

Total protein estimation. Total serum proteins for normalization of DcR1 levels from ELISA was done by Bradford assay. The procedure was carried out according to manufacturer's recommendations. In double distilled water, serum samples were diluted upto 1500 times. The standard curve was generated by using protein Bovine Serum Albumin (BSA). Standard protein BSA and samples were mixed in ratio 4 : 1 with coomassie brilliant blue G – 250 dye (Bradford reagent) followed by incubation at room temperature for about 15 minutes on shaker. The absorbance was taken at 595 nm in 680XR model of Microplate reader (Biorad, Hercules, CA, USA). Standard curve was generated with quadratic fit or linear models[11].

ELISA. ELISA for DcR1 was performed according to the manufacturer's protocol (Abcam, Cat no ab46018). Sample serum assays were performed in duplicate. Standard DcR1 was assayed over a concentration range of 10000–312.5 pg/ml in duplicates for each experiment. The assay recognizes both natural and recombinant human DcR1 and the sensitivity of assay was $<$147 pg/ml. Appropriate blanks were also incorporated into experimental design. Normalization was done with total protein.

Statistical analysis. The assumption of normality was tested with the help of Normal Quantile plot (Q-Q plot) and it was observed that data was not normally distributed. Mann-Whitney U-test was, therefore, applied for comparing the two groups. For comparing more than two groups, Kruskal Wallis one-way analysis of variance (ANOVA) followed by post-hoc was applied for multiple comparisons. The $p \leq 0.05$ was considered significant. The measure R^2 (Coefficient of determination) was used to determine the goodness of standard curve fit for ELISA and total protein. All statistical analysis such as linear regression, quadratic fit and test of significance were performed with statistical product and service solutions (SPSS; IBM SPSS Statistics 20.0, Chicago, Illinois, USA) 20.0 software. Receiver operating characteristic (ROC) curve, which is defined as a plot of true positive rate (test sensitivity) versus false positive (1-specificity) rate for different cut-off points of DcR1 levels was drawn for predicted model. Area under the ROC curve is considered as an effective measure of inherent validity of a diagnostic test.

1. Brown, R. C., Lockwood, A. H. & Sonawane, B. R. Neurodegenerative Diseases, An Overview of Environmental Risk Factors. *Environ Health Perspect* **113**, 1250–1256 (2005).
2. Owen, C. G., Fletcher, A. E., Donoghue, M. & Rudnicka, A. R. How big is the burden of visual loss caused by age related macular degeneration in the United Kingdom? *Br J Ophthalmol.* **87**, 312–317 (2003).
3. Azad, R., Chandra, P. & Gupta, R. The economic implications of the use of anti-vascular endothelial growth factor drugs in age-related macular degeneration. *Indian Journal of Ophthalmology.* **55**, 441–443 (2007).
4. Wang, A. L. *et al.* Autophagy and exosomes in the aged retinal pigment epithelium, Possible relevance to drusen formation and age-related macular degeneration. *PLoS ONE* **4**, e4160 (2008).
5. Bhattacharya, S., Chaum, S., Johnson, D. A. & Johnson, L. R. Age-Related Susceptibility to Apoptosis in Human Retinal Pigment Epithelial Cells Is Triggered by Disruption of p53–Mdm2 Association. *Invest. Ophthalmol.* **53**, 8350–8366 (2012).
6. Sharma, N. K. *et al.* Association between CFH Y402H polymorphism and age related macular degeneration in North Indian cohort. *PLoS ONE* **8**, e70193 (2013).
7. Sharma, N. K. *et al.* Single Nucleotide Polymorphism and Serum Levels Of VEGFR2 are Associated With Age Related Macular Degeneration. *Curr Neurovasc Res.* **9**, 256–65 (2012).
8. Sharma, N. K. *et al.* New Biomarker for Neovascular Age Related Macular Degeneration, Eotaxin-2. *DNA Cell Biol.* **31**, 1618–1627 (2012).
9. Anand, A. *et al.* Single Nucleotide Polymorphisms in MCP-1 and Its Receptor Are Associated with the Risk of Age Related Macular Degeneration. *PLoS ONE* **7**, e49905 (2012).
10. Klein, R. *et al.* Risk alleles in CFH and ARMS2 and the long-term natural history of age-related macular degeneration, the Beaver Dam Eye Study. *JAMA Ophthalmol.* **131**, 383–92 (2013).
11. Johnstone, W. R., Frew, A. J. & Smyth, M. J. The TRAIL apoptotic pathway in cancer onset, progression and therapy. *Nature* **8**, 782–798 (2008).
12. Hageman, G. S. *et al.* An integrated hypothesis that considers drusen as biomarkers of immune-mediated processes at the RPE-Bruch's membrane interface in aging and age-related macular degeneration. Prog. Retin. *Eye Res.* **20**, 705–732 (2001).
13. Crabb, J. W. *et al.* Drusen proteome analysis: an approach to the etiology of age-related macular degeneration. *Proc. Natl. Acad. Sci.* **99**, 14682–14687 (2002).

14. Dunaief, J. L., Dentchev, T., Ying, G. & Milam, A. H. The Role of Apoptosis in Age-Related Macular Degeneration. *Arch Ophthalmol.* **120**,1435–1442 (2002).
15. Ozoren, N. & El-Deiry, W. S. Cell surface death receptor signaling in normal and cancer cells. *Semin Cancer Biol.* **13**, 135–147 (2003).
16. Yamanaka, T. *et al.* Chemotherapeutic agents augment TRAIL-induced apoptosis in human hepatocellular carcinoma cell lines. *Hepatology* **32**, 482–490 (2000).
17. Toscano, F. *et al.* P53-mediated upregulation of DcR1 impairs oxaliplatin/TRAIL-induced synergistic anti-tumour potential in colon cancer cells. *Oncogene* **27**, 4161–71(2008).
18. Chavala, S. H. *et al.* Retinal angiogenesis suppression through small molecule activation of p53. *J Clin Invest.* **123**, 4170–4181 (2013).
19. Chang, B. *et al.* Retinal degeneration mutants in the mouse. *Vision Res.* **42**, 517–25 (2002).
20. Chang, B. *et al.* Age-related retinal degeneration (arrd2) in a novel mouse model due to a nonsense mutation in the Mdm1 gene. *Hum Mol Genet.* **17**, 3929–41 (2008).
21. Hawes, N. L. *et al.* Retinal degeneration 6 (rd6): a new mouse model for human retinitis punctata albescens. *Invest Ophthalmol Vis Sci.* **41**, 3149–57 (2000).
22. Li, Z. Y. & Milam, A. H. Apoptosis in retinitis pigmentosa. Anderson RELaVail MMHollyfield JGeds.Degenerative Diseases of the Retina. *New York, NY Plenum Press* 1–8 (1995).
23. Xu, G. Z., Li, W. W. & Tso, M. O. Apoptosis in human retinal degenerations. *Trans Am Ophthalmol Soc.* **94**, 411–430 (1996).
24. Kerrigan, M. S., Zack, D. J., Quigley, H. A., Smith, S. D. & Pease, M. E. TUNEL-positive ganglion cells in human primary open-angle glaucoma. *Arch Ophthalmol.* **115**, 1031–1035 (1997).
25. Johnstone, R. W., Ruefli, A. A. & Lowe, S. W. Apoptosis, a link between cancer genetics and chemotherapy. *Cell* **108**, 153–164 (2002).

Acknowledgments

The study was carried out at Department of Neurology, PGIMER, Chandigarh, India. We acknowledge Indian Council of Medical research, India for providing funds (45/11/2010-HUM/BMS). The funders had no role in study design, data collection and analysis, decision to publish, or preparation of the manuscript.

Author contributions

A.A. conceptualized the study and framework. N.K.S. and A.A. conducted the study, data analysis interpreted the results and wrote the manuscript. S.K.S., A.K.B., N.J. and P.K.G. contributed to the data analysis and prepared some figures. A.G., S.P. and R.D.S. contributed to the interpretation and reviewed the manuscript. All authors reviewed the manuscript.

Additional information

Competing financial interests: The authors declare no competing financial interests.

How to cite this article: Anand, A. *et al.* Does DcR1 (TNF-related apoptosis-inducing-ligand Receptor 3) have any role in human AMD pathogenesis? *Sci. Rep.* **4**, 4114; DOI:10.1038/srep04114 (2014).

This work is licensed under a Creative Commons Attribution-NonCommercial-NoDerivs 3.0 Unported license. To view a copy of this license, visit http://creativecommons.org/licenses/by-nc-nd/3.0

Preclinical non-human models to combat dementia

Avijit Banik and Akshay Anand

Neuroscience Research Lab, Department of Neurology, Post Graduate Institute of Medical Education and Research, Chandigarh, INDIA

ABSTRACT

Dementia is characterized by a certain degree of memory loss with disabled intellectual functioning, which mostly presents as Alzheimer's disease. The underlying causes range from gene mutations, lifestyle factors, and other environmental influences to brain injuries and normal aging. Although there have been many rodent and non-human primate models created by various drugs, neurotoxins and genetic ablation but the current scenario does not exhibit a well characterized animal model to evaluate novel compounds and various treatment strategies for dementia. Therefore, a comprehensive model exhibiting the pathologies and neuro-behavioral parameters close to this syndrome is very much needed. This report discusses the various experimental strategies to create animal models of dementia.

KEYWORDS: Dementia, Alzheimer's disease, Memory loss, Spatial memory, Animal model

Corresponding Author: Akshay Anand, Ph.D, Department of Neurology, Post Graduate institute of Medical Education and Research, Chandigarh, INDIA - 160012, Tel: +91 172 2756090, Fax: +91 172 2744401, E-mail: akshay1anand@rediffmail.com

doi : 10.5214/ans.0972.7531.200109

Introduction

Dementia, one of the major medical illnesses at older age, where the patient's language, attention and memory are compromised. Based on the etiology it can be reversible or irreversible; the onset could be sudden or gradual and the effect could be short term or long term. Amnesia is one of the characteristic feature of dementia and could be anterograde or retrograde depending on the forgotten events which are recently stored or from distant past.[1] Dementia is not a mere consequence of normal aging, rather an acquired impairment of cognition leading to person's inability to deal with activities in daily living compromising social activities, occupational functioning and relationships without affecting the consciousness.[2] Around 7% of the 65 year old population is affected by dementia and this incidence reaches 30 to 50% by the age of 85.[3] As of 2009 report of Alzheimer's Disease International, it is estimated that as many as 35.6 million people are living with dementia worldwide and this number is expected to be double by 2030 and will reach 115.4 million by 2050. Much of those living in developing countries are estimated to be 58% and it may rise to 71% by 2050.[4] In India more than 3 million people are estimated to be suffering from this and by 2030 this estimate is expected to be double.[5]

Alzheimer's disease (AD) is the major cause of dementia whereas, vascular dementia, dementia with Lewy bodies, fronto-temporal dementia etc also lead to memory deficits.[6] The diagnosis for dementia is based on clinical criterion related to memory, attention, orientation, judgment, language, motor and spatial skills. In last two decades the research efforts have focused on the multiple causes for the pathogenesis of the disease, leading to the emergence of robust functional and morphological biomarkers that can be evaluated in patients non-invasively through neuroimaging techniques and that have largely increased the sensitivity and specificity of its diagnosis.[7,8] Although there is a huge treatment gap as more than 75% of the patients suffering from dementia have not been diagnosed and therefore do not posses access to treatment and supportive cares.[4]

With the monumental impact of this disease on our socio-economic status the need to focus on the scientific evaluation of the disease on non-human models to validate the disease diagnosis, pathophysiology and neurobehavioral outcomes has heightened. This has led to the development of several disease model organisms for AD ranging from *Drosophila,* vertebrates like Zebrafish to several rodents and non-human primates. Several transgenic animals are also created for AD by manipulating a single or multiple genes at their expression level to mimic the pathological symptoms of the disease. Here, we have attempted to summarize various strategies to create the model animals for dementia and AD and this effort would give us a comprehensive overview on the scientific approaches taken together for understanding the disease at the molecular and physiological context and further for developing various therapeutic strategies.

Animal models for Dementia

The recent strategies in the development of animal models for dementia have paved the way to validate the efficacy, safety and protectiveness of several anti-dementia drugs before they could reach the clinical trials. A reliable animal model of memory loss with certain characteristics have been established in multiple ways by exposing the animals to a predetermined brain injury[9] or intracranial infusion of certain neurotoxins.[10] Approaches have been adopted to create some suitable transgenic rodent models of Alzheimer's disease by genetically introducing certain mutant genes associated with the disease. A number of behavioral parameters are analyzed in multiple assessments tasks ranging from their normal exploratory locomotor activities to motor coordination and memory analysis in spatial mazes with varying degree of difficulties offered to the animals.[11] Contrary to this, even the lower animals like zebrafish,[12] snails[13] are effectively studied to understand the underlying mechanisms involved in cellular and molecular conservations for memory disorders. There have been certain mutations also studied in *Drosophila* to evaluate their roles in pharmacological and genetic basis of cognition.[14]

NMDA receptor antagonism

The neurotransmitters and their receptors, which are actively involved in memory pathways, are widely targeted by their antagonists to impair learning and memory in animal models. NMDA (N-methyl-D-aspartic acid) receptor antagonists play

significant role in producing reversible or irreversible transient cognitive impairment in many experimental models to understand the molecular pathways involved in memory mechanisms and further to evaluate the screening of several anti-dementia drugs on these model animals.[15] There is a strong evidence that blocking the NMDA receptors at an early stage of neonatal life results in severe neurodegeneration due to lack of stimulation in the neurons.[16] Continuous NMDA antagonism results in irreversible damages in synaptic formations, more specifically blocks the induction of long term potentiation (LTP) through CA1 hippocampal pathway.[17] This in turn induces the abnormalities in hemispheric communications. Even constant administration at higher doses, these NMDAR antagonists develop permanent damage in the rodent brains termed as "Olney's Lesions".[18] A number of experimental NMDAR antagonists such as AP5 (D,L-2-amino-5-phosphonopentanoic acid), MK-801 (Dizocilpine maleate), NPC 12626 (2-amino-4,5-(1,2-cyclohexyl)-7-phosphonoheptanoic acid), PCP (1-(1-phenylcyclohexyl) piperidine), Ketamine have been used successfully to create the rodent models of memory loss to further investigate their molecular mechanisms involved[19] (Table 1). A series of cognitive parameters are analysed on these models using different behavioral apparatus viz., Morris water maze, radial arm maze, plus maze, active avoidance and passive avoidance tests. Even though blockade of NMDA transmission may be helpful to set up an animal model for the study of memory dysfunction, memantine, an NMDA channel blocker, is currently used for the treatment of AD. Hence the relationship between NMDA transmission and AD pathophysiology is not linear and simple, and needs further investigation.

Neurodegeneration by site specific delivery of neurotoxins

Selective neurodegeneration by various neurotoxins has also been tried in primates and rodents to elucidate the pathogenic mechanisms involved in Alzheimer's disease. Kainic acid, Domoic acid and Ibotenic acid are widely used neurotoxins, delivered through intracranial injections for specific neuron loss in hippocampal or other cortical areas (Table 2).[20,21] Mostly, these toxins induce glutamic acid mediated neuro-excitotoxicity by altering the calcium homeostasis in brain leading to inactivation of Ca2+ and CaM-mediated adenylate cyclase pathway, which in turn leads to neurdegeneration and loss of memory.[22,10] *In-vitro* treatment of kainic acid (KA) in primary striatal neurons induces excitotoxicity through p53 mediated mitochondrial dysfunction, production of reactive oxygen species, and apoptosis of neurons.[23] These findings are further validated with the impaired cognitive functions in rats when intra hippocampally administered.[24] Domoic acid (DA), the harmful neurotoxin extracted from algal blooms, can also cause severe anterograde amnesia when microinjected into the rat hippocampus.[21] Ibotenic

Table 1: Neuropathological and behavioral features of NMDAR antagonists induced animal models of memory loss

NMDAR antagonists	Site of Delivery	Subjects	Experimental outcome	References
AP5	Chronic intraventricular infusion	Male Lister rats	Spatial memory impairment in Morris water maze task	[43]
AP5	Basolateral Amygdala	Male Wistar rats	Impairment of inhibition effect in taste memory trace	[44]
AP5	Hippocampal CA3 region	Male & Female C57BL/6 mice	Attenuation of acquisition and long-term memory retrieval in spatial pattern completion task	[45]
MK-801	Intraperitoneal administration	Harlan Wistar rats	spatial cognition deficits in the cone field test	[46]
MK-801	Exposed to water, containing drug	Male Zebrafish	Cognitive impairment in inhibitory avoidance test and social interaction task	[47]
PCP	Subcutaneous administration	Male and female Sprague-Dawley rats on postnatal days of 7, 9 and 11	At adulthood impaired cognition in spatial reference and working memory task	[48]
PCP	Subcutaneous administration	Male mice of C57BL/6N, C57BL/6J, ddY, and ICR	Strain differences in enhanced immobility in the forced swim test (ddY>>C57BL/6N and 6J>ICR). Impairment of recognition memory but no strain difference in the novel object recognition test	[49]
Ketamine	Intraperitoneal administration	Male hooded Lister rats	dose-dependent working memory impairment in odor span task	[50]
Ketamine	Intravenous administration on postnatal days 5-6	Rhesus monkeys	At 10 months of age impairment in learning, motivation, color discrimination, and short-term memory tasks. Cognitive impairment persistant over 3 and one-half years of age	[51]
NPC 12626	Intraperitoneal administration	Male Sprague Dawley rats	At higher dose, the choice accuracy at all retention intervals is disrupted	[52]
NPC 12626	Mantle cavity, into the hemocoel	Land snail (*Cepaea nemoralis*)	Reduction in the pronociceptive effects evaluated Thermal response latency test	[53]

Table 2: Neuropathological and behavioral features of toxins induced animal models for memory loss

Toxins	Pathogenic Mechanisms	Subjects	Experimental outcome	References
Kainic Acid	Overproduction of reactive oxygen species, mitochondrial dysfunction	Rats	Impairment in learning and memory in Y maze task	[24]
Kainic Acid	Decreased expression of NMDA receptor subunit 2B in hippocampus	Rats	No hippocampal neuronal loss, spatial memory inpairment	[54]
Domoic Acid	Degeneration of CA3 and CA1 pyramidal cells and dentate gyrus granule cells through loss of $Ca2^{+}$ homeostasis	Rats	Severe anterograde amnesia analysed by Morris water maze task	[21]
Domoic Acid	Increased conc. of intracellular Ca2+ led to reduced level of cyclic AMP, inducing cytotoxicity	Rats	Neurodegeneration and Memory impairment	[10]
Domoic Acid	Mild neuropathologic changes (I.P) Lesions in hippocampus (I.V); hippocampus and cerebral cortex (oral) Neuronal degeneration (I.P/I.C) Lesion in the hippocampus and cerebral cortex (oral)	Monkeys administered I.P/I.V /Orally Rats administered I.P/I.C /Orally	No behavioral impairments Memory deficit in Morris water maze test (I.P) Learning impairment in radial arm maze (I.C) No behavioral impairments (oral)	[55]
Ibotenic Acid	Reduction of choline acetyltransferase and acetylcholine esterase in the hippocampus	Rats	Memory impairment in maze tests	[67]
Ibotenic Acid	Lesion in the nucleus basalis of Meynert	C57BL/6 mice	Working memory impairment in 8-arm radial maze	[56]

I.P: Intraperitoneal; I.V: Intravenous; I.C: Intracranial

acid, synthesized by mushrooms *Amanita muscaria* and *Amanita pantherina,* has been reported to disrupt the cholinergic network when delivered in rat brain and further impairs cognitive performance in water maze.[11] Together these neurotoxins provide methods to induce memory loss resulting in validation of novel therapeutics.

Memory impairment by mechanical brain injury

Animal models for Traumatic brain injury (TBI) have a profuse clinical significance to understanding the pathophysiology of injured neurons and how they combat in response to trauma. TBI is often associated with memory impairment characterized by primary or secondary neuronal loss leading to alterations in synaptic plasticity.[25] The recent strategies in development of this model target site specific injury to the brain parenchyma or hippocampal/parahippocampal regions of rodents[26,27] and also primates.[28,29] Gao *et al.* have reported the moderate parasagittal fluid percussion method to induce TBI in rats leading to memory loss in Morris water maze tests.[30] Other studies reported in the 90s demonstrate that formation of lesion in specific region of the brain, such as dorsal hippocampus compromises about 40% of the total hippocampus volume leading to significant learning and memory impairment.[31,32] Recently, several modified approaches have been tested upon on rodents to induce the brain injury such as, pellet shot from a modified air rifle for penetrating injury to the brain parenchyma[33] or, detonation of an open field explosive to create a low level blast trauma without systemic injuries to the brain.[34] All these models showed significant cognitive and behavioral impairments along with neuropathological characteristics found acutely in the brain injury.

Transgenic mice

Transgenic models of Alzheimer's disease in mice have been successfully produced by targeting multiple genes closely related to the disease pathologies and several symptoms associated with the disease. This is the most useful system in exist to understand the pathophysiology of the disease and investigate new promising drugs for AD. In last two decades there have been several successful attempts made to create transgenic models with similar signs and symptoms very close to the disease. The clinical implications of these models are enormous and by using them in experimental trials a number of effective molecules have been identified and vigorously tested upon to come out with the most suitable therapeutic composition which could reduce the pathological burden of the disease rather than the symptomatic relief. A number of mutations associated with FAD targeting APP, PS1 and PS2 genes responsible for the pathogenesis of AD, have been identified till date and they are successfully captured in mice to develop the extracellular deposition of insoluble β-amyloid plaques, a pathological hallmark of AD (**Table 3**).

One of the mostly targeted molecules, APP (amyloid β precursor protein) with desired mutation could produce toxic amyloid plaques in the brain leading to cognitive impairment. These mutations in APP are widely investigated to understand the underlying mechanisms in Aβ metabolism, aggregation, and deposition.[35] The PDAPP mice were the first transgenics for AD that expressed several neuropathological features of the disease. It could successfully develop Aβ deposition in temporal and hippocampal regions, leading to amyloid angiopathy, microgliosis and astrocytosis and further behavioral impairments. All these properties have paved the way to make PDAPP one of the attractive models to

Table 3: Neuropathological and behavioral features of several transgenic mice models of Alzheimer's disease

Transgenics	Traget Site	Functional Outcome	References
Amyloid precursor protein (PDAPP)	Swedish, London, Indiana- isoforms of Human APP: V717F	Amyloid depotition in brain tissues and impaired performance in learning and memory tasks	[57]
Amyloid precursor protein (PDAPP)	Human APP770: V717F	Confocal and electron microscopy images show neuritic plaques with a dense amyloid core surrounded by astroglial cells. Abundant Extracellular amyloid fibrils also found	[58]
$APPs_w$ or Tg2576	Human APP695: double mutation K670N, M671L	Significant over expression of Aβ peptides and learning and memory deficit at 9-10 months of age	[59]
APP23	Human APP695: double mutation K670N, M671L	Aβ plaques at 6 months, hyperphosphorylated tau tangles and neuronal loss followed by cognitive impairment	[60]
Presenilin 1 (PS1)	Human PS: M146L or M146V	Increased production of beta-amyloid (Aβ) and hyper-phosphorylation of tau protein in hippocampus and decrease in level of presynaptic synaptophysin	[61]
Presenilin 2 (PS2)	Human PSEN2: N141I or M239V	Overexpression of Presenilin 2 and increased production of Abeta-42 leading to activation of caspase-3 and Cox-2. Also behavioral deficit in water maze task	[62]
APP/PS1	Human/mouse APPswe: double mutation K595N, M596L Human PS1: A246E	High levels of Aβ(1-40) and Aβ(1-42) detected among different brain regions and significant memory deficits in radial arm water maze test	[63]
3xTg: PS1/APP/Tau	PS1(M146V), APP(Swe), and tau(P301L)	Amyloid plaques and neurofibrillary tangles formed. Synaptic abnormalities and cognitive deficit	[41]
Beta site APP cleaving enzyme (BACE)	β-Secretase	Increased load of Aβ peptides deposition in the cortex, hippocampus and in brain vasculature. Also impaired spatial acquisition in water maze test	[64]
Apolipoprotein E (apoE7/apoE4)	Apo E4: C112R, or L28P and C112R ApoE7: Q244K or Q245K	Significant increase in levels of serum lipid and impaired memory performance in behavioral tasks	[65]
Tau	Microtubule-associated tau protein (T44): P301L	Increase in the level of phosphorylated tau at the surface of rough endoplasmic reticulum membranes in brain tissue	[66]

evaluate the valid mode of diagnosis and treatment of AD.[36] Interestingly another line of transgenic mice with double mutations in APP and Presenilin (PS1) have shown spatial memory deficits in water maze analysis followed by a higher extracellular amyloid-β deposition and intracellular deposition of hyperphosphorylated tau proteins.[37] The mutations only in the Presenilin gene do not exhibit Aβ deposition unless coupled with APP mutation.[38] However, functional reduction of Presenilin alone by 50% has led to significant cognitive impairment in *Drosophila,* demonstrate that Presenilin homeostasis is one of the important mechanisms involved in memory network.[14] Although most of these models engineered till date do not undergo significant cell loss but only a few of the selective transgenic models with very early and aggressive neuropathology sustain neuronal loss.

Several lines of evidence reveal that there is microglial activation prior to amyloid-β deposition in brain suggesting that the immunogenic reactions followed by production of cytokines and neurotoxin induced neurodegeneration preceed amyloid-β pathology in the brain.[39,40] There is a triple transgenic line created recently in an attempt to mimic the most symptomatic and neuropathological phenotypes of the disease by targeting PS1, APP and Tau protein together. The pathological findings suggest that there are synaptic abnormalities and deposition of both plaques and tangles, leading to cognitive deficits.[41] Beta site APP cleaving enzyme (BACE1), one of the important proteases, breaks down the APP into soluble amyloid peptide. The mutation in BACE1 may lead to abnormal break down of APP, forming insoluble plaques in the brain. The BACE1 knock-in along with APP transgene have shown the faster neural degradation in mice brain.[42]

Conclusions

50 years back biologists and psychologists were least likely to believe that various pathophysiological complications leading to dementia could be studied experimentally. But in last two decades there have been extensive analysis done on non-human models to uncover the neurophysiological and molecular events leading to dementia. There have been several strategies to establish these experimental animal models including intracranial delivery of certain neurotoxins, administration of antagonists for neurotransmitter receptors, site specific mechanical injury to the brain and transgenics. Fortunately, transgenic mice that are generated with specific mutations indicate the molecular pathways involved in dementia. Also, these models can mimic the neuro-pathological and behavioral symptoms of the disease. Considering the rapid progress in the field, these animal models have contributed tremendously in preclinical studies and paved way to bridge the gap for human translation. Therefore the clinical significance of these models is immense and selection of a validated

model organism for preclinical testing remains a real challenge.

The article complies with International Committee of Medical Journal Editor's uniform requirements for the manuscripts.

Competing interests – None,
Source of Funding – None

Received Date : 13 December, 2012

Revised Date : 30 December, 2012

Accepted Date : 07 January, 2013

References

1. Fauci AS, Braunwald E, Kasper DL. Harrison's principles of internal medicine. McGraw-Hill Professional, United States 2008; 17.
2. Gerhard EW, Leyhe T, Klöppel S, *et al*. New developments in the diagnosis of dementia. Dtsch Arztebl Int. 2010; 107: 677–683.
3. Geldmacher DS and Whitehouse PJ. Evaluation of dementia. N Eng J Med. 1996, 5: 330–305.
4. Alzheimer's Disease International: World Alzheimer Report (ADI:WAR) 2009.
5. Alzheimer's and Related Disorders Society of India (ARDSI) 2008.
6. Basu S and Bhattacharya KB. Dementia Current Status. Post Grad Med. 2003; 17: 543–541.
7. Trojanowski JQ, Vandeerstichele H, Korecka M, *et al.* Update on the biomarker core of the Alzheimer's disease neuroimaging initiative subjects: Alzheimer's Disease Neuroimaging Initiative. Alzheimers Dement 2010; 6(3): 230–238.
8. Maalouf M, Ringman JM, Shi J. An update on the diagnosis and management of dementing conditions. Rev Neurol Dis. 2011; 8(3–4):e68–87.
9. Albensi BC and Janigro D. Traumatic brain injury and its effects on synaptic plasticity. Brain Inj. 2003; 17(8): 653–663.
10. Nijjar MS and Nijjar SS. Domoic acid-induced neurodegeneration resulting in memory loss is mediated by Ca2+ overload and inhibition of Ca2+ calmodulin-stimulated adenylate cyclase in rat brain. Int J Mol Med. 2000; 6(4): 377–389.
11. Crawley JN and Paylor R. A proposed test battery and constellations of specific behavioral paradigms to investigate the behavioral phenotypes of transgenic and knockout mice. Horm Behav. 1997; 31(3): 197–211.
12. Kim YH, Lee Y, Kim D, *et al*. Scopolamine-induced learning impairment reversed by physostigmine in zebrafish. Neurosci Res. 2010; 67: 156–161.
13. Solntseva SV and Nikitin VP. Reversible and irreversible stages in the development of amnesia after disruption of the reactivation of associative memory in snails. Neurosci Behav Physio. 2010; 40: 679–686.
14. McBride SM, Choi CH, Schoenfeld BP, *et al*. Pharmacological and genetic reversal of age-dependent cognitive deficits attributable to decreased presenilin function. J Neurosci. 2010; 30(28): 9510–9522.
15. Gunduz-Bruce H. The acute effects of NMDA antagonism: from the rodent to the human brain. Brain Res Rev. 2009; 60(2): 279–286.
16. Haberny KA, Paule MG, Scallet AC, *et al*. Ontogeny of the N-methyl-D-aspartate (NMDA) receptor system and susceptibility to neurotoxicity. Toxicol Sci 2002; 68(1): 9–17.
17. Bannerman DM, Good MA, Butcher SP, *et al*. Distinct components of spatial learning revealed by prior training and NMDA receptor blockade. Nature. 1995; 378: 182–186.
18. Olney J, Labruyere J, Wang G, *et al*. NMDA antagonist neurotoxicity: mechanism and prevention. Science. 1991; 254(5037): 1515–1518.
19. Neill JC, Barnes S, Cook S, *et al*. Animal models of cognitive dysfunction and negative symptoms of schizophrenia: focus on NMDA receptor antagonism. Pharmacol Ther. 2010; 128(3): 419–432.
20. Ciriza I, Carrero P, Frye CA, *et al*. Reduced metabolites mediate neuroprotective effects of progesterone in the adult rat hippocampus. The synthetic progestin medroxyprogesterone acetate (Provera) is not neuroprotective. J Neurobiol. 2006; 66: 916–928.
21. Sutherland RJ, Hoesing JM, Whishaw IQ. Domoic acid, an environmental toxin, produces hippocampal damage and severe memory impairment. Neurosci Lett. 1990; 120: 221–223.
22. Krogsgaard-Larsen P and Hansen JJ. Naturally-occurring excitatory amino acids as neurotoxins and leads in drug design. Toxicol Lett. 1992; 64–65: 409–416.
23. Dong XX, Wang YR, Qin S, *et al*. p53 Mediates autophagy activation and mitochondria dysfunction in kainic acid-induced excitotoxicity in primary striatal neurons. Neuroscience. 2012; 207: 52–64.
24. Srivastava N, Seth K, Srivastava N, *et al*. Functional restoration using basic fibroblast growth factor (bFGF) infusion in kainic acid induced cognitive dysfunction in rat: neurobehavioural and neurochemical studies. Neurochem Res. 2008; 33: 1169–1177.
25. Albensi BC. Models of brain injury and alterations in synaptic plasticity. J Neurosci Res. 2001; 65(4): 279–283.
26. Clark RE, Zola SM, Squire LR. Impaired recognition memory in rats after damage to the hippocampus. J Neurosci. 2000; 20: 8853–8860.
27. Gould TJ, Rowe WB, Heman KL, *et al*. Effects of hippocampal lesions on patterned motor learning in the rat. Brain Res Bull. 2002; 58: 581–586.
28. Nemanic S, Alvarado MC, Bachevalier J. The hippocampal/ parahippocampal regions and recognition memory: insights from visual paired comparison versus object delayed nonmatching in monkeys. J Neurosci. 2004; 24: 2013–2026.
29. Zola SM, Squire LR, Teng E, *et al.* Impaired recognition memory in monkeys after damage limited to the hippocampal region. J Neurosci. 2000; 20: 451–463.
30. Gao J, Prough DS, McAdoo DJ, *et al*. Transplantation of primed human fetal neural stem cells improves cognitive function in rats after traumatic brain injury. Exp Neurol. 2006; 201: 281–92.
31. Moser EI, Moser MB and Andersen P. Spatial learning impairment parallels the magnitude of dorsal hippocampal lesions, but is hardly present following ventral lesions. J Neurosci. 1993; 13: 3916–3925.
32. Moser MB, Moser EI, Forrest E, *et al.* Spatial learning with a minislab in the dorsal hippocampus. Proc Natl Acad Sci USA 1995; 92: 9697–9701.
33. Plantman S, Ng KC, Lu J, *et al.* Characterization of a novel rat model of penetrating traumatic brain injury. J Neurotrauma. 2012; 29(6): 1219–1232.
34. Rubovitch V, Ten-Bosch M, Zohar O, *et al*. A mouse model of blast-induced mild traumatic brain injury. Exp Neurol. 2011; 232(2): 280–289.
35. Hsiao K. Transgenic mice expressing Alzheimer amyloid precursor proteins. Exp Gerontol. 1998; 33: 883–889.
36. Basak JM and Holtzman DM. APP-Based Transgenic Models: The PDAPP Model. Neuromethods 2011; 48: 371–385.
37. Lee HJ, Lee JK, Lee H, *et al*. Human umbilical cord blood-derived mesenchymal stem cells improve neuropathology and cognitive impairment in an Alzheimer's disease mouse model through modulation of neuroinflammation. Neurobiol Aging. 2010; 33: 588–602.
38. Higgins LS. Animal models of Alzheimer's disease. Mol Med Today. 1999; 5: 274–276.
39. El Khoury JB, Moore KJ, Means TK, *et al*. CD36 mediates the innate host response to beta-amyloid. J Exp Med. 2003; 197: 1657–1666.
40. Meda L, Cassatella MA, Szendrei GI, *et al*. Activation of microglial cells by beta-amyloid protein and interferon-gamma. Nature. 1995; 374: 647–650.
41. Oddo S, Caccamo A, Shepherd JD, *et al*. Triple-transgenic model of Alzheimer's disease with plaques and tangles: intracellular Abeta and synaptic dysfunction. Neuron. 2003; 39: 409–421.
42. Rockenstein E, Mante M, Alford M, *et al*. High betasecretase activity elicits neurodegeneration in transgenic mice despite reductions in amyloid-beta levels: implications for the treatment of Alzheimer disease. J Biol Chem. 2005; 280: 32957–32967.
43. Morris RG. Synaptic plasticity and learning: selective impairment of learning rats and blockade of long-term potentiation *in vivo* by the N-methyl-D-aspartate receptor antagonist AP5. J Neurosci. 1989; 9: 3040–3057.
44. Traverso LM, Quintero E, Vargas JP, *et al*. Taste memory trace disruption by AP5 administration in basolateral amygdala. Neuroreport. 2010; 21(2): 99–103.
45. Fellini L, Florian C, Courtey J, *et al*. Pharmacological intervention of hippocampal CA3 NMDA receptors impairs acquisition and long-term memory retrieval of spatial pattern completion task. Learn Mem. 2009; 16(6): 387–394.
46. Bouger PC and van der Staay FJ. Rats with scopolamine- or MK-801-induced spatial discrimination deficits in the cone

field task: animal models for impaired spatial orientation performance. Eur Neuropsychopharmacol. 2005; 15(3): 331–346.
47. Seibt KJ, Piato AL, da Luz Oliveira R, *et al*. Antipsychotic drugs reverse MK-801-induced cognitive and social interaction deficits in zebrafish (Danio rerio). Behav Brain Res. 2011; 224(1): 135–139.
48. Andersen JD and Pouzet B. Spatial memory deficits induced by perinatal treatment of rats with PCP and reversal effect of D-serine. Neuropsychopharmacology. 2004; 29(6): 1080–1090.
49. Mouri A, Koseki T, Narusawa S, *et al*. Mouse strain differences in phencyclidine-induced behavioural changes. Int J Neuropsychopharmacol. 2011; 9: 1–13.
50. Rushforth SL, Steckler T and Shoaib M. Nicotine improves working memory span capacity in rats following sub-chronic ketamine exposure. Neuropsychopharmacology. 2011; 36(13): 2774–2781.
51. Paule MG, Li M, Allen RR, *et al*. Ketamine anesthesia during the first week of life can cause long-lasting cognitive deficits in rhesus monkeys. Neurotoxicol Teratol. 2011; 33(2): 220–230.
52. Pontecorvo MJ, Clissold DB, White MF, *et al*. N-methyl-D-aspartate antagonists and working memory performance: comparison with the effects of scopolamine, propranolol, diazepam, and phenylisopropyladenosine. Behav Neurosci. 1991; 105(4): 521–535.
53. Kavaliers M, Choleris E and Saucier DM. The NMDA receptor antagonist, NPC 12626, reduces the pronociceptive effects of orphanin FQ and kappa opiate antinociception in the land snail, *Cepaea nemoralis*. Peptides. 1997; 18(7): 943–947.
54. Sun QJ, Duan RS, Wang AH, *et al*. Alterations of NR2B and PSD-95 expression in hippocampus of kainic acid-exposed rats with behavioural deficits. Behav Brain Res. 2009; 201(2): 292–299.
55. Grant KS, Burbacher TM, Faustman EM, *et al*. Domoic acid: neurobehavioral consequences of exposure to a prevalent marine biotoxin. Neurotoxicol Teratol. 2010; 32(2): 132–141.
56. Wang, Matsumoto Y, Shindo T, *et al*. Neural stem cells transplantation in cortex in a mouse model of Alzheimer's disease. J Med Invest. 2006; 53: 61–69.
57. Morgan D. Learning and memory deficits in APP transgenic mouse models of amyloid deposition. Neurochem Res. 2003; 28: 1029–1034.
58. Masliah E, Sisk A, Mallory M, *et al*. Comparison of neurodegenerative pathology in transgenic mice overexpressing V717F beta-amyloid precursor protein and Alzheimer's disease. J Neurosci. 1996; 16(18): 5795–5811.
59. Hsiao K, Chapman P, Nilsen S, *et al*. Correlative memory deficits, Abeta elevation, and amyloid plaques in transgenic mice. Science. 1996; 274(5284): 99–102.
60. Van Dam D, Vloeberghs E, Abramowski D, *et al*. APP23 mice as a model of Alzheimer's disease: an example of a transgenic approach to modeling a CNS disorder. CNS Spectr. 2005; 10(3): 207–222.
61. Yang X, Yang Y, Liu J, *et al*. Increased phosphorylation of Tau and synaptic protein loss in the aged transgenic mice expressing familiar Alzheimer's disease-linked Presenilin 1 mutation. Neurochem Res. 2011; 37: 15–22.
62. Hwang DY, Chae KR, Kang TS, *et al*. Alterations in behavior, amyloid beta-42, caspase-3, and Cox-2 in mutant PS2 transgenic mouse model of Alzheimer's disease. FASEB J. 2002; 16: 805–813.
63. Xiong H, Callaghan D, Wodzinska J, *et al*. Biochemical and behavioral characterization of the double transgenic mouse model (APPswe/PS1dE9) of Alzheimer's disease. Neurosci Bull. 2011; 27: 221–232.
64. Ozmen L, Woolley M, Albientz A, *et al*. BACE/APPV717F double-transgenic mice develop cerebral amyloidosis and inflammation. Neurodegener Dis. 2005; 2: 284–298.
65. Sun M and Qi Z. The human apoE7 and apoE4 transgenic mice models. Sci China Series C Life Sci. 2001; 44: 652–660.
66. Perreault S, Bousquet O, Lauzon M, *et al*. Increased association between rough endoplasmic reticulum membranes and mitochondria in transgenic mice that express P301L tau. J Neuropathol Exp Neurol. 2009; 68: 503–551.
67. Kim JH, Hahm DH, Lee HJ, *et al*. Acori graminei rhizoma ameliorated ibotenic acid-induced amnesia in rats. Evid Based Complement Alternat Med. 2009; 6: 457–464.

frontiers in
NEUROLOGY

REVIEW ARTICLE
published: 11 May 2012
doi: 10.3389/fneur.2012.00075

Preclinical models to investigate retinal ischemia: advances and drawbacks

Gillipsie Minhas[1], Ryuichi Morishita[2] and Akshay Anand[1]*

[1] Neuroscience Research Lab, Department of Neurology, Postgraduate Institute of Medical Education and Research, Chandigarh, India
[2] Division of Clinical Gene Therapy, Graduate School of Medicine, Osaka University Medical School, Osaka, Japan

Edited by:
Kenneth Shindler, University of Pennsylvania, USA

Reviewed by:
Yaping Joyce Liao, Stanford University School of Medicine, USA
Reas Khan Sulaimankutty, University of Pennsylvania, USA

***Correspondence:**
Akshay Anand, Neuroscience Research Lab, Department of Neurology, Postgraduate Institute of Medical Education and Research, Chandigarh-160012, India.
e-mail: akshay1anand@rediffmail.com

Retinal ischemia is a major cause of blindness worldwide. It is associated with various disorders such as diabetic retinopathy, glaucoma, optic neuropathies, stroke, and other retinopathies. Retinal ischemia is a clinical condition that occurs due to lack of appropriate supply of blood to the retina. As the retina has a higher metabolic demand, any hindrance in the blood supply to it can lead to decreased supply of oxygen, thus causing retinal ischemia. The pathology of retinal ischemia is still not clearly known. To get a better insight into the pathophysiology of retinal ischemia, the role of animal models is indispensable. The standard treatment care for retinal ischemia has limited potential. Transplantation of stem cells provide neuroprotection and to replenish damaged cells is an emerging therapeutic approach to treat retinal ischemia. In this review we provide an overview of major animal models of retinal ischemia along with the current and preclinical treatments in use.

Keywords: animal model, retinal ischemia, stem cells, therapeutics

INTRODUCTION

The term "ischemia" implies reduction in the blood supply to a tissue resulting in insufficiency to meet the metabolic requirements. Thus, retinal ischemia is the clinical condition when the blood supply to the retina is obstructed. The retina is an extension of central nervous system (CNS) and thus shares many embryological, functional, and anatomical characteristics with brain. The response to ischemia in retinal neurons is similar to those in other parts of CNS. Nevertheless, retina is more resistant to ischemic injury than the brain (Tso and Jampol, 1982).

As far as the blood supply to the retina is concerned, the mammalian retina has a dual circulation system. The major portion of blood supply goes to the choroid, i.e., 65–85% of the total supply, whereas the remaining goes to the retina through central retinal artery, which originates from ophthalmic artery (Henkind et al., 1979). **Figure 1** depicts the blood supply to the eye. The extent of retinal ischemia and the region of retina affected depends on the blood supply that is obstructed (Saint-Geniez and D'Amore, 2004). The retina has a high metabolic demand. Any hindrance in the blood supply affects the exchange of substrates and products, leading to many morphological and functional changes in retina. The pathophysiology of retinal ischemia is not completely known but involves imbalance in ion transport, changes in neurotransmitter levels, oxidative stress, and finally cell death. Thus, there is a need to study the pathophysiology involved so that better therapeutic agents can be tested. As retina can be studied non-invasively the investigations into retinal ischemia may lead to a better understanding of cerebral ischemia.

NEED FOR ANIMAL MODELS

Although humans and animals have varying phenotype, they share strikingly common physiological and anatomical details. Therefore, to understand the human physiology and to test new treatments through preclinical investigations, animal experimentation has always been a core of basic and clinical research. The importance of developing animal models for retinal ischemia originates from the limitations found in the use of *in vitro* models. Retinal ischemia at molecular and biochemical levels can be studied in depth using an *in vitro* model of ischemia but the pathophysiological details can only be understood using an appropriate animal model. An ideal animal model for retinal ischemia should have parallelism with humans at anatomical, vascular, and retinal levels besides offering ease in handling and manipulation.

ANIMAL MODELS OF RETINA ISCHEMIA

ELEVATION OF INTRAOCULAR PRESSURE

The model often used to cause retinal ischemia is by increasing intraocular pressure (IOP). This model involves elevation of the IOP above the systemic arterial pressure for a fixed duration of time (Peachey et al., 1993). High IOP results in global ischemia as it hampers the blood supply from both uveal and retinal circulation. In rodents, different groups have shown that IOP-induced retinal ischemia mimics the features observed in human central retinal artery occlusion (CRAO) and primary open angle glaucoma (Smith and Baird, 1952; Buchi et al., 1991).

The animal model of retinal ischemia model was first described by Smith and Baird (1952) and was further validated by Flower and Patz (1971) in cats. In rodents, the elevated IOP-induced retinal ischemia injury was induced in rats by Buchi et al. (1991). In all these studies, the IOP was increased through cannulation of the anterior chamber with a 26-gauge needle connected to an elevated chamber containing normal saline. The IOP was raised to 110 mm Hg. This method has been used in a wide range of experiments to study the alteration in protein expression, ion channel imbalance, excitotoxicity in various animal models (Hirrlinger et al., 2010; Joachim et al., 2011). Ji et al. (2005) used this model

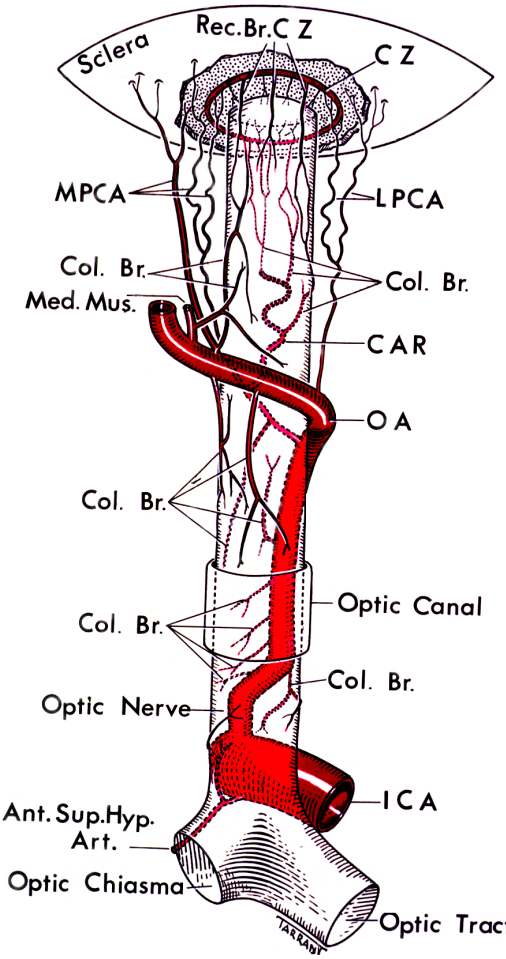


FIGURE 1 | The figure depicting the circle of Zinn-Haller and the blood supply to eye (Hayreh, 1963).

in mice to investigate the mechanism behind the retinal ganglion cell death due to retinal ischemia.

The advantages of using this model are that it is temporary and reversible, easy to create, and reproduce and there is minimal requirement of surgery or special equipments. But there is a limitation to this model that the elevated IOP can itself cause damage and hence, lead to incorrect interpretation of the data (Peachey et al., 1993).

MIDDLE CEREBRAL ARTERY OCCLUSION

It has been reported that the cerebral stroke incidents are invariably accompanied with temporary (amaurosis fugax) or permanent vision loss. A purely vascular model of retinal ischemia is the middle cerebral artery occlusion (MCAO). As the ophthalmic artery which is the source of blood supply to the inner retina originates proximal to the origin of middle cerebral artery (MCA), any hindrance in the blood flow in MCA obstructs the flow to the ipsilateral retina. This method involves occlusion of blood supply by the use of a filament inserted through external carotid artery (ECA) and internal carotid artery (ICA) and advanced into the MCA.

This procedure was first time demonstrated by Block et al. (1997) in rats that led to MCAO induced retinal ischemia. Later the same model was used to depict damage to retina through MCAO in mice (Steele et al., 2008). This model is a non-invasive and does not disrupt the blood–retina barrier or cause any mechanical damage to the retina (Kaja et al., 2003). The MCAO model has other advantages including reproducibility making it permissive for reperfusion related investigations.

CHRONIC CAROTID OCCLUSION

Retinal ischemia can also be caused by carotid artery disease in humans. This model was first induced by Block et al. (1992) in rats in order to show that the bilateral common carotid artery occlusion in rats causes functional damage to the retina. The electroretinogram studies have also shown a decrease in amplitude of b-wave 7 days after the bilateral carotid artery occlusion or two-vessel occlusion (2VO). The b-wave represents the bipolar and Muller cell activity (Barnett and Osborne, 1995). Not only functional, 2VO model also causes structural damage to the retina. In another study in rats, Lavinsky et al. (2006) showed that in the animals that showed functional damage, the retinal thickness was found to be decreased and the layers that are most affected included inner and outer plexiform layers.

The 2VO model for retinal ischemia leads to permanent occlusion without any reperfusion. Due to collateral blood circulation partial blood supply to retina is retained through Circle of Willis leading to variable retinal damage.

PHOTOTHROMBOSIS OF RETINAL VESSELS

The photothrombosis or photocoagulation induced retinal ischemia model is a simple and non-invasive method. It is comparatively a new method to perform vessel occlusion. This method was first described in adult rat retina by Mosinger and Olney (1989), where the authors injected Rose Bengal, a photosensitive dye intravenously and then exposed the retina to light of a fixed wavelength (550 nm) leading to photothrombosis. Miller et al. (1994) used this same method in a non-human primate model, cynomolgus monkey (*Macaca fascicularis*), where a laser at 577 nm was used for causing occlusion. Buchi et al. (1994) used this model to study morphological and histological changes in retina. Schimdt-Kastner also used Photothrombosis to induce ischemia in rat retina and showed the ganglion cell death (Schmidt-Kastner and Eysel, 1994). Another photosensitive dye, apart from Rose Bengal, that can be used in this model, is chloro-aluminum sulfonated phthalocyanine (Kliman et al., 1994).

Like any other method, this too has its own advantages and disadvantages. Photothrombosis leads to variability in retinal damage and hence irregular damage due to variation in light exposure. It leads to permanent ischemia and can therefore not be used to study damage due to reperfusion. This method results in damage due to free-radicals.

OCCLUSION OF CENTRAL RETINAL ARTERY

The central retinal artery is the first intraorbital branch of ophthalmic artery. The CRAO causes complete inner retinal ischemia.

In humans, the clinical features were first described by von Graefe (1859). The CRAO model has been used to induce retinal ischemia in different species. Hayreh induced transient CRAO in rhesus monkeys by clamping the central retinal artery for different time durations. This study also showed that the damage induced depends on the tolerance time for the particular species (Hayreh et al., 1980). Zhang et al. (2005) created this model in rats by intravenous injection of Rose Bengal and treating the animals with green laser. This model is used to study the pathways involved in transient retinal ischemia by mimicking the clinical features of CRAO in humans. In another study in CRAO model in rhesus monkeys, amino acid profiling was done to evaluate the role of glutamate excitotoxicity in ischemia (Kwon et al., 2005). The mouse model showing similar changes as human CRAO has been generated, where central retinal artery was occluded by laser photoactivation of Rose Bengal. The occlusion of 6–24 h showed molecular and histological changes (Goldenberg-Cohen et al., 2008). CRAO can also be achieved by another method which leads to ischemia – reperfusion model. In this model a suture is placed behind the eye globe and then obstructing the blood flow by pressing the tube through which both ends of suture are passed (Prasad et al., 2010).

ENDOTHELIN ADMINISTRATION

Endothelin-1 or ET-1 is a 21 amino acid long peptide with vasoconstrictor activity. It was first purified and characterized in 1988 from the conditioned medium of cultures of porcine aortic endothelial cells (Yanagisawa et al., 1988). In humans, cardiovascular disease, renal, and ocular disorders have been associated with endothelin-1. The vasoconstrictor activity of endothelin has been demonstrated in retinal arteries in rats. In a study by Bursell et al. (1995) an approximate 17% reduction in diameter after 10^{-7} M concentration of ET-1 was shown. Sakaue et al. also studied the effect of endothelin on the retinal vessels after intravitreal administration of ET-1 in rabbit eyes. The authors showed a dose-dependent response, where the concentration of 10^{-6} M caused vasoconstriction and lower concentrations caused vasodilation first with vasoconstrictions later, leading to hypoxia and retinal ischemia (Sakaue et al., 1992; Sato et al., 1993; Takei et al., 1993). In another study, ET-1 administration was used to obstruct the central retinal artery causing ganglion cell loss in retina (Masuzawa et al., 2006).

No problems such as inflammation or infection are associated with this model, but this has a limitation of ET-1 dose. Also it may show some undesirable effect due to systemic circulation to other tissues.

CURRENT AND POTENTIAL THERAPEUTIC STRATEGIES FOR RETINAL ISCHEMIA

Current treatments for retinal ischemia involve recovery of the blood circulation in retina that will prevent further damage and permanent vision loss. Combination of strategies are being used to treat retinal ischemia including intravitreal or retinal vein administration of anticoagulants such as tissue-plasminogen activator (t-PA), hemodilution, pan-retinal laser photocoagulation, or anti-VEGF antibodies (Lucentis or Avastin). Ischemic conditions in retina have been shown to up-regulate the expression of vascular endothelial growth factor or VEGF, a potent angiogenic factor. This change in VEGF levels leads to retinal neovascularization or growth of abnormal blood vessels. Neutralizing VEGF through monoclonal antibodies has been shown to block neovascularization. This technique was tested in a primate model of retinal ischemia induced by laser. The study showed that VEGF was inhibited *in vivo* when proteins containing human (Flt) or mouse (Flk) VEGF receptors attached to IgG were administered (Aiello et al., 1995). This showed almost complete inhibition of neovascularization. Laser photocoagulation or pan-retinal laser treatment is used to decrease the neovascularization or growth of abnormal blood vessels, thus decreasing the damage to the retina.

All these strategies that are being used have their own limitations. The anticoagulants and vasodilators are effective only in limited cases of retinal ischemia, such as CRAO patients, while the laser treatment is effective only when given early (Rumelt et al., 1999). This unavailability of effective treatment options has led to development of various other neuroprotective agents. Other possible therapeutic agents include NMDA receptor blockers or inhibitors, catalase and thioredoxin (free-radical scavengers), calcium channel blockers, and many others. These novel drugs and chemical compounds have been tested in different animal models of retinal ischemia, showing positive outcome and potential as future therapeutics. Various antagonists and blockers have been demonstrated to reduce the damage caused through ischemia. NMDA receptor antagonists have shown neuroprotective effect in retinal ischemia animal models. Different NMDA receptor blockers that have been tested in preclinical studies are dextromethorphan, MK-801, memantine (Cao et al., 1994; Lam et al., 1997; Osborne et al., 1999). Blockers of calcium channels have also been tested in animal models and have shown to decrease neurotoxicity (Melena et al., 1999). Retinal ischemia damage is exacerbated by free-radicals. Free-radicals are generated by reoxidation of compounds during reperfusion and leads to oxidative stress (Gilgun-Sherki et al., 2002). Thus, different free-radical scavengers can be used for treatment. Rios et al. compared the free-radical scavengers – SOD or superoxide dismutase and DMTU or dimethylthiourea. In an IOP-induced retinal ischemia model in rats, intravitreal administration of both the compounds has shown to potential in recovery. In this model, DMTU led to 40% functional recovery while SOD treatment showed a 99% recovery when assessed through electroretinogram (Rios et al., 1999).

Apart from these, growth factors such as CNTF, bFGF, NGF, BDNF, PEDF, HGF have been tested in retinal ischemia–reperfusion models for therapeutic potential (Unoki and LaVail, 1994; Ogata et al., 2001; Shibuki et al., 2002). These therapeutic agents have short half-life and thus require repeated administration resulting in side-effects. This limitation can be overcome by the delivery of the gene of neurotrophic factors directly using gene therapy. Viral vectors have been used successfully to transfect cells in eye (Bennett et al., 1994; Flannery et al., 1997; Di Polo et al., 1998). Wu et al. used recombinant Adeno-associated virus (AAV) vector to transfer GDNF intravitreally in rats subjected to elevated IOP. GDNF is a known neurotrophic factor

that reduces ischemic injury (Wu et al., 2004). It has also been shown in different studies that GDNF protects photoreceptors and inhibits apoptosis. Another group of neuroprotectants that have shown positive results in animal models by inhibiting apoptosis are the inhibitors of apoptosis (IAP) which inhibit caspases. Most tested IAP is the XIAP which blocks caspases 3, 7, and 9 (Deveraux et al., 1997; Xu et al., 1999; Eberhardt et al., 2000; Holcik et al., 2001; McKinnon et al., 2002; Petrin et al., 2003). Renwick et al. reported that XIAP overexpression protects the retina from transient ischemia induced by elevation of IOP in rats. In this study the authors intravitreally administered AAV vector expressing XIAP and demonstrated structural and functional protection in retinal ischemia model (Renwick et al., 2006). But it has a limitation of being ineffective in the cases where retinal ischemia occurs suddenly.

ROLE OF STEM CELL THERAPY IN RETINAL ISCHEMIA

The treatment strategies discussed in the previous section have limited potential. Stem cells are an emerging branch used in the treatment of a wide variety of disorders (Lenka and Anand, 2009). The use of stem cells from different sources are being studied and clinical trials are being carried out for disorders such as diabetes, spinal cord injury, fractures, cardiovascular, and neurological disorders. Replenishment of neuronal and retinal cells by stem cell transplantation is therefore a promising approach to treat retinal ischemia.

The stem cells have an ability to self-renew and differentiate into specialized cells. They can act through various mechanisms. Stem cells can induce angiogenesis and thus, increase vascularization. Stem cells can also enhance the endogenous repair mechanisms, reduce inflammation, and release trophic factors. In the case of retinal ischemia, the eye is easily accessible for transplantation of stem cells. Thus, the stem cell therapy has a huge potential to restore visual function in case of retinal ischemia (Cogliati and Swaroop, 2009).

Stem cells from various sources have been used for treatment. Most commonly used are the stem cells from the bone-marrow as they are easier to obtain. Two types of cell population is present in the bone-marrow – hematopoietic progenitor cells and hematopoietic stem cells. The sub-population of hematopoietic stem cells has been shown to differentiate into lineage-negative and lineage-positive sub-types. This division is according to their ability to differentiate. The cells in lineage-negative fraction can lead to vascular endothelial cells or the endothelial precursor cells after the differentiation. These progenitor cells can then mobilize from the bone-marrow and home to target sites of angiogenesis in different injuries. Bone-marrow mesenchymal stem cells (BM-MSCs) differentiate into retinal neural cells *in vivo* and *in vitro*, and when implanted at a site of injury in experimental animal models, they show the ability to migrate to the injury site, initiate tissue repair, and restore function (Goes et al., 2008).

Another source of stem cells for the therapeutic purposes is those obtained from the early embryos. These embryonic stem cells have two characteristic properties, their ability to replicate indefinitely and their pluripotency. Thus the embryonic stem cells can differentiate into various cell types. These cells have also been tested in the cerebral ischemia model, showing structural as well as functional recovery (Wei et al., 2005). Various research groups have shown the potential of these stem cells in neurodegenerative diseases including retinal damage. The use of embryonic stem cells for transplantation has its own limitations. The foremost is the ethical concerns over its use and secondly there is a risk of immune rejection. To overcome these limitations, another stem cell source from non-pluripotent cells was discovered. In 2006, Takahashi and Yamanaka identified four transcription factors – Oct3/4, Sox-2, Klf-4, c-myc. These factors can reprogram the DNA leading to the formation of stem cells from a non-pluripotent cell. These stem cells are known as induced pluripotent stem cells or iPCs (Takahashi and Yamanaka, 2006). iPCs have been used in various animal models and have shown to form different cell types. In humans, iPCs have been isolated from the patients with neurodegenerative disorders such as Parkinson's disease, muscular dystrophy, amyotrophic lateral sclerosis (Dimos et al., 2008; Park et al., 2008). iPCs have been used to generate human neuronal cells, photoreceptors, and retinal pigmented epithelium cells (Takahashi and Yamanaka, 2006; Hirami et al., 2009; Karumbayaram et al., 2009). Another source of stem cells that is being tested as a potential therapy is the umbilical cord blood. It has a large percentage of hematopoietic stem cells, higher than those found in bone-marrow and also these cells show lesser immune rejection.

Earlier the CNS was thought to be a non-renewable tissue in mammals. Neural stem cells are normally found in the developing CNS, but studies have shown that these are also present in adult CNS. These cells are found in restricted region of CNS, such as hippocampus, subventricular zone, spinal cord, and ependyma and

Table 1 | Advantages and limitations of different animal models of retinal ischemia.

Animal model	Advantages	Limitations
Elevation of intraocular pressure	Temporary and reversible; easy to create and reproduce; minimal requirement of surgery or special equipments	High IOP can cause damage
Middle cerebral artery occlusion	Transient (can study reperfusion); reproducible	Requires specialized skills; incomplete ischemia; alter blood flow to the brain
Chronic carotid occlusion	Reproducible; easy	Variable damage; permanent ischemia
Photothrombosis of retinal vessels	Simple	Variable degrees of exposure and variable damage; permanent ischemia; free-radical damage
Occlusion of central retinal artery	Complete retinal ischemia	–
Endothelin administration	No inflammation or infection	Can enter systemic circulation

can form astrocytes, neurons, and oligodendrocytes. The neural stem cells were first isolated from adult rat hippocampus (Palmer et al., 1997). These cells have shown the ability to migrate and differentiate into neuronal cells in retinal injury (Nishida et al., 2000). But more studies need to be done to estimate the efficiency of the neural stem cells.

The stem cell transplantation in retina has some limitations, such as poor cell homing, cell migration, and integration. Thus, many of the transplanted cells do not reach the retina. A study has shown that only 1% of the cells transplanted intraocularly reach the retina (Johnson et al., 2010).

CONCLUSION

Retinal ischemia is the clinical condition caused by insufficient supply of blood to retina and is found in many of the disorders. Retina, like the CNS originates from the ectoderm. Thus, with the use of animal models of retinal ischemia pathophysiology can be studied and therapeutic agents can be tested. Each of the animal models described in this review has its own advantages and limitations. **Table 1** summarizes the advantages and limitations of the retinal ischemia models discussed in this review. Thus, the choice of animal models for pre-clinical testing will depend on the research problem involved.

REFERENCES

Aiello, L. P., Pierce, E. A., Foley, E. D., Takagi, H., Chen, H., Riddle, L., Ferrara, N., King, G. L., and Smith, L. E. (1995). Suppression of retinal neovascularization in vivo by inhibition of vascular endothelial growth factor (VEGF) using soluble VEGF-receptor chimeric proteins. *Proc. Natl. Acad. Sci. U.S.A.* 92, 10457–10461.

Barnett, N. L., and Osborne, N. N. (1995). Suppression of retinal neovascularization in vivo by inhibition of vascular endothelial growth factor (VEGF) using soluble VEGF-receptor chimeric proteins. *Exp. Eye Res.* 61, 83–90.

Bennett, J., Wilson, J., Sun, D., Forbes, B., and Maguire, A. (1994). Adenovirus vector-mediated in vivo gene transfer into adult murine retina. *Invest. Ophthalmol. Vis. Sci.* 35, 2535–2542.

Block, F., Grommes, C., and Kosinski, C. (1997). Retinal ischemia induced by the intraluminal suture methods in rats. *Neurosci. Lett.* 232, 45–48.

Block, F., Schwarz, M., and Sontag, K. -H. (1992). Retinal ischemia induced by occlusion of both common carotid arteries in rats as demonstrated by electroretinography. *Neurosci. Lett.* 144, 124–126.

Buchi, E. R., Lam, T. T., Suvaizdis, I., and Tso, M. O. (1994). Injuries induced by diffuse photodynamic action in retina and choroid of albino rats. Morphologic study of an experimental model. *Retina (Philadelphia, Pa.)* 14, 370–378.

Buchi, E. R., Suivaizdis, I., and Fu, J. (1991). Pressure-induced retinal ischemia in rats: an experimental model for quantitative study. *Ophthalmologica* 203, 138–147.

Bursell, S. E., Clermont, A. C., Oren, B., and King, G. L. (1995). The in vivo effect of endothelins on retinal circulation in nondiabetic and diabetic rats. *Invest. Ophthalmol. Vis. Sci.* 36, 596–607.

Cao, W., Zaharia, M., Drumheller, A., Casanova, C., Lafond, G., Brunette, J. R., and Jolicoeur, F. B. (1994). Effects of dextromethorphan on ischemia induced ERG changes in rabbit. *Curr. Eye Res.* 13, 97–102.

Cogliati, T., and Swaroop, A. (2009). Stems cells and neuronal repair. *Ann. Neurosci.* 16, 143–145.

Deveraux, Q. L., Takahashi, R., Salvesen, G. S., and Reed, J. C. (1997). X-linked IAP is a direct inhibitor of cell-death proteases. *Nature* 388, 300–304.

Di Polo, A., Aigner, L. J., Dunn, R. J., Bray, G. M., and Aguayo, A. J. (1998). Prolonged delivery of brain-derived neurotrophic factor by adenovirus-infected Muller cells temporarily rescues injured retinal ganglion cells. *Proc. Natl. Acad. Sci. U.S.A.* 95, 3978–3983.

Dimos, J. T., Rodolfa, K. T., and Niakan, K. K. (2008). Induced pluripotent stem cells generated from patients with ALS can be differentiated into motor neurons. *Science* 321, 1218–1221.

Eberhardt, O., Coelln, R. V., Kugler, S., Lindenau, J., Rathke-Hartlieb, S., Gerhardt, E., Haid, S., Isenmann, S., Gravel, C., Srinivasan, A., Bähr, M., Weller, M., Dichgans, J., and Schulz, J. B. (2000). Protection by synergistic effects of adenovirus-mediated X-chromosome-linked inhibitor of apoptosis and glial cell line-derived neurotrophic factor gene transfer in the 1-methyl-4-phenyl-1,2,3,6-tetrahydropyridine model of Parkinson's disease. *J. Neurosci.* 20, 9126–9134.

Flannery, J. G., Zolotukhin, S., Vaquero, M. I., LaVail, M. M., Muzyczka, N., and Hauswirth, W. W. (1997). Efficient photoreceptor-targeted gene expression in vivo by recombinant adeno-associated virus. *Proc. Natl. Acad. Sci. U.S.A.* 94, 6916–6921.

Flower, R. W., and Patz, A. (1971). The effect of hyperbaric oxygenation on retinal ischemia. *Invest. Ophthalmol. Vis. Sci.* 10, 605–616.

Gilgun-Sherki, Y., Rosenbaum, Z., Melamed, E., and Offen, D. (2002). Antioxidant therapy in acute central nervous system injury: current state. *Pharmacol. Rev.* 54, 271–284.

Goes, A. M., Castanheira, P., Torquetti, L., and Nehemy, M. B. (2008). Retinal incorporation and differentiation of mesenchymal stem cells intravitreally injected in the injured retina of rats. *Arq. Bras. Oftalmol.* 71, 644–650.

Goldenberg-Cohen, N., Dadon, S., Avraham, B.-C. R., Kramer, M., Hasanreisoglu, M., Eldar, I., Weinberger, D., and Bahar, I. (2008). Molecular and histological changes following central retinal artery occlusion in a mouse model. *Exp. Eye Res.* 87, 327–333.

Hayreh, S. S. (1963). The central artery of the retina its role in the blood supply of the optic nerve. *Br. J. Ophthalmol.* 47, 651–663.

Hayreh, S. S., Kolder, H. E., and Weingeist, T. (1980). Central retinal artery occlusion and retinal tolerance time. *Ophthalmology* 87, 75–78.

Henkind, P., Hansen, R. I., and Szalay, J. (1979). "Ocular circulation," in *Physiology of the Human Eye and Visual System*, ed. R. E. Records (New York: Harper and Row), 98–155.

Hirami, Y., Osakada, F., and Takahashi, K. (2009). Generation of retinal cells from mouse and human induced pluripotent stem cells. *Neurosci. Lett.* 458, 126–131.

Hirrlinger, P. G., Elke, U., Ianors, I., Andreas, R., and Thomas, P. (2010). Alterations in protein expression and membrane properties during Müller cell gliosis in a murine model of transient retinal ischemia. *Neurosci. Lett.* 472, 73–78.

Holcik, M., Gibson, H., and Korneluk, R. G. (2001). XIAP: apoptotic brake and promising therapeutic target. *Apoptosis* 6, 253–261.

Ji, J., Chang, P., Pennesi, M. E., Yang, Z., Zhang, J., Li, D., Wu, S. M., and Gross, R. L. (2005). Effects of elevated intraocular pressure on mouse retinal ganglion cells. *Vision Res.* 45, 169–179.

Joachim, S. C., Wax, M. B., Boehm, N., Dirk, D., Pfeiffer, N., and Grus, F. H. (2011). Up-regulation of antibody response to heat shock proteins and tissue antigens in an ocular ischemia model. *Invest. Ophthalmol. Vis. Sci.* 52, 3468–3474.

Johnson, T. V., Bull, N. D., and Martin, K. R. (2010). Identification of barriers to retinal engraftment of transplanted stem cells. *Invest. Ophthalmol. Vis. Sci.* 51, 960–970.

Kaja, S., Yang, S. H., and Wei, J. (2003). Estrogen protects the inner retina from apoptosis and ischemia-induced loss of Vesl-1L/Homer-1c immunoreactive synaptic connections. *Invest. Ophthalmol. Vis. Sci.* 44, 3155–3162.

Karumbayaram, S., Novitch, B. G., and Patterson, M. (2009). Directed differentiation of human-induced pluripotent stem cells generates active motor neurons. *Stem Cells* 27, 806–811.

Kliman, G. H., Puliafito, C. A., Grossman, G. A., and Gregory, W. A. (1994). Retinal and choroidal vessel closure using phthalocyanine photodynamic therapy. *Lasers Surg. Med.* 15, 11–18.

Kwon, Y. H., Rickman, D. W., Baruah, S., Zimmerman, M. B., Kim, C.-S., Boldt, H. C., Russell, S. R., and Hayreh, S. S. (2005). Vitreous and retinal amino acid concentrations in experimental central retinal artery occlusion in the primate. *Eye* 19, 455–463.

Lam, T. T., Siew, E., Chu, R., and Tso, M. O. (1997). Ameliorative effect of MK-801 on retinal ischemia. *J. Ocul. Pharmacol. Ther.* 13, 129–137.

Lavinsky, D., Arterni, N. S., Achaval, M., and Netto, C. A. (2006). Chronic bilateral common carotid artery occlusion: a model for ocular ischemic syndrome in the rat. *Graefes Arch. Clin. Exp. Ophthalmol.* 244, 199–204.

Lenka, N., and Anand, A. (2009). Advancements in stem cell research: an Indian perspective – I. *Ann. Neurosci.* 16, 97.

Masuzawa, K., Jesmin, S., Maeda, S., Kaji, Y., Oshika, T., Zaedi, S., and Shimojo, N. (2006). A model of retinal ischemia-reperfusion injury in rats by subconjuctival injection of endothelin-1. *Exp. Biol. Med.* 231, 1085–1089.

McKinnon, S. J., Lehman, D. M., Tahzib, N. G., Ransom, N. L., Reitsamer, H. A., Liston, P., LaCasse, E., Li, Q., Korneluk, R. G., and Hauswirth, W. W. (2002). Baculoviral IAP repeat-containing-4 protects optic nerve axons in a rat glaucoma model. *Mol. Ther.* 5, 780–787.

Melena, J., Wood, J. P. M., and Osborne, N. N. (1999). Betaxolol, a B1-adrenoceptor antagonist, has an affinity for L-type Ca^{2+} channels. *Eur. J. Pharmacol.* 378, 317–322.

Miller, J. W., Adamis, A. P., Shima, D. T., D'Amore, P. A., Moulton, R. S., O'Reilly, M. S., Folkman, J., Dvorak, H. F., Brown, L. F., and Berse, B. (1994). Vascular endothelial growth factor/vascular permeability factor is temporally and spatially correlated with ocular angiogenesis in a primate model. *Am. J. Pathol.* 145, 574–584.

Mosinger, J. L., and Olney, J. W. (1989). Photothrombosis-induced ischemic neuronal degeneration in the rat retina. *Exp. Neurol.* 105, 110–113.

Nishida, A., Zakahashi, M., Tauihara, H., Nakamo, I., Tahahashi, J. B., Mizoguchi, A., Ide, C., and Honda, Y. (2000). Incorporation and differentiation of hippocampus-derived neural stem cells transplanted in injured adult rat retina. *Invest. Ophthalmol. Vis. Sci.* 41, 4268–4269.

Ogata, N., Wang, L., Jo, N., Tombran-Tink, J., Takahashi, K., Mrazek, D., and Matsumura, M. (2001). Pigment epithelium derived factor as a neuroprotective agent against ischemic retinal injury. *Curr. Eye Res.* 22, 245–252.

Osborne, N. N., DeSantis, L., Bae, J. H., Ugarte, M., Wood, J. P. M., Nash, M. S., and Chidlow, G. (1999). Topically applied betaxolol attenuates NMDA-induced toxicity to ganglion cells and the effects of ischemia to the retina. *Exp. Eye Res.* 69, 331–342.

Palmer, T. D., Takahashi, J., and Gage, F. H. (1997). The adult rat hippocampus contains primordial neural stem cells. *Mol. Cell. Neurosci.* 8, 389–404.

Park, I. H., Arora, N., Huo, H., Maherali, N., Ahfeldt, T., Shimamura, A., Lensch, M. W., Chad, C., Hochedlinger, K., and Daley, G. Q. (2008). Disease-specific induced pluripotent stem cells. *Cell* 134, 877–886.

Peachey, N. S., Green, D. J., and Ripps, H. (1993). Ocular ischemia and the effects of allopurinol on functional recovery in the retina of the arterially perfused cat eye. *Invest. Ophthalmol. Vis. Sci.* 34, 58–65.

Petrin, D., Baker, A., Coupland, S. G., Liston, P., Narang, M., Damji, K., Leonard, B., Chiodo, V. A., Timmers, A., Hauswirth, W., Korneluk, R. G., and Tsilfidis, C. (2003). Structural and functional protection of photoreceptors from MNU-induced retinal degeneration by the X-linked inhibitor of apoptosis. *Invest. Ophthalmol. Vis. Sci.* 44, 2757–2763.

Prasad, S. S., Kojic, L., Wen, Y. H., Chen, Z., Xiong, W., Jia, W., and Cyander, M. S. (2010). Retinal gene expression after central retinal artery ligation: effects of ischemia and reperfusion. *Invest. Ophthalmol. Vis. Sci.* 51, 6207–6219.

Renwick, J., Narang, M. A., Coupland, S. G., Xuan, J. Y., Baker, A. N., Brousseau, J., Petrin, D., Munger, R., Leonard, B. C., Hauswirth, W. W., Korneluk, R. G., and Tsilfidis, C. (2006). XIAP-mediated neuroprotection in retinal ischemia. *Gene Ther.* 13, 339–347.

Rios, L., Cluzel, J., Vennat, J. C., Menerath, J. M., and Doly, M. J. (1999). Comparison of intraocular treatment of DMTU and SOD following retinal ischemia in rats. *J. Ocul. Pharmacol. Ther.* 15, 547–556.

Rumelt, S., Dorenboim, Y., and Rehany, U. (1999). Aggressive systematic treatment for central retinal artery occlusion. *Am. J. Ophthalmol.* 128, 733–738.

Saint-Geniez, M., and D'Amore, P. A. (2004). Development and pathology of the hyaloid, choroidal and retinal vasculature. *Int. J. Dev. Biol.* 48, 1045–1058.

Sakaue, H., Kiryu, J., Takeuchi, A., Yamamoto, F., and Honda, Y. (1992). Effects of endothelin on retinal blood vessels. *Nippon Ganka Gakkai Zasshi* 96, 469–472.

Sato, T., Takei, K., Nonoyama, T., Miyauchi, T., Goto, K., and Hommura, S. (1993). Endothelin-1-induced vasoconstriction in retinal blood vessels in the rabbit. *Nippon Ganka Gakkai Zasshi* 97, 683–689.

Schmidt-Kastner, R., and Eysel, U. T. (1994). Ischemic damage visualized in flat mounts of rat retina after photochemically induced thrombosis. *Brain Res. Bull.* 34, 487–491.

Shibuki, H., Katai, N., Kuroiwa, S., Kurokawa, T., Arai, J., Matsumoto, K., Nakamura, T., and Yoshimura, N. (2002). Expression and neuroprotective effect of hepatocyte growth factor in retinal ischemia-reperfusion injury. *Invest. Ophthalmol. Vis. Sci.* 43, 528–536.

Smith, G. G., and Baird, C. D. (1952). Survival time of retinal cells when deprived of their blood supply by increased intraocular pressure. *Am. J. Ophthalmol.* 35, 133–136.

Steele, E. C., Guo, Q., and Namura, S. (2008). Filamentous middle cerebral artery occlusion causes ischemic damage to retina in mice. *Stroke* 39, 2099–2104.

Takahashi, K., and Yamanaka, S. (2006). Induction of pluripotent stem cells from mouse embryonic and adult fibroblast cultures by defined factors. *Cell* 126, 663–676.

Takei, K., Sato, T., Nonoyama, T., Miyauchi, T., Goto, K., and Hommura, S. (1993). A new model of transient complete obstruction of retinal vessels induced by endothelin-1 injection into the posterior vitreous body in rabbits. *Graefes Arch. Clin. Exp. Ophthalmol.* 231, 476–481.

Tso, M. O., and Jampol, L. M. (1982). Pathophysiology of hypertensive retinopathy. *Ophthalmology* 89, 1132–1145.

Unoki, K., and LaVail, M. M. (1994). Protection of the rat retina from ischemic injury by brain-derived neurotrophic factor, ciliary neurotrophic factor, and basic fibroblast growth factor. *Invest. Ophthalmol. Vis. Sci.* 35, 907–915.

von Graefe, A. (1859). Ueber Embolie der Arteria centralis retinae als Ursache plotzlicher Erblindung. *Albrecht Von Graefes Arch. Ophthalmol.* 5, 136–157.

Wei, L., Cui, L., Snider, B. J., Rivkin, M., Yu, S. S., Lee, C. S., Adams, L. D., Johnso, E. M., Yu, S. P., and Choi, D. W. (2005). Transplantation of embryonic stem cells overexpressing Bcl-2 promotes functional recovery after transient cerebral ischemia. *Neurobiol. Dis.* 19, 183–193.

Wu, W.-C., Lai, C.-C., Chen, S.-L., Sun, M.-H., Xiao, X., Chen, T.-L., Tsai, R. J.-F., Kuo, S.-W., and Tsao, Y.-P. (2004). GDNF gene therapy attenuates retinal ischemic injuries in rats. *Mol. Vis.* 10, 93–102.

Xu, D., Bureau, Y., McIntyre, D. C., Nicholson, D. W., Liston, P., Zhu, Y., Fong, W. G., Crocker, S. J., Korneluk, R. G., and Robertson, G. S. (1999). Attenuation of ischemia-induced cellular and behavioural deficits by X chromosome-linked inhibitor of apoptosis protein overexpression in the rat hippocampus. *J. Neurosci.* 19, 5026–5033.

Yanagisawa, M., Kurihara, H., Kimura, S., Tomobe, Y., Kobayashi, M., Mitsui, Y., Yazaki, Y., Goto, K., and Masaki, T. (1988). A novel potent vasoconstrictor peptide produced by vascular endothelial cells. *Nature* 332, 411–415.

Zhang, Y., Cho, C.-H., Atchaneeyasakul, L.-O., McFarland, T., Appukuttan, B., and Stout, J. T. (2005). Activation of the mitochondrial apoptotic pathway in a rat model of central retinal artery occlusion. *Invest. Ophthalmol. Vis. Sci.* 46, 2133–2139.

Conflict of Interest Statement: The authors declare that the research was conducted in the absence of any commercial or financial relationships that could be construed as a potential conflict of interest.

Received: 12 January 2012; accepted: 16 April 2012; published online: 11 May 2012.

Citation: Minhas G, Morishita R and Anand A (2012) Preclinical models to investigate retinal ischemia: advances and drawbacks. Front. Neur. ***3****:75. doi: 10.3389/fneur.2012.00075*

This article was submitted to Frontiers in Neuro-Ophthalmology, a specialty of Frontiers in Neurology.

Copyright © 2012 Minhas, Morishita and Anand. This is an open-access article distributed under the terms of the Creative Commons Attribution Non Commercial License, which permits non-commercial use, distribution, and reproduction in other forums, provided the original authors and source are credited.

8

Animal Models of Retinal Ischemia

Gillipsie Minhas and Akshay Anand*
Neuroscience Research Lab, Department of Neurology
Postgraduate Institute of Medical Education and Research, Chandigarh
India

1. Introduction

Retinal ischemia is a frequent source of irreparable visual impairment and even loss of sight, affecting over a hundred million individuals in the world. It is associated with a wide range of clinical retinal disorders, like ischemic optic neuropathies, obstructive retinopathies, carotid occlusive disorders, diabetic retinopathy and glaucoma. Retinal ischemia occurs when the blood supply to retina is inadequate to meet the metabolic requirements of the retina. If treatment is not given to fix this imbalance, the outcome is irreversible, ischemic and apoptotic cascades resulting in cell death. Appropriate study models, particularly animal models, are necessary for further understanding the etiology, pathology, and evolution of retinal ischemia and also in order to help in the evaluation, development, and improvement of therapeutic strategies. Accordingly, quite a few *in-vivo* and *ex-vivo* mammalian models have been developed to study this syndrome. The rat models of retinal ischemia are frequently used, because the distribution of retinal and choroidal blood supply is quite similar to that in humans.

The retina has been extensively used for the study of pathophysiology of ischemia and mechanism of damage triggered by ischemia and excitotoxicity. Compared to all the other tissues, retina has a higher metabolic rate; any disturbance in blood supply can have an effect on the supply of oxygen and the substrates leading to retinal ischemia. The retina has a dual blood supply. The photoreceptors and most of the outer plexiform layer (OPL) are nourished by choriocapillaries, while the inner retinal layers are nourished by the central retinal artery. The actual effects of retinal ischemia vary, depending on the position of the occlusion. It is clear that occlusion of the retinal artery leads to inner retinal ischemia only, but occlusion of ophthalmic artery leads to global retinal ischemia, as it supplies blood to the central retinal artery as well as choriocapillaries.

2. Retinal architecture

The retina of mammals is a functionally specialised tissue. It is capable of light detection and perception as well as processing and transmission of the information received to the central nervous system. It has two major elements – the neurosensory retina and the pigment epithelium (RPE). During the embryonic development, the RPE and neural development are

* Corresponding Author

derived from the same layer, i.e. the neuroectoderm, although they are morphologically not similar. Hence, they are considered collectively as "retina".

The retina is made up of three principal layers of nuclei, which are, from internal to external, the thin ganglion cell layer, the inner nuclear layer and the outer nuclear layer (Figure 1). The ganglion cell layer consists of cell bodies of various classes of ganglion cells and amacrine cells. The inner nuclear layer is the layer with nuclei of bipolar cells, amacrine cells, horizontal cells and Muller cells. And the outer layer is the one which contains the nuclei of rod and cone photoreceptors. There are also two plexiform or synaptic layers that are not filled with any cell nuclei. The inner plexiform layer (IPL) lies between the ganglion cells and inner nuclear layer and the outer plexiform layer (OPL) is sandwiched between the outer and inner nuclear layer. These synaptic layers contain axons and dendrites, which aid in early visual processing and also help in adjusting to different light intensities.

The retina contains a rich assortment of cell types including light-sensing photoreceptors. The outermost layer of the cells in the retina is the RPE. It is a simple cuboidal epithelium, containing melanosomes that help in quenching photons that are not absorbed and therefore, minimise light scattering. RPE also has other biological functions like maintenance of choroidal vasculature and blood-retinal barrier. The retinal photoreceptor cells are specialised neurons found in the outer retina. The diversity of inner retinal neurons is really complex. Bipolar cells span from the OPL to the IPL, in which they form synapses with photoreceptor cells and ganglion cells respectively. The nuclei of bipolar cells are found in the inner nuclear layer. Amacrine cells in themselves as a group are considerable in number as well as diversity. These are present in both inner nuclear layer plus the ganglion cell layer where they are involved in relaying impulses (Masland, 1988). Another type of cells that also occur in the retina are the ganglion cells. Ganglion cells have long axons that are pass through the optic nerve (Berson, 2007). Glial cells are also found in the retina. These cells support the retinal microenvironment. These include Muller cells, astrocytes and microglia. Another type of cell found in the ganglion cell layer and optic nerve head are the astrocytes. These cells contribute to the blood retinal barrier (Kaur *et al*., 2008).

3. Retinal blood supply

As mentioned earlier, the cause of retinal ischemia is insufficient supply of blood, which is unable to meet the metabolic demands of the retina. When occlusion occurs in any tissue, anatomy of blood supply plays a significant role. The retina has a higher metabolic rate, even than that of the brain. The retina is a specialised extension of central nervous system and has a complex and dual blood supply, i.e the choroidal and the retinal. The choroid gets the maximum blood supply (around 65-85% of total supply to the eye), whereas the retina gets just 20-30%blood (Henkind, *et al*., 1979). The photoreceptors in the outer nuclear layer and the outer plexiform layer are nourished indirectly from the choriocapillaries; whereas, the inner retinal layers are nourished by branches of central retinal artery, which arises from the ophthalmic artery as the central retinal artery enters the retina, it divides into four main branches. The retinal blood vessels also help in maintaining the blood-retinal barrier. Outer retinal layer ischemia is caused by occlusion in choriocapillaries. On the other hand, complete retinal ischemia and infarction require ophthalmic artery occlusion (Saint-Geniez and D'Amore, 2004).

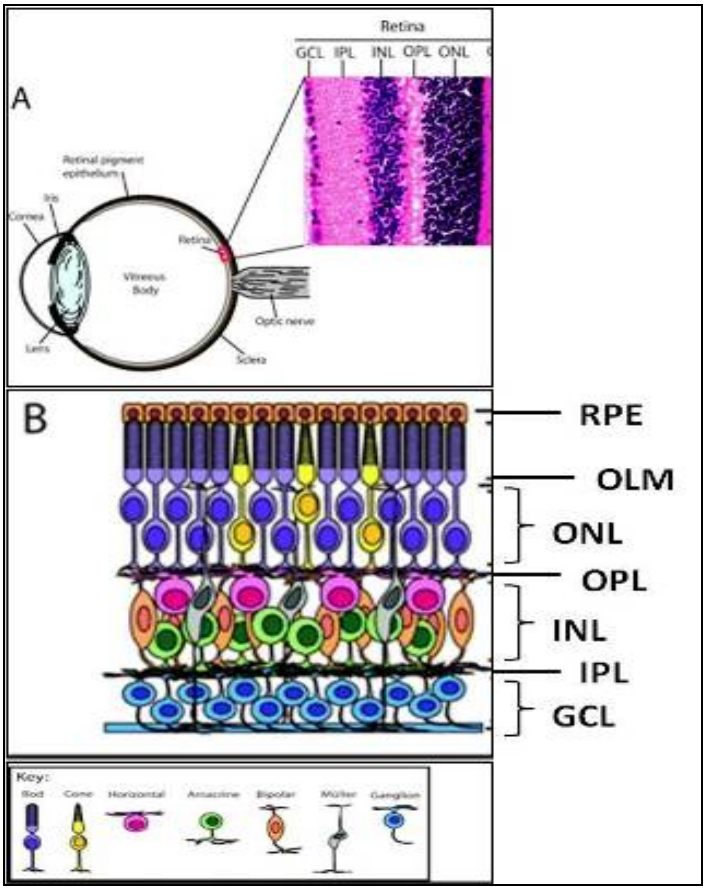


Fig. 1. Different cell layers in retina (where RPE – Retina Pigmented Epithelium, OLM – Outer Limiting Membrane, ONL – Outer Nuclear Layer, OPL – Outer Plexiform Layer, INL – Inner Nuclear Layer, IPL – Inner Plexiform Layer, GCL – Ganglion Cell Layer) *(reproduced and readapted with permission – Poche & Reese, 2009)*

4. Correlation between the brain and the retina

The retina shares many functional, embryological and anatomic characteristics with the brain. In humans, the eye starts developing at about 3 weeks of pregnancy. The eye is mainly derived from three types of embryonic tissue – neuroectoderm forms retina, pigment cell layers and optic nerves, mesoderm leads to cornea, sclera and blood vessels and the ectoderm forms the lens. At 22 days of embryonic stage, a pair of optic vesicles is formed on each side of the forebrain. These vesicles form connections with the developing central nervous system through stalk-like structures. As the development progresses, these stalks become thinner and form optic nerves. Thus, it is a representative of the CNS. The mesoderm in the embryo forms the blood vessels – the hyaloid artery and vein, that nourishes the developing lens, which later on in development transform to the central artery

and the vein. The retina can be visualised directly, thus, it can be used to study stroke. Many retinal conditions are associated with stroke, such as occlusion of middle cerebral artery also leads to retinal ischemia, as can be seen in figure 2, where it shows that the ophthalmic artery originates nearby to the MCA. Thus, the mechanisms that affect the eye and the brain are linked to some extent. But, the examination of retina to predict future stroke incidence is still doubtful.

Retinal neurons and glia show same response to ischemia as the neurons in the other part of the CNS. Retina also has a blood-retinal barrier similar to the blood-brain barrier (Tso & Jampol, 1982). These two also differ in the resistance to the ischemic injury. The retina can survive much longer than the brain. Also, the retina shows geographical difference in sensitivity to ischemia, the outer retinal layers being more prone to the injury than the inner ones.

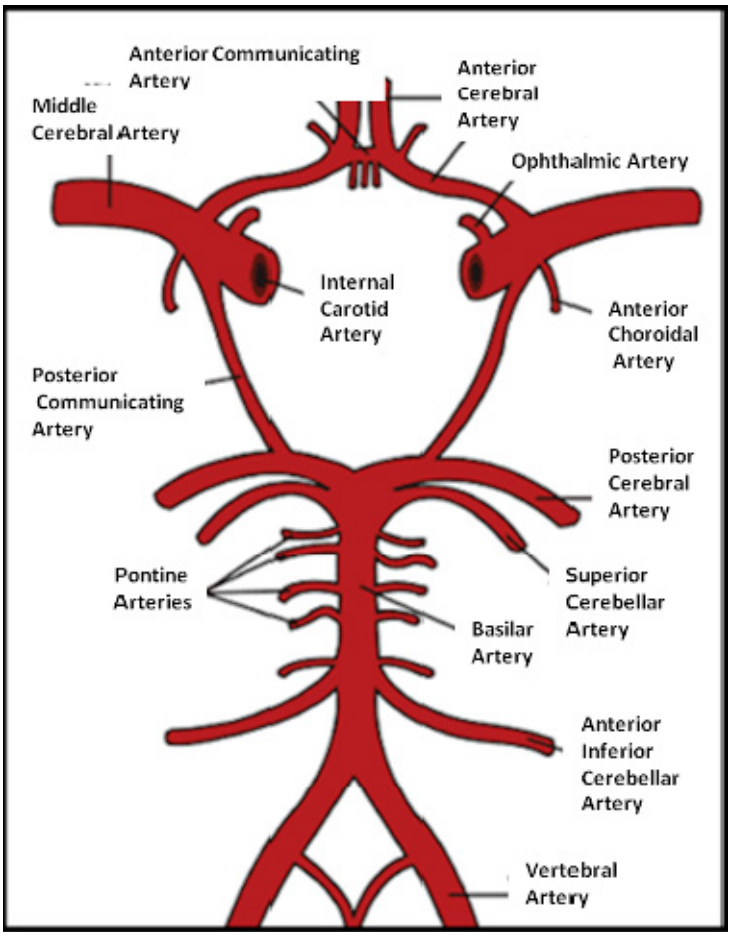


Fig. 2. The figure depicting Circle of Willis showing blood supply to brain and retina (*Reproduced with permission from M. F. Block, 1997)*

5. Susceptibility to retinal ischemia

Various changeable and non-changeable factors are involved in ischemia, such as age, family history, ethnic group, and previous medical history. Kawai *et al* studied the different risk factors related to neuronal injury using an intraocular pressure rat model. The number of retinal ganglion cells (RGCs) keeps on decreasing with age and the residual RGCs become more susceptible to damage. Calorie intake has also been proven to be a factor involved in ischemia. The diet restriction has a neuroprotective effect and thus, leads to lesser damage to RGCs. As seen in the case of glaucoma, pre-existing diabetes is a reason for greater harm to RGCs (Kawai *et al*, 2001).

Genetic background is one of the principal determinants of susceptibility to retinal neovascularisation and breakdown of blood retinal barrier. Vulnerability to ischemia-induced retinal neovascularisation depends on the strain of animal model used. Strain difference in rat model leads to variation in expression of VEGF and thus, causes an increase in permeability and leakage of fluid and plasma proteins, resulting in edema. It has been demonstrated that Brown-Norway rats are more susceptible to Sprague-Dawley rats (Gao *et al*., 2002).

It is seen that a certain percentage of cell death that occurs in transient cerebral and retinal ischemia occurs by means of apoptosis. An apoptosis cascade involves both pro-apoptotic and anti-apoptotic genes. One of these is p53, which is a DNA-binding transcription factor involved in DNA damage and repair. Ischemia leads to increase in expression of p53. The p53 causes selective vulnerability of inner retina to transient ischemia. Also, it is observed that transgenic mice lacking in p53 are resistant to excitotoxicity. Mice heterozygous for null mutation in p53 gene are resistant to retinal ischemia. From the above discussion, it is safe to say that p53 can be one more target for therapeutic strategy for retinal ischemia (Zhang *et al*., 2005).

6. Pathophysiology of retinal ischemia

Retina has a really high metabolic rate. Glucose and oxygen deprivation can harm the whole retina, but all cells are not equally vulnerable. The loss of cells due to ischemia is irregular. The retinal cells that lie near the blood vessels are exposed to an environment rich in oxygen and thus, are more prone to the ischemic damage. But, another thing to consider is that these cells are the first one to be cured on reperfusion. Temporary interruption of blood circulation prevents the exchange of metabolic substrates and products, affecting cells in retina. However, in addition, there are many indirect effects which are sustained even after restoration of blood supply. These effects may be systemic, such as respiratory or vasomotor centre failure or the outcome can also be localised, i.e. impaired reperfusion, edema or breakdown of blood-brain barrier. Thus, evidently, these effects are so complicated that it is hard to identify the order of events leading to damage.

Retinal ischemia causes a number of morphological and functional changes. These changes are a product of combined and inter-related pathophysiological pathways – leading to imbalance in ion transport, changes in neurotransmitter levels, neuronal depolarisation, oxidative stress, and energy failure. The occurrence of ischemia leads to a complex cascade of response to energy failure and ATP depletion which eventually causes cell death. Studies have shown that substrate deprivation is the less damaging as compared to oxygen deprivation, which reduces protein synthesis. The irreversible damage increases with an increase in the duration of oxygen deprivation. The cells which are the most affected are the

photoreceptor cells as these have the maximum oxidative metabolic rates. But when both substrate and oxygen deprivation are combined, a reduction in the ATP synthesis is observed. This leads to energy metabolism failure. The process can be explained as follows - decrease in ATP levels disrupt the Na^+/K^+ ATPase transporter, leading to disruption of membrane potential and ion gradients, preventing the repolarisation of axons and synaptic membranes. There are many studies which testify to the discharge of various neurotransmitters, e.g. GABA, glycine, dopamine, acetylcholine, after the occurrence of ischemia. During the ischemia the receptors for different neurotransmitters, present on the retina, are opened in response to the elevated levels of their ligands, e.g. GABA, glycine, extracellularly. Under normal circumstances, neurotransmitter levels are low extracellularly. Glutamate is recognized as the major excitatory retinal neurotransmitter. It is released by photoreceptor bipolar cells and the ganglion cells. During retinal ischemia glutamate gets accumulated in the extracellular space (Louzada-Junior *et al*., 1992). Lucas and Newhouse showed the occurrence of glutamate excitotoxicity in ischemia. Neurons in inner retina and ganglion cells are more susceptible to ischemia due to the incidence of high levels of glutamate receptors. Glutamate causes neurotoxicity by several different mechanisms, i.e., increase in Ca^{2+} ion levels, Na^+ influx, which depolarises the plasma membranes. There are a number of receptors which can activate glutamate neurotoxicity. These can be NMDA as well as non-NMDA based receptors (Lucas & Newhouse, 1957). In 1992, Osborne stated the role of NMDA – based excitotoxicity in retinal ischemia. NMDA receptors are Ca^{2+} permeable, and thus, increase in glutamate levels raises the Ca^{2+} ion levels intracellularly. Excess glutamate causes Na^+ influx, which is followed by Cl^- influx, which cannot be countered by outward efflux as the membranes are impermeable to most intracellular anions. Therefore, transport of cations and Cl^- ions increases the intracellular osmolarity, causing osmotic shock, edema and cell lysis and death (Osborne *et al*., 1992). The voltage gated Ca^{2+} channels are also opened, leading to rise in intracellular levels of Ca^{2+} ions, which inhibit the mitochondrial metabolism. Another group also validated the involvement of NMDA as well as non-NMDA based receptors in retinal degeneration. Romano *et al*., in an *in-vitro* model of ischemia in the retina from a chick embryo reported by using the blockers of both NMDA and non-NMDA receptors that the damage to the retina is due to overexcitation of the receptors (Romano *et al*., 1998). Ueda *et al* also showed that the NMDA caused damage to blood vessels in the retina. They created a rat model by injecting NMDA into the eye, which led to loss of retinal ganglion cells and thinning of the inner plexiform layer, thus damaging the inner retinal layers and also led to loss of endothelial cells in the blood vessels in the retina (Ueda *et al*., 2010).

Reperfusion, i.e. restoration of blood supply after the ischemic injury, can also lead to cell damage. Oxygen restoration to the deprived tissue can add up to the injury caused by ischemia (Jennings *et al*., 1960). Also, it has been shown that LDH, marker of cell death increases after oxygen restoration (Sims *et al*., 1992).

7. *In-vitro* models of retinal ischemia

Most of the cell culture models for ischemia utilise primary nerve cell cultures, that are exposed to insults associated with ischemia *in-vivo*, e.g., glutamate neurotoxicity, glucose and oxygen deprivation. One of the approach involved chemical ischemia in immortalised rat retinal ganglion cell line (RGC-5). They used iodoacetic acid (IAA), a known inhibitor of enzyme glyceraldehyde 3-phosphate dehydrogenase. This IAA treatment induces changes

seen in retinal ischemia, such as disturbance in membrane potential, ATP loss and reactive oxygen species generation (Malur *et al*., 2008). Another way of inducing ischemic-like changes *in-vitro* is to incubate retinal pigmented epithelium (RPE) cells with oligomycin (an ATP synthase inhibitor) and sodium cyanide (inhibits cytochrome-c oxidase), along with IAA (Palmero *et al*., 2000). In-vitro model can also be induced by glucose/oxygen deprivation.

These in-vitro models can be used for testing and identifying novel neuroprotective compounds. Many herbal products are nowadays being used, the Chinese herbal medicines, in a large number of disorders, e.g. coronary heart disease, cardiovascular disease and traumatic wounds. Romano *et al* examined the neuroprotective activity of an extract from Chinese safflower (*Cartnamus tinchoris*, Honghua). An *in-vitro* model of retinal ischemia was made from chick embryo retina. The ischemia was generated by removing glucose from the media and growing the culture in nitrogen atmosphere. It was seen that Honghua protected the retina from the effects of toxins like NMDA and also from the ischemic conditions (Romano, *et al*., 1993).

Another herbal extract that has been used in Korea and China are derived from the shrub, *Thuja orientalis*. It has been shown to be effective in disorders such as, gout, diarrhoea and rheumatism. It was demonstrated by Jung *et al* in the transformed retinal ganglion cell line (RGC-5) *in vitro* that the extract of *Thuja orientalis* has anti-oxidant properties. In this study, RGC-5 cells were exposed to H_2O_2 to create oxidative stress. The major component found in this extract with anti-oxidant properties is the isoquercitrin, which can be in future used for treating glaucoma, but requires further investigation (Jung, *et al*., 2010). The roots of another plant, *Scutellaria baicalensis*, are also used in China. It contains three flavnoids – wogonin, baicalin, baicalein. These flavenoids are natural free-radical scavengers. Out of the three flavenoids found, baicalin has been shown to have neuroprotective action, but the mode of its action is unknown. The role of baicalin was observed in *in vitro* model in RGC-5 cell line, where it reduces the damage caused by reactive species and apoptosis (Jung *et al*., 2008). Matteucci *et al* have also tested the curcumin, the phenolic extract obtained from *Curcuma longa* in primary retinal cell cultures. It showed protective effect for both the retinal as well as hippocampal neurons from NMDA excitotoxicity. The mode of action of curcumin may be through the increase in production of NMDA receptor subunits (Matteucci, *et al*., 2011). But these *in-vitro* models have some limitations of their own, such as getting sufficient quantities of cells and obtaining reproducible and comparable data. Also, the *in vitro* models do not correlate much to the *in vivo* conditions as these do not provide apt physiological environment and are based on chemical interactions.

8. Need for animal models

Animal models have been a mainstay of basic and applied research. Animal testing has been used since second century where early writings by Greeks discuss its use. Dissection and experimentation has been used to get knowledge about anatomy and physiology in humans. The use of animal models has allowed the fast progression of scientific discovery. Animal models have had a central place in medical research, in developing new therapeutic strategies for treating human diseases as well as in preclinical trials. The aim of using animal models is to achieve better understanding of pathways involved in the disease without causing any harm to the human being. A number of animal models are available for studying the mechanisms of retinal ischemia. The vascular supply and pathways involved

in retinal ischemia in animal models must be better understood for developing new therapies for human disorders.
In-vitro models have always been used to get insight of biochemical and molecular events caused by ischemia; but animal models are essential in understanding pathophysiology of retinal ischemia. In all animal models of retinal ischemia, the retinal circulation is obstructed to study the balance between energy supply and demands, vascular and neuronal changes. Different species such as monkeys, rabbits, rodents, cats, dogs have been used as animal models. In choosing an animal model, several factors are considered like anatomy of vascular circulation and retina, relevance to humans and also the availability of the animals.

9. Desirable characteristics in animal models

Animal models are used to understand the mechanism behind a particular disease and also to discover new as well as validate the already therapeutics for it. Animal models can either be spontaneous or induced and can be developed in any species which fits best for the disease to be studied and the purpose of our study.
The model should show up same characteristics and symptoms as seen in human disorders. The model should have common features with the humans, such as anatomy, vascular system and retina in case of animal models for retinal ischemia. But at the same time these animals should be easy to manipulate, i.e. they should have small size, high reproducibility and easy for genetic manipulation. For testing the therapeutics, the animal models being used should mimic the humans and give same response as desired in the humans, so that the humans will show similar response. Other desirable characteristics include low cost, easy availability, easy to handle and breed and less prone to infections or diseases other than the desired one.

10. Animal models of retina ischemia

10.1 Raising the intraocular pressure

It is the most widely used method to study the mechanisms involved in retinal ischemia. Peachey *et al*. demonstrated that the high intraocular pressure (IOP) induced retinal ischemia model has been established as an important model system. IOP model creates ischemia by elevating and maintaining the intraocular pressure above the systemic arterial pressure (Peachey *et al*., 1993). Flower *et al* described the retinal ischemia model in cats. The IOP was raised to 110mm Hg by cannulation of anterior chamber with a 26-gauge needle, which is connected through nylon tubing to an elevated container with normal saline. This increase in intraocular pressure blocks the retinal blood circulation and thus, leads to ischemia (Flower *et al*., 1971). Following a similar procedure, a model of pressure-induced retinal ischemia/reperfusion injury was established in rats (Buchi *et al*., 1991).
It has been used to study changes in protein expression, excitotoxicity and alteration in membrane properties in various different models. IOP animal models have also been used to study changes in serum antibody reactivities after ischemia. Joachim *et al*. created IOP model by raising the pressure to 130mm Hg for an hour to check the antibody response to ischemia/reperfusion injury (Joachim, *et al*., 2011). On the other hand, Hirelinger *et al*. investigated the involvement of ion imbalance and role of Muller cells in degeneration of retina in a mouse IOP model (Hirelinger, *et al*., 2010).

Baicalin, a flavenoid found in roots of *Scutellaria biacalensis*, when was administered in rats intraperitoneally showed protection from the retinal ischemia'reperfusion injury, as was seen *in vitro.* The baicalin was given before subjecting the animals to raised intraocular pressure of 120mm Hg for 50 minutes (Jung, *et al*., 2008).
The principle limitation of this model include that the raised intraocular pressure itself can contribute to the resulting retinal damage. Thus, this model is complicated by a combination of ischemic as well as pressure-induced injury.

10.2 Cerebral artery occlusion

Acute thrombotic/embolic stroke in humans are often associated with temporary diminishment (amaurois fugax) or even permanent loss of vision. Middle cerebral artery occlusion (MCAO) is a purely vascular model of retinal ischemia that reproduces transient human vision loss. MCAO in rodents is one of the most widely used experimental paradigms to induce focal cerebral ischemia. This model occludes arterial blood flow intraluminally and allows reperfusion by removing the inserted filament. The ophthalmic artery that mainly supplies the inner retina originates from the internal carotid artery proximal to the origin of the middle cerebral artery. Therefore, it is expected that MCAO simultaneously obstructs blood flow in the ipsilateral retina. Block *et al* demonstrated the first evidence of retinal ischemia by MCAO in rats (Block *et al*., 1992). Steele *et al* have shown for the first time that MCAO simultaneously obstructs blood flow in ipsilateral retina in mice (Steele *et al*., 2008).
Kaja *et al* indicates that the MCAO/ reperfusion model is more appropriate than other retinal ischemia models such as high intraocular pressure or optic nerve ligation models to study the cellular and molecular changes in retina after stroke (Kaja *et al*., 2003). This model is non-invasive with respect to the eye and does not induce blood-retina barrier disruption or mechanical damage to retina. The model is reproducible and easily reversible and involves vascular structure of the entire eye. Therefore, MCAO is a more relevant model for studying changes and testing the efficacy of therapeutic strategies for retinal ischemia.
This model has been used to validate the effect of a various herbs of Chinese origin. The extracts from wolfberries *(Lycium barbarum,* Gougizi*)* mostly consist of polysaccharides and are believed to be good for the eye. It has also been shown previously in many studies that these extracts have protective effect against liver damage, ageing and oxidation (Ha, *et al*., 2005, Li, *et al*., 2007, Yu, *et al*., 2007).The group created a model by occluding the internal carotid artery in rats. The extracts were given orally for 1 week before the occlusion. This study showed that this pre-treatment with the extracts protected the retina from various conditions linked with retinal ischemia, such as, neuronal death, apoptosis, glial cell activation and blood-retinal barrier disruption (Li, *et al*., 2011).

10.3 Chronic carotid ligation

In two-vessel occlusion model, the occlusion is permanent and long-lasting and reperfusion does not occur. This model reduces the cortical/hippocampal blood flow to 25-50% of the normal levels in 2.5 hours post occlusion (Yamamoto *et al*., 2006). The blood flow in the retina may be more severely reduced than in the brain. Davidson *et al* have also shown that the two-vessel occlusion, i.e. the bilateral carotid artery occlusion causes an early loss of the pupillary reflex in 50% of the animals (Davidson *et al*., 2000). The 2-VO model mimics the ocular pathology of human carotid artery disease. The internal carotid artery (ICA) which

begins at the bifurcation of the common carotid artery (CCA) provides the major blood supply to brain. It also provides the blood supply to the eye through the ophthalmic artery.
Many studies have shown that bilateral common carotid artery occlusion in rat causes functional impairment of retina (Block *et al*., 1992). The electroretinogram have also demonstrated that b-wave amplitude representing bipolar and Muller cell activity in response to light exposure is decreased 7 days after the onset of 2VO (Barnett and Osborne, 1995). These functional changes are accompanied by structural damage. In animals that lost their pupillary reflex, the total retinal thickness decreased from approximately 120 µm to around 87 µm. The most affected layers being the synaptic zones in inner plexiform as well as the outer plexiform layer (Lavinsky *et al*., 2006).
In this model, occlusion of both CCAs cuts off blood supply to the retina, however, some retinal perfusion is maintained by retrograde blood flow to ophthalmic artery through the Circle of Willis. The degree of retinal damage also varies greatly within the same experiment, due to heterogeneity in tolerance towards ischemia in individual animal.

10.4 Photocoagulation of retinal vessels

There are only a few studies at present that report the ischemia of less than 5 minutes, which is often observed during the ocular surgeries. The faults that are present in other methods, such as invasiveness and inflammation in raising the intraocular pressure or ligation of optic vessels that causes changes in retina unrelated to ischemia, can be reduced by direct laser exposure of the main retinal vessels.
Kalamkarov *et al.* induced the characteristics of retinal ischemia in rats by direct laser coagulation of blood vessels using argon laser (Kalamkarov *et al*., 2000). Selective occlusion of vessels using laser permits creation of local and extensive retinal ischemia by choosing various retinal vessels and by modifying the exposure dose. In this technique, Rose Bengal, an iodinated photosensitive dye is injected intravenously through tail vein. The eyes are then exposed to 7 minutes of intense light (550nm, which is the absorption peak for this dye). Retinal vein occlusion was simulated in non-human primate model, i.e. cynomolgus monkey (*Maccaca fascicularis*). Dye yellow (577nm) laser light was used to occlude all branch retinal veins in the eye (Miller *et al*., 1994). Photodynamic thrombosis with green argon laser light and Rose Bengal dye was also used to create retinal ischemia model in pigs by occluding the retinal veins.
Laser coagulated Sprague Dawley rats were used to validate the effect of Hongua *in vivo*. In this model, Honghua extract was injected intravitreally, before they were subjected to Rose Bengal dye and laser (550nm). It is hypothesised that as the major component in the Honghua extract is glucose, the neuroprotective effect of the same could be due to availability of energy source after ischemia (Romano, *et al*., 1993). Another Chinese herbal medicine – Fufang Xuehuantong capsule was also studied by Yuan *et al*. They created a rat model for retinal vein occlusion by using laser photocoagulation and then validated the therapeutic benefits Chinese herbal medicine by quantitating the expression of various growth factors in the animal model (Yuan *et al*., 2011).

10.5 Central retinal artery occlusion

In humans, CRAO results in severe retinal ischemia, resulting in irreversible damage within hours. A minimal invasive model of transient retinal ischemia was introduced by Dangeliene *et al*., which involves photothrombotic central retinal artery occlusion (CRAO)

using intravenous injection of Rose Bengal and green laser irradiation of CRA in rats (Dangeliene *et al*., 2000). Rose Bengal is a photosensitive dye that releases oxygen free radicals when irradiated by the laser. This active oxygen results in intraluminal thrombus formation and thus, occlusion of CRA. Another retinal ischemia-reperfusion model through the occlusion of central retinal artery involves placing a suture behind the eye globe, including the CRA and ciliary artery. Both ends of the suture were then passed through a small plastic tube and ischemia is caused by pressing the tube against the artery. Prasad *et al* used the central retinal artery ligation model in rats to compare between different occlusion times as well as different time-period of reperfusion. They studied gene expression of various transcription-related genes after 30 and 90 minutes of occlusion and at 3 hours and 12 hours of reperfusion (Prasad *et al*., 2010).

10.6 Endothelin administration

Transient obstruction of central retinal artery can also be obtained by injecting vasoconstrictive drug. This method is less invasive, simple and does not require any special equipment. Endothelin-1 (ET-1) is a potent vasoconstrictive peptide produced by the vascular endothelial cells. Endothelin is found naturally in various tissues and is involved in a variety of biological activities. It has been linked with pathophysiology of various human disorders, e.g. cardiovascular, renal and ocular. Endothelin-1 can cause apoptosis of neurons in the CNS (Syed, *et al*., 2006). Endothelin-1 causes cell death through mechanism involving free-radicals (Oku, *et al*., 2008). Sugiyama *et al* have shown the association of endothelin with glaucoma. The authors investigated the effect of ET-1 on rabbit eye and observed that the intravenous as well as intravitreal administration of ET-1 reduces both the intraocular pressure and the blood flow in the optic nerve (Sugiyama, *et al*., 1995). Granstam *et al* demonstrated similar effects of endothelin in a cat model (Granstam, *et al*., 1992). Masuzawa *et al* have shown that a high dose of ET-1 when injected under the conjunctiva obstructs the central retinal artery without any damage to other tissues. Endothelin-1 causes retinal ganglion cell loss and activates glial cells (Masuzawa *et al*., 2006). It has also been seen that the intravitreal administration of ET-1 affects the retinal arteries directly. A dose of 10^{-7} M ET-1 led to decrease in the diameter by 17% (Bursell, *et al*., 1995).

Endothelin-1 also causes constriction of arteries *in-vitro*. Yu *et al* showed that ET-1 dose causes constriction even in cryopreserved human retinal arterioles. But the relation between the dose and the related activity is still not known (Yu, *et al*., 1998).

Thus, in this method there is no problem regarding inflammation or infection. But, like any other method being used, this method too is not completely free from drawbacks. The dose of endothelin-1 used is quite high, which may pass into the systemic circulation and exert some undesired effects in other tissues.

11. Current and potential therapeutic strategies for retinal ischemia

Many strategies have been used but have not been successful or have shown various limitations and are at experimental stage. Current treatments available for retinal ischemia include intravitreal or retinal vein administration of tissue-plasminogen activator (t-PA), hemodilution, pan-retinal laser photocoagulation or anti-VEGF antibodies or medication (Lucentis or Avastin). Occlusion of retinal vessels or retinal ischemia leads to retinal neovascularisation. Laser photocoagulation is used to decrease the neovascularisation in retina and thus, the oxygen demand. The decrease in overall oxygen requirement will stop

ischemia and hence, further damage to the eye. Ischemic conditions also cause up-regulation of expression of angiogenic factors, such as vascular endothelial growth factor or VEGF. VEGF is involved in angiogenesis and causes abnormal vessels growth or neovascularisation. To reduce the damage of ischemia, oxygen supply to retina has to be improved. Therefore, anti-VEGF drugs can be directly injected in the eye, e.g. the drugs that have been most tested in animal models include, bevacizumab, ranibizumab, pegaptanib sodium. Corticosteroids, such as, dexamethasone, are also under experimentation, as these inhibit VEGF and inflammatory factors (Lattanzio, *et al*., 2011). Another technique that holds promise is the use of anti-VEGF antibodies. Neutralising anti-VEGF monoclonal antibodies have been demonstrated to block neovascularisation when administered in a primate model of laser-induced retinal ischemia. Aiello *et al* showed the in-vivo inhibition of VEGF with the help of VEGF- neutralising proteins-containing extracellular domain of human (Flt) or mouse (Flk) VEGF receptors attached to IgG. These chimeric proteins showed 100% reduction in neovascularisation with human Flt and 95% with murine Flk domains. The suppression of VEGF was dose-dependent (Aeillo *et al*., 1995).

There are many other drugs and chemical compounds which have been tested in animal models of retinal ischemia with positive results and hope for future therapeutics. Cao *et al* in 1994 provided the evidence for the neuroprotective effect of NMDA antagonists in retinal ischemia. They showed that the NMDA receptor antagonist, dextromethorphan has a protective effect after retinal ischemia. However, it is not still clear whether dextromethorphan works via NMDA receptors. Other NMDA antagonists, such as MK-801 or memantine also protect from retinal ischemia (Lam *et al*., 1997 and Osborne, 1999). Blockers of voltage-gated Ca^{2+} channels, e.g. nifediprine and betaxolol also decrease neurotoxicity by reducing Ca^{2+} ions influx (Melena *et al*., 1999).

Another approach can be the use of the free- radical scavengers. Free-radicals play an important role in the damage caused by retina ischemia. Free-radicals are formed when reduced compounds, which accumulate during ischemia, are reoxidised during reperfusion. This free radical burst causes oxidative stress (Gilgun Sherki, 2002). Intravenous injection of SOD reduces the development of edema in rat model. SOD or superoxide dismutase is a well-known scavenger of superoxide radicals. Another compound that can be used is dimethylthiourea or DMTU, which is a synthetic compound that traps $OH^{\cdot}$, H_2O_2 and other free radicals. Intravitreal injections of both SOD and DMTU have been shown to lead to recovery in IOP-induced ischemia rat model. DMTU (75µg/eye) resulted in 40% functional recovery when assessed through electroretinogram. SOD, on the other hand, leads to 99% functional recovery on post-treatment and 81% on pre-treatment. Thus, all these chemical compounds and drugs that decrease or reverse the cause of ischemia can be helpful in reducing the damage to some extent.

RNA interference (RNAi) is a natural phenomenon in mammals, which is involved in silencing of gene expression. It involves a double-stranded RNA which cleaves any RNA complimentary to it. RNAi has been proposed to be used in therapeutics by downregulating the expression of specific genes. Reich *et al* used the technique of RNA interference in retinal cells *in vitro*, as well as *in vivo* in the mouse retina. They used this technique to downregulate the VEGF expression, which is known to be upregulated in retinal ischemia (Reich *et al*., 2003). RNAi can be further investigated and tested for other genes, e.g. cytokines that are upregulated in the pathophysiology of retinal ischemia.

Stem cell therapy is a promising technique for tissue repair and regeneration. Advances in the field of stem cells have lead to their use in treatment of various disorders (Lenka &

Anand, 2010, Rajarathna, 2009). Stem cells basically are unspecialised cells which are capable of self – renewal and under specific defined environment these cells can form functionally specialised cells. The stem cells can either be obtained from early embryos or certain tissues in adults, such as umbilical cord and peripheral blood, bone marrow. They work through either replacing damaged cells or through the factors released by them. Stem cells have been used in various vascular neurodegenerative diseases and most of the ocular disorders involve problem in either of the two. Eye is an accessible organ and with large number of animal models available, the use of stem cells poses a promise for preserving functionality (Cogliati & Swaroop, 2009).

Adult bone marrow contains hematopoietic stem cells (HSCs) and hematopoietic progenitor cells (HPCs), which can differentiate into various cell types of myeloid and endothelial lineages. Bone-marrow contains stem cells which can either differentiate into Lin+ (hematopoietic lineage) or Lin- (non-hematopoietic lineage). Lin- population contains progenitor cells that differentiate into vascular endothelial cells, i.e. the endothelial progenitor cells (EPCs). Many preclinical and clinical studies have shown bone-marrow derived cells contribute to neoangiogenesis during wound healing, retinal ischemia, myocardial infarction, neonatal growth and tumor growth. Lin- population have been shown to express neuronal markers after transplantation in brain or retina in various mouse models. Bone-marrow cells differentiate into neuronal cells, astrocytes *in-vitro* and also *in-vivo* when injected intravenously into brain of mouse model (Mezey, *et al*., 2000). Also, it has been shown that BMCs can differentiate into retinal neural cells *in-vivo* (Woodbury, *et al*., 2000). Lin- bone-marrow stem cells when injected intravitreally into photocoagulated retina of a mouse model, migrated to astrocytes and formed retinal vessels. Ischemic conditions release cytokines that recruit EPCs to the site. Ischemia results in up-regulation of angiogenic factor, vascular endothelial growth factor or VEGF-A, which has its receptors Flk-1 and Flt-1 on EPCs, HSCs and HPCs, thus leading to their migration to the site (Kalka, *et al*., 2000). But their importance in clinics is still unknown as the success depends on their functional incorporation.

Mesenchymal stem cells (MSCs) also found in bone marrow and other tissues such as cord blood, peripheral blood, fallopian tube, and fetal liver and lung have been used in over a range of different clinical trials (US NIH clinical trial database – www.clinicaltrials.gov), including those in fractures, diabetes, heart and liver disease and neurological disorders. MSCs have the potential to differentiate into neurons, especially retinal neurons. These cells also secrete molecules that modify the environment for the surrounding cells. MSCs for instance, express a number of neuroprotective factors, such as BDNF, CNTF, IGF, bFGF and NGF, which protect the injured retina. MSCs have another remarkable property, i.e. the homing potential; they can migrate to pathological areas (Prabhakar, *et al*., 2010). They can migrate from blood circulation to brain, spinal cord, and eye (Kan, *et al*., 2005). Thus, MSCs have shown neuroprotection in various neurodegenerative models, but clinical translation is still questionable.

Another source of stem cell therapy is the embryonic stem cells (ESCs), obtained from the inner cell mass of blastocyst. ESCs can differentiate into various cell types, such as hematopoietic cells, astrocytes, hepatocytes, glial cells, neurons. Wei *et al*., 2005, showed that the transplantation of human embryonic cells in MCAO stroke model led to structural as well as functional recovery. Transplanted ESCs differentiated into neurons, astrocytes, oligodendrocytes and endothelial cells. These ESC – derived endothelial cells can form vascular-like structures *in-vivo* as well as *in-vitro*, thus induce angiogenesis (Levenberg, *et*

al., 2002). Embryonic stem cells have issue of ethical restrictions as well as immune rejection. Thus, alternate source of stem cells was identified from non-pluripotent cells. Every nucleated cell in an individual has identical genome, except the gametes. Different cell types are identified on the basis of the genes that are expressed. In 2006, four transcription factors – *Oct 3/4, Sox-2, Klf-4* and *c-myc*, that are capable of reprogramming DNA were identified (Takahashi & Yamanaka, 2006). Forced expression of these specific genes in a non-pluripotent cell lead to a pluripotent stem cell, known as induced pluripotent stem cell (iPC). Human iPCs have been derived successfully from patients with neurological disorders – Parkinson's disease, muscular dystrophy, Huntington's (Park *et al*., 2008). iPC from the skin cells of an amylotrophic lateral sclerosis (ALS) patient have been differentiated into motor neurons (Dimos *et al*., 2008). Takahashi group for the first time generated photoreceptor cells from the embryonic stem cells (Takahashi & Yamanaka, 2006). The same method has been used to create human photoreceptor and retinal pigmented epithelium phenotype (Hirami *et al*., 2009). Human neuronal cells can also be generated from iPC (Karumbayaram *et al*., 2009). Human umbilical cord blood is a well known source of hematopoietic stem cells and has been used in various disorders. Umbilical cord blood contains higher percentage of hematopoietic stem cells than the bone marrow and also poses a lesser risk of immune rejection. The cells from cord blood have the potential to form retinal neuronal cells.

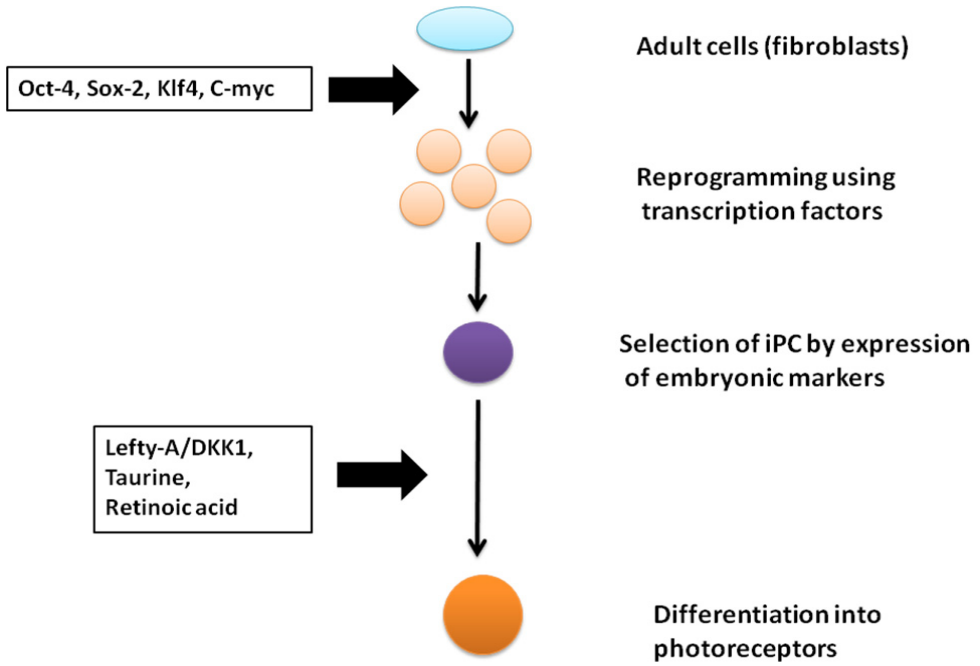


Fig. 3. Formation of iPC from adult somatic cell

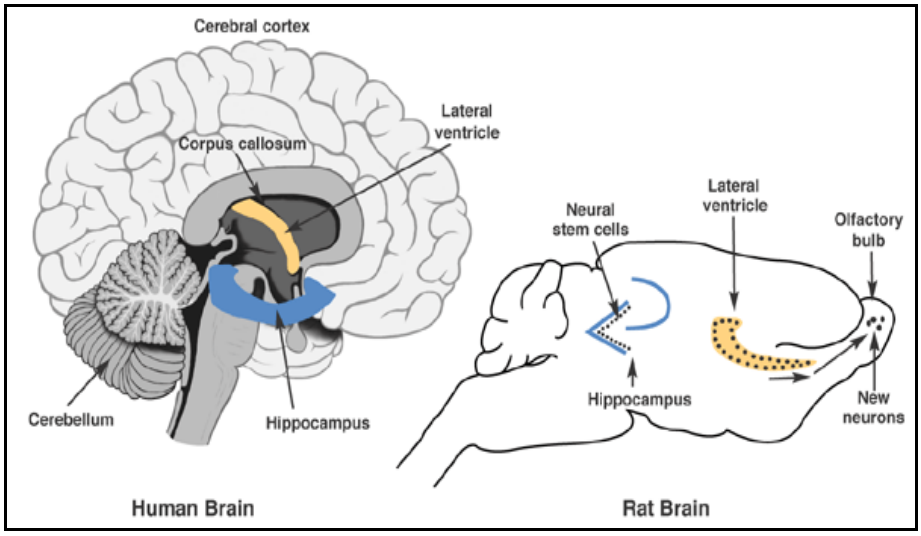


Fig. 4. Different sources of neural stem cells (NSCs) in human and rat brain *(Reproduced with permission http://pubs.niaaa.nih.gov/publications/arh27-2/197-204.htm)*

The mammalian central nervous system was considered is a non-renewable tissue. But studies have demonstrated that neural stem cells (NSCs) do exist not only in developing CNS, but also in adult nervous system of all mammals and are capable of differentiating into neurons, astrocytes and oligodendrocytes. Neural stem or progenitor cells can be isolated from various parts of CNS, such as hippocampus, subventricular zone, spinal cord and ependyma. Palmer *et al* for the first time isolated NSCs from the hippocampus of an adult rat. These hippocampus-derived NSCs have an ability to migrate and differentiate into neuronal lineage in injured retina, but are unable to form retina-specific cells (Nishida *et al*., 2000). Embryonic retina derived neural progenitors can differentiate into photoreceptors *in-vitro* (Ahmad *et al*., 2004). NSCs have an advantage over the embryonic stem cells with respect to their clinical translation, i.e. NSC can be expanded through numerous passages in-vitro and can be easily manipulated (English & Anand, 2010) . But, further studies are required to derive retinal neurons from the NSCs.

But there are some limitations and barriers for stem cell transplantation in retina, as retina shows poor cell integration. Like any other part in the central nervous system, the retina too is rigid to cell migration. Thus, most of the cells that are transplanted do not reach the retina. It has been shown that only 1% of intraocularly transplanted cells reach the retina (Johnson, *et al*., 2010).The stem cell therapy holds a promising future in retinal disorders, but the problems need to be dealt with before clinical translation.

Another therapeutic approach that shows a promising future is the concept of personalised therapy, where the candidate genes linked with various eye disorders can be identified and the genetic make-up of an individual can be used for disease prediction and treatment.

12. Conclusion

Retinal ischemia is a common cause for visual impairment and vision loss. It is a condition related with many different human disorders, such as diabetic retinopathy, glaucoma, and it

occurs when the blood supply is not sufficient to meet the demand. The retina and brain share common development pathway. Retina, like CNS, originates from ectoderm, however, it can be non-invasively studied. Also, as the retinal blood vessels share many features with the cerebral blood vessels, the investigations can be extrapolated to brain pathology. Thus, studying the retina, through the retinal ischemia models can help in understanding the mechanism and pathophysiology of stroke as well as in validating potential therapeutics. But all the methods discussed here have their own strengths and limitations. Out of all the above mentioned animal models, pressure elevation model is commonly used as it is easily reproducible and it mimics many human disorders – central retinal artery occlusion (CRAO), glaucoma, occlusion of ophthalmic artery. For example, some methods require penetration of a needle through the cornea, and must be fixed in the anterior chamber for one hour. The invasiveness can lead to inflammation and other damages. Similarly, unilateral and bilateral occlusion of carotid artery requires specialised skills in vascular surgery. It may cause incomplete ischemia and all of these procedures alter blood flow to the brain. Likewise, photocoagulation is simple but has many disadvantages including variable degrees of exposure and hence, variable damage. Besides, the ischemic damage caused is permanent because of which reperfusion cannot be studied. The choice of animal models for pre-clinical testing, therefore, depends on the research questions which have been raised.

13. References

Ahmad, I., Das, A. V., James, J., Bhattacharya S. & Zhao, X. (2004). Neural stem cells in the mammalian eye: types and regulation. *Seminar in Cell and Developmental Biology*, Vol. 15, No. 1, pp. 53-62

Barnett, N. L. & Osborne, N. N. (1995). Suppression of retinal neovascularization in vivo by inhibition of vascular endothelial growth factor (VEGF) using soluble VEGF-receptor chimeric proteins. *Experimental Eye Research*, Vol. 61, pp. 83–90

Berson, D. M. (2007). Phototransduction in ganglion - cell photoreceptors. *Pflugers Archives*, Vol. 454, pp. 849-855

Block, F., Grommes, C. & Kosinski, C. (1997). Retinal ischemia induced by the intraluminal suture methods in rats. *Neuroscience Letters*, Vol. 232, pp. 45-48

Block, F. & Schwarz, M. (1997). Effects of antioxidants on ischemic retinal dysfunction. *Experimental Eye Research*, Vol. 64, pp. 559–564

Block, F., Schwarz, M. & Sontag, K.H. (1992). Retinal ischemia induced by occlusion of both common carotid arteries in rats as demonstrated by electroretinography. *Neuroscience Letters*, Vol. 144, pp. 124–126

Buchi, E. R., Suivaizdis, I. & Fu, J. (1991). Pressure-induced retinal ischemia in rats: an experimental model for quantitative study. *Ophthalmologica*, Vol. 203, pp. 138–147

Bursell, S. E., Clermont, A. C., Oren, B. & King, G. L. (1995). The *in vivo* effect of endothelins on retinal circulation in nondiabetic and diabetic rats. *Investigative Ophthalmology and Visual Science*, Vol. 36, No. 3, pp. 596–607

Cao, W., Zaharia, M., Drumheller, A., Casanova, C., Lafond, G., Brunette, J. R. & Jolicoeur, F. B. (1994). Effects of dextromethorphan on ischemia induced ERG changes in rabbit. *Current Eye Research*, Vol. 13, No. 2, pp. 97-102

Cogliati, T. & Swaroop, A. (2009). Stems cells and neuronal repair. *Annals of Neurosciences*, Vol. 16, No. 4, pp. 143-145

Daugeliene, L. Niwa, M. & Hara, A. (2000). Transient ischemic injury in the rat retina caused by thrombotic occlusion-thrombolytic reperfusion. *Investigative Ophthalmology and Visual Science*, Vol. 41, pp. 2743–2747

Davidson, C. M., Pappas, B. A., Stevens, W. D., Fortin, T. & Bennett, S. A. L. (2000). Chronic cerebral hypoperfusion: loss of papillary reflex, visual impairment and retinal neurodegeneration. *Brain Research*, Vol. 859, No. 1, pp. 96-103

Dimos, J. T., Rodolfa, K. T. & Niakan, K. K. (2008). Induced pluripotent stem cells generated from patients with ALS can be differentiated into motor neurons. *Science,* Vol. 321, pp. 1218–1221

English, D. & Anand, A. (2010). Neural stem cell therapy – how the hype began. *Annals of Neurosciences*. Vol. 17, No. 1.

Flower, R .W. & Patz, A. (1971). The effect of hyperbaric oxygenation on retinal ischemia. *Ophthalmology and Visual Science*. Vol. 10, No. 8, pp. 605-616.

Gao, G., Li, Y. , Fant, J., Craig, E., Crosson, S., Becerra, P. & Ma, J. (2002). Difference in ischemic regulation of vascular endothelial growth factor and pigment epithelium-derived factor in Brown Norway and Sprague Dawley rats contributing to different susceptibilities to retinal neovascularization. *Diabetes*. Vol. 51, No. 4, pp. 1218-1225.

Gilgun-Sherki, Y., Rosenbaum, Z., Melamed, E. & Offen, D. (2002). Antioxidant therapy in acute central nervous system injury: current state. *Pharmacological Reviews*. Vol. 54, No. 2, pp. 271-284.

Granstam, E., Wang, L. & Bill, A. (1992). Ocular effects of endothelin-1 in the cat. *Current Eye Research*. Vol. 11, No. 4, pp. 325-332.

Ha, K. T., Yoon, S. J., Choi, D. Y., Kim, D. W. & Kim, J. K. (2005). Protective effect of *Lycium chinense* fruit on carbon tetrachloride-induced hepatotoxicity. *Journal of Ethnopharmacology*. Vol. 96, pp. 529–535.

Hein, T. W. , Rosa, R. H., Jr., Yuan, Z. , Roberts, E. & Kuo, L. (2010). Divergent roles of nitric oxide and rho kinase in vasomotor regulation of human retinal arterioles. *Investigative Ophthalmology and Visual Sciences*. Vol. 51, No. 3, pp. 1583-1590.

Henkind , P., Hansen, R. I. & Szalay, J. (1979). Ocular circulation. In "Physiology of the human eye and visual system" (Ed. Records, R.E.), pp. 98-155. Harper & Row, New York.

Hirami, Y., Osakada F, Takahashi K, *et al*. (2009). Generation of retinal cells from mouse and human induced pluripotent stem cells. *Neuroscience Letters*. Vol. 458, pp. 126–131.

Hirrlinger, P. G., Elke, U., Ianors, I., Andreas, R. & Thomas, P. (2010). Alterations in protein expression and membrane properties during Müller cell gliosis in a murine model of transient retinal ischemia. *Neuroscience Letters*. Vol. 472, pp. 73–78.

Jennings, R. B., Sommers, H. M., Smyth, G. A., Flack, H. A. & Linn, H. (1960). Myocardial necrosis induced by temporary occlusion of a coronary artery in the dog. *Archives of Pathology*. Vol. 70, pp. 68–78.

Joachim, S. C., Wax, M. B., Boehm, N., Dirk, D., Pfeiffer N & Grus FH. (2011). Up-regulation of antibody response to heat shock proteins and tissue antigens in an ocular ischemia model. *Investigative Ophthalmology and Visual Sciences*

Jung, S. H., Kang, K. D., Ji, D., Fawcett, R. J., Safa, R., Kamalden, T. A. & Osborne, N. N.(2008). The flavonoid baicalin counteracts ischemic and oxidative insults to retinal cells and lipid peroxidation to brain membranes. *Neurochemistry International*. Vol. 53, No. 6-8, pp. 325-337.

Jung, S. H., Kim, B. J., Lee, E. H. & Osborne, N. N. (2010). Isoquercitrin is the most effective antioxidant in the plant *Thuja orientalis* and able to counteract oxidative-induced damage to a transformed cell line (RGC-5 cells). *Neurochemistry International*. Vol. 57, No. 7, pp. 713-721.

Kaja, S., Yang, S. H. & J. Wei *et al*. (2003). Estrogen protects the inner retina from apoptosis and ischemia-induced loss of Vesl-1L/Homer-1c immunoreactive synaptic connections. *Investigative Ophthalmology and Visual Science*, Vol. 44, pp. 3155-3162, .

Kalamkarov, G.R., Tsapenko, I. V., Zueva, M.V., Ivanov, A. N., Konstantinova, T. S., Burgova, A. E., Rezvykh S. V., Fedorov, A. A. & Shevchenko, T. F. (2008). Experimental model of acute ischemia of the retina in rats. *Bulletin of Experimental Biology and Medicine*. Vol. 145, No. 6, pp. 688-691.

Kalka, C., Masuda, H. & Takahashi, T. (2000). Vascular endothelial growth factor (165) gene transfer augments circulating endothelial progenitor cells in human subjects. *Circulation Research*. Vol. 86, No. 1198-1202.

Kan, I., Melamed, E. & Offen, D. (2005). Integral therapeutic potential of bone marrow mesenchymal stem cells. *Current Drug Targets*. Vol. 6, No. 1, pp. 31-41.

Karumbayaram, S., Novitch, B. G., Patterson, M. (2009). Directed differentiation of human-induced pluripotent stem cells generates active motor neurons. *Stem Cells,* Vol. 27, pp. 806–811.

Kaur, C., Foulds, W. S. & Ling, E. A. (2008). Blood-retinal barrier in hypoxic ischemic condition: basic concepts, clinical features and management. *Progress in Retina and Eye Research*, Vol. 27, pp. 622-647

Kawai, S., Vora, S., Das, S., Gachie, E., Becker, B. & Neufeld, A. H. (2001). Modeling of risk factors for the degeneration of retinal ganglion cells after ischemia/reperfusion in rats: effects of age, caloric restriction, diabetes, pigmentation, and glaucoma. *The FASEB Journal,* Vol. 15, pp. 1285-1287

Lam, T. T., Siew, E., Chu, R. & Tso, M. O. (1997). Ameliorative effect of MK-801 on retinal ischemia. *Journal of Ocular Pharmacology Therapeutics*, Vol. 13, pp. 129–137

Lavinsky, D., Arterni, N. S., Achaval, M. & Netto, C. A. (2006). Chronic bilateral common carotid artery occlusion: a model for ocular ischemic syndrome in the rat. *Graefe's Archive for Clinical and Exaperimental Opthalmology*, Vol. 244, No. 2, pp. 199-204

Lenka, N. & Anand, A. (2010). Advancements in stem cell research: an Indian perspective – I. *Annals of Neurosciences*, Vol. 17, No. 3

Levenberg, S., Golub, J. S., Amit, M., Itskovitz-Eldor, J. & Langer, R. (2002). Endothelial cells derived from human embryonic stem cells. *Proceedings of National Academy of Sciences, USA*, Vol. 99, No. 7, pp. 4391-4396

Li, S-Y., Yang, D., Yeung, C-M., Yu, W-Y., Chang, R. C-C., So, K-F., Wong, D. & Lo, A. C. Y. (2011). *Lycium barbarum* polysaccharides reduce neuronal damage, blood-retinal barrier disruption and oxidative stress in retinal ischemia/reperfusion injury. *PLoS ONE*, Vol. 6, No. 1, pp. e16380

Li, X. M., Ma, Y. L. & Liu, X. J. (2007). Effect of the *Lycium barbarum* polysaccharides on age-related oxidative stress in aged mice. *Journal of Ethnopharmacology*, Vol. 111, pp. 504–511.

Louzada-Junior, P., Dias, J. J., Santos, W. F., Lachat, J. J., Bradford, H. F. & Coutinho-Netto, J. (1992). Glutamate release in experimental ischaemia of the retina: an approach using microdialysis. *Journal of Neurochemistry*, Vol. 59, pp. 358–363

Lucas, D. R., Newhouse, J. P. (1957). The toxic effect of sodium L-glutamate on the inner layers of the retina. *Archives of Ophthalmology*, Vol. 58, pp. 193–201

Masland, R. H. (1998). Amacrine cells. *Trends in Neuroscience*, Vol. 11, pp. 405-410

Masuzawa, K., Jesmin, S., Maeda, S., Kaji, Y., Oshika, T., Zaedi, S. & Shimojo, N. (2006). A model of retinal ischemia-reperfusion injury in rats by subconjuctival injection of Endothelin-1. *Experimental Biology and Medicine*, Vol. 231, pp. 1085–1089

Matteucci, A., Cammarota, R. , Paradisi, S. , Varano, M. , Balduzzi, M. , Leo, L., Bellenchi, G.C. , de Nuccio, C., Carnovale-Scalzo, G. , Scorcia, G., Frank, C., Mallozzi, C. , di Stasi, A. M. , Visentin, S. & Malchiodi-Albedi, F. (2011) . Curcumin Protects against NMDA-Induced Toxicity: A Possible Role for NR2A Subunit. *Investigative Ophthalmology and Visual Sciences,* Vol. 52, No. 2, pp. 1070-1077

Melena, J., Wood, J. P. M. & Osborne, N. N. (1999). Betaxolol, a B1- adrenoceptor antagonist, has an affinity for L-type Ca^{2+} channels. *European Journal of Pharmacology*, Vol. 378, pp. 317–322

Mezey,E., Chandross, K. J., Harta, G., Maki, R. A. & McKercher, S. R. (2000). Turning blood into brain: cells bearing neuronal antigens generated *in vivo* from bone marrow, *Science*, Vol. 290, pp. 1779-1782

Miller, J. W., Adamis, A. P., Shima, D. T., D'Amore P. A., Moulton, R. S., O'Reilly, M. S., Folkman, J., Dvorak, H. F., Brown, L. F., Berse, B., Yeo, T-K., & Yeot, K-T. (1994) . Vascular endothelial growth factor/vascular permeability factor is temporally and spatially correlated with ocular angiogenesis in a primate model. *American Journal of Pathology*, Vol. 145, No. 3

Mishida, A., Zakahashi, M., Tauihara, H., Nakamo, I., Tahahashi, J. B., Mizoguchi, A., Ide, C. & Honda, Y. (2000). Incorporation and differentiation of hippocampus-derived neural stem cells transplanted in injured adult rat retina. *Investigative Opthalmology and Visual Sciences*, Vol. 41, No. 13, pp. 4268-4269

Osborne, N. N., DeSantis, L., Bae, J. H., Ugarte, M., Wood, J. P. M., Nash, M. S. & Chidlow, G. (1999a). Topically applied betaxolol attenuates NMDA-induced toxicity to ganglion cells and the effects of ischaemia to the retina. *Experimental Eye Research*, Vol. 69, pp. 331–342

Osborne, N. N., Safa, R., Nash & M. S. (1999b). Photoreceptors are preferentially affected in the rat retina following permanent occlusion of the carotid arteries. *Vision Research*, Vol. 39, pp. 3995–4002

Palmer, T. D., Takahashi, J. & Gage, F. H. (1997). The adult rat hippocampus contains primordial neural stem cells. *Molecular and Cellular Neuroscience*, Vol. 8, No. 6, pp. 389-404

Palmero, M., Bellot , J. L., Castillo, M., Garcia-Cabanes, C., Miquel, J. & Orts, A. (2000). An *in-vitro* model of ischemic-like stress in retinal pigmented epithelium cells:

protective effects of antioxidants. *Mechanisms of Ageing and Development*, Vol. 114, No. 3, pp. 185-190

Park, I. H., Arora, N., Huo, H., Maherali, N., Ahfeldt, T., Shimamura, A., Lensch, M. W., Chad, C., Hochedlinger, K. & Daley, G. Q. (2008). Disease-specific induced pluripotent stem cells. *Cell,* Vol. 134, pp. 877–86

Paul, A. L., Piercet, E. A., Foleyt, E. D., Takagittil, H., Chen, H., Riddle, L., Ferrara, N., Kingttii, G. L. & Smitht, L. E. H.. (1995). Suppression of retinal neovascularization in vivo by inhibition of vascular endothelial growth factor (VEGF) using soluble VEGF-receptor chimeric proteins. *Proceedings of National Academy of Science, USA,* Vol. 92, pp. 10457-10461

Peachey, N. S., Green, D. J. & Ripps, H. (1993). Ocular ischemia and the effects of allopurinol on functional recovery in the retina of the arterially perfused cat eye. *Investigative Ophthalmology and Visual Science*, Vol. 34, pp. 58–65

Plate, K. H., Breier, G., Weich, H. A., Risau, W. (1992). Vascular endothelial growth factor is a potential tumour angiogenesis factor in human gliomas *in vivo*. *Nature*, Vol. 359, pp. 845-848

Poché, R. A. & Reese, B. E. (2009).Retinal horizontal cells: challenging paradigms of neural development and cancer biology. *Development*, Vol. 136, pp. 2141-2151

Prabhakar, S., Muthaian, R., Chhabra, R. & Anand, A. (2010). Analysis of homing potential of marrow-derived mononuclear cells in an experimentally-induced brain stroke mouse model. *Brain Injury,* Vol. 24, No. 12, pp. 1485-1490

Prasad, S. S., Kojic, L., Wen, Y. H., Chen, Z., Xiong, W., Jia, W. & Cyander, M. S. (2010). Retinal gene expression after central retinal artery ligation: Effects of ischemia and reperfusion. *Investigative Ophthalmology and Visual Science*, Vol. 51, No. 12, pp. 6207-6219

Rajarathna,T. (2009). Advancements in stem cell research: an Indian perspective – II. *Annals of Neurosciences*, Vol. 16, No. 3, pp. 97

Reich, S. J. , Fosnot, J. , Kuroki, A. , Tang, W. , Yang , X. , Maguire, A. M. , Bennett, J. & Tolentino, M. J. (2003) . Small interfering RNA (siRNA) targeting *VEGF* effectively inhibits ocular neovascularization in a mouse model. *Molecular Vision*, Vol. 9, pp. 210-216

Rios, L., Jacques, C., Vennat, J-C., Menerath, J-M., & Doly, M. (1999). Comparison of intraocular treatment of DMTU and SOD following retinal ischemia in rats. *Journal of Ocular Pharmacology and Therapeutics,* Vol. 15, No. 6, pp. 547-556

Romano, C., Price, M. T., Almli, T. & Olney, J. W. (1998). Excitotoxic neurodegeneration induced by deprivation of oxygen and glucose in isolated retina. *Investigative Ophthalmology and Visual Science,* Vol. 39, pp. 416-423

Romano, C., Price, M., Bai, H. Y. & Olney, J. W. (1993). Neuroprotectants in Honghua: glucose attenuates retinal ischemic damage. *Investigative Ophthalmology and Visual Science*, Vol. 34, No. 1, pp. 72-80

Saint-Geniez, M. & D'Amore, P.A. (2004). Development and pathology of the hyaloid, choroidal and retinal vasculature. *International Journal of Developmental Biology*, Vol. 48, pp. 1045-1058

Shima, D. T., Adamis, A. P., Ferrara, N., Allende, R., Yeo, K., & D'Amore, P. A. (1995). Hypoxic induction of endothelial cell growth factors in retinal cells: identification

and characterization of vascular endothelial growth factor as the mitogen. *Molecular Medicine,* Vol. 2, pp. 64-75

Shweiki, D., Itin, A., Softer, D. & Keshet, E. (1992). Vascular endothelial growth factor induced by hypoxia may mediate hypoxia-initiated angiogenesis. *Nature*, Vol. 359, pp. 843-845

Sims, S. R. (1992). Energy metabolism and selective neuronal vulnerability following global cerebral ischemia. *Neurochemical Research*, Vol. 17, pp. 923–931

Steele, E. C., Guo, Q. & Namura, S. (2008). Filamentous middle cerebral artery occlusion causes ischemic damage to retina in mice. *Stroke*, Vol. 39, No. 7, pp. 2099-2104

Sugiyama, T., Moriya, S., Oku, H. & Azuma, I. (1995). Association of endothelin-1 with normal tension Glaucoma – clinical and fundamental studies. *Survey of Opthalmology*, Vol. 39, No. 1, pp. S49-S56

Syed, H., Safa, R., Chidlow, G. & N. N. Osborne. (2006). Sulfisoxazole, an endothelin receptor antagonist, protects retinal neurones from insults of ischemia/reperfusion or lipopolysaccharide. *Neurochemistry International*, Vol. 48, No. 8, pp. 708–717

Szabo, M. E., Droy-Lefaix, M. T., Doly, M. & Braquet, P. (1991). Free radical-mediated effects in reperfusion injury: a histologic study with SOD and EGb 761 in rat retina. *Ophthalmic Research*, Vol. 23, pp. 225-234

Szabo, M. E., Droy-Lefoix, M. T., Doly, M., Carre, C. & Braquer, P. (1991). Ischemia and reperfusion-induced histologic changes in the rat retina: demonstration of a free radical-mediated mechanism. *Investigative Ophthalmology & Visual Science*, Vol. 32, No. 5, pp. 1471-1478

Takahashi, K. & Yamanaka, S. (2006).Induction of pluripotent stem cells from mouse embryonic and adult fibroblast cultures by defined factors. *Cell,* Vol. 126, pp. 663–676

Tso, M. O. & Jampol, L. M. (1982). Pathophysiology of hypertensive retinopathy. *Ophthalmology*, Vol. 89, pp. 1132-1145

Ueda, K., Makahara, T., Hoshino, M., Mori, A. & Sakamoto, K. (2010). Retinal blood vessels are damaged in rat model of NMDA-induced retinal degeneration. *Neuroscience Letters*, Vol. 485, No. 1, pp. 55-59

Wei, L., Cui, L., Snider, B. J., Rivkin, M., Yu, S. S., Lee, C. S., Adams, L. D. Johnson, E. M., Yu, S. P. & Choi, D. W. (2005). Transplantation of embryonic stem cells overexpressing Bcl-2 promotes functional recovery after transient cerebral ischemia. *Neurobiology of Disease,* Vol. 19, No. 1-2, pp. 183-193

Woodbury, D., Schwarz, E. J., Prockop, D. J. & Black I. B. (2000). Adult rat and human bone marrow stromal cells differentiate into neurons. *Journal of Neuroscience Research*, Vol. 61, pp. 364-370

Yamamoto, H., Schimdt-Kasmer, R., Hamasaki, D. I., Yamamoto, H. & Parel, J. M. (2006). Complex neurodegeneration in retina following moderate ischemia induced by bilateral common carotid artery occlusion in Wistar rats. *Experimental Eye Research*, Vol. 82, No. 5, pp. 767-779

Yu, D. Y., Su, E. N., Cringle, S. J., Alder, V. A., Yu, P. K. & Desantis, L. (1998). Effect of betaxolol, timolol and nimodipine on human and pig retinal arterioles. *Experimental Eye Research*, Vol. 67, pp. 73–81

Yu, M. S., Lai, C. S., Ho, Y. S., Zee, S. Y. & So, K. F.(2007). Characterization of the effects of anti-aging medicine *Fructus lycii* on beta-amyloid peptide neurotoxicity. *International Journal of Molecular Medicine*, Vol. 20, pp. 261–268

Yuan, Y-Z., Yuan, F., Xu, Q-Y., Yu, J., Li, L. & Zhang, J-L. (2011). Effect of Fufang Xuehuantong capsule on a rat model of retinal vein occlusion. *Chinese Journal of Integrative Medicine*. Vol. 17, No. 4, pp. 296-301

Zhang, S. X., Ma, J., Sima, J., Chen, Y., Hu, M. S., Ottlecz, A., & Lambrou, G. N. (2005). Genetic difference in susceptibility to the blood-retina barrier breakdown in diabetes and oxygen-induced retinopathy. *American Journal of Pathology*, Vol. 166, No. 1, pp. 313–321

Brain Injury, November 2010; 24(12): 1485–1490

informa
healthcare

ORIGINAL ARTICLE

Analysis of homing potential of marrow-derived mononuclear cells in an experimentally-induced brain stroke mouse model

SUDESH PRABHAKAR[1], RUPADEVI MUTHAIAN[1], RAJESH CHABBRA[2], & AKSHAY ANAND[1]

[1]*Department of Neurology, and* [2]*Department of Neurosurgery, Post Graduate Institute of Medical Education and Research, Chandigarh, India*

(Received 30 November 2009; accepted 5 August 2010)

Brain Inj Downloaded from informahealthcare.com by University of California Irvine on 10/30/14
For personal use only.

Abstract

Primary objective: To analyse the efficacy of bone marrow-derived mononuclear cells (MNCs) in traversing the blood–brain barrier (BBB) in an experimental model of stroke.

Methods and procedures: The middle cerebral artery occlusion (MCAo) mouse model was established and behavioural and histological analysis was performed, subsequently the carboxyfluorescein diacetate (CFDA)-labelled MNCs were transplanted through the tail vein immediately after 23 hours of reperfusion. The fluorescence microscopic analysis of the brain sections was analysed in both acute and sub-acute phases of transplantation.

Results: The neurological deficit was confirmed by TTC staining and contra lateral turning behaviour. After 2 and 7 days of transplantation, the CFDA-labelled MNCs were observed in the infarcted regions along the line of cortex.

Conclusion: The presence of the CFDA-labelled cells in the ischaemic injured brain lesions proved homing of the implanted MNCs in the infarcted regions of the brain. The successful homing of MNCs may pave way for future clinical trials using MNC in stroke.

Keywords: *Ischemic stroke, MCAO model, stem cell transplantation, marrow-derived mononuclear cells*

Introduction

Stroke is the third most common cause of death worldwide, a neurological syndrome, clinically defined and characterized by rapidly progressing symptoms and signs of focal loss of cerebral function [1]. Approximately 80% of stroke comprises of variant ischemia which results from either thrombotic or embolic occlusion of a major cerebral artery, especially the middle cerebral artery (MCA). Consequently, blood flow reduction occurs which triggers a series of multi-step pathophysiologic events characterized by ischemic cascade [2]. Asians have a higher prevalence of stroke when compared to coronary heart disease. Epidemiological survey conducted on an Indian population has revealed that there was a higher prevalence of cerebral haemorrhage in the community compared to that reported from Western countries [3].

Despite the increase in research investigations, no specific medical therapy has been developed for stroke, even though many promising experimental compounds have reached the Phase III clinical trials [1]. More than 700 drugs have been studied to date which are found to be effective in animal

Correspondence: Akshay Anand, PhD, Assistant Professor, Department of Neurology, Post Graduate Institute of Medical Education and Research, Sector-12, Chandigarh 160012, India. Tel: 91-172 2756090. Fax: 91 172 2748399. E-mail: akshay1anand@rediffmail.com. website: www.neurologypgi.org

ISSN 0269–9052 print/ISSN 1362–301X online © 2010 Informa UK Ltd.
DOI: 10.3109/02699052.2010.520298

Copyright Informa Healthcare 2010
Non-commercial distribution
Unauthorized use prohibited.
Authorized users can download, display, view and print a single copy for personal use.
RIGHTSLINK

stroke models, but none has been proven useful except for a few free radical tapering agents and the thrombolytics [2].

Despite tremendous research in utilizing various sources of stem cells like mesenchymal stem cells, umbilical cord blood cells and amniotic epithelial cells, the homing potential has not been adequately investigated. Presently, the Indian government has initiated several studies using mononuclear cells for various clinical trials. In order to understand the therapeutic potential of bone marrow-derived mononuclear cells in the therapeutic management of stroke, this study analysed the homing efficiency of bone marrow mononuclear cells after experimentally-induced stroke in mouse. It has been believed that the changes in the molecules responsible for cellular trafficking to hypoxic site are responsible for the trapping of mononuclear cells in the ischaemic site [4]. The nerve growth factor of bone marrow mononuclear cells tends to increase peripheral nerve regeneration by its secreting potential [5]. This is possible if there is successful homing of bone marrow-derived mononuclear cells after which efforts can be focused on the signalling cascade involved in the regulation of matrix metalloproteinases or chemokine/chemokine receptors, which participate in the homing of bone marrow mononuclear cells to ischemic site.

Brain Inj Downloaded from informahealthcare.com by University of California Irvine on 10/30/14
For personal use only.

Materials and methods

Animals

This study was approved by and performed in accordance with the guidelines of the Institutional Animal Ethical Committee, Post Graduate Institute of Medical Education and Research, Chandigarh, India. Healthy adult male Swiss albino mice ($n = 15$) with an average weight of 25–30 grams and an age of 6–8 weeks were randomly divided into four groups: (1) Sham group; (2) MCAO group; (3) Transplantation group, 2 days and (4) 7 days. The mice were barrier housed two per cage in a temperature ($24 \pm 2^{\circ}$C) and light controlled environment with a 12 : 12 hour light–dark cycle and provided free access to food and water.

Surgical procedure

An experimental stroke mouse model was established by intraluminal suture method, adapted to rat MCAo developed by Zea-Longa et al. [6]. For induction and maintenance of anaesthesia, a ketamine (80 mg/kg) and xylazine (10 mg/kg) cocktail was diluted in normal saline in the ratio of 1 : 10. After placing the animals in the supine position, the skin incision was made in the neck region, following which the muscle was retracted laterally. The right common carotid artery (CCA), external carotid artery (ECA) and internal carotid artery (ICA) were isolated from the vagus nerve. The arteriotomy was made in the ECA to facilitate the insertion of monofilament. A poly-L-lysine coated 6-0 monofilament was carefully advanced up to 11 mm [7] from the carotid artery bifurcation or until resistance was felt. After 60 min of the occlusion period, a loose knot was placed on the ECA stump, below the arteriotomy, and the filament was then carefully removed. Finally, the knot was tightened and reperfusion was confirmed before closing the incision. For sham control, the right CCA, ECA and ICA were exposed via midline incision, but not disrupted, the suture was not inserted and, after 60 min, the incision was closed. Duration of anaesthesia was similar in both MCAo and sham groups.

Behavioural analysis

The neurological status of each animal was evaluated by confirming the turning behaviour towards the side contra-lateral to the ischemic hemisphere, immediately after recovery from anaesthesia, which persisted up to 4 hours after MCAo. This was an acute behavioural response after MCAo and was considered as a precocious index of neurological deficit and neuronal damage.

Histological analysis

After 23 hours of reperfusion, the animals were euthanized by administration of a high dose of ketamine and xylazine and the brain was dissected out carefully and was frozen at -80°C for 15 minutes. The frozen brain was sliced into coronal sections with 1 millimetre thickness and stained at 37°C for 20 minutes with saline solution containing 1% of 2, 3, 5 triphenyltetrazolium chloride (TTC). The cross-sectional area of infarction in each brain slice was examined under a dissection microscope. The stained slices then were transferred into 10% formaldehyde solution for fixation. Images of the brain sections were captured.

Isolation of mononuclear cells

The bone marrow cells were collected by flushing out the aspirates from the tibiae and femur of the mouse with the help of low serum-containing medium using 26G needles. RBCs were lysed using RBC lysis buffer, following which these cells were subjected to density gradient isolation of mononuclear cells. An isolation phase of mononuclear cells requires several manipulation and centrifugation phases of bone marrow aspirates [8]. One millilitre of Ficoll solution was placed in a

RIGHTSLINK

15 millilitre centrifuge tube and the bone marrow cells were layered on it carefully and centrifuged at 1800 rpm for 30 minutes in order to isolate low density mononuclear cells. Mononuclear cells were transferred and washed twice with culture medium at 3500 rpm for 10 minutes. The cells were then suspended in 500 microlitres of PBS for further use. Trypan blue dye was used to confirm the viability of transplanted cells which were counted using an haemocytometer. Flow cytometric analysis of mononuclear cells was performed to examine the purity and the presence of the mononuclear cell population before transplantation.

Transplantation

For transplantation, CFDA-labelled mononuclear cells were used to track the transplanted cells in the brain. The mononuclear cells were suspended in phosphate buffered saline (PBS) containing CFDA solution and incubated at 37°C for 15 minutes, accompanied with mild shaking. After 15 minutes, the cells were pelleted at 2000 rpm at 4°C and, subsequently, suspended in pre-warmed PBS at 37°C for 30 minutes. Cells were then washed with PBS at 2000 rpm at 4°C before transplantation. Approximately 2×10^5 to 5×10^5 labelled cells in 500 microlitres total fluid volume were injected with a 26G needle into a tail vein after 24 hours of MCAo.

Immunohistochemical analysis

The mice were sacrificed after 2 and 7 days of transplantation. The brains were removed and cryosectioned at a thickness of 8–10 micrometres. The sections were mounted on poly-L-lysine coated slides and then fixed in Histochoice for 10–15 minutes. The coronal sections were examined under fluorescence microscopy.

Brain Inj Downloaded from informahealthcare.com by University of California Irvine on 10/30/14
For personal use only.

Results

Establishment of model: Behavioural analysis

In the present study, after creating the transient ischemia through middle cerebral artery occlusion, the behavioural analysis of contra-lateral turning confirmed the lesion was performed. The intraluminal thread method of ischemia in mice did not produce subarachnoid haemorrhage and seizures.

Histological analysis

The coronal brain sections of MCA-occluded animals showed a consistent pattern of ischemic damage, which was characterized by reduced or absence of TTC stain (Figure 1), whereas the sham-operated animals were devoid of ischemia. Significant correlation between infarction size and neurological deficit was observed.

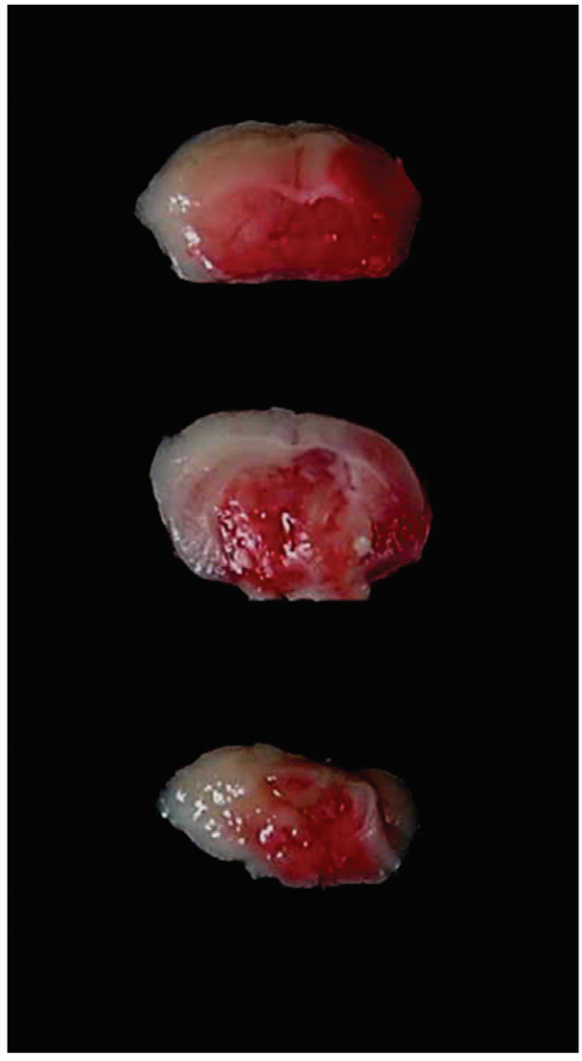


Figure 1. The images of TTC stained coronal sections of brain showing infarction after 60 minutes of occlusion and 23 hours of reperfusion. The white portion represents the ischemic injury in MCAO mice.

MNCs home to infarcted region

The pure population of mononuclear cells were confirmed by FACS analysis (Figure 2). The mononuclear cells equivalent to the 200–400 forward scatter correlates to the cell volume and 200–400 side scatter corresponding to the complexity of the molecule. The CFDA-labelled mononuclear cells were observed in the infarcted regions along the line of cortex after a period of 2 days (Figures 3(*a*) and (*b*)) and 7 days (Figures 3(*c*) and (*d*)) corresponding to acute and sub-acute phase. This is an index to determine the short-term fate

RIGHTSLINK

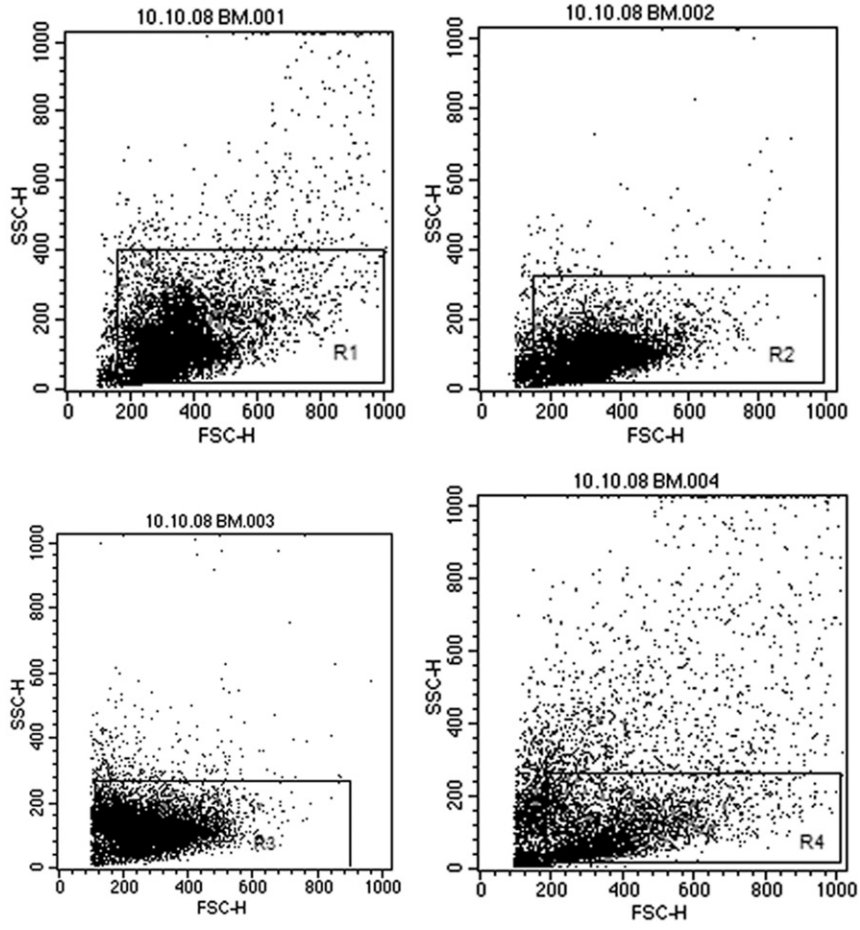


Figure 2. FACS analysis corroborated the purity and presence of mononuclear cells derived from mouse bone marrow.

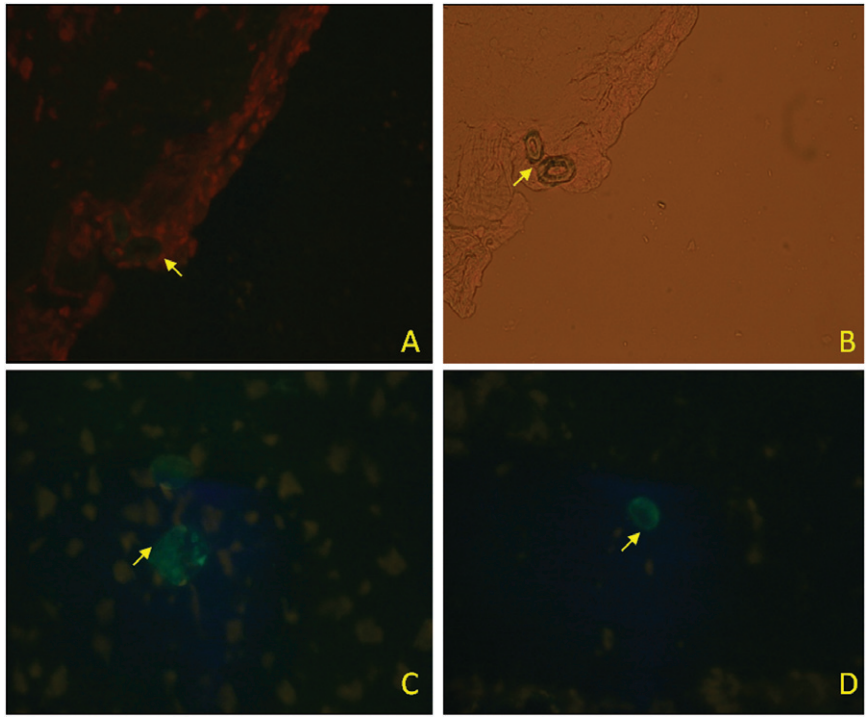


Figure 3. CFDA-labelled cells were detected in the coronal brain sections under fluorescence microscopy after 2 (*a* and *b*) and 7 (*c* and *d*) days of transplantation.

Brain Inj Downloaded from informahealthcare.com by University of California Irvine on 10/30/14
For personal use only.

of mononuclear cells, proving the homing behaviour of mononuclear cells to the ischemic site.

Discussion

Although various sources of stem cells have been discussed recently in the current literature for neural therapy and repair, yet mononuclear cells are the most attractive type that have been used and led to several clinical trials for neurodegenerative diseases which have been initiated in this country. Techniques for inducing transient MCAo by an intraluminal thread method have been extensively used in experimental models of ischemic stroke since it induces relatively bigger and reproducible infarct volumes. A reliable focal stroke model of transient regional ischemia in rats reported in the literature [6] was less invasive than conventional methods. Several variations and applications of this technique have been reported in order to refine and validate this technique. The aim of the present study was to establish a transient MCAo model in mice and to evaluate the efficacy of homing of MNCs to the ischemic site in the acute phase of the experimental stroke mouse model. The advantages of this model are its reproducibility and ease of reperfusion. However, it is sometimes difficult to detect neurological deficits after cerebral ischemia in rodents [9]. In the present study, mice showed contra-lateral turning behaviour, immediately after surgery, which was considered as a marker of behavioural deficit and was distinctly correlated with infarction evaluated later. In contrast, previous reports have analysed the correlation between the severity of behavioural deficits and histological findings. Various tests to monitor the behaviour include average forelimb and hind limb placing scores, asymmetric limb use for wall movement, Morris water-maze test and probe trial performance and infarct volume measurement. It was found that the infarct size significantly correlated with only two behavioural measures (forelimb placing performance correlated with subcortical infarct volume) while performance on the water-maze test also correlated with subcortical infarct volume [10]. Hence, further investigations will reveal the importance of behavioural deficit in bringing infarct volume changes in experimental stroke.

This study confirmed the infarcted site with the staining of TTC, an oxidation-reduction indicator. Therefore, the tissue with normal levels of the enzyme is stained red, whereas ischemic and infarcted tissue remains unstained owing to loss of the enzyme [11]. The present study demonstrates the homing behaviour of bone marrow-derived mononuclear cells caused by successful trafficking through the BBB which may have been driven by chemotaxis. The detailed molecular mechanism needs further investigation. This study shows that intravenous infusion of bone marrow-derived mononuclear cells, 24 hours after transient MCAo in mice, results in accumulation of CFDA-labelled cells in the infarcted region of the brain. This illustrates that mononuclear cells are not only able to cross the blood–brain barrier but also survive there for up to a week. The mechanism of homing and cell cycle kinetics has been investigated [12] and molecular imaging of bone marrow mononuclear cell homing in ischemic myocardium has been analysed [13].

The data presented here has some limitations, like absence of MCAo validation by laser Doppler flow meter coupled with a limited choice of time points analysed for study. However, this study was still able to demonstrate that bone marrow MNCs can successfully migrate to the infarcted area across the blood–brain barrier in mice.

Conclusion

Since there is a sudden increase in MNC-based clinical trials, a dose-dependent investigation along with side-to-side comparison of various routes of delivery is warranted. As the majority of the studies have been done in rats, this is a rare study conducted in mice which is important because extrapolation of data is easy with the availability of several mice knock outs. This study establishes the proof that MNCs can indeed cross the mice BBB and reach the infarcted area at early time points. Further studies can investigate the biology of MNCs in neuronal repair with analysis of behavioural outcomes at other time points using additional validation tools including laser doppler.

Acknowledgement

This study was supported by the Department of Biotechnology (DBT), New Delhi, India.

Declaration of interest: The authors report no conflicts of interest. The authors alone are responsible for the content and writing of the paper.

References

1. Feuerstein GZ, Wang X. Animal models of stroke. Molecular Medicine Today 2000;6:133–135.
2. Durukan A, Tatlisumak T. Acute ischaemic stroke: Overview of major experimental rodent models, pathophysiology, and therapy of focal cerebral ischaemia. Pharmacology, Biochemistry and Behavior 2007;87:179–197.
3. Banerjee TK, Das SK. Epidemiology of stroke in India. Neurology Asia 2006;11:1–4.

Brain Inj Downloaded from informahealthcare.com by University of California Irvine on 10/30/14
For personal use only.

RIGHTSLINK

4. Bosco MC, Puppo M, Blengio F, Fraone T, Cappello P, Giovarelli M, Varesio L. Monocytes and dendritic cells in a hypoxic environment: Spotlights on chemotaxis and migration. Immunobiology 2008;213:733–749.
5. Ribeiro-Resende VT, Pimentel-Coelho PM, Mesentier-Louro LA, Mendez RM, Mello-Silva JP, Cabral-da-Silva MC, de Mello FG, de Melo Reis RA, Mendez-Otero R. Trophic activity derived from bone marrow mononuclear cells increases peripheral nerve regeneration by acting on both neuronal and glial cell populations. Neuroscience 2009;2:540–549.
6. Zea Longa E, Wenstein PR, Carlson S, Cummins R. Reversible middle cerebral artery occlusion without craniectomy in rats. Stroke 1989;20:84–91.
7. Shah ZA, Khodadad N, Judy K, Kathy K, Sylvain D. Use of an optimized transient occlusion of the middle cerebral artery protocol of the mouse stroke model. Journal of Stroke and Cerebrovascular Diseases 2006;15:133–138.
8. Kawasaki Oyama RS, Braile DM, Caldas HC, Leal JC, Goloni-Bertollo EM, Pavarino-Bertelli EC, Abbud Filho M, Santos ID. Blood mesenchymal stem cell culture from the umbilical cord with and without Ficoll-paque density gradient method. Revista Brasileira de Cirurgia Cardiovascular 2008;23:29–34.
9. Belayev L, Khoutorova L, Zhao W, Vigdorchik A, Belayev A, Busto R, Magal E, Ginsberg MD. Neuroprotective effect of darbepoetin alfa, a novel recombinant erythropoietic protein, in focal cerebral ischaemia in rats. Stroke 2005;36: 1065–1070.
10. Robin LR, Gerald PS, Ren X, Edward DH. A comparison of long-term functional outcome after 2 middle cerebral artery occlusion models in rats. Stroke 2001;32: 2648–2657.
11. Kazuo Isayama MD, Lawrence H, Pitts MD, Merry C, Nishimura BS. Evaluation of 2,3,5-triphenyltetrazolium chloride staining to delineate rat brain infarcts. Stroke 1991;2:1394–1398.
12. Srour EF, Jetmore A, Wolber FM, Plett PA, Abonour R, Yoder MC, Orschell-Tratcoff CM. Homing, cell cycle kinetics and fate of transplanted hematopoietic stem cells. Leukemia 2001;15: 1681–1684.
13. Sheikh AY, Lin SA, Cao F, van der Bogt KE, Chu P, Chang CP, Contag CH, Robbins RC, Wu JC. Molecular imaging of bone marrow mononuclear cell homing and engraftment in ischaemic myocardium. Stem Cells 2007;25: 2677–2684.

Brain Inj Downloaded from informahealthcare.com by University of California Irvine on 10/30/14
For personal use only.

Pharmacology, Biochemistry and Behavior 97 (2010) 192–197

Contents lists available at ScienceDirect

Pharmacology, Biochemistry and Behavior

journal homepage: www.elsevier.com/locate/pharmbiochembeh

Neuroprotective effect of *Bacopa monniera* on ischemia induced brain injury

Manish Kumar Saraf [a,b,1], Sudesh Prabhakar [a,1], Akshay Anand [a,*]

[a] Department of Neurology, Post Graduate Institute of Medical Education and Research, Sector-12, Chandigarh, 160012, India
[b] University of Texas Medical Branch, Galveston, TX 77555, USA

ARTICLE INFO

Article history:
Received 30 March 2010
Received in revised form 4 June 2010
Accepted 25 July 2010
Available online 1 August 2010

Keywords:
Bacopa monniera
Brain ischemia
Neuroprotection
Oxidative stress

ABSTRACT

Purpose: Brain stroke is a leading cause of death without effective treatment. *B. monniera*, an Indian herbal medicine, exerts antioxidant activity and antistress activity by modulating the antioxidative defence system. We wanted to test if *B. monniera* could alleviate the ischemia induced brain injury and cognitive dysfunction in Wistar rats.
Procedure: We studied the effect of *B. monniera* (120 mg kg^{-1}, 160 mg kg^{-1} and 240 mg kg^{-1} P.O.) on transient intracarotid artery (ICA) occlusion induced ischemia by testing the neurobehavioral and biochemical parameters on treated and control rats.
Findings: B. monniera attenuated the reduced transfer latency in ischemic rats in a step through test and showed a protective effect on ischemia induced memory impairment in the plus maze task. It also showed a marginal improvement in neurodeficit score and fore limb muscle grip strength. *B. monniera* reduced the infarct size in the ischemic brain. It also decreased nitrite, nitrate and lipid peroxidation and significantly improved catalase activity.
Conclusion: These observations suggest the neuroprotective and antioxidant activity of *B. monniera* on ischemia induced brain injury and pave the way for future investigations.
© 2010 Elsevier Inc. All rights reserved.

1. Introduction

Stroke is one of the leading causes of death worldwide (Rensink et al., 2009). World Health Organization (WHO) data reflects 5.7 million deaths from cerebrovascular diseases out of 58 million global deaths in 2005. The number of people with transient ischemic attack (TIA) is estimated to be even greater. There are studies which indicate that the incidence of second stroke is higher in survivors of TIA (Sacco et al., 2006). Brain stroke is a sudden loss of brain function usually caused by a blockade or leakage of a blood vessel. It develops from a complex cascade of cellular events that ultimately leads to cerebral infarction (Hou and MacManus, 2002) and causes sudden loss of vision, balance, coordination, speech and memory (O'Brien et al., 2003). Severe strokes may also lead to sudden death.

Reactive oxygen species (ROS) are formed during cerebral ischemia due to calcium overload-induced inhibition of mitochondrial electron transport chain and activation of phospholipase A2 (Moskowitz et al., 1984). Reperfusion of the ischemic brain may further aggravate neuronal injury by increasing free radical formation (del Zoppo and Hallenbeck, 2000). Moreover, free radicals may also promote lipid peroxidation (Kumar and Gupta, 2002) which ultimately alters the integrity of the plasma membrane. ROS such as peroxynitrite (Epe et al., 1996) and hydroxyl radical (Delaney et al., 1997) are reported to produce DNA nicking. ROS are also documented to activate lysosomal enzymes, which may contribute to neuronal injury (Ollinger and Brunk, 1995). Additionally, mitochondrial damages due to ROS release may contribute to delayed cell death after cerebral ischemia and reperfusion (Fiskum, 2000).

Bacopa monniera, an Indian herbal drug (Syn. Brahmi) displays antioxidant (Tripathi et al., 1996), antistress (Chowdhuri et al., 2002) and anxiolytic (Shanker and Singh, 2000; Singh and Singh, 1980) activities. It has also been shown to exert antioxidant effects through chelating of metal ions, breaking oxidative chain reaction (Tripathi et al., 1996), improving activities of antioxidative defence enzymes (Bhattacharya et al., 2000a) and scavenging of free radicals (Russo et al., 2003). It exhibits an antistress activity in rat by modulating the activities of Hsp70, P450 and SOD (Chowdhuri et al., 2002), repairing the damaged neurons by enhanced kinase activity, neuronal synthesis coupled with restoration of synaptic activity and nerve impulse transmission (Kishore and Singh, 2005; Singh and Dhawan, 1997), which could be partly responsible for its cognition facilitation activity. The memory enhancing effects have been attributed to the active constituent bacosides A (Chatterji et al., 1965) and B (Dhawan and Singh, 2002). This facilitates the effect on retention capacity in avoidance response in rats (Singh et al., 1988) and ability to reverse amnesic effects of neurotoxin, scopolamine and electric shock (Bhattacharya et al., 2000b).

Therapeutic agents such as tissue plasminogen activator, antioxidants, and glutamate receptor blockers show limited efficacy in

* Corresponding author. Tel.: +91 172 2756094; fax: +91 172 2748399.
E-mail address: akshay1anand@rediffmail.com (A. Anand).
URL: http://www.neurologypgi.org (A. Anand).
[1] These authors contributed equally.

0091-3057/$ – see front matter © 2010 Elsevier Inc. All rights reserved.
doi:10.1016/j.pbb.2010.07.017

stroke and therefore a number of studies have been initiated for the improvement of therapeutic strategies of brain stroke. Several herbal drugs have also shown a promising neuroprotective effect in rodents (Chen et al., 2003; Kim et al., 2008; Lee et al., 2003; Sun et al., 2008; Tian et al., 2008; Zhou et al., 2009). There are some herbal drugs which have shown a dual role of exerting antiamnesic and neuroprotective effects (Kim et al., 2008; Lin et al., 2005; Siripurapu et al., 2005; Wang et al., 2005, 2008; Yun et al., 2007). *B. monniera* is also reported to provide neuroprotection against cigarette smoke induced apoptosis (Anbarasi et al., 2005a,b,c, 2006a,b) and aluminium induced oxidative stress (Jyoti et al., 2007). In addition, our own earlier investigations have revealed antiamnesic effects of *B. monniera* using several amnesic agents. Therefore, in this study we wanted to expand our investigation with this drug and explore its effect on ischemia induced brain injury by studying its association with behavioral parameters.

2. Materials and methods

2.1. Materials and subjects

Male Wistar rats weighing 200–250 g were used in the present study. They were housed individually with *ad labium* access to food and water under controlled laboratory conditions and were exposed to a 12 h cycle of light and dark. The experiments were conducted in a semi-sound proof laboratory. The dried powder of *B. monniera* (Brahmi) standardized extract, containing 55.34% of bacosides, was obtained from Lumen Marketing Company, Chennai. The suspension of *B. monniera* extract was prepared in 5% w/v Tween 80. Sodium selenite was prepared in normal saline.

2.2. Transient global ischemia

All experiments were performed in accordance with the guidelines of the institute animal ethical committee. Adequate measures were taken to minimize pain or discomfort with animal experimental procedures. Rat was anaesthetized with ketamine (50 mg/ml) and xylazine (50 mg/ml) cocktail (9:1) injected intra-peritoneally combined with analgesic (diclofenac sodium). A small cut was made on the neck region and the neck muscle was retracted for isolation of the common carotid artery. The internal carotid artery was subsequently isolated. 30 min of ischemia was given to the rat by blocking the internal carotid artery with a micro-vascular clip. After the ischemic period, the neck muscle was tied and an antibiotic was applied. The test drug solution or suspension was administered to the respective group of rats described below for a period of seven days. Group 1 (sham) rats were injected with vehicle (5% Tween 80 10 ml kg^{-1} orally). The ischemia was produced in groups 2 to 6. After the induction of 30 min ischemia, group 2 rats were administered with vehicle (5% Tween 80 10 ml kg^{-1} orally for 8 days). Sodium selenite (2 mg kg^{-1} i.p.) was injected in group 3. *B. monniea* at 120 mg kg^{-1}, 160 mg kg^{-1} and 240 mg kg^{-1} was administered orally for 8 days to ischemic rats of groups 4 to 6 respectively. 7 additional days of post ischemic survival time was provided. On the 7th and 8th days behavioral studies were carried out. Rats were sacrificed by an overdose of anesthesia on the 8th day after completion of behavioral tests. The isolated brains were frozen for TTC staining and biochemical tests.

2.3. Neurobehavioral test

2.3.1. Neurodeficit score

The neurological status of the animals was evaluated using the methods described by Bederson et al. (1986). Accordingly, four categories of neurological findings were noted: 0 = no observed neurological deficit; 1 = contralateral forelimb flexion with wrist flexion and shoulder adduction; 2 = reduced resistance to lateral push; and 3 = circling movements towards the ipsilateral side.

2.3.1.1. Rota rod test. Sensorimotor performance was evaluated using a rota rod test. All animals were tested for their ability to remain on the rotating bar at a speed of 14 rpm. Each animal was provided a minimum of three trials. After 8 post ischemic days the animals were tested for motor impairment after administration of test drugs. Latency to fall off the rotating rod was noted for each trial with a 5 min maximum to termination of the trials.

2.3.2. Hanging wire

The experimental animals were suspended by its forelimbs on a wire stretched between 2 posts, 45 cm above a foam sheet. The time (in seconds), until the animal fell down, was recorded. 2 min of cut off time was designated. This task was used as a measure of grasping ability and forelimb strength.

2.3.3. Pole fall

The rat was placed in a pole of 1 inch diameter 45 cm above a foam sheet. The time (in seconds) until the animal fell down was recorded. A maximum of 2 min was designated as cut off time. This task was used as a measure of grasping ability and forelimb strength.

2.4. Memory test

2.4.1. Elevated plus maze

Plus maze for rat consists of a central platform connected to two open arms and two enclosed arms. The maze is elevated to a height of 50 cm from the floor. During training trials the animal was placed at the end of an open arm, facing away from the central platform of the maze. The time taken by the animal to move from open arm and cross the line marked in enclosed arm with all four paws was recorded as transfer latency time (TL). In case the rats did not enter the enclosed arm within 90 s, it was gently pushed into the enclosed arm and a TL of 90 s was assigned to it. The animal was allowed to remain in the maze for the duration of 10 s. The TL measured on the plus maze on the first day serves as an index of acquisition, whereas the TL measured after 24 h of acquisition trial was taken as an index of retrieval.

2.4.2. Passive avoidance paradigm

The tendency of rodents to avoid bright light and prefer a darker side is the principle of this technique. The test apparatus consists of a small illuminated chamber connected to a large dark chamber via a door. The latency time to enter the dark compartment from the light compartment within 180 s was noted as an index of acquisition. Once the animal enters into the dark chamber, a brief electric foot shock was delivered. After 2 and 24 h the retention test was performed and the time taken by the animal to enter the dark compartment from the illuminated compartment was noted. Prolongation of this step through latency time indicated acquisition and retrieval of the memory for the foot shock received by the animal.

2.5. Cerebral infarct size

Frozen brain was sectioned into uniform slices of about 2 mm thickness. The slices were incubated in 2% TTC (triphenyl tetrazolium chloride) solution at 37 °C in a PBS buffer for 10 min. The slices were preserved in 10% normal formal saline solution. The slices were arranged in a glass plate in a row and the images were captured. We used software Image J (Version 3.00, University of Texas Health Science Center, San Antonio) for measurement of the area of infarction (yellow area) and the total area of the section (pink area + yellow area). The percentage of the area of infarction was calculated as [(yellow area/total area) × 100].

2.6. Biochemical investigation

We used 8 rats per group for behavioral tests. After completion of the behavioral test, the brain was isolated. At least 3 brains per group were used for histological studies and the remaining 5 brains were used for biochemical tests. We did not pool the brain for biochemical tests. The small amount of a homogenized sample of the individual brain was aliquoted in various tubes and used for various biochemical tests.

2.6.1. Nitric oxide estimation

The brain was analyzed for nitric oxide, SOD, GPx, catalase and lipid peroxidase assay. Nitric oxide was estimated by an indirect measurement of nitrite, nitrate and total nitrite in rat brain extract supernatants obtained after centrifugation. Cadmium beads were added to the supernatant for total nitrite estimation and incubated overnight. The clear supernatant was treated with a mixture of coloring reagents I (1% sulfanilamide in 3 N HCl) and II (0.1% NED·2 HCl) and incubated for 10 min at room temperature. The absorbance was noted at 620 nm and 550 nm respectively. The nitrite and total nitrite level were normalized to the total protein estimated by Bradford method.

2.6.2. SOD estimation

SOD level was measured by superoxide dismutase estimation kit (Sigma, USA) in brain homogenates. The protocol was adapted to kit instructions and was normalized by total protein. Total protein was estimated by Bradford method.

2.6.3. GPx estimation

The GPx level was measured by glutathioperoxidase estimation kit (Sigma) in brain homogenates. The standard protocol as described in the kit was followed. The GPx level was estimated, which was normalized by total protein. The total protein was estimated by Bradford method.

2.6.4. Lipid peroxidase estimation

The lipid peroxidation in the homogenate was determined by the method of Wills (1966). The tissue homogenate with 0.1 M of Tris–HCl buffer was incubated at 37 °C for 2 h. After incubation 10% w/v ice cold TCA was added. The reaction mixture was centrifuged at 8000 *g* for 10 min. 0.67% TBA was added to the supernatant and the tubes were kept in a boiling water bath for 10 min till the pink color appeared. The absorbance was measured at 550 nm and the amount of malondialdehyde content was calculated using the molar extinction coefficient of MDA-TBA chromophore ($1.56\times10^5\ M^{-1}\ cm^{-1}$). The results were expressed as nmol of MDA/mg protein.

2.6.5. Catalase estimation

Catalase activity was assayed in the postmitochondrial supernatant by the method of Luck (1971). An appropriate amount of sample was added to the cuvette containing hydrogen peroxide phosphate buffer. The contents were mixed thoroughly. The decrease in absorbance was followed at 240 nm for 3 min at a 30 s interval. The activity of enzyme was expressed as μmol of H_2O_2 decomposed/min/mg protein, using the molar extinction coefficient of H_2O_2 ($0.71\ M^{-1}\ cm^{-1}$).

2.7. Statistical analysis

Behavioral data was analyzed by ANOVA followed by post hoc 'least significant difference' (LSD). '*' indicates a significant difference for treated group vs control group at $p<0.05$. '$' indicates a significant difference for treated group vs ischemic group at $p<0.05$. Biochemical data were analyzed by ANOVA followed by least significant difference (LSD). 'a' indicates a significant difference for treated group vs control group at $p<0.05$. 'b' indicates a significant difference for treated group vs ischemic group at $p<0.05$.

3. Results

The rat model of ischemia was established by temporary blocking of the internal carotid artery for 10 min, 30 min, 60 min and 120 min and assessing the cognitive and neurological status (data not shown). We then chose to extend our investigations with 30 min ischemia as the investigative measure as it creates infarction and cognitive impairment without severe paralytic symptoms.

3.1. B. monniera attenuates ischemia induced memory deficits

We tested the effect of different doses of *B. monniera* at 120 mg, 160 mg and 240 mg kg^{-1} orally and sodium selenite 2 mg kg^{-1} intraperitoneally for 8 days in ischemic rats. There was a reduction in the transfer latency in ischemic animals using a step through test which was attenuated by *B. monniera* and sodium selenite treatment (Fig. 1A). In the plus maze task, *B. monniera* showed more protective effects as compared to sodium selenite on ischemia induced impairment in the retrieval of memory (Fig. 1B).

3.2. B. monniera improved neurological score and reduced infarct size in ischemic rat

Neurobehavioral tests such as neurodeficit scoring, pole fall and hanging wire results showed impairment in neurobehavioral scale using ischemic rats (Table 1). Some of the neurobehavioral outcomes (such as neurodeficit score and fore limb muscle grip strength) of these rats showed a moderate improvement by *B. monniera* treatment while muscle grip strength measured by pole fall remained unaffected in the *B. monniera* treated group. We also observed that *B. monniera* and sodium selenite reduced the infarct size measured by TTC staining of frozen brain section of the rat (Fig. 2A).

3.3. B. monniera exerts antioxidant effect in ischemic rat

The total nitrite was elevated in ischemic rats. Sodium selenium treatment and *B. monniera* treatment reduced the enhanced total nitrite in ischemic rat as compared to untreated ischemic rat (Fig. 2B). Similar to sodium selenite, *B. monniera* also reduced the lipid peroxidation in ischemic rat as compared to untreated ischemic rats (Fig. 2C). The catalase activity was significantly enhanced in selenite and *B. monniera* (240 mg kg^{-1} orally) co-treated rats while the lower dose of *B. monniera* (120 mg kg^{-1} and 160 mg kg^{-1} orally) did not affect the catalase activity as compared to controls (Fig. 2D). The superoxide dismutase activity was unaffected in treated and untreated ischemic rats (Fig. 2E). *B. monniera* gradually improved the glutathione activity though the GPx activity was not significantly affected in ischemic rat (Fig. 2F).

4. Discussion

B. monniera (Brahmi) is a popular drug prescribed by the Indian alternative medicine system practitioners in India since time immemorial. The exact mechanism of action of *B. monniera* could be attributed to a combination of cholinergic modulation (Das et al., 2002; Kishore and Singh, 2005) and antioxidant effects (Bhattacharya et al., 2000a). In the absence of tangible results with the single molecule approach, herbal extracts comprising several molecules are being tested for neuroprotective and therapeutic effects. The neuroprotective effect of three oral doses of *B. monniera* namely, 120 mg kg^{-1}, 160 mg kg^{-1} and 240 mg kg^{-1} was tested in ischemic rats including sodium selenite as reference. In this study, we report that all doses of *B. monniera* (120 mg kg^{-1}, 160 mg kg^{-1} and 240 mg kg^{-1} orally) reversed the ischemia induced memory impairment in the plus maze and passive avoidance tasks better than that of sodium selenite. This finding is supported by our previous studies where *B. monniera* reversed L-NNA (Saraf et al., 2009), scopolamine

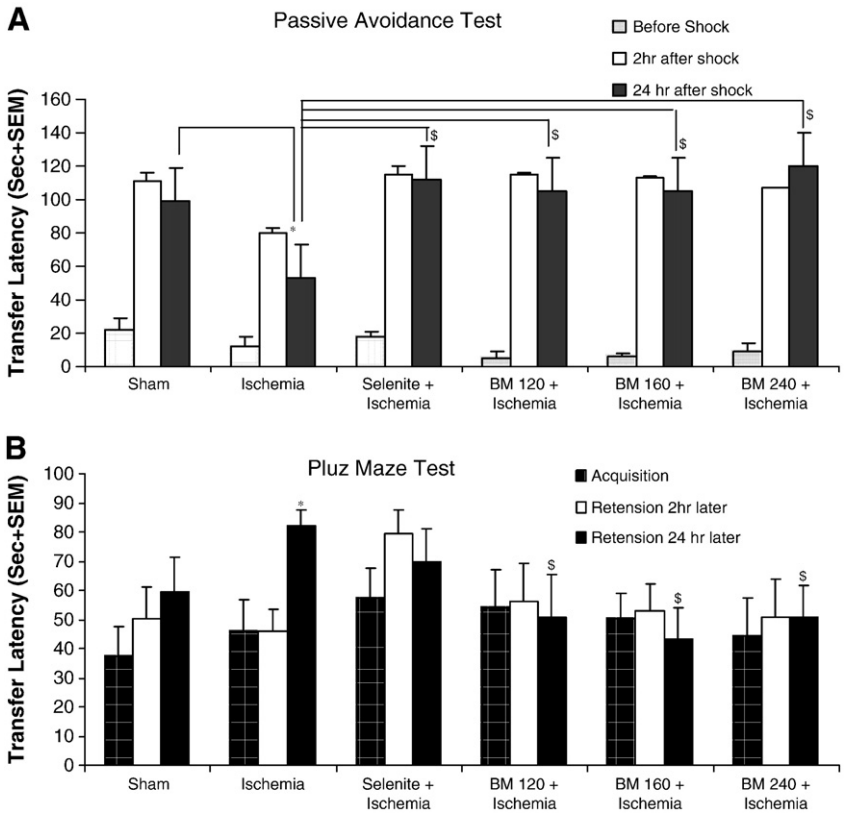


Fig. 1. *B. monniera* attenuates ischemia induced memory deficit. (A) *B. monniera* (120 mg kg^{-1}, 160 mg kg^{-1} and 240 mg kg^{-1} orally) and sodium selenite significantly reverse the reduction in transfer latency as compared to ischemic rats noted after 24 h of delivery of electric shock in passive avoidance test. Transfer latency was not significantly different in treated rat and ischemic rats as compared to control rat before and 2 h after delivery of foot shock. (B) *B. monniera* (120 mg kg^{-1}, 160 mg kg^{-1} and 240 mg kg^{-1} orally), but not sodium selenite, significantly attenuates the impairment in retention as compared to ischemic rat measured 24 h later in the plus maze test. The acquisition and retention 2 h later were unaffected in ischemic and treated rats as compared to control rats. Data were analyzed by ANOVA followed by post hoc 'least significant difference' (LSD). '*' indicates a significant difference for treated group vs control group at $p<0.05$. '$' indicates a significant difference for treated group vs ischemic group at $p<0.05$.

(Saraf et al., 2007) and diazepam induced acquisition and retrieval of memory (Prabhakar et al., 2008). It is reported to improve the performance of rats in various learning situations (Singh and Dhawan, 1982). *B. monniera* extract also reverses Y-maze performance and open field hyperlocomotion behavioral changes and reduces the level of amyloid especially Abeta 1-40 and 1-42 (Holcomb et al., 2006). It provides protection from phenytoin (an antiepileptic drug) induced deficit in cognitive function of mice by similar behavioral tasks (Vohora et al., 2000) lending versatility to its mechanism of action.

In this study, *B. monniera* reduced the infarct size similar to sodium selenite thereby validating the neuroprotective effects of this drug. Moreover, we also found improvement in the neurological scores such as neurodeficit score and fore limb muscle grip strength when *B. monniera* was administered. These observations clearly suggest a protective effect of *B. monniera.* In the previous study *B. monniera* has been documented to provide neuroprotection against cigarette smoke induced apoptosis (Anbarasi et al., 2005a,b,c, 2006a,b) and aluminium induced oxidative stress (Jyoti et al., 2007). Several other herbal drugs have also shown the promising neuroprotective effect in rodents (Chen et al., 2003; Kim et al., 2008; Lee et al., 2003; Sun et al., 2008; Tian et al., 2008; Zhou et al., 2009). Some of those have shown both antiamnesic effects and neuroprotective effects (Kim et al., 2008; Lin et al., 2005; Siripurapu et al., 2005; Wang et al., 2005; Wang et al., 2008; Yun et al., 2007).

The biochemical investigations of the current study have revealed that *B. monniera* reduces the total nitrite and lipid peroxidation, which suggests that *B. monniera* may reduce the formation of a free radical. We also noticed that it enhanced catalase enzyme activity along with mild improvement in glutathione peroxidase activity, although such improvement in glutathione peroxidase activity was not significant. On the other hand, Chowdhuri et al. (2002) reported that the bacoside of *B. monniera* (BBM) attenuates the stress induced suppression of hsp70 expression only in the hippocampus and the cerebral cortex while the cerebellum and the rest of the brain remain unaffected. Moreover the alteration in SOD activity is not homogenous in the

Table 1
B. monniera improves the neurobehavioral outcome in ischemic rats. Neurobehavioral tests such as neurodeficit scoring, pole fall and hanging wire results in impairment of neurobehavioral deficit in ischemic rat. Some of the neurobehavioral outcomes (such as neurodeficit score and fore limb muscle grip strength) showed moderate improvement by *B. monniera* treatment while muscle grip strength measured by pole fall remained unaffected in *B. monniera* treated group.

Group no.	Group name	Neurodeficit mean score	Hanging wire (mean fall time in seconds)	Pole fall (mean fall time in seconds)	Rota rod (mean fall time in seconds)
1	Sham (control)	0	84.23 ± 14.66	31.38 ± 12.6	2.74 ± 0.12
2	Ischemia	3	44.57 ± 18.29	14.92 ± 10.2	1.9 ± 0.047
3	Selenite + ischemia	1	60.78 ± 4.37	31.43 ± 7.46	2.0 ± 0.072
4	BM 120 + ischemia	1.48	78.12 ± 15.62	20.12 ± 9.77	1.38 ± 0.042
5	BM 160 + ischemia	1.71	78.78 ± 9.3	21.85 ± 10.3	1.78 ± 0.069
6	BM 240 + ischemia	1.25	51.23 ± 16.7	21.4 ± 14.2	2.0 ± 0.039

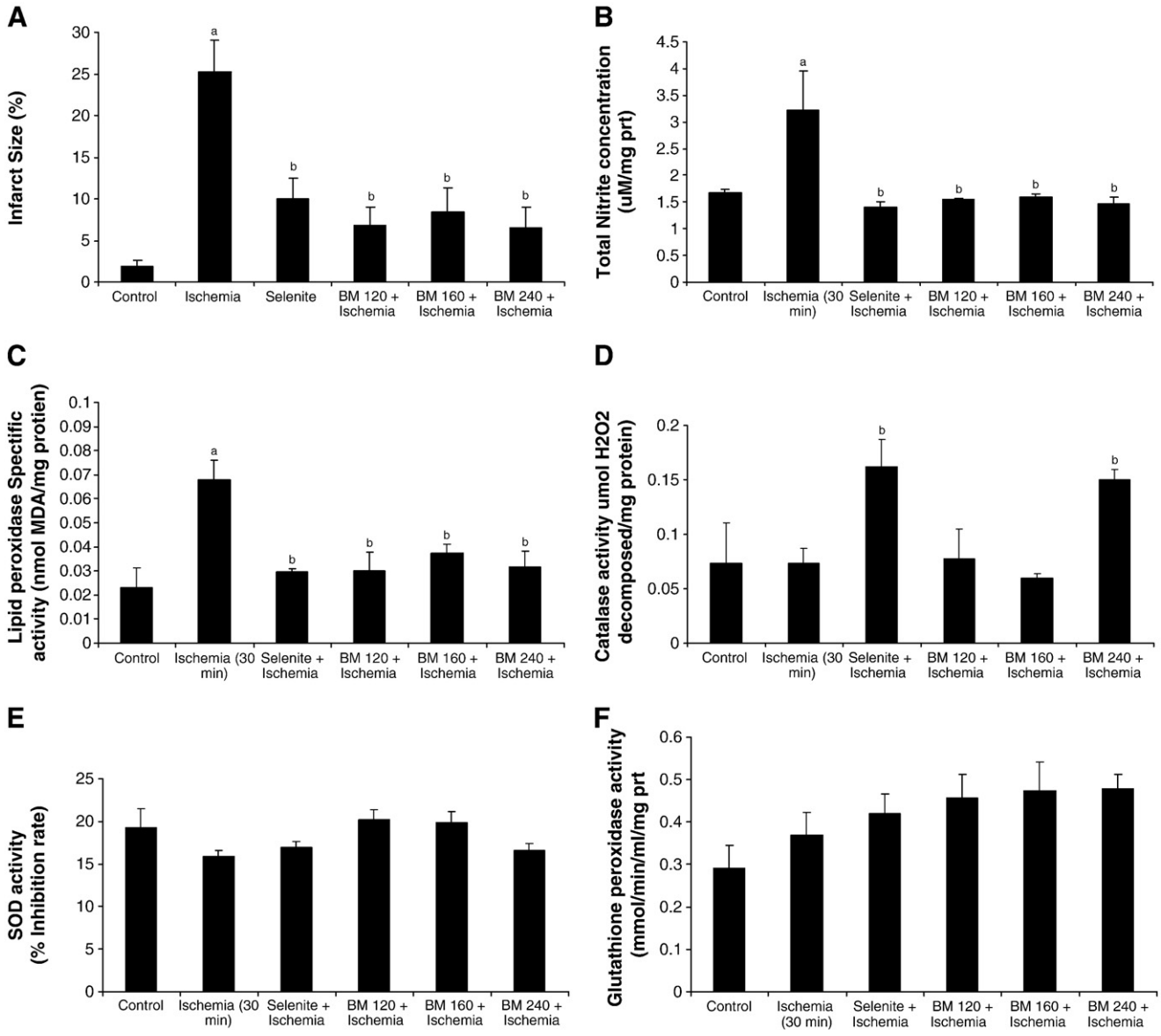


Fig. 2. *B. monniera* attenuates ischemia induced infarction by suppressing molecules involved in oxidative stress. (A) Histogram of size of infarction in control and treated ischemic rats. (B) *B. monniera* and sodium selenite reduced the enhanced total nitrite in ischemic rat as compared to untreated ischemic rat. (C) Similar to sodium selenium, *B. monniera* also reduced the lipid peroxidation in ischemic rat as compared to non-treated ischemic rat. (D) The catalase activity was significantly enhanced in selenite and *B. monniera* (240 mg kg^{-1} orally) treated rats while the lower dose of *B. monniera* (120 mg kg^{-1} and 160 mg kg^{-1} orally) did not affect the catalase activity as compared to control. (E) The superoxide dismutase activity was unaffected in treated and untreated ischemic rats. (F) *B. monniera* gradually improved the glutathione activity as compared to control, though the GPx activity was not significantly affected in ischemic rat. Data were analyzed by ANOVA followed by a least significant difference (LSD). 'a' indicates significant difference for treated group vs control group at $p<0.05$. 'b' indicates a significant difference for treated group vs ischemic group at $p<0.05$.

hippocampus, cortex, cerebellum and the rest of the brain. In this study, we measured the SOD activity in the whole brain rather than any specific part of the brain which explains, in some extent, the absence of change of SOD activity. Chowdhuri et al. (2002) also argued that BBM and stress, when imparted alone, increase the cytochrome P450 but when BBM is administered to the stressed animal it attenuates cytochrome P450 (Chowdhuri et al., 2002). These observations suggest that *B. monniera* may be involved in potentiating the antioxidative defence mechanisms by involving lipid peroxidase and catalase enzymes. This postulation is evidenced by several reports in which *B. monniera* attenuates the cigarette smoke induced neural injury and the cognitive deficit possibly by exhibiting free radical scavenging and anti-lipid peroxidative effects that protect the brain from oxidative damage. It is also known to augment vitamin C, vitamin E, and vitamin A and the activities of glutathione, superoxide dismutase, catalase, glutathione peroxidase and glutathione reductase (Anbarasi et al., 2006b). These investigations establish many leads for future investigations which may include P450, ROS and calcium estimations. Metal ions such as aluminium (Deloncle et al., 2002, 1990, 1995Deloncle and Guillard, 1990), zinc (Choi, 1996; Cuajungco and Lees, 1996; Kim et al., 1999; Koh and Choi, 1994), lead (Han et al., 2007; Nowak et al., 2008) and pollutant (Anbarasi et al., 2006a,c) are contributing factors of the oxidative mechanism that are potential targets which can be screened for mediation by *B. monniera.*

5. Conclusion

On the basis of our findings, we conclude that *B. monniera* attenuates the ischemia induced memory and other neurological deficits including infarct size by exerting antioxidant effects, however, additional investigation on P450, ROS, calcium etc. can uncover the mechanism. Further investigations with purified active constituents of

B. monniera may also validate its neuroprotective and antiamnesic effects. It also suggests that the pursuit of reductionist or single molecule approach should not be a paradigm barrier in clinical translation particularly if herbal extracts promise therapeutic solutions.

Acknowledgement

The work was partially supported by the Indian Council of Medical Education and Research, New Delhi, India (grant no. 45/4/2005/BMS/TRM).

References

Anbarasi K, Vani G, Balakrishna K, Devi CS. Creatine kinase isoenzyme patterns upon chronic exposure to cigarette smoke: protective effect of bacoside A. Vascul Pharmacol 2005a;42:57–61.

Anbarasi K, Vani G, Balakrishna K, Devi CS. Effect of bacoside A on membrane-bound ATPases in the brain of rats exposed to cigarette smoke. J Biochem Mol Toxicol 2005b;19:59–65.

Anbarasi K, Vani G, Devi CS. Protective effect of bacoside A on cigarette smoking-induced brain mitochondrial dysfunction in rats. J Environ Pathol Toxicol Oncol 2005c;24:225–34.

Anbarasi K, Kathirvel G, Vani G, Jayaraman G, Shyamala Devi CS. Cigarette smoking induces heat shock protein 70 kDa expression and apoptosis in rat brain: modulation by bacoside A. Neuroscience 2006a;138:1127–35.

Anbarasi K, Vani G, Balakrishna K, Devi CS. Effect of bacoside A on brain antioxidant status in cigarette smoke exposed rats. Life Sci 2006b;78:1378–84.

Bederson JB, Pitts LH, Tsuji M, Nishimura MC, Davis RL, Bartkowski H. Rat middle cerebral artery occlusion: evaluation of the model and development of a neurologic examination. Stroke 1986;17:472–6.

Bhattacharya SK, Bhattacharya A, Kumar A, Ghosal S. Antioxidant activity of *Bacopa monniera* in rat frontal cortex, striatum and hippocampus. Phytother Res 2000a;14:174–9.

Bhattacharya SK, Kumar A, Ghosal S. Effect of *Bacopa monniera* on animal models of Alzheimer's disease and perturbed central cholinergic markers of cognition in rats. In: Siva Sanka DV, editor. Molecular aspects of Asian medicines. New York: PJD Publication; 2000b.

Chatterji N, Rastogi RP, Dhar ML. Chemical examination of *Bacopa monniera* Wettst. Part II: the constitution of bacoside A. Ind. J. Chem. 1965;3:24–9.

Chen M, Wang Y, Liu Y, Hou XY, Zhang QG, Meng FJ, et al. Possible mechanisms underlying the protective effects of SY-21, an extract of a traditional Chinese herb, on transient brain ischemia/reperfusion-induced neuronal death in rat hippocampus. Brain Res 2003;989:180–6.

Choi DW. Zinc neurotoxicity may contribute to selective neuronal death following transient global cerebral ischemia. Cold Spring Harb Symp Quant Biol 1996;61:385–7.

Chowdhuri DK, Parmar D, Kakkar P, Shukla R, Seth PK, Srimal RC. Antistress effects of bacosides of *Bacopa monnieri:* modulation of Hsp70 expression, superoxide dismutase and cytochrome P450 activity in rat brain. Phytother Res 2002;16:639–45.

Cuajungco MP, Lees GJ. Prevention of zinc neurotoxicity in vivo by N, N, N′, N′-tetrakis (2-pyridylmethyl) ethylene-diamine (TPEN). NeuroReport 1996;7:1301–4.

Das A, Shanker G, Nath C, Pal R, Singh S, Singh H. A comparative study in rodents of standardized extracts of *Bacopa monniera* and *Ginkgo biloba*: anticholinesterase and cognitive enhancing activities. Pharmacol Biochem Behav 2002;73:893–900.

del Zoppo GJ, Hallenbeck JM. Advances in the vascular pathophysiology of ischemic stroke. Thromb Res 2000;98:73–81.

Delaney CA, Green IC, Lowe JE, Cunningham JM, Butler AR, Renton L, et al. Use of the comet assay to investigate possible interactions of nitric oxide and reactive oxygen species in the induction of DNA damage and inhibition of function in an insulin-secreting cell line. Mutat Res 1997;375:137–46.

Deloncle R, Guillard O. Mechanism of Alzheimer's disease: arguments for a neurotransmitter-aluminium complex implication. Neurochem Res 1990;15:1239–45.

Deloncle R, Guillard O, Clanet F, Courtois P, Piriou A. Aluminum transfer as glutamate complex through blood-brain barrier. Possible implication in dialysis encephalopathy. Biol Trace Elem Res 1990;25:39–45.

Deloncle R, Guillard O, Huguet F, Clanet F. Modification of the blood-brain barrier through chronic intoxication by aluminum glutamate. Possible role in the etiology of Alzheimer's disease. Biol Trace Elem Res 1995;47:227–33.

Deloncle R, Fauconneau B, Piriou A, Huguet F, Guillard O. Aluminum L-glutamate complex in rat brain cortex: in vivo prevention of aluminum deposit by magnesium D-aspartate. Brain Res 2002;946:247–52.

Dhawan BN, Singh HK. Nootropic and some other effects of *Bacopa monniera* Linn. (Brahmi). Ann Neurosci 2002;6:34–40.

Epe B, Ballmaier D, Roussyn I, Briviba K, Sies H. DNA damage by peroxynitrite characterized with DNA repair enzymes. Nucleic Acids Res 1996;24:4105–10.

Fiskum G. Mitochondrial participation in ischemic and traumatic neural cell death. J Neurotrauma 2000;17:843–55.

Han JM, Chang BJ, Li TZ, Choe NH, Quan FS, Jang BJ, et al. Protective effects of ascorbic acid against lead-induced apoptotic neurodegeneration in the developing rat hippocampus in vivo. Brain Res 2007;1185:68–74.

Holcomb LA, Dhanasekaran M, Hitt AR, Young KA, Riggs M, Manyam BV. *Bacopa monniera* extract reduces amyloid levels in PSAPP mice. J Alzheimers Dis 2006;9:243–51.

Hou ST, MacManus JP. Molecular mechanisms of cerebral ischemia-induced neuronal death. Int Rev Cytol 2002;221:93-148.

Jyoti A, Sethi P, Sharma D. *Bacopa monniera* prevents from aluminium neurotoxicity in the cerebral cortex of rat brain. J Ethnopharmacol 2007;111:56–62.

Kim EY, Koh JY, Kim YH, Sohn S, Joe E, Gwag BJ. Zn2+ entry produces oxidative neuronal necrosis in cortical cell cultures. Eur J Neurosci 1999;11:327–34.

Kim YT, Yi YJ, Kim MY, Bu Y, Jin ZH, Choi H, et al. Neuroprotection and enhancement of spatial memory by herbal mixture HT008-1 in rat global brain ischemia model. Am J Chin Med 2008;36:287–99.

Kishore K, Singh M. Effect of bacosides, alcoholic extract of *Bacopa monniera* Linn. (Brahmi), on experimental amnesia in mice. Indian J Exp Biol 2005;43:640–5.

Koh JY, Choi DW. Zinc toxicity on cultured cortical neurons: involvement of N-methyl-D-aspartate receptors. Neuroscience 1994;60:1049–57.

Kumar MH, Gupta YK. Antioxidant property of *Celastrus paniculatus* willd.: a possible mechanism in enhancing cognition. Phytomedicine 2002;9:302–11.

Lee B, Choi Y, Kim H, Kim SY, Hahm DH, Lee HJ, et al. Protective effects of methanol extract of Acori graminei rhizoma and Uncariae ramulus et Uncus on ischemia-induced neuronal death and cognitive impairments in the rat. Life Sci 2003;74:435–50.

Lin Z, Yan Y, Zhu D, Yu B, Wang Q. Protective effects of FBD—an experimental Chinese traditional medicinal formula on memory dysfunction in mice induced by cerebral ischemia–reperfusion. J Ethnopharmacol 2005;97:477–83.

Luck H. Catalase. In: Bergmeyer HO, editor. Methods of Enzymatic analysis. New York, London: Academic Press; 1971. p. 885–93.

Moskowitz N, Schook W, Puszkin S. Regulation of endogenous calcium-dependent synaptic membrane phospholipase A2. Brain Res 1984;290:273–9.

Nowak P, Szczerbak G, Nitka D, Kostrzewa RM, Josko J, Brus R. Cortical dopaminergic neurotransmission in rats intoxicated with lead during pregnancy. Nitric oxide and hydroxyl radicals formation involvement. Neurotoxicol Teratol 2008;30(5):428–32.

O'Brien JT, Erkinjuntti T, Reisberg B, Roman G, Sawada T, Pantoni L, et al. Vascular cognitive impairment. Lancet Neurol 2003;2:89–98.

Ollinger K, Brunk UT. Cellular injury induced by oxidative stress is mediated through lysosomal damage. Free Radic Biol Med 1995;19:565–74.

Prabhakar S, Saraf MK, Pandhi P, Anand A. *Bacopa monniera* exerts antiamnesic effect on diazepam-induced anterograde amnesia in mice. Psychopharmacology (Berl) 2008;200:27–37.

Rensink M, Schuurmans M, Lindeman E, Hafsteinsdottir T. Task-oriented training in rehabilitation after stroke: systematic review. J Adv Nurs 2009;65(4):737–54.

Russo A, Izzo AA, Borrelli F, Renis M, Vanella A. Free radical scavenging capacity and protective effect of *Bacopa monniera* L. on DNA damage. Phytother Res 2003;17:870–5.

Sacco RL, Adams R, Albers G, Alberts MJ, Benavente O, Furie K, et al. Guidelines for prevention of stroke in patients with ischemic stroke or transient ischemic attack: a statement for healthcare professionals from the American Heart Association/American Stroke Association Council on Stroke: co-sponsored by the Council on Cardiovascular Radiology and Intervention: the American Academy of Neurology affirms the value of this guideline. Stroke 2006;37:577–617.

Saraf MK, Prabhakar S, Khanduja KL, Anand A. Antiamnesic action of *Bacopa monniera* is mediated through protein kinase-CREB. Pathway in amnesic mice induced by Scopolamine. San Diego, CA, USA: Society for Neuroscience; 2007. p. 156. 19/U3.

Saraf MK, Prabhakar S, Anand A. *Bacopa monniera* alleviates N-nitro-L-arginine-induced but not MK-801-induced amnesia: a mouse Morris water maze study. Neuroscience 2009;160(1):149–55.

Shanker G, Singh HK. Anxiolytic profile of standardized Brahmi extract. Ind J Phamacol 2000;32:152.

Singh HK, Dhawan BN. Effect of *Bacopa monniera* Linn. (Brahmi) extract on avoidance responses in rat. J Ethnopharmacol 1982;5:205–14.

Singh HK, Dhawan BN. Neuropsychopharmacological effects of the ayurvedic nootropic *Bacopa monniera* Linn. (Brahmi). Ind J Pharmacol 1997;29S:359–65.

Singh RH, Singh L. Studies on the antioxidant anxiety effect of the Medhay Rasayan drug Brahmi (*Bacopa monniera* Linn)—Part II (experimental studies). J Res Ind Med. Yoga Homeo 1980;14:1–6.

Singh HK, Rastogi RP, Srimal RC, Dhawan BN. Effects of bacosides A and B on avoidance response in rats. Phytother Res 1988;2:70–5.

Siripurapu KB, Gupta P, Bhatia G, Maurya R, Nath C, Palit G. Adaptogenic and anti-amnesic properties of *Evolvulus alsinoides* in rodents. Pharmacol Biochem Behav 2005;81:424–32.

Sun YF, Pei DS, Zhang QX, Zhang GY. Neuroprotection of GST, an extract of traditional Chinese herb, against ischemic brain injury induced by transient brain ischemia and reperfusion in rat hippocampus. Neurol Res 2008;30:471–5.

Tian J, Li G, Liu Z, Zhang S, Qu G, Jiang W, et al. ND-309, a novel compound, ameliorates cerebral infarction in rats by antioxidant action. Neurosci Lett 2008;442:279–83.

Tripathi YB, Chaurasia S, Tripathi E, Upadhyay A, Dubey GP. *Bacopa monniera* Linn. as an antioxidant: mechanism of action. Indian J Exp Biol 1996;34:523–6.

Vohora D, Pal SN, Pillai KK. Protection from phenytoin-induced cognitive deficit by *Bacopa monniera*, a reputed Indian nootropic plant. J Ethnopharmacol 2000;71:383–90.

Wang Z, Li YM, Gong XJ, Lin J, Zou JM. Effects of Naomaitai capsule on learning and memory and content of Ach in rat model produced by cerebral ischemia–reperfusion. Zhongguo Zhong Yao Za Zhi 2005;30:459–62.

Wang ZF, Yan J, Fu Y, Tang XC, Feng S, He XC, et al. Pharmacodynamic study of FS-0311: a novel highly potent, selective acetylcholinesterase inhibitor. Cell Mol Neurobiol 2008;28:245–61.

Wills ED. Mechanisms of lipid peroxide formation in animal tissues. Biochem J 1966;99(3):667–76.

Yun YJ, Lee B, Hahm DH, Kang SK, Han SM, Lee HJ, et al. Neuroprotective effect of palmul-chongmyeong-tang on ischemia-induced learning and memory deficits in the rat. Biol Pharm Bull 2007;30:337–42.

Zhou Y, Peng L, Zhang WD, Kong DY. Effect of triterpenoid saponins from *Bacopa monniera* on scopolamine-induced memory impairment in mice. Planta Med 2009;75:568–74.

Neurochem Res (2010) 35:1172–1181
DOI 10.1007/s11064-010-0171-x

ORIGINAL PAPER

Antiamnesic Effect of *B. monniera* on L-NNA Induced Amnesia Involves Calmodulin

Akshay Anand · Manish Kumar Saraf · Sudesh Prabhakar

Accepted: 9 April 2010 / Published online: 30 April 2010
© Springer Science+Business Media, LLC 2010

Abstract Amnesia may result from ageing, chronic drug abuse or head injury and there are limited therapeutic strategies to such conditions. We have shown that *Bacopa monniera*, a memory enhancing drug can reverse both diazepam and scopolamine induced amnesia in mice. In order to understand the downstream effects of *B. monniera*, this study was designed to investigate how *B. monniera* antagonizes MK801, an NMDA receptor antagonist and N_{ω}-Nitro-L-arginine (L-NNA), a nitric oxide synthase inhibitor. We compared the degree of reversal *B. monniera* imparts on MK801 and L-NNA induced anterograde amnesia in experimental mice. Our data revealed that L-NNA induced anterograde amnesia was significantly reversed by *B. monniera*, however, it did not attenuate the MK 801 induced anterograde amnesia. *B. monniera* significantly increased calmodulin (CaM) and pCREB/CREB levels when the whole brain lysates of *B. monniera* pretreated amnesic mice were compared with those of L-NNA treated mice. We conclude that antiamnesic effect *B. monniera* on L-NNA induced amnesia may be mediated by NO pathyway involving CaM, which is required for LTP sustenance. These studies evoke interest in their future development as potential antiamnesic drugs.

Keywords Amnesia · *Bacopa monniera* · CREB · Calmodulin · L-NNA · MK801

Introduction

Dementia affects around 7% of the general population older than 65 years which doubles every 5 years, to reach 30–50% by the age of 85 [23, 36, 37, 43]. Amnesia develops as a consequence of various neurological problems such as Alzheimer's disease. The interference in the long term potentiation (LTP) process, a biological mechanism of learning and memory [14, 34], produces amnesia. Competitive NMDA receptor antagonists such as AP5, NPC and non-competitive NMDA receptor antagonist such as phencyclidine, ketamine and MK801 block LTP induction [13, 25, 28] and produce amnesia as evidenced by various behavioral experiments [6, 27]. MK 801 has been used as an amnesic agent for testing antiamnesic effect of cannabidiol-rich extracts [20], SB-399885 (a 5-HT6 receptor blocker), [45] and thioperamide (a histamine-H3 receptor antagonist) [10]. Further it is known that activation of NMDA receptors produces nitric oxide by activation of nitric oxide synthase (NOS). Nitric oxide acts as retrograde messenger that further potentiates LTP process [29, 40, 58]. Administration of 7-nitro-imidazole nitric oxide synthase (NOS) inhibitors, has been reported to

Akshay Anand and Manish Kumar Saraf are equal authors.

A. Anand
Neuroscience Research Lab, Department of Neurology, Post Graduate Institute of Medical Education and Research, Sector-12, Chandigarh 160012, India

M. K. Saraf
Neuroscience Research Lab, Post Graduate Institute of Medical Education and Research, Sector-12, Chandigarh 160012, India
e-mail: mksaraf@utmb.edu

M. K. Saraf
Internal Medicine, University of Texas Medical Branch, Galveston, TX 77555, USA

S. Prabhakar (✉)
Department of Neurology, Post Graduate Institute of Medical Education and Research, Sector-12, Chandigarh 160012, India
e-mail: pgineurology@gmail.com
URL: http://www.pgimer.nic.in/code/profiles/sprabhakar.htm

block hippocampal LTP and induce impairment of learning and memory in rats [30, 57, 59]. Aminoguanidine and L-N-iminoethyl-lysine, inducible NOS inhibitors, are found to exacerbate the deficit in cognitive performance, as assessed by Morris water maze (MWM) and increase neuronal loss in vulnerable regions (CA3 and CA1) of hippocampus in rats after traumatic brain injury [57]. The bilateral intra hippocampal microinjection of nitro-arginine (NO-arg), an NOS inhibitor, produces retrograde amnesia in the inhibitory avoidance task [9].

Metabolic enhancers, choline esterase inhibitors etc., are the currently available drugs useful for treatments of amnesia and have limited efficacy with attending side effects. *B. monniera* Linn (Syn. Brahmi), has been used as a memory-enhancing agent although its precise mechanism of action is not known. The behavioral animal studies have shown that administration of *B. monniera* improves motor learning [48]. Similarly, *B. monniera* extract has been shown to improve acquisition, retention, and delayed extinction of newly acquired behavior in a brightness discrimination reaction task [55]. The memory enhancing effects have been attributed to the active constituent bacosides A [16] and B [19] and have been shown to exert facilitatory effect on mental retention in avoidance response in rats [56] and reverse amnesic effects of scopolamine and electric-shock [11, 12]. *B. monniera* is reported to provide neuroprotection against cigarette smoke induced apoptosis [1–5] and aluminum induced oxidative stress [33]. We have earlier reported that *B. monniera* attenuates both scopolamine [51] and diazepam induced memory deficits [47] with calmodulin playing a dominant tole in evoking antiamnesic effects of *B. monniera* on scopolamine induced amnesia. Knowing that NMDA receptor and NOS are important target sites of LTP, we wanted to investigate the downstream signaling pathway of *B. monniera* mediated reversal of MK-801 (NMDA antagonist) and N_{ω}-nitro-l-arginine (L-NNA; NOS inhibitor)-induced amnesia.

Materials and Methods

Swiss albino mice (male, age 3–5 months, weight 25–35 g) were used in the present study. They were housed in an animal house and provided free access of water and standard diet, and exposed to 12 h light and dark cycle. The experiments were conducted between 900 to 1800 hours in a semi soundproof laboratory.

Drugs and Chemicals

N_{ω}-nitro-l-arginine (L-NNA) and MK 801 (Sigma–Aldrich, New Delhi) were dissolved in normal saline. Standardized extract of *Bacopa monniera* (Lumen marketing company Chennai), composed of Bacosides (55.35%), was suspended in Tween 80 (5% v/v in normal saline). We used MAP kinase assay kit (Chemicon International USA), pCREB assay kit (Bisource USA), CREB assay kit (Bisource USA), cAMP assay kit (Calbiochem USA), total protein kit (Biorad Laboratories, USA). Sigma–Aldrich, USA was the main source of chemicals such as aprotinin, leuceptin, pepstatin, PMSF, EDTA, tris HCl, sodium hydrochloride, snake venom serum, cadmium beds, sulfanilamide, NED, $MnCl_2$, Trichloroacetic acid, CaM deficient PDE, goat serum, calcium chloride, magnesium sulfate, $NaHCO_3$, Na_2CO_3, Trizma base, DAB, Tween 20 etc. Anti-NOS2 antibody was purchased from Santacruz Biotech, USA and goat anti-rabbit IgG HRP labeled was got from Sigma–Aldrich, USA.

Behavioral Evaluation

Morris water maze was employed to evaluate learning and memory [42]. It consisted of a circular water tank (2 m diameter and 45 cm height), filled with water that was made opaque with a white colored dye. The tank was divided into four equal quadrants. A tiny platform (10 cm^2) was placed one centimeter below the level of water in the center of one of these four quadrants designated as target quadrant. The position of platform was kept unaltered throughout all the training sessions. In the present study, quadrant-2 (Q2) was considered as the target quadrant. Each animal was subjected to four consecutive trials on each day with a gap of 5 min, during which they were allowed to escape onto the hidden platform. In case the animal was unable to locate the hidden platform within 120 s period, it was gently guided to the platform and allowed to remain there for 20 s. Escape latency time (ELT) was noted as the index of acquisition. Each animal was subjected to the four acquisition trials per day for six consecutive days.

In order to study the effect of drug on acquisition, drug solution was administered before acquisition trials for six consecutive days. The experimental mice were screened with rota-rod to test the muscle coordination activity of mice before conducting the maze experiments [24]. Mice, showing abnormal swimming pattern in water maze, and low muscle coordination activity in rota rod test were excluded from study. The study was divided in eight groups. The number of mice in each group was 7. The details of drug treatment are described in the table (Table 1).

Mice in Group I were administered normal saline (10 ml kg^{-1}) orally 60 min before and normal saline (10 ml kg^{-1}) intraperitoneally 30 min before acquisition (day 1–6). Five percent Tween 80 was used as a diluent for preparation of *B. monniera* suspension. Group II mice were treated with 5% Tween 80 (10 ml kg^{-1} oral), 60 min

Table 1 Regimen for Administration of vehicle and pharmacological agents

Group	No.	Treatment
Control	I	NS (10 ml kg^{-1} PO) 60 min before + NS (10 ml kg^{-1} ip) 30 min before acquisition trials (day 1 to day 6)
5% Tween 80 per se	II	5% TWEEN 80 (10 ml kg^{-1} PO) 60 min before + NS (10 ml kg^{-1} ip) 30 min before acquisition trials (day 1 to day 6)
L-NNA	III	5% TWEEN 80 (10 ml kg^{-1} PO) 60 min before + L-NNA (30 mg kg^{-1} ip) 30 min before acquisition trials (day 1 to day 6)
B. monniera + L-NNA	IV	BM (80 mg kg^{-1} PO) 60 min before + L-NNA (30 mg kg^{-1} ip) 30 min before acquisition trials (day 1 to day 6)
MK 801	V	5% Tween 80 (10 ml kg^{-1} PO) 60 min before + MK (0.17 mg kg^{-1} ip) 30 min before acquisition trials (day 1 to day 6)
B. monniera + MK 801	VI	BM (120 mg kg^{-1} PO) 60 min before + MK (0.17 mg kg^{-1} ip) 30 min before acquisition trials (day 1 to day 6)
B. monniera—per se	VII–VIII	BM (80 mg and 120 mg kg^{-1} PO) 60 min before acquisition trials (day 1 to day 6)

BM Bacopa monniera standardized extract suspension, *NS* normal saline

before and normal saline (10 ml kg^{-1} ip) 30 min before acquisition to observe the per se effect of 5% Tween 80 on normal acquisition of memory. Group III mice were treated with Tween-80 (10 ml kg^{-1}, orally) 60 min before and L-NNA (30 mg kg^{-1} i.p.) 30 min before acquisition trials; group IV mice were administered standardized extract of *B. monniera* (80 mg kg^{-1} oral) 60 min before and L-NNA (30 mg kg^{-1} i.p.) 30 min before acquisition trials. Group V mice were treated with 5% Tween 80 (10 ml kg^{-1}) orally 60 min before and MK801 i.e. 0.17 mg/kg^{1} i.p. 30 min before acquisition trials. In order to assess anti-amnesic effect of *B. monniera* on MK801 induced anterograde amnesia, group VI mice were administered standardized extract of *B. monniera* (120 mg kg^{-1} oral) 60 min before and MK801 (0.17 mg kg^{-1} i.p.) 30 min before acquisition trials. We also studied per se effect of *B. monniera* on acquisition of memory under groups VII and VIII. This included *B. monniera* suspension of 80 and 120 mg kg^{-1}, respectively administered 60 min before trial with normal saline (10 ml kg^{-1} ip) 30 min before trials.

Biochemical Investigations

Nitric Oxide Estimation

The frozen brains of mouse were homogenized with lysis buffer containing 0.01 M Tris HCl (pH 7.6), 0.1 M Sodium chloride, 0.001 M EDTA and protease inhibitors such as aprotinin 2.0 μg/ml, leupeptin 10 μg/ml, pepstatin 5 μg/ml and 0.1 mM PMSF. Nitric oxide was estimated by indirect measurement of nitrite, nitrate and total nitrite in mouse brain extract on supernatants. Cadmium beads were added to supernatant for total nitrite estimation and incubated overnight. The clear supernatant was treated with mixture of coloring reagent I (1% Sulfanilamide in 3 N HCl) and II (0.1% NED.2HCl) and incubated for 10 min at room temperature. The absorbance was noted at 620 and 550 nm, respectively. The nitrite and total nitrite level was normalized to total protein estimated by Bradford method.

Phosphodiesterase Assay

Mouse brains were homogenized with lysis buffer and the clear supernatant separated after centrifugation. The reaction mixture, comprising of Tris 40 mM, 5 mM $MnCl_2$, mouse brain extract and 10 mM cAMP was incubated for 10 min at 37°C and then heated for 2 min to terminate the reaction. Snake venom serum (1 mg/ml) was added and incubated for 10 min at 30°C. Trichloroacetic acid 50% was added and the inorganic phosphorus (P_i) release was estimated by Fiske and Subbaraw method [22]. In brief, the supernatant was mixed with ammonium molybdate solution and distilled water followed by ANSA solution. The plate was read at 660 nm. The phosphodiesterase (PDE) activity of sample was expressed in nmol P_i liberated/min/mg protein.

Ca/Calmodulin Assay

Calmodulin was estimated by the method described by Lin et al. (1974). Test samples containing Tris HCl- pH 8.0 4 mM, calcium chloride 50 μM magnesium sulfate 5 mM, CaM deficient PDE 0.5 unit, clear supernatant, cAMP 10 mM and distilled water were prepared. After preparation, these samples were incubated for 30 min at 30°C, heated for 2 min in boiling water bath. Snake venom serum (1 mg/ml) was added to each sample and incubated for 10 min at 30°C. The reaction was stopped by addition of 50% Trichloroacetic acid. Calmodulin activity of sample was expressed in nmol of Pi liberated cAMP hydrolyzed/min/mg protein.

cAMP Assay

cAMP level was estimated using cAMP Direct immunoassay kit (Calbiochem, USA). The kit uses a polyclonal antibody to cAMP that binds to cAMP in samples in a competitive manner. Briefly, the tissue powder was homogenized in 10 volumes of 0.1 N HCl to stop endogenous phosphodiesterase activity, centrifuged at 600×*g* at 4°C and clear supernatant obtained for cAMP estimation. It was followed by incubation with rabbit cAMP polyclonal antibody for 2 h at room temperature. The excess reagents were washed away and substrate was added. After a short incubation time, the reaction was stopped and the yellow color generated read on a microplate reader at 405 nm. The intensity of the color is proportional to the concentration of cAMP in standards and samples. The standard curve was obtained as Percent Bound (B/Bo) versus concentration of cAMP.

MAP Kinase Assay

The MAP kinase activity in mouse brains was estimated by employing non-radioactive MAP Kinase (ERK1/2) Activity Assay Kit (Chemicon International, USA). Briefly, about 250 µl of mouse brain homogenate was mixed with 250 µl of MAP kinase sample buffer at 4°C for cell lysis and vortexed for estimation. The total protein was estimated by Bradford method.

Mice brains were homogenized with 500 µl of common lysis buffer, containing Tris HCl 10 mM (pH 7.4), EDTA 0.5 mM, aprotinin 2.0 µg/ml, leupeptin 10 µg/ml, pepstatin 5 µg/ml and PMSF 0.1 mM to estimate MAP kinase, iNOS, pCREB and CREB assay.

iNOS Assay

The capture antibody solution was prepared in coating buffer (containing $NaHCO_3$ 0.068 M, Na_2CO_3 0.032 M; pH 8.9) at 1:200 dilution. The microplate was coated with capture anti-NOS2 antibody (Santacruz Biotech, USA) overnight at 4°C. The plate was washed with 10 mM phosphate buffer saline (PBS), containing NaCl 150 mM, Na_2HPO_4 8.1 mM, NaH_2PO_4 1.9 mM; pH 7.2–7.4 for 5 min. About 100 µl of 5% BSA was prepared in PBS as blocking solution and then incubated for 2 h at 37°C. The plates were washed with PBS buffer. After washing the rabbit anti-iNOS 0.9 antibody (Santacruz Biotech, USA) was added at a dilution of 1:200 in buffer containing NaCl%, Trizma base 20 mM, BSA 0.1%, Tween 20 0.04% and incubated for 1 h at 37°C. After washing, goat anti-rabbit IgG HRP labeled (Sigma, USA) was added and incubated for 1 h at 37°C. The excess secondary antibody was removed by washing the plates with PBS. After addition of TMB substrate, the plate was incubated for 5 min at the room temperature. The reaction was stopped and absorbance read at 492 and 450 nm and normalized to total protein.

Total-CREB and pCREB Assay

CREB Total and CREB [pS133] kit (BioSource, USA), based on a solid phase sandwich Enzyme Linked-Immuno-Sorbent Assay (ELISA) were used for the measurement of level of CREB and pCREB level in mouse brain extract. The protocol, as described in the kit was followed.

Immunohistochemistry

Six micrometer sections of the mid portion of mouse brain, embedded in tissue frozen medium, were obtained. The frozen sections were incubated with 0.3% H_2O_2 in PBS buffer for 10 min. After washing the sections with PBS, 5% goat serum was applied as blocking solution (prepared in PBSTB, Tween-20 0.2%, BSA 0.5%) for 1 h in a humidified chamber. Rabbit anti-NOS2 (Santacruz Biotech, USA; 1:100 diluted in PBSTB) was added and incubated overnight at 4°C. The excess primary antibody was removed by washing. Goat anti-rabbit IgG-HRP (Sigma USA; 1:100 diluted in PBSTB) was added and incubated for 1 h at room temperature. After washing, the substrate solution containing DAB stock 1%, 50 µl H_2O_2 0.3% in PBS buffer, was added and incubated at room temperature. The sections were washed with PBS and then air-dried before mounting. Similarly, pCREB was immunostained by applying rabbit anti-pCREB (Santacuz Biotech, USA; 1:100 diluted in PBSTB) antibody.

Statistical Analysis

All results were expressed as mean ± SEM (Standard Error of the Mean). We analyzed the behavioral results of Morris water maze using ANOVA followed by post hoc "Tukey's" at $P < 0.05$ for multiple comparisons among the groups. 'a' indicates significance at $P < 0.05$ of particular day's escape latency time (i.e., ELT of day 2–day 6) versus ELT (escape latency time) on day 1 of same group. We also compared the ELT of treated group with control's ELT and with amnesic agent's ELT in each time point (i.e., day 1–day 6). 'b' indicates significance at $P < 0.05$ of particular day of ELT versus same day control group's ELT. 'c' indicates significance of ELT of particular day versus same day's ELT of amnesic agent group. The biochemical results were analyzed by ANOVA followed by post hoc test i.e., LSD (least significance difference). 'e' indicates significance at $P < 0.05$ of treated group versus control group. 'f' indicates significance at $P < 0.05$ of treated group versus amnesic agent's group.

Results

B. monniera Reverses L-NNA Induced Amnesia but not MK 801 Induced Amnesia

N_{ω}-nitro-l-arginine (L-NNA) (30 mg kg^{-1} i.p.) significantly impaired progressive decrease in ELT during successive acquisition trials on day 3 ($F = 3.0$), day 4 ($F = 4.5$) and day 5 ($F = 6.9$) at $P < 0.05$ as compared to control group (Fig. 1a). These observations suggest that L-NNA impairs the process of acquisition of new memory by producing anterograde amnesia. *B. monniera* (80 mg kg^{-1} oral) administration progressively decreased ELT in L-NNA (30 mg kg^{-1} i.p.) treated mice ($F = 3.04$, $P < 0.05$) and reversed L-NNA (30 mg kg^{-1} i.p.) induced impairment of progressive decrease in ELT with ongoing acquisition trials (Fig. 1a), suggesting that *B. monniera* reverses L-NNA (30 mg kg^{-1} i.p.) induced anterograde amnesia.

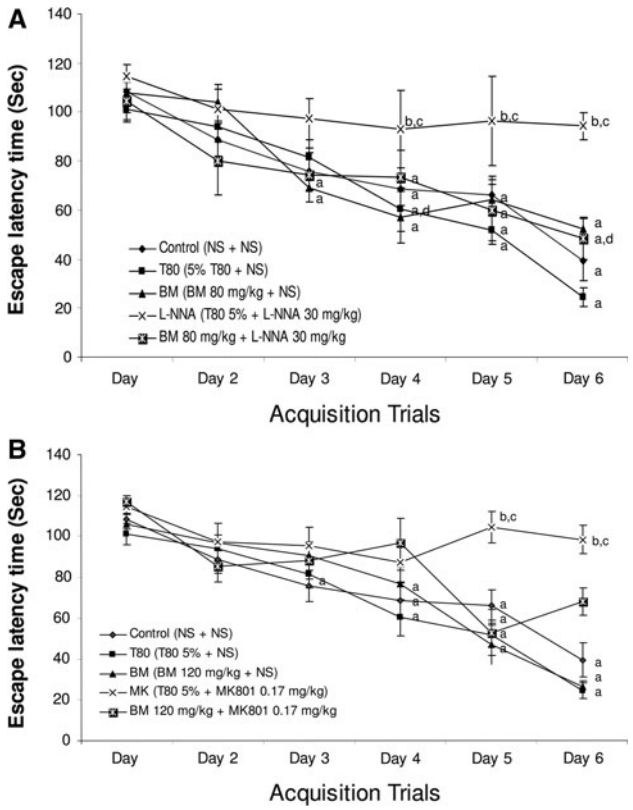


Fig. 1 *Bacopa monniera* attenuates L-NNA induced anterograde amnesia and did not alleviate MK801 induced anterograde amnesia. In acquisition trials, each value represents mean escape latency time ± SEM. **a** L-NNA (30 mg/kg ip) impairs acquisition which is attenuated by *B. monniera* (80 mg/kg oral) as compared to L-NNA, while *B. monniera* (80 mg/kg oral) and 5% tween 80 (10 ml/kg ip) does not modify the acquisition of memory. **b** MK801 at 0.17 mg/kg ip produces anterograde amnesia. *B. monniera* at 120 mg/kg oral did not attenuate anterogrode amnesia induced by MK801 induced anterograde amnesia. *B. monniera* 120 mg/kg oral and 5% tween 80 do not alter normal acquisition. We have analyzed the results using ANOVA followed by post hoc "Dunnet's" test at $P < 0.05$ for multiple comparisons among the groups. '*a*' indicates significance at $P < 0.05$ of particular day's ELT (i.e., ELT of day 2–day 6) versus ELT on day 1 of same group. '*b*' indicates significance at $P < 0.05$ of particular day of ELT versus same day control group's ELT. '*c*' indicates significance of ELT of particular day versus same day's ELT of 5% tween 80 group. '*d*' indicates significance of ELT of particular day versus same day's ELT of L-NNA or MK801 group

Mice were treated once daily with MK801 (0.17 mg kg^{-1} i.p.) from day 1 to day 6. During acquisition trials of Morris water maze test, these mice did not show progressive decrease in ELT from day 1 to day 6 which was opposite to control group ELT. We compared the ELT of day 2, day 3, day 4, day 5 and day 6 with ELT of day 1 of MK 801 treated group and were not found to be significantly different. At F 1.37, the significance levels read 0.63, 0.53, 0.16, 0.95, 0.71, respectively, which indicates that there was no consistent learning in mice from day 1 to day 6. We also compared the day 4, day 5 and day 6 ELT of MK 801 treated group with control group ELT of day 4, day 5 and day 6, respectively and we found ELT of day 4 to day 6 in MK 801 treated group ($F = 3.09$, 4.53, 6.93 respectively, $P < 0.05$) were significant different as compared to control group (Fig. 1b). These observations suggest that MK801 impairs the process of acquisition of new memory by producing anterograde amnesia. *B. monniera* (120 mg kg^{-1} oral) did not alter MK801 (0.17 mg kg^{-1} i.p.) induced impairment of progressive decrease in ELT with ongoing acquisition trials. We did not find significant difference between these groups on day 4 ($F = 3.086$; $P = 0.98$), day 5 ($F = 4.535$, $P = 0.265$) and day 6 ($F = 6.933$, $P = 0.297$) at $P < 0.05$ (Fig. 1b). 5% Tween 80 ($F = 20.28$, $P < 0.05$) and *B. monniera* (120 mg kg^{-1} oral, $F = 16.25$, $P < 0.05$; 80 mg kg^{-1} oral, $F = 4.65$, $P < 0.05$ versus day 1) significantly reduced the ELT as compared to day 1 and therefore these treatments do not affect normal acquisition (Fig. 1a, b) memory in Morris water maze test.

B. monniera Attenuates L-NNA Suppressed CaM Activity

N_{ω}-nitro-l-arginine (L-NNA) partially affected the calmodulin activity, but it is not statistically different from control ($P = 0.165$, $F = 1.34$). *B. monniera* significantly ($P < 0.05$; $F = 1.34$) attenuated the L-NNA suppressed calmodulin activity as compared to L-NNA. The attenuation, in *B. monniera* and L-NNA group, was not significantly different from control group ($P = 0.432$; $F = 1.34$). MK801 did not ($P = 0.241$; F 1.34) affect the calmodulin levels and similarly *B. monniera* along with MK 801 did not alter ($P = 0.252$; F 1.34) the calmodulin activity. *B. monniera* did not alter calmodulin, when administered alone ($P = 0.442$; F 1.34) (Fig. 2a).

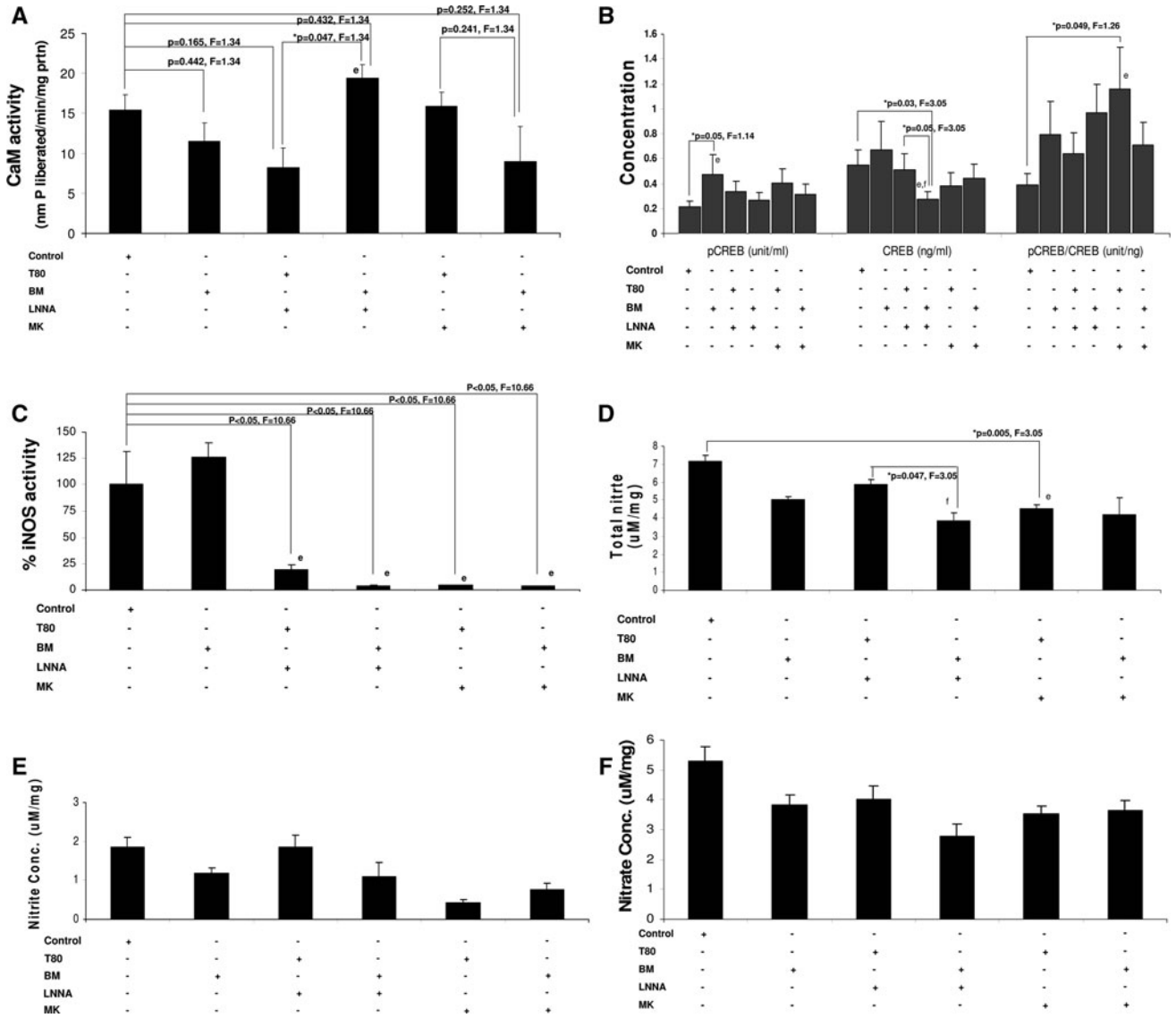


Fig. 2 Effect of *Bacopa monniera* on calmodulin, phosphorylated-CREB, total CREB and iNOS. **a** *B. monniera* with L-NNA upregulates calmodulin activity as compared to L-NNA group, while its administration with MK801 did not affect calmodulin. **b** *B. monniera* alone significantly enhances the pCREB expression as compared to control while in-combination with L-NNA or MK801 shows no significant improvement in pCREB. *B. monniera* also reduces CREB when it administered with L-NNA. Ratio of pCREB/CREB is higher in *B. monniera*—L-NNA group and MK801 group. **c** iNOS expression, measured by ELISA, was reduced in L-NNA and MK 801 with or without *B. monniera* -treated brain as compared control. **d–f** Total nitrite, Nitrite and Nitrate level in control and treated brain. Data was analyzed by ANOVA followed by LSD. '*e*' indicates significant difference for treated group vs control group at $P < 0.05$, '*f*' indicates significant difference for treated group versus L-NNA or MK801 group at $P < 0.05$. These values were obtained after normalization with total protein

Effect of *B. monniera* on pCREB and CREB

pCREB level was not significantly changed in L-NNA, MK801, *B. monniera* + *L-NNA* and *B. monniera* + MK 801 group as compared to control group. In these groups the p value is higher than 0.05 at $F = 1.14$. On the other hand *B. monniera* per se administration significantly increased the pCREB level as compared to control ($P = 0.05$, $F = 1.14$).

The level of CREB was reduced when *B. monniera* was administered with L-NNA as compared to control group ($P = 0.03$, $F = 3.05$) and as compared to L-NNA group ($P = 0.05$, $F = 3.05$). The CREB level remained unaltered with L-NNA ($P = 0.670$, $F = 5.252$) and MK 801 treatment ($P = 0.082$, $F = 5.252$). Moreover, it was not affected by *B. monniera* in MK 801 pretreated group ($P = 0.228$, $F = 5.252$). *B. monniera* alone did not ($P = 0.148$, $F = 5.252$) produce any effect of CREB level

(Fig. 2b). The pCREB immunoreactivity was qualitatively subdued in brain sections from MK 801 treated mice as compared to controls while pCREB immunostaining was not affected by L-NNA and *B. monniera* treatment as compared to controls (Fig not shown). The ratio of pCREB/CREB was partially higher in *B. monniera* and L-NNA treated mice as compared to control mice. It was also significant higher in MK801 treated mice as compared to control mice.

Effect of *B. monniera* on iNOS, Nitrite, Nitrate, and cAMP

The iNOS immunoreactivity was less prominent in brain sections from MK 801, L-NNA treated mice with or without *B. monniera* pretreatment as compared to controls (data not shown). iNOS expression was significantly ($P < 0.05$, $F = 10.66$) reduced with L-NNA and MK 801 treatment. *B. monniera* did not reverse the suppressed iNOS expression in L-either NNA or MK 801 amnesic mouse. The suppression in *B. monniera* + L-NNA and *B. monniera* + MK801 was significantly ($P < 0.05$, $F = 10.66$) when compared to control (Fig. 2c).

Total nitrite ($P = 0.005$; $F = 3.05$) was reduced with MK801 treatment which was not reversed by *B. monniera* pretreatment. *B. monniera* significantly reduced the total nitrite when administered with L-NNA as compared to L-NNA alone treated group ($P = 0.047$; $F = 3.05$). L-NNA alone did not change the total nitrite as compared to control. Moreover *B. monniera* per se did not produce any effect on total nitrite (Fig. 2d). Nitrate and nitrite level were either partially reduced or remained unchanged with L-NNA and MK801 treatment with or with out *B. monniera*. *B. monniera* per se did not change nitrate, nitrite and total nitrite level (Fig. 2e, f).

Effect of *B. monniera* on cAMP and PDE

When cAMP levels were compared between L-NNA, MK 801 and control groups, there was no significant difference. We report $P > 0.05$ at F 1.27 when compared to controls. Moreover, *B. monniera* also did not alter the cAMP levels when it was administered alone or when it was administered with L-NNA and MK801. We did not find any significant difference among these groups even after multiple comparison (Fig. 3a). The P and F value for such comparisons that were not significant were not mentioned.

Similar results were obtained when we measured PDE level. It was unaltered in both L-NNA treatment with or without *B. monniera*. However, MK 801 reduced the PDE level ($P < 0.05$, $F = 1.85$) but it was not attenuated by *B. monniera*. When we compared *B. monniera* + MK 801 with control group, we did not find statistical difference ($P = 0.057$; $F = 1.85$) (Fig. 3b).

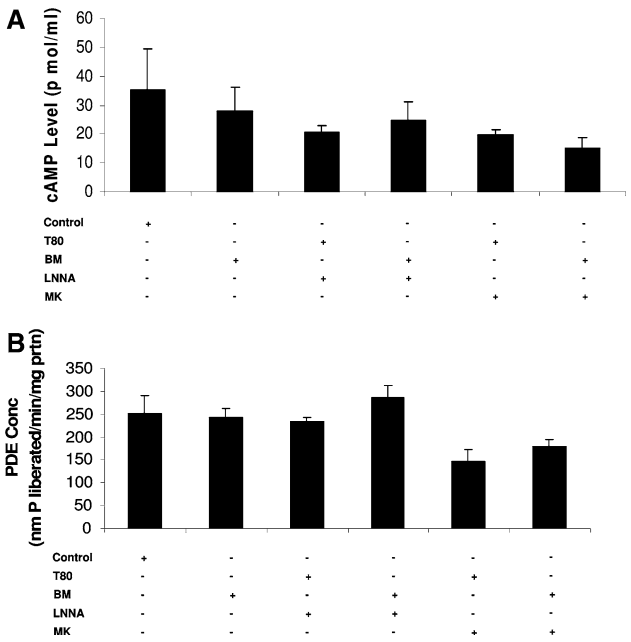


Fig. 3 Effect of *B. monniera* on cyclic adenosine monophosphate (cAMP) and PDE. **a** The level of cAMP level in control and treated group which remains unchanged in treated group as compared to control. **b** PDE level was not attenuated in *B. monniera-L-NNA* group by *B. monniera.* Data were analyzed by ANOVA followed by Bonferroni and LSD test. '*e*' indicates significant difference for treated group versus control group at $P < 0.05$, '*f*' indicates significant difference for treated group versus L-NNA or MK801 group at $P < 0.05$. These values were obtained after normalization with total protein

Discussion

NMDA receptor and NOS are integral component of LTP which require for post synaptic activation and maintenance of long term potentiation (LTP) process. The blockage of NMDA receptor and inhibition of NOS enzyme interfere the LTP process. Earlier we reported the antiamnesic effect of *B. monniera* against scopolamine [51] and diazepam induced memory deficit [47]. For better understanding the mechanism of *B. monniera's* antiamnesic effect, we analysed the effect of *B. monniera* on MK801 and L-NNA induced deficit in memory. In this study we report that L-NNA, a nitric oxide synthase (NOS) inhibitor, produces anterograde amnesia. In order to explore the role of post synaptic molecules in amnesia, we performed investigations in the whole brain extracts of L-NNA treated mice. Due to complexity of interactions in downstream pathway of LTP [49], we investigated only the well cited downstream molecules of LTP. In this study, *B. monniera* acts to significantly mask the L-NNA induced anterograde

amnesia as shown by our water maze experiments. Calmodulin, a Calcium binding protein, is an intergral component of CaM kinase cascade [41, 53] and mediates long term potentiation [38] as well as synaptic strength [31] by activating the CaM kinase II [50], is significantly upregulated by this drug. Amyloid beta, responsible for Alzheimer's disease, prevents the activation of calcium/calmodulin-dependent protein kinase II and AMPA receptor phosphorylation and thereby inhibiting the hippocampal long-term potentiation [62].

Pharmacological and genetic manipulations have indicated a strong role of CREB and pCREB in memory consolidation [7, 8, 15, 18, 39, 46]. *B. monniera* downregulated CREB in L-NNA-*B. monniera* treated mice, while cAMP, PDE, pCREB, nitrite and nitrate remained unaffected. In this study learning is expected to enhance the expression of pCREB but it was not significantly altered when compared between amnesic mice and *B. monniera* treated mice. This could be partly because CREB is more important for long term memory than shot term memory [17, 26, 32, 60]. It is also possible that L-NNA induced reduction of Ca^{++} is not sufficiently rescued by *B. monniera* to upregulate CREB. pCREB/CREB level being an index of phosphorylation of CREB into pCREB was further analysed and found to be higher in *B. monniera* pretreated mice than L-NNA treated mice. These findings suggest the involvement of calmodulin mediated CREB pathway in bringing about the antiamnesic effects of *B. monniera* on L-NNA treated mice. It is worthwhile to review some studies where similar paradigms have been used to understand the memory enhancing drugs.

MK 801 and TCP, a non competitive NMDA receptor antagonists, are reported to induce impairment of both acquisition and retrieval in different paradigms of learning and memory [21, 35]. Our demonstration of MK801 induction of amnesia in mice is corroborated with similar studies where MK801 was used to produce memory deficits [6, 27, 44, 52, 54, 61] as testing platform to screen antiamnesic effects of novel drugs. Our results, however, did not lead to reversal of MK801 induced amnesia by *B. monniera* when evaluated by Morris water maze tasks. MK801 suppressed iNOS, nitrite and total nitrite with mild reduction in nitrate, cAMP, and PDE but did not affect CREB, pCREB and Calmodulin. *B. monniera* neither induced CaM when co administered with MK 801, like it did when it was co-administered with L NNA, nor it disinhibited the iNOS, nitrite, nitrate, total nitrite, cAMP and PDE levels. pCREB/CREB levels were also unaffected in the *B monniera*-MK 801 treated mice. These finding suggest that *B. monniera* does not reverse the effect of MK801 at both behavioural and molecular level even at a higher dose of 120 mg/kg.

We explain the findings by suggesting that *B. monniera* exerts restorative effect rather than memory enhancing effect because no positive per se effect of *B. monniera* was seen in these studies. We can speculate that *B. monniera* exerts anti-amnesic effect on L-NNA induced amnesia without affecting NMDA receptor and by improving the release of nitric oxide and restoring the LTP.

Although the value of molecular analogs in drug discovery can not be disregarded, however, the potential of traditional knowledge herbs such as *B. monniera* also needs deeper investigation, particularly when the current reductionist approach has not resulted in tangible therapies. These may include further studies on downstream signaling mechanisms and LTP processes.

Conclusions

This is the first report of antiamnesic effects of *B. monniera* on L-NNA induced anterograde amnesia. *B. monniera* is not able to delink the MK801 from its NMDA receptor thereby affecting the successful restoration of LTP. We therefore postulate that NOS mediated pathway plays a more dominant role in *B. monniera* mediated reversal of amnesia. On the basis of our findings, we conclude that LNNA induced amnesia may be mediated by CaM. Further investigations with additional CaM antagonists coupled with purification of active constituents of *B. monniera* that potentiate such antiamnesic responses can uncover their value for translation to clinic. Given these findings from a herb, it is important to realize that pursuit of reductionist approach should be cautiously adopted in scientific approaches. Compromises between biological utility and molecular specificity will remain inherent in target selection for CNS drugs.

References

1. Anbarasi K, Kathirvel G, Vani G, Jayaraman G, Shyamala Devi CS (2006) Cigarette smoking induces heat shock protein 70 kDa expression and apoptosis in rat brain: modulation by bacoside A. Neuroscience 138:1127–1135
2. Anbarasi K, Vani G, Balakrishna K, Devi CS (2005) Creatine kinase isoenzyme patterns upon chronic exposure to cigarette smoke: protective effect of Bacoside A. Vasc Pharmacol 42:57–61
3. Anbarasi K, Vani G, Balakrishna K, Devi CS (2005) Effect of bacoside A on membrane-bound ATPases in the brain of rats exposed to cigarette smoke. J Biochem Mol Toxicol 19:59–65
4. Anbarasi K, Vani G, Balakrishna K, Devi CS (2006) Effect of bacoside A on brain antioxidant status in cigarette smoke exposed rats. Life Sci 78:1378–1384
5. Anbarasi K, Vani G, Devi CS (2005) Protective effect of bacoside A on cigarette smoking-induced brain mitochondrial dysfunction in rats. J Environ Pathol Toxicol Oncol 24:225–234
6. Bannerman DM, Good MA, Butcher SP, Ramsay M, Morris RG (1995) Distinct components of spatial learning revealed by prior training and NMDA receptor blockade. Nature 378:182–186

7. Barco A, Alarcon JM, Kandel ER (2002) Expression of constitutively active CREB protein facilitates the late phase of long-term potentiation by enhancing synaptic capture. Cell 108:689–703
8. Barco A, Pittenger C, Kandel ER (2003) CREB, memory enhancement and the treatment of memory disorders: promises, pitfalls and prospects. Expert Opin Ther Targets 7:101–114
9. Bernabeu R, de Stein ML, Fin C, Izquierdo I, Medina JH (1995) Role of hippocampal NO in the acquisition and consolidation of inhibitory avoidance learning. Neuroreport 6:1498–1500
10. Bernaerts P, Lamberty Y, Tirelli E (2004) Histamine H3 antagonist thioperamide dose-dependently enhances memory consolidation and reverses amnesia induced by dizocilpine or scopolamine in a one-trial inhibitory avoidance task in mice. Behav Brain Res 154:211–219
11. Bhattacharya SK, Bhattacharya A, Kumar A, Ghosal S (2000) Antioxidant activity of *Bacopa monniera* in rat frontal cortex, striatum and hippocampus. Phytother Res 14:174–179
12. Bhattacharya SK, Kumar A, Ghosal S (2001) Effect of *Bacopa monniera* on animal models of Alzheimer's disease and perturbed central cholinergic markers of cognition in rats. In: Mori A, Satoh T (eds) Emerging drugs: molecular aspects of Asian medicines. PJD Publication, Westbury, pp 21–32
13. Bliss TV, Collingridge GL (1993) A synaptic model of memory: long-term potentiation in the hippocampus. Nature 361:31–39
14. Bliss TV, Lomo T (1973) Long-lasting potentiation of synaptic transmission in the dentate area of the anaesthetized rabbit following stimulation of the perforant path. J Physiol 232:331–356
15. Casadio A, Martin KC, Giustetto M, Zhu H, Chen M, Bartsch D et al (1999) A transient, neuron-wide form of CREB-mediated long-term facilitation can be stabilized at specific synapses by local protein synthesis. Cell 99:221–237
16. Chatterji N, Rastogi RP, Dhar ML (1965) Chemical examination of Bacopa monniera Wettst. Part II: the constitution of Bacoside A. Ind J Chem 3:24–29
17. Dash PK, Hochner B, Kandel ER (1990) Injection of the cAMP-responsive element into the nucleus of Aplysia sensory neurons blocks long-term facilitation. Nature 345:718–721
18. Davis GW, Schuster CM, Goodman CS (1996) Genetic dissection of structural and functional components of synaptic plasticity. III. CREB is necessary for presynaptic functional plasticity. Neuron 17:669–679
19. Dhawan BN, Singh HK (2002) Nootropic and some other effects of *Bacopa monniera* Linn. (Brahmi). Ann Neurosci 6:34–40
20. Fadda P, Robinson L, Fratta W, Pertwee RG, Riedel G (2006) Scopolamine and MK801-induced working memory deficits in rats are not reversed by CBD-rich cannabis extracts. Behav Brain Res 168:307–311
21. Filliat P, Blanchet G (1995) Effects of TCP on spatial memory: comparison with MK-801. Pharmacol Biochem Behav 51:429–434
22. Fiske CH, Subbaraw Y (1925) The colorimetric determination of phosphorus. J Biol Chem 66:375–400
23. Geldmacher DS, Whitehouse PJ (1996) Evaluation of dementia. N Engl J Med 335:330–336
24. Ghelardini C, Galeotti N, Gualtieri F, Romanelli MN, Bucherelli C, Baldi E et al (2002) DM235 (sunifiram): a novel nootropic with potential as a cognitive enhancer. Naunyn Schmiedebergs Arch Pharmacol 365:419–426
25. Gruart A, Munoz MD, Delgado-Garcia JM (2006) Involvement of the CA3-CA1 synapse in the acquisition of associative learning in behaving mice. J Neurosci 26:1077–1087
26. Guzowski JF, McGaugh JL (1997) Antisense oligodeoxynucleotide-mediated disruption of hippocampal cAMP response element binding protein levels impairs consolidation of memory for water maze training. Proc Natl Acad Sci USA 94:2693–2698
27. Han CJ, Pierre-Louis J, Scheff A, Robinson JK (2000) A performance-dependent adjustment of the retention interval in a delayed non-matching-to-position paradigm differentiates effects of amnestic drugs in rats. Eur J Pharmacol 403:87–93
28. Harney SC, Rowan M, Anwyl R (2006) Long-term depression of NMDA receptor-mediated synaptic transmission is dependent on activation of metabotropic glutamate receptors and is altered to long-term potentiation by low intracellular calcium buffering. J Neurosci 26:1128–1132
29. Hawkins RD, Son H, Arancio O (1998) Nitric oxide as a retrograde messenger during long-term potentiation in hippocampus. Prog Brain Res 118:155–172
30. Holscher C (1994) Inhibitors of metabotropic glutamate receptors produce amnestic effects in chicks. Neuroreport 5:1037–1040
31. Huang FL, Huang KP, Boucheron C (2007) Long-term enrichment enhances the cognitive behavior of the aging neurogranin null mice without affecting their hippocampal LTP. Learn Mem 14:512–519
32. Josselyn SA, Shi C, Carlezon WA Jr, Neve RL, Nestler EJ, Davis M (2001) Long-term memory is facilitated by cAMP response element-binding protein overexpression in the amygdala. J Neurosci 21:2404–2412
33. Jyoti A, Sethi P, Sharma D (2007) *Bacopa monniera* prevents from aluminium neurotoxicity in the cerebral cortex of rat brain. J Ethnopharmacol 111:56–62
34. Kang KR, Lee SY (2001) Effect of serum and hydrogen peroxide on the Ca2+/calmodulin-dependent phosphorylation of eukaryotic elongation factor 2(eEF-2) in Chinese hamster ovary cells. Exp Mol Med 33:198–204
35. Kant GJ, Wylie RM, Vasilakis AA, Ghosh S (1996) Effects of triazolam and diazepam on learning and memory as assessed using a water maze. Pharmacol Biochem Behav 53:317–322
36. Lin YM, Liu YP, Cheung WY (1974) Purification and characterization of protein activator of cyclic nucleotide phosphodiesterase from bovine brain. Methods Enzymol 38:262–273
37. Lobo A, Launer LJ, Fratiglioni L, Andersen K, Di Carlo A, Breteler MM et al (2000) Prevalence of dementia and major subtypes in Europe: a collaborative study of population-based cohorts. Neurologic Diseases in the Elderly Research Group. Neurology 54:S4–9
38. Manabe T (2008) Molecular mechanisms for memory formation. Brain Nerve 60:707–715
39. Matynia A, Kushner SA, Silva AJ (2002) Genetic approaches to molecular and cellular cognition: a focus on LTP and learning and memory. Annu Rev Genet 36:687–720
40. Medina JH, Izquierdo I (1995) Retrograde messengers, long-term potentiation and memory. Brain Res Brain Res Rev 21:185–194
41. Mizuno K, Antunes-Martins A, Ris L, Peters M, Godaux E, Giese KP (2007) Calcium/calmodulin kinase kinase beta has a male-specific role in memory formation. Neuroscience 145:393–402
42. Morris R (1984) Developments of a water-maze procedure for studying spatial learning in the rat. J Neurosci Methods 11:47–60
43. O'Brien JT, Erkinjuntti T, Reisberg B, Roman G, Sawada T, Pantoni L et al (2003) Vascular cognitive impairment. Lancet Neurol 2:89–98
44. Pedreira ME, Perez-Cuesta LM, Maldonado H (2002) Reactivation and reconsolidation of long-term memory in the crab Chasmagnathus: protein synthesis requirement and mediation by NMDA-type glutamatergic receptors. J Neurosci 22:8305–8311
45. Perez-Garcia G, Meneses A (2005) Oral administration of the 5-HT6 receptor antagonists SB-357134 and SB-399885 improves memory formation in an autoshaping learning task. Pharmacol Biochem Behav 81:673–682
46. Pittenger C, Kandel E (1998) A genetic switch for long-term memory. C R Acad Sci III 321:91–96

47. Prabhakar S, Saraf MK, Pandhi P, Anand A (2008) *Bacopa monniera* exerts antiamnesic effect on diazepam-induced anterograde amnesia in mice. Psychopharmacology (Berl) 200:27–37
48. Prakash JC, Sirsi M (1962) Comparative study of the effects of Brahmi (*Bacopa monniera*) and chlorpromazine on motor learning in rats. J Sci Ind Res 21:93–96
49. Sanes JR, Lichtman JW (1999) Can molecules explain long-term potentiation? Nat Neurosci 2:597–604
50. Sanhueza M, McIntyre CC, Lisman JE (2007) Reversal of synaptic memory by Ca2+/calmodulin-dependent protein kinase II inhibitor. J Neurosci 27:5190–5199
51. Saraf MK, Prabhakar S, Khanduja KL, Anand A (2007) Antiamnesic action of Bacopa monniera is mediated through protein kinase-CREB pathway in amnesic mice induced by Scopolamine. In: Society for Neuroscience, San Diego, 156.119/U153
52. Saucier D, Cain DP (1995) Spatial learning without NMDA receptor-dependent long-term potentiation. Nature 378:186–189
53. Schmitt JM, Guire ES, Saneyoshi T, Soderling TR (2005) Calmodulin-dependent kinase kinase/calmodulin kinase I activity gates extracellular-regulated kinase-dependent long-term potentiation. J Neurosci 25:1281–1290
54. Si K, Lindquist S, Kandel E (2004) A possible epigenetic mechanism for the persistence of memory. Cold Spring Harb Symp Quant Biol 69:497–498
55. Singh HK, Dhawan BN (1997) Neuropsychopharmacological effects of the ayurvedic nootropic *Bacopa monniera* Linn. (Brahmi). Ind J Pharmacol 29S:359–365
56. Singh HK, Rastogi RP, Srimal RC, Dhawan BN (1988) Effects of Bacosides A and B on avoidance response in rats. Phytother Res 2:70–75
57. Sinz EH, Kochanek PM, Dixon CE, Clark RS, Carcillo JA, Schiding JK et al (1999) Inducible nitric oxide synthase is an endogenous neuroprotectant after traumatic brain injury in rats and mice. J Clin Invest 104:647–656
58. Stevens CF, Wang Y (1993) Reversal of long-term potentiation by inhibitors of haem oxygenase. Nature 364:147–149
59. Tong XK, Hamel E (1999) Regional cholinergic denervation of cortical microvessels and nitric oxide synthase-containing neurons in Alzheimer's disease. Neuroscience 92:163–175
60. Yin JC, Del Vecchio M, Zhou H, Tully T (1995) CREB as a memory modulator: induced expression of a dCREB2 activator isoform enhances long-term memory in Drosophila. Cell 81:107–115
61. Zhang WN, Bast T, Feldon J (2001) The ventral hippocampus and fear conditioning in rats: different anterograde amnesias of fear after infusion of N-methyl-D-aspartate or its noncompetitive antagonist MK-801 into the ventral hippocampus. Behav Brain Res 126:159–174
62. Zhao D, Watson JB, Xie CW (2004) Amyloid beta prevents activation of calcium/calmodulin-dependent protein kinase II and AMPA receptor phosphorylation during hippocampal long-term potentiation. J Neurophysiol 92:2853–2858

Neurochem Res (2010) 35:279–287
DOI 10.1007/s11064-009-0051-4

ORIGINAL PAPER

Scopolamine Induced Amnesia is Reversed by *Bacopa monniera* Through Participation of Kinase-CREB Pathway

Manish Kumar Saraf · Akshay Anand · Sudesh Prabhakar

Accepted: 13 August 2009 / Published online: 16 September 2009
© Springer Science+Business Media, LLC 2009

Abstract Scopolamine, an anticholinergic drug, is reported to produce amnesia by interference of long term potentiation and has been used for discerning the efficacy of various antiamnesic drugs. The intoxication with anticholinergics and benzodiazepines tend to produce neurodegeneration which cause memory deficits. Our earlier reports have shown the antiamnesic drug, *B. monniera* to be capable of alleviating diazepam induced memory deficits. We have now tested how scopolamine affects downstream signaling molecules of long term potentiation and if *B. monniera* can also modulate the scopolamine induced amnesia. We used Morris water maze scale to test the amnesic effect of scopolamine and its reversal by *B. monniera*. Rota-rod test was used to screen muscle coordination activity of mice before water maze investigations were carried out. The results showed that scopolamine downregulated protein kinase C and iNOS without affecting cAMP, protein kinase A, calmodulin, MAP kinase, nitrite, CREB and pCREB. *B. monniera* reversed the scopolamine induced amnesia by significantly improving calmodulin and by partially attenuating protein kinase C and pCREB. These observations suggest involvement of calmodulin in evoking antiamnesic effects of *B. monniera*.

Keywords Amnesia · *Bacopa monniera* · Calmodulin · CREB · Scopolamine · Water maze

Manish Kumar Saraf and Akshay Anand are equal authors.

M. K. Saraf · A. Anand · S. Prabhakar (✉)
Neuroscience Research Lab, Department of Neurology, Post Graduate Institute of Medical Education and Research, Sector-12, Chandigarh 160012, India
e-mail: pgineurology@gmail.com
URL: www.pgimer.nic.in

Introduction

Dementia is one of the causes of memory loss [17], which affects 7% population older than 65 years and upto 30–50% population by the age of 85 years. This is growing with increase in life span [17, 25, 29]. Cholinergic antagonism is reported to produce cognition deficit which imitates Alzheimer's disease [14] similar to hippocampal lesion induced cognitive deficits [1, 46]. The degeneration of glutamatergic neurons, in addition to cholinergic neurons [3], is reported in hippocampus and cortex of AD (Alzheimer disease) patients [4, 16]. Long term potentiation (LTP) which is a well accepted mechanism of learning and memory is activated due to high frequency presynaptic stimulation [7, 8]. It subsequently activates postsynaptic downstream signalling which comprises of retrograde messengers, kinases, calmodulin, cAMP response element binding protein etc. [22, 23]. Scopolamine, an acetylcholine receptor antagonist, has been reported to impair LTP [30, 34], and also used as amnesic agent but the down stream signalling pathway of scopolamine induced amnesia is elusive. Before understanding the amnesic drugs it is worthwhile to review the drugs such as Galantamine (a cholinesterase inhibitor) which is isolated from *Galanthus nivalis* and *Lycoris radiate* [20, 21] and is licensed in the United Kingdom for treatment of mild to moderate Alzheimer's disease [12, 44]. *B. monniera* (Brahmi) is another popular drug used by alternative medicine practitioners in India. The preliminary study evaluated that *B. monniera* alcoholic extract increased the learning ability of rats [38]. Subsequent studies indicated that cognition-facilitating effect of standardized extract of *B. monniera* was due to two prominent constituents, bacoside-A [10, 40] and bacoside-B [6, 40]. *B. monniera* also exhibited antioxidant [43], antistress [11] and anxiolytic [37, 41] activities in

animals. *B. monniera* along with *ginkgo biloba* extract exerts significant anticholinesterase and antidementic properties in mice and attenuates the scopolamine induced cognition deficit in passive avoidance test [13] exhibiting cholinergic characteristics [19]. *B. monniera* also provides protection from phenytoin (an antiepileptic drug) induced deficit in cognitive function of mice [45]. Bacosides, the prominent constituent of *B. monniera*, has been reported to alleviate the amnesic effects of scopolamine [33, 39]. However, there are also reports where it is shown to improve the cognitive deficit possibly by exhibiting free radical scavenging and anti-lipid peroxidative effects [2] that protect the brain from oxidative damage, and by augmenting the anti-oxidative defence system of glutathione, vitamin C, vitamin E, and vitamin A and the activities of superoxide dismutase (SOD), catalase, glutathione peroxidase (GPX) and glutathione reductase (GR) besides maintaining the levels of trace elements such as copper, iron, zinc and selenium [2]. *B. monniera* extract also reduces the level of amyloid especially Abeta 1–40 and 1–42 in doubly transgenic mouse model of rapid amyloid deposition and reverses Y-maze performance and open field hyperlocomotion behavioral changes [19].

We have earlier reported that *B. monniera* attenuates diazepam induced memory deficits [32]. For better understanding of mechanism of *B. monniera* we have investigated the effect of *B. monniera* on scopolamine-induced amnesia at both molecular and behavioral level.

Experimental Procedure

Animals and Drugs

All experiments were performed in accordance with the guidelines of Institute animal ethical committee and European Communities Council Directive (86/609/EEC). Adequate measures were taken to minimize pain or discomfort with animal experimental procedures. Swiss albino mice (male, age matched, weight 25–35 g) were housed four per cage with ad libitum access to food and water under controlled laboratory conditions. Experiments were conducted between 9.00 and 18.00 h in a semi soundproof laboratory. All the drugs solutions were prepared before use. The standardized extract of *B. monniera* (Lumen marketing company, Chennai), containing *bacosides* A and B, was suspended in Tween 80 (5% % v/v in normal saline), while scopolamine (Sigma–Aldrich, New Delhi) was dissolved in normal saline. Healthy mice were screened on the basis of the swimming ability and normal behavior. Rota-rod test in mice 'before and after administration of scopolamine' was used to validate muscle co-ordination activity of mice. Mice, showing the normal fall time of 4 min from rotating rod at 15 rpm speed were selected for memory evaluation (Data not shown). If animal showed abnormal muscle coordination before or after drug administration, they were not included in the study.

Behavioral Evaluation

Apparatus

Morris water maze [27] was used to assess learning and memory in experimental mice. We followed the methodology of Morris water maze described in our earlier study [32, 36]. It consisted of a circular water tank (2 m diameter and 45 cm height), filled with opaque water. A platform (10 cm^2) was placed one centimeter below the level of water in the center of one of four quadrants, which was considered as the target quadrant. The position of platform was kept unaltered throughout the acquisition trials. During acquisition trial mouse was allowed to search the platform and spent at least 20 s there. In the event the animal was unable to locate the hidden platform within 120 s, it was gently guided to it. Escape latency time (ELT) to locate the hidden platform in water maze was noted as an index of acquisition. Each animal was subjected to the four acquisition trials per day for six consecutive days. The study was divided in eleven groups. Each group comprised of seven mice. Rota-rod test was performed to screen test the muscle coordination activity of mice before subjecting them to water maze evaluation. Mice, showing abnormal swimming pattern in water maze, coupled with low muscle coordination activity in rota-rod test were excluded from study. For the study of drug on acquisition, it was administered before acquisition trial for 6 days.

Drug Treatment Schedule During Morris Water Test

Mice (Group I) were administered normal saline (10 ml kg^{-1}) intraperitoneally 30 min before acquisition (day 1–6). Group II mice were injected with *B. monniera* (120 mg kg^{-1}) and group III mice were injected with 5% Tween- 80 (10 ml kg^{-1}) orally 60 min before acquisition trial to study per-se effect of *B. monniera* and diluent 5% Tween 80 on normal acquisition of memory. In order to study the effect of scopolamine on acquisition of memory, group IV mice were treated with scopolamine i.e., 0.1 mg kg^{-1} i.p. respectively, 30 min before acquisition trials. To assess anti-amnesic effect of *B. monniera* on scopolamine induced anterograde amnesia, group V mice were administered a constant dose of *B. monniera* 120 mg kg^{-1} orally and scopolamine 0.1 mg kg^{-1} i.p. 60 and 30 min, respectively, before acquisition trials.

Neurochemical Analysis

Ca/Calmodulin Assay

Calmodulin was estimated by the method described by Lin et al. [24]. Brain sample was mixed with the buffer solution containing Tris–HCl 4 mM, calcium chloride 50 μM, magnesium sulfate 5 mM, CaM deficient Phosphodiesterase 0.5 unit, and cAMP 10 mM. Incubated it for 30 min at 30° and heated for 2 min in water bath. After addition of Snake venom serum (1 mg/ml) the sample mixer was incubated for 10 min at 30°C. The reaction was stopped by addition of 50% Trichloroacetic acid. OD (optical density) of clear supernatant was determined. Calmodulin activity of sample was expressed in nmol of Pi liberated cAMP hydrolyzed/min/mg protein.

Cyclic Adenosine Monophosphate (cAMP) Assay

cAMP level was estimated using cAMP direct immunoassay kit (Calbiochem, USA). The tissue powder was homogenized in 10 volumes of 0.1 N HCl, centrifuged it at 600*g* at 4^{O}C and clear supernatant obtained for cAMP estimation. The rabbit cAMP polyclonal antibody was incubated for 2 h. The standard curve was obtained as Percent Bound (B/Bo) versus concentration of cAMP.

Protein Kinase A and Protein Kinase C Assay

The pooled brain of mice was homogenized with 500 μl of common lysis buffer, containing Tris–HCl 10 mM (pH 7.4), EDTA (0.5 mM), aprotinin 2.5 μl/ml, leuceptin 10 μg/ml, pepstatin A 1.25 μg/ml, protease inhibitor cocktail 50 μl/ml was used to estimate PKA, PKC, MAP kinase assay, and western blotting of pCREB and CREB protein.

Mouse brain samples were mixed with protein kinase buffer containing Tris HCl pH (7.4), EGTA 1 mM, Triton X-100, beta-mercaptoethanol 20 mM, common lysis buffer and vortexed it gently. The solution was centrifuged at 14,000*g* for 5 min at 4°C. The supernatant was re-centrifuged at 100,000*g* for 1 h at 4°C. The clear supernatant was obtained and stored at 4°C for assay. The total protein was estimated by Bradford method. Protein kinase-non radioactive assay kit (Calbiochem, USA) was used to estimate the protein kinase A and C in supernatant of mouse brain. PKA component mixture contained reaction buffer, 1 mM ATP, 20 μM cAMP. PKC reaction mixture consisted of reaction buffer, 20 mM Calcium chloride, 1 mM ATP, 500 μg/ml phosphatidyl serine and 20 mM EGTA. The component mixture was transferred to microplate, preincubated at 25°C for 5 min. Mouse brain supernatant was added and vortexed. The reaction mixture was transferred into synthetic PKA/PKC pseudosubstrate coated plate and incubated for 20 min at room temperature. The reaction was stopped by adding 20% phosphoric acid. The biotinylated antibody of phosphorylated pseudosubstrate was added to each well after washing and incubating for 60 min at room temperature. The plate was washed and substrate solution added to each well and incubated for 4 min at room temperature. O.D was taken at 492 nm using microplate reader.

MAP Kinase Assay

The MAP kinase activity of mouse brain sample was estimated by employing non-radioactive MAP Kinase (ERK1/2) Activity Assay Kit (Chemicon International, USA). About 250 μl of mouse brain homogenate was mixed with 250 μl of MAP kinase sample buffer at 4°C for cell lysis and vortexed. The supernatant was aliquoted and stored. The total protein was estimated by Bradford method.

Inducible Nitric Oxide Sythase (Inos) Assay

The capture antibody solution was prepared in coating buffer (containing $NaHCO_3$ 0.068 M, Na_2CO_3 0.032 M; pH 8.9) at 1:200 dilution. The microplate was coated with diluted capture anti-NOS2 antibody (Santacruz Biotech, USA) overnight at 4°C. The plate was washed with 10 mM phosphate buffer saline (PBS), containing NaCl 150 mM, Na_2HPO_4 8.1 mM, NaH_2PO_4 1.9 mM; pH 7.2–7.4 for 5 min. About 100 μl of 5% BSA was prepared in PBS as blocking solution and then incubated for 2 h at 37°C. The plates were washed with PBS buffer. After washing the rabbit anti-iNOS antibody (Santacruz Biotech, USA) was added at a dilution of 1:200 in buffer containing NaCl 0.9%, Trizma base 20 mM, BSA 0.1%, Tween 20 0.04% and incubated for 1 h at 37°C. After washing goat anti-rabbit IgG HRP labeled (Sigma, USA) was added and incubated for 1 h at 37°C. The excess secondary antibody was removed by washing the plates with PBS. After addition of TMB substrate, the plate was incubated for 5 min at the room temperature. The reaction was stopped by stop solution. The absorbance of plates was read at 492 and 450 nm and normalized to total protein.

Total-CREB and pCREB Assay

CREB Total and CREB [pS133] kit (BioSource, USA), based on a solid phase sandwich Enzyme Linked-Immuno-Sorbent Assay (ELISA) was used for the

measurement of level of CREB and pCREB level in mouse brain extract.

Statistical Analysis

We have analyzed the results of Morris water maze using ANOVA followed by post hoc "Dunnet's" test at $P < 0.05$ for multiple comparisons among the groups. '*a*' indicates significance at $P < 0.05$ of particular day's ELT (i.e., ELT of day 2–6) versus ELT on day 1 of same group. We also compared the ELT of treated group with control's ELT and with scopolamine's ELT in each time point (i.e., day 1–6). '*b*' indicates significance at $P < 0.05$ of particular day of ELT versus same day control group's ELT. '*c*' indicates significance of ELT of particular day versus same day's ELT of tween 80 5% group. '*d*' indicates significance of ELT of particular day versus same day's ELT of scopolamine (0.1 mg/kg ip) group. All results were expressed as mean + SEM. (Standard error mean). The biochemical results were analyzed by ANOVA followed by post hoc tests such as least significance difference (LSD) and Bonferroni test. '*e*' indicates significance at $P < 0.05$ of treated group versus control group. '*f*' indicates significance at $P < 0.05$ of treated group versus scopolamine group.

Results

B. monniera Attenuates Scopolamine Induced Anterograde Amnesia

Control mice showed significant decrease in ELT with successive acquisition trials on day 1–6 ($a = P < 0.05$ vs. ELT on day 1, $F = 11.26$). 5% Tween 80 did not affect normal acquisition memory ($a = P < 0.05$ vs. ELT on day 1, $F = 20.61$). *B. monniera* (120 mg kg^{-1} oral) alone neither enhanced nor impaired the normal acquisition and retrieval of memory ($a = P < 0.05$ vs. ELT on day 1, $F = 16.56$). Scopolamine at 0.1 mg kg^{-1} i.p significantly impaired acquisition by impairing gradual reduction in ELT. This group was significantly different from control group and 5% Tween 80 group ($b = P < 0.05$ and $c = P < 0.05$, F values 1.01, 1.26, 2.89, 3.28, 8.4 and 16.38 on day 1–6, respectively). *B. monniera* (120 mg kg^{-1} oral) co-administered with scopolamine at 0.1 mg kg^{-1} i.p showed a gradual decline in ELT which was significantly different when compared to scopolamine treated group ($d = P < 0.05$ versus the same day's ELT of Scopolamine group, F values 1.1, 1.26, 2.89, 3.28, 8.4, 16.38 on day 1–6, respectively) (Fig. 1).

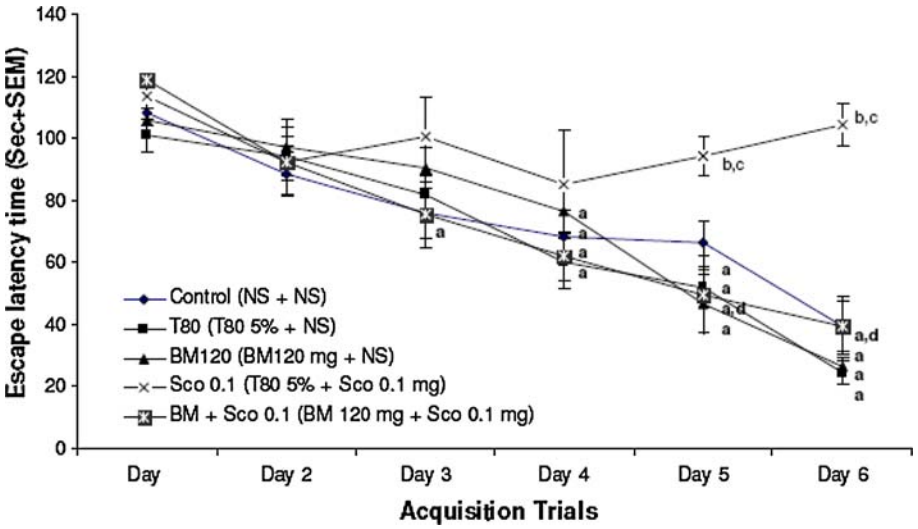


Fig. 1 Attenuation of Scopolamine induced anterograde amnesia by *Bacopa monniera.* In acquisition trials, each value represents mean escape latency time ±SEM. *Control* group shows normal acquisition of memory. Scopolamine at 0.1 mg/kg ip produces anterograde amnesia. *B. monniera* at 120 mg/kg oral prominently attenuates anterogrode amnesia induced by scopolamine at 0.1 mg/kg ip. *B. monniera* 120 mg/kg oral and 5% tween 80 do not alter normal acquisition. We have analyzed the results using ANOVA followed by post hoc "Dunnet's" test at $P < 0.05$ for multiple comparisons among the groups. '*a*' indicates significance at $P < 0.05$ of particular day's ELT (i.e., ELT of day 2–day 6) versus ELT on day 1 of same group. '*b*' indicates significance at $P < 0.05$ of particular day of ELT versus same day control group's ELT. '*c*' indicates significance of ELT of particular day versus same day's ELT of 5% tween 80 group. '*d*' indicates significance of ELT of particular day versus same day's ELT of scopolamine group

Scopolamine Suppresses PKC and iNOS Activity in Mouse Brains

Scopolamine significantly reduced protein kinase C ($e = P < 0.05$, F value 7.01; Fig. 2a) and iNOS ($e = P < 0.05$, F value 8.50; Fig. 2e) as compared to controls but did not alter cAMP (Fig. 2b), Protein kinase A (Fig. 2c), MAP kinase (Fig. 2d) and pCREB (Fig. 3b) even when co-administered with *B. monniera*.

B. monniera Enhances Calmodulin Level With Concomitant Loss of PKC Suppression

B. monniera significantly improved the calmodulin as compared to scopolamine ($f = P < 0.05$, F value 2.84; Fig. 3a) even though Scopolamine did not significantly suppress calmodulin as compared to control ($P = 0.384$, F value 2.84; Fig. 3a). Scopolamine neither altered total-CREB level nor changed pCREB level as compared to

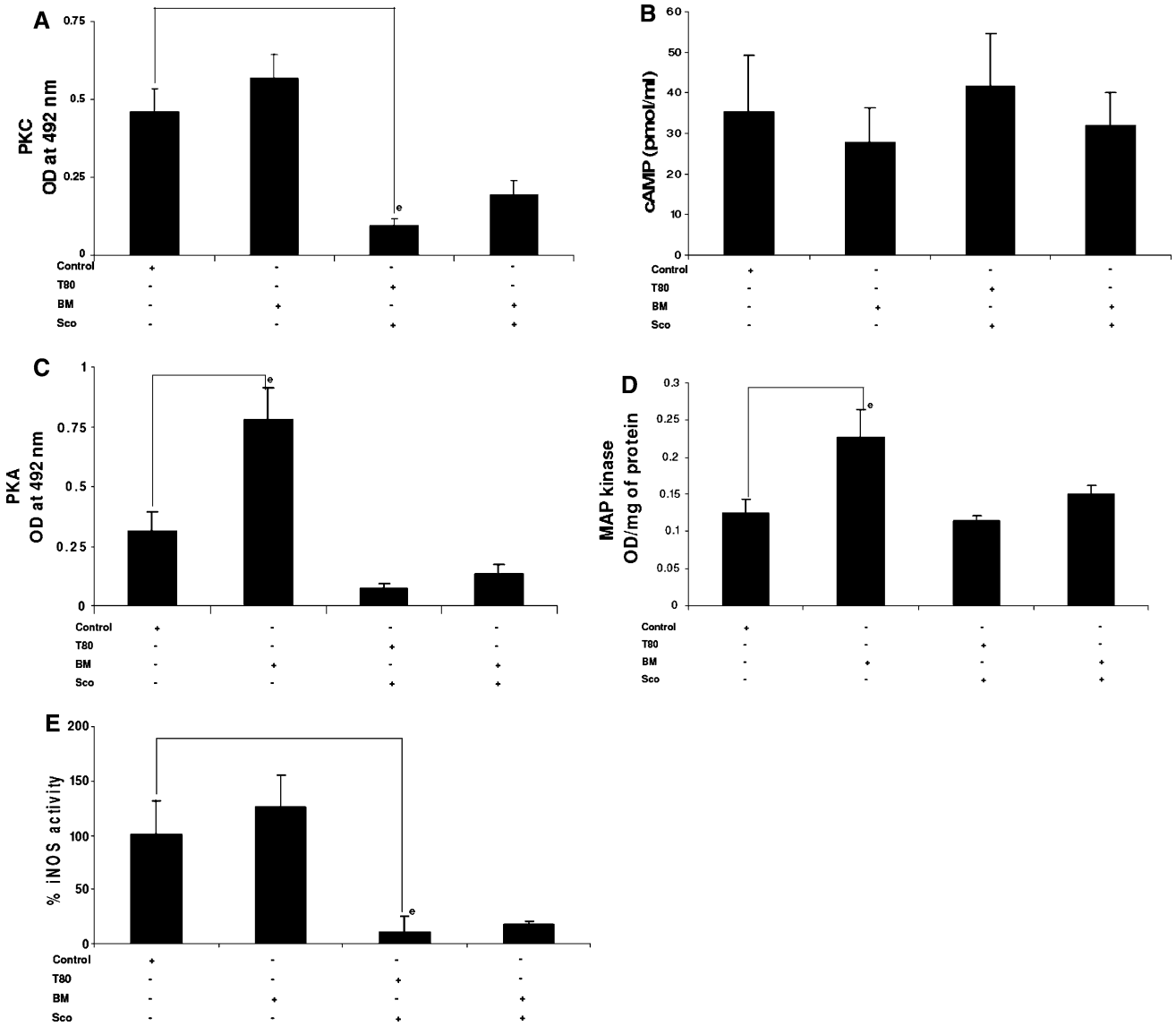


Fig. 2 Effect of *Bacopa monniera* on protein kinase C (PKC), cyclic adenosine monophosphate (cAMP), protein kinase A (PKA) and MAP kinase evaluated from whole brain homogenates. **a** Scopolamine significantly reduces PKC level. *B. monniera* along with scopolamine attenuates scopolamine suppressed PKC level when compared to control. **b** The level of cAMP levels are unchanged. **c** *B. monniera* with scopolamine does not significantly improve PKA while its *per-se* effect is significant in enhancing the PKA level. **d** *B. monniera* alone significantly up-regulates MAPkinase as compared to control. *B. monniera* co-administration with scopolamine dose not affect MAP kinase. **e** Scopolamine significantly suppresses the inducible nitric oxide (iNOS) expression as compared to control. The combined administration of *B. monniera* and scopolamine does not attenuate scopolamine iNOS expression as compared to scopolamine. Data was analyzed by ANOVA followed by Bonferroni and LSD test. '*e*' indicates significant difference for treated group versus control group at $P < 0.05$, '*f*' indicates significant difference for treated group versus scopolamine group at $P < 0.05$. These values were obtained after normalization with total protein

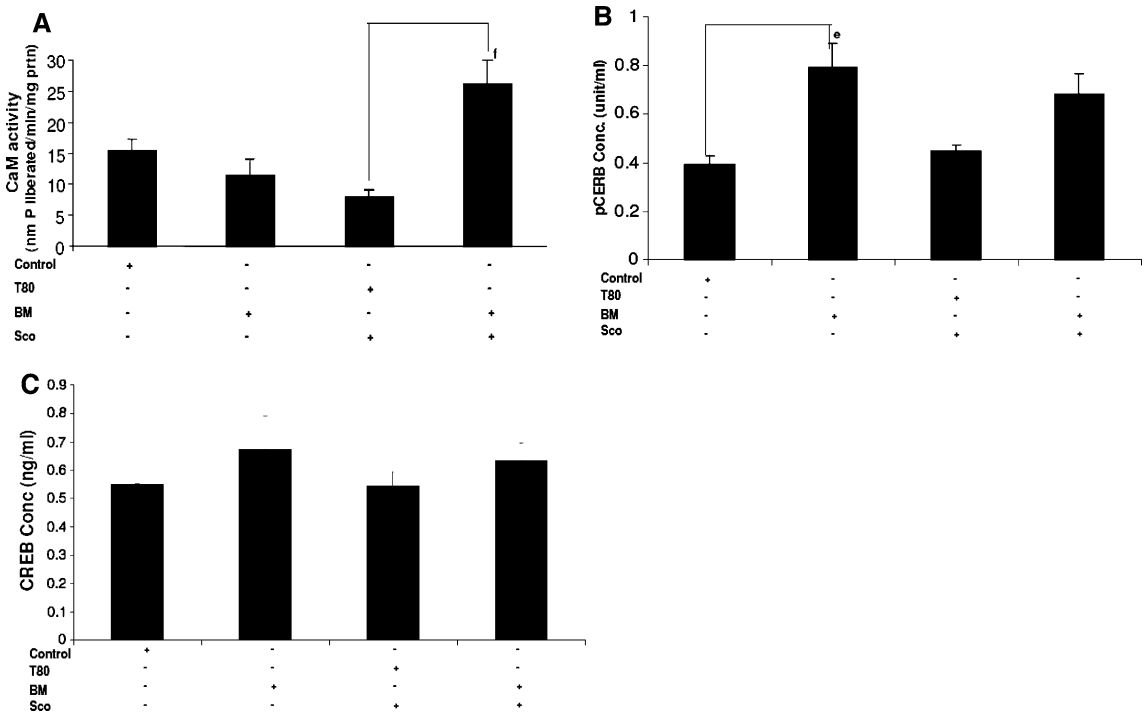


Fig. 3 Effect of *Bacopa monniera* on calmodulin, phosphorylated-CREB, total CREB in whole brain homogenates. **a** *B. monniera* with scopolamine upregulates calmodulin activity as compared to scopolamine group. **b** *B. monniera* alone significantly enhances the pCREB expression as compared to control while in combination with scopolamine shows partial increment as compared to scopolamine. **c** CREB expression does not alter among all treated groups as compared of control group. Data was analyzed by ANOVA followed by LSD and Bonferroni. '*e*' indicates significant difference for treated group versus control group at $P < 0.05$, '*f*' indicates significant difference for treated group versus scopolamine group at $P < 0.05$. These values were obtained after normalization with total protein

control group when analyzed by ELISA. *B. monniera* co-administered with scopolamine, partially improved the pCREB expression as compared to scopolamine ($P = 0.10$, F value 4.17; Fig. 3b) as measured by ELISA. Total CREB content remained unchanged in *B. monniera* with or without scopolamine (Fig. 3c). When administered per-se it significantly upregulated protein kinase A ($e = P < 0.05$, F value 7.18; Fig. 2c), MAP kinase ($e = P < 0.05$, F value 5.25; Fig. 2d) and pCREB as compared to control ($e = P < 0.05$, F value 4.17; Fig. 3b) without affecting cAMP, protein kinase C and iNOS (Fig. 2b, c, e).

Discussion

The central cholinergic system is known to regulate the cognitive function. The impairment of cholinergic neuron in hipocampus is the main feature of Alzheimer's disease. In this study scopolamine, acetylcholine receptor antagonist, significantly impaired the process of acquisition by producing anterograde amnesia. In order to explore the role of post synaptic molecules in amnesia, we analysed the whole brain extracts of scopolamine treated mice. Due to complexity of interactions in downstream molecules of LTP [35], we limited our investigations to most cited candidates of LTP. Our results showed that Scopolamine significantly suppressed Protein kinase C and iNOS and mildly decreased CaM activity without significantly altering cAMP, protein kinase A, MAP kinase, pCREB and CREB. It suggests that the blockade of acetylcholine receptors by scopolamine downregulates protein kinase C and iNOS producing anterograde amnesia. Our utilization of scopolamine to evaluate the antiamnesic efficacy of *B. monniera* is in consonance with previous approaches [5, 18, 31, 42, 47] and has provided an opportunity to understand *B. monniera*'s mechanism of action in more detail. *B. monniera* was able to reverse anterograde amnesia induced by scopolamine allows us to propose the contribution of cholinergic system and Kinase-CREB pathway for antiamnesic effect of *B. monniera* as supported by some of the earlier reports [13, 28]. *B. monniera* is reported to reverse neurotoxin and colchicines induced depletion of acetyholine and suppression of choline esterase activity and muscarinic receptor binding in frontal cortex and hippocampus [33]. Moreover, it is documented to inhibit the acetylcholine esterase activity dose dependently [13].

It is known that Calmodulin activates protein kinase C and nitric oxide synthase enzyme and potentiates the retrograde messenger pathway. The significant finding

resulting from this investigation showed enhanced Calmodulin activity as a result of *B. monniera* pre treatment. We found that Scopolamine reduced the protein kinase C in brain without significantly altering either CREB or Calmodulin. As CREB is a molecular marker of long term potentiation and memory formation [15] it was analysed in *B. monniera* treated and untreated animals without any significant change. It is known that drugs affecting cAMP and protein kinase A are known to modulate memory consolidation in hippocampus [9] indicating substantial contribution of protein kinase A in memory. However, our results are in variance with these findings. On the contrary, *B. monniera* was found to enhance MAP kinase, pCREB and PKA activity when administered per-se without bringing any significant improvement in normal memory. Such 'molecular-behavioral partitioning' can be explained by stating that *B. monniera* exerts restorative effect on conditions of spatial memory deficits and not on normal memories. Further experimentation with other amnesic agents or models may provide deeper insight about activity of *B. monniera* or its mechanism of action. Further, it is known that scopolamine prevents the increase of PKC elicited by oxiracetam. PKC activation is therefore believed to be a common mechanism amongst cognition stimulating drugs from different chemical classes [26]. Expectedly, when memory deficits are produced by scopolamine there is marked downregulation of PKC and iNOS. We postulate that CaM plays a dominant role in LTP, apparently downstream of PKC and iNOS and upon activation may restore the memory loss without their de suppression. This effect of *B. monniera* could also be partly ascribed to the denovo effect of *B. monniera* on CaM RNA synthesis which leads to its sustained expression. It could thus be a postulated that CaM is a candidate molecule whose role in attenuation of memory deficits needs further investigation.

In order to further examine the participation of retrograde messenger mediated pathway in the reversal of memory, we also analyzed nitric oxide, which is synthesized in postsynaptic neurons and acts as retrograde messenger in LTP. We found that scopolamine reduced the expression of iNOS which remained unaffected when treated by *B. monniera*. It is possible that *B. monniera* does not directly involve nitric oxide mediated retrograde messenger pathway while exerting its antiamnesic effect. Retrograde messengers such as nitric oxide rapidly maintain LTP by increasing release of presynaptic glutamate, while kinase pathway potentiates the postsynaptic synthesis of proteins required for synaptic plasticity and maintenance of LTP. It is possible that scopolamine interrupts LTP by suppressing iNOS. It is well known that while the low amount of nitric oxide interrupts LTP and its higher amount causes exitotoxicity due to formation of free radical, therefore the balance in nitric oxide level is critical for neuronal homeostasis. Contrary to popular belief that *B. monniera* is a memory enhancer, it possesses a vital role in alleviating memory deficits than memory enhancement per se, however, these results should be interpreted with caution because these experiments have been limited to evaluation of short term memory and the data is based on sub-chronic administration of *B. monniera* alone. It is possible that the chronic effects of *B. monniera* could improve behaviour implicated by upregulation of PKA, MAPK and pCREB.

Because the reported increase of protein kinase A, MAP kinase and pCREB do not lead to memory enhancement, it can also be argued that *B. monniera* enhances memory that can not be evaluated by Morris water maze. While these results are not discrepant it is tempting to delink the enhancement of BM induced CREB/Calmodulin from failure of scopolamine to alter these molecules when amnesia is induced. It is not necessary that LTP reduction caused due to amnesic drugs will surely lead to disruption of CREB or Calmodulin. Other reasons that may have confounded the results include the sampling of whole brain homogenates instead of specific brains regions involved in long term memory consolidation.

On the basis of our findings, we can conclude that *B. monniera* induced suppression of scopolamine related amnesia may be mediated by PKC and CaM. Further investigations with additional CaM agonists and/or antagonists of PKC coupled with screening of active constituents of *B monniera* that potentiate such antiamnesic responses, can uncover their potential for translation to clinic. This study provides a basis for designing a future study that can address *B. monniera's* effects on synaptogenesis and synaptic plasticity. Moreover, it will be equally interesting to identify the *B. monniera's* the role in prefrontal cortex and amygdale, in addition to its role in hippocampus, in LTP. However, it is also important to realize that pursuit of reductionist or single molecule approach should not be a scientific barrier in translation when herbal extracts can deliver therapeutic solutions. The use of herbal drugs in potentiating anti-amnesic responses seeks to dilute the current reductionism in experimental science evoking interest in their future development as potential memory enhancing drugs.

Acknowledgments The work was partially supported by Department of Biotechnology, New Delhi (India) (No. BT/PR3533/Med/12/152/2002). The authors wish to thank Dr. Nusrat and Dr. S Sharma for valuable discussions.

References

1. Anagnostaras SG, Maren S, Fanselow MS (1995) Scopolamine selectively disrupts the acquisition of contextual fear conditioning in rats. Neurobiol Learn Mem 64:191–194

2. Anbarasi K, Vani G, Balakrishna K, Devi CS (2006) Effect of bacoside A on brain antioxidant status in cigarette smoke exposed rats. Life Sci 78:1378–1384
3. Araujo DM, Lapchak PA, Robitaille Y, Gauthier S, Quirion R (1988) Differential alteration of various cholinergic markers in cortical and subcortical regions of human brain in Alzheimer's disease. J Neurochem 50:1914–1923
4. Aronica E, Dickson DW, Kress Y, Morrison JH, Zukin RS (1998) Non-plaque dystrophic dendrites in Alzheimer hippocampus: a new pathological structure revealed by glutamate receptor immunocytochemistry. Neuroscience 82:979–991
5. Bao HY, Zhang J, Yeo SJ, Myung CS, Kim HM, Kim JM et al (2005) Memory enhancing and neuroprotective effects of selected ginsenosides. Arch Pharm Res 28:335–342
6. Basu N, Rastogi RP, Dhar ML (1967) Chemical examination of *Bacopa monniera* Wettst Part III: the constitution of Bacoside-B. Indian J Chem 5:84
7. Bliss TV, Collingridge GL (1993) A synaptic model of memory: long-term potentiation in the hippocampus. Nature 361:31–39
8. Bliss TV, Lomo T (1973) Long-lasting potentiation of synaptic transmission in the dentate area of the anaesthetized rabbit following stimulation of the perforant path. J Physiol 232:331–356
9. Bonini JS, Da Silva WC, Bevilaqua LR, Medina JH, Izquierdo I, Cammarota M (2007) On the participation of hippocampal PKC in acquisition, consolidation and reconsolidation of spatial memory. Neuroscience 147:37–45
10. Chatterji N, Rastogi RP, Dhar ML (1965) Chemical examination of *Bacopa monniera* Wettst. Part II: the constitution of Bacoside A. Indian J Chem 3:24–29
11. Chowdhuri DK, Parmar D, Kakkar P, Shukla R, Seth PK, Srimal RC (2002) Antistress effects of bacosides of *Bacopa monnieri*: modulation of Hsp70 expression, superoxide dismutase and cytochrome P450 activity in rat brain. Phytother Res 16:639–645
12. Clegg A, Bryant J, Nicholson T, McIntyre L, De Broe S, Gerard K et al (2002) Clinical and cost-effectiveness of donepezil, rivastigmine, and galantamine for Alzheimer's disease. A systematic review. Int J Technol Assess Health Care 18:497–507
13. Das A, Shanker G, Nath C, Pal R, Singh S, Singh H (2002) A comparative study in rodents of standardized extracts of *Bacopa monniera* and Ginkgo biloba: anticholinesterase and cognitive enhancing activities. Pharmacol Biochem Behav 73:893–900
14. Ebert U, Kirch W (1998) Scopolamine model of dementia: electroencephalogram findings and cognitive performance. Eur J Clin Invest 28:944–949
15. Evans MS, Viola-McCabe KE (1996) Midazolam inhibits long-term potentiation through modulation of GABAA receptors. Neuropharmacology 35:347–357
16. Francis PT, Palmer AM, Snape M, Wilcock GK (1999) The cholinergic hypothesis of Alzheimer's disease: a review of progress. J Neurol Neurosurg Psychiatry 66:134–147
17. Geldmacher DS, Whitehouse PJ (1996) Evaluation of dementia. N Eng J Med 5:330–335
18. Ho SC, Ho YF, Lai TH, Liu TH, Wu RY (2005) Traditional Chinese herbs against hypertension enhance memory acquisition. Am J Chin Med 33:787–795
19. Holcomb LA, Dhanasekaran M, Hitt AR, Young KA, Riggs M, Manyam BV (2006) *Bacopa monniera* extract reduces amyloid levels in PSAPP mice. J Alzheimers Dis 9:243–251
20. Howes MJ, Houghton PJ (2003) Plants used in Chinese and Indian traditional medicine for improvement of memory and cognitive function. Pharmacol Biochem Behav 75:513–527
21. Howes MJ, Perry NS, Houghton PJ (2003) Plants with traditional uses and activities, relevant to the management of Alzheimer's disease and other cognitive disorders. Phytother Res 17:1–18
22. Kandel ER (2004) The molecular biology of memory storage: a dialog between genes and synapses. Biosci Rep 24:475–522
23. Kandel ER (2005) Eric Kandel: a life in learning and memory. Drug Discov Today 10:302–304
24. Lin YM, Liu YP, Cheung WY (1974) Purification and characterization of protein activator of cyclic nucleotide phosphodiesterase from bovine brain. Methods Enzymol 38:262–273
25. Lobo A, Launer LJ, Fratiglioni L, Andersen K, Di Carlo A, Breteler MM et al (2000) Prevalence of dementia and major subtypes in Europe: a collaborative study of population-based cohorts. Neurologic diseases in the elderly research group. Neurology 54:S4–S9
26. Lucchi L, Pascale A, Battaini F, Govoni S, Trabucchi M (1993) Cognition stimulating drugs modulate protein kinase C activity in cerebral cortex and hippocampus of adult rats. Life Sci 53:1821–1832
27. Morris R (1984) Developments of a water-maze procedure for studying spatial learning in the rat. J Neurosci Methods 11:47–60
28. Nathan PJ, Tanner S, Lloyd J, Harrison B, Curran L, Oliver C et al (2004) Effects of a combined extract of *Ginkgo biloba* and *Bacopa monniera* on cognitive function in healthy humans. Hum Psychopharmacol 19:91–96
29. O'Brien JT, Erkinjuntti T, Reisberg B, Roman G, Sawada T, Pantoni L et al (2003) Vascular cognitive impairment. Lancet Neurol 2:89–98
30. Ovsepian SV, Anwyl R, Rowan MJ (2004) Endogenous acetylcholine lowers the threshold for long-term potentiation induction in the CA1 area through muscarinic receptor activation: in vivo study. Eur J Neurosci 20:1267–1275
31. Parle M, Dhingra D, Kulkarni SK (2004) Memory-strengthening activity of *Glycyrrhiza glabra* in exteroceptive and interoceptive behavioral models. J Med Food 7:462–466
32. Prabhakar S, Saraf MK, Pandhi P, Anand A (2008) *Bacopa monniera* exerts antiamnesic effect on diazepam-induced anterograde amnesia in mice. Psychopharmacology (Berl)
33. Russo A, Borrelli F (2005) *Bacopa monniera*, a reputed nootropic plant: an overview. Phytomedicine 12:305–317
34. Sanchez G, Alvares Lde O, Oberholzer MV, Genro B, Quillfeldt J, da Costa JC et al (2009) M4 muscarinic receptors are involved in modulation of neurotransmission at synapses of Schaffer collaterals on CA1 hippocampal neurons in rats. J Neurosci Res 87:691–700
35. Sanes JR, Lichtman JW (1999) Can molecules explain long-term potentiation? Nat Neurosci 2:597–604
36. Saraf MK, Kishore K, Thomas KM, Sharma A, Singh M (2003) Role of platelet activating factor in triazolobenzodiazepines-induced retrograde amnesia. Behav Brain Res 142:31–40
37. Shanker G, Singh HK (2000) Anxiolytic profile of standardized Brahmi extract. Ind J Phamacol 32:152
38. Singh HK, Dhawan BN (1982) Effect of *Bacopa monniera* Linn. (brahmi) extract on avoidance responses in rat. J Ethnopharmacol 5:205–214
39. Singh HK, Dhawan BN (1997) Neuropsychopharmacological effects of the ayurvedic nootropic *Bacopa monniera* Linn. (Brahmi). Indian J Pharmacol 29S:359–365
40. Singh HK, Rastogi RP, Srimal RC, Dhawan BN (1988) Effects of Bacosides A and B on avoidance response in rats. Phytotherap Res 2:70–75
41. Singh RH, Singh RL (1980) Studies on the antioxidant anxiety effect of the Medhay Rasayan drug Brahmi (*Bacopa monniera* Linn)- Part II (experimental studies). J Res Ind Med Yoga Homeo 14:1–6
42. Siripurapu KB, Gupta P, Bhatia G, Maurya R, Nath C, Palit G (2005) Adaptogenic and anti-amnesic properties of *Evolvulus alsinoides* in rodents. Pharmacol Biochem Behav 81:424–432
43. Tripathi YB, Chaurasia S, Tripathi E, Upadhyay A, Dubey GP (1996) *Bacopa monniera* Linn. as an antioxidant: mechanism of action. Indian J Exp Biol 34:523–526

44. Tully T, Bourtchouladze R, Scott R, Tallman J (2003) Targeting the CREB pathway for memory enhancers. Nat Rev Drug Discov 2:267–277
45. Vohora D, Pal SN, Pillai KK (2000) Protection from phenytoin-induced cognitive deficit by *Bacopa monniera*, a reputed Indian nootropic plant. J Ethnopharmacol 71:383–390
46. Watts J, Stevens R, Robinson C (1981) Effects of scopolamine on radial maze performance in rats. Physiol Behav 26:845–851
47. Yamazaki T, Yaguchi M, Nakajima Y, Hosono T, Niiho Y, Hibi Y et al (2005) Effects of an aqueous extract of Puerariae flos (Thomsonide) on impairment of passive avoidance behavior in mice. J Ethnopharmacol 100:244–248

Neuroscience 160 (2009) 149–155

BACOPA MONNIERA ALLEVIATES N_ω-NITRO-L-ARGININE-INDUCED BUT NOT MK-801-INDUCED AMNESIA: A MOUSE MORRIS WATER MAZE STUDY

M. K. SARAF, S. PRABHAKAR AND A. ANAND*

Neuroscience Research Laboratory, Department of Neurology, Post Graduate Institute of Medical Education and Research, Sector 12, Chandigarh 160012, India

Abstract—*N*-methyl-D-aspartate (NMDA) receptor and nitric oxide syntheses are the emerging target sites for development of novel drug molecules because their modulation affects the long term potentiation (LTP) process. NMDA receptor antagonists and nitric oxide synthase inhibitors induce amnesia in animals and therefore have been employed for evaluation of efficacy of several novel antiamnesic agents. *Bacopa monniera* Linn (syn. Brahmi) is commonly used in the ancient Indian medical system for improvement of memory deficit. We have earlier described the involvement of GABAergic and cholinergic system to account for the antiamnesic effects of *B. monniera* on diazepam- and scopolamine-induced amnesia. In extension to our previous study this study was designed to investigate the downstream mechanism of *B. monniera* by evaluation of its effect on MK-801 (an NMDA receptor antagonist) and N_ω-nitro-L-arginine (L-NNA) (a nitric oxide inhibitor) induced memory deficit. We used a Morris water maze scale and compared the degree of reversal of amnesia induced by the two agents. Male Swiss albino mice were subjected to a Rotarod muscle incoordination test followed by water maze tasks. Our data revealed that L-NNA and MK-801 produced anterograde and retrograde amnesia and *B. monniera* significantly attenuated the L-NNA-induced anterograde amnesia, partially reversing L-NNA-induced retrograde amnesia. On the other hand, *B. monniera* neither attenuated the MK-801-induced anterograde amnesia nor improved retrograde amnesia caused by it. **© 2009 IBRO. Published by Elsevier Ltd. All rights reserved.**

Key words: amnesia, *Bacopa monniera*, L-NNA, MK-801, Morris water maze.

The interference in long term potentiation (LTP) (Bliss and Lomo, 1973; Kang and Lee, 2001) is documented to affect the synaptic plasticity. The blockade of postsynaptic receptors such as AMPA receptors, *N*-methyl-D-aspartate (NMDA) receptors and metabotropic receptors thus impairs the LTP and synaptic plasticity. Both competitive (i.e. AP5, NPC and 12,626) and non-competitive NMDA receptor antagonists (i.e. phencyclidine, ketamine and MK-801) block LTP induction (Bliss and Collingridge, 1993; Gruart et al., 2006; Harney et al., 2006) and produce amnesia (Bannerman et al., 1995; Han et al., 2000). MK-801, a prominent NMDA receptor blocker, is reported to impair both acquisition and retrieval in different paradigms of learning and memory (Filliat and Blanchet, 1995; Kant et al., 1996). It has, therefore, been used as an experimental drug to induce amnesia in animals for evaluation of various antiamnesic agents such as cannabinoid-rich extracts (Fadda et al., 2006), SB-399885 (Perez-Garcia and Meneses, 2005) and thioperamide (Bernaerts et al., 2004). Similarly, 7-nitro-imidazole (a nitric oxide synthase (NOS) inhibitor) has been reported to block hippocampal LTP and induce impairment of learning and memory in rats (Holscher, 1994; Sinz et al., 1999; Tong and Hamel, 1999).

In the absence of tangible results with single molecule approach, extracts comprising several molecules are now being tested for antiamnesic effects. Galantamine (a cholinesterase inhibitor), isolated from *Galanthus nivalis* and *Lycoris radiate* (Howes and Houghton, 2003; Howes et al., 2003) recently became licensed in the United Kingdom for treatment of mild to moderate Alzheimer's disease (Clegg et al., 2002; Tully et al., 2003). *Bacopa monniera* Linn (syn. Brahmi) is another such herbal drug which has been used for several centuries for treatment of neurological diseases in the Indian Ayurvedic system of medicine. *B. monniera* extract was later studied and found to reduce the level of amyloid, especially Abeta 1–40 and 1–42 in doubly transgenic mouse model of rapid amyloid deposition and brought favorable Y-maze performance and open field hyperlocomotion behavioral changes (Holcomb et al., 2006). The animal studies show that the *B. monniera* standard extract improves the cognition deficit as evaluated by various animal models. It has been shown to improve acquisition and retention in a brightness discrimination reaction task (Singh, 1997) and reverses amnesic effects of neurotoxin, scopolamine, electric-shock and immobilization stress (Bhattacharya et al., 2001) and attenuates motor learning deficit (Prakash and Sirsi, 1962). Like animal studies, the clinical studies also provide equally robust evidence of *B. monniera's* action on cognitive function (Stough et al., 2001). In a clinical study Sharma et al. reported *B. monniera's* effect on revitalizing the intellectual functions of children (Sharma, 1987). We have earlier reported that *B. monniera* attenuates both scopolamine-induced (Saraf et al., 2007) and diazepam-induced memory deficit (Prabhakar et al., 2008) which suggests the involvement of cholinergic and GABAergic system in modulation of learning and memory (Saraf et al., 2008). Since NMDA receptor and NOS are the important components of LTP, this study was designed to test the downstream effects of *B. monniera* on MK-801 (NMDA antagonist) and N_ω-nitro-L-arginine (L-NNA; NOS inhibitor)-induced amnesia.

*Corresponding author. Tel: +91-172-2756094; fax: +91-172-2748399.
E-mail address: akshay1anand@rediffmail.com (A. Anand); URL: http://www.pgimer.nic.in/Akshay%20Anand.htm.

Abbreviations: ELT, escape latency time; L-NAME, N^G-nitro-L-arginine methyl ester; L-NNA, N_ω-nitro-L-arginine; LTP, long term potentiation; NMDA, *N*-methyl-D-aspartate; NOS, nitric oxide synthase; Q (with number), quadrant.

0306-4522/09 $ - see front matter © 2009 IBRO. Published by Elsevier Ltd. All rights reserved.
doi:10.1016/j.neuroscience.2009.02.005

EXPERIMENTAL PROCEDURES

Male Swiss albino mice were used in the present study. They were housed in an animal house with free access to water and standard diet, and exposed to a 12-h light/dark cycle. The experiments were conducted between 09:00 and 18:00 h in a semi-soundproof laboratory. L-NNA and MK-801 were dissolved in normal saline. Standardized extract of *Bacopa monniera*, containing 55.35% bacosides, was suspended in Tween 80 (5% v/v in normal saline).

Behavioral evaluation

Morris water maze was employed to evaluate learning and memory (Morris, 1984). This model has several advantages over other models including the radial arm maze. These include (1) absence of motivational stimuli such as food and water deprivation, electrical stimulations and buzzer sounds which are required in active/passive avoidance tasks and may interfere the normal process of memory; these are not required in this setup; (2) animals can be trained in a shorter time (1 week) while the arm maze studies require several weeks of training; (3) intra-maze cues like odor trains are eliminated in the pool; (4) larger dose response studies can be conducted in a week's time; and (5) from a theoretical point of view, the water maze is an aversively motivated task, while the arm maze is appetitive motivated task. This test allows studies of spatial working memory and reference memory (Vogel, 2002). Olton and coworkers had suggested the role of the hippocampus in spatial memory using these behavioral tests (Olton and Samuelson, 1976; Olton et al., 1979). It has, therefore, been extensively used for evaluation of spatial memory deficit (Bermudez-Rattoni et al., 1991; McNamara and Skelton, 1991, 1992; Anand et al., 2007) induced by benzodiazepine (McNamara and Skelton, 1992; Shimizu et al., 1998; Saraf et al., 2003; Anand et al., 2007). This model suitably combines evaluation of both spatial memory along with locomotor activity. Therefore, it can be used for evaluation of drugs which not only affect spatial memory but also impair locomotor activity.

It consists of a circular water tank filled with water that is made opaque with a white-colored dye. The tank was divided into four equal quadrants with the help of two threads, running at right angle to each other over the rim of the pool. A tiny platform (10 cm^2) was placed 1 cm below the level of water in the center of one of these four quadrants designated as target quadrant. The position of platform was kept unaltered throughout all the training sessions. In the present study, quadrant 2 (Q2) was considered as the target quadrant. Each animal was subjected to four consecutive trials on each day with a gap of 5 min, during which they were allowed to escape on to the hidden platform. In case the animal was unable to locate the hidden platform within 120 s period, it was gently guided to the platform and allowed to remain there for 20 s. Escape latency time (ELT), as a quantitative measure to locate the hidden platform in water maze, was noted as the index of acquisition. Each animal was subjected to the four acquisition trials per day for six consecutive days. On seventh day, platform was removed and time spent by the animal in each of four quadrants (Q1, Q2, Q3, Q4) was noted. The time spent by the animal in target quadrant searching for the hidden platform was noted as an index of retrieval.

In order to study the effect of drug on acquisition, drug solution was administered before acquisition trials for six consecutive days and the diluent was administered before retrieval trial on day 7. Drug solution was administered before retrieval trial on day 7 to study its effect on retrieval of memory. The experimental mice were screened with a Rota-rod to test the muscle coordination activity of mice before conducting the maze experiments (Ghelardini et al., 2002). Mice, showing abnormal swimming pattern in water maze, and low muscle coordination activity in Rota-rod test were excluded from study. Each group comprised seven mice.

Mice in group I were administered normal saline (10 ml kg^{-1}) intraperitoneally 30 min before acquisition (day 1–6) and retrieval trial (day 7). Five percent Tween 80 was used as a diluent for preparation of *B. monniera* suspension. Group II mice were administered 5% Tween 80 (10 ml kg^{-1}) orally 60 min before acquisition and retrieval trial to record the per se effect of 10% Tween 80 on normal acquisition and retrieval of memory. Group III mice were treated with L-NNA (30 mg kg^{-1} i.p.) 30 min before acquisition trials and normal saline (10 ml kg^{-1} i.p.) 30 min before retrieval trial. Group IV mice were administered normal saline (10 ml kg^{-1} i.p.) 30 min before acquisition trials and L-NNA (30 mg kg^{-1} i.p.) 30 min before retrieval trial in order to evaluate the effect of L-NNA on retrieval process. Group V mice were administered standardized extract of *B. monniera* (80 mg kg^{-1} oral) 60 min before and L-NNA (30 mg kg^{-1} i.p.) 30 min before acquisition trials. group VI mice were treated with 5% Tween 80 (10 ml/kg i.p.) 60 min before and normal saline (10 ml/kg i.p.) 30 min before acquisition trials, and standardized extract of *B. monniera* (80 mg kg^{-1} oral) and L-NNA (30 mg kg^{-1} i.p.) were administered 60 and 30 min before retrieval trial respectively. group VII, VIII and IX mice were treated with varying doses of MK-801, i.e. 0.25, 0.17 and 0.1 mg/kg^{-1} i.p. 30 min before acquisition trials and normal saline (10 ml kg^{-1} i.p.) 30 min before retrieval trial. Group X mice were administered normal saline (10 ml kg^{-1} i.p.) 30 min before acquisition trials and MK-801 (0.25 mg kg^{-1} i.p.) 30 min before retrieval trial in order to evaluate its effect on retrieval process. Group XI mice were administered standardized extract of *B. monniera* (120 mg kg^{-1} oral) 60 min before and MK-801 (0.17 mg kg^{-1} i.p.) 30 min before acquisition trials. Group XII mice were treated with 5% Tween 80 (10 ml/kg i.p.) 60 min before and normal saline (10 ml/kg i.p.) 30 min before acquisition trials, and standardized extracts of *B. monniera* (120 mg kg^{-1} oral) and MK-801 (0.25 mg kg^{-1} i.p.) were administered 60 and 30 min before retrieval trial respectively. We also studied per se the effect of *B. monniera* on acquisition and retrieval of memory in group XIII and XIV mice with *B. monniera* suspension 80 and 120 mg kg^{-1} orally respectively 60 min before and normal saline (10 ml kg^{-1} i.p.) 30 min before trials.

Statistical analysis

We have analyzed the behavioral results of the Morris water maze using SPSS statistical software and applied one-way ANOVA followed by Tukey's post hoc analysis at $P<0.05$ for multiple comparisons among the groups. During retrieval trials, each value represents mean±SEM.

RESULTS

B. monniera reverses L-NNA induced amnesia

L-NNA (30 mg kg^{-1} i.p.) did not lead to a progressive decrease in ELT during successive acquisition trials ($F=0.46$ and P-values were 0.96, 0.88, 0.76, 0.86. 0.8 on day 2 to day 6 respectively) as compared to day 1 ELT. ELT of the L-NNA-treated group was significantly different from the ELT of the control group on day 3 ($F=3.0$), day 4 ($F=4.5$) and day 5 ($F=6.9$) at $P<0.05$ (Fig. 1a). L-NNA (30 mg kg^{-1} i.p.)-treated mice did not spend more time in the target quadrant ($F=1.81$ and P-values were 0.99, 0.5, 0.25 versus Q1, Q3 and Q4 respectively). L-NNA reduced the time an animal spent in the target quadrant ($F=2.74$ at $P<0.05$) as compared to control (Fig. 1b). These observations suggest that L-NNA impairs the process of acquisition of new memory by producing anterograde amnesia and it also produces retrograde amnesia by impairing retrieval process of the trained mice. *B. monniera* (80 mg kg^{-1} oral) administration progressively decreased ELT in L-NNA (30 mg kg^{-1} i.p.)-treated mice with ongoing acquisition trials

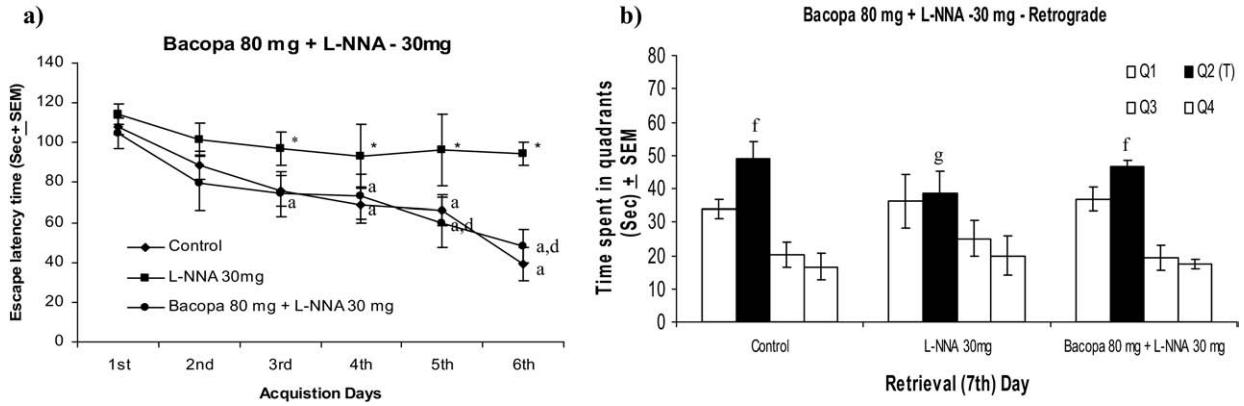


Fig. 1. *B. monniera* attenuates L-NNA-induced anterograde amnesia and retrograde amnesia. In acquisition trials, each value represents mean ELT±SEM. Control group shows significant ($F=17.42$, $P<0.05$ versus day 1) gradual reduction in ELT with acquisition days as compared to day 1 ELT. (a) L-NNA (30 mg/kg i.p.) impairs acquisition ($F=3.0$, 4.5, 6.9 on days 4–6 respectively at $P<0.05$) as compared to control which is reversed ($F=3.04$, $P<0.05$) by *B. monniera* (80 mg/kg oral). (b) L-NNA impairs ($F=2.74$ at $P<0.05$) retrieval of memory as compared to control. *B. monniera* partially reverses L-NNA-induced retrograde amnesia as compared to L-NNA group. ANOVA, followed by post hoc "Tukey" analysis at $P<0.05$ was applied for multiple comparisons among the groups. "a" Indicates significance of a particular day's ELT (i.e. ELT of day 2–day 6) versus ELT on day 1 of same group. "*" Indicates significance of particular day of ELT versus same-day control group's ELT. "d" Indicates significance of ELT of particular day versus same day's ELT of L-NNA. "f" Indicates significance of time spent of target quadrant as compared to other quadrants, i.e. Q1, Q3 and Q4. "g" Indicates significance versus control group's time spent in target quadrant (Q2).

($F=3.04$, $P<0.05$) as compared to day 1 and reversed the L-NNA—induced impairment of progressive decrease in ELT with ongoing acquisition trials (Fig. 1a). *B. monniera* (80 mg kg^{-1} oral) also increased preferential stay of L-NNA (30 mg kg^{-1} i.p.)-treated mice in target quadrant ($F=29.05$ and *P*-values were 0.12, 0.0, 0.0 versus Q1, Q3 and Q4 respectively). The *F* and "*P*" value was 2.74 and 0.22 respectively at the time of post hoc "LSD" analysis while these values were 2.74 and 0.805 respectively, when post hoc "Tukey" analysis was done (Fig. 1b). Together these findings suggest that *B. monniera* reverses L-NNA induced anterograde amnesia as well as partially relieving retrograde amnesia.

The control mice showed expected decrease in ELT ($F=17.42$, $P<0.05$ versus day 1) with successive acquisition trials (Figs. 1a, 2a–e, 3a) and enhancement in time spent in the target quadrant ($F=12.30$, $P<0.05$ vs. Q1, Q2, Q3) as compared to the time spent in the other quadrants during retrieval trial (Figs. 1b, 1e, 2b, 3b).

B. monniera does not attenuate MK-801-induced amnesia

MK-801, at 0.25 mg kg^{-1} i.p. ($F=1.46$; $P=0.9$, 0.6, 0.25, 0.97, 0.56 on days 2–6 respectively versus day 1) and 0.17 mg kg^{-1} i.p. ($F=1.37$; $P=0.64$, 0.53, 0.16, 0.95, 0.71 on days 2–6 respectively versus day 1) did not alter the ELT during successive acquisition trials as compared to day 1. ELT of these mice were significantly different from control mice ($F=3.09$, 4.53, 6.93 on day 4 to day 6 respectively, $P<0.05$) (Fig. 2a, b). The lower dose of MK-801 (0.1 mg kg^{-1} i.p.) did not impair the progressive decrease in ELT ($F=22.1$, $P=0.9$, 0.45, 0.0, 0.0, 0.0 on days 2–6 versus day 1), because it did not produce anterograde amnesia (Fig. 2c). MK-801 (0.25 mg kg^{-1} i.p.) significantly reduced ($F=2.74$, $P<0.05$ versus control) the preferential stay of mice in the target quadrant (Q2) during the retrieval trial as compared to the control group (Fig. 2e). These observations suggest that MK-801 impairs the process of acquisition of new memory by producing anterograde amnesia. It also produces retrograde amnesia by impairing retrieval process of trained mice. *B. monniera* (120 mg kg^{-1} oral) did not alter MK-801 (0.17 mg kg^{-1} i.p.)-induced impairment of a progressive decrease in ELT ($F=1.48$, $P=0.9$, 0.6, 0.4, 0.79, 0.27 on days 2–6 respectively versus day 1; $F=1.0$ at $P=1$ on day 1, $F=1.3$ at $P=0.97$ on day 2, $F=2.2$ at $P=0.3$ on day 3, $F=3.1$ at $P=0.76$ on day 4, $F=4.5$ at $P=0.98$ on day 5, $F=6.9$ at $P=0.3$ on day 6 versus MK-801-treated group) with ongoing acquisition trials (Fig. 2d). It also did not enhance ($F=2.74$, $P=0.77$) the preferential stay of mice in the target quadrant (Q2) during the retrieval trial with amnesia induced by MK-801 at 0.25 mg kg^{-1} i.p. (Fig. 2e).

B. monniera and 5% Tween 80 per se effect

Five percent Tween 80 ($F=20.28$, $P<0.05$) and *B. monniera* (120 mg kg^{-1} oral, $F=16.25$, $P<0.05$; 80 mg kg^{-1} oral, $F=4.65$, $P<0.05$ versus day 1) significantly reduced the ELT as compared to day 1 just like the control mice. These mice did not spend more time (*F*-values were 35.15, 11.39. 4.39 respectively for Tween 80, *B. monniera* 120 and 80 mg kg^{-1} group) in the target quadrant. Therefore, these mice did not significantly affect normal acquisition (Fig. 3a) and retrieval of memory (Fig. 3b) as compared to control mice.

DISCUSSION

NOS is an integral component of retrograde messenger system, i.e. a nitric oxide–mediated pathway of LTP. NOS is inhibited by *N*G-nitro-L-arginine methyl ester (L-NAME), *N*-monomethyl-L-arginine (L-NMMA), Nw-nitro-L-arginine and 7-nitroindazole. There are several reports which suggest that the inhibition of NO synthesis produces amnesia

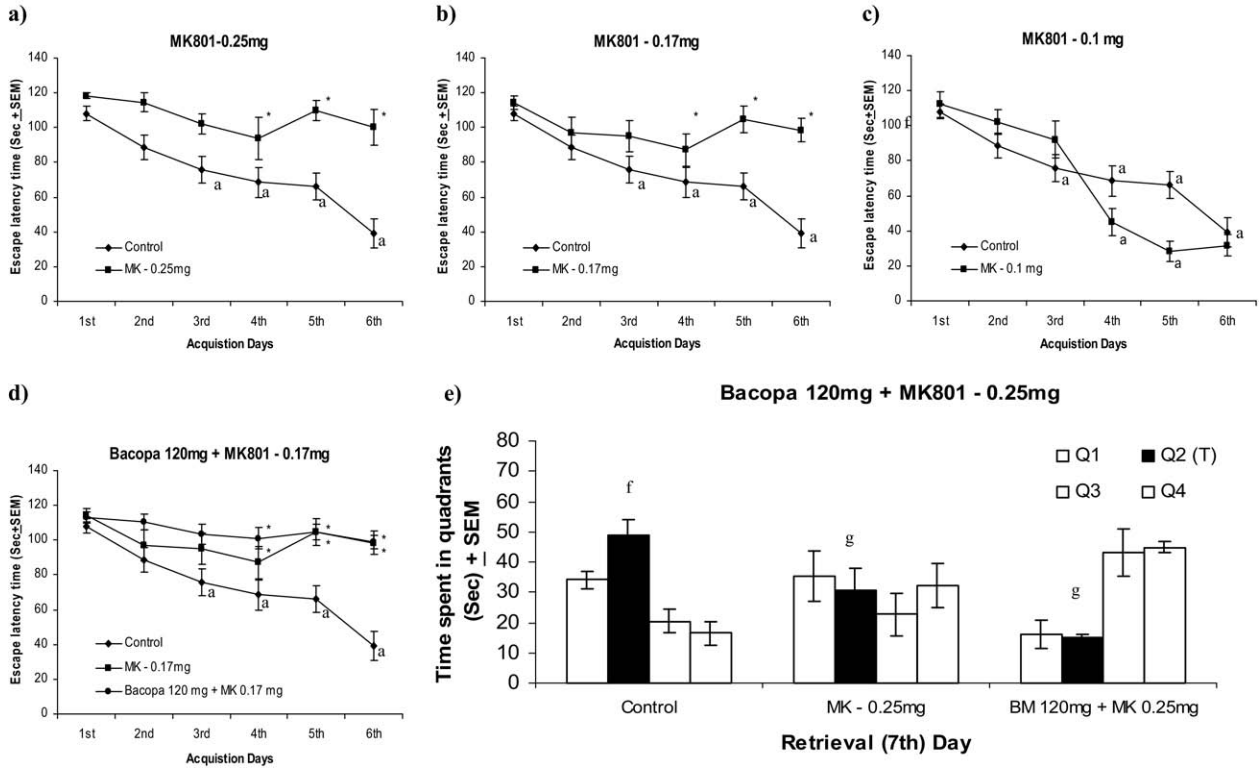


Fig. 2. *B. monniera* did not alleviate MK-801-induced anterograde and retrograde amnesia. In acquisition trials, each value represents mean ELT±SEM. Control group shows significant gradual reduction in ELT with acquisition days as compared to day 1 ELT. (a–c) MK-801 at 0.17 mg/kg and 0.25 mg/kg i.p. impairs ($F=3.09, 4.53, 6.93$ on day 4 to day 6 respectively, $P<0.05$) the gradual decrease in ELT and produces anterograde amnesia as compared to control. MK-801 at 0.1 mg/kg i.p. shows a decrease in ELT and does not impair the acquisition of memory as compared to control. (d) *B. monniera* at 120 mg/kg oral did not attenuate anterograde amnesia induced by MK-801 (0.17 mg/kg i.p.). (e) MK-801 0.25 mg/kg i.p. significantly impaired ($F=2.74$, $P<0.05$) retrieval of memory as compared to control. *B. monniera* did not attenuate the MK-801-induced retrograde amnesia. ANOVA, followed by post hoc "Tukey" analysis at $P<0.05$ was applied for multiple comparisons among the groups. "a" Indicates significance of particular day's ELT (i.e. ELT of day 2–day 6) versus ELT on day 1 of same group. "*" Indicates significance at $P<0.05$ of particular day of ELT versus same-day control group's ELT. "d" Indicates significance of ELT of particular day versus same day's ELT of MK-801. "f" Indicates significance versus time spent in other quadrants, i.e. Q1, Q3 and Q4. "g" Indicates significance versus control group's time spent in target quadrant (Q2). "h" Indicates significance versus MK-801 group's time spent in target quadrant (Q2).

(Holscher, 1994), disrupts spatial learning and olfactory memory (Bohme et al., 1993; Hawkins et al., 1998), blunts behavioural performance during task acquisition and decreases locomotor activity in habituation tasks (Yamada et al., 1995). Aminoguanidine and L-*N*-iminoethyl-lysine, NOS inhibitors, are also found to exacerbate similar deficits in cognitive performance during Morris water maze test (Sinz et al., 1999). Similarly, nitro-arginine (NO-arg), a NOS inhibitor, produces retrograde amnesia in the inhibitory avoidance task (Bernabeu et al., 1995). In this study we report that L-NNA, another NOS inhibitor, produced anterograde amnesia because its administration before acquisition trials significantly attenuated the normal decrease in ELT during ongoing acquisition trials. It also produced retrograde amnesia because its administration before retrieval trial prevented the preferential stay of mice in target quadrant during retrieval trial. This suggests that L-NNA produces both anterograde and retrograde amnesia.

NMDA receptor is another important component of LTP which is required for induction and maintenance of LTP. NMDA antagonist blocks LTP induction (Bliss and Collingridge, 1993; Sinz et al., 1999; Izumi et al., 2005; Parwani et al., 2005; Gruart et al., 2006; Harney et al., 2006; Satou et al., 2006) and produces amnesia as shown by various behavioral experiments (Bannerman et al., 1995; Saucier and Cain, 1995; Han et al., 2000; Zhang et al., 2001; Pedreira et al., 2002; Si et al., 2004). Our investigations revealed that MK-801 produced anterograde amnesia by impairing gradual reduction in ELT. It is known that retrograde amnesia caused by MK-801 and TCP, the two NMDA receptor antagonists, induces impairment in acquisition and retrieval (Filliat and Blanchet, 1995; Kant et al., 1996). Similarly, other NMDA antagonists also show amnesic properties, for example, HA-966 impairs visual recognition memory in rhesus monkeys (Matsuoka and Aigner, 1996) and CPP [(±)-3-(2-carboxypiperazin-4-yl)-propyl-1-phosphonic acid] impairs the memory in passive avoidance tasks (Mohamed et al., 2000).

B. monniera

Linn (syn. *B. monniera* Wettst, *Herpestis monniera* Linn.) is a very popular and frequently used drug by alternative medicine practitioners in India. It has been used as a

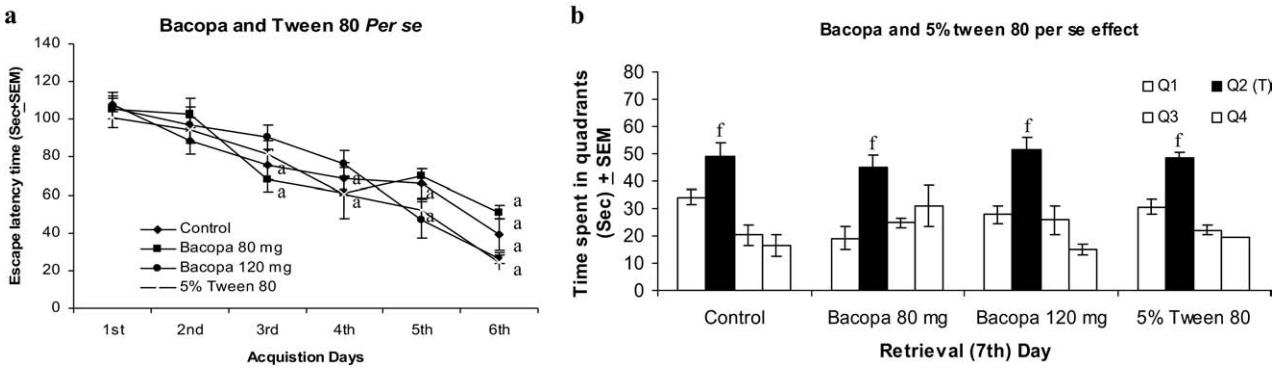


Fig. 3. Effect of *B. monniera* on normal acquisition and retrieval of memory. In acquisition trials, each value represents mean ELT±SEM. Control group shows gradual reduction in ELT with acquisition days as compared to day 1 ELT. (a) *B. monniera* at 80 and 120 mg/kg does not alter acquisition as compared to control. Similarly 5% Tween 80 does not alter an acquisition as compared to control. (b) *B. monniera* at 80 and 120 mg/kg oral and 5% Tween 80 do not affect the retrieval as compared to control. ANOVA, followed by post hoc "Tukey" test was applied at $P<0.05$ for multiple comparisons among the groups. "a" Indicates significance at $P<0.05$ of particular day's ELT (i.e. ELT of day 2–day 6) versus ELT on day 1 of same group. "*" Indicates significance at $P<0.05$ of particular day of ELT versus same-day control group's ELT. "g" Indicates significance at $P<0.05$ versus control group's time spent in target quadrant (Q2).

memory-enhancing agent in the centuries-old Ayurvedic system. Its beneficial effects have been attributed to the active constituent saponin, as bacosides A (Chatterji et al., 1965), bacoside B (Dhawan and Singh, 2002), and bacosaponins (Garai et al., 1996a,b). The exact mechanism of action of *B. monniera* is not known, however, there is evidence that its mechanism of action could be attributed to a combination of cholinergic modulation (Das et al., 2002; Kishore and Singh, 2005) and antioxidant effects (Bhattacharya et al., 2000). However, there are also reports where it is shown to improve the cognitive deficit possibly by exhibiting free radical scavenging and anti-lipid peroxidative effects (Anbarasi et al., 2006b). In earlier studies we have shown that *B. monniera* reverses both scopolamine-induced (Saraf et al., 2007) and diazepam-induced memory deficit (Prabhakar et al., 2008) which suggests the involvement of a cholinergic and GABAergic system in modulation of learning and memory (Saraf et al., 2008). In order to understand the downstream effect of *B. monniera*, we examined the antiamnesic effects of *B. monniera* on MK-801- and L-NNA-induced deficits in memory. We found that *B. monniera* acts to significantly mask the L-NNA-induced anterograde amnesia while only partially attenuating retrograde amnesia induced by it, however, it was not able to relieve the amnesic effects caused by MK-801.

Several traditional drugs including Chinese herbs such as *Achyranthes bidentata*, *Ophiopogon japonicus*, and *Cnidium monnieri* have been reported to ameliorate MK-801-induced amnesia by using a passive avoidance task in rats (Lin et al., 2003). In contrast to the Chinese study our report revealed that *B. monniera* did not attenuate MK-801-induced anterograde amnesia even at higher doses. *B. monniera* failed to reverse retrograde amnesia induced by MK-801 as evidenced by lack of significant improvement of preferential stay of mice in the target quadrant. No per se effect of vehicles (such as 5% Tween 80) and *B. monniera* (80 and 120 mg kg^{-1} oral) was observed on normal acquisition and retrieval of memory. The fact that 80 mg/kg oral dose of *B. monniera* could reverse L-NNA-induced amnesia and a higher dose of 120 mg/kg could not attenuate the MK-801-induced amnesia indicates that *B. monniera* exerts an antiamnesic effect by relieving the NOS inhibitory effects of L-NNA and not by acting at NMDA receptors. It is possible that *B. monniera* restores the release of nitric oxide by reducing the inhibition of NOS activity, possibly maintaining the neuronal LTP process. Pitsikas et al. (2003) reported that molsidomine, a nitric oxide donor, was able to attenuate NOS inhibitor (i.e. L-NAME)–induced acquisition deficits (Pitsikas et al., 2003) and age-related memory deficits (Pitsikas et al., 2005). On the other hand NOS inhibitors (i.e. aminoguanidine and L-*N*-iminoethyl-lysine) were responsible for increasing neuronal loss in vulnerable regions (CA3 and CA1) of hippocampus in rats (Sinz et al., 1999) and exacerbating the deficits in cognitive performance during Morris water maze tests. It is possible that L-NNA increases the endogenous neuronal loss which is ameliorated by *B. monniera* by reviving the neuronal activity required for normal a LTP mechanism. This is supported by the report where *B. monniera* has been shown to reduce brain damage and neuronal apoptosis during cigarette smoking (Anbarasi et al., 2006a). Creatine kinase, a sensitive marker of cerebral brain damage, is also reported to be downregulated by it. *B. monniera* protects the brain from oxidative damage (Dhanasekaran et al., 2007) by maintaining the functional integrity of mitochondria (Anbarasi et al., 2005b) and membrane ionic balance (Anbarasi et al., 2005a), as well as by augmenting the antioxidative defense system (Anbarasi et al., 2006b) which could be helpful in rescue of memory loss. However, this needs detailed evaluation but it appears certain that *B. monniera* is not able to delink the MK-801 from its NMDA receptor thereby affecting the successful restoration of LTP. We therefore postulate that the NOS-mediated pathway plays a more dominant role in *B. monniera*–mediated reversal of amnesia.

CONCLUSION

We conclude that *B. monniera* has the capacity to attenuate the anterograde amnesia induced by L-NNA without engaging the NMDA pathway.

Acknowledgments—This study was supported by the Department of Biotechnology, New Delhi, India.

REFERENCES

Anand A, Saraf MK, Prabhakar S (2007) Sustained inhibition of brotizolam induced anterograde amnesia by norharmane and retrograde amnesia by L-glutamic acid in mice. Behav Brain Res 182:12–20.

Anbarasi K, Kathirvel G, Vani G, Jayaraman G, Shyamala Devi CS, 2006a) Cigarette smoking induces heat shock protein 70 kDa expression and apoptosis in rat brain: modulation by bacoside A. Neuroscience 138:1127–1135.

Anbarasi K, Vani G, Balakrishna K, Devi CS (2006b) Effect of bacoside A on brain antioxidant status in cigarette smoke exposed rats. Life Sci 78:1378–1384.

Anbarasi K, Vani G, Balakrishna K, Devi CS (2005a) Effect of bacoside A on membrane-bound ATPases in the brain of rats exposed to cigarette smoke. J Biochem Mol Toxicol 19:59–65.

Anbarasi K, Vani G, Devi CS (2005b) Protective effect of bacoside A on cigarette smoking-induced brain mitochondrial dysfunction in rats. J Environ Pathol Toxicol Oncol 24:225–234.

Bannerman DM, Good MA, Butcher SP, Ramsay M, Morris RG (1995) Distinct components of spatial learning revealed by prior training and NMDA receptor blockade. Nature 378:182–186.

Bermudez-Rattoni F, Introini-Collison IB, McGaugh JL (1991) Reversible inactivation of the insular cortex by tetrodotoxin produces retrograde and anterograde amnesia for inhibitory avoidance and spatial learning. Proc Natl Acad Sci U S A 88:5379–5382.

Bernabeu R, de Stein ML, Fin C, Izquierdo I, Medina JH (1995) Role of hippocampal NO in the acquisition and consolidation of inhibitory avoidance learning. Neuroreport 6:1498–1500.

Bernaerts P, Lamberty Y, Tirelli E (2004) Histamine H3 antagonist thioperamide dose-dependently enhances memory consolidation and reverses amnesia induced by dizocilpine or scopolamine in a one-trial inhibitory avoidance task in mice. Behav Brain Res 154:211–219.

Bhattacharya SK, Bhattacharya A, Kumar A, Ghosal S (2000) Antioxidant activity of Bacopa monniera in rat frontal cortex, striatum and hippocampus. Phytother Res 14:174–179.

Bhattacharya SK, Kumar A, Ghosal S (2001) Effect of *Bacopa monniera* on animal models of Alzheimer's disease and perturbed central cholinergic markers of cognition in rats. In: Emerging drugs—molecular aspects of Asian medicines, vol. 1 (Mori A, Satoh T, eds), pp 21–32. Westbury, NY: PJD Publications.

Bliss TV, Collingridge GL (1993) A synaptic model of memory: long-term potentiation in the hippocampus. Nature 361:31–39.

Bliss TV, Lomo T (1973) Long-lasting potentiation of synaptic transmission in the dentate area of the anaesthetized rabbit following stimulation of the perforant path. J Physiol 232:331–356.

Bohme GA, Bon C, Lemaire M, Reibaud M, Piot O, Stutzmann JM, Doble A, Blanchard JC (1993) Altered synaptic plasticity and memory formation in nitric oxide synthase inhibitor-treated rats. Proc Natl Acad Sci U S A 90:9191–9194.

Chatterji N, Rastogi RP, Dhar ML (1965) Chemical examination of *Bacopa monniera* Wettst. Part II. The constitution of bacoside A. Ind J Chem 3:24–29.

Clegg A, Bryant J, Nicholson T, McIntyre L, De Broe S, Gerard K, Waugh N (2002) Clinical and cost-effectiveness of donepezil, rivastigmine, and galantamine for Alzheimer's disease. A systematic review. Int J Technol Assess Health Care 18:497–507.

Das A, Shanker G, Nath C, Pal R, Singh S, Singh H (2002) A comparative study in rodents of standardized extracts of Bacopa monniera and Ginkgo biloba: anticholinesterase and cognitive enhancing activities. Pharmacol Biochem Behav 73:893–900.

Dhanasekaran M, Tharakan B, Holcomb LA, Hitt AR, Young KA, Manyam BV (2007) Neuroprotective mechanisms of ayurvedic antidementia botanical Bacopa monniera. Phytother Res 21:965–969.

Dhawan BN, Singh HK (2002) Nootropic and some other effects of *Bacopa monniera* Linn. (Brahmi) Ann Neurosci 6:34–40.

Fadda P, Robinson L, Fratta W, Pertwee RG, Riedel G (2006) Scopolamine and MK801-induced working memory deficits in rats are not reversed by CBD-rich cannabis extracts. Behav Brain Res 168:307–311.

Filliat P, Blanchet G (1995) Effects of TCP on spatial memory: comparison with MK-801. Pharmacol Biochem Behav 51:429–434.

Garai S, Mahato SB, Ohtani K, Yamasaki K (1996a) Bacopasaponin D—a pseudojujubogenin glycoside from Bacopa monniera. Phytochemistry 43:447–449.

Garai S, Mahato SB, Ohtani K, Yamasaki K (1996b) Dammarane-type triterpenoid saponins from Bacopa monniera. Phytochemistry 42: 815–820.

Ghelardini C, Galeotti N, Gualtieri F, Romanelli MN, Bucherelli C, Baldi E, Bartolini A (2002) DM235 (sunifiram): a novel nootropic with potential as a cognitive enhancer. Naunyn Schmiedebergs Arch Pharmacol 365:419–426.

Gruart A, Munoz MD, Delgado-Garcia JM (2006) Involvement of the CA3-CA1 synapse in the acquisition of associative learning in behaving mice. J Neurosci 26:1077–1087.

Han CJ, Pierre-Louis J, Scheff A, Robinson JK (2000) A performance-dependent adjustment of the retention interval in a delayed nonmatching-to-position paradigm differentiates effects of amnestic drugs in rats. Eur J Pharmacol 403:87–93.

Harney SC, Rowan M, Anwyl R (2006) Long-term depression of NMDA receptor-mediated synaptic transmission is dependent on activation of metabotropic glutamate receptors and is altered to long-term potentiation by low intracellular calcium buffering. J Neurosci 26:1128–1132.

Hawkins RD, Son H, Arancio O (1998) Nitric oxide as a retrograde messenger during long-term potentiation in hippocampus. Prog Brain Res 118:155–172.

Holcomb LA, Dhanasekaran M, Hitt AR, Young KA, Riggs M, Manyam BV (2006) Bacopa monniera extract reduces amyloid levels in PSAPP mice. J Alzheimers Dis 9:243–251.

Holscher C (1994) Inhibitors of metabotropic glutamate receptors produce amnestic effects in chicks. Neuroreport 5:1037–1040.

Howes MJ, Houghton PJ (2003) Plants used in Chinese and Indian traditional medicine for improvement of memory and cognitive function. Pharmacol Biochem Behav 75:513–527.

Howes MJ, Perry NS, Houghton PJ (2003) Plants with traditional uses and activities, relevant to the management of Alzheimer's disease and other cognitive disorders. Phytother Res 17:1–18.

Izumi Y, Izumi M, Matsukawa M, Funatsu M, Zorumski CF (2005) Ammonia-mediated LTP inhibition: effects of NMDA receptor antagonists and L-carnitine. Neurobiol Dis 20:615–624.

Kang KR, Lee SY (2001) Effect of serum and hydrogen peroxide on the Ca^{2+}/calmodulin-dependent phosphorylation of eukaryotic elongation factor 2(eEF-2) in Chinese hamster ovary cells. Exp Mol Med 33:198–204.

Kant GJ, Wylie RM, Vasilakis AA, Ghosh S (1996) Effects of triazolam and diazepam on learning and memory as assessed using a water maze. Pharmacol Biochem Behav 53:317–322.

Kishore K, Singh M (2005) Effect of bacosides, alcoholic extract of Bacopa monniera Linn. (Brahmi), on experimental amnesia in mice. Indian J Exp Biol 43:640–645.

Lin YC, Wu CR, Lin CJ, Hsieh MT (2003) The ameliorating effects of cognition-enhancing Chinese herbs on scopolamine- and MK-801-induced amnesia in rats. Am J Chin Med 31:543–549.

Matsuoka N, Aigner TG (1996) The glycine/NMDA receptor antagonist HA-966 impairs visual recognition memory in rhesus monkeys. Brain Res 731:72–78.

McNamara RK, Skelton RW (1991) Diazepam impairs acquisition but not performance in the Morris water maze. Pharmacol Biochem Behav 38:651–658.

McNamara RK, Skelton RW (1992) Like diazepam, CL 218,872, a selective ligand for the benzodiazepine omega 1 receptor subtype, impairs place learning in the Morris water maze. Psychopharmacology (Berl) 107:347–351.

Mohamed AF, Matsumoto K, Tabata K, Takayama H, Kitajima M, Watanabe H (2000) Effects of Uncaria tomentosa total alkaloid and its components on experimental amnesia in mice: elucidation using the passive avoidance test. J Pharm Pharmacol 52:1553–1561.

Morris R (1984) Developments of a water-maze procedure for studying spatial learning in the rat. J Neurosci Methods 11:47–60.

Olton DS, Becker J, Handelman G (1979) Hippocampus. Space and memory. Behav Brain Sci 2:313–365.

Olton DS, Samuelson RJ (1976) Remembrance of places passed: spatial memory in rats. Exp Psychol An Behav Proc 2:97–116.

Parwani A, Weiler MA, Blaxton TA, Warfel D, Hardin M, Frey K, Lahti AC (2005) The effects of a subanesthetic dose of ketamine on verbal memory in normal volunteers. Psychopharmacology 183:265–274.

Pedreira ME, Perez-Cuesta LM, Maldonado H (2002) Reactivation and reconsolidation of long-term memory in the crab Chasmagnathus: protein synthesis requirement and mediation by NMDA-type glutamatergic receptors. J Neurosci 22:8305–8311.

Perez-Garcia G, Meneses A (2005) Oral administration of the 5-HT6 receptor antagonists SB-357134 and SB-399885 improves memory formation in an autoshaping learning task. Pharmacol Biochem Behav 81:673–682.

Pitsikas N, Rigamonti AE, Cella SG, Muller EE (2003) The 5-HT 1A receptor antagonist. WAY 100635 improves rats performance in different models of amnesia evaluated by the object recognition task. Brain Res 983:215–222.

Pitsikas N, Rigamonti AE, Cella SG, Sakellaridis N, Muller EE (2005) The nitric oxide donor molsidomine antagonizes age-related memory deficits in the rat. Neurobiol Aging 26:259–264.

Prabhakar S, Saraf MK, Pandhi P, Anand A (2008) *Bacopa* monniera exerts antiamnesic effect on diazepam-induced anterograde amnesia in mice. Psychopharmacology 200:27–37.

Prakash JC, Sirsi M (1962) Comparative study of the effects of Brahmi (*Bacopa monniera*) and chlorpromazine on motor learning in rats. J Sci Ins Res 21:93–96.

Saraf MK, Kishore K, Thomas KM, Sharma A, Singh M (2003) Role of platelet activating factor in triazolobenzodiazepines-induced retrograde amnesia. Behav Brain Res 142:31–40.

Saraf MK, Prabhakar S, Anand A (2008) A possible link between cholinergic and GABAergic system in induction of amnesia. Proceedings of the 18th meeting of the European Neurological Society, Journal of Neurology, Nice, France. Springer, 255, pp 163.

Saraf MK, Prabhakar S, Khanduja KL, Anand A (2007) Antiamnesic action of *Bacopa* monniera is mediated through protein kinase-CREB. In: Pathway in amnesic mice induced by scopolamine. Proceedings of the Society for Neuroscience, San Diego, CA, USA, pp 156.119/U153.

Satou M, Hoshikawa R, Sato Y, Okawa K (2006) An in vitro study of long-term potentiation in the carp (Cyprinus carpio L.) olfactory bulb. J Comp Physiol A Neuroethol Sens Neural Behav Physiol 192:135–150.

Saucier D, Cain DP (1995) Spatial learning without NMDA receptor-dependent long-term potentiation. Nature 378:186–189.

Sharma R, Chaturvedi C, Tewari PV (1987) Efficacy of *Bacopa monniera* in revitalizing intellectual functions in children. J Res Edu Ind Med 23:1–12.

Shimizu K, Matsubara K, Uezono T, Kimura K, Shiono H (1998) Reduced dorsal hippocampal glutamate release significantly correlates with the spatial memory deficits produced by benzodiazepines and ethanol. Neuroscience 83:701–706.

Si K, Lindquist S, Kandel E (2004) A possible epigenetic mechanism for the persistence of memory. Cold Spring Harb Symp Quant Biol 69:497–498.

Singh HK, Dhawan BN (1997) Neuropsychopharmacological effects of the ayurvedic nootropic *Bacopa monniera* Linn. (Brahmi) Ind. J Pharmacol 29S:359–365.

Sinz EH, Kochanek PM, Dixon CE, Clark RS, Carcillo JA, Schiding JK, Chen M, Wisniewski SR, Carlos TM, Williams D, DeKosky ST, Watkins SC, Marion DW, Billiar TR (1999) Inducible nitric oxide synthase is an endogenous neuroprotectant after traumatic brain injury in rats and mice. J Clin Invest 104:647–656.

Stough C, Lloyd J, Clarke J, Downey LA, Hutchison CW, Rodgers T, Nathan PJ (2001) The chronic effects of an extract of Bacopa monniera (Brahmi) on cognitive function in healthy human subjects. Psychopharmacology 156:481–484.

Tong XK, Hamel E (1999) Regional cholinergic denervation of cortical microvessels and nitric oxide synthase-containing neurons in Alzheimer's disease. Neuroscience 92:163–175.

Tully T, Bourtchouladze R, Scott R, Tallman J (2003) Targeting the CREB pathway for memory enhancers. Nat Rev Drug Discov 2:267–277.

Vogel HG (2002) Drug effects on learning and memory. In: Drug discovery and evaluation: Pharmacological assays (Vogel WH, Schölkens BA, Sandow J, Müller G, co-eds), pp 595–643. Heidelberg, Berlin: Springer-Verlag.

Yamada K, Noda Y, Nakayama S, Komori Y, Sugihara H, Hasegawa T, Nabeshima T (1995) Role of nitric oxide in learning and memory and in monoamine metabolism in the rat brain. Br J Pharmacol 115:852–858.

Zhang WN, Bast T, Feldon J (2001) The ventral hippocampus and fear conditioning in rats: different anterograde amnesias of fear after infusion of N-methyl-D-aspartate or its noncompetitive antagonist MK-801 into the ventral hippocampus. Behav Brain Res 126: 159–174.

(Accepted 4 February 2009)
(Available online 11 February 2009)

Neuroscience 155 (2008) 476–484

BACOPA MONNIERA AMELIORATES AMNESIC EFFECTS OF DIAZEPAM QUALIFYING BEHAVIORAL–MOLECULAR PARTITIONING

M. K. SARAF,[a1] S. PRABHAKAR,[a1] P. PANDHI[b] AND A. ANAND[a]*

[a]*Department of Neurology, Neuroscience Research Laboratory, Post Graduate Institute of Medical Education and Research, Sector-12, Chandigarh, 160012, India*

[b]*Department of Pharmacology, Post Graduate Institute of Medical Education and Research, Sector-12, Chandigarh, 160012, India*

Abstract—Benzodiazepines are known to produce amnesia by involvement of GABAergic system and by interference of long term potentiation (LTP). In this study, we examined effect of *Bacopa monniera* on downstream molecules of LTP after diazepam-induced amnesia in mice. We used a Morris water maze scale for evaluating the effect of *Bacopa monniera* after screening for muscle coordination by rota rod. The index of acquisition and retrieval was recorded as escape latency time (ELT). Behavioral results showed that *Bacopa monniera* (120 mg kg^{-1} oral) significantly reversed diazepam- (1.75 mg kg^{-1} i.p.) induced amnesia in Morris water maze task. The molecular studies revealed that diazepam upregulated mitogen activated protein kinase (MAP kinase), phosphorylated CREB (pCREB) and inducible nitric oxide synthase (iNOS), while it downregulated nitrite, nitrate, total nitrite, cAMP response element binding protein (CREB) expression, phosphodiesterase, cyclic adenosine monophosphate (cAMP) without affecting calmodulin levels. *Bacopa monniera* suppressed the diazepam induced upregulation of MAP kinase, pCREB and iNOS and attenuated the downregulation of nitrite. It did not affect the cAMP, PDE, nitrate, total nitrite, total CREB level. These behavioral findings displayed the reversal of diazepam-induced amnesia by *Bacopa monniera* without qualifying the molecular details although some downstream molecules of LTP may be involved. **© 2008 IBRO. Published by Elsevier Ltd. All rights reserved.**

Key words: amnesia, benzodiazepine, behavioral-molecular, *Bacopa monniera*, diazepam, water maze.

Diazepam, frequently prescribed for disorders such as seizure, insomnia and anesthesia may result in cognitive dysfunction (Lister, 1985; Mejo, 1992). It acts on benzodiazepine site of GABA/benzodiazepine receptor complex, impairs both prospective memory and retrospective memory (Rich et al., 2005). Benzodiazepines including diazepam cause amnesia in animals (Tomaz et al., 1992; Saraf et al., 2003; Zhou et al., 2007). The mechanism of benzodiazepine action is known to occur through the GABA receptors (Robin and Trieger, 2002). Benzodiazepine (Zhou et al., 2007) binding sites are present on GABA receptors in hippocampal neurons (Xu and Sastry, 2005). The blocking of long term potentiation (LTP) in slices of hippocampus and piriform cortex by benzodiazepines has been suggested to occur by increased action on GABA-mediated inhibitory potentials possibly mediating the amnesic effects of benzodiazepines (del Cerro et al., 1992). Diazepam, when applied before LTP, potentiates the amplitude and prolongs the decay of GABA(A) receptor-mediated inhibitory postsynaptic currents (IPSCs). This is further confirmed by studies where flumazenil, a benzodiazepine receptor antagonist, has been shown to block the diazepam induced-enhancement of the IPSC suggesting the involvement of benzodiazepine in LTP of the GABAergic IPSC in rat hippocampal CA1 neurons (Xu and Sastry, 2005). Diazepam is therefore very useful candidate in evaluation of anti-amnesic drugs (Parle and Dhingra, 2003; Dhingra et al., 2004; Parle et al., 2004).

Bacopa monniera, also known as brahmi, is known to improve the performance of rats in various learning situations such as shock-motivated brightness-discrimination reaction, an active conditioned flight reaction, the continuous avoidance response (Singh and Dhawan, 1982) and attenuates the scopolamine-, sodium nitrite– and BN 52021– (a platelet activating factor receptor antagonist) induced amnesia in mouse on Morris water maze task (Kishore and Singh, 2005). *Bacopa* extract contains two prominent constituents namely bacoside-A (Chatterji et al., 1965; Singh et al., 1988) and bacoside-B (Basu et al., 1967; Singh et al., 1988). It has also been shown to exert antioxidant effects through chelating of metal ions, breaking oxidative chain reaction (Tripathi et al., 1996), improving activities of antioxidative defense enzymes (Bhattacharya et al., 2000) and scavenging the free radicals (Russo et al., 2003). It also modulates the activities of Hsp70 (heat shock protein 70), cytochrome P450 and superoxide dismutase (Chowdhuri et al., 2002), which could constitute part of cellular response to stress in the brain. It improves the neuronal function of impaired neuron by enhancing protein kinase activity (Singh and Dhawan, 1997), which could be partly responsible for its cognition facilitation activity. *Bacopa* along with *Ginkgo biloba* extract has been suggested to exert significant anti-cholinesterase and anti-dementic properties in mice and attenuates the scopolamine-induced cognition deficit in passive avoid-

[1] M.K.S. and S.P.: Equal authors.

*Corresponding author. Tel: +91-172-2756094; fax: +91-172-2748399.
E-mail address: akshay@neurologypgi.com, URL: www.neurologypgi.com (A. Anand).
E-mail address: msaraf@scientist.com (M. K. Saraf).

Abbreviations: cAMP, cyclic adenosine monophosphate; CREB, cAMP response element binding protein; ELT, escape latency time; ERK, extracellular signal-regulated kinase; iNOS, inducible nitric oxide synthase; IPSC, inhibitory postsynaptic current; LSD, least significance difference; LTP, long term potentiation; MAP kinase, mitogen activated protein kinase; Nf1, neurofibromin1; PBS, phosphate buffer saline; pCREB, phosphorylated CREB; PDE, phosphodiesterase; P_i, inorganic phosphorus.

0306-4522/08$32.00+0.00 © 2008 IBRO. Published by Elsevier Ltd. All rights reserved.
doi:10.1016/j.neuroscience.2008.05.043

ance test (Das et al., 2002) providing evidence of its cholinergic characteristics (Meziane et al., 1998). Bacoside-A is the prominent constituent of *Bacopa* extract that has been reported to alleviate the amnesic effects of neurotoxin, scopolamine, electric-shock and immobilization stress (Dhawan and Singh, 1996; Russo and Borrelli, 2005). Like animal studies, the clinical studies also provide equally robust evidence of *Bacopa*'s action on cognitive function. In a clinical study Sharma et al., reported *Bacopa*'s effect on revitalizing the intellectual functions of children (Sharma et al., 1987). Some studies have suggested that the choice of dose and duration of *Bacopa*'s treatment is critical for bringing its optimal effects. For example, chronic administration of 300 mg oral *Bacopa* for about 5–12 weeks substantially improves the higher order cognitive process in healthy humans (Stough et al., 2001). In a phase I trial study BacoMind, containing *Bacopa* extract, does not show prominent adverse affect in healthy human volunteers (Pravina et al., 2007).

Retrograde messengers and kinase pathways are the component of downstream signaling of LTP. The previous studies utilizing pharmacological agents or genetically modified transgenic mouse corroborate the role of calmodulin pathway, protein kinase A pathway, Ras/Raf/MAPK pathway and cAMP response element binding protein (CREB) on LTP and on learning and memory (Matynia et al., 2002; Barco et al., 2003; Lynch, 2004). The experiments reported here were designed to examine effect of *Bacopa monniera* on diazepam-induced amnesia and test the hypothesis if there is modulation of such LTP downstream molecules that are responsible for antiamnesic effects of *Bacopa monniera* and compare the results with behavioral results.

EXPERIMENTAL PROCEDURES

Animals

Male Swiss albino mice (age matched, weight 25–35 g) were housed in standard mouse cage and provided free access to water and standard diet and exposed to a 12-h light/dark cycle. Experiments were carried out between 09:00–18:00 h in a semi-soundproof laboratory in accordance with the European Communities Council Directive (86/609/EEC) and Institute Animals ethical committee. We used the minimum number of animals in the experimental protocol which was consistent to obtain statistical significant results. Moreover we also took suitable precautions to minimize animal suffering according to institute animal ethical guidelines. Healthy mice, showing good swimming ability and normal behavior, were screened. Diazepam (Ranbaxy Laboratory Ltd., Mumbai, India) was dissolved in normal saline and the dose of administration was determined. Standardized extract of *Bacopa monniera* (donated by Dr. H. K. Singh, Pharmacology Division, Central Drug Research Laboratory, Lucknow) contained 55.35% bacosides and was suspended in Tween 80 (5% v/v in normal saline) before administration.

Morris water maze

Morris water maze tasks were performed to evaluate spatial learning and memory (Morris, 1984) and according to method described in our earlier paper (Anand et al., 2007). Briefly, quadrant 2 (Q2) was designated as the target quadrant where a platform was placed about 1 cm below the level of opaque water, filled in circular water tank of 2 m dia. Each animal was subjected to four consecutive trials on each day. When the animal was unable to locate the hidden platform in 120 s period, it was gently guided to the platform and allowed to remain there for 10 s. Escape latency time (ELT), as a quantitative measure to locate the hidden platform in water maze, was recorded as an index of acquisition. Rota-rod test was performed to screen test the muscle coordination activity of mice before subjecting them to water maze evaluation. Mice, showing abnormal swimming pattern in water maze, coupled with low muscle coordination activity in rota rod test were excluded from study.

In order to study the effect of experimental drug on acquisition, the drug solution was administered before acquisition trials for six consecutive days. In order to study the per se effect of vehicle, the corresponding diluent was administered before acquisition trials. In the present study, five groups were included. Each experimental and control group comprised six mice. Mice (Group I) were administered normal saline (10 ml kg^{-1}) orally 60 min before trial and intraperitoneally 30 min before trial. Tween 80 solution (0.5% v/v; 10 ml kg^{-1} oral) was administered 60 min before and normal saline (10 ml kg^{-1} i.p.) 30 min before trials in group II mice. Group III mice were administered diazepam (1.75 mg kg^{-1} i.p.) 30 min before trials. In order to study the effect of *Bacopa monniera*, mice were orally administered standardized extract of *Bacopa monniera* (Group IV 120 mg kg^{-1} oral) 60 min before trials and amnesic dose of diazepam (1.75 mg/kg i.p.) 30 min before trials. Group V mice were administered *Bacopa monniera* suspension (120 mg kg^{-1} orally) 60 min before and normal saline (10 ml kg^{-1} i.p.) 30 min before trials in order to investigate its per se effect on learning and retrieval of memory.

Neurochemical analysis

Mouse brain was isolated after completion of Morris water maze studies and thereafter preserved it for neurochemical analysis.

Nitric oxide estimation

The frozen brains of mouse were homogenized with lysis buffer (containing 0.01 M Tris–HCl (pH 7.6), 0.1 M sodium chloride, 0.001 M EDTA and protease inhibitors such as aprotinin 2.0 μg/ml, leupeptin 10 μg/ml, pepstatin 5 μg/ml and 0.1 mM PMSF. Nitric oxide was estimated by indirect measurement of nitrite, nitrate and total nitrite in mouse brain extract supernatants obtained after centrifugation. Cadmium beads were added to supernatant for total nitrite estimation and incubated overnight. The clear supernatant was treated with mixture of coloring reagent I (1% sulfanilamide in 3 N HCl) and II (0.1% NED.2HCl) and incubated for 10 min at room temperature. The absorbance was noted at 620 nm and 550 nm respectively. The nitrite and total nitrite level was normalized to total protein estimated by Bradford method.

Phosphodiesterase (PDE) assay

The frozen brains of mice were homogenized with lysis buffer and the clear supernatant was separated after centrifugation. The reaction mixture, comprising Tris 40 mM, 5 mM $MnCl_2$, mouse brain extract and 10 mM cyclic adenosine monophosphate (cAMP) was incubated for 10 min at 37 °C and then heated for 2 min to terminate the reaction. Snake venom serum was added (1 mg/ml) and incubated for 10 min at 30 °C. Fifty percent trichloroacetic acid was added and the inorganic phosphorus (P_i) release was estimated by Fiske and Subbaraw method (Fiske and Subbaraw, 1925). In brief, the supernatant was mixed with ammonium molybdate solution and distilled water followed by ANSA solution. The plate was read at 660 nm. The level of phosphorus was derived from standard curve of potassium phosphate. The PDE activity of sample was expressed in nmol P_i liberated/min/mg protein.

Ca/calmodulin assay

Calmodulin was estimated by the method described by Lin et al. (1974). Test samples containing Tris–HCl, pH 8.0, 4 mM, calcium chloride 50 μM, magnesium sulfate 5 mM, CaM deficient PDE 0.5 unit, clear supernatant, cAMP 10 mM and distilled water were prepared. After preparation, these samples were incubated for 30 min at 30 °C, heated for 2 min in a boiling waterbath. Snake venom serum (1 mg/ml) was added to each samples and incubated for 10 min at 30 °C. The reaction was stopped by addition of 50% trichloroacetic acid. The clear supernatant was obtained after centrifugation at 5000 rpm for 10 min. Calmodulin activity of sample was expressed in nmol of Pi liberated cAMP hydrolyzed/min/mg protein.

cAMP assay

cAMP level was estimated using cAMP Direct immunoassay kit (Calbiochem, San Diego, CA, USA). The kit uses a polyclonal antibody to cAMP that binds to cAMP in samples in a competitive manner. Briefly, the tissue powder was homogenized in 10 volumes of 0.1 N HCl to stop endogenous PDE activity, centrifuged at 600×g at 4 °C and clear supernatant obtained for cAMP estimation. It was followed by incubation with rabbit cAMP polyclonal antibody for 2 h at room temperature. The excess reagents were washed away and substrate was added. After a short incubation time, the reaction was stopped and the yellow color generated read on a microplate reader at 405 nm. The intensity of the color is proportional to the concentration of cAMP in standards and samples. The standard curve was obtained as percent bound (B/Bo) versus concentration of cAMP.

Mitogen activated protein kinase (MAP kinase) assay

The weighted brains of mice were homogenized with 500 μl of common lysis buffer, containing Tris–HCl 10 mM (pH 7.4), EDTA 0.5 mM, aprotinin 2.0 μg/ml, leupeptin 10 μg/ml, pepstatin 5 μg/ml and PMSF 0.1 mM to estimate MAP kinase, inducible nitric oxide synthase (iNOS), phosphorylated CREB (pCREB) and CREB protein.

The MAP kinase activity, in mouse brain sample, was estimated by employing non-radioactive MAP Kinase (extracellular signal-regulated kinase (ERK) 1/2) Activity Assay Kit (Chemicon International, Temecula, CA, USA). About 250 μl of frozen mouse brain homogenate was mixed with 250 μl of MAP kinase sample buffer at 4 °C for cell lysis and vortexed. The supernatant was aliquoted and stored. The total protein was estimated by Bradford method.

iNOS assay

The capture antibody solution was prepared in coating buffer (containing $NaHCO_3$ 0.068 M, Na_2CO_3 0.032 M; pH 8.9) at 1:200 dilution. The microplate was coated with diluted capture anti-NOS2 antibody (Santa Cruz Biotech, Santa Cruz, CA, USA) overnight at 4 °C. The plate was washed with 10 mM phosphate buffer saline (PBS), containing NaCl 150 mM, Na_2HPO_4 8.1 mM, NaH_2PO_4 1.9 mM; pH 7.2–7.4 for 5 min. About 100 μl of 5% BSA was prepared in PBS as blocking solution and then incubated for 2 h at 37 °C. The plates were washed with PBS buffer. After washing, the rabbit anti-iNOS antibody (Santa Cruz Biotech) was added at a dilution of 1:200 in buffer containing NaCl 0.9%, Trizma base 20 mM, BSA 0.1%, Tween 20 0.04% and incubated for 1 h at 37 °C. After washing, goat anti-rabbit IgG HRP labeled (Sigma, St. Louis, MO, USA) was added and incubated for 1 h at 37 °C. The excess secondary antibody was removed by washing the plates with PBS. After addition of TMB substrate, the plate was incubated for 5 min at the room temperature. The reaction was stopped by stop solution. The absorbance of plates was read at 492 nm and 450 nm and normalized to total protein.

Total-CREB and pCREB assay

Total CREB and pCREB kit (BioSource, Camarillo, CA, USA), based on a solid phase sandwich enzyme-linked immunosorbent assay (ELISA) was used for the measurement of CREB and pCREB level in mouse brain extract. The protocol, as described in the kit was followed.

Data analysis

All results were expressed as mean±S.E.M. (standard error mean). We analyzed the behavioral results of Morris water maze using ANOVA followed by post hoc Dunnett's at $P<0.05$ for multiple comparisons among the groups. 'a' Indicates significance at $P<0.05$ of particular day's ELT (i.e. ELT of day 2–day 6) versus ELT on day 1 of same group. We also compared the ELT of treated group with control's ELT and with diazepam's ELT in each time point (i.e. day 1–day 6). 'b' Indicates significance at $P<0.05$ of particular day of ELT versus same day control group's ELT. 'c' Indicates significance of ELT of particular day versus same day's ELT of diazepam group. The biochemical results were analyzed by ANOVA followed by post hoc test i.e. LSD (least significance difference). '*' Indicates significance at $P<0.05$ of treated group versus control group. '#' Indicates significance at $P\leq0.05$ of treated group versus diazepam group.

RESULTS

Bacopa monniera reverses diazepam induced anterograde amnesia

Control group I mice showed significant decrease in ELT with successive acquisition trials at days 1–6. Administration of diazepam at 1.75 mg kg^{-1} i.p. 30 min before acquisition trials significantly attenuated the decrease in ELT during successive acquisition trials (a=$P<0.05$; $F=1.077$, analyzed by ANOVA followed by Dunnett test). These were significantly differ from control group's ELT of same day, analyzed by ANOVA followed by LSD post hoc test for multiple comparison (b=$P<0.05$, $F=3.47$ on days 4–6 respectively). These observations suggest that diazepam impairs acquisition by producing anterograde amnesia. *Bacopa* 120 mg/kg p.o. (a=$P<0.001$ vs. ELT on day 1, $F=6.51$) reverses diazepam- (1.75 mg/kg i.p.) induced deficit in decrease in ELT (c=$P<0.05$ versus same day's ELT of diazepam group, $F=3.073$, 1.049, 18.511 on days 4–6 respectively). It suggests that *Bacopa monniera* reversed diazepam induced anterograde amnesia. The suspension of *Bacopa monniera* extract was prepared in 5% v/v Tween 80 solution. Five percent Tween 80 and *Bacopa monniera* (120 mg kg^{-1}oral) did not affect the normal acquisition ('a' indicates significance at $P<0.05$ of particular day's ELT versus ELT on day 1 of same group) (Fig. 1).

Effect of *Bacopa* on total CREB and pCREB

Diazepam partially reduced the total CREB ($F=11.33$, $P=0.085$), while it significantly augmented the pCREB level ($F=6.86$, $P<0.001$). *Bacopa* per se neither affected total CREB ($F=11.33$, $P=0.904$) nor altered pCREB ($F=6.86$, $P=0.67$) when compared with control mice. *Bacopa* upon co-administration with diazepam reduced the total CREB level ($F=11.33$, $P=0.011$) and pCREB level

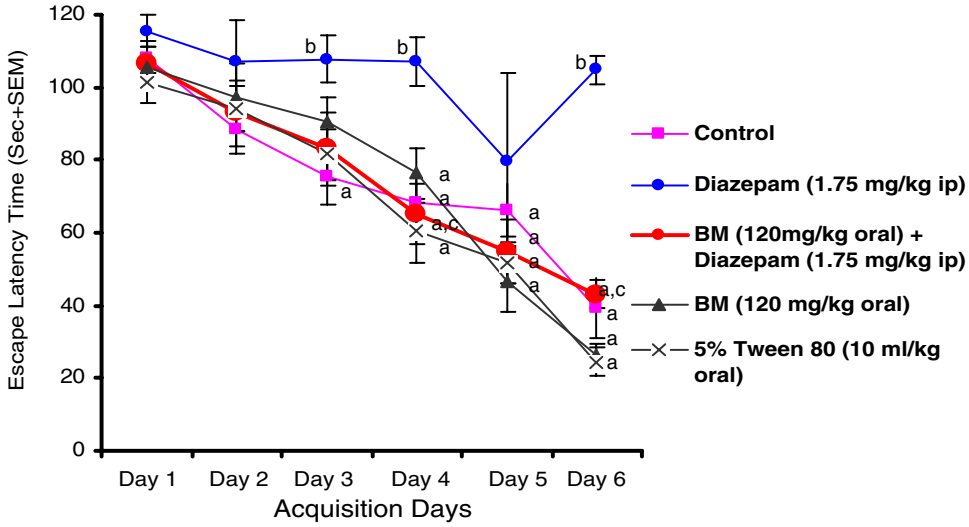


Fig. 1. Attenuation of diazepam induced anterograde amnesia by *Bacopa monniera.* In acquisition trials, each value represents mean ELT±S.E.M. Control group shows normal acquisition of memory. Diazepam at 1.75 mg/kg i.p. produces anterograde amnesia. *Bacopa* at 120 mg/kg oral significantly attenuates diazepam- (1.75 mg/kg i.p.) induced anterograde amnesia. *Bacopa* (120 mg/kg oral) and 5% tween 80 (10 ml/kg oral) do not alter normal acquisition. 'a' indicates significance at $P<0.05$ of particular day's ELT (i.e. ELT of day 2–day 6) versus ELT on day 1 of same group. We also compared the ELT of the treated group with control's ELT and with diazepam's ELT in each time point (i.e. day 1–day 6). 'b' indicates significance at $P=0.05$ of a particular day of ELT versus the same day control group's ELT. 'c' indicates significance of ELT of a particular day versus the same day's ELT of diazepam (1.75 mg/kg i.p.) group. The data were analyzed by ANOVA followed by post hoc test i.e. Dunnett's test for multiple comparison.

($F=6.86$, $P=0.002$) as compared with diazepam-treated mice (Fig. 2).

Effect of *Bacopa* on calmodulin and MAP kinase

Diazepam and *Bacopa*, when administered individually, upregulated MAP kinase ($F=6.512$, $P<0.05$). *Bacopa* with diazepam significantly reversed diazepam-induced enhancement of MAP kinase as compared with diazepam ($F=6.512$, $P=0.03$). Diazepam alone or in combination with *Bacopa monniera* did not alter the calmodulin levels ($F=1.67$) (Fig. 3).

Effect of *Bacopa* on cAMP and PDE

Bacopa, when administered with diazepam, mildly reduced cAMP level ($F=1.86$, $P=0.782$) and PDE activity ($F=1.857$, $P=0.082$) as compared with control. Such reductions in *Bacopa* with diazepam group were not significantly different from diazepam group. Diazepam partially reduced the cAMP ($F=1.86$, $P=0.556$) and PDE ($F=1.857$, $P=0.335$) level when compared with control mice. However, *Bacopa* per se did not alter either of the two (Fig. 4).

Effect of *Bacopa* on nitrite, nitrate, total nitrite and iNOS

Diazepam partially reduced nitrate ($F=1.86$, $P=0.28$), nitrite levels ($F=1.698$, $P=0.055$) and significantly reduced total nitrite ($F=3.05$, $P=0.013$) level. *Bacopa* along with diazepam attenuated diazepam-induced nitrite ($F=1.698$, $P=0.017$) without affecting total nitrite ($F=3.05$, $P=0.132$) and nitrate level ($F=1.86$, $P=0.408$). Diazepam also enhanced the expression of iNOS ($F=10.6$, $P<0.05$) as compared with control which was attenuated by *Bacopa* when it was co-administered with it as compared with diazepam ($F=10.6$, $P=0.05$) (Fig. 5).

The expression of pCREB and iNOS, detected by immunohistochemistry and Western blotting, was not substantially altered in treated groups as compared with control group (data not shown).

DISCUSSION

In order to investigate the behavioral and molecular effects of *Bacopa monniera* on diazepam-induced amnesia we used Morris water maze scale. It offers several advantages over other models of learning and memory: 1) absence of motivational stimuli such as food and water deprivation, electrical stimulations and buzzer sounds (as required in passive avoidance task), which may potentially affect memory evaluation test 2) As the herbal drugs take some time to metabolize, extended treatment regimen produces better results in Morris water test. 3) The animal requires a few days of training in the Morris water maze instead of several weeks of training in the arm maze. 3) Intramaze cues like odor trains are eliminated in the pool; 4) large dose response studies can be conducted in a week's time (Vogel, 2002).

Bacopa is earlier reported to exert antiamnesic effects (Dhanasekaran et al., 2007) by combination of its antioxidant and cholinergic activities (Tripathi et al., 1996; Bhattacharya et al., 1999, 2000; Das et al., 2002) but the precise mechanism remains elusive. As benzodiazepines have also been reported to block LTP in slices of hippocampus and piriform cortex due to increased action on GABA-mediated inhibitory potentials (del Cerro et al.,

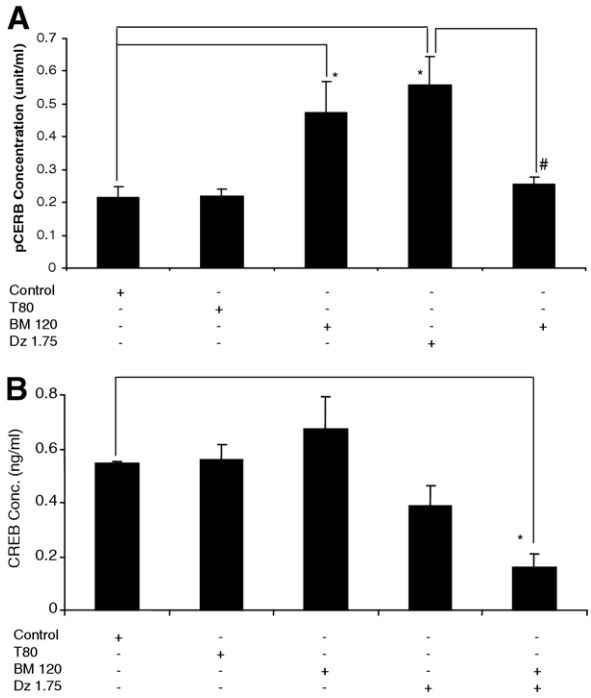


Fig. 2. Effect of *Bacopa monniera* and diazepam on phosphorylated-CREB and total CREB. (A) *Bacopa*, when administered with diazepam, reverses the diazepam induced enhancement of pCREB expression as compared with diazepam. *Bacopa* also increases pCREB expression when administered alone. (B) *Bacopa* with diazepam mildly decreases total CREB expression as compared with diazepam. This reduction is significantly differed from control group. Diazepam mildly reduces the total CREB expression. Data were analyzed by ANOVA followed by LSD. * Indicates significant difference for treated group vs. control group at $P<0.05$, # indicates significant difference for treated group vs. diazepam group at $P<0.05$.

1992) it is possible that benzodiazepines cause amnesia through LTP interference. The behavioral study revealed that diazepam produced amnesia which was significantly reversed by *Bacopa.* It is known that benzodiazepine exerts amnesic effect possibly mediated by GABA-Bz system through activation of GABA receptors (Robin and Trieger, 2002). It is possible that *Bacopa* modulates the same system in exerting antiamnesic effects.

The present study provided us with an opportunity of dissecting the effect of diazepam on downstream signaling molecules of LTP in this context. This investigation revealed diazepam induced upregulation of MAP kinase, pCREB and iNOS, and downregulation of nitrite, nitrate, total nitrite, CREB expression, PDE, cAMP without affecting calmodulin levels. Even though there were positive behavioral results. Such surprising findings were consistent with the results of Mantelas et al. (2003), who found that the activation of GABA-A receptors leads to increased expression of nNOS and pCREB. On the other hand, Huopaniemi et al., 2004 documented that diazepam reduces the expression levels of calcium/calmodulin-dependent protein kinase II, BDNF, MAP kinase phosphatase (Huopaniemi et al., 2004). It is known that diazepam inhibits the induction or maintenance of LTP (Hu et al., 2006) and potentiates LTD. Muscimol, a naturally occurring compound isolated from *Amanita muscaria*, and benzodiazepines act on $GABA_A$ receptors and induce LTD in rat hippocampus slice (Korpi and Seeburg, 1993; Akhondzadeh and Stone, 1995, 1999). Combined with the report that it impairs spatial memory independent of LTP suppression (McNamara et al., 1993) the resulting weak synaptic stimulation leading to LTD might involve NMDA receptor along with low level of calcium, protein kinases, etc. Benzodiazepine is believed to switch synaptic process from long term potentiation to long term depression (LTD) and it is quite possible that different components of existing mechanisms are engaged by molecules constituting the herbs that are either yet to be studied or too complex to associate with corresponding behavioral patterns. This could be partly resolved by screening of active constituents that constitute *Bacopa.*

It is known that the mutation of Nf1 (neurofibromin1) gene leads to neurofibromatosis I, the commonest single-gene genetic disorder resulting in learning disabilities. $Nf1^{+/-}$ mice show impairments in the water maze and contextual discrimination. The electrophysiological studies also indicate LTP deficits in $Nf1^{+/-}$ mice which could be due to increased GABA-mediated inhibition (Costa et al., 2001; Matynia et al., 2002). The K-$Ras^{+/-}$ mutation could also rescue these learning impairment and LTP deficits. These data suggest that Ras/Nf1 signaling modulates inhibition and that inhibition may have a role in regulating LTP (Costa et al., 2002; Costa and Silva, 2002; Matynia et al., 2002). MAPK belongs to superfamily of signaling cascades comprising ERKs, JNKs (c-Jun kinases) and the

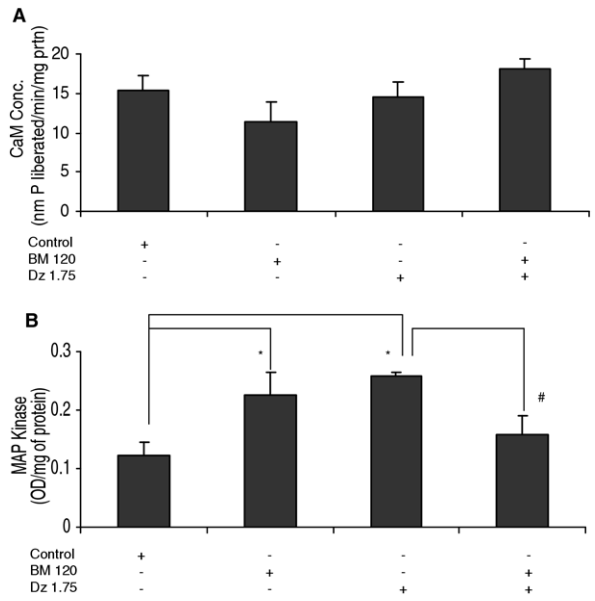


Fig. 3. Effect of *Bacopa monniera* and diazepam on Ca^{2+}/calmodulin and MAP kinase. (A) Diazepam and *Bacopa*, when administered alone or together, do not significantly affect calmodulin as compared with control. (B) Diazepam and *Bacopa* alone partially enhance MAP kinase as compared with control. *Bacopa*, when administered with diazepam, partially reduces the enhanced level of MAP kinase as compared with diazepam group. Data were analyzed by ANOVA followed by LSD. * Indicates significant difference for treated group vs. control group at $P<0.05$, # indicates significant difference for treated group vs. diazepam group at $P<0.05$.

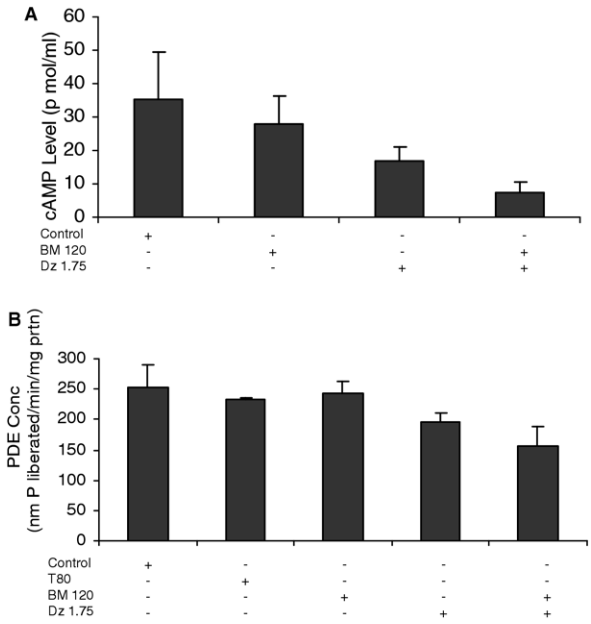


Fig. 4. Effect of *Bacopa monniera* and diazepam on cAMP and PDE. (A) Diazepam and *Bacopa*, when administered alone or together, do not significantly affect cAMP level as compared with control. (B) Diazepam alone partially reduce the PDE activity while *Bacopa*, when administered with diazepam, also suppresses PDE activity as compared with control. Data were analyzed by ANOVA followed by LSD. * Indicates significant difference for treated group vs. control group at $P<0.05$, # indicates significant difference for treated group vs. diazepam group at $P<0.05$.

p38 stress activated protein kinases. The two ERK MAPK isoforms, p44 MAPK and p42 MAPK, are referred to as ERK1 and ERK2, respectively (Sweatt, 2001; Adams and Sweatt, 2002). Increased ERK1/2 phosphorylation and nuclear translocation were observed after learning in the water maze, indicating the involvement of ERK in the LTP machinery (Blum et al., 1999; Adams and Sweatt, 2002; Matynia et al., 2002). These observations were later conformed by using SL327 in mice (Selcher et al., 1999). Dash and coworkers demonstrate that ERK activation occurs in the hippocampus during learning (Selcher et al., 1999; Dash et al., 2002b; Hebert and Dash, 2002). In this study, we report that *Bacopa monniera* suppressed the diazepam induced upregulation of MAP kinase, pCREB and iNOS possibly to reverse amnesia partly in consonance with the anticipated change of ERK 1/2 phosphorylation. Koyama et al. (2004) reported that N-(4-acetyl-1-piperazinyl)-p-fluorobenzamide monohydrate (FK960), a novel anti-dementia drug, increases the phosphorylation of ERK and CREB, which are blocked by PD98059, a ERK kinase inhibitor (Koyama et al., 2004). Nefiracetam, a nootropic drug has been reported to alleviate the cerebral ischemia–induced memory impairment in the water maze task along with attenuation of decrease in CaM-stimulated adenyl cyclase activity, cAMP content, PKA, and phosphorylation of CREB, but it did not reduce the infarct size (Takeo et al., 2003). The usefulness of CREB per se as a target for the development of memory-enhancing drugs is controversial (Barco et al., 2003). EGb761, extract of *Ginkgo biloba* facilitates the acquisition of conditioned fear by activating ERK1/2 (Yang et al., 2007). In the cell culture study, aniracetam, a nootropic drug, attenuates apoptosis of as-

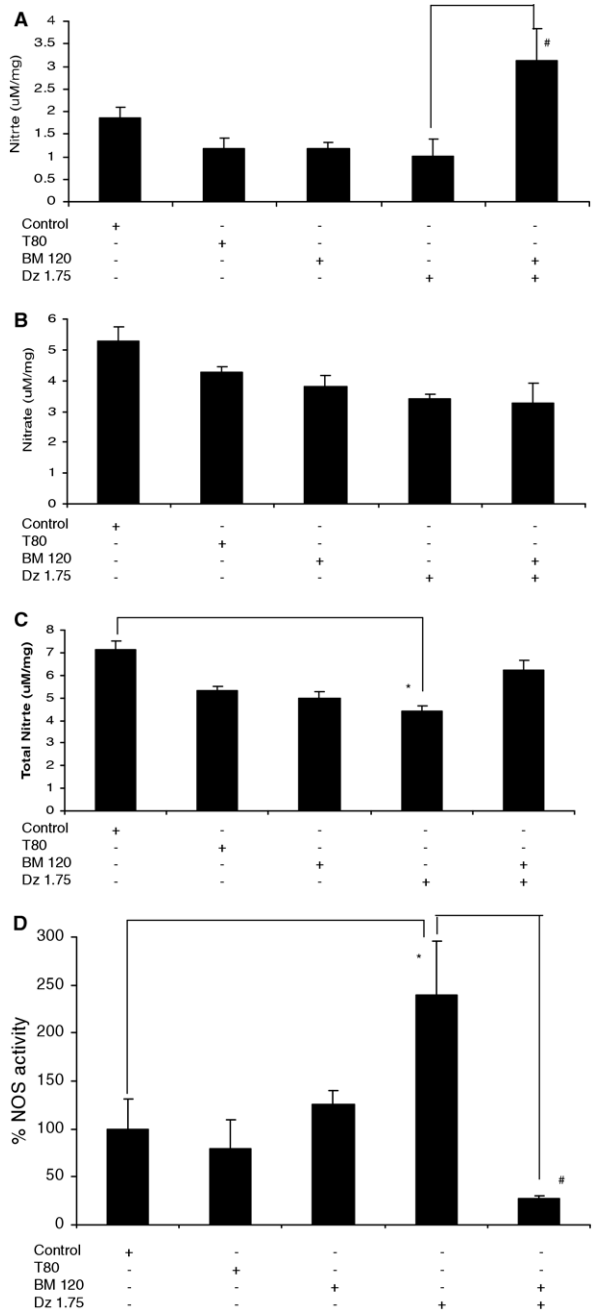


Fig. 5. Modulation of diazepam suppressed nitrite, nitrate and total nitrite level and iNOS expression by *Bacopa monniera.* (A–C) Diazepam suppression of nitrite, nitrate and total nitrite levels. *Bacopa* significantly attenuates diazepam induced suppression of nitrite level and mildly alleviates diazepam induced suppression of total nitrite level as compared with diazepam group. Nitrate level is not affected in *Bacopa* and diazepam groups as compared with control group. (D) *Bacopa* attenuates the diazepam enhanced iNOS expression as compared with diazepam. Data were analyzed by ANOVA followed by LSD. * Indicates significant difference for treated group vs. control group at $P<0.05$, # indicates significant difference for treated group vs. diazepam group at $P<0.05$.

trocytes subjected to simulated ischemia which was earlier accelerated by PD98059, a MAP/ERK inhibitor, suggesting the involvement of MAPK pathway in the downstream of aniracetam mechanism (Gabryel et al., 2002). In general, the finding uncovers the complexity of the correlation between the molecular finding and behavioral results, like other earlier findings (Dash et al., 2002a; Balschun et al., 2003). The role of LTP machinery may also vary across strains. One of the ERK1$^{-/-}$ mouse strains showed no alterations in ERK2 protein levels or phosphorylation, LTP, general activity, motor skills, or learning and memory as assessed by fear conditioning and passive avoidance tasks (Matynia et al., 2002; Mazzucchelli et al., 2002). These results were later challenged in a second ERK1$^{-/-}$ mouse line in which alterations in the phosphorylation levels of ERK2 were enhanced, and LTP in the nucleus accumbens, but not the hippocampus or amygdala. Similarly, these mice showed enhanced learning or memory observed in active and passive avoidance tests (Selcher et al., 2001; Matynia et al., 2002). PDE inhibitor is known to inhibit the metabolism of cAMP and increase the level of cAMP. In the present study we did not find rise in cAMP even though there was inhibition of PDE. Diazepam causes a biphasic and concentration-dependent inhibition of forskolin-stimulated adenylyl cyclase activity in MCF-7 membranes of breast cancer cells, the first phase of inhibition at picomolar to nanomolar drug concentrations and at micromolar concentrations of diazepam the steep decrease in adenylyl cyclase activity (Niles and Wang, 1999). It is our assumption that acute treatment with diazepam, a PDE inhibitor (Juan-Fita et al., 2006), might raise cAMP while the subchronic treatment did not show a rise in cAMP level due to inhibition of adenylyl cyclase activity (Tenn and Niles, 1997; Niles and Wang, 1999). *Bacopa monniera* did not affect cAMP, PDE, nitrate and calmodulin. In the present study, diazepam upregulated iNOS while it significantly downregulated total nitrite and partially reduced nitrite and nitrate. On the other hand L-NAME, a nitric oxide inhibitor, is reported to reverse the stress-induced changes in total brain nitrate/nitrite content in rat (Masood et al., 2003). Nitrite also enhance (3H)diazepam binding which contributes a role to postsynaptic inhibition (Tallman and Gallager, 1979). *Bacopa monniera* attenuated the downregulation of nitrite without affecting total nitrite and nitrate in this study.

Given the clear behavioral evidence of the role of *Bacopa* in reversing drug-induced amnesia despite any significant involvement of LTP molecules, it is important to review the approach applied in evolving targets of memory enhancement. Foremost among them is the need to overcome the belief that the reductionism paradigm is an essential component of advancement in drug discovery research. It may be helpful to exploit the traditional knowledge based on symptomatic improvement in order to facilitate drug discovery process irrespective of clear molecular definitions because it may be possible that the proportion of candidate molecules may reverse memory deficits more effectively than intervention of single molecules or active constituents.

Acknowledgments—The work was partially supported by the Department of Biotechnology, New Delhi (India) (No. BT/PR3533/Med/12/152/2002).

REFERENCES

Adams JP, Sweatt JD (2002) Molecular psychology: roles for the ERK MAP kinase cascade in memory. Annu Rev Pharmacol Toxicol 42:135–163.

Akhondzadeh S, Stone T (1999) Prevention of muscimol-induced long-term depression by brain-derived neurotrophic factor. Prog Neuropsychopharmacol Biol Psychiatry 23:1215–1226.

Akhondzadeh S, Stone TW (1995) Induction of a novel form of hippocampal long-term depression by muscimol: involvement of GABAA but not glutamate receptors. Br J Pharmacol 115:527–533.

Anand A, Saraf MK, Prabhakar S (2007) Sustained inhibition of brotizolam induced anterograde amnesia by norharmane and retrograde amnesia by l-glutamic acid in mice. Behav Brain Res 182:12–20.

Balschun D, Wolfer DP, Gass P, Mantamadiotis T, Welzl H, Schutz G, Frey JU, Lipp HP (2003) Does cAMP response element-binding protein have a pivotal role in hippocampal synaptic plasticity and hippocampus-dependent memory? J Neurosci 23:6304–6314.

Barco A, Pittenger C, Kandel ER (2003) CREB, memory enhancement and the treatment of memory disorders: promises, pitfalls and prospects. Expert Opin Ther Targets 7:101–114.

Basu N, Rastogi RP, Dhar ML (1967) Chemical examination of *Bacopa monniera* Wettst part III: The constitution of bacoside-B. Indian J Chem 5:84.

Bhattacharya SK, Bhattacharya A, Kumar A, Ghosal S (2000) Antioxidant activity of Bacopa monniera in rat frontal cortex, striatum and hippocampus. Phytother Res 14:174–179.

Bhattacharya SK, Kumar A, Ghosal S (1999) Effect of *Bacopa monniera* on animal models of Alzheimer's disease and perturbed central cholinergic markers of cognition in rats In: Molecular aspects of Asian medicines (Siva Sanka DV, ed), pp 27–58. New York: PJD Publication.

Blum S, Moore AN, Adams F, Dash PK (1999) A mitogen-activated protein kinase cascade in the CA1/CA2 subfield of the dorsal hippocampus is essential for long-term spatial memory. J Neurosci 19:3535–3544.

Chatterji N, Rastogi RP, Dhar ML (1965) Chemical examination of *Bacopa monniera* Wettst. Part II: The constitution of bacoside A. Ind J Chem 3:24–29.

Chowdhuri DK, Parmar D, Kakkar P, Shukla R, Seth PK, Srimal RC (2002) Antistress effects of bacosides of Bacopa monniera: modulation of Hsp70 expression, superoxide dismutase and cytochrome P450 activity in rat brain. Phytother Res 16:639–645.

Costa RM, Federov NB, Kogan JH, Murphy GG, Stern J, Ohno M, Kucherlapati R, Jacks T, Silva AJ (2002) Mechanism for the learning deficits in a mouse model of neurofibromatosis type 1. Nature 415:526–530.

Costa RM, Silva AJ (2002) Molecular and cellular mechanisms underlying the cognitive deficits associated with neurofibromatosis 1. J Child Neurol 17:622–626; discussion 627–629, 646–651.

Costa RM, Yang T, Huynh DP, Pulst SM, Viskochil DH, Silva AJ, Brannan CI (2001) Learning deficits, but normal development and tumor predisposition, in mice lacking exon 23a of Nf1. Nat Genet 27:399–405.

Das A, Shanker G, Nath C, Pal R, Singh S, Singh H (2002) A comparative study in rodents of standardized extracts of Bacopa monniera and Ginkgo biloba: anticholinesterase and cognitive enhancing activities. Pharmacol Biochem Behav 73:893–900.

Dash PK, Mach SA, Blum S, Moore AN (2002a) Intrahippocampal wortmannin infusion enhances long-term spatial and contextual memories. Learn Mem 9:167–177.

Dash PK, Mach SA, Moore AN (2002b) The role of extracellular signal-regulated kinase in cognitive and motor deficits following experimental traumatic brain injury. Neuroscience 114:755–767.

del Cerro S, Jung M, Lynch G (1992) Benzodiazepines block long-term potentiation in slices of hippocampus and piriform cortex. Neuroscience 49:1–6.

Dhanasekaran M, Tharakan B, Holcomb LA, Hitt AR, Young KA, Manyam BV (2007) Neuroprotective mechanisms of ayurvedic antidementia botanical Bacopa monniera. Phytother Res 21: 965–969.

Dhawan BN, Singh HK (1996) Pharmacology of ayurvedic nootropic Bacopa monniera. Proceedings of the Int. Conv. Biol. Psychiat., Bombay, pp. Abstr. No. NR 59.

Dhingra D, Parle M, Kulkarni SK (2004) Memory enhancing activity of Glycyrrhiza glabra in mice. J Ethnopharmacol 91:361–365.

Fiske CH, Subbaraw Y (1925) The colorimetric determination of phosphorus. J Biol Chem 66:375–400.

Gabryel B, Adamczyk J, Huzarska M, Pudelko A, Trzeciak HI (2002) Aniracetam attenuates apoptosis of astrocytes subjected to simulated ischemia in vitro. Neurotoxicology 23:385–395.

Hebert AE, Dash PK (2002) Extracellular signal-regulated kinase activity in the entorhinal cortex is necessary for long-term spatial memory. Learn Mem 9:156–166.

Hu XD, Ge YX, Hu NW, Zhang HM, Zhou LJ, Zhang T, Li WM, Han YF, Liu XG (2006) Diazepam inhibits the induction and maintenance of LTP of C-fiber evoked field potentials in spinal dorsal horn of rats. Neuropharmacology 50:238–244.

Huopaniemi L, Keist R, Randolph A, Certa U, Rudolph U (2004) Diazepam-induced adaptive plasticity revealed by alpha1 GABAA receptor-specific expression profiling. J Neurochem 88:1059–1067.

Juan-Fita MJ, Vargas ML, Hernandez J (2006) Diazepam enhances inotropic responses to dopamine in rat ventricular myocardium. Anesth Analg 102:676–681.

Kishore K, Singh M (2005) Effect of bacosides, alcoholic extract of Bacopa monniera Linn. (brahmi), on experimental amnesia in mice. Indian J Exp Biol 43:640–645.

Korpi ER, Seeburg PH (1993) Natural mutation of GABAA receptor alpha 6 subunit alters benzodiazepine affinity but not allosteric GABA effects. Eur J Pharmacol 247:23–27.

Koyama Y, Egawa H, Osakada M, Baba A, Matsuda T (2004) Increase by FK960, a novel cognitive enhancer, in glial cell line-derived neurotrophic factor production in cultured rat astrocytes. Biochem Pharmacol 68:275–282.

Lin YM, Liu YP, Cheung WY (1974) Purification and characterization of protein activator of cyclic nucleotide phosphodiesterase from bovine brain. Methods Enzymol 38:262–273.

Lister RG (1985) The amnesic action of benzodiazepines in man. Neurosci Biobehav Rev 9:87–94.

Lynch MA (2004) Long-term potentiation and memory. Physiol Rev 84:87–136.

Mantelas A, Stamatakis A, Kazanis I, Philippidis H, Stylianopoulou F (2003) Control of neuronal nitric oxide synthase and brain-derived neurotrophic factor levels by GABA-A receptors in the developing rat cortex. Brain Res Dev Brain Res 145:185–195.

Masood A, Banerjee B, Vijayan VK, Ray A (2003) Modulation of stress-induced neurobehavioral changes by nitric oxide in rats. Eur J Pharmacol 458:135–139.

Matynia A, Kushner SA, Silva AJ (2002) Genetic approaches to molecular and cellular cognition: a focus on LTP and learning and memory. Annu Rev Genet 36:687–720.

Mazzucchelli C, Vantaggiato C, Ciamei A, Fasano S, Pakhotin P, Krezel W, Welzl H, Wolfer DP, Pages G, Valverde O, Marowsky A, Porrazzo A, Orban PC, Maldonado R, Ehrengruber MU, Cestari V, Lipp HP, Chapman PF, Pouyssegur J, Brambilla R (2002) Knockout of ERK1 MAP kinase enhances synaptic plasticity in the striatum and facilitates striatal-mediated learning and memory. Neuron 34:807–820.

McNamara RK, dePape GE, Skelton RW (1993) Differential effects of benzodiazepine receptor agonists on hippocampal long-term potentiation and spatial learning in the Morris water maze. Brain Res 626:63–70.

Mejo SL (1992) Anterograde amnesia linked to benzodiazepines. Nurse Pract 17:49–50.

Meziane H, Dodart JC, Mathis C, Little S, Clemens J, Paul SM, Ungerer A (1998) Memory-enhancing effects of secreted forms of the beta-amyloid precursor protein in normal and amnestic mice. Proc Natl Acad Sci U S A 95:12683–12688.

Morris R (1984) Developments of a water-maze procedure for studying spatial learning in the rat. J Neurosci Methods 11:47–60.

Niles LP, Wang J (1999) Diazepam inhibits forskolin-stimulated adenylyl cyclase activity in human tumour cells. Pharmacol Toxicol 85:153–156.

Parle M, Dhingra D (2003) Ascorbic Acid: a promising memory-enhancer in mice. J Pharmacol Sci 93:129–135.

Parle M, Dhingra D, Kulkarni SK (2004) Memory-strengthening activity of Glycyrrhiza glabra in exteroceptive and interoceptive behavioral models. J Med Food 7:462–466.

Pravina K, Ravindra KR, Goudar KS, Vinod DR, Joshua AJ, Wasim P, Venkateshwarlu K, Saxena VS, Amit A (2007) Safety evaluation of BacoMind in healthy volunteers: a phase I study. Phytomedicine 14:301–308.

Rich JB, Svoboda E, Brown GG (2005) Diazepam-induced prospective memory impairment and its relation to retrospective memory, attention, and arousal. Hum Psychopharmacol 21:101–108.

Robin C, Trieger N (2002) Paradoxical reactions to benzodiazepines in intravenous sedation: a report of 2 cases and review of the literature. Anesth Prog 49:128–132.

Russo A, Borrelli F (2005) Bacopa monniera, a reputed nootropic plant: an overview. Phytomedicine 12:305–317.

Russo A, Izzo AA, Borrelli F, Renis M, Vanella A (2003) Free radical scavenging capacity and protective effect of Bacopa monniera L. on DNA damage. Phytother Res 17:870–875.

Saraf MK, Kishore K, Thomas KM, Sharma A, Singh M (2003) Role of platelet activating factor in triazolobenzodiazepines-induced retrograde amnesia. Behav Brain Res 142:31–40.

Selcher JC, Atkins CM, Trzaskos JM, Paylor R, Sweatt JD (1999) A necessity for MAP kinase activation in mammalian spatial learning. Learn Mem 6:478–490.

Selcher JC, Nekrasova T, Paylor R, Landreth GE, Sweatt JD (2001) Mice lacking the ERK1 isoform of MAP kinase are unimpaired in emotional learning. Learn Mem 8:11–19.

Sharma R, Chaturvedi C, Tewari PV (1987) Efficacy of *Bacopa monniera* in revitalizing intellectual functions in children. J Res Educ Ind Med 23:1–12.

Singh HK, Dhawan BN (1982) Effect of Bacopa monniera Linn. (brahmi) extract on avoidance responses in rat. J Ethnopharmacol 5:205–214.

Singh HK, Dhawan BN (1997) Neuropsychopharmacological effects of the ayurvedic nootropic *Bacopa monniera* Linn. (brahmi). Ind J Pharmacol 29S:359–365.

Singh HK, Rastogi RP, Srimal RC, Dhawan BN (1988) Effects of bacosides A and B on avoidance response in rats. Phytother Res 2:70–75.

Stough C, Lloyd J, Clarke J, Downey LA, Hutchison CW, Rodgers T, Nathan PJ (2001) The chronic effects of an extract of Bacopa monniera (brahmi) on cognitive function in healthy human subjects. Psychopharmacology (Berl) 156:481–484.

Sweatt JD (2001) The neuronal MAP kinase cascade: a biochemical signal integration system subserving synaptic plasticity and memory. J Neurochem 76:1–10.

Takeo S, Niimura M, Miyake-Takagi K, Nagakura A, Fukatsu T, Ando T, Takagi N, Tanonaka K, Hara J (2003) A possible mechanism for improvement by a cognition-enhancer nefiracetam of spatial memory function and cAMP-mediated signal transduction system in sustained cerebral ischaemia in rats. Br J Pharmacol 138:642–654.

Tallman JF, Gallager DW (1979) Modulation of benzodiazepine binding site sensitivity. Pharmacol Biochem Behav 10:809–813.

Tenn CC, Niles LP (1997) Sensitization of G protein-coupled benzodiazepine receptors in the striatum of 6-hydroxydopamine-lesioned rats. J Neurochem 69:1920–1926.

Tomaz C, Dickinson-Anson H, McGaugh JL (1992) Basolateral amygdala lesions block diazepam-induced anterograde amnesia in an inhibitory avoidance task. Proc Natl Acad Sci U S A 89:3615–3619.

Tripathi YB, Chaurasia S, Tripathi E, Upadhyay A, Dubey GP (1996) Bacopa monniera Linn. as an antioxidant: mechanism of action. Indian J Exp Biol 34:523–526.

Vogel HG (2002) Drug effects on learning and memory: Drug discovery and evaluation: pharmacological assays, pp 595–643. Berlin, Germany: Springer-Verlag.

Xu JY, Sastry BR (2005) Benzodiazepine involvement in LTP of the GABA-ergic IPSC in rat hippocampal CA1 neurons. Brain Res 1062:134–143.

Yang YL, Su YW, Ng MC, Chao PK, Tung LC, Lu KT (2007) Extract of Ginkgo biloba EGb761 facilitates extinction of conditioned fear measured by fear-potentiated startle. Neuropsychopharmacology 32:332–342.

Zhou Y, Shen YH, Zhang C, Su J, Liu RH, Zhang WD (2007) Triterpene saponins from Bacopa monnieri and their antidepressant effects in two mice models. J Nat Prod 70:652–655.

(Accepted 30 May 2008)
(Available online 7 June 2008)

Available online at www.sciencedirect.com
ScienceDirect
Behavioural Brain Research 182 (2007) 12–20
BEHAVIOURAL BRAIN RESEARCH
www.elsevier.com/locate/bbr

Research report

Sustained inhibition of brotizolam induced anterograde amnesia by norharmane and retrograde amnesia by L-glutamic acid in mice

Akshay Anand [1,2], Manish Kumar Saraf [1,3], Sudesh Prabhakar *

Department of Neurology, Post Graduate Institute of Medical Education and Research, Sector-12, Chandigarh 160012, India[4]

Received 3 November 2006; received in revised form 21 April 2007; accepted 27 April 2007
Available online 3 May 2007

Abstract

Benzodiazepines such as diazepam, lorazepam, are reported to produce anterograde amnesia but these do not affect the retrieval mechanism. Triazodiazepines such as alprazolam, triazolam and brotizolam produce both anterograde and retrograde amnesia. Because benzodiazepine receptor antagonists are known to reverse anterograde amnesia, we wanted to test if inverse agonist can also improve learning and memory. The present study was designed to investigate the effect of norharmane (benzodiazepine receptor inverse agonist) and L-glutamic acid (glutamate receptor agonist) on brotizolam induced anterograde and retrograde amnesia using Morris water maze task in mice. Norharmane reversed anterograde amnesia induced by brotizolam and did not reverse retrograde amnesia induced by it. L-Glutamic acid attenuated retrograde amnesia but did not affect anterograde amnesia induced by brotizolam. These results provide an opportunity to understand the mechanisms of anterograde and retrograde amnesia which may occur with interaction of presynaptic molecules or LTP modulation.
© 2007 Elsevier B.V. All rights reserved.

Keywords: Amnesia; Brotizolam; Benzodiazepine receptor; L-Glutamic acid; Morris water maze; Memory; Norharmane

1. Introduction

Amnesia may develop either as an consequence of various neurological problems such as stroke, multiple cerebral infarcts, head trauma and Alzheimer's disease [1,2] or consumption of alcohol [3,4], chronic drug abuse [5,6] and certain chemical agents utilization [5,7,8]. Anterograde amnesia, an impairment to store new memories [9], can result from acute brain syndrome [10] and retrograde amnesia, a failure to retrieve old memories [11,12], can emerge out as an symptom of Korsakoff's disease, Alzheimer's disease and may be associated with other diseases such as Parkinson's disease, Huntington's chorea, head injury and use of certain drugs [2,13]. Most of earlier benzodiazepines such as diazepam, halazepam [14,15] are reported to produce anterograde amnesia without affecting the retrieval mechanism [16] while triazolodiazepines, a newer subclass of benzodiazepines, such as alprazolam and triazolam are known to produce both anterograde and retrograde amnesia [10,17,18]. Brotizolam, another triazolodiazepine and benzodiazepine receptor agonist [19–21], also functions as platelet activating factor (PAF) receptor antagonist [18,22–25] and exerts hypnotic and sedative activity [26,27]. It has a significant anterograde and retrograde properties [18]. Benzodiazepine receptor antagonists such as flumazenil [17] and CGS 8216 attenuate amnesia induced by various benzodiazepines and triazolodiazepines [28].

There are several reports describing betacarbolines like FG 7142 [29], and beta CCM (methyl beta-carboline-3-carboxylate) [30,31] has been shown to exert inverse agonist properties and reported to alleviate memory deficits caused [32–34] due to EGCG or alcohol treated subjects [35–37]. Norharmane, an endogenous β-carboline, is a normal body constituent [38] and is abundantly present in cigarette smoke and cooked foodstuff [39,40] as well as in animals [38,41,42]. Norharmane, a benzodiazepine receptor inverse agonist [43], is known to interact with a variety of receptors especially benzodiazepines present in hippocampal, neocortical and hypothalamic, thalamic, accumbens

* Corresponding author. Tel.: +91 172 2756691; fax: +91 172 27544401.
E-mail addresses: akshay@neurologypgi.com (A. Anand), manishsaraf123@rediffmail.com (M.K. Saraf), sudesh@prabhakars.com (S. Prabhakar).
[1] These authors have equal authorship.
[2] Tel.: +91 172 2756094; fax: +91 172 2748399.
[3] Tel.: +91 172 2756090.
[4] Website: www.neurologypgi.com.

0166-4328/$ – see front matter © 2007 Elsevier B.V. All rights reserved.
doi:10.1016/j.bbr.2007.04.022

and amygdaloid nuclei [42,44], however, there is no report of its beneficial effects on learning and memory. Coffee, which contains norharman, harman and beta-carboline alkaloids, can reduce the incidence of Parkinson's disease due to inhibition of monoaminooxidase [45,46]. Although similar studies explored its MAO inhibition properties, its interaction with benzodiazepine receptor agonist is not adequately investigated in the context of its inverse agonism. Similarly, Glutamate receptor is another important player in hippocampal long-term potentiation and memory. Glutamic acid, a glutamate receptor agonist enhances retention of memory [47] but has not been shown to alleviate brotizolam induced memory deficits. The present study investigated the effect of norharmane and L-glutamic acid on brotizolam induced anterograde and retrograde amnesia.

2. Material and methods

2.1. Animals

Swiss albino mice (20–40 g) of either sex were used in the present study. They were kept in an animal house and provided free access of water and standard diet. They were exposed to 12 h light and dark cycle. The experiments were conducted between 10:00 and 17:30 h in a semi soundproof laboratory.

2.2. Acquisition and retrieval trials using morris water maze

Morris water maze [48] was employed to evaluate learning and memory. It consisted of a circular water tank (150 cm diameter and 45 cm height), filled with water maintained at 25 °C. The water was made opaque with white colored dye. Tank was divided into four equal quadrants with the help of two threads, running at right angle to each other over the rim of the pool. A platform (10 cm^2) of 29 cm height was submerged in the center of one of these four quadrants. The position of platform was kept unaltered throughout the training session. In the present study, quadrant-1 (Q1) was designated as the target quadrant. Each animal was subjected to four consecutive trials on each day with a gap of 5 min, during which they were allowed to seek the hidden platform and allowed to remain there for 20 s. In case the animal was unable to locate the hidden platform within 120 s, it was gently guided to the platform and allowed to remain there for 20 s. Escape latency time to locate the hidden platform in water maze was noted as an index of memory acquisition. Each animal was subjected to the four acquisition trials per day for 4 consecutive days. On fifth day, platform was removed and time spent by the animal in each of four quadrants (Q1, Q2, Q3 and Q4) was noted. The time spent by the animal in the target quadrant while searching the hidden platform was noted as an index of retrieval.

2.3. Drugs and chemicals

All the drug solutions were freshly prepared before use. Brotizolam (Boehringer Ingelheim Pharmaceutical Inc.) was dissolved in 0.3% propylene glycol (PG). L-Glutamic acid hydrochloride (Sigma–Aldrich, New Delhi) was dissolved in distilled water and the pH was adjusted to 6.8–7.0 by addition of 10 M sodium hydroxide solution. Distilled water was used as solvent for norharmane hydrochloride (Sigma–Aldrich, New Delhi) and diazepam (Ranbaxy Laboratories Limited, New Delhi).

2.4. Experimental protocol

For producing anterograde amnesia, the drug was administered before each acquisition trial on days 1–4 and an appropriate vehicle was administered before the respective retrieval trial on 5th day. Retrograde amnesia was produced by administering the drug before retrieval trial on the 5th day. The *per se* effect of the drug was analyzed by administering the drug before acquisition and retrieval trial. In the present study, 23 groups, comprising of six mice each, were studied (Table 1).

2.4.1. Diazepam treated groups (Groups I–III)

Mice (Group I) were administered distilled water (10 ml kg^{-1} i.p.) 30 min before acquisition trials (days 1–4) and retrieval trial (day 5). Group II mice were administered diazepam (1 mg kg^{-1} i.p.), dissolved in distilled water, 30 min before acquisition trials and distilled water (10 ml kg^{-1} i.p.) 30 min before retrieval trial. Group III mice were administered distilled water (10 ml kg^{-1} i.p.) 30 min before acquisition trials and diazepam (1 mg kg^{-1} i.p.) 30 min before retrieval trial.

2.4.2. Brotizolam treated groups (Groups IV–XIII)

Group IV mice were administered 3% PG (10 ml kg^{-1} i.p.), used to dissolve brotizolam, 30 min before acquisition trials and retrieval trials. Groups V, VI, VII, VIII, IX and X mice were administered different doses of brotizolam, i.e. 0.75, 0.50, 0.25, 0.10, 0.05 and 0.01 mg kg^{-1} i.p., 30 min before acquisition trials, respectively, and were administered 3% PG (10 ml kg^{-1} i.p.) 30 min before retrieval trial. Groups XI, XII and XIII mice were administered 3% PG (10 ml kg^{-1} i.p.) 30 min before acquisition trials and mice were administered with 0.25, 0.10, 0.01 mg kg^{-1} i.p. brotizoam 30 min before retrieval trial, respectively.

2.4.3. Norharmane treated groups (Groups XIV–XIX)

Group XIV mice were administered norharmane (20 mg kg^{-1} i.p.) 40 min before acquisition and retrieval trials. Group XV mice were administered norharmane (10 mg kg^{-1} i.p.) 40 min before and diazepam (1 mg kg^{-1} i.p.) 30 min before acquisition trials, and were administered distilled water (10 ml kg^{-1} i.p.) 40 min before retrieval trial. Group XVI mice were administered norharmane (20 mg kg^{-1} i.p.) 40 min before and diazepam (1 mg kg^{-1} i.p.) 30 min before acquisition trials, and were administered distilled water (10 ml kg^{-1} i.p.) 40 min before retrieval trial.

Group XVII mice were administered norharmane (20 mg kg^{-1} i.p) 40 min before combined with brotizolam (0.1 mg kg^{-1} i.p.) 30 min before acquisition trials, respectively, and were administered distilled water (10 ml kg^{-1} i.p.) 40 min before and 3% PG (10 ml kg^{-1} i.p.) 30 min before retrieval trial, respectively. Group XVIII mice were administered higher dose of norharmane (40 mg kg^{-1} i.p.) combined with brotizolam (0.1 mg kg^{-1} i.p.) and were administered distilled water (10 ml kg^{-1} i.p.) 40 min before and 3% PG (10 ml kg^{-1} i.p.) 30 min before retrieval trial. Group XIX mice were administered distilled water (10 ml kg^{-1} i.p.) 40 min before and 3% PG (10 ml kg^{-1} i.p.) 30 min before acquisition trials. These mice were administered norharmane (20 mg kg^{-1} i.p.) 40 min before and brotizolam (0.1 mg kg^{-1} i.p.) 30 min before retrieval trial.

2.4.4. L-Glutamic acid treated group (Groups XX–XXIII)

Group XX mice were administered L-glutamic acid (2 g kg^{-1} i.p.) 40 min before acquisition and retrieval trials. Group XXI mice were administered L-glutamic acid (2 g kg^{-1} i.p.) 40 min before and diazepam (1 mg kg^{-1} i.p.) 30 min before acquisition trials, and were administered distilled water (10 ml kg^{-1} i.p.) 40 min before retrieval trial. Group XXII mice were administered L-glutamic acid (2 g kg^{-1} i.p.) 40 min combined with brotizolam (0.1mg kg^{-1} i.p.) 30 min before acquisition trials. Distilled water was administered 40 min before (10 ml kg^{-1} i.p.) and 3% PG 30 min before retrieval trial. Group XXIII mice were administered distilled water (10 ml kg^{-1} i.p.) 40 min before and 3% PG (10 ml kg^{-1} i.p.) 30 min before acquisition trials. These mice were administered L-glutamic acid (2 g kg^{-1} i.p.) 40 min before and brotizolam (0.1 mg kg^{-1} i.p.) 30 min before retrieval trial, respectively.

3. Statistical analysis

All results were expressed as mean ± S.E.M. Data was analyzed using one-way ANOVA followed by Dunnett's test. $p < 0.05$ was considered to be statistically significant. In acquisition trials, each value represents mean ± S.E.M. 'a' $p < 0.05$ versus ELT on day 1. 'b' $p < 0.05$ versus ELT of control group for the same day. During retrieval trials, each value represents mean ± S.E.M. 'a' $p < 0.05$ versus time spent in other quadrants,

Table 1
Experimental protocol

Treatment	Group	Dose and duration prior to acquisition trials (days 1–4)	Figure	Dose and duration prior to retrieval trial (day 5)	Figure
Control	I	DW (10 ml kg^{-1} i.p.) 30 min before acquisition	Figs. 1a, 2a, 3a	DW (10 ml kg^{-1} i.p.) 30 min before retrieval	Figs. 1b, 2b, 3b
Diazepam anterograde	II	Dz (1 mg kg^{-1} i.p.) 30 min before acquisition	Figs. 2a and 3a	DW (10 ml kg^{-1} i.p.) 30 min before retrieval	Not shown
Diazepam retrograde	III	DW (10 ml kg^{-1} i.p.) 30 min before acquisition	Not shown	Dz (1 mg kg^{-1} i.p.) 30 min before retrieval	Figs. 2b and 3b
Three percent PG *per se*	IV	PG (10 ml kg^{-1} i.p.) 30 min before acquisition	Fig. 1a	PG (10 ml kg^{-1} i.p.) 30 min before retrieval	Fig. 1b
Brotizolam anterograde	V	Bz (0.75 mg kg^{-1} i.p.) 30 min before acquisition	Not shown	PG (10 ml kg^{-1} i.p.) 30 min before retrieval	Not shown
Brotizolam anterograde	VI	Bz (0.50 mg kg^{-1} i.p.) 30 min before acquisition	Not shown	PG (10 ml kg^{-1} i.p.) 30 min before retrieval	Not shown
Brotizolam anterograde	VII	Bz (0.25 mg kg^{-1} i.p.) 30 min before acquisition	Fig. 1a	PG (10 ml kg^{-1} i.p.) 30 min before retrieval	Fig. 1b
Brotizolam anterograde	VIII	Bz (0.10 mg kg^{-1} i.p.) 30 min before acquisition	Fig. 1a	PG (10 ml kg^{-1} i.p.) 30 min before retrieval	Fig. 1b
Brotizolam anterograde	IX	Bz (0.05 mg kg^{-1} i.p.) 30 min before acquisition	Fig. 1a	PG (10 ml kg^{-1} i.p.) 30 min before retrieval	Fig. 1b
Brotizolam anterograde	X	Bz (0.01 mg kg^{-1} i.p.) 30 min before acquisition	Fig. 1a	PG (10 ml kg^{-1} i.p.) 30 min before retrieval	Fig. 1b
Brotizolam retrograde	XI	PG (10 ml kg^{-1} i.p.) 30 min before acquisition	Fig. 1c	Bz (0.25 mg kg^{-1} i.p.) 30 min before retrieval	Fig. 1d
Brotizolam retrograde	XII	PG (10 ml kg^{-1} i.p.) 30 min before acquisition	Fig. 1c	Bz (0.10 mg kg^{-1} i.p.) 30 min before retrieval	Fig. 1d
Brotizolam retrograde	XIII	PG (10 ml kg^{-1} i.p.) 30 min before acquisition	Fig. 1c	Bz (0.01 mg kg^{-1} i.p.) 30 min before retrieval	Fig. 1d
Norharman *per se*	XIV	NH (20 ml kg^{-1} i.p.) 40 min before acquisition	Fig. 2a	NH (20 ml kg^{-1} i.p.) 40 min before retrieval	Fig. 2b
Norharman 10 mg + diazepam anterograde	XV	NH (10 kg^{-1} i.p.) 40 min before acquisition + diazepam (1 mg kg^{-1} i.p.) 30 min before acquisition	Not shown	DW (10 ml k retrieval g^{-1} i.p.) 40 min before retrieval	Not shown
Norharman 20 mg + diazepam − anterograde	XVI	NH (20 kg^{-1} i.p.) 40 min before acquisition + diazepam (1 mg kg^{-1} i.p.) 30 min before acquisition	Fig. 2a	DW (10 ml kg^{-1} i.p.) 40 min before retrieval	Not shown
Norharman 20 mg + brotizolam − anterograde	XVII	NH (20 kg^{-1} i.p.) 40 min before acquisition + brotizolam (0.1 mg kg^{-1} i.p.) 30 min before acquisition	Not shown	DW (10 ml kg^{-1} i.p.) 40 min before + 3% PG 30 min before retrieval	Not shown
Norharman 40 mg + brotizolam − anterograde	XVIII	NH (40 kg^{-1} i.p.) 40 min before acquisition + brotizolam (0.1 mg kg^{-1} i.p.) 30 min before acquisition	Fig. 2a	DW (10 ml kg^{-1} i.p.) 40 min before + 3% PG 30 min before retrieval	Not shown
Norharman (20 mg) + brotizolam − retrograde	XIX	DW (10 ml kg^{-1} i.p.) 40 min before acquisition + 3% PG 30 min before acquisition	Not shown	NH (20 kg^{-1} i.p.) 40 min before + brotizolam (0.1 mg kg^{-1} i.p.) 30 min before retrieval	Fig. 2b
L-Glutamic acid *per se*	XX	GA (2 g kg^{-1} i.p.) 40 min before acquisition	Fig. 3a	GA (2 g kg^{-1} i.p.) 40 min before retrieval	Fig. 3b
L-Glutamic acid 2 g + diazepam − anterograde	XXI	GA (2 g kg^{-1} i.p.) 40 min before acquisition + diazepam (1 mg kg^{-1} i.p.) 30 min before acquisition	Fig. 3a	DW (10 ml kg^{-1} i.p.) 40 min before retrieval	Not shown
L-Glutamic acid 2 g + brotizolam − anterograde	XXII	GA (2 g kg^{-1} i.p.) 40 min before acquisition + brotizolam (0.1 mg kg^{-1} i.p.) 30 min before acquisition	Fig. 3a	DW (10 ml kg^{-1} i.p.) 40 min before retrieval + 3% PG 30 min before retrieval	Not shown
L-Glutamic acid + brotizolam − 2 g retrograde	XXIII	DW (10 ml kg^{-1} i.p.) 40 min before acquisition + 3% PG 30 min before acquisition	Not shown	GA (2 g kg^{-1} i.p.) 40 min before retrieval + brotizolam (0.1 mg kg^{-1} i.p.) 30 min before retrieval	Fig. 3b

Regimen for administration of vehicle and pharmacological agents. Bz: Brotizolam, DW: Distilled Water, Dz: Diazepam, GA:L-Glutamic Acid, NH: Norharman, PG: 3% Propyleneglycol.

i.e. Q2, Q3 and Q4. $^{*}p < 0.05$ versus time spent in target quadrant (Q1) in control group.

4. Results

4.1. Diazepam produces anterograde amnesia and brotizolam produces anterograde and retrograde amnesia both

Lower doses of brotizolam, i.e. 0.01 mg kg^{-1} i.p. produced no significant effect on decrease in ELT during successive acquisition trials (Fig. 1a) and the time spent in the target quadrant (Fig. 1b). Administration of brotizolam at higher doses (0.25, 0.10 and 0.05 mg kg^{-1} i.p.) significantly attenuated the decrease in ELT recorded during acquisition trials (Fig. 1a) and markedly reduced the time spent in target quadrant (Fig. 1b). These observations suggest that brotizolam produces dose dependent anterograde amnesia.

The different doses of brotizolam (0.25, 0.1 and 0.01 mg kg^{-1} i.p.), administered before retrieval trials, reduced time spent in target quadrant in a dose dependent manner (Fig. 1d) in trained mice which had previously shown progressive decrease in ELT during successive acquisition trials (Fig. 1c). Moreover, lower doses of 0.01 mg kg^{-1} i.p. of brotizolam produced no significant effect on time spent in the target quadrant while comparatively higher doses (0.25 and 0.1 mg kg^{-1} i.p.) of brotizolam markedly reduced the time spent by trained mice in target quadrant (Fig. 1d). These observations suggest that brotizolam produces dose dependent retrograde amnesia. Mice, treated with higher doses of brotizolam (0.50 and 0.75 mg kg^{-1}), were excluded from study because it impaired the swimming ability.

Anterograde administration of diazepam (1 mg kg^{-1} i.p.) attenuated the decrease in ELT during acquisition trials (Figs. 2a and 3a) and markedly reduced the time spent in target quadrant (Data not shown). It should be noted that failure of retrieval of memory during retrieval trial was due to diazepam-induced impairment of acquisition. Administration of diazepam (1 mg kg^{-1} i.p.) 30 min before retrieval trials to mice which were trained previously for 4 consecutive acquisition days, produced no significant effect on time spent in the target quadrant (Figs. 2b and 3b). These observations suggest that diazepam does not produce retrograde amnesia.

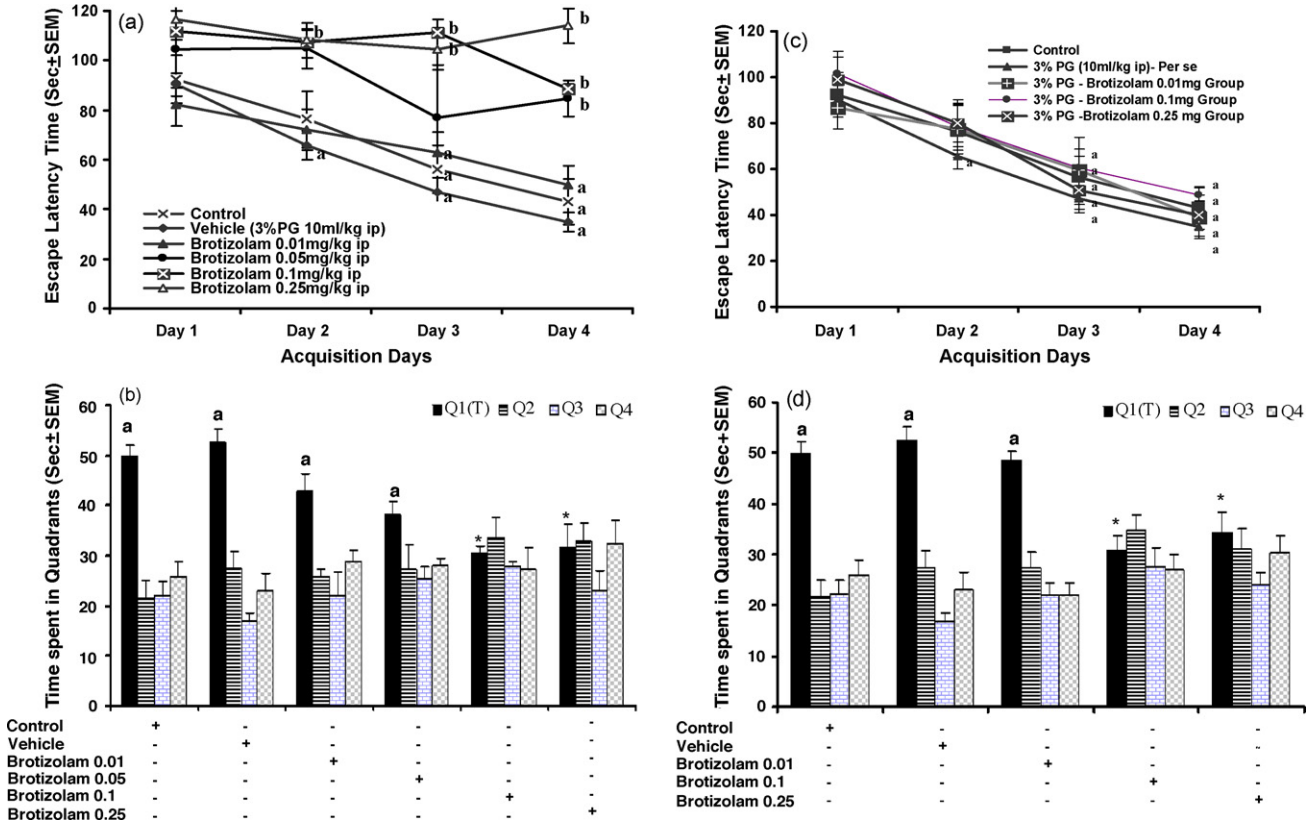


Fig. 1. Effect of brotizolam on acquisition and retrieval of memory. Control represents administration of distilled water (10 ml kg^{-1} i.p.) 30 min before acquisition trials (days 1–4) and retrieval trial (day 5). Vehicle represents administration of 3% propylene glycol (10 ml kg^{-1} i.p.) 30 min before acquisition and retrieval trial. (a) Brotizolam produces dose dependent anterograde amnesia when it (0.01, 0.05, 0.1 and 0.25 mg kg^{-1} i.p.) was administered 30 min before acquisition trials. (b) The dose dependent anterograde amnesic effect of brotizolam is also corroborated by impaired retrieval. (c) Shows normal acquisition in mice. These mice were administered 3% propylene glycol (10 ml kg^{-1} i.p.) before acquisition trials. (d) Brotizolam produces dose dependent retrograde amnesia in the trained mice when brotizolam (0.01, 0.1 and 0.25 mg kg^{-1} i.p.) was administered 30 min before retrieval trials. Data was analyzed using one-way ANOVA followed by Dunnett's test and Duncun test and $p < 0.05$ was considered to be statistically significant. 'a' $p < 0.05$ vs. ELT on day 1. 'b' $p < 0.05$ vs. ELT of control group for the same day during acquisition trials. 'a' $p < 0.05$ vs. time spent in other quadrants, i.e. Q2, Q3 and Q4. $^{*}p < 0.05$ vs. time spent in target quadrant (Q1) in control group during retrieval trials.

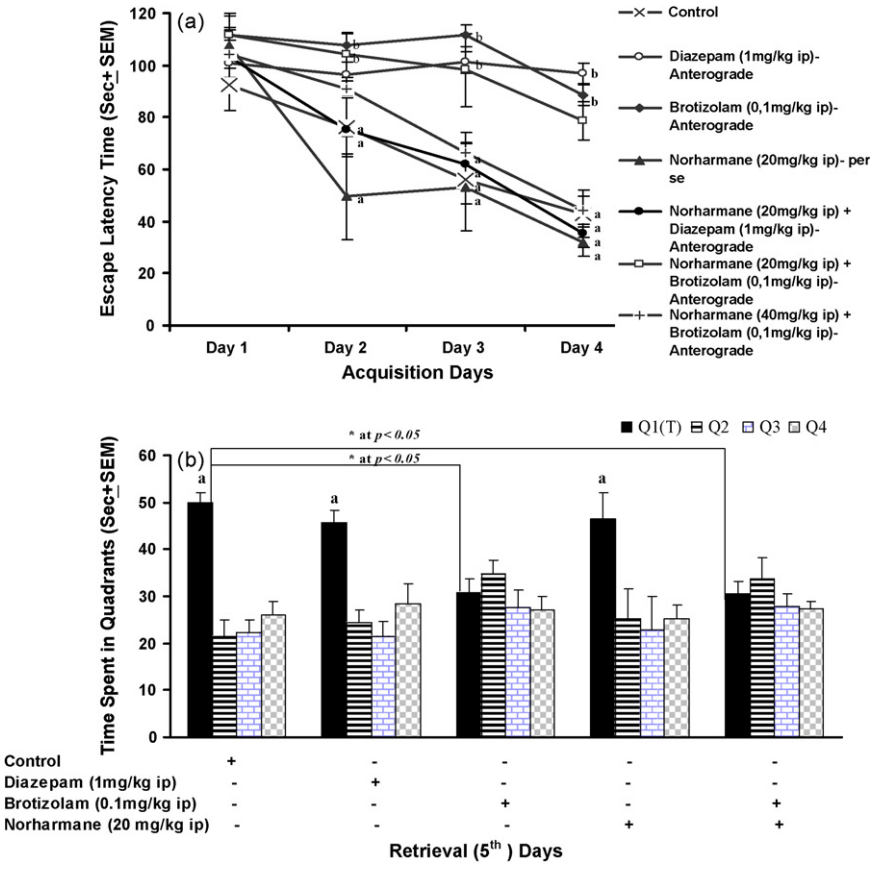


Fig. 2. Effect of norharman on diazepam and brotizolam induced amnesia. Control represents administration of distilled water (10 ml kg^{-1} i.p.) 30 min before acquisition and retrieval trial. (a) Norharmane significantly attenuates diazepam and brotizolam induced anterograde amnesia when administered prior to acquisition trials. (b) Brotizom produces retrograde amnesia which is unaffected by norharmane while diazepam dose not produce retrograde amnesia when these agents are administered prior to retrieval trial to learned mice. Data was analyzed using one-way ANOVA followed by Dunnett's test and $p < 0.05$ was considered to be statistically significant. 'a' $p < 0.05$ vs. ELT on day 1. 'b' $p < 0.05$ vs. ELT of control group for the same day during acquisition trials. 'a' $p < 0.05$ vs. time spent in other quadrants, i.e. Q2, Q3 and Q4. $^{*}p < 0.05$ vs. time spent in target quadrant (Q1) in control group during retrieval trials.

4.2. Norharmane attenuates diazepam and brotizolam induced anterograde amnesia

Norharmane at 10 mg kg^{-1} i.p., administered 40 min before acquisition trials (data not shown), did not reverse diazepam (1 mg kg^{-1} i.p.) induced attenuation of decrease in ELT while at 20 mg kg^{-1} i.p. It significantly prevented diazepam (1 mg kg^{-1} i.p.) induced attenuation of decrease in ELT (Fig. 2a). This suggests that norharmane attenuates diazepam induced anterograde amnesia.

Norharmane at 40 mg kg^{-1} i.p., administered before acquisition trial, also significantly prevented brotizolam (0.1 mg kg^{-1} i.p.) induced attenuation of decrease in ELT with ongoing acquisition trials (Fig. 2a). The attenuating effect of norharmane at 20 mg kg^{-1} i.p. on brotizolam (0.1 mg kg^{-1} i.p.) induced anterograde amnesia was less pronounced (Fig. 2a). This latter dose when administered before retrieval trial, did not alter the brotizolam (0.1 mg kg^{-1} i.p.) induced decrease in time spent in the target quadrant (Fig. 2b). These observations suggest that norharmane attenuates brotizolam induced anterograde amnesia but does not affect brotizolam induced retrograde amnesia.

4.3. L-Glutamic acid reverses brotizolam induced retrograde amnesia

L-Glutamic acid at 2 g kg^{-1} i.p., when administered 40 min before acquisition trials, did not produce significant effect on diazepam (1 mg kg^{-1} i.p.) and brotizolam (0.1 mg kg^{-1} i.p.) induced attenuation of decrease in ELT (Fig. 3a) while it significantly prevented brotizolam (0.1 mg kg^{-1} i.p.) induced decrease in time spent in the target quadrant (Fig. 3b).

4.4. Three percent PG, norharman and L-glutamic acid do not affect normal acquisition of memory

ELT significantly decreased over successive days with acquisition trials on days 1–4 in mice in the control group which were administered distilled water (10 ml kg^{-1} i.p.) 30 min before acquisition trials (Figs. 1a, c, 2a and 3a). Mice, administered distilled water (10 ml kg^{-1} i.p.) 30 min before retrieval trial spent significantly more time in the target quadrant (Q1) as compared to time spent in the other quadrants (Q2, Q3 and Q4) during retrieval trial (Figs. 1b, d, 2b and 3b). Three percent PG (10 ml kg^{-1} i.p.), administered 30 min before acquisition and

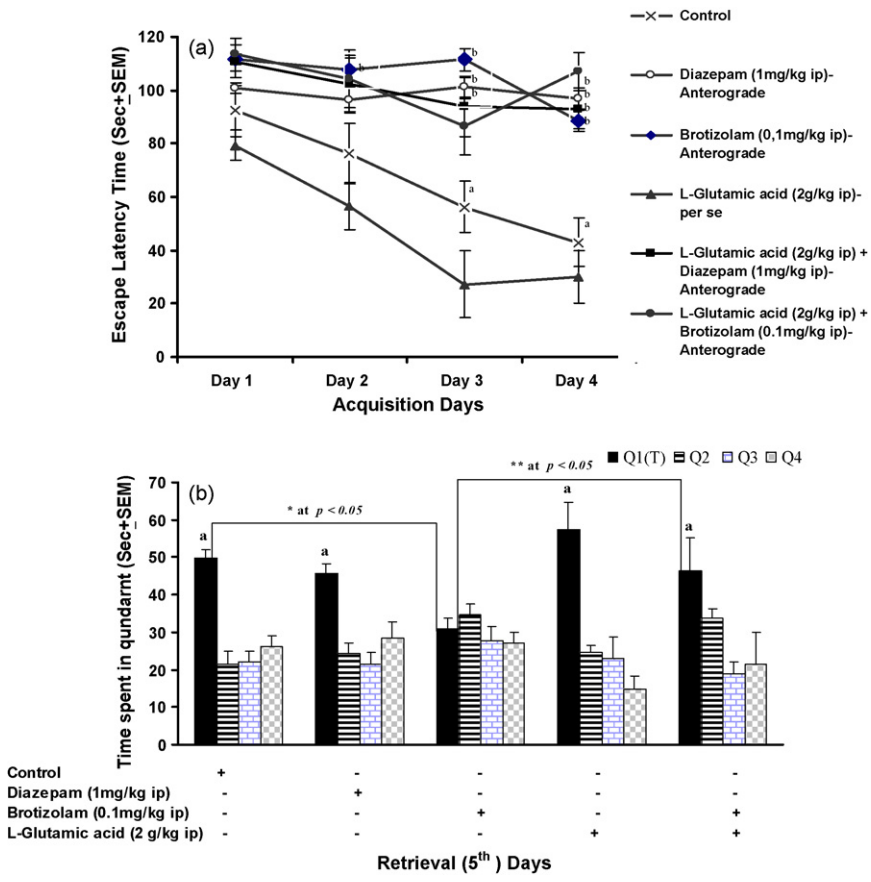


Fig. 3. Effect of L-glutamic acid on diazepam and brotizolam induced amnesia. Control represents administration of distilled water (10 ml kg^{-1} i.p.) 30 min before acquisition and retrieval trial. (a) L-Glutamic acid does not attenuate diazepam and brotizolam induced anterograde amnesia when administered prior to acquisition trials. (b) Brotizom produces retrograde amnesia which is significantly reversed by L-glutamic acid while diazepam dose not produce retrograde amnesia when these agents administered prior to retrieval trial to learned mice. Data was analyzed using one-way ANOVA followed by Dunnett's test and $p < 0.05$ was considered to be statistically significant. 'a' $p < 0.05$ vs. ELT on day 1. 'b' $p < 0.05$ vs. ELT of control group for the same day during acquisition trials. 'a' $p < 0.05$ vs. time spent in other quadrants, i.e. Q2, Q3 and Q4. $^{*}p < 0.05$ vs. time spent in target quadrant (Q1) in control group during retrieval trials.

retrieval trials, did not produce significant effect on decrease in ELT during successive acquisition trials (Figs. 1a and 2a) and the time spent in the target quadrant (Q1) (Figs. 1b and 2b). Norharmane (20 mg kg^{-1} i.p.), administered 30 min before acquisition and retrieval trial, did not produce significant effect on decrease in ELT during successive acquisition trials and the time spent in the target quadrant during retrieval trial as compared to the control group treated with distilled water (Fig. 2a and b). These observations suggest that norharmane exerts no direct effect on normal acquisition and retrieval of memory.

Similarly, L-glutamic acid (2 g kg^{-1} i.p.), when administered 30 min before acquisition and retrieval trials did not produce any effect on decrease in ELT during successive acquisition trials or the time spent in the target quadrant (Q1) during retrieval trial (Fig. 3a and b). These observations suggest that L-glutamic acid has no direct effect on normal acquisition and retrieval of memory.

5. Discussion

This report constitutes the result of series of experiments following our documentation of anti amnesic effects of flumazenil on brotizolam induced anterograde amnesia using water maze mouse model. We reported that such anti-amnesic effects were presumably exerted through the mediation of Benzodiazepine receptor as displayed by known antagonistic properties of flumazenil [18]. In order to examine the effect of other modifiers of this receptor we tested the inverse agonist characteristic of norharmane with brotizolam and diazepam. The present study revealed that both diazepam and brotizolam administration in mice significantly attenuates the normal decrease in ELT during acquisition trials and brotizolam, but not diazepam, prevents the preferential stay of mice in the target quandrant during retrieval trial. While diazepam produced only anterograde amnesia and brotizolam produced both anterograde and retrograde amnesia. Similar amnesic effects have been earlier reported by using various benzodiazepines [49] such as diazepam, halazepam [14], lorazepam and chlordiazepoxide [14] in rodents. In this study brotizolam required moderate doses (0.1 mg kg^{-1} i.p.) to produce the complete anterograde amnesia. Similar studies with alprazolam [17] and brotizolam [18] have produced both anterograde and retrograde amnesia in mice. Ro 15-4513 and beta-CCM, benzodiazepine inverse agonists are also reported to show anti-amnesic affect by increasing retention and prolonged

the step-down latencies in amnesic mice treated with ethanol [50]. Beta-CCM also antagonizes EGCG-induced amnesia in the passive avoidance test [35] and alleviates the memory deficits of alcohol-treated subjects [36]. Beta-carboline like beta-CCM is also known to enhance learning performance upon diazepam induced anterograde amnesia [31]. Since norharmane is a benzodiazepine receptor inverse agonist [43] we investigated the effect of norharmane on brotizolam induced amnesia. This study showed that norharmane prevented brotizolam induced anterograde amnesia. We were also able to examine the effect of norharmane on a standard benzodiazepine receptor agonist such as diazepam and found it to reverse anterograde amnesia caused by it. These observations suggest that the anti-amnesic effect of norharmane on diazepam and brotizolam induced anterograde amnesia indirectly support the role of benzodiazepine receptor in evoking amnesia. Similar observations have been reported using flumazenil [21] and CGS8216 (a benzodiazepine receptor antagonists) [28] with benzodiazepines [32–34]. Beta-carbolines (an inverse agonist of benzodiazepine receptors) also improves cognitive performance impaired by benzodiazepine [14,30]. However, norharmane which can also bind to other neurotransmitter receptors in the brain, including 5-HT and dopamine receptors and possess MAO-A or MAO-B inhibition properties can engage an alternative mechanism through which norharmane exhibits antiamnesic effect. Norharmane, however, did not prevent brotizolam induced retrograde amnesia, suggesting that this is mediated through a mechanism independent of the interaction with either MAO-A or benzodiazepine receptors. It lends credence to earlier studies with flumazenil (a benzodiazepine receptor antagonist) and brotizolam [18] where the retrograde amnesia was not reversed even by blocking benzodiazepine receptor.

Glutamate receptor agonist facilitates long-term potentiation by activating postsynaptic glutamate receptors such as NMDA (*N*-methyl-D-aspartate) receptor and therefore induces the memory process [47,51–54]. In this study, retrograde amnesia induced by brotizolam was reversed by glutamic acid but not by norharmane. L-Glutamic acid did not reverse anterograde amnesia which was reversed by norharmane. It is possible that anterograde amnesia induced by diazepam or brotizolam proceeds with the involvement of presynaptic circuits and glutamic acid participates in the processing of the memory retrieval by involvement of postsynaptic connexions. It is known that Glutamate receptor agonists such as monosodium glutamate, glutamic acid may be beneficial in lower concentration [47,55] but are harmful in higher concentration due to prolonged activity of glutamate receptors and may subsequently cause neurodegeneration [56–58]. Glutamic acid reverses $Pb^{(2+)}$-induced NMDA receptor damage [59] and modulates the cytotoxic effect of tumor necrosis factor in the HL-60 cell line [60] providing an indirect evidence for its role in memory consolidation. L-Glutamic acid has been studied to enhance retention in mice on a shock avoidance-learning paradigm. In Y-maze study, Glutamic acid has not only been shown to improve learning in normal mice but in also antagonizing the amnesic effect of diazepam and GABA in step-down test that suggests that increasing GABA-ergic neuronal transmission is unfavorable to learning and memory, but increasing Glutaminergic transmission is contrary to the former [61]. D-Cycloserine, NMDA receptor agonist, has also been reported to improve the acquisition of rats treated with scopolamine in water maze task [62]. Moreover, D-cycloserine along with milacemide, a glycine prodrug, has also been noted to reverse learning impairments induced by beta 25–35-amyloid peptide [63]. The blockers of glutamate receptors, aminophosphonovaleric acid (AP5) and cyano-nitroquinoxaline-dione (CNQX) impair retention in step-down avoidance task [64] suggesting a prominent role of NMDA receptor in the process of learning and memory. Dizocilpine, a NMDA receptor antagonist, has also been documented to produce amnesia in the Y-maze task and step-down type passive avoidance [65]. It has been reported that brotizolam blocks PAF receptor [18,22–25] and activates benzodiazepine receptor [19–21]. Shimizu et al. have described that triazolam, triazolodiazepine, impairs spatial memory in rats by reducing glutamate release in the dorsal hippocampus [66] thus providing an indirect evidence of the role of glutamic acid in LTP. In the previous studies, we had reported that phenyl methane sulfonyl fluoride (PMSF), a PAF acetyl hydrolase inhibitor, reversed brotizolam induced retrograde amnesia possibly by reducing metabolism of PAF. Triazolam induced retrograde amnesia is also demonstrated to reverse by PAF and cigarete smoke extract. In this study, L-glutamic acid reversed brotizolam induced retrograde amnesia. We could neither conclude that PAF receptor mediated LTP modulation is directly responsible for anti-amnesic effect of L-glutamic acid nor establish that it is not. We can not rule out the possibility that L-glutamic acid supplements synaptic glutamate receptor potentiation thereby increasing the synaptic concentration of PAF from postsynaptic neurons, relieve PAF blockade and subsequently revive the LTP but only additional experiments can determine this. Similarly, we recognize the possibility of involvement of other mechanisms independent of PAF receptor in evoking anti-amnesic effects of L-glutamic acid.

6. Conclusion

We conclude that anterograde amnesia induced by brotizolam and effectively attenuated by norharmane, and retrograde amnesia induced by brotizolam and reversed by L-glutamic acid, constitutes a significant finding that could help in understanding memory enhancing agents and their targets.

Acknowledgements

This study was supported by Medical Education and Research Cell, Post Graduate Institute of Medical Education and Research, Chandigargh, India. We are grateful to Prof. Manjeet Singh, Former Head, Department of Pharmaceutical Science and Drug Research, Punjabi University, Patiala for the gift of brotizolam. We are also thankfully obliged to Mr. R.C. Goyal, Statistician, PGIMER, Chandigarh, India for data analysis. We are thankful to Prof. P. Pandhi, Head, Department of Pharmacology for logistic support.

References

[1] Llorente-Vizcaino A, Cejudo-Bolivar JC. Memories and Alzheimer's disease. Rev Neurol 2001;32:1163–72.
[2] Basu S, Bhattacharya KB. Dementia current status. Post Grad Med 2003;17:543–51.
[3] Fama R, Marsh L, Sullivan EV. Dissociation of remote and anterograde memory impairment and neural correlates in alcoholic Korsakoff syndrome. J Int Neuropsychol Soc 2004;10:427–41.
[4] McIntosh C, Chick J. Alcohol and the nervous system. J Neurol Neurosurg Psychiatry 2004;75(Suppl. 3):iii16–21.
[5] Vik PW, Cellucci T, Jarchow A, Hedt J. Cognitive impairment in substance abuse. Psychiatr Clin North Am 2004;27:97–109, ix.
[6] Chun MM. Drug-induced amnesia impairs implicit relational memory. Trends Cogn Sci 2005;9:355–7.
[7] Barros DM, Carlis V, Maidana M, Silva ES, Baisch AL, Ramirez MR, et al. Interactions between anandamide-induced anterograde amnesia and post-training memory modulatory systems. Brain Res 2004;1016:66–71.
[8] Ji JZ, Zhang XH, Li BM. Deficient spatial memory induced by blockade of beta-adrenoceptors in the hippocampal CA1 region. Behav Neurosci 2003;117:1378–84.
[9] Mejo SL. Anterograde amnesia linked to benzodiazepines. Nurse Pract 1992;17(44):49–50.
[10] Hung DZ, Tsai WJ, Deng JF. Anterograde amnesia in triazolam overdose despite flumazenil treatment: a case report. Hum Exp Toxicol 1992;11:289–90.
[11] Di Renzi E, Lucchelli F, Muggia S, Spinnler H. Is memory loss without anatomical damage tantamount to a psychogenic deficit? The case of pure retrograde amnesia. Neuropsychologia 1997;35:781–94.
[12] Squire LR, Clark RE, Knowlton BJ. Retrograde amnesia. Hippocampus 2001;11:50–5.
[13] Rossato JI, Bonini JS, Coitinho AS, Vianna MR, Medina JH, Cammarota M, et al. Retrograde amnesia induced by drugs acting on different molecular systems. Behav Neurosci 2004;118:563–8.
[14] Jensen LH, Stephens DN, Sarter M, Petersen EN. Bidirectional effects of beta-carbolines and benzodiazepines on cognitive processes. Brain Res Bull 1987;19:359–64.
[15] Patel JB, Ciofolo VB, Iorio LC. Benzodiazepine blockade of passive-avoidance task in mice: a state-dependent phenomenon. Psychopharmacology (Berl) 1979;61:25–8.
[16] Ghoneim MM, Mewaldt SP. Benzodiazepines and human memory: a review. Anesthesiology 1990;72:926–38.
[17] Singh N, Sharma A, Singh M. Possible mechanism of alprazolam-induced amnesia in mice. Pharmacology 1998;56:46–50.
[18] Saraf MK, Kishore K, Thomas KM, Sharma A, Singh M. Role of platelet activating factor in triazolobenzodiazepines-induced retrograde amnesia. Behav Brain Res 2003;142:31–40.
[19] Jin YH, Munakata M, Morimoto H, Akaike N. Effects of benzodiazepine receptor agonists in neurones acutely dissociated from the rat neostriatum. Neuroreport 1997;8:3197–200.
[20] Hirouchi M, Mizutani H, Kohno Y, Kuriyama K. Characteristics of the association of brotizolam, a thieno-triazolo diazepine derivative, with the benzodiazepine receptor: a selective and high affinity ligand of the central type I benzodiazepine receptor. Jpn J Pharmacol 1992;59:387–91.
[21] Sanger DJ, Perrault G, Morel E, Joly D, Zivkovic B. Animal models of anxiety and the development of novel anxiolytic drugs. Prog Neuropsychopharmacol Biol Psychiatry 1991;15:205–12.
[22] Casals-Stenzel J. Thieno-triazolo-1,4-diazepines as antagonists of platelet-activating factor: present status. Lipids 1991;26:1157–61.
[23] Paulson SK, Wolf JL, Novotney-Barry A, Cox CP. Pharmacologic characterization of the rabbit neutrophil receptor for platelet-activating factor. Proc Soc Exp Biol Med 1990;195:247–54.
[24] Tahraoui L, Floch A, Mondot S, Cavero I. High affinity specific binding sites for tritiated platelet-activating factor in canine platelet membranes: counterparts of platelet-activating factor receptors mediating platelet aggregation. Mol Pharmacol 1988;34:145–51.
[25] Robaut C, Durand G, James C, Lave D, Sedivy P, Floch A, et al. PAF binding sites. Characterization by [3H]52770 RP, a pyrrolo[1,2-c]thiazole derivative, in rabbit platelets. Biochem Pharmacol 1987;36:3221–9.
[26] Leonard JP, Heinrich-Nols J, Roth TG. Nocturnal psychometric assessment of the hypnotic activity of low and normal doses of brotizolam. Arzneimittelforschung 1996;46:462–7.
[27] Leonard JP, Heinrich-Nols J, Roth TG. Dynamics of the hypnotic effect of 0.125 mg and 0.250 mg brotizolam. The lower dosage is adequate for treatment of sleep disorders. Fortschr Med 1996;114:179–82.
[28] Cain DP. Prior non-spatial pretraining eliminates sensorimotor disturbances and impairments in water maze learning caused by diazepam. Psychopharmacology (Berl) 1997;130:313–9.
[29] Leidenheimer NJ, Schechter MD. Evidence for noradrenergic involvement in mediating the FG 7142 discriminative stimulus. Pharmacol Biochem Behav 1992;43:77–83.
[30] Venault P, Chapouthier G, de Carvalho LP, Simiand J, Morre M, Dodd RH, et al. Benzodiazepine impairs and beta-carboline enhances performance in learning and memory tasks. Nature 1986;321:864–6.
[31] Venault P, Chapouthier G, Simiand J, Dodd RH, Rossier J. Enhancement of performance by methyl beta-carboline-3-carboxylate, in learning and memory tasks. Brain Res Bull 1987;19:365–70.
[32] Hodges H, Green S. Effects of chlordiazepoxide on cued radial maze performance in rats. Psychopharmacology (Berl) 1986;88:460–6.
[33] Jensen RA, Martinez JL, Vasquez BJ, McGaugh JL. Benzodiazepines alter acquisition and retention of an inhibitory avoidance response in mice. Psychopharmacology (Berl) 1979;64:125–9.
[34] Lister RG. The amnesic action of benzodiazepines in man. Neurosci Biobehav Rev 1985;9:87–94.
[35] Vignes M, Maurice T, Lante F, Nedjar M, Thethi K, Guiramand J, et al. Anxiolytic properties of green tea polyphenol (–)-epigallocatechin gallate (EGCG). Brain Res 2006;1110:102–15.
[36] Beracochea D. Animal models of amnesia of alcoholic origin: an amnesia without memory impairment. Therapie 2000;55:493–501.
[37] Beracochea D, Celerier A, Pierard C. BetaCCM but not physostigmine enhancement of memory retrieval depends on emotional processes in mice. Psychopharmacology (Berl) 2004;176:66–73.
[38] Fekkes D, Schouten MJ, Pepplinkhuizen L, Bruinvels J, Lauwers W, Brinkman UA. Norharman, a normal body constituent. Lancet 1992;339:506.
[39] Totsuka Y, Ushiyama H, Ishihara J, Sinha R, Goto S, Sugimura T, et al. Quantification of the co-mutagenic beta-carbolines, norharman and harman, in cigarette smoke condensates and cooked foods. Cancer Lett 1999;143:139–43.
[40] Adachi J, Mizoi Y, Naito T, Yamamoto K, Fujiwara S, Ninomiya I. Determination of beta-carbolines in foodstuffs by high-performance liquid chromatography and high-performance liquid chromatography-mass spectrometry. J Chromatogr 1991;538:331–9.
[41] Fekkes D, Bode WT. Occurrence and partition of the beta-carboline norharman in rat organs. Life Sci 1993;52:2045–54.
[42] Baum SS, Hill R, Rommelspacher H. Norharman-induced changes of extracellular concentrations of dopamine in the nucleus accumbens of rats. Life Sci 1995;56:1715–20.
[43] Mingo NS, Burnham WM. Secondary generalization in non-kindled rats following acute administration of GABA-complex and adenosine antagonists. Electroencephalogr Clin Neurophysiol 1990;75:444–51.
[44] Pawlik M, Kaulen P, Baumgarten HG, Rommelspacher H. Quantitative autoradiography of [3H]norharman [(3H]beta-carboline) binding sites in the rat brain. J Chem Neuroanat 1990;3:19–24.
[45] Herraiz T, Chaparro C. Human monoamine oxidase enzyme inhibition by coffee and beta-carbolines norharman and harman isolated from coffee. Life Sci 2006;78:795–802.
[46] Herraiz T, Chaparro C. Human monoamine oxidase is inhibited by tobacco smoke: beta-carboline alkaloids act as potent and reversible inhibitors. Biochem Biophys Res Commun 2005;326:378–86.
[47] Flood JF, Baker ML, Davis JL. Modulation of memory processing by glutamic acid receptor agonists and antagonists. Brain Res 1990;521:197–202.
[48] Morris R. Developments of a water-maze procedure for studying spatial learning in the rat. J Neurosci Methods 1984;11:47–60.

[49] Gamzu ER. Animal model studies of benzodiazepine-induced amnesia. Psychopharmacol Ser 1988;6:218–29.
[50] Nabeshima T, Tohyama K, Kameyama T. Reversal of alcohol-induced amnesia by the benzodiazepine inverse agonist Ro 15-4513. Eur J Pharmacol 1988;155:211–7.
[51] Mangiavacchi S, Wolf ME. Stimulation of *N*-methyl-D-aspartate receptors, AMPA receptors or metabotropic glutamate receptors leads to rapid internalization of AMPA receptors in cultured nucleus accumbens neurons. Eur J Neurosci 2004;20:649–57.
[52] Lozovaya NA, Grebenyuk SE, Tsintsadze T, Feng B, Monaghan DT, Krishtal OA. Extrasynaptic NR2B and NR2D subunits of NMDA receptors shape 'superslow' afterburst EPSC in rat hippocampus. J Physiol 2004;558:451–63.
[53] Fujii S, Sasaki H, Mikoshiba K, Kuroda Y, Yamazaki Y, Mostafa Taufiq A, et al. A chemical LTP induced by co-activation of metabotropic and *N*-methyl-D-aspartate glutamate receptors in hippocampal CA1 neurons. Brain Res 2004;999:20–8.
[54] Fujii S, Mikoshiba K, Kuroda Y, Ahmed TM, Kato H. Cooperativity between activation of metabotropic glutamate receptors and NMDA receptors in the induction of LTP in hippocampal CA1 neurons. Neurosci Res 2003;46:509–21.
[55] Gribanova NV, Rakitina TV, Zhokhov SS, Pustoshilova NM, Lipkin VM, Kostanian IA. L-Glutamic acid modulates the cytotoxic effect of tumor necrosis factor in the HL-60 cell line. Bioorg Khim 2005;31:602–8.
[56] Sanabria ER, Pereira MF, Dolnikoff MS, Andrade IS, Ferreira AT, Cavalheiro EA, et al. Deficit in hippocampal long-term potentiation in monosodium glutamate-treated rats. Brain Res Bull 2002;59:47–51.
[57] Ishikawa K, Kubo T, Shibanoki S, Matsumoto A, Hata H, Asai S. Hippocampal degeneration inducing impairment of learning in rats: model of dementia? Behav Brain Res 1997;83:39–44.
[58] Marmo E. L-Glutamic acid as a neurotransmitter in the CNS. Med Res Rev 1988;8:441–58.
[59] Xu SZ, Rajanna B. Glutamic acid reverses Pb2+-induced reductions of NMDA receptor subunits in vitro. Neurotoxicology 2006;27:169–75.
[60] Kostanian IA, Nurieva RI, Novolotskaia EV, Astapova MV, Dranitsyna SM, Zav'ialov VP, et al. Effect of L-glutamic acid on the reception of cytokines by HL-60 cells. Bioorg Khim 1998;24:3–9.
[61] Pan JC, Zhang SS. Antagonism of piracetam on the amnestic effect of diazepam in mice. Yao Xue Xue Bao 1996;31:91–4.
[62] Sirvio J, Ekonsalo T, Riekkinen Jr P, Lahtinen H, Riekkinen Sr P. D-Cycloserine, a modulator of the *N*-methyl-D-aspartate receptor, improves spatial learning in rats treated with muscarinic antagonist. Neurosci Lett 1992;146:215–8.
[63] Maurice T, Lockhart BP, Su TP, Privat A. Reversion of beta 25–35-amyloid peptide-induced amnesia by NMDA receptor-associated glycine site agonists. Brain Res 1996;731:249–53.
[64] Jerusalinsky D, Ferreira MB, Walz R, Da Silva RC, Bianchin M, Ruschel AC, et al. Amnesia by post-training infusion of glutamate receptor antagonists into the amygdala, hippocampus, and entorhinal cortex. Behav Neural Biol 1992;58:76–80.
[65] Maurice T, Privat A. SA4503, a novel cognitive enhancer with sigma1 receptor agonist properties, facilitates NMDA receptor-dependent learning in mice. Eur J Pharmacol 1997;328:9–18.
[66] Shimizu K, Matsubara K, Uezono T, Kimura K, Shiono H. Reduced dorsal hippocampal glutamate release significantly correlates with the spatial memory deficits produced by benzodiazepines and ethanol. Neuroscience 1998;83:701–6.

© 2004 Nature Publishing Group http://www.nature.com/naturemedicine

Mouse models of visual deficits

To the editor:

In their recent article[1], Ambati and colleagues present important data that provides insight into cell involvement in age-related macular degeneration (AMD). However, they erroneously state that there is "no animal model of drusen deposition or spontaneously occurring CNV [choroidal neovascularization] resembling that seen in patients with AMD." Jackson Laboratories (Bar Harbor, Maine, USA) has a strain of mouse (C57BLKS-*Bst*/J) in which, "after seven months of age, 19% of heterozygotes have focal, nonrhegmatogenous, retinal detachment accompanied by subretinal neovascularization." These symptoms of this strain were originally reported by Smith *et al.*[2]. Although Ambati *et al.* present an exciting finding of a new model for AMD, it would benefit the readers to be aware that there is at least another model of CNV that may also suit their research interests.

Nilanjana Sengupta & Sergio Caballero
Department of Pharmacology and Therapeutics, PO Box 100267, University of Florida, Gainesville, Florida 32610-0267, USA.
jhimli@ufl.edu

1. Ambati, J. *et al. Nat. Med.* **9**, 1390–1397 (2003).
2. Smith, R.S. *et al. Proc. Natl. Acad. Sci. USA* **97**, 2191–2195 (2000).

Ambati *et al.* reply:

We thank Sengupta and Caballero for their interest in our work. Although a small fraction of $Bst^{+/-}$ mice spontaneously develop choroidal neovascularization (CNV), Sengupta and Caballero do not mention that a majority of these heterozygous mice show many other severe ocular disturbances[1–3]. Nearly 60% of $Bst^{+/-}$ mice have abnormal pupillary light responses owing to unilateral or bilateral atrophy of the optic nerves. The mean number of retinal ganglion cells is reduced by 70% as a result of delayed fusion of the optic fissure. In addition to optic nerve malformation (coloboma), several foci of the neural retina are characterized by folds, dysplasia and thinning. Ectopic ganglion cell axons and photoreceptor nuclei are further examples of disorganization. Persistence of the hyaloid vessels is another ocular disturbance in $Bst^{+/-}$ mice.

Although the optic nerve pathology in $Bst^{+/-}$ mice is vaguely reminiscent of autosomal dominant optic atrophy (DOA) in humans, it also includes numerous other ocular abnormalities not resembling those seen in DOA. In addition, the mouse ortholog of the human *OPA1* gene, which is mutated in DOA, has been excluded from the mouse *Bst* locus[4]. Given that the CNV phenotype in $Bst^{+/-}$ mice is even more distant than the optic nerve abnormality from the respective human conditions, CNV in these mice is likely to be as uninstructive about the pathogenesis of the human condition as, say, the appearance of lens opacities in these mice is to be about age-related cataract in patients. The ocular phenotype of patients with early or late AMD bears no resemblance to the panoply of structural abnormalities in $Bst^{+/-}$ mice, which probably result from global embryonic dysfunction rather than specific perturbations of cellular pathways. Nevertheless, given the rare occurrence of spontaneous CNV in mice, study of this angiogenic process will provide insight into the secondary effects of CNV on photoreceptor disruption, which ultimately leads to deficits in visual perception.

Jayakrishna Ambati[1], Akshay Anand[2], Eiji Sakurai[1], William A Kuziel[3], Barrett J Rollins[4] & Balamurali K Ambati[5]

[1]Department of Ophthalmology & Visual Sciences, University of Kentucky, Lexington, Kentucky 40536-0284, USA. [2]Department of Neurology, Postgraduate Institute of Medical Education and Research, Chandigarh, 160 012 India. [3]Protein Design Labs, 34801 Campus Drive, Fremont, California 94555, USA. [4]Dana Farber Cancer Institute, Harvard Medical School, Boston, Massachusetts 02115, USA. [5]Department of Ophthalmology, Medical College of Georgia, Augusta, Georgia 30907, USA.
e-mail: jamba2@uky.edu

1. Rice, D.S. *et al. Invest. Ophthalmol. Vis. Sci.* **38**, 2112–2124 (1997).
2. Tang, Q., Rice, D.S. & Goldowitz, D. *Dev. Biol.* **207**, 239–255 (1999).
3. Smith, R.S. *et al. Proc. Natl. Acad. Sci. USA* **97**, 2191–2195 (2000).
4. Delettre, C., Lenaers, G., Belenguer, P. & Hamel, C.P. *BMC Genet* **4**, 8 (2003).

nature medicine

An animal model of age-related macular degeneration in senescent Ccl-2- or Ccr-2-deficient mice

Jayakrishna Ambati[1], Akshay Anand[1], Stefan Fernandez[2], Eiji Sakurai[1], Bert C Lynn[3], William A Kuziel[4], Barrett J Rollins[5] & Balamurali K Ambati[6]

The study and treatment of age-related macular degeneration (AMD), a leading cause of blindness, has been hampered by a lack of animal models. Here we report that mice deficient either in monocyte chemoattractant protein-1 (Ccl-2; also known as MCP-1) or its cognate C-C chemokine receptor-2 (Ccr-2) develop cardinal features of AMD, including accumulation of lipofuscin in and drusen beneath the retinal pigmented epithelium (RPE), photoreceptor atrophy and choroidal neovascularization (CNV). Complement and IgG deposition in RPE and choroid accompanies senescence in this model, as in human AMD. RPE or choroidal endothelial production of Ccl-2 induced by complement C5a and IgG may mediate choroidal macrophage infiltration into aged wild-type choroids. Wild-type choroidal macrophages degrade C5 and IgG in eye sections of *Ccl2*$^{-/-}$ or *Ccr2*$^{-/-}$ mice. Impaired macrophage recruitment may allow accumulation of C5a and IgG, which induces vascular endothelial growth factor (VEGF) production by RPE, possibly mediating development of CNV. These models implicate macrophage dysfunction in AMD pathogenesis and may be useful as a platform for validating therapies.

© 2003 Nature Publishing Group http://www.nature.com/naturemedicine

AMD is the principal cause of irreversible, registered legal blindness on three continents[1]. It is characterized by progressive degeneration of the retina, RPE and underlying choroid (the highly vascular tissue beneath the RPE), which results in severe vision loss. The earliest clinically visible abnormality in AMD is the accumulation of drusen (lipoproteinaceous deposits) in the extracellular matrix between the RPE and the choroid. Drusen deposition is a significant risk factor for progression to CNV, the exudative hallmark of late AMD, and vision loss. To date, there is no animal model of drusen deposition or spontaneously occurring CNV resembling that seen in patients with AMD.

Existing animal models attempting to simulate AMD through high-fat diets and phototoxicity[2,3], senescence acceleration[4] or candidate gene manipulation[5–7] do not fully replicate the clinical, histologic and angiographic features of the human condition. Because macrophage dysfunction may have a role in AMD, we examined the eyes of mice that are deficient in Ccl-2 or its receptor Ccr-2 and consequently possess defects in macrophage mobilization[8,9]. We observed that senescent Ccl-2- and Ccr-2-deficient mice (9–27 months old) exhibited morphological, ultrastructural and functional features characteristic of human AMD.

RESULTS

Drusen and lipofuscin in *Ccl2*$^{-/-}$ and *Ccr2*$^{-/-}$ mice

Eyes from 64 *Ccl2*$^{-/-}$ and *Ccr2*$^{-/-}$ mice and 40 age-matched wild-type mice, ranging from 3 to 27 months of age, were subjected to ocular fundus examination. Of these, eyes from 25 *Ccl2*$^{-/-}$, 21 *Ccr2*$^{-/-}$ and 18 age-matched wild-type mice (6 younger than 12 months, 7 between 12 and 24 months and 5 older than 24 months) were extensively examined histopathologically. Before 9 months of age, the fundi of *Ccl2*$^{-/-}$ and *Ccr2*$^{-/-}$ mice were indistinguishable from those of wild-type mice. After 9 months, subretinal deposits with ophthalmoscopic and pathologic features of drusen in AMD patients were observed in all mice of both knockout strains, and increased in number with age as in humans (**Fig. 1a,b** and **Supplementary Figure 1** online). In contrast, no such changes were visible in wild-type mice even at 24 months of age ($n = 5$). We also noted that the Bruch membrane (the extracellular matrix between the RPE and choroid) was markedly thickened in senescent Ccl-2- and Ccr-2-deficient mice compared with age-matched wild-type mice, and that its collagen and elastin layers were severely disrupted with internal fragmentation characteristic of AMD[10] (**Fig. 1c,d** and **Supplementary Figure 1** online). As in human AMD patients[11], intense immunostaining of tissue inhibitor of metalloproteinases-3 (TIMP-3), which is produced by the RPE and thought to contribute to thickening of the Bruch membrane, was observed in aged knockout mice (**Fig. 1e**). As the *Ccl2*$^{-/-}$ and *Ccr2*$^{-/-}$ mice aged, increasing amounts of lipofuscin granules (autofluorescent lysosomal residual bodies that accumulate with age in RPE cells of humans and have been implicated in AMD development[12]) were observed in swollen and vacuolated RPE cells (**Fig. 1f**) at 9 months and thereafter. Ultrastructural analysis of these RPE cells showed

[1]Department of Ophthalmology, University of Kentucky, 740 South Limestone Street, Lexington, Kentucky 40536-0284, USA. [2]Department of Microbiology and Immunology, University of Kentucky, MS423 Medical Science Building, Lexington, Kentucky 40506-0286, USA. [3]Department of Chemistry, University of Kentucky, A053 ASTeCC Building, Lexington, Kentucky 40506-0286, USA. [4]Institute for Cellular and Molecular Biology, University of Texas, Austin, Texas 78712-1095, USA. [5]Dana Farber Cancer Institute, Brigham & Women's Hospital, Harvard Medical School, 44 Binney Street Mayer 430, Boston, Massachusetts 02115, USA. [6]Department of Ophthalmology, Medical College of Georgia, Augusta, Georgia 30907, USA. Correspondence should be addressed to J.A. (jamba2@uky.edu).

Published online 19 October 2003; doi:10.1038/nm950

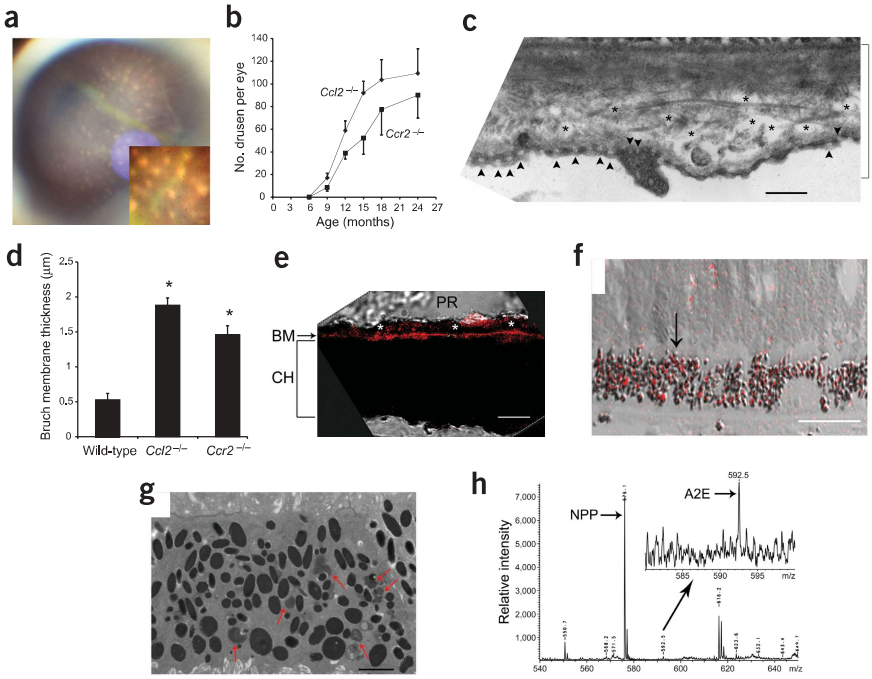


Figure 1 *Ccl2*$^{-/-}$ and *Ccr2*$^{-/-}$ mice develop early AMD. (**a**) Fundus photo of 15-month-old *Ccl2*$^{-/-}$ mouse. Inset shows higher magnification. (**b**) Drusen deposits in knockout mice increase with age ($n = 4$). (**c**) Collagen and elastin fibers (asterisks) of thickened Bruch membrane (indicated by bracket) in 9-month-old *Ccl2*$^{-/-}$ mouse are disrupted, and choriocapillaries are highly fenestrated (arrowheads). (**d**) Bruch membrane is thickened in 10- to 12-month-old knockout mice ($n = 5$). *, $P < 0.05$ compared with wild-type. (**e**) TIMP-3 (red) immunoreactivity in RPE (asterisks) and Bruch membrane (BM) of 14-month-old *Ccl2*$^{-/-}$ mouse. There was no staining in photoreceptors (PR) or choroid (CH). (**f**) Lipofuscin autofluorescence (red) in light micrograph of RPE (arrow) of 15-month-old *Ccl2*$^{-/-}$ mouse. (**g**) Lipofuscin granules (arrows) in electron micrograph of 15-month-old *Ccl2*$^{-/-}$ mouse. (**h**) MALDI spectrum of RPE of 12-month-old *Ccl2*$^{-/-}$ mouse, showing A2E signal. NPP, *N*-perfluoroalkyl pyridine. Scale bar = 0.5 μm (**c**), 50 μm (**e**), 10 μm (**f**), or 2 μm (**g**).

substantial intracellular accumulation of dense bodies (**Fig. 1g** and **Supplementary Figure 1** online), including large ellipsoid and spherical structures of high electron density that presumably represent melanosomes and melanolipofuscin fusion particles, respectively, and numerous smaller structures of variable density representing lipofuscin granules. We tested RPE extracts for the presence of N-retinylidene-N-retinylethanolamine (A2E), the principal lipofuscin fluorophore[13], by matrix-assisted laser desorption/ionization– time-of-flight (MALDI-TOF) mass spectrometry. RPE extracts from 12-month-old knockouts contained 25 pmol of A2E per eye (**Fig. 1h**). No A2E was detected in the RPE of age-matched wild-type mice. Lipofuscin accumulation is thought to promote RPE dysfunction in AMD[14,15].

Retinal degeneration and CNV in *Ccl2*$^{-/-}$ and *Ccr2*$^{-/-}$ mice

As the *Ccl2*$^{-/-}$ and *Ccr2*$^{-/-}$ mice aged, they exhibited several features, including progressive outer retinal degeneration and CNV, that were similar to features of patients with late AMD[10]. Despite evidence of RPE and choroidal pathology, differences in neural retinal morphol-

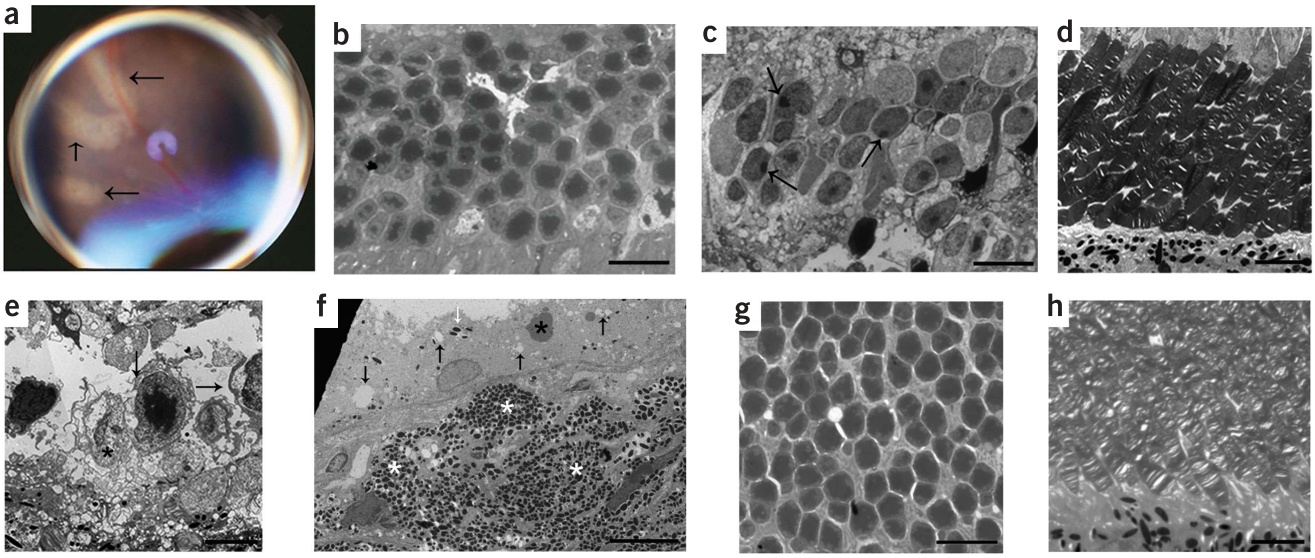


Figure 2 *Ccl2*$^{-/-}$ and *Ccr2*$^{-/-}$ mice develop retinal degeneration. (**a**) Fundus of an 18-month-old *Ccr2*$^{-/-}$ mouse shows geographic atrophy (arrows). (**b**) Electron micrograph of healthy photoreceptor cell bodies in 14-month-old wild-type mouse. (**c**) Attenuated photoreceptors with pyknotic nuclei (arrows) in 16-month-old *Ccl2*$^{-/-}$ mouse. (**d**) Orderly arrays of photoreceptor outer segments in 14-month-old wild-type mouse. (**e**) Marked degeneration and segments (asterisk) with pigment-laden RPE cells (arrows) amidst disorganized tissue in 16-month-old *Ccl2*$^{-/-}$ mouse. (**f**) RPE of 16-month-old *Ccl2*$^{-/-}$ mouse shows marked vacuolization (arrows), degenerated nucleus (black asterisk) and few pigment granules (white arrow). Choroid is filled with abundant melanocytes (white asterisks) but no choriocapillaris vessels. (**g**,**h**) Retina in *Ccl2*$^{-/-}$ mouse outside these atrophic areas contains normal photoreceptor cell bodies (**g**) and outer segments (**h**). Scale bar = 10 μm (**b**,**c**,**f**,**g**) or 5 μm (**d**,**e**,**h**).

© 2003 Nature Publishing Group http://www.nature.com/naturemedicine

© 2003 Nature Publishing Group http://www.nature.com/naturemedicine

ogy between knockout and wild-type mice were not observed before 16 months of age. At 16 months and thereafter, both knockout strains had confluent areas of visible atrophy similar to the 'geographic' atrophy seen in advanced AMD (**Fig. 2a**). These areas were characterized by cell loss in the outer nuclear layer of the retina and atrophy of photoreceptor segments (**Fig. 2b–e**), as well as attenuation of the RPE and choriocapillaris (**Fig. 2f**) as in late AMD[10]. In these regions, the RPE was hypopigmented and devoid of basal infoldings, and there was prominent vacuolization and degeneration of most intracellular organelles. The choriocapillaris was nearly obliterated, with few or no patent inner choroidal vessels observed in the areas corresponding to fundus atrophy. Regions outside these areas did not display such atrophy (**Fig. 2g,h**).

Current animal models of CNV (the neovascular form of AMD that accounts for >80% of visual loss in patients with AMD) rely on laser injury to fracture the Bruch membrane[16,17], or viral transfection of VEGF into RPE cells[18–20]. Although these models are useful for experimental study, they are poor facsimiles of the human condition. Thus, it is notable that we identified CNV with frank evidence of angiographic leakage in 4 of 15 *Ccl2*$^{-/-}$ and 3 of 13 *Ccr2*$^{-/-}$ mice older than 18 months, and in none of 16 age-matched wild-type mice. This frequency of conversion to the neovascular stage is comparable to the rate of progression from drusen deposition to CNV in humans with AMD[1]. At earlier stages (15–19 months), CNV had breached the outer, but not the inner, aspect of the Bruch membrane (intrachoroidal neovascularization), showing angiographic leakage of indocyanine green but not fluorescein (**Fig. 3a–c** and **Supplementary Fig. 2** online). This nascent angiogenesis later (18–27 months) completely breached the Bruch membrane and caused RPE and photoreceptor disruption as a result of the accumulation of subretinal fluid leakage from these immature vessels, which was visible on fluorescein angiography (**Fig. 3d–f** and **Supplementary Fig. 3** online). VEGF was overexpressed in the RPE in senescent Ccl-2- and Ccr-2-deficient mice, but not in age-matched wild-type mice (**Fig. 3g,h**), consistent with its putative role as the angiogenic factor driving CNV.

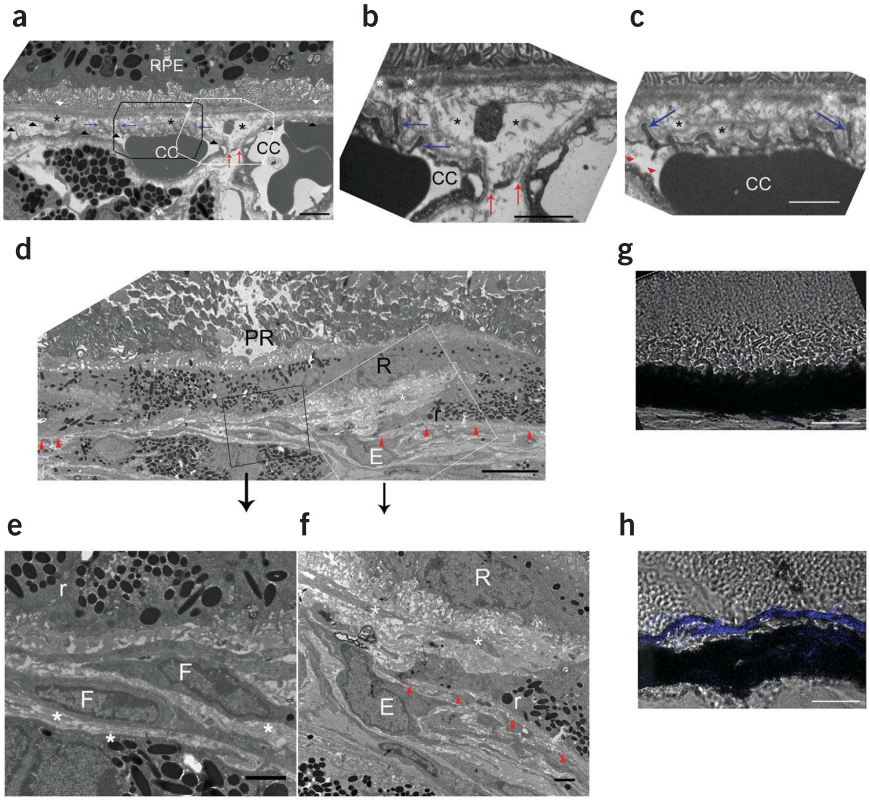


Figure 3 *Ccl2*$^{-/-}$ and *Ccr2*$^{-/-}$ mice develop neovascular AMD and overexpress VEGF in RPE. (**a–c**) Electron micrograph of a 20-month-old *Ccl2*$^{-/-}$ mouse shows dilated choriocapillaries (CC) inserting processes (blue arrows) into Bruch membrane with fragmented collagen and elastin layers (asterisks). Inner Bruch membrane (white arrowheads) is intact, whereas outer Bruch membrane (black arrowheads) is breached by choriocapillary processes (blue arrows) and fractures (red arrows). White and black areas in **a** are magnified in **b** and **c**, respectively, showing breaks (red arrows) in outer Bruch membrane and endothelial processes (blue arrows) inserted into Bruch membrane, disrupting outer collagenous (black asterisk) and elastin and inner collagenous layers (white asterisks). Large fenestrae (arrowheads) are also visible. (**c**). (**d–f**) CNV in 24-month-old *Ccr2*$^{-/-}$ mouse, showing an endothelial cell (E) and fibrocytes (white asterisks) invading sub-RPE space through a defect in the Bruch membrane (arrowheads), disrupting overlying photoreceptors (PR). High-magnification insets show fibrocytes (F) invading Bruch membrane and disrupting overlying RPE (r) extracellular matrix (**e**), and an endothelial cell (E) and fibrocyte processes (asterisks) that have broken through a discontinuity in the Bruch membrane (arrowheads) to displace an RPE cell (R) from its intact monolayer (r; **f**). (**g,h**) VEGF (blue staining) is minimally present in RPE of 18-month-old wild-type mouse (**g**) but is markedly expressed in RPE and choroid of 18-month-old *Ccl2*$^{-/-}$ mouse (**h**). Scale bar = 2 μm (**a,e,f**), 1 μm (**b,c**), 10 μm (**d**) or 100 μm (**g,h**).

Complement and IgG deposition in *Ccl2*$^{-/-}$ and *Ccr2*$^{-/-}$ mice

Recent evidence suggests that complement activation and immune complex deposition occur in eyes of humans with AMD[21–23]. We identified the deposition of many of these proteins in aging *Ccl2*$^{-/-}$ and *Ccr2*$^{-/-}$ mice. Complement component C5 (**Fig. 4a**), IgG (**Fig. 4b,c**), the complement regulatory proteins vitronectin and CD46 (membrane cofactor protein; **Fig. 4d,e**), serum amyloid P component (SAP; a potential activator of the complement cascade; **Fig. 4f**) and advanced glycation endproducts (AGE; data not shown) were present in the RPE or choroids of both strains of knockout mice, but not in age-matched wild-type mice, similar to their distribution in eyes of humans with AMD[21,24]. We found evidence of IgG light chain deposition, which increased with age, in the RPE and choroids of knockout mice (**Fig. 4g**). Colocalization of IgG and C3c in choroidal vessel walls (**Fig. 4c**) not only suggests the presence of immune complexes[25,26], but also reflects ongoing immune deposit formation because C3c, a split product of surface-bound C3b, is cleared within hours[25]. The presence of CD46 (a membrane-bound regulator that facilitates inactivation of the activated complement components C3b and C4b) and vitronectin (a fluid-phase regulator that binds to the terminal complement complex to regulate complement-mediated lysis) and the localization of complement intermediates suggests that complement activation occurs to completion. These deposits were identified in six of seven *Ccl2*$^{-/-}$ and four of six *Ccr2*$^{-/-}$ mice as young as 6 months of age. This predates the changes visible on fundus exam-

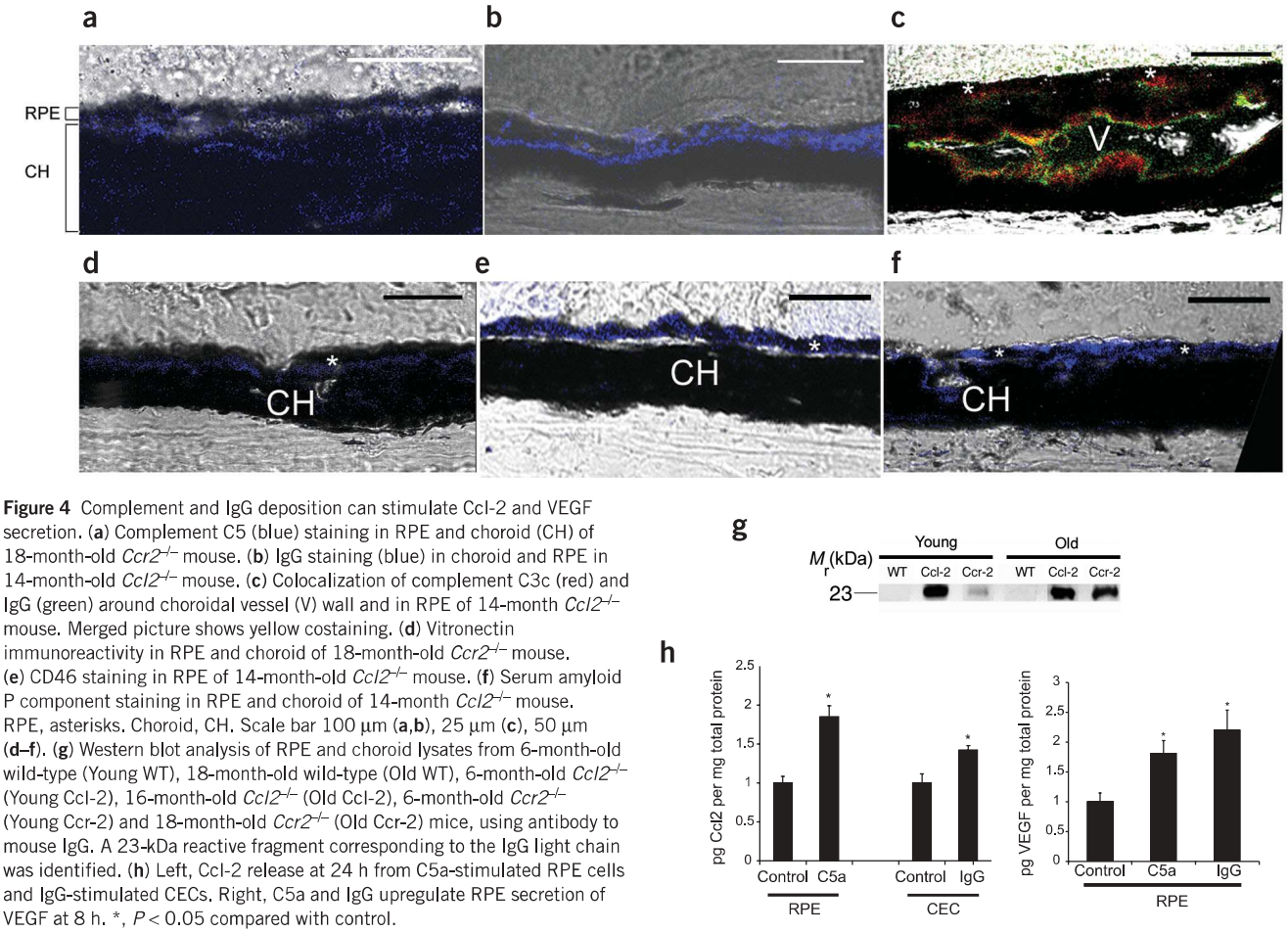


Figure 4 Complement and IgG deposition can stimulate Ccl-2 and VEGF secretion. (**a**) Complement C5 (blue) staining in RPE and choroid (CH) of 18-month-old *Ccr2*$^{-/-}$ mouse. (**b**) IgG staining (blue) in choroid and RPE in 14-month-old *Ccl2*$^{-/-}$ mouse. (**c**) Colocalization of complement C3c (red) and IgG (green) around choroidal vessel (V) wall and in RPE of 14-month *Ccl2*$^{-/-}$ mouse. Merged picture shows yellow costaining. (**d**) Vitronectin immunoreactivity in RPE and choroid of 18-month-old *Ccr2*$^{-/-}$ mouse. (**e**) CD46 staining in RPE of 14-month-old *Ccl2*$^{-/-}$ mouse. (**f**) Serum amyloid P component staining in RPE and choroid of 14-month *Ccl2*$^{-/-}$ mouse. RPE, asterisks. Choroid, CH. Scale bar 100 µm (**a**,**b**), 25 µm (**c**), 50 µm (**d**–**f**). (**g**) Western blot analysis of RPE and choroid lysates from 6-month-old wild-type (Young WT), 18-month-old wild-type (Old WT), 6-month-old *Ccl2*$^{-/-}$ (Young Ccl-2), 16-month-old *Ccl2*$^{-/-}$ (Old Ccl-2), 6-month-old *Ccr2*$^{-/-}$ (Young Ccr-2) and 18-month-old *Ccr2*$^{-/-}$ (Old Ccr-2) mice, using antibody to mouse IgG. A 23-kDa reactive fragment corresponding to the IgG light chain was identified. (**h**) Left, Ccl-2 release at 24 h from C5a-stimulated RPE cells and IgG-stimulated CECs. Right, C5a and IgG upregulate RPE secretion of VEGF at 8 h. *, $P < 0.05$ compared with control.

ination and is consistent with a potential causal role. Such deposits were not identified in wild-type mice.

In other immune complex deposition disorders, it has been postulated that these proteins serve as an inflammatory focus by inciting macrophage recruitment through Fc and complement receptor binding, triggering humoral activation and phagocytosis. Consistent with this hypothesis, we found that Ccl-2 secretion by human RPE and choroidal endothelial cells (CEC) was upregulated by C5a (the activated form of C5) and IgG, respectively (**Fig. 4h**). AGE also stimulates human RPE cell secretion of Ccl-2 (ref. 27).

These data may explain the presence of subretinal deposits in Ccl-2- and Ccr-2-deficient mice, which are impaired in recruiting macrophages requisite for clearance and degradation of drusen and other debris[28]. Consistent with this hypothesis, there was an age-dependent increase in the expression of Ccl-2 in the RPE (**Fig. 5a**,**b**) and in macrophage infiltration in the choroids of wild-type mice (**Fig. 5c–e**). Using flow cytometry, we found that aging was associated with a marked increase (15-fold) in the number of macrophages in the choroids of wild-type mice, compared with only a modest (2- to 3-fold) increase in knockout mice (**Fig. 5e**). These data suggest that macrophage recruitment in aged wild-type mice is principally directed along the Ccl-2–Ccr-2 axis. Along with overexpression of C5 in the RPE and choroids of *Ccl2*$^{-/-}$ and *Ccr2*$^{-/-}$ mice, we found marked upregulation of the C5a receptor (C5aR) in both strains of knockout mice starting at an early age, and in wild-type mice at a later age (**Fig. 5f**). We interpret these findings to suggest that in the wild-type animal, ongoing stimulation by C5a upregulates C5aR expression[29], which leads to Ccl-2 production and subsequent clearance of C5 and molecules tagged by this opsonin. In knockout mice, the inability to summon sufficient numbers of or appropriately stimulated macrophages would lead to continued C5 deposition.

We found that both C5a and IgG stimulated human RPE cells to increase their secretion of the potent angiogenic cytokine VEGF (**Fig. 4h**), which is consistent with the VEGF overexpression by the RPE in senescent Ccl-2- or Ccr-2-deficient mice (**Fig. 3h**). AGE also upregulates human RPE[30] and CEC[31] secretion of VEGF. Together, these processes may underlie the development of CNV and highly fenestrated choroidal capillaries (**Figs. 1c** and **3e**), both of which can be induced by VEGF[18–20,32] in these mice.

Macrophages adhere to and degrade C5a and IgG

We used cell culture inserts to examine the migration of macrophages across a porous membrane coated with collagen IV (CIV, an abundant constituent of the Bruch membrane), in response to Ccl-2. We coated the membranes with C5a or IgG to determine whether macrophages recruited to these protein-deposition sites by locally secreted Ccl-2 are immobilized when they contact these proteins in the extracellular matrix. We found that Ccl-2-induced macrophage chemotaxis was inhibited both by C5a and IgG (**Fig. 6a**). Such immobilization indicated that macrophages adhere to C5a- or IgG-coated surfaces. Using CIV-coated multispot slides coated with C5a or IgG, we found that macrophages adhered to these proteins in

© 2003 Nature Publishing Group http://www.nature.com/naturemedicine

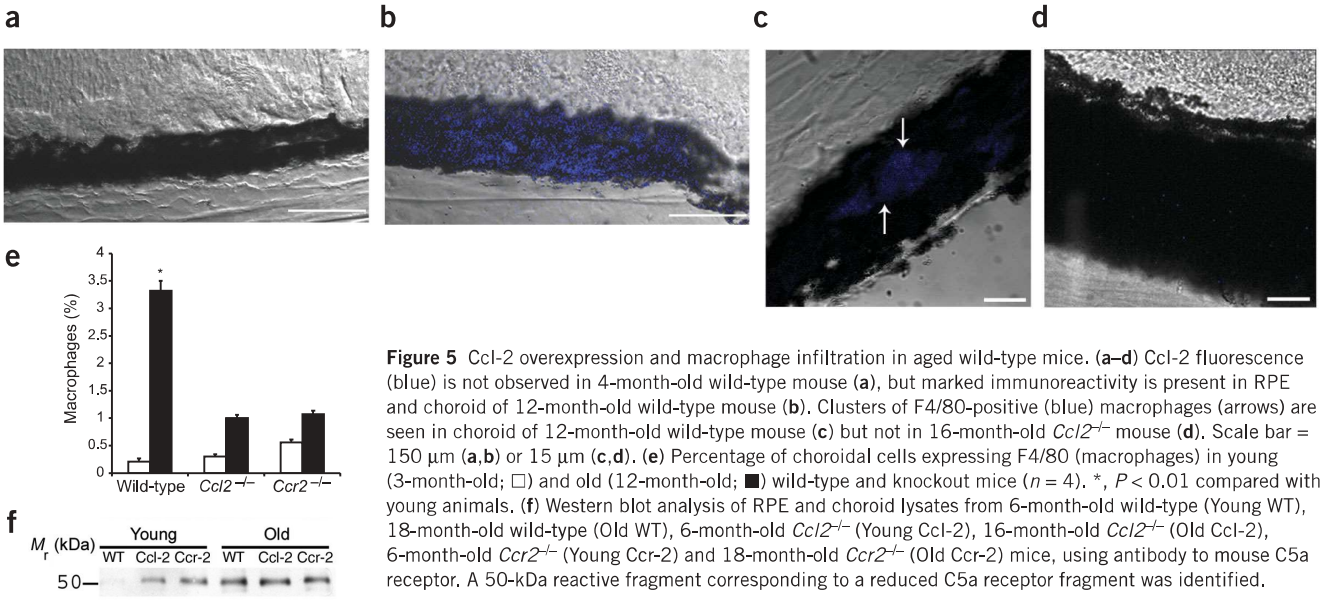


Figure 5 Ccl-2 overexpression and macrophage infiltration in aged wild-type mice. (**a–d**) Ccl-2 fluorescence (blue) is not observed in 4-month-old wild-type mouse (**a**), but marked immunoreactivity is present in RPE and choroid of 12-month-old wild-type mouse (**b**). Clusters of F4/80-positive (blue) macrophages (arrows) are seen in choroid of 12-month-old wild-type mouse (**c**) but not in 16-month-old *Ccl2*$^{-/-}$ mouse (**d**). Scale bar = 150 μm (**a**,**b**) or 15 μm (**c**,**d**). (**e**) Percentage of choroidal cells expressing F4/80 (macrophages) in young (3-month-old; □) and old (12-month-old; ■) wild-type and knockout mice ($n = 4$). *, $P < 0.01$ compared with young animals. (**f**) Western blot analysis of RPE and choroid lysates from 6-month-old wild-type (Young WT), 18-month-old wild-type (Old WT), 6-month-old *Ccl2*$^{-/-}$ (Young Ccl-2), 16-month-old *Ccl2*$^{-/-}$ (Old Ccl-2), 6-month-old *Ccr2*$^{-/-}$ (Young Ccr-2) and 18-month-old *Ccr2*$^{-/-}$ (Old Ccr-2) mice, using antibody to mouse C5a receptor. A 50-kDa reactive fragment corresponding to a reduced C5a receptor fragment was identified.

a dose-dependent fashion (**Fig. 6b**). Collectively, these data suggest that macrophages recruited by Ccl-2 become immobilized when they contact C5a or IgG and associate with them in the extracellular matrix.

Because macrophages were immobilized by and adhered to C5 and IgG *in vitro*, and because aging was associated with macrophage infiltration into the choroids of wild-type mice, we postulated that these cells could scavenge immune complexes in the eyes of *Ccl2*$^{-/-}$ or *Ccr2*$^{-/-}$ mice. To test this hypothesis, we purified macrophages from aged wild-type choroids by magnetic cell sorting and plated them on unfixed eye sections from *Ccl2*$^{-/-}$ or *Ccr2*$^{-/-}$ mice, which were rich in C5 and IgG deposits in their RPE and choroids. Incubation with wild-type macrophages for 24 h markedly reduced the total RPE and choroidal area occupied by C5 or IgG, compared with untreated sections (**Fig. 6c**,**d** and **Supplementary Fig. 4** online). Within 2 h, macrophages were spread out over the tissue and intimately associated with protein deposits (**Fig. 6e–g**). These results indicate that macrophages clear C5 and IgG deposits *in situ*, and suggest a pivotal role for macrophage deficiency in the accumulation of complement components and immunoglobulins in *Ccl2*$^{-/-}$ and *Ccr2*$^{-/-}$ mice.

DISCUSSION

We have described the first animal model of AMD that recapitulates the key elements of the human condition, using senescent mice lacking the macrophage chemoattractant Ccl-2 or its cognate receptor Ccr-2. The presence of similar pathology in two ligand-receptor strains that are defective in induced macrophage trafficking strengthens the hypothesis that macrophage dysfunction has a role in its pathogenesis. The accumulation of complement components, complement regulatory proteins and IgG in these mice, as in humans with AMD, suggests that impaired macrophage recruitment allows accretion of proteins associated with complement activation and immune

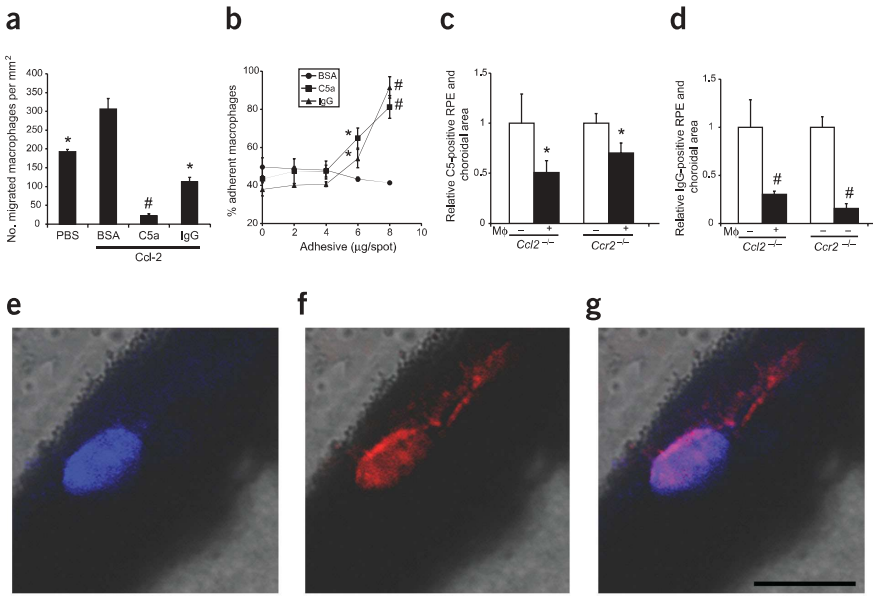


Figure 6 Macrophages are immobilized by, adhere to and degrade C5 and IgG. (**a**) Migration of wild-type peritoneal macrophages toward Ccl-2, across membranes coated with CIV and BSA, C5a or IgG ($n = 3$). *, $P < 0.05$; #, $P < 0.01$ compared with BSA. (**b**) Adhesion of wild-type peritoneal macrophages to slides coated with CIV and C5a or IgG ($n = 3$). *, $P < 0.05$; #, $P < 0.01$ compared to BSA. (**c**,**d**) Choroidal macrophages of 12-month-old wild-type mice clear C5 and IgG *in situ*. Quantitation shows significantly less C5 (**c**) and IgG (**d**) immunoreactivity in sections from 12- to 14-month-old knockout mice incubated with macrophages (Mϕ), compared with sections without macrophages ($n = 4$–7). *, $P < 0.05$; #, $P < 0.01$. (**e–g**) Confocal images from 12-month-old *Ccr2*$^{-/-}$ mouse eye section incubated with wild-type choroidal macrophages for 2 h. **e**, An F4/80-positive (blue) macrophage adheres to the section. **f**, IgG-immunoreactive material (red) appears closely associated with and engulfed by macrophage in the merged image (**g**). Scale bar = 15 μm.

© 2003 Nature Publishing Group http://www.nature.com/naturemedicine

© 2003 Nature Publishing Group http://www.nature.com/naturemedicine

complex deposition. The inability to summon macrophages is thus associated with the senescence-associated development of features strongly reminiscent of human AMD, which was corroborated by several lines of evidence. In particular, we have shown that Ccl-2-driven macrophages are immobilized by and adhere to C5a and IgG *in vitro*, and that macrophages degrade these proteins *in situ*. Combined with the observation of a marked deficiency of macrophages in the choroids of aged knockout mice, these data suggest that impaired macrophage mobilization *in vivo* prevents clearance of these proteins, as these cells are known to scavenge immune complexes through complement opsonization *in vivo*.

Because deposition of complement-related proteins and IgG precedes the accumulation of drusen and lipofuscin, it is likely that the AMD-like pathology is due, at least in part, to complement activation and immune complex deposition, rather than the converse. Because RPE cells in AMD eyes that are immunoreactive for complement-related proteins and IgG exhibit anatomic prelethal signs[22,23], accumulation of these proteins may compromise RPE function. The presence of IgG and complement C3 and C5 intermediates is strongly suggestive of the presence of immune complexes, and is consistent with the presence of circulating retinal autoantibodies in patients with AMD[33,34]. Furthermore, patients with membranoproliferative glomerulonephritis, in which complement activation and immune complex deposition cause glomerular injury, develop drusen deposits resembling those in AMD in ultrastructure and composition (including C5 and IgG deposition[35]), as well as CNV[36]. Collectively, these findings support the concept that complement activation and immune complex deposition may injure the RPE in AMD. RPE injury, which may be manifested by secondary photoreceptor degradation, can also be triggered by excessive accumulation of lipofuscin[5]. SAP and TIMP-3 may also impair drusen clearance by functioning as protease inhibitors[21]. RPE overexpression of VEGF, stimulated by complement components and IgG, combined with fragmentation of the Bruch membrane, provides an environment permissive for CNV.

The stimulus for complement activation in eyes of humans with AMD is unknown, but recognition of AMD as an inflammatory disease has stimulated interest in possible infectious etiologies. In particular, *Chlamydia pneumoniae* infection has been associated with AMD by seroepidemiology[37,38]. Both diseases are chronic, subclinical and inflammatory in nature. Because *Chlamydia pneumoniae* upregulates Ccl-2 secretion by endothelial cells and monocytes[39], the susceptibility of *Ccl2*$^{-/-}$ or *Ccr2*$^{-/-}$ mice to microbial infections might provoke complement activation and immune complex deposition. Pathologic deposits associated with Alzheimer disease and atherosclerosis, the latter of which has been linked to *Chlamydia pneumoniae*, contain C5 and IgG[21] and stimulate Ccl-2 secretion[40–42].

It is unclear whether endogenous macrophages that accumulate in the choroids of patients with AMD[43] serve protective or destructive functions. While they may aid in drusen clearance[28], they also may promote development of CNV[44], similar to their proposed role in the laser-injury model[45,46]. These findings suggest that macrophages can serve in both pro- and anti-inflammatory capacities, and that dysregulation of clearance functions may fuel disease progression. We recognize the apparent paradox between the presence of macrophages beneath drusen and CNV in patients with AMD, and the relative paucity of the macrophages as a potential pathogenic factor in the development of AMD-like pathology in this model. This could be resolved by findings showing that macrophages in human AMD are inadequate in number or in the ability to degrade protein deposits and resorb drusen. Further studies are required to dissect the molecular phenotypes of choroidal macrophages in various stages of the disease.

The occurrence of AMD-like pathology in these knockout mice does not prove a role for Ccl-2, Ccr-2 or macrophage recruitment in human AMD, as other molecular perturbations could create identical pathological phenotypes. Conclusive evidence of a causative role for Ccl-2 or Ccr-2 may emerge from ongoing functional rescue experiments. In addition, we have not excluded the possibility that Ccl-2 or Ccr-2 may protect against AMD through mechanisms other than macrophage recruitment, such as induction of RPE-trophic or antiangiogenic factors. However, such functions have not been described for either protein.

The presence of both atrophic and neovascular pathologies in *Ccl2*$^{-/-}$ and *Ccr2*$^{-/-}$ mice at an age corresponding to human senescence makes these mice attractive models for investigating both early and late AMD. Because the mouse retina does not contain a specialized macula, however, this model is not an exact replica of the human condition. But the pathology in human AMD, while pronounced in the macular area, is not confined to this central region[47], and the features observed in aged *Ccl2*$^{-/-}$ and *Ccr2*$^{-/-}$ mice closely resemble those of the clinical condition in anatomical appearance, biochemical composition and functional disruption. More importantly, they define a system for molecular dissection of the determinants of AMD pathogenesis, and provide a platform on which to develop and validate new therapeutic strategies. These findings also raise the question of whether genetic polymorphisms associated with higher levels of Ccl-2 or Ccr-2 protect individuals from AMD, and should prompt a search for underexpressing mutations in patients with AMD.

METHODS

Animals. Wild-type C57BL/6 mice were purchased from Jackson Laboratories, and *Ccl2*$^{-/-}$ and *Ccr2*$^{-/-}$ strains, generated as described previously[8,9] were backcrossed ten times to C57BL/6 mice. Mice were then anesthetized by intramuscular injection of ketamine (50 mg/kg) and xylazine (10 mg/kg). Experiments were approved by the University of Kentucky Institutional Animal Care and Use Committee.

Fundus photography and angiography. Photographs and angiograms were taken with a TRC-50IA camera (Topcon) after intraperitoneal injection of fluorescein sodium (Akorn; 60 mg/kg) or indocyanine green (Sigma-Aldrich; 6 mg/kg), and evaluated by two masked readers.

Immunohistochemistry and electron microscopy. Frozen sections fixed in Histochoice MB (Amresco) and blocked with 5% donkey serum (Jackson Immunoresearch) were stained with rabbit antibody to mouse C3c (1:1,000; gift of J.D. Lambris, University of Pennsylvania), mouse antibody to mouse C5 (1:1,000; gift of J.D. Lambris), rabbit antibody to human CD46 (1:500; Santa Cruz Biotechnology), goat antibody to mouse Ccl-2 (15 μg/ml; R&D Systems), goat antibody to human SAP (1:500; Santa Cruz Biotechnology), rabbit antibody to mouse TIMP-3 (1:2,500; gift of B.H.F. Weber, University of Wuerzburg), goat antibody to mouse VEGF (15 μg/ml; R&D Systems), rabbit polyclonal antibody to AGE (1:1,000, gift of A. Gugliucci, Touro University) or goat antibody to human vitronectin (1:500; Santa Cruz Biotechnology). Bound antibodies were detected with Cy3-conjugated goat or Cy5-conjugated donkey secondary antibodies (1:100; Jackson Immunoresearch). Alternatively, sections were stained directly with FITC-conjugated goat antibody to mouse IgG (1:100; BD PharMingen), Cy5-conjugated donkey antibody to mouse IgG (1:100; Jackson Immunoresearch) or Cy5-conjugated F4/80 (5 μg/ml; Serotec). A mouse-on-mouse kit (Vector Laboratories) was used for C5 staining. Lipofuscin autofluorescence was detected through the Cy3 channel. Transmission electron microscopic studies were conducted on uranyl acetate– and lead citrate–stained ultrathin sections. Bruch membrane thickness was determined 150 μm from the optic nerve by taking the average measurements of the thinnest and thickest parts.

Western blotting. Equal amounts of total protein from RPE and choroids were resolved with 4–20% SDS-PAGE and transferred to nitrocellulose membranes

for western blotting with antibody to mouse C5aR (gift of J.D. Lambris) or mouse IgG (Transduction Laboratories).

Flow cytometry. Single-cell suspensions of RPE and choroids were incubated in Fc block (0.5 mg/ml; BD PharMingen) for 15 min on ice and stained with Cy5-F4/80 antibody (1:30). Live cells were detected by gating on forward versus side scatter, followed by analysis of F4/80 in the fluorescence channel (FACSCalibur, BD Biosciences).

Migration. Wild-type peritoneal macrophage migration (10^5 cells/well) toward 30 nM of mouse Ccl-2 (R&D Systems) was assayed using 24-well Transwell chambers (Corning) separated by a 5-μm polycarbonate filter coated with 50 μg/ml collagen IV (CIV; Fluka), with or without overlay of human C5a (50 nM; Calbiochem), mouse IgG (50 μg/well; Jackson Immunoresearch) or BSA (50 μg/well; Sigma-Aldrich). Migrated cells were counted after 3 h of incubation at 37 °C.

Adherence. Wild-type peritoneal macrophages (10^5 cells/spot) were plated on multispot glass slides (Shandon) coated with 50 μg/ml CIV and overlaid with human C5a, mouse IgG or BSA (0–8 μg/spot). Adherence was quantitated using CyQuantGR (Molecular Probes) after incubation at 37 °C for 1 h.

Degradation. Frozen, unfixed eye sections from knockout mice were transferred to 24-well culture plates, incubated with or without wild-type (12-month-old) choroidal macrophages (10^4 cells/well), which were purified by magnetic cell sorting using MicroBeads conjugated with CD11b antibody (clone M1/70.15.11.5; Miltenyi Biotec), for up to 24 h at 37 °C. Sections were fixed with Histochoice MB, stained for C5, IgG or F4/80, and imaged by scanning confocal microscopy. Relative areas of C5 or IgG immunoreactivity were measured for four to seven sections using image-analysis software (Photoshop 6.0; Adobe Systems).

Cell stimulation. Serum-starved human CECs (gift of D.R. Hinton, University of Southern California) and human RPE cells were stimulated with human C5a (50 ng/ml) or immobilized human IgG (50 μg/well; Sigma-Aldrich) after attaining 80% confluence. Ccl-2 and VEGF levels were measured by ELISA (R&D Systems) at 8 and 24 h and normalized to total protein levels.

MALDI-TOF mass spectrometry. RPE extracts and standards of synthetic A2E (gifts of E. Rodriguez-Boulan, New York University, and G.H. Travis, University of California, Los Angeles) were dissolved in 50% methanol and 50% water (Fisher Scientific), transferred to C18 PrepSep solid-phase extraction columns (Fisher) and eluted with 1 ml methanol containing 0.1% trifluoroacetic acid (Fisher). *N*-perfluoroalkyl pyridine (gift of S. Rankin, University of Kentucky; 250 ng) was added to samples as an external standard. The MALDI target was prepared by adding 0.5 μl sample to deposited 0.5 μl matrix (α-cyano-4-hydroxycinnamic acid; Sigma-Aldrich). Positive ion spectra were acquired on a Bruker Autoflex MALDI-TOF mass spectrometer (Bruker Daltonic). The A2E response (m/z 592.5) was normalized to the *N*-perfluoroalkyl pyridine response (m/z 576.1).

Statistics. Data are represented as mean ± s.e.m. of at least three independent experiments, and were compared using the two-tailed Student t-test. The null hypothesis was rejected at $P < 0.05$.

Note: Supplementary information is available on the Nature Medicine website.

ACKNOWLEDGMENTS

We thank M.G. Engle, M. Jennes and R. King for assistance with histology and electron microscopy; G. Chen for maintaining cell cultures; M.H. Hanson for photography; J. Husemann for technical advice; H.E. Grossniklaus for expertise in interpreting electron micrographs; and A.P. Adamis, S. Bondada, D.C. Collins, R. Mohan, E.J. Smart, V. Kumar, P.A. Pearson, A.M. Rao, G.S. Rao and J.G. Woodward for valuable discussions. J.A. was supported by a Foundation Fighting Blindness Career Development Award, the Dennis W. Jahnigen Career Development Award administered by the American Geriatrics Society and funded by the John A. Hartford Foundation and Atlantic Philanthropies, grants from Prevent Blindness America and Fight for Sight and a physician-scientist award from University of Kentucky; E.S. was supported by a Fight For Sight postdoctoral fellowship; and B.K.A. was supported by a Knights-Templar Eye Foundation grant.

COMPETING INTERESTS STATEMENT

The authors declare competing financial interests (see the *Nature Medicine* website for details).

Received 9 July; accepted 23 September 2003
Published online at http://www.nature.com/naturemedicine/

1. Smith, W. *et al.* Risk factors for age-related macular degeneration: pooled findings from three continents. *Ophthalmology* **108**, 697–704 (2001).
2. Dithmar, S. *et al.* Murine high-fat diet and laser photochemical model of basal deposits in Bruch membrane. *Arch. Ophthalmol.* **119**, 1643–1649 (2001).
3. Cousins, S.W. *et al.* The role of aging, high fat diet and blue light exposure in an experimental mouse model for basal laminar deposit formation. *Exp. Eye Res.* **75**, 543–553 (2002).
4. Majji, A.B. *et al.* Age-related retinal pigment epithelium and Bruch's membrane degeneration in senescence-accelerated mouse. *Invest. Ophthalmol. Vis. Sci.* **41**, 3936–3942 (2000).
5. Weng, J. *et al.* Insights into the function of Rim protein in photoreceptors and etiology of Stargardt's disease from the phenotype in abcr knockout mice. *Cell* **98**, 13–23 (1999).
6. Dithmar, S., Curcio, C.A., Le, N.A., Brown, S. & Grossniklaus, H.E. Ultrastructural changes in Bruch's membrane of apolipoprotein E-deficient mice. *Invest. Ophthalmol. Vis. Sci.* **41**, 2035–2042 (2000).
7. Rakoczy, P.E. *et al.* Progressive age-related changes similar to age-related macular degeneration in a transgenic mouse model. *Am. J. Pathol.* **161**, 1515–1524 (2002).
8. Lu, B. *et al.* Abnormalities in monocyte recruitment and cytokine expression in monocyte chemoattractant protein 1-deficient mice. *J. Exp. Med.* **187**, 601-608 (1998).
9. Kuziel, W.A. *et al.* Severe reduction in leukocyte adhesion and monocyte extravasation in mice deficient in CC chemokine receptor 2. *Proc. Natl. Acad. Sci. USA* **94**, 12053–12058 (1997).
10. Green, W.R. & Enger, C. Age-related macular degeneration histopathologic studies. The 1992 Lorenz E. Zimmerman Lecture. *Ophthalmology* **100**, 1519–1535 (1993).
11. Kamei, M. & Hollyfield, J.G. TIMP-3 in Bruch's membrane: changes during aging and in age-related macular degeneration. *Invest. Ophthalmol. Vis. Sci.* **40**, 2367–2375 (1999).
12. Delori, F.C., Fleckner, M.R., Goger, D.G., Weiter, J.J. & Dorey, C.K. Autofluorescence distribution associated with drusen in age-related macular degeneration. *Invest. Ophthalmol. Vis. Sci.* **41**, 496–504 (2000).
13. Eldred, G.E. & Lasky, M.R. Retinal age pigments generated by self-assembling lysosomotropic detergents. *Nature* **361**, 724–726 (1993).
14. Suter, M. *et al.* Age-related macular degeneration. The lipofuscin component *N*-retinyl-*N*-retinylidene ethanolamine detaches proapoptotic proteins from mitochondria and induces apoptosis in mammalian retinal pigment epithelial cells. *J. Biol. Chem.* **275**, 39625–39630 (2000).
15. Finnemann, S.C., Leung, L.W. & Rodriguez-Boulan, E. The lipofuscin component A2E selectively inhibits phagolysosomal degradation of photoreceptor phospholipid by the retinal pigment epithelium. *Proc. Natl. Acad. Sci. USA* **99**, 3842–3847 (2002).
16. Ryan, S.J. Subretinal neovascularization. Natural history of an experimental model. *Arch. Ophthalmol.* **100**, 1804–1809 (1982).
17. Tobe, T. *et al.* Targeted disruption of the FGF2 gene does not prevent choroidal neovascularization in a murine model. *Am. J. Pathol.* **153**, 1641–1646 (1998).
18. Spilsbury, K., Garrett, K.L., Shen, W.Y., Constable, I.J. & Rakoczy, P.E. Overexpression of vascular endothelial growth factor (VEGF) in the retinal pigment epithelium leads to the development of choroidal neovascularization. *Am. J. Pathol.* **157**, 135–144 (2000).
19. Baffi, J., Byrnes, G., Chan, C.C. & Csaky, K.G. Choroidal neovascularization in the rat induced by adenovirus mediated expression of vascular endothelial growth factor. *Invest. Ophthalmol. Vis. Sci.* **41**, 3582–3589 (2000).
20. Schwesinger, C. *et al.* Intrachoroidal neovascularization in transgenic mice overexpressing vascular endothelial growth factor in the retinal pigment epithelium. *Am. J. Pathol.* **158**, 1161–1172 (2001).
21. Mullins, R.F., Russell, S.R., Anderson, D.H. & Hageman, G.S. Drusen associated with aging and age-related macular degeneration contain proteins common to extracellular deposits associated with atherosclerosis, elastosis, amyloidosis, and dense deposit disease. *FASEB J.* **14**, 835–846 (2000).
22. Johnson, L.V., Ozaki, S., Staples, M.K., Erickson, P.A. & Anderson, D.H. A potential role for immune complex pathogenesis in drusen formation. *Exp. Eye Res.* **70**, 441–449 (2000).
23. Anderson, D.H., Mullins, R.F., Hageman, G.S. & Johnson, L.V. A role for local inflammation in the formation of drusen in the aging eye. *Am. J. Ophthalmol.* **134**, 411–431 (2002).
24. Ishibashi, T. *et al.* Advanced glycation end products in age-related macular degeneration. *Arch. Ophthalmol.* **116**, 1629–1632 (1998).
25. Schulze, M. *et al.* Glomerular C3c localization indicates ongoing immune deposit formation and complement activation in experimental glomerulonephritis. *Am. J. Pathol.* **142**, 179–187 (1993).
26. Brons, R.H. *et al.* Detection of immune deposits in skin lesions of patients with Wegener's granulomatosis. *Ann. Rheum. Dis.* **60**, 1097–1102 (2001).
27. Bian, Z.M. *et al.* Glycated serum albumin induces chemokine gene expression in human retinal pigment epithelial cells. *J. Leukoc. Biol.* **60**, 405–414 (1996).
28. Duvall, J. & Tso, M.O. Cellular mechanisms of resolution of drusen after laser coagulation. An experimental study. *Arch. Ophthalmol.* **103**, 694–703 (1985).

© 2003 Nature Publishing Group http://www.nature.com/naturemedicine

29. Riedemann, N.C. *et al.* Expression and function of the C5a receptor in rat alveolar epithelial cells. *J. Immunol.* **168**, 1919–1925 (2002).
30. Lu, M. *et al.* Advanced glycation end products increase retinal vascular endothelial growth factor expression. *J. Clin. Invest.* **101**, 1219–1224 (1998).
31. Hoffmann, S., Friedrichs, U., Eichler, W., Rosenthal, A. & Wiedemann, P. Advanced glycation end products induce choroidal endothelial cell proliferation, matrix metalloproteinase-2 and VEGF upregulation *in vitro*. *Graefes Arch. Clin. Exp. Ophthalmol.* **240**, 996–1002 (2002).
32. Roberts, W.G. & Palade, G.E. Neovasculature induced by vascular endothelial growth factor is fenestrated. *Cancer Res.* **57**, 765–772 (1997).
33. Penfold, P.L., Provis, J.M., Furby, J.H., Gatenby, P.A. & Billson, F.A. Autoantibodies to retinal astrocytes associated with age-related macular degeneration. *Graefes Arch. Clin. Exp. Ophthalmol.* **228**, 270–274 (1990).
34. Gurne, D.H., Tso, M.O., Edward, D.P. & Ripps, H. Antiretinal antibodies in serum of patients with age-related macular degeneration. *Ophthalmology* **98**, 602–607 (1991).
35. Mullins, R.F., Aptsiauri, N. & Hageman, G.S. Structure and composition of drusen associated with glomerulonephritis: implications for the role of complement activation in drusen biogenesis. *Eye* **15**, 390–395 (2001).
36. Leys, A. *et al.* Subretinal neovascular membranes associated with chronic membranoproliferative glomerulonephritis type II. *Graefes Arch. Clin. Exp. Ophthalmol.* **228**, 499–504 (1990).
37. Ishida, O. *et al.* Is *Chlamydia pneumoniae* infection a risk factor for age related macular degeneration? *Br. J. Ophthalmol.* **87**, 523–524 (2003).
38. Kalayoglu, M.V., Galvan, C., Mahdi, O.S., Byrne, G.I. & Mansour, S. Serological association between *Chlamydia pneumoniae* infection and age-related macular degeneration. *Arch. Ophthalmol.* **121**, 478–482 (2003).
39. Kothe, H. *et al.* Hydroxymethylglutaryl coenzyme A reductase inhibitors modify the inflammatory response of human macrophages and endothelial cells infected with *Chlamydia pneumoniae*. *Circulation* **101**, 1760–1763 (2000).
40. Meda, L. *et al.* β-amyloid (25-35) peptide and interferon-γ synergistically induce the production of the chemotactic cytokine MCP-1/JE in monocytes and microglial cells. *J. Immunol.* **157**, 1213–1218 (1996).
41. Boring, L., Gosling, J., Cleary, M. & Charo, I.F. Decreased lesion formation in CCR2$^{-/-}$ mice reveals a role for chemokines in the initiation of atherosclerosis. *Nature* **394**, 894–897 (1998).
42. Gu, L. *et al.* Absence of monocyte chemoattractant protein-1 reduces atherosclerosis in low density lipoprotein receptor-deficient mice. *Mol. Cell* **2**, 275–281 (1998).
43. Penfold, P.L., Madigan, M.C., Gillies, M.C. & Provis, J.M. Immunological and aetiological aspects of macular degeneration. *Prog. Retin. Eye Res.* **20**, 385–414 (2001).
44. Grossniklaus, H.E. *et al.* Macrophage and retinal pigment epithelium expression of angiogenic cytokines in choroidal neovascularization. *Mol. Vis.* **8**, 119–126 (2002).
45. Sakurai, E. *et al.* Targeted disruption of the CD18 or ICAM-1 gene inhibits choroidal neovascularization. *Invest. Ophthalmol. Vis. Sci.* **44**, 2743–2749 (2003).
46. Sakurai, E., Anand, A., Ambati, B.K., van Rooijen, N. & Ambati, J. Macrophage depletion inhibits experimental choroidal neovascularization. *Invest. Ophthalmol. Vis. Sci.* **44**, 3578–3585 (2003).
47. Ambati, J., Ambati, B.K., Yoo, S.H., Ianchulev, S. & Adamis, A.P. Age-related macular degeneration: etiology, pathogenesis, and therapeutic strategies. *Surv. Ophthalmol.* **48**, 257–293 (2003).

© 2003 Nature Publishing Group http://www.nature.com/naturemedicine

View publication stats

Macrophage Depletion Inhibits Experimental Choroidal Neovascularization

Eiji Sakurai,[1] *Akshay Anand,*[1] *Balamurali K. Ambati,*[2] *Nico van Rooijen,*[3] *and Jayakrishna Ambati*[1]

Objective. To investigate the role of macrophages in the development of laser-induced choroidal neovascularization (CNV) by selective depletion with liposomal clodronate (Cl_2MDP-LIP).

Methods. Laser photocoagulation was used to induce CNV in wild-type C57BL/6J mice. Animals were treated with intravenous (IV) and/or subconjunctival (SC) Cl_2MDP-LIP or PBS-LIP at the following time points: 2 days before, immediately after, 2 days before and immediately after, or 2 days after laser injury. CNV responses were compared on the basis of en masse volumetric measurements and fluorescein angiography after laser photocoagulation. Macrophages were identified by immunostaining for F4/80, and vascular endothelial growth factor (VEGF) expression was quantified by ELISA.

Results. Macrophages invaded the site of laser injury within 1 day of photocoagulation and peaked at 3 days. IV Cl_2MDP-LIP significantly decreased the volume of CNV and angiographic leakage when administered 2 days before and/or immediately after laser injury, but not when administered 2 days after injury. SC Cl_2MDP-LIP significantly decreased lesion volume when coadministered with IV PBS-LIP but not IV Cl_2MDP-LIP. IV Cl_2MDP-LIP was significantly more beneficial when administered 2 days before laser injury than immediately after, but combining SC Cl_2MDP-LIP with IV treatment eliminated this difference. Reduction in CNV volume correlated with VEGF protein levels and number of infiltrating macrophages.

Conclusions. Generalized macrophage depletion reduced the size and leakage of laser-induced CNV and was associated with decreased macrophage infiltration and VEGF protein. These findings define the role of the macrophage as a critical component in initiating the laser-induced CNV response. (*Invest Ophthalmol Vis Sci.* 2003;44:3578–3585) DOI:10.1167/iovs.03-0097

From the [1]Department of Ophthalmology, University of Kentucky, Lexington, Kentucky; the [2]Department of Ophthalmology, Medical College of Georgia, Augusta, Georgia; and the [3]Department of Cell Biology and Immunology, Vrije Universiteit, Amsterdam, The Netherlands.

Supported by Career Development Awards from Foundation Fighting Blindness (JA) and American Geriatrics Society (JA), a Prevent Blindness America/Fight for Sight Grant-in-Aid (JA), the University of Kentucky Physician Scientist Award (JA), and Knights-Templar Eye Foundation (BKA).

Submitted for publication January 29, 2003; revised March 26, 2003; accepted April 7, 2003.

Disclosure: **E. Sakurai**, None; **A. Anand**, None; **B.K. Ambati**, None; **N. van Rooijen**, None; **J. Ambati**, None

The publication costs of this article were defrayed in part by page charge payment. This article must therefore be marked "*advertisement*" in accordance with 18 U.S.C. §1734 solely to indicate this fact.

Corresponding author: Jayakrishna Ambati, Department of Ophthalmology, University of Kentucky, 801 Rose Street, Lexington, KY 40536-0284; jamba2@uky.edu.

Age-related macular degeneration (AMD) is the leading cause of irreversible blindness among the elderly in most industrialized nations,[1] yet little is known about the molecular mechanisms of choroidal neovascularization (CNV), the angiogenic process responsible for most severe visual loss in patients with AMD.[2]

The presence of macrophages in histologic studies of CNV has elicited interest in their role in the development of neovascular AMD. The spatiotemporal distribution of macrophages correlates with arborizing CNV in humans[3] and in animal models.[4] In patients with AMD, macrophages are in proximity to thinned and perforated areas of Bruch's membrane[5,6] and participate in digesting the outer collagenous zone of Bruch's membrane,[6] both of which facilitate the subretinal entry of CNV.

To test directly the hypothesis that macrophages play a causal rather than coincidental role in the development of CNV, we used the technique of pharmacological macrophage depletion with liposomal clodronate (Cl_2MDP-LIP) in the laser-induced model of CNV, which captures many salient pathologic and molecular features of neovascular AMD. Although free Cl_2MDP does not penetrate cell membranes and has a short circulating half-life, Cl_2MDP-LIP is phagocytosed by macrophages and rapidly induces apoptosis[7,8] without secretion of proinflammatory cytokines by the dying macrophages.[9] Moreover, Cl_2MDP-LIP appears to have a very selective effect on macrophages and phagocytic dendritic cells. Neutrophils and lymphocytes are not directly affected by this drug.[10–12]

We sought to assess the differential contribution of macrophages in the local (submandibular) lymph nodes versus that of the circulating, splenic, and hepatic macrophages to the development of CNV in this model. We administered Cl_2MDP-LIP by intravenous (IV) injection, which leads to near complete depletion of splenic and hepatic macrophages and marginal zone dendritic cells within 24 hours, persisting for 1 to 2 weeks in mice,[10] and/or subconjunctival (SC) injection, which leads to the depletion of macrophages from the draining submandibular lymph nodes.[13]

We attempted to differentiate the contribution of circulating versus resident retinal macrophages to CNV. Cl_2MDP-LIP does not cross the blood–brain barrier (and presumably the blood–retinal barrier) until it is damaged by an inflammatory response.[14] Therefore, we administered IV Cl_2MDP-LIP before laser injury and/or after laser injury, because the latter but not the former would permit the drug access to resident macrophages in the retina. We also correlated the macrophage response to laser injury with the level of vascular endothelial growth factor (VEGF), which is operative in the development of CNV[15–21] to deduce a mechanism for the effect of macrophage depletion in this process.

Methods

Animals

All animal experiments were in accordance with the guidelines of the University of Kentucky IACUC and ARVO Statement for the Use of

Investigative Ophthalmology & Visual Science, August 2003, Vol. 44, No. 8
Copyright © Association for Research in Vision and Ophthalmology

Downloaded from iovs.arvojournals.org on 02/12/2021

Animals in Ophthalmic and Vision Research. Male wild-type C57BL/6 mice (Jackson Laboratories, Bar Harbor, ME) between 6 and 8 weeks of age were used to minimize variability, because age[22] and sex (Tanemura M, et al. *IOVS* 2001;42:ARVO Abstract 530) can influence susceptibility to CNV. For all procedures, anesthesia was achieved by intramuscular injection of 50 mg/kg ketamine HCl (Fort Dodge Animal Health, Fort Dodge, IA) and 10 mg/kg xylazine (Phoenix Scientific, St. Joseph, MO), and pupils were dilated with topical 1% tropicamide (Alcon, Fort Worth, TX).

Induction of CNV

Laser photocoagulation (532 nm, 200 mW, 100 ms, 75 μm; OcuLight GL, Iridex, Mountain View, CA) was performed on both eyes of each animal on day 0 by a single individual masked to drug group assignment. Laser spots were applied in a standardized fashion around the optic nerve, using a slit lamp delivery system and a coverslip as a contact lens. The morphologic end point of the laser injury was the appearance of a cavitation bubble, a sign thought to correlate with the disruption of Bruch's membrane.

Liposomes

Clodronate (dichloromethylene diphosphonate; Cl_2MDP) was a gift of Roche Diagnostics GmbH, Mannheim, Germany. Clodronate-liposomes (Cl_2MDP-LIP) were prepared[11] as follows. In short, 86 mg phosphatidylcholine (Lipoid EPC; Lipoid, Ludwigshafen, Germany) and 8 mg cholesterol (Sigma-Aldrich, St. Louis, MO) were combined with 10 mL of a clodronate (0.7 M) solution and sonicated gently. The resultant liposomes were then washed to eliminate free drug. Empty liposomes were prepared under the same conditions with phosphate-buffered saline (PBS; Invitrogen/Gibco, Grand Island, NY) instead of the clodronate solution. Animals received 200 μL Cl_2MDP-LIP or PBS-LIP through the tail vein with a 30-gauge needle on day −2 (group 1), day 0 (immediately after laser injury; group 2), day –2 and day 0 (group 3), or day +2 (group 4). At these same time points, animals received 10 μL Cl_2MDP-LIP in one eye and 10 μL PBS-LIP in the other injected into the subconjunctival space with a syringe (Hamilton, Reno, NV). Injections were performed in a masked fashion.

Fluorescein Angiography

Fluorescein angiography was performed with a camera and imaging system (TRC 50 IA camera; ImageNet 2.01 system; Topcon, Paramus, NJ) at 1 week after laser photocoagulation. The photographs were captured with a 20-D lens in contact with the fundus camera lens after intraperitoneal injection of 0.1 mL of 2.5% fluorescein sodium (Akorn, Decatur, IL). A retina specialist not involved in the laser photocoagulation or angiography evaluated the fluorescein angiograms at a single sitting in masked fashion.

Volume of CNV

One week after laser injury, eyes were enucleated and fixed with 4% paraformaldehyde for 30 minutes at 4°C. Eye cups obtained by removing anterior segments were washed three times in PBS, followed by dehydration and rehydration through a methanol series. After blocking twice with buffer (PBS containing 1% bovine serum albumin (BSA; Sigma-Aldrich) and 0.5% Triton X-100 (Sigma-Aldrich) for 30 minutes at room temperature, eye cups were incubated overnight at 4°C with 0.5% FITC-isolectin B4 (Vector Laboratories, Burlingame, CA), which binds to terminal β-D-galactose residues on the surface of endothelial cells and selectively labels the murine vasculature, diluted with PBS containing 0.2% BSA and 0.1% Triton X-100. After two washings with PBS containing 0.1% Triton X-100, the neurosensory retina was gently detached and severed from the optic nerve. Four relaxing radial incisions were made, and the remaining RPE-choroid-sclera complex was flatmounted in antifade medium (Immu-Mount Vectashield Mounting Medium; Vector Laboratories) and coverslipped.

Flatmounts were examined with a scanning laser confocal microscope (TCS SP; Leica, Heidelberg, Germany). Vessels were visualized by exciting with blue argon laser wavelength (488 nm) and capturing emission between 515 to 545 nm. A 40× oil-immersion objective was used for all imaging studies. Horizontal optical sections (1 μm step) were obtained from the surface of the RPE-choroid-sclera complex. The deepest focal plane in which the surrounding choroidal vascular network connecting to the lesion could be identified was judged to be the floor of the lesion. Any vessel in the laser treated area and superficial to this reference plane was judged as CNV. Images of each section were digitally stored. The area of CNV-related fluorescence was measured by computerized image analysis with the microscope software (TCS SP; Leica). The summation of whole fluorescent area in each horizontal section was used as an index for the volume of CNV. Imaging was performed by an operator masked to treatment group assignment.

Immunostaining

At various times during the first week after laser injury, animals were injected with 1 mL FITC-isolectin B4 through the tail vein, and retinal-RPE-choroid-scleral or RPE-choroid-scleral flatmounts were prepared 30 minutes later. These were stained with antibodies against F4/80 (5 μg/mL; Serotec, Oxford, UK), expressed by retinal microglia and all mouse macrophages save those in lymphoid organs[23] or leukocyte common antigen CD45.2 (5 μg/mL; eBioscience, San Diego, CA), which also identifies retinal microglia.[24] Flatmounts were examined by scanning laser confocal microscopy. An optical density plot of the selected area was generated by a histogram graphing tool in the image-analysis software (Photoshop, ver. 6.0; Adobe Systems, Mountain View, CA) to obtain a quantitative index of macrophage numbers, as described previously.[25,26] Image analysis was performed by an operator masked to treatment group assignment.

VEGF ELISA

At 3 days after injury by 12 laser spots, the RPE-choroid complex was sonicated in lysis buffer (20 mM imidazole HCl, 10 mM KCl, 1 mM $MgCl_2$, 10 mM EGTA, 1% Triton X-100, 10 mM NaF, 1 mM Na molybdate, and 1 mM EDTA with protease inhibitor; Sigma-Aldrich) on ice for 15 minutes. VEGF protein levels in the supernatant were determined by an ELISA kit (threshold of detection 3 pg/mL; R&D Systems, Minneapolis, MN) that recognizes all splice variants, at 450 to 570 nm (Emax; Molecular Devices, Sunnyvale, CA), and normalized to total protein (Bio-Rad, Hercules, CA). Duplicate measurements were performed in a masked fashion by an operator not involved in photocoagulation, imaging, or fluorescein angiography.

Statistics

Volume of CNV. The dependent variable in the analysis was the average lesion volume per eye per mouse. A linear mixed model for a split plot design was constructed with two whole plot (between mice) factors. These are treatments (i.e., timing of the treatments relative to the laser injury) and intravenous (IV) administration (Cl_2MDP-LIP or PBS-LIP). The split plot (within mice) factor was subcutaneous (SC) administration (Cl_2MDP-LIP or PBS-LIP). Post hoc comparison of means consisted of either a pair-wise comparison of means or a contrast among the means constructed with error terms, depending on whether the contrast was between or within mice, respectively. Because the variability among mice treated with IV Cl_2MDP-LIP differed substantially from the variability among mice treated with IV PBS-LIP, the linear mixed model contained different variance components for these groups. Statistical significance was determined at the 0.05 level.

F4/80 and VEGF. Quantitative immunostaining and VEGF protein data were analyzed by ANOVA with the Dunnett multiple comparison test. Results were considered significant at $P < 0.05$.

Downloaded from iovs.arvojournals.org on 02/12/2021

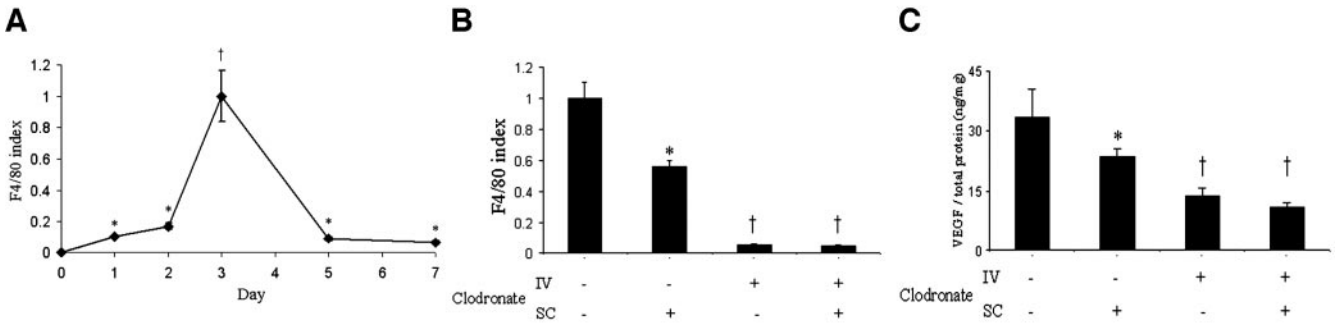


FIGURE 1. Cl_2MDP-LIP inhibited macrophage recruitment and VEGF protein expression after laser injury. (**A**) F4/80-positive macrophages were detected in the RPE-choroid of laser lesions within 1 day after laser injury and peaked in number at day 3. The index was normalized to peak response. $^*P < 0.01$ and $\dagger P < 0.001$ compared with day 0. (**B**) IV Cl_2MDP-LIP nearly abolished the peak macrophage response at day 3 in the RPE-choroid of laser lesions. SC Cl_2MDP-LIP partially inhibited macrophage recruitment when combined with IV PBS-LIP treatment but conferred no benefit when added to IV Cl_2MDP-LIP. $^*P < 0.01$ and $\dagger P < 0.001$ compared with no Cl_2MDP-LIP (PBS-LIP) treatment. (**C**) VEGF protein expression peaked at day 3 (data not shown). IV Cl_2MDP-LIP inhibited the VEGF protein expression response at day 3 in the RPE-choroid of laser lesions. SC Cl_2MDP-LIP partially inhibited VEGF levels when combined with IV PBS treatment but confered no benefit when added to IV Cl_2MDP-LIP. Data are expressed as the mean ± SEM. $^*P < 0.01$ and $\dagger P < 0.001$ compared with no Cl_2MDP-LIP (PBS-LIP) treatment. $n = 5$ per group.

RESULTS

Macrophages invaded the site of laser injury within 1 day, with a peak response at 3 days, followed by rapid disappearance by 5 to 7 days (Fig. 1A). IV Cl_2MDP-LIP administration nearly abolished macrophage recruitment, whereas SC Cl_2MDP-LIP blunted the macrophage response when administered with IV PBS-LIP, but did not confer added benefit to IV Cl_2MDP-LIP (Fig. 1B). The peak macrophage number paralleled the maximal amount of VEGF protein detected in the laser lesion at 3 days ($r^2 = 0.988$; Fig. 1C) and the volume of CNV at 7 days ($r^2 = 0.986$).

Confocal planar analysis revealed marked spatial colocalization of macrophages and endothelial cells at the site of laser injury (Fig. 2). In addition, IV Cl_2MDP-LIP, and SC Cl_2MDP-LIP to a lesser extent, decreased both the peak number of macrophages and endothelial cell coverage in parallel. We also observed that, whereas macrophages were found in areas without endothelial cells, the converse was rarely the case, supporting the notion that temporally macrophages precede and promote endothelial cell proliferation. During the first 3 days after laser injury, macrophages were concentrated in the choroidal base and central substance of the CNV lesion, but were sparse near its retinal apex (Fig. 3). Also, there was no difference in the density of macrophages and retinal microglia in the retina adjacent to the laser scar compared with the remainder of the retina, using either F4/80 (Fig. 3C) or CD45.2 (similar data not shown).

The stereotypical CNV response to laser injury was markedly inhibited by IV Cl_2MDP-LIP and to a lesser extent by SC Cl_2MDP-LIP (Fig. 4). Combined IV and SC Cl_2MDP-LIP treatment 2 days before laser injury decreased CNV volume by 90.8% ± 3.1% ($P < 0.0001$), immediately after laser injury by 79.2% ± 11.1% ($P < 0.0001$), and before and immediately after laser injury by 91.7% ± 4.7% ($P < 0.0001$), compared with combined IV and SC PBS-LIP treatment (Fig. 5). However, when IV and SC Cl_2MDP-LIP were administered 2 days after laser injury CNV volume was not significantly reduced ($P = 0.11$). IV Cl_2MDP-LIP treatment reduced CNV volumes in eyes treated with SC Cl_2MDP-LIP or SC PBS-LIP. When coadministered with IV PBS-LIP, SC Cl_2MDP-LIP treatment 2 days before laser injury decreased CNV volumes by 24.5% ± 7.2% ($P = 0.05$), immediately after laser injury by 27.8% ± 8.2% ($P = 0.05$), and before and immediately after laser injury by 35.5% ± 7.9% ($P = 0.007$), compared with SC PBS-LIP; however, SC Cl_2MDP-LIP did not augment the antiangiogenic effect of IV Cl_2MDP-LIP.

Pair-wise comparison of the different groups (timing of administration) revealed that IV Cl_2MDP-LIP was more effective when administered 2 days before laser injury than immediately after ($P = 0.05$) or 2 days after ($P < 0.0001$; Fig. 5E). Administering IV Cl_2MDP-LIP immediately after laser injury did not provide added benefit when it was administered 2 days before as well ($P = 0.83$). When SC Cl_2MDP-LIP was combined with IV Cl_2MDP-LIP, drug treatment 2 days before was no more effective than immediately after ($P = 0.20$), but both were more effective than 2 days after ($P < 0.0001$).

At 1 week after laser photocoagulation, fewer lesions in Cl_2MDP-treated animals exhibited fluorescein leakage (Fig. 6). Greater suppression of angiographic leakage was found when Cl_2MDP-LIP was administered both before and immediately after laser injury.

DISCUSSION

To our knowledge, this study is the first to demonstrate that macrophage depletion by Cl_2MDP-LIP inhibits the development of laser-induced CNV, validating our hypothesis that macrophages play a pivotal role in this process. Cl_2MDP-LIP decreased the peak macrophage response in parallel with VEGF protein levels and total CNV volume. Cl_2MDP-LIP administered before and/or immediately after laser injury inhibited CNV, whereas it did not exhibit any effect when administered 2 days after laser injury. This is presumably because macrophage depletion occurs roughly 24 hours after Cl_2MDP-LIP exposure, by which time the peak macrophage response at the site of laser injury has occurred. These data show that macrophages, which previous histopathological studies of experimental and clinical CNV have shown to be closely associated with new vessels, play a causal not a coincidental role in the development of laser-induced CNV.

IV Cl_2MDP-LIP–induced inhibition of CNV was not augmented by SC Cl_2MDP-LIP, whereas the latter was observed to inhibit CNV partially when coadministered with IV PBS-LIP. The total volume of SC Cl_2MDP-LIP administered to any single animal did not exceed 20 μL, which is insufficient to deplete splenic or hepatic macrophages.[13] In a model of experimental autoimmune pigment-epithelial uveitis (EAPU), IV Cl_2MDP-LIP, but not SC Cl_2MDP-LIP, inhibited EAPU,[27] suggesting that SC

Downloaded from iovs.arvojournals.org on 02/12/2021

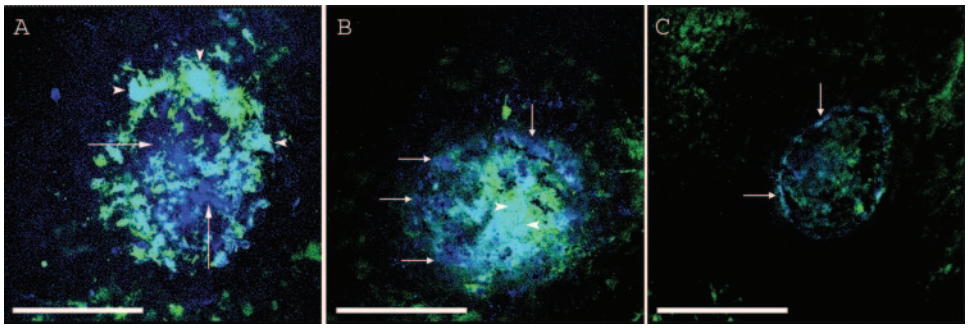


FIGURE 2. Macrophages recruited after laser injury colocalized with endothelial cells, and both responses were inhibited by Cl_2MDP-LIP. (**A**) Three days after laser injury in an animal treated with IV PBS-LIP, macrophages (*arrows*) stained by Cy5-F4/80 (*blue*) colocalized (*arrowheads*) with endothelial cells stained by FITC-Isolectin B4 (*green*). Colocalization by merging yielded a *cyan* color. (**B**) SC Cl_2MDP-LIP partially inhibited the number of macrophages (*arrows*) and CNV volume. (**C**) IV Cl_2MDP-LIP nearly abolished macrophage (*arrows*) and CNV response. The 1-μm sections with the greatest density of F4/80+ staining within laser scars are shown. Scale bar, 50 μm.

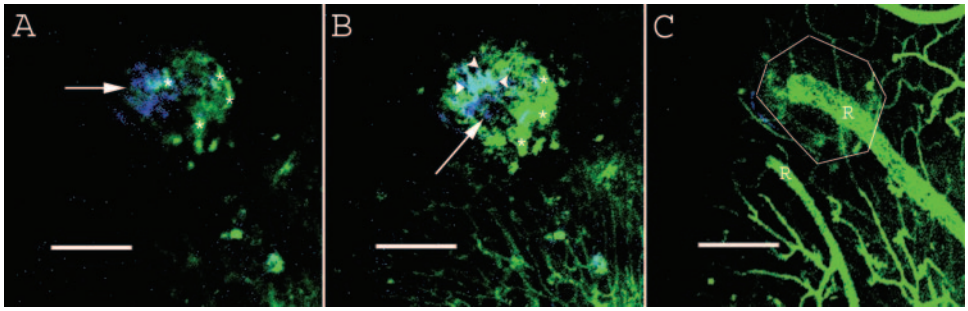


FIGURE 3. Macrophages in CNV were not recruited from the resident retinal population. (**A**) Three days after laser injury, numerous macrophages (*arrow*) stained by Cy5-F4/80 (*blue*) were present near the choroidal base of the CNV lesion (endothelial cells stained by FITC-Isolectin B4 appear *green* ✻). (**B**) The highest density of macrophages (*arrow*), many of which colocalized with endothelial cells (✻) (merge yields *cyan* color; *arrowheads*) was present in the middle of the CNV lesion. (**C**) A paucity of macrophages were found at the retinal surface of the CNV lesion (perimeter outlined in *white*) and in the adjacent retina (R). One-micrometer-thick sections are shown. Scale bar, 50 μm.

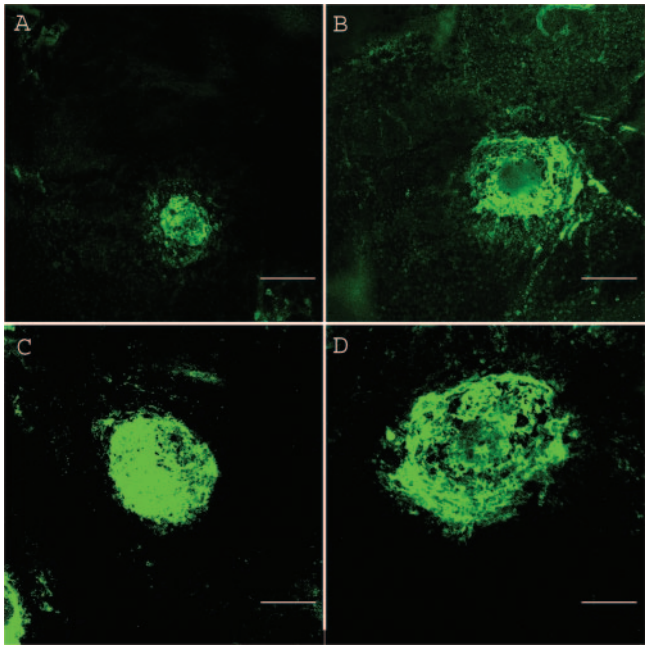


FIGURE 4. Cl_2MDP-LIP inhibited CNV 1 week after laser injury. IV Cl_2MDP-LIP administered 2 days before and immediately after laser injury suppressed CNV volume (**A**) to a greater degree than when administered 2 days after laser injury (**B**). SC Cl_2MDP-LIP administered 2 days before and immediately after laser injury in the presence of IV PBS-LIP partially inhibited CNV volume (**C**) compared with IV and SC PBS-LIP treatments at the same times (**D**). Stacked confocal images (1 μm sections) of FITC-isolectin B4 labeled tissue within laser scars are shown. Scale bar, 100 μm.

Downloaded from iovs.arvojournals.org on 02/12/2021

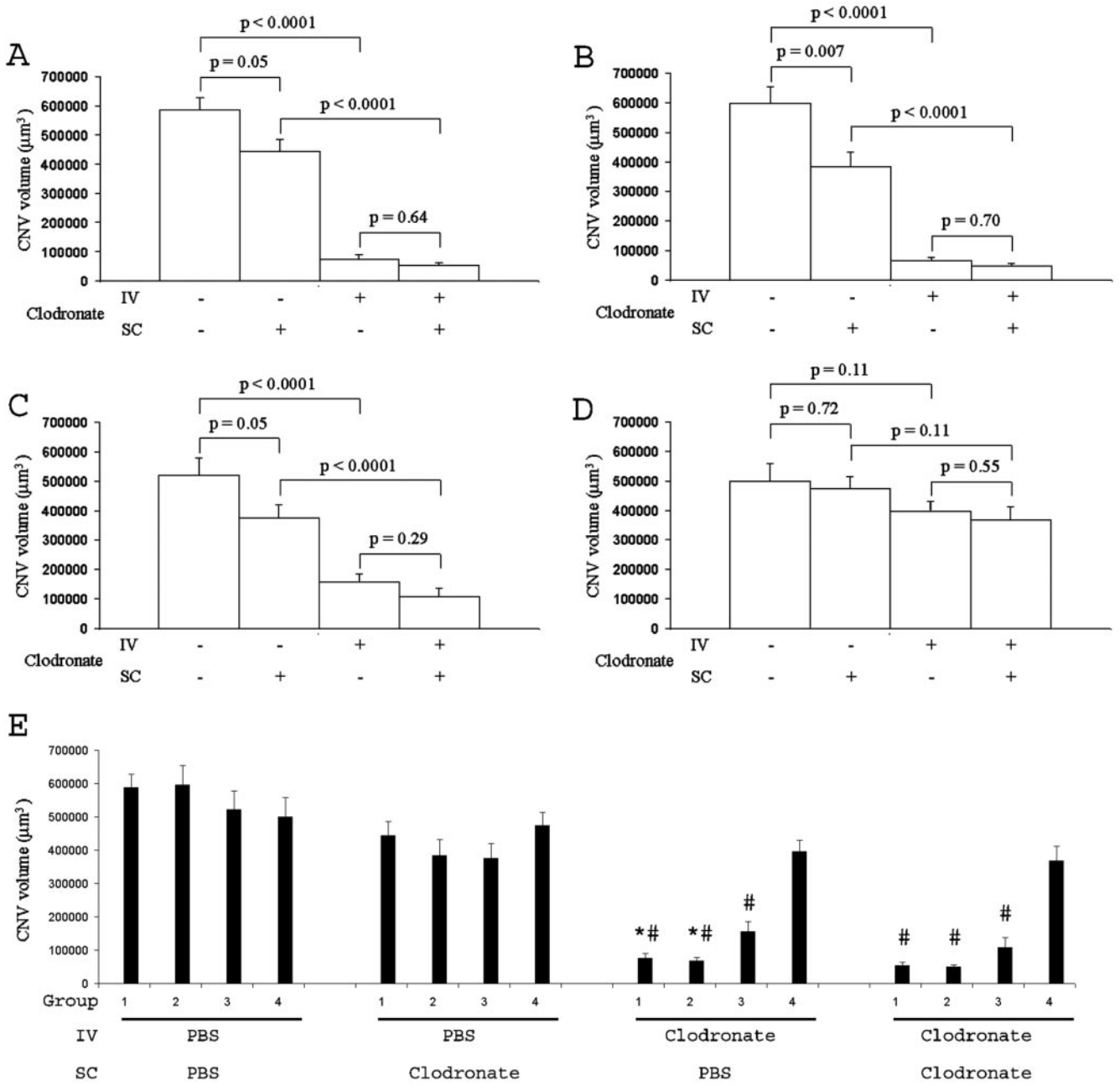


FIGURE 5. CNV volume was markedly diminished in Cl_2MDP-LIP–treated mice 1 week after laser injury. Cl_2MDP-LIP administered 2 days before laser injury (**A**), 2 days before and immediately after laser injury (**B**), and immediately after laser injury (**C**) demonstrated potent inhibition of CNV volume when Cl_2MDP-LIP was administered IV and mild inhibition when it was administered SC. SC Cl_2MDP-LIP did not provide added inhibition when administered with IV Cl_2MDP-LIP, but provided moderate inhibition when coadministered with IV PBS-LIP. Neither route of administration provided significant inhibition when administered 2 days after laser injury (**D**). (**E**) Pair-wise comparison of CNV volumes between group 1 (treatment 2 days before), group 2 (2 days before and immediately after), group 3 (immediately after), and group 4 (2 days after) are presented. IV Cl_2MDP-LIP was more effective when administered 2 days before laser injury (group 1 or 2) than immediately after (group 3) or 2 days after (group 4). When SC Cl_2MDP-LIP was combined with IV Cl_2MDP-LIP, drug treatments 2 days before (group 1 or 2) or immediately after (group 3) were more effective than at 2 days after (group 4). Administering IV Cl_2MDP-LIP immediately after laser injury did not provide added benefit when it was administered 2 days before, as well (group 1 versus group 2). $^*P < 0.05$ versus group 3, $\#P < 0.0001$ versus group 4. All other differences NS. $n = 5$ for all groups.

delivery of liposomes does not exert a systemic effect. Therefore, the observed beneficial effect of SC Cl_2MDP-LIP on CNV may be attributed to depletion of regional lymph node macrophages. In aggregate, these observations suggest that the predominant pool of macrophages that infiltrate areas of laser-induced CNV is derived from the systemic circulation, although submandibular nodes make a minor contribution.

The origin of macrophages observed after laser injury has been the subject of much inquiry.[4,28–30] We found that administering IV Cl_2MDP-LIP immediately after laser injury, which provides access to resident macrophages, did not augment the inhibition of CNV induced by IV Cl_2MDP-LIP 2 days before injury. We also found no infiltration of macrophages and microglia in the retina adjacent to the laser scar. Our data provide

Downloaded from iovs.arvojournals.org on 02/12/2021

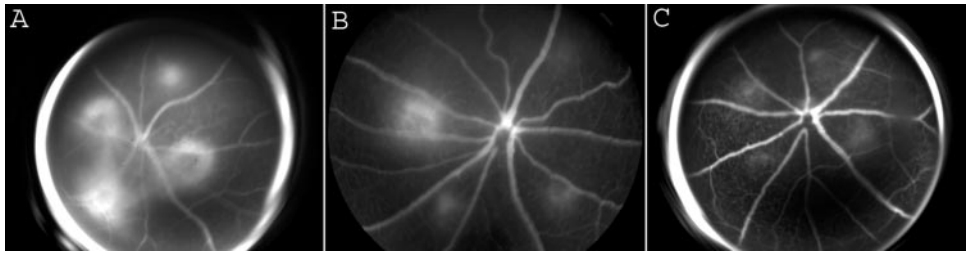


FIGURE 6. Cl_2MDP-LIP decreased angiographic leakage of laser-induced CNV. Representative late phase (6–8 minutes) fluorescein angiograms 1 week after laser injury of mice treated with IV PBS-LIP before and immediately after (**A**), with IV Cl_2MDP-LIP 2 days before (**B**), and with IV Cl_2MDP-LIP 2 days before and immediately after (**C**) laser injury.

direct anatomic and functional evidence that circulating rather than resident macrophages are the primary culprit in laser-induced CNV. This is consistent with the in vitro finding of polarized secretion of macrophage chemoattractant protein (MCP)-1 from the RPE into the choroid rather than the retina[31] and the in vivo finding of MCP-1 in RPE and choroid, but not in the retina, of eyes with AMD.[32]

A consensus has yet to emerge in quantifying experimental CNV: Both anatomic and functional metrics have been used. The former include measuring thickness and area on serial sections or volumes by confocal microscopy on RPE-choroidal flatmounts, aided by an endothelial cell marker. En masse volumetric measurements are less susceptible to nonorthogonality and loss or poor quality of sections than serial sectioning. Fluorescein angiography, which correlates with visual acuity in patients with AMD[33–35] and also permits longitudinal evaluation of the evolution of the laser lesions unlike histopathological examination, reflects on the leakage of these lesions, which presumably correlates with their activity. We used both anatomic and functional metrics of measuring CNV to corroborate our findings: Cl_2MDP-LIP inhibited both the anatomic volume and the angiographic leakage of laser-induced CNV.

We have shown that the leukocyte adhesion molecules CD18 and intercellular adhesion molecule (ICAM)-1 play a key role in laser-induced CNV.[36] Because liposomes do not interfere with leukocyte adhesion[37] or rolling[38] and PBS-LIP did not inhibit CNV, the antiangiogenic effects of Cl_2MDP-LIP can be attributed to depletion of macrophages alone. We infer therefore that the paracrine signals produced by macrophages promote the development of CNV. A likely signaling candidate is VEGF, as its levels were suppressed by Cl_2MDP-LIP in tandem with the number of macrophages, particularly because VEGF has been shown to be operative in CNV.[15–21]

We postulate that Cl_2MDP-LIP aborted the early-phase response to laser injury, mediated by macrophage migration, perhaps in response to overexpression of MCP-1, a stereotyped wounding response[39] that also occurs in RPE cells of AMD eyes (Spandau U, et al. *IOVS* 2000;41:ARVO Abstract 4440).[32] In support of this hypothesis, we have demonstrated that genetic ablation of MCP-1 or its cognate receptor CCR2 markedly inhibits laser-induced CNV (data not shown). However, the inhibition of CNV volume in MCP-1– or CCR2-deficient mice (~75%) did not match the near abolition induced by maximal Cl_2MDP-LIP treatment, probably due to depletion by Cl_2MDP-LIP of macrophages responsive not only to MCP-1 but to other chemokines, such as macrophage inflammatory proteins-1α and -β, that may play minor roles in recruiting macrophages.

Administering Cl_2MDP-LIP before or immediately after injury sharply reduced the number of macrophages in the site of laser injury, preventing the paracrine effects of these cells on endothelial cell migration and proliferation. VEGF, a major product of activated macrophages was reduced in parallel with the decrease in the number of macrophages. Laser photocoagulation leads to VEGF production by RPE cells,[40] predominantly on the choroidal side,[41] which itself can act as a macrophage chemoattractant.[42,43] However, because VEGF was reduced by Cl_2MDP-LIP, it seems that macrophages contribute perhaps more toward upregulation of VEGF than RPE or that RPE secretion of VEGF may be induced, in part, by macrophage–RPE interaction. Through their own VEGF release[44] macrophages can amplify the local VEGF response. Also macrophage-derived cytokines can stimulate VEGF production in RPE cells[45] and choroidal fibroblasts.[46] Macrophages can perpetuate their ingress by stimulating RPE cells to secrete MCP-1 into the choroid in a polarized gradient.[31] In addition to VEGF, macrophages also may produce matrix metalloproteinases (MMPs) directly[47] or through VEGF, which induces MMP expression in endothelial cells,[48] These MMPs, which have been found in CNV in AMD,[49] can facilitate endothelial cell migration during angiogenesis.

These findings may have some relevance to CNV in AMD, for although the laser injury model may involve processes not relevant to AMD, it captures many of the important features of the human condition. Laser photocoagulation that disrupts Bruch's membrane can induce CNV in humans.[50] Both in experimental models and in AMD, newly formed vessels that are functionally incompetent[51,52] project into the subretinal space through defects in Bruch's membrane. Aggregation of leukocytes near arborizing neovascular tufts[3,4,45] is another shared feature of experimental and clinical CNV. Immunostaining has demonstrated the presence of VEGF and its receptors,[40,53] basic fibroblast growth factor,[54,55] transforming growth factor-β,[54,56] tumor necrosis factor-α,[45] Fas, and Fas-ligand[57,58] in cells of the CNV membranes in both conditions.

Because angiogenesis is a complex process with multiple redundant and intertwined cascades, it is remarkable that macrophage depletion alone nearly abolished CNV. This suggests, at least in this model of CNV, that macrophages and cytokines derived from them are requisite in this process and buttresses the growing body of evidence implicating leukocytes in the initiation of angiogenesis. Although macrophage inactivation could lead to immunosuppression, no overt infection was observed in our study involving transient macrophage depletion or by other investigators.[9,11] Although the clinical implications of transient, partial depletion of macrophages with Cl_2MDP-LIP will be apparent only in human trials, MCP-1 or CCR2 may be attractive molecular targets, particularly with local drug delivery.[59]

Acknowledgments

The authors thank Robinette King and Guojin Chen for technical assistance; Richard J. Kryscio, University of Kentucky Biostatistics Consulting Unit, for statistical analyses; and Ambati M. Rao, Delwood C. Collins, and P. Andrew Pearson for ongoing support.

References

1. Smith W, Assink J, Klein R, et al. Risk factors for age-related macular degeneration: pooled findings from three continents. *Ophthalmology.* 2001;108:697–704.
2. Macular Photocoagulation Study Group. Argon laser photocoagulation for neovascular maculopathy: five-year results from randomized clinical trials. *Arch Ophthalmol.* 1991;109:1109–1114.

Downloaded from iovs.arvojournals.org on 02/12/2021

3. Grossniklaus HE, Cingle KA, Yoon YD, Ketkar N, L'Hernault N, Brown S. Correlation of histologic 2-dimensional reconstruction and confocal scanning laser microscopic imaging of choroidal neovascularization in eyes with age-related maculopathy. *Arch Ophthalmol.* 2000;118:625–629.
4. Nishimura T, Goodnight R, Prendergast RA, Ryan SJ. Activated macrophages in experimental subretinal neovascularization. *Ophthalmologica.* 1990;200:39–44.
5. Killingsworth MC, Sarks JP, Sarks SH. Macrophages related to Bruch's membrane in age-related macular degeneration. *Eye.* 1990; 4:613–621.
6. van der Schaft TL, Mooy CM, de Bruijn WC, de Jong PT. Early stages of age-related macular degeneration: an immunofluorescence and electron microscopy study. *Br J Ophthalmol.* 1993;77: 657–661.
7. Naito M, Nagai H, Kawano S, et al. Liposome-encapsulated dichloromethylene diphosphonate induces macrophage apoptosis in vivo and in vitro. *J Leukoc Biol.* 1996;60:337–344.
8. van Rooijen N, Sanders A, van den Berg TK. Apoptosis of macrophages induced by liposome-mediated intracellular delivery of clodronate and propamidine. *J Immunol Methods.* 1996;193: 93–99.
9. van Rooijen N, Sanders A. Elimination, blocking, and activation of macrophages: three of a kind? *J Leukoc Biol.* 1997;62:702–709.
10. van Rooijen N, Kors N, Kraal G. Macrophage subset repopulation in the spleen: differential kinetics after liposome-mediated elimination. *J Leukoc Biol.* 1989;45:97–104.
11. Van Rooijen N, Sanders A. Liposome mediated depletion of macrophages: mechanism of action, preparation of liposomes and applications. *J Immunol Methods.* 1994;174:83–93.
12. Alves-Rosa F, Stanganelli C, Cabrera J, van Rooijen N, Palermo MS, Isturiz MA. Treatment with liposome-encapsulated clodronate as a new strategic approach in the management of immune thrombocytopenic purpura in a mouse model. *Blood.* 2000;96:2834–2840.
13. Van der Veen G, Broersma L, Van Rooijen N, Van Rij G, Van der Gaag R. Cytotoxic T lymphocytes and antibodies after orthotropic penetrating keratoplasty in rats treated with dichloromethylene diphosphonate encapsulated liposomes. *Curr Eye Res.* 1998;17: 1018–1026.
14. Huitinga I, Damoiseaux JG, van Rooijen N, Dopp EA, Dijkstra CD. Liposome mediated affection of monocytes. *Immunobiology.* 1992;185:11–19.
15. Cui JZ, Kimura H, Spee C, Thumann G, Hinton DR, Ryan SJ. Natural history of choroidal neovascularization induced by vascular endothelial growth factor in the primate. *Graefes Arch Clin Exp Ophthalmol.* 2000;238:326–333.
16. Spilsbury K, Garrett KL, Shen WY, Constable IJ, Rakoczy PE. Overexpression of vascular endothelial growth factor (VEGF) in the retinal pigment epithelium leads to the development of choroidal neovascularization. *Am J Pathol.* 2000;157:135–144.
17. Schwesinger C, Yee C, Rohan RM, et al. Intrachoroidal neovascularization in transgenic mice overexpressing vascular endothelial growth factor in the retinal pigment epithelium. *Am J Pathol.* 2001;158:1161–1172.
18. Baffi J, Byrnes G, Chan CC, Csaky KG. Choroidal neovascularization in the rat induced by adenovirus mediated expression of vascular endothelial growth factor. *Invest Ophthalmol Vis Sci.* 2000;41:3582–3589.
19. Honda M, Sakamoto T, Ishibashi T, Inomata H, Ueno H. Experimental subretinal neovascularization is inhibited by adenovirus-mediated soluble VEGF/flt-1 receptor gene transfection: a role of VEGF and possible treatment for SRN in age-related macular degeneration. *Gene Ther.* 2000;7:978–985.
20. Kwak N, Okamoto N, Wood JM, Campochiaro PA. VEGF is major stimulator in model of choroidal neovascularization. *Invest Ophthalmol Vis Sci.* 2000;41:3158–3164.
21. Krzystolik MG, Afshari MA, Adamis AP, et al. Prevention of experimental choroidal neovascularization with intravitreal anti-vascular endothelial growth factor antibody fragment. *Arch Ophthalmol.* 2002;120:338–346.
22. Espinosa-Heidmann DG, Suner I, Hernandez EP, Frazier WD, Csaky KG, Cousins SW. Age as an independent risk factor for severity of experimental choroidal neovascularization. *Invest Ophthalmol Vis Sci.* 2002;43:1567–1573.
23. Austyn JM, Gordon S. F4/80, a monoclonal antibody directed specifically against the mouse macrophage. *Eur J Immunol.* 1981; 11:805–815.
24. Chen L, Yang P, Kijlstra A. Distribution, markers, and functions of retinal microglia. *Ocul Immunol Inflamm.* 2002;10:27–39.
25. Lehr HA, van der Loos CM, Teeling P, Gown AM. Complete chromogen separation and analysis in double immunohistochemical stains using Photoshop-based image analysis. *J Histochem Cytochem.* 1999;47:119–126.
26. Lehr HA, Mankoff DA, Corwin D, Santeusanio G, Gown AM. Application of Photoshop-based image analysis to quantification of hormone receptor expression in breast cancer. *J Histochem Cytochem.* 1997;45:1559–1565.
27. Broekhuyse RM, Huitinga I, Kuhlmann ED, Rooijen NV, Winkens HJ. Differential effect of macrophage depletion on two forms of experimental uveitis evoked by pigment epithelial membrane protein (EAPU), and by melanin-protein (EMIU). *Exp Eye Res.* 1997; 65:841–848.
28. Gloor BP. On the question of the origin of macrophages in the retina and the vitreous following photocoagulation (autoradiographic investigations by means of 3H-thymidine). *Albrecht Von Graefes Arch Klin Exp Ophthalmol.* 1974;190:183–194.
29. Ishikawa Y, Momoeda S, Yoshitomi F. Origin of macrophage in photocoagulated rabbit retina. *Jpn J Ophthalmol.* 1983;27:138–148.
30. Tso MO. Photic maculopathy in rhesus monkey: a light and electron microscopic study. *Invest Ophthalmol.* 1973;12:17–34.
31. Holtkamp GM, De Vos AF, Peek R, Kijlsta A. Analysis of the secretion pattern of monocyte chemotactic protein-1 (MCP-1) and transforming growth factor-beta 2 (TGF-beta2) by human retinal pigment epithelial cells. *Clin Exp Immunol.* 1999;118:35–40.
32. Grossniklaus HE, Ling JX, Wallace TM, et al. Macrophage and retinal pigment epithelium expression of angiogenic cytokines in choroidal neovascularization. *Mol Vis.* 2002;8:119–126.
33. Miller JW, Schmidt-Erfurth U, Sickenberg M, et al. Photodynamic therapy with verteporfin for choroidal neovascularization caused by age-related macular degeneration: results of a single treatment in a phase 1 and 2 study. *Arch Ophthalmol.* 1999;117:1161–1173.
34. Treatment of Age Related Macular Degeneration with Photodynamic Therapy (TAP) Study Group. Photodynamic therapy of subfoveal choroidal neovascularization in age-related macular degeneration with verteporfin: one-year results of 2 randomized clinical trials: TAP report. *Arch Ophthalmol.* 1999;117:1329–1345.
35. Treatment of Age Related Macular Degeneration with Photodynamic Therapy (TAP) Study Group. Photodynamic therapy of subfoveal choroidal neovascularization in age-related macular degeneration with verteporfin: two-year results of 2 randomized clinical trials: TAP Report 2. *Arch Ophthalmol.* 2001;119:198–207.
36. Sakurai E, Taguchi H, Anand A, et al. Targeted disruption of the CD18 or ICAM-1 gene inhibits choroidal neovascularization. *Invest Ophthalmol Vis Sci.* 2003;44:2743–2749.
37. Baatz H, Puchta J, Reszka R, Pleyer U. Macrophage depletion prevents leukocyte adhesion and disease induction in experimental melanin-protein induced uveitis. *Exp Eye Res.* 2001;73:101–109.
38. Malhotra R, Taylor NR, Bird MI. Anionic phospholipids bind to L-selectin (but not E-selectin) at a site distinct from the carbohydrate-binding site. *Biochem J.* 1996;314:297–303.
39. DiPietro LA, Polverini PJ, Rahbe SM, Kovacs EJ. Modulation of JE/MCP-1 expression in dermal wound repair. *Am J Pathol.* 1995; 146:868–875.
40. Wada M, Ogata N, Otsuji T, Uyama M. Expression of vascular endothelial growth factor and its receptor (KDR/flk-1) mRNA in experimental choroidal neovascularization. *Curr Eye Res.* 1999; 18:203–213.
41. Blaauwgeers HG, Holtkamp GM, Rutten H, et al. Polarized vascular endothelial growth factor secretion by human retinal pigment epithelium and localization of vascular endothelial growth factor receptors on the inner choriocapillaris: evidence for a trophic paracrine relation. *Am J Pathol.* 1999;155:421–428.

Downloaded from iovs.arvojournals.org on 02/12/2021

42. Clauss M, Weich H, Breier G, et al. The vascular endothelial growth factor receptor Flt-1 mediates biological activities: implications for a functional role of placenta growth factor in monocyte activation and chemotaxis. *J Biol Chem.* 1996;271:17629–17634.
43. Barleon B, Sozzani S, Zhou D, Weich HA, Mantovani A, Marme D. Migration of human monocytes in response to vascular endothelial growth factor (VEGF) is mediated via the VEGF receptor flt-1. *Blood.* 1996;87:3336–3343.
44. Harmey JH, Dimitriadis E, Kay E, Redmond HP, Bouchier-Hayes D. Regulation of macrophage production of vascular endothelial growth factor (VEGF) by hypoxia and transforming growth factor beta-1. *Ann Surg Oncol.* 1998;5:271–278.
45. Oh H, Takagi H, Takagi C, et al. The potential angiogenic role of macrophages in the formation of choroidal neovascular membranes. *Invest Ophthalmol Vis Sci.* 1999;40:1891–1898.
46. Kvanta A. Expression and regulation of vascular endothelial growth factor in choroidal fibroblasts. *Curr Eye Res.* 1995;14: 1015–1020.
47. Banda MJ, Werb Z. Mouse macrophage elastase: purification and characterization as a metalloproteinase. *Biochem J.* 1981;193: 589–605.
48. Lamoreaux WJ, Fitzgerald ME, Reiner A, Hasty KA, Charles ST. Vascular endothelial growth factor increases release of gelatinase A and decreases release of tissue inhibitor of metalloproteinases by microvascular endothelial cells in vitro. *Microvasc Res.* 1998;55: 29–42.
49. Steen B, Sejersen S, Berglin L, Seregard S, Kvanta A. Matrix metalloproteinases and metalloproteinase inhibitors in choroidal neovascular membranes. *Invest Ophthalmol Vis Sci.* 1998;39:2194–2200.
50. Francois J, De Laey JJ, Cambie E, Hanssens M, Victoria-Troncoso V. Neovascularization after argon laser photocoagulation of macular lesions. *Am J Ophthalmol.* 1975;79:206–210.
51. Tobe T, Ortega S, Luna JD, et al. Targeted disruption of the FGF2 gene does not prevent choroidal neovascularization in a murine model. *Am J Pathol.* 1998;153:1641–1646.
52. Sarks SH, Van Driel D, Maxwell L, Killingsworth M. Softening of drusen and subretinal neovascularization. *Trans Ophthalmol Soc UK.* 1980;100:414–422.
53. Otani A, Takagi H, Oh H, et al. Vascular endothelial growth factor family and receptor expression in human choroidal neovascular membranes. *Microvasc Res.* 2002;64:162–169.
54. Amin R, Puklin JE, Frank RN. Growth factor localization in choroidal neovascular membranes of age-related macular degeneration. *Invest Ophthalmol Vis Sci.* 1994;35:3178–3188.
55. Ogata N, Matsushima M, Takada Y, et al. Expression of basic fibroblast growth factor mRNA in developing choroidal neovascularization. *Curr Eye Res.* 1996;15:1008–1018.
56. Ogata N, Yamamoto C, Miyashiro M, Yamada H, Matsushima M, Uyama M. Expression of transforming growth factor-β mRNA in experimental choroidal neovascularization. *Curr Eye Res.* 1997; 16:9–18.
57. Hinton DR, He S, Lopez PF. Apoptosis in surgically excised choroidal neovascular membranes in age-related macular degeneration. *Arch Ophthalmol.* 1998;116:203–209.
58. Kaplan HJ, Leibole MA, Tezel T, Ferguson TA. Fas ligand (CD95 ligand) controls angiogenesis beneath the retina. *Nat Med.* 1999; 5:292–297.
59. Ambati J, Gragoudas ES, Miller JW, et al. Transscleral delivery of bioactive protein to the choroid and retina. *Invest Ophthalmol Vis Sci.* 2000;41:1186–1191.

Downloaded from iovs.arvojournals.org on 02/12/2021

Targeted Disruption of the CD18 or ICAM-1 Gene Inhibits Choroidal Neovascularization

Eiji Sakurai,[1,2] *Hogara Taguchi,*[2,3] *Akshay Anand,*[1] *Balamurali K. Ambati,*[3,4] *Evangelos S. Gragoudas,*[3] *Joan W. Miller,*[3] *Anthony P. Adamis,*[3,5] *and Jayakrishna Ambati*[1,3]

Purpose. To investigate the role of the leukocyte adhesion molecules CD18 and intercellular adhesion molecule (ICAM)-1 in the development of choroidal neovascularization (CNV).

Methods. Laser photocoagulation was used to induce CNV in wild-type C57BL/6J mice and species-specific counterparts with targeted homozygous disruption of the CD18 or ICAM-1 gene. Expression of CD18 and ICAM-1 after laser injury was assessed by immunostaining. CNV responses were compared on the basis of en masse volumetric measurements obtained by confocal microscopy 2 weeks after laser injury and by determination of fluorescein angiographic leakage at 1, 2, and 4 weeks after laser injury.

Results. The site of laser injury showed upregulation of ICAM-1 and invasion by CD18-positive leukocytes within 1 day of laser injury. Significantly fewer lesions exhibited fluorescein leakage defined to be pathologically significant in CD18-deficient mice at weeks 1, 2, and 4 weeks and in ICAM-1–deficient mice at 1 and 4 weeks, compared with the control. There were a significantly greater number of lesions without fluorescein leakage in CD18-deficient mice than in the other two groups at all time points. The volume of CNV in CD18- and ICAM-1–deficient mice was significantly less than in wild type.

Conclusions. These data suggest a nonredundant role for leukocyte adhesion to vascular endothelium in the development of laser-induced choroidal neovascularization. (*Invest Ophthalmol Vis Sci.* 2003;44:2743–2749) DOI:10.1167/iovs.02-1246

From the [1]Department of Ophthalmology, University of Kentucky, Lexington, Kentucky; the [3]Department of Ophthalmology, Massachusetts Eye and Ear Infirmary, Harvard Medical School, Boston, Massachusetts; the [4]Department of Ophthalmology, Medical College of Georgia, Augusta, Georgia; and [5]Eyetech Research Center, Woburn, MA.

[2]Contributed equally to the work and therefore should be considered equivalent authors.

Supported by the American Ophthalmological Society Knapp Testimonial Fund (JA), a Foundation Fighting Blindness Career Development Award (JA), a Prevent Blindness America/Fight for Sight Grant-in-Aid (JA), a University of Kentucky Physician Scientist Award (JA), the Knights-Templar Eye Foundation (BKA), the Roberta Siegel Research Fund (APA), a Research to Prevent Blindness Senior Investigator Award (ESG), the Massachusetts Lions Eye Research Fund (APA, JWM), and the National Eye Institute (APA).

Submitted for publication December 5, 2002; revised January 16, 2003; accepted January 26, 2003.

Disclosure: **E. Sakurai**, None; **H. Taguchi**, None; **A. Anand**, None; **B.K. Ambati**, None; **E.S. Gragoudas**, None; **J.W. Miller**, None; **A.P. Adamis**, Eyetech Pharmaceuticals (E); **J. Ambati**, None

The publication costs of this article were defrayed in part by page charge payment. This article must therefore be marked "*advertisement*" in accordance with 18 U.S.C. §1734 solely to indicate this fact.

Corresponding author: Jayakrishna Ambati, Department of Ophthalmology, University of Kentucky, 740 S. Limestone Street, Lexington, KY 40536-0284; jamba2@uky.edu.

Age-related macular degeneration (AMD) is the leading cause of irreversible blindness among the elderly in most industrialized nations.[1] Yet, little is known about the molecular mechanisms of choroidal neovascularization (CNV), the angiogenic process responsible for most of the severe vision loss in patients with AMD.[2]

Leukocytes have been implicated in the pathogenesis of AMD, because their spatiotemporal distribution correlates with arborizing CNV in humans[3] and in animal models.[4] Macrophages are found in proximity to thinned and perforated areas of Bruch's membrane[5,6] and participate in the digestion of the outer collagenous zone of Bruch's membrane,[5] both of which facilitate the subretinal entry of CNV. There is growing evidence that leukocyte-mediated angiogenesis involves the interaction of cellular adhesion molecules and vascular endothelial growth factor (VEGF),[7,8] which itself is operative in CNV.[9–11] VEGF induces the expression of intercellular adhesion molecule (ICAM)-1 on tumor and retinal vascular endothelium and regulates leukocyte adhesion to endothelial cells.[12,13] ICAM-1 blockade decreases VEGF-induced leukostasis in the retina[13,14] and angiogenesis in the cornea.[8] These systems are intertwined: leukocytes, which possess receptors for and migrate in response to VEGF,[15] can also produce and release VEGF.[16]

The laser photocoagulation model of induced CNV captures many salient pathologic and molecular features of neovascular AMD. Therefore, we investigated the effects of ICAM-1 and its cognate receptor CD18 in a murine model of laser-induced CNV.

Methods

Animals

All animal experiments were in accordance with the guidelines of the University of Kentucky and Massachusetts Eye and Ear Infirmary Animal Care Committees and the ARVO Statement for the Use of Animals in Ophthalmic and Vision Research. CD18- (C57BL/6J-*Itgb2*^{tm1Bay}) and ICAM-1–deficient (C57BL/6J-*Icam1*^{tm1Bay}) mice, backcrossed onto the C57BL/6J background over 10 generations, were purchased from Jackson Laboratories (Bar Harbor, ME), as were wild-type C57BL/6J mice, which served as the control. Thus, these mice were expected to be more than 99.9% similar at all unlinked loci. Species specificity is important because genetic background determines susceptibility to neovascularization.[17] Only male mice between 4 and 6 weeks of age were used, to minimize variability, because age[18] and sex (Tanemura M, Miyamoto N, Mandai M, Honda Y, ARVO Abstract 530, 2001) can influence susceptibility to CNV. Genotypes were confirmed by PCR of genomic DNA extracted from tail snips. For all procedures, anesthesia was achieved by intramuscular injection of 50 mg/kg ketamine hydrochloride (Abbott, North Chicago, IL) and 10 mg/kg xylazine (Bayer, Shawnee Mission, KS), and pupils were dilated with topical 0.5% tropicamide (Alcon, Humacao, Puerto Rico).

Induction of CNV

Laser photocoagulation (630 nm, 400 mW, 0.05 second, 50 μm; model 920 Argon/Dye; Coherent Medical, Santa Clara, CA) was performed on

Copyright © Association for Research in Vision and Ophthalmology

both eyes of each animal ($n = 10$ per group) by an operator masked to its genetic identity.[19] Four laser spots were applied in a peripapillary distribution in a standardized fashion, two to three disc diameters from the optic nerve, using a slit lamp delivery system and a coverslip as a contact lens. The morphologic end point of the laser injury was the appearance of a cavitation bubble, a sign thought to correlate with the disruption of Bruch's membrane.

Fluorescein Angiography

Fluorescein angiography was performed by an operator masked to the genetic identity of the animal, with a commercial camera and imaging system (TRC 50 VT camera and IMAGEnet 1.53 system; Topcon, Paramus, NJ), at 1, 2, and 4 weeks after laser photocoagulation. The photographs were captured with a 20-D lens in contact with the fundus camera lens, after intraperitoneal injection of 0.1 mL of 1% fluorescein sodium (Akorn, Decatur, IL).

Two masked retina specialists not involved in laser photocoagulation or angiography evaluated the fluorescein angiograms at a single sitting. Lesions were graded on an ordinal scale based on the spatial and temporal evolution of fluorescein leakage as follows: 0 (nonleaky): no leakage, faint hyperfluorescence, or mottled fluorescence without leakage; 1 (questionable leakage): hyperfluorescent lesion without progressive increase in size or intensity; 2A (leaky): hyperfluorescence increasing in intensity but not in size; no definite leakage; 2B (pathologically significant leakage): hyperfluorescence increasing in intensity and in size; definite leakage.

Volume of CNV

Two weeks after laser injury, eyes were enucleated and fixed with 4% paraformaldehyde for 30 minutes at 4°C. Eyecups obtained by removing anterior segments were washed three times in phosphate-buffered saline (PBS; Invitrogen-Life Technologies, Grand Island, NY), followed by dehydration and rehydration through a methanol series. After blocking was performed twice with buffer (PBS containing 1% bovine serum albumin [BSA; Sigma, St. Louis, MO]) and 0.5% Triton X-100 [Sigma]) for 30 minutes at room temperature (RT), eyecups were incubated overnight at 4°C with 0.5% fluorescein *Griffonia simplicifolia* lectin I (Vector Laboratories, Burlingame, CA), which binds to terminal β-D-galactose residues on the surface of endothelial cells and selectively labels the murine vasculature, diluted with PBS containing 0.2% BSA and 0.1% Triton X-100. After two washings with PBS containing 0.1% Triton X-100, the neurosensory retina was gently detached and severed from the optic nerve. Four relaxing radial incisions were made, and the remaining RPE-choroid-sclera complex was flatmounted (Immu-Mount Vectashield Mounting Medium; Vector) and coverslipped.

Flatmounts were examined with a scanning laser confocal microscope (TCS SP; Leica, Heidelberg, Germany). Vessels were visualized by exciting with blue argon laser wavelength (488 nm) and capturing emission between 515 and 545 nm. A 40× oil-immersion objective was used for all imaging studies. Horizontal optical sections (1-μm thickness step) were obtained from the surface of the RPE-choroid-sclera complex. The deepest focal plane in which the surrounding choroidal vascular network connecting to the lesion could be identified was judged to be the floor of the lesion. Any vessel in the laser-treated area and superficial to this reference plane was judged as CNV. Images of each section were digitally stored. The area of CNV-related fluorescence was measured by computerized image analysis with the microscope software (TCS SP; Leica). The summation of whole fluorescent area in each horizontal section was used as an index for the volume of CNV.

Immunostaining

Enucleated eyes were fixed (Histochoice MB; Amresco, Inc., Solon, OH) for 48 hours, and 7-μm paraffin sections were cut. Immunostaining was performed on deparaffinized sections preincubated with serum-free protein block (Dako, Carpinteria, CA) for 30 minutes at RT. Endogenous alkaline phosphatase activity was quenched with levamisole. Sections were then incubated for 1 hour at RT with rat anti-mouse CD18 (M18/2; Chemicon, Temecula, CA), rat anti-mouse ICAM-1 (KAT-1; R&D Systems, Minneapolis, MN), or rabbit anti-human von Willebrand Factor (A0082; Dako). Tissues were then incubated with diluted primary antibody (2–10 μg/mL) for 1 hour at RT. Diluted biotinylated secondary IgG (2–10 μg/mL) was applied for 30 minutes at RT. Signal amplification was obtained with a kit (Vectastain Indirect; Vector) followed by a streptavidin-biotin-alkaline phosphatase complex (ABC Kit; Vector). Color development was performed (Vector Red; Vector) and sections counterstained with hematoxylin. Specificity of staining was assessed by omitting the primary antibody.

Statistics

Fluorescein Angiography. Differences in incidence of grade-0 or -2B lesions between groups were analyzed by repeated-measures nested logistic regression. Because the probability development of CNV in each laser lesion is influenced by the group to which the lesion belongs, the mouse, the eye, and the laser spot, the nested design consisted of four measures (laser spots) per eye within two measures (eyes) per mouse within five measures (animals) per group. As the dependent variable (lesion grade) is ordinal with four levels, logistic regression considering both a between-subjects design (three groups, each with five animals) and a within-subjects design (two eyes and three time points) was performed. Because of the within-subjects part of the design, a repeated-measures analysis with the three factors (group, eye, time point) as main effects, and with two-way interactions was undertaken. Correlations between groups and lesion grades were analyzed by a multivariate permutation test. Two-tailed differences with a type I error not exceeding 0.05 were considered significant.

Volume of CNV. The mean lesion volumes were compared by using a linear mixed model with a split-plot, repeated-measures design. The whole-plot factor was the genetic group to which the animal belonged, and the split-plot factor was the eye. Statistical significance was determined at the 0.05 level. Post hoc comparison of means was constructed with a Bonferroni adjustment for multiple comparisons ($P < 0.017$).

Results

In wild-type C57BL/6J mice, numerous CD18- and ICAM-1–positive cells were concentrated at the site of the laser lesion as early as 1 day after injury and persisted up to 4 days (Fig. 1). These findings were restricted to the sites of injury and not generalized throughout the eye.

The volume of CNV in CD18-deficient mice was reduced by 67.0% ± 10.9% ($P < 0.0001$) and by 75.7% ± 8.6% ($P < 0.0001$) in ICAM-1–deficient mice, compared with wild-type C57BL/6J mice at 2 weeks after laser injury (Fig. 2). There was no statistically significant difference in CNV volume between the two knockout strains or between eyes within genetically identical groups. Both flatmounts and serial sections taken at 2 weeks after injury showed markedly smaller CNV membranes in CD18- and ICAM-1–deficient animals compared with those in wild types (Fig. 3).

At 1, 2, and 4 weeks after laser photocoagulation, pathologically significant leakage (grade-2B lesions) developed in most of the wild-type mice, but in significantly fewer CD18-deficient mice (Fig. 4). At weeks 1 and 4, significantly fewer lesions in the ICAM-1–deficient mice were grade-2B compared with wild-type animals, with a similar trend approaching significance at week 2. Fewer CD18-deficient mice ($P = 0.002$) and ICAM-1–deficient mice ($P = 0.028$) had three or more grade-2B lesions in each eye compared with the wild type (Fig. 5). At weeks 1 and 2, there was a significantly greater number of nonleaky (grade 0) lesions in the CD18-deficient mice than in the other two groups, with a similar trend approaching significance at

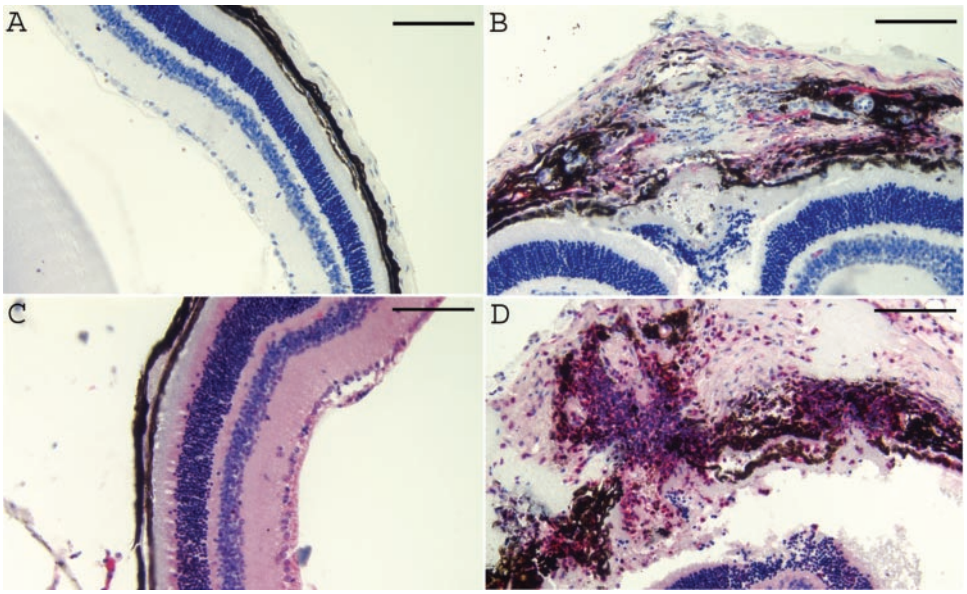


FIGURE 1. CD18- and ICAM-1–positive cells in CNV within 1 day of laser injury. (**A**, **C**) Unlasered areas showing normal neurosensory retina, retinal pigment epithelium (RPE), choroid, and sclera stained with red fluorescent dye and rat anti-mouse ICAM-1 (**A**) or rat anti-mouse CD18 (**C**). (**B**) Laser lesion (same section of eye as in (**A**) shows disruption and migration of RPE with high density of ICAM-1–expressing cells (presumed RPE and choroidal endothelial cells, stained with red fluorescent dye and rat anti-mouse ICAM-1), 1 day after injury. (**D**) Laser lesion (same section of eye as in (**C**) showing numerous CD18-positive cells (stained with red fluorescent dye and rat anti-mouse CD18) corresponding to surface of round *blue* cells (presumed leukocytes), 1 day after injury. Sections counterstained with hematoxylin (**A**, **B**) or hematoxylin and eosin (**C**, **D**). Scale bar, 100 μm. Original magnification, ×200.

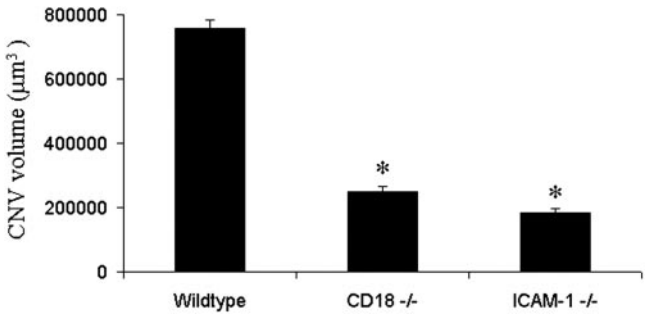


FIGURE 2. CNV volume was markedly diminished in CD18 and ICAM-1–deficient mice 2 weeks after laser injury. The volume per lesion (mean ± SEM) in $CD18^{-/-}$ (250,322.7 ± 15,071.9) and in $ICAM\text{-}1^{-/-}$ mice (184,744.8 ± 11,897.7) was significantly less than in wild-type animals (758,916.5 ± 26,077.6). $^{*}P < 0.0001$; $n = 5$ in all groups.

week 4 (Fig. 6). A trend toward a greater number of grade-0 lesions in the ICAM-1–deficient mice than in the control mice was observed. Odds ratios highlight the significant differences between proportions of grade-0 or -2B lesions between groups at all time points (Table 1). There were no significant intragroup differences in the proportion of grade-0 or -2B lesions at any time point in any of the three groups. No significant regression of CNV, as evaluated by fluorescein angiography, was observed within any group at the three time points. There was a high correlation between the group and the lesion grades ($r = 0.544$, $P < 0.001$).

DISCUSSION

In our study, CD18 or ICAM-1–deficient mice had smaller CNV membranes that also exhibit decreased fluorescein leakage than wild-type mice. This is consistent with the findings of ICAM-1 expression in the endothelial cells of CNV membranes in patients with AMD[20] (Nozaki M, Ozeki H, Ogura Y, ARVO Abstract 1229, 2001) and in laser-induced CNV in rats,[21] buttressing the growing body of evidence implicating leukocytes and leukocyte adhesion molecules in the initiation of angiogenesis.

The inhibition of CNV, although marked, was incomplete in both knockout groups, suggesting the presence of alternate mechanisms of angiogenesis. Nevertheless, the substantial inhibition of CNV in this model supports the hypothesis that

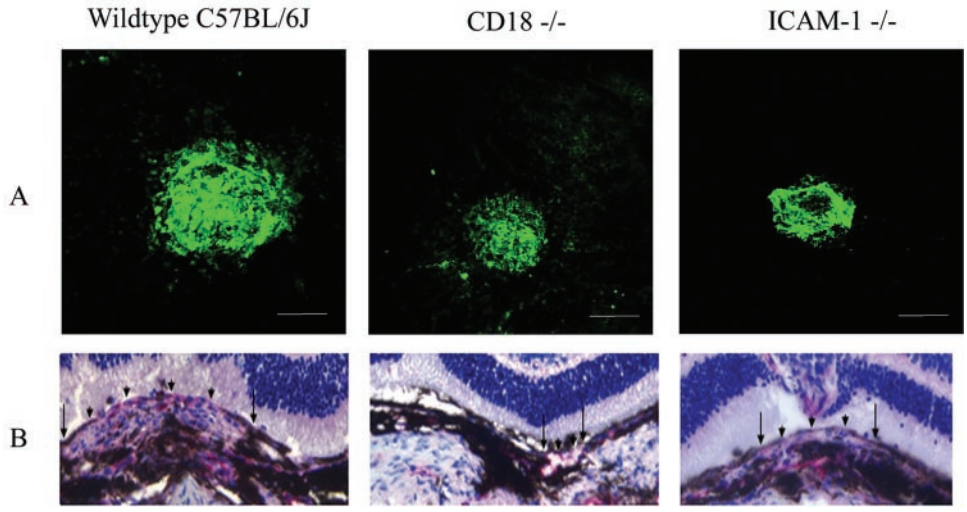


FIGURE 3. CNV size was markedly diminished in CD18- and ICAM-1–deficient mice 2 weeks after laser injury. (**A**) Stacked confocal images of fluorescein *Griffonia simplicifolia* lectin I-labeled tissue within laser scars show CNV membranes with a significantly smaller number in the mutant mice than in wild type. (**B**) Serial sections labeled with von Willebrand factor showed smaller CNV membranes, both in thickness and area. The section with the maximum diameter (*arrows*) for each CNV lesion, with thickness demonstrated by *arrowheads* along its surface, is shown. Scale bar, 100 μm.

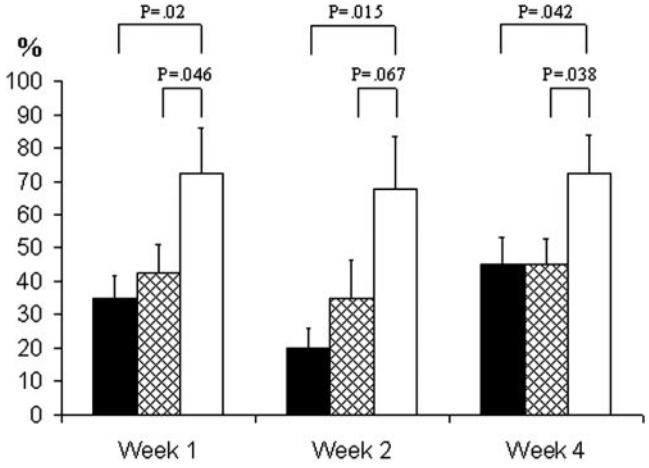


FIGURE 4. Significantly fewer grade-2B lesions occurred in CD18- and ICAM-1–deficient mice than in background C57BL/6J mice. Percentage of grade-2B lesions (mean ± SEM) in CD18-deficient (■), ICAM-1–deficient (▨), and wild-type (□) mice ($n = 5$ for all groups).

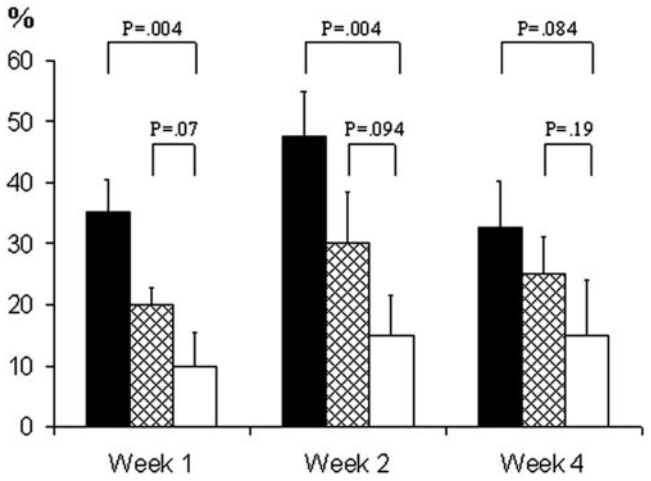


FIGURE 6. Significantly greater numbers of grade-0 lesions occurred in CD18-deficient mice compared with the control. Percentage of grade-0 lesions (mean ± SEM) in CD18-deficient (■), ICAM-1–deficient (▨), and wild-type (□) mice ($n = 5$ for all groups).

CD18 and ICAM-1 play a key role in initiating or at least facilitating CNV, particularly because cells expressing these markers are abundant in the site of CNV early after laser injury. Further, the extent of the requirement for CD18 and ICAM-1 in CNV may be more than demonstrated herein because genetic ablation is incomplete in these leaky knockouts.[22,23] In addition, the full contribution of leukocytes to CNV induction may not have been extracted in this paradigm because leukocyte adhesion sometimes can be CD18 independent.[24]

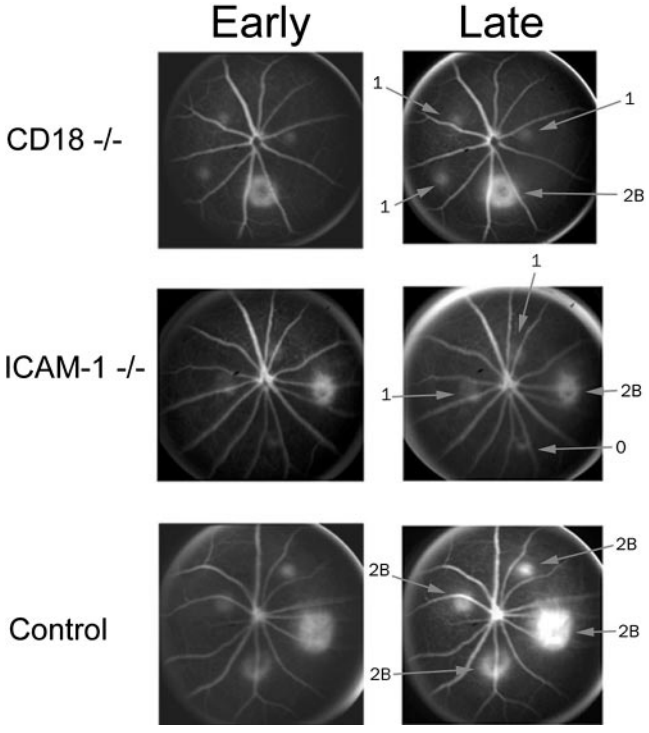


FIGURE 5. More control mice had three or more grade-2B lesions than did CD18- or ICAM-1–deficient mice. Representative early-phase (1–3 minutes) and late-phase (8–10 minutes) fluorescein angiograms of a CD18$^{-/-}$, ICAM-1$^{-/-}$, and wild-type C57BL/6J mouse. *Arrows*: lesion grades.

We found significantly greater inhibition of CNV-associated angiographic leakage in CD18-deficient than in ICAM-1–deficient mice, perhaps due to variations in the degree of hypomorphism in gene expression between the two groups, because these mutations are not completely null. Blockade of CD18 results in greater inhibition of leukocyte adhesion to RPE cells in response to inflammatory cytokines than blockade of ICAM-1.[25] This suggests that CD18 may recognize ligands other than ICAM-1, as appears to be the case in the accumulation of dendritic cells in the lung.[26] CD18 may bind to fibronectin,[27] which is found in the basement membrane of CNV in AMD.[5,28] Also, due to alternative RNA splicing, ICAM-1–deficient mice are not completely devoid of cell surface ICAM-1 expression[23] and contain normal levels of circulating soluble ICAM-1,[29] which can promote angiogenesis.[30]

A consensus has yet to evolve in quantifying experimental CNV. Both anatomic and functional metrics have been used. The former include measuring thickness and area on serial sections or volumes by confocal microscopy on RPE-choroidal flatmounts, aided by an endothelial cell marker. En masse volumetric measurements are less susceptible to nonorthogonality and loss/poor quality of sections than serial sectioning. Fluorescein angiography has been used to comment on the leakage of these lesions, presumably correlating with their activity due to incompetence of the immature vessels.

We used both anatomic and functional metrics of measuring CNV to reinforce the fidelity of our findings. Although both clinical[31,32] and experimental[33] CNV typically demonstrates fluorescein leakage, both types of CNV can be angiographically silent,[33–36] which correlates with envelopment by RPE.[37] In addition, fluorescein leakage correlates with visual acuity in patients with AMD,[38–40] and also permits longitudinal evaluation of the evolution of the laser lesions, unlike histopathological examination. Therefore, we defined grade-2B lesions, which have an angiographic and clinical appearance akin to classic CNV,[41] as pathologically significant. Notably, these are the type of lesion affected most by CD18 and ICAM-1 adhesion. Confocal microscopy disclosed the presence of CNV in grade-1, -2A, and -2B lesions but not in grade-0 lesions (Taguchi H, Kim RY, Razavi S, Connolly EJ, Gragoudas ES, Miller JW, ARVO Abstract 880, 2000). However, the hyperfluorescence of grade 1, and perhaps grade 2A, lesions may be due to transmission through RPE defects.

TABLE 1. Event Rates of Grade 0 and Grade 2B Lesions over 4-Week Period in CD18 or ICAM-1–Deficient Mice Compared with C57BL/6J Mice

	Grade 0 Lesions			Grade 2B Lesions		
Group	**Odds Ratio**	**95% CI**	***P***	**Odds Ratio**	**95% CI**	***P***
Control	1.00	—	—	1.00	—	—
$CD18^{-/-}$	5.29	1.7–16.4	0.004	0.11	0.02–0.58	0.01
$ICAM\text{-}1^{-/-}$	2.66	0.85–8.33	0.094	0.16	0.03–0.77	0.02

Although the laser-induced model of CNV may involve processes not relevant to AMD, it captures many of the important features of the human condition. Laser photocoagulation that disrupts Bruch's membrane can induce CNV in humans.[42] Both in experimental models and in AMD, newly formed vessels that are functionally incompetent[19,41,43] project into the subretinal space through defects in Bruch's membrane. Aggregation of leukocytes near arborizing neovascular tufts[3,4,44–46] is another shared feature of experimental and clinical CNV. Immunostaining has demonstrated the presence of VEGF and its receptors,[47,48] basic fibroblast growth factor,[49,50] transforming growth factor-β,[49,51] tumor necrosis factor-α,[45] Fas, and Fas-ligand[52,53] in cells composing the CNV membranes in both conditions.

We postulate that laser photocoagulation incites inflammation, leading to endothelial upregulation of ICAM-1, which binds to CD18, mediating firm leukocyte-endothelial adhesion and transmigration.[54] Laser photocoagulation leads to production of VEGF by RPE cells,[48] predominantly on the choroidal side.[55] In addition to stimulating proliferation of adjacent choroidal vascular endothelium, VEGF can upregulate ICAM-1 expression on endothelium.[12,13] Circulating leukocytes, which migrate in response to VEGF,[16] can then bind to this activated endothelium and to RPE.[25] Through their own release of VEGF,[16] leukocytes can amplify the locally produced VEGF response as they bind to the endothelium. Also leukocyte-derived cytokines can stimulate VEGF production in RPE cells[45] and choroidal fibroblasts.[56] Leukocytes can perpetuate their ingress by stimulating RPE cells to secrete the chemotaxins IL-8 and monocyte chemotactic protein-1 into the choroid in a polarized gradient[57,58] and to express ICAM-1 preferentially on the choroidal surface.[25] Leukocytes may also produce matrix metalloproteinases (MMPs) directly[59,60] or by releasing VEGF, which induces expression of MMP in endothelial cells.[61] These MMPs, which have been found in CNV in AMD,[62] can facilitate endothelial cell migration during angiogenesis.

In conclusion, the development of CNV is inhibited in mice deficient in the CD18 or ICAM-1 gene. Our observations suggest that CD18- and ICAM-1–mediated leukocyte adhesion are nonredundant events in the development of clinically apparent CNV, which is the principal cause of vision loss in AMD.[2] These findings may be relevant to neovascularization elsewhere in the body, where leukocytes and growing vessels are often found in proximity.[63] Because leukocytes are the principal purveyors of host defense, targeted methods of inhibiting adhesion molecules such as local drug delivery[64] would be desirable.

Acknowledgments

The authors thank Matthias Krause for critical review; Robinette King, Guojin Chen, and Edward Connolly for technical assistance; Ambati M. Rao and Delwood C. Collins for continued support; and Richard J. Kryscio, University of Kentucky Biostatistics Consulting Unit, and Wenjun Li, Massachusetts Eye and Ear Infirmary Biostatistics Center, for statistical analyses.

References

1. Klein R, Wang Q, Klein BE, Moss SE, Meuer SM. The relationship of age-related maculopathy, cataract, and glaucoma to visual acuity. *Invest Ophthalmol Vis Sci.* 1995;36:182–191.
2. Macular Photocoagulation Study Group. Argon laser photocoagulation for neovascular maculopathy: five-year results from randomized clinical trials. *Arch Ophthalmol.* 1991;109:1109–1114.
3. Grossniklaus HE, Cingle KA, Yoon YD, Ketkar N, L'Hernault N, Brown S. Correlation of histologic 2-dimensional reconstruction and confocal scanning laser microscopic imaging of choroidal neovascularization in eyes with age-related maculopathy. *Arch Ophthalmol.* 2000;118:625–629.
4. Nishimura T, Goodnight R, Prendergast RA, Ryan SJ. Activated macrophages in experimental subretinal neovascularization. *Ophthalmologica.* 1990;200:39–44.
5. van der Schaft TL, Mooy CM, de Bruijn WC, de Jong PT. Early stages of age-related macular degeneration: an immunofluorescence and electron microscopy study. *Br J Ophthalmol.* 1993;77:657–661.
6. Killingsworth MC, Sarks JP, Sarks SH. Macrophages related to Bruch's membrane in age-related macular degeneration. *Eye.* 1990;4:613–621.
7. Melder RJ, Koenig GC, Witwer BP, Safabakhsh N, Munn LL, Jain RK. During angiogenesis, vascular endothelial growth factor and basic fibroblast growth factor regulate natural killer cell adhesion to tumor endothelium. *Nat Med.* 1996;2:992–997.
8. Moromizato Y, Stechschulte S, Miyamoto K, et al. CD18 and ICAM-1-dependent corneal neovascularization and inflammation after limbal injury. *Am J Pathol.* 2000;157:1277–1281.
9. Spilsbury K, Garrett KL, Shen WY, Constable IJ, Rakoczy PE. Overexpression of vascular endothelial growth factor (VEGF) in the retinal pigment epithelium leads to the development of choroidal neovascularization. *Am J Pathol.* 2000;157:135–144.
10. Baffi J, Byrnes G, Chan CC, Csaky KG. Choroidal neovascularization in the rat induced by adenovirus mediated expression of vascular endothelial growth factor. *Invest Ophthalmol Vis Sci.* 2000;41:3582–3589.
11. Krzystolik MG, Afshari MA, Adamis AP, et al. Prevention of experimental choroidal neovascularization with intravitreal anti-vascular endothelial growth factor antibody fragment. *Arch Ophthalmol.* 2002;120:338–346.
12. Radisavljevic Z, Avraham H, Avraham S. Vascular endothelial growth factor up-regulates ICAM-1 expression via the phosphatidylinositol 3 OH-kinase/AKT/nitric oxide pathway and modulates migration of brain microvascular endothelial cells. *J Biol Chem.* 2000;275:20770–20774.
13. Miyamoto K, Khosrof S, Bursell SE, et al. Vascular endothelial growth factor (VEGF)-induced retinal vascular permeability is mediated by intercellular adhesion molecule-1 (ICAM-1). *Am J Pathol.* 2000;156:1733–1739.
14. Miyamoto K, Khosrof S, Bursell SE, et al. Prevention of leukostasis and vascular leakage in streptozotocin-induced diabetic retinopathy via intercellular adhesion molecule-1 inhibition. *Proc Natl Acad Sci USA.* 1999;96:10836–10841.
15. Clauss M, Weich H, Breier G, et al. The vascular endothelial growth factor receptor Flt-1 mediates biological activities. Implications for a functional role of placenta growth factor in monocyte activation and chemotaxis. *J Biol Chem.* 1996;271:17629–17634.

16. Harmey JH, Dimitriadis E, Kay E, Redmond HP, Bouchier-Hayes D. Regulation of macrophage production of vascular endothelial growth factor (VEGF) by hypoxia and transforming growth factor beta-1. *Ann Surg Oncol.* 1998;5:271–278.
17. Rohan RM, Fernandez A, Udagawa T, Yuan J, D'Amato RJ. Genetic heterogeneity of angiogenesis in mice. *FASEB J.* 2000;14: 871–876.
18. Espinosa-Heidmann DG, Suner I, Hernandez EP, Frazier WD, Csaky KG, Cousins SW. Age as an independent risk factor for severity of experimental choroidal neovascularization. *Invest Ophthalmol Vis Sci.* 2002;43:1567–1573.
19. Tobe T, Ortega S, Luna JD, et al. Targeted disruption of the FGF2 gene does not prevent choroidal neovascularization in a murine model. *Am J Pathol.* 1998;153:1641–1646.
20. Heidenkummer HP, Kampik A. Surgical extraction of subretinal pseudotumors in age related macular degeneration. Clinical, morphologic and immunohistochemical results. *Ophthalmologe.* 1995;92:631–639.
21. Shen WY, Yu MJ, Barry CJ, Constable IJ, Rakoczy PE. Expression of cell adhesion molecules and vascular endothelial growth factor in experimental choroidal neovascularisation in the rat. *Br J Ophthalmol.* 1998;82:1063–1071.
22. Wilson RW, Ballantyne CM, Smith CW, et al. Gene targeting yields a CD18-mutant mouse for study of inflammation. *J Immunol.* 1993;151:1571–1578.
23. King PD, Sandberg ET, Selvakumar A, Fang P, Beaudet AL, Dupont B. Novel isoforms of murine intercellular adhesion molecule-1 generated by alternative RNA splicing. *J Immunol.* 1995;154: 6080–6093.
24. Mizgerd JP, Kubo H, Kutkoski GJ, et al. Neutrophil emigration in the skin, lungs, and peritoneum: different requirements for CD11/CD18 revealed by CD18-deficient mice. *J Exp Med.* 1997;186: 1357–1364.
25. Elner SG, Elner VM, Pavilack MA, et al. Modulation and function of intercellular adhesion molecule-1 (CD54) on human retinal pigment epithelial cells. *Lab Invest.* 1992;66:200–211.
26. Schneeberger EE, Vu Q, LeBlanc BW, Doerschuk CM. The accumulation of dendritic cells in the lung is impaired in CD18-/- but not in ICAM-1-/- mutant mice. *J Immunol.* 2000;164:2472–2478.
27. Rey-Ladino JA, Pyszniak AM, Takei F. Dominant-negative effect of the lymphocyte function-associated antigen-1 beta (CD18) cytoplasmic domain on leukocyte adhesion to ICAM-1 and fibronectin. *J Immunol.* 1998;160:3494–3501.
28. Das A, Puklin JE, Frank RN, Zhang NL. Ultrastructural immunocytochemistry of subretinal neovascular membranes in age-related macular degeneration. *Ophthalmology.* 1992;99:1368–1376.
29. van Den Engel NK, Heidenthal E, Vinke A, Kolb H, Martin S. Circulating forms of intercellular adhesion molecule (ICAM)-1 in mice lacking membranous ICAM-1. *Blood.* 2000;95:1350–1355.
30. Gho YS, Kleinman HK, Sosne G. Angiogenic activity of human soluble intercellular adhesion molecule-1. *Cancer Res.* 1999;59: 5128–5132.
31. Teeters VW, Bird AC. A clinical study of the vascularity of senile disciform macular degeneration. *Am J Ophthalmol.* 1973;75:53–65.
32. Gass JD. Pathogenesis of disciform detachment of the neuroepithelium. *Am J Ophthalmol.* 1967;63:(suppl):1–139.
33. Ryan SJ. Subretinal neovascularization: natural history of an experimental model. *Arch Ophthalmol.* 1982;100:1804–1809.
34. Green WR, Key SN III. Senile macular degeneration: a histopathologic study. *Trans Am Ophthalmol Soc.* 1977;75:180–254.
35. Schneider S, Greven CM, Green WR. Photocoagulation of well-defined choroidal neovascularization in age-related macular degeneration: clinicopathologic correlation. *Retina.* 1998;18:242–250.
36. Miller H, Miller B, Ryan SJ. Correlation of choroidal subretinal neovascularization with fluorescein angiography. *Am J Ophthalmol.* 1985;99:263–271.
37. Miller H, Miller B, Ryan SJ. The role of retinal pigment epithelium in the involution of subretinal neovascularization. *Invest Ophthalmol Vis Sci.* 1986;27:1644–1652.
38. Miller JW, Schmidt-Erfurth U, Sickenberg M, et al. Photodynamic therapy with verteporfin for choroidal neovascularization caused by age-related macular degeneration: results of a single treatment in a phase 1 and 2 study. *Arch Ophthalmol.* 1999;117:1161–1173.
39. Treatment of Age Related Macular Degeneration with Photodynamic Therapy (TAP) Study Group. Photodynamic therapy of subfoveal choroidal neovascularization in age-related macular degeneration with verteporfin: one-year results of 2 randomized clinical trials—TAP report. *Arch Ophthalmol.* 1999;117:1329–1345.
40. Treatment of Age Related Macular Degeneration with Photodynamic Therapy (TAP) Study Group. Photodynamic therapy of subfoveal choroidal neovascularization in age-related macular degeneration with verteporfin: two-year results of 2 randomized clinical trials—TAP Report 2. *Arch Ophthalmol.* 2001;119:198–207.
41. Miller H, Miller B, Ishibashi T, Ryan SJ. Pathogenesis of laser-induced choroidal subretinal neovascularization. *Invest Ophthalmol Vis Sci.* 1990;31:899–908.
42. Francois J, De Laey JJ, Cambie E, Hanssens M, Victoria-Troncoso V. Neovascularization after argon laser photocoagulation of macular lesions. *Am J Ophthalmol.* 1975;79:206–210.
43. Sarks SH, Van Driel D, Maxwell L, Killingsworth M. Softening of drusen and subretinal neovascularization. *Trans Ophthalmol Soc UK.* 1980;100:414–422.
44. Penfold PL, Provis JM, Billson FA. Age-related macular degeneration: ultrastructural studies of the relationship of leucocytes to angiogenesis. *Graefes Arch Clin Exp Ophthalmol.* 1987; 225:70–76.
45. Oh H, Takagi H, Takagi C, et al. The potential angiogenic role of macrophages in the formation of choroidal neovascular membranes. *Invest Ophthalmol Vis Sci.* 1999;40:1891–1898.
46. Pollack A, Korte GE, Heriot WJ, Henkind P. Ultrastructure of Bruch's membrane after krypton laser photocoagulation. II. Repair of Bruch's membrane and the role of macrophages. *Arch Ophthalmol.* 1986;104:1377–1382.
47. Otani A, Takagi H, Oh H, et al. Vascular endothelial growth factor family and receptor expression in human choroidal neovascular membranes. *Microvasc Res.* 2002;64:162–169.
48. Wada M, Ogata N, Otsuji T, Uyama M. Expression of vascular endothelial growth factor and its receptor (KDR/flk-1) mRNA in experimental choroidal neovascularization. *Curr Eye Res.* 1999; 18:203–213.
49. Amin R, Puklin JE, Frank RN. Growth factor localization in choroidal neovascular membranes of age-related macular degeneration. *Invest Ophthalmol Vis Sci.* 1994;35:3178–3188.
50. Ogata N, Matsushima M, Takada Y, et al. Expression of basic fibroblast growth factor mRNA in developing choroidal neovascularization. *Curr Eye Res.* 1996;15:1008–1018.
51. Ogata N, Yamamoto C, Miyashiro M, Yamada H, Matsushima M, Uyama M. Expression of transforming growth factor-β mRNA in experimental choroidal neovascularization. *Curr Eye Res.* 1997; 16:9–18.
52. Hinton DR, He S, Lopez PF. Apoptosis in surgically excised choroidal neovascular membranes in age-related macular degeneration. *Arch Ophthalmol.* 1998;116:203–209.
53. Kaplan HJ, Leibole MA, Tezel T, Ferguson TA. Fas ligand (CD95 ligand) controls angiogenesis beneath the retina. *Nat Med.* 1999; 5:292–297.
54. Sligh JE Jr, Ballantyne CM, Rich SS, et al. Inflammatory and immune responses are impaired in mice deficient in intercellular adhesion molecule 1. *Proc Natl Acad Sci USA.* 1993;90:8529–8533.
55. Blaauwgeers HG, Holtkamp GM, Rutten H, et al. Polarized vascular endothelial growth factor secretion by human retinal pigment epithelium and localization of vascular endothelial growth factor receptors on the inner choriocapillaris. Evidence for a trophic paracrine relation. *Am J Pathol.* 1999;155:421–428.
56. Kvanta A. Expression and regulation of vascular endothelial growth factor in choroidal fibroblasts. *Curr Eye Res.* 1995;14: 1015–1020.
57. Holtkamp GM, Van Rossem M, de Vos AF, Willekens B, Peek R, Kijlstra A. Polarized secretion of IL-6 and IL-8 by human

retinal pigment epithelial cells. *Clin Exp Immunol.* 1998;112: 34–43.

58. Holtkamp GM, De Vos AF, Peek R, Kijlsta A. Analysis of the secretion pattern of monocyte chemotactic protein-1 (MCP-1) and transforming growth factor-beta 2 (TGF-β2) by human retinal pigment epithelial cells. *Clin Exp Immunol.* 1999;118:35–40.
59. Peppin GJ, Weiss SJ. Activation of the endogenous metalloproteinase, gelatinase, by triggered human neutrophils. *Proc Natl Acad Sci USA.* 1986;83:4322–4326.
60. Banda MJ, Werb Z. Mouse macrophage elastase: purification and characterization as a metalloproteinase. *Biochem J.* 1981;193:589–605.
61. Lamoreaux WJ, Fitzgerald ME, Reiner A, Hasty KA, Charles ST. Vascular endothelial growth factor increases release of gelatinase A and decreases release of tissue inhibitor of metalloproteinases by microvascular endothelial cells in vitro. *Microvasc Res.* 1998;55: 29–42.
62. Steen B, Sejersen S, Berglin L, Seregard S, Kvanta A. Matrix metalloproteinases and metalloproteinase inhibitors in choroidal neovascular membranes. *Invest Ophthalmol Vis Sci.* 1998;39:2194–2200.
63. Knighton DR, Hunt TK, Scheuenstuhl H, Halliday BJ, Werb Z, Banda MJ. Oxygen tension regulates the expression of angiogenesis factor by macrophages. *Science.* 1983;221:1283–1285.
64. Ambati J, Gragoudas ES, Miller JW, et al. Transscleral delivery of bioactive protein to the choroid and retina. *Invest Ophthalmol Vis Sci.* 2000;41:1186–1191.

Sustained Inhibition of Corneal Neovascularization by Genetic Ablation of CCR5

Balamurali K. Ambati,[1,2] *Akshay Anand,*[3] *Antonia M. Joussen,*[2,4] *William A. Kuziel,*[5] *Anthony P. Adamis,*[2,6] *and Jayakrishna Ambati*[2,3]

Purpose. To determine whether genetic ablation of the CC chemokine receptor CCR5 (involved in leukocyte and endothelial chemotaxis) inhibits the development of corneal neovascularization.

Methods. Wild-type C57BL/6J mice and species-specific counterparts with targeted homozygous disruption of the CCR5 gene underwent chemical and mechanical denudation of corneal and limbal epithelium. Corneas were harvested 2 and 4 weeks after injury. Neovascularization was quantified by CD31 immunostaining. Expression of VEGF protein was quantified by ELISA.

Results. The mean percentages of neovascularized corneal area in control mice and CCR5-deficient mice 2 weeks after denudation were 58.3% and 38.5% ($P = 0.05$), respectively. At 4 weeks after denudation, the corresponding percentages were 67.6% and 44.0% ($P = 0.028$). In CCR5-deficient mice, VEGF protein levels were reduced 51.1% at 2 weeks ($P = 0.05$) after injury and 37.3% at 4 weeks ($P = 0.03$).

Conclusions. CCR5-deficient mice showed a persistent 34% to 35% inhibition of corneal neovascularization for up to 4 weeks. This inhibition correlates with reduced expression of VEGF. These data implicate CCR5 as one essential component in the development of corneal neovascularization. (*Invest Ophthalmol Vis Sci.* 2003;44:590–593) DOI:10.1167/iovs.02-0685

Corneal neovascularization (CNV) is a central feature in the pathogenesis of many blinding corneal disorders and a major sight-threatening complication in corneal infections and chemical injury and after keratoplasty, in which neovascularization adversely impacts corneal graft survival.[1]

From the [1]Department of Ophthalmology, Medical College of Georgia, Augusta, Georgia; the [3]Department of Ophthalmology, University of Kentucky, Lexington, Kentucky; the [4]Department of Vitreoretinal Surgery, Center of Ophthalmology, University of Cologne, Cologne, Germany; the [5]Section of Molecular Genetics and Microbiology and Institute for Cellular and Molecular Biology, University of Texas, Austin, Texas; the [2]Department of Ophthalmology, Massachusetts Eye and Ear Infirmary, Harvard Medical School, Boston, Massachusetts; and [6]Eyetech Pharmaceuticals, Woburn, Massachusetts.

Supported by the Heed Ophthalmic Foundation (BKA), American Ophthalmological Society-Knapp Testimonial Fund (JA), a Foundation Fighting Blindness Career Development Award (JA), University of Kentucky Physician-Scientist Award (JA), Grant Jo 324/2-1 from the German Research Foundation (AMJ), the National Eye Institute (APA), Massachusetts Lions Eye Research Fund (APA), and the Roberta Siegel Research Fund (APA).

Submitted for publication July 9, 2002; revised August 19, 2002; accepted September 29, 2002.

Disclosure: **B.K. Ambati**, None; **A. Anand**, None; **A.M. Joussen**, None; **W.A. Kuziel**, None; **A.P. Adamis**, Eyetech Pharmaceuticals (E); **J. Ambati**, None

The publication costs of this article were defrayed in part by page charge payment. This article must therefore be marked "*advertisement*" in accordance with 18 U.S.C. §1734 solely to indicate this fact.

Corresponding author: Jayakrishna Ambati, Department of Ophthalmology, University of Kentucky, 801 Rose Street, Lexington, KY 40536-0284; jamba2@uky.edu.

Although the molecular mechanisms underlying CNV have not been fully deciphered, vascular endothelial growth factor (VEGF) seems to play an indispensable role. It induces CNV when applied exogenously[2] and is the principal endogenous angiogenic force in the neovascularization that follows limbal injury.[3] Transmigrating and invading corneal leukocytes appear to provide much of the requisite VEGF that drives CNV.[3]

The recruitment of leukocytes to inflammatory sites is mediated by chemokines. Chemokines bind to specific receptors that, despite some redundancy, show specificity for individual chemokines. Evidence is emerging that individual chemokines attract specific leukocyte populations through processes determined by ligand specificity and the expression patterns of the corresponding receptors.[4] CCR5 receptor ligands include the macrophage inflammatory proteins (MIPs) 1α and 1β, which recruit both macrophages and neutrophils.[5,6]

Endothelial cell migration and proliferation are also essential to angiogenesis, and these processes are known to be influenced by vascular endothelial growth factor (VEGF) and basic fibroblast growth factor (bFGF).[7,8] Further, endothelial cell chemotaxis and/or proliferation can be stimulated by chemokines, including interleukin (IL)-8, monocyte chemotactic protein (MCP)-1, regulated on activation normal T-cell expressed and secreted (RANTES), and MIP-1α and -1β.[9,10]

Previous work has confirmed that corneal angiogenesis is driven in large part by inflammatory mediators.[11,12] MIP-1α has been associated with CNV in helminth keratitis,[13] shown to be required for the development of CNV in HSV keratitis[14,15] and demonstrated to be angiogenic in Kaposi's sarcoma–associated herpes virus infection.[16] It has also been associated with angiogenesis in corneal allograft rejection.[17,18] Its receptor, CCR5, also found on endothelial cells, is a receptor for CC chemokines that are involved in angiogenesis, including RANTES and MIP-1α and -1β.[10,19]

We therefore examined the role of CCR5 in a clinically relevant ocular model of corneal injury by studying the neovascular response of animals genetically deficient in these molecules.

Methods

All animal experiments were approved by the Massachusetts Eye and Ear Infirmary Animal Care Committee and the University of Kentucky Animal Care Committee and conformed to the ARVO Statement for the Use of Animals in Ophthalmic and Vision Research. Mice were anesthetized by intramuscular injection of 50 mg/kg ketamine hydrochloride (Abbott Laboratories, N. Chicago, IL) and 10 mg/kg xylazine (Bayer, Shawnee Mission, KS). Animals were killed by a lethal dose of pentobarbital (150 mg/kg).

Animals

Wild-type C57BL/6J mice (Jackson Laboratories, Bar Harbor, ME) were used as controls. To create the CCR-knockout strain, the entire CCR5 coding region was replaced by insertion of a neomycin-resistant expression cassette, as described previously.[20,21] Although the original knockout strains were generated on a mixed C57BL/6 × 129/Ola genetic background, the mice used in the experiments described

Investigative Ophthalmology & Visual Science, February 2003, Vol. 44, No. 2
Copyright © Association for Research in Vision and Ophthalmology

herein represent the progeny of the eighth generation backcross of the knockout mutations to inbred C57BL/6 animals. Because the CCR2 and CCR5 genes are very closely linked, a wild-type control strain for both knockout strains was developed by backcrossing the wild-type CCR5 locus from 129/Ola to the C57BL/6 background for eight generations. This control strain minimizes the genetic differences flanking the targeted allele. Wild-type C57BL/6 and 129/Ola CCR5 genes were distinguished by the presence of a *Bgl*II restriction fragment length polymorphism.[20]

Genotype Analysis

The genotype of all experimental animals was determined on tail DNA samples. CCR5 knockout alleles were identified by PCR analysis with a set of four primers. Wild-type CCR5 alleles were identified by synthesis of a 450-bp PCR product with primers complementary to sequences on each side of the crossover site (primer 1, 5′-AAGCAGGAGGATCGT-GAGCTTGAC-3′, and primer 2, 5′-GAAACAAGTTGTTGTGCACCTCAG-3′). Disrupted CCR5 alleles were identified by synthesis of a 350-bp PCR product with a primer that is complementary to a sequence in the neomycin resistance coding region (primer 3, 5′-TTCCATTGCT-CAGCGGTGCT-3′) combined with a primer complementary to a CCR5 sequence downstream of the crossover site (primer 4, 5′-TGTTTCCTC-CTCTAGCCTTCACTATG-3′).

Experimental Design

Both groups of mice (control, CCR5 knockout) underwent corneal injury. Corneas were harvested 2 and 4 weeks after injury. An image analyzer was used by a masked investigator to quantify neovascularization in immunostained corneas.

Model of Corneal Neovascularization

Topical proparacaine and 2 μL of 0.15 M NaOH were applied to the right cornea of each mouse. The corneal and limbal epithelia were removed with a Tooke corneal knife (Katena Products, Denville, NJ) in a rotary motion parallel to the limbus. Erythromycin ophthalmic ointment was instilled immediately after epithelial denudation.

Labeling of Corneal Neovascularization

Immunohistochemical staining for vascular endothelial cells was performed on corneal flatmounts. Fresh corneas were dissected, rinsed in PBS for 30 minutes, and fixed in 100% acetone (Sigma, St. Louis, MO) for 20 minutes. After the corneas were washed in PBS, nonspecific binding was blocked with 0.1 M PBS, 2% albumin (Sigma) for 1 hour at room temperature. Incubation with FITC-coupled monoclonal anti-mouse CD31 antibody (Pharmingen) at a concentration of 1:500 in 0.1 M PBS, 2% albumin at 4°C overnight was followed by subsequent washes in PBS at room temperature. Corneas were mounted with an antifading agent (Gelmount; Biomeda, Inc, San Francisco, CA) and visualized with a fluorescence microscope (Leica, Wetzlar, Germany).

Quantification of Corneal Neovascularization

Digital quantification of corneal neovascularization has been described.[22,23] Images of the corneal vasculature were captured with a CD-330 charge-coupled device (CCD) camera (Dage-MIT, Inc., Michigan City, IN) attached to a fluorescence microscope (MZ FLIII; Leica Microsystems Inc., Deerfield, IL). The images were analyzed on computer (Openlab; Improvision Inc., Lexington, MA), resolved at 624 × 480 pixels, and converted to tagged information file format (TIFF) files. The neovascularization was quantified by setting a threshold level of fluorescence above which only vessels were captured. The entire mounted cornea was analyzed to minimize sampling bias. The quantification of the neovascularization was performed in masked fashion. The total corneal area was outlined, with the innermost vessel of the limbal arcade used as the border. The total area of neovascularization was then normalized to the total corneal area, and the percentage of the cornea covered by vessels was calculated.

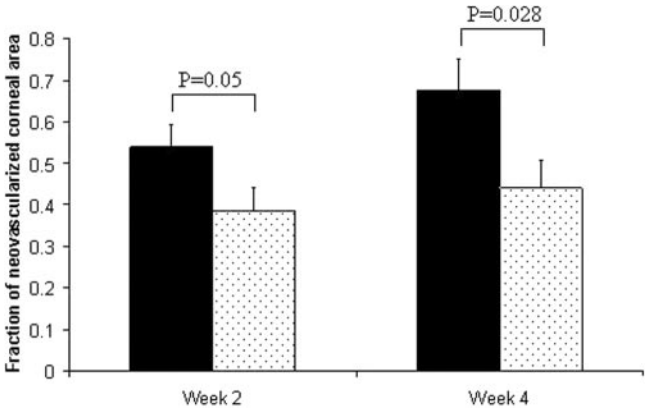


FIGURE 1. Mean ± SEM fraction of corneal neovascularization, 2 and 4 weeks after denudation in control (■) and CCR5-deficient (▨) mice.

Corneal Harvest for ELISA

At 1, 3, 14, and 21 days, scraped corneas were dissected and placed in 60 μL lysis buffer (20 mM imidazole hydrochloride, 10 mM potassium chloride, 1 mM magnesium chloride, 10 mM EGTA, 1% Triton, 10 mM sodium fluoride, 1 mM sodium molybdate, and 1 mM EDTA [pH 6.8]), supplemented with protease inhibitor (Sigma) followed by homogenization. The lysate was cleared of debris by centrifugation at 14,000 rpm for 15 minutes (4°C), and the supernatant was collected. Total protein was determined with a Bradford protein assay (Bio-Rad, Hercules, CA).

VEGF ELISA

VEGF was determined by a commercially available ELISA kit (R&D Systems, Minneapolis, MN) which recognizes the 164-amino-acid splice variant of mouse VEGF. The assay was performed according to the manufacturer's instructions. Briefly, standards or tissue samples (50 μL) were pipetted into an antibody-coated 96-well plate containing 50 μL of assay diluent and incubated for 2 hours at RT on a shaker. The wells were then washed five times with wash buffer, 100 μL of VEGF conjugate was added, and the samples were again incubated for 2 hours at RT. Samples were washed five times, 100 μL substrate buffer was added, the samples were incubated for 30 minutes at RT, the reaction was stopped, and the absorption was measured with an ELISA reader (Emax; Molecular Devices, Sunnyvale, CA) at 450 nm with lambda correction at 570 nm. All measurements were performed in duplicate. The lower limit of ELISA was 3.0 pg/mL. The tissue sample concentration was calculated from the standard curve and corrected for total protein.

Statistics

Data were analyzed by the Kruskal-Wallis test with the Dunn test for multiple comparisons (SPSS, Inc., Chicago, IL). Type I error not exceeding 0.05 was deemed significant.

RESULTS

Data on (mean ± SEM) percentages of neovascularized cornea area in mice 2 and 4 weeks after corneal scraping and implantation are presented in Figure 1.

Percentage Area of Corneal Neovascularization

At 2 weeks after denudation, $CCR5^{-/-}$ mice ($n = 8$) had 34.0% less ($P = 0.05$) neovascularized corneal area than control mice ($n = 13$). At 4 weeks after denudation, $CCR5^{-/-}$ mice ($n = 6$) had 34.9% less neovascularized corneal area than control mice ($P = 0.028$). Representative images are shown in Figure 2.

VEGF Expression

Data are presented in Figure 3. CCR5$^{-/-}$ mice had 51.1% less corneal VEGF than control mice at 14 days after scraping (P = 0.05) and 37.3% less VEGF at 21 days after scraping (P = 0.03).

Discussion

In this study, CCR5-deficient mice experienced a sustained inhibition of corneal neovascularization after chemical and mechanical denudation of corneal epithelium, an effect correlated with reduced VEGF expression. These data implicate CCR5 as one of the components in the development of corneal neovascularization, probably because of the effects of this receptor and ligands on endothelial cells and macrophages. Endothelial cells possess CCR5[19,24,25] and undergo chemotaxis in response to RANTES, MIP-1α, and MIP-1β (ligands for CCR5).[10]

Macrophage involvement in corneal neovascularization is well known[24] and infiltration of these cells, which is closely associated with neovascularization, peaks 2 weeks after corneal injury.[25] Use of manumycin, a Ras farnesyltransferase inhibitor, inhibits CNV and infiltration of macrophages (but not that of neutrophils).[26] Pharmacologic depletion of macrophages dramatically limits CNV in corneal allograft rejection.[27] Increased expression of VEGF after corneal injury has been localized to infiltrating inflammatory cells, especially macrophages, after corneal injury,[3] which probably accounts for the reduced expression of VEGF observed in this study.

CCR5 plays a role in chemotaxis of mature macrophages, because MIP-1α is chemotactic for differentiated macrophages.[28,29] MIP-1α is correlated with corneal infiltration of leukocytes, and antibodies to MIP-1α reduce corneal opacification in herpetic keratitis.[30] Previous reports have found upregulation of MIP-1α after alkali injury, *Pseudomonas* infection, and HSV infection.[30–32] A proximate role of MIP-1α, and thus CCR5, is likely, because it is produced by the corneal stroma in response to injury.[31,33]

Because inhibition of CNV in CCR5-deficient mice is only approximately one third, it is clear that other mechanisms are involved. However, we may speculate as to the reasons for the persistent inhibition of corneal neovascularization observed in CCR5$^{-/-}$ mice. First, CCR5 may be involved in migration and proliferation of endothelial cells. Second, the reduced expression of VEGF in this model (and thus diminished angiogenic stimulus) may have been due to decreased macrophage infiltration.

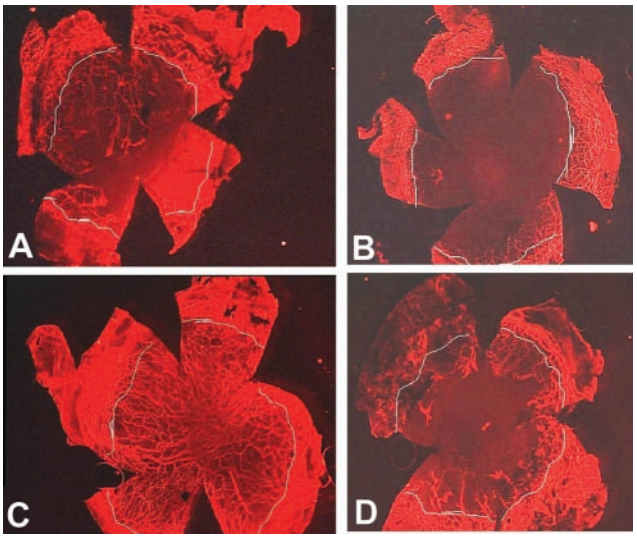


Figure 2. Representative photographs of corneal flatmounts of control (**A, C**) and CCR5-deficient (**B, D**) mouse eyes, 2 (**A, B**) and 4 (**C, D**) weeks after corneal injury, stained with FITC-coupled monoclonal murine anti-CD31 antibody to visualize endothelial cells.

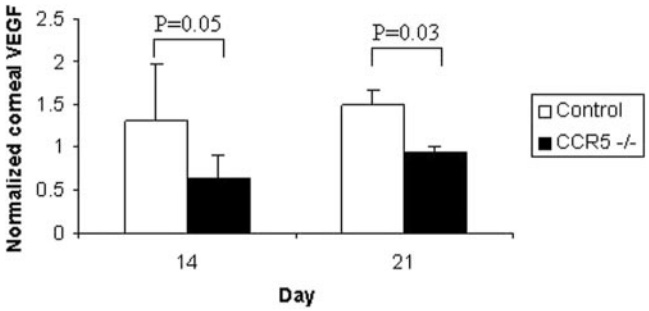


Figure 3. Mean VEGF ± SEM protein expression, normalized to total corneal protein, 2 and 4 weeks after denudation in control (■) and CCR5-deficient (□) mice.

In the present study, neovascularization was persistently inhibited in CCR5-deficient mice, which points the way toward a possible therapeutic target for pharmacologic agents. That this inhibition was demonstrated in a mechanical and chemical corneal trauma increases its clinical relevance. The method of inducing neovascularization affects pharmacologic efficacy—for example, integrin antagonists inhibit bFGF-induced corneal neovascularization but not that caused by chemical injury.[34]

In summary, this finding could advance the management of blinding disorders such as Stevens-Johnson syndrome, cicatricial pemphigoid, corneal allograft rejection, and corneal injury from infection, trauma, or alkali. Future research should also characterize the effect of and the complex molecular interplay among chemokines, leukocytes, and neovascularization and extend this model to other sites of ocular neovascularization.

References

1. Epstein RJ, Stulting RD, Hendricks RL, Harris DM. Corneal neovascularization: pathogenesis and inhibition. *Cornea.* 1987;6:250–257.
2. Kenyon BM, Voest EE, Chen CC, Flynn E, Folkman J, D'Amato RJ. A model of angiogenesis in the mouse cornea. *Invest Ophthalmol Vis Sci.* 1996;37:1625–1632.
3. Amano S, Rohan R, Kuroki M, Tolentino M, Adamis AP. Requirement for vascular endothelial growth factor in wound- and inflammation-related corneal neovascularization. *Invest Ophthalmol Vis Sci.* 1998;39:18–22.
4. Kim CH, Broxmeyer HE. Chemokines: signal lamps for trafficking of T and B cells for development and effector function. *J Leukoc Biol.* 1999;65:6–15.
5. Raport CJ, Gosling J, Schweickart VL, Gray PW, Charo IF. Molecular cloning and functional characterization of a novel human CC chemokine receptor (CCR5) for RANTES, MIP-1beta, and MIP-1alpha. *J Biol Chem.* 1996;271:17161–17166.
6. Samson M, LaRosa G, Libert F, et al. The second extracellular loop of CCR5 is the major determinant of ligand specificity. *J Biol Chem.* 1997;272:24934–24941.
7. Risau W. Mechanisms of angiogenesis. *Nature.* 1997;386:671–674.
8. Lindner V, Majack RA, Reidy MA. Basic fibroblast growth factor stimulates endothelial regrowth and proliferation in denuded arteries. *J Clin Invest.* 1990;85:2004–2008.
9. Koch AE, Polverini PJ, Kunkel SL, et al. Interleukin-8 as a macrophage-derived mediator of angiogenesis. *Science.* 1992;258:1798–1801.
10. Berger O, Gan X, Gujuluva C, et al. CXC and CC chemokine receptors on coronary and brain endothelia. *Mol Med.* 1999;5:795–805.

11. Moromizato Y, Stechschulte S, Miyamoto K, et al. CD18 and ICAM-1-dependent corneal neovascularization and inflammation after limbal injury. *Am J Pathol.* 2000;157:1277–1281.
12. Philipp W, Speicher L, Humpel C. Expression of vascular endothelial growth factor and its receptors in inflamed and vascularized human corneas. *Invest Ophthalmol Vis Sci.* 2000;41:2514–2522.
13. Pearlman E, Hall LR, Higgins AW, et al. The role of eosinophils and neutrophils in helminth-induced keratitis. *Invest Ophthalmol Vis Sci.* 1998;39:1176–1182.
14. Chang E, Galle L, Maggs D, Estes DM, Mitchell WJ. Pathogenesis of herpes simplex virus type 1-induced corneal inflammation in perforin-deficient mice. *J Virol.* 2000;74:11832–11840.
15. Tumpey TM, Cheng H, Cook DN, Smithies O, Oakes JE, Lausch RN. Absence of macrophage inflammatory protein-1α prevents the development of blinding herpes stromal keratitis. *J Virol.* 1998;72:3705–3710.
16. Boshoff C, Endo Y, Collins PD, et al. Angiogenic and HIV-inhibitory functions of KSHV-encoded chemokines. *Science.* 1997;278:290–294.
17. Torres PF, De Vos AF, van der Gaag R, Martins B, Kijlstra A. Cytokine mRNA expression during experimental corneal allograft rejection. *Exp Eye Res.* 1996;63:453–461.
18. King WJ, Comer RM, Hudde T, Larkin DF, George AJ. Cytokine and chemokine expression kinetics after corneal transplantation. *Transplantation.* 2000;70:1225–1233.
19. Schecter AD, Calderon TM, Berman AB, et al. Human vascular smooth muscle cells possess functional CCR5. *J Biol Chem.* 2000;275:5466–5471.
20. Kuziel WA, Maeda N. CCR2 and CCR5. In: Mak TW, ed. *The Gene Knockout Facts Book.* London: Academic Press; 1998:118–121.
21. Huffnagle GB, McNeil LK, McDonald RA, et al. Cutting edge: role of C-C chemokine receptor 5 in organ-specific and innate immunity to Cryptococcus neoformans. *J Immunol.* 1999;163:4642–4646.
22. Proia AD, Chandler DB, Haynes WL, et al. Quantitation of corneal neovascularization using computerized image analysis. *Lab Invest.* 1988;58:473–479.
23. Goede V, Schmidt T, Kimmina S, Kozian D, Augustin HG. Analysis of blood vessel maturation processes during cyclic ovarian angiogenesis. *Lab Invest.* 1998;78:1385–1394.
24. Polverini PJ, Cotran PS, Gimbrone MA Jr, Unanue ER. Activated macrophages induce vascular proliferation. *Nature.* 1977;269:804–806.
25. Ding Z, He Y, Wei H. A morphological study of experimental corneal neovascularization [in Chinese]. *Chung Hua Yen Ko Tsa Chih.* 1995;31:49–51.
26. Sonoda K, Sakamoto T, Yoshikawa H, et al. Inhibition of corneal inflammation by the topical use of Ras farnesyltransferase inhibitors: selective inhibition of macrophage localization. *Invest Ophthalmol Vis Sci.* 1998;39:2245–2251.
27. Van der Veen G, Broersma L, Dijkstra CD, Van Rooijen N, Van Rij G, Van der Gaag R. Prevention of corneal allograft rejection in rats treated with subconjunctival injections of liposomes containing dichloromethylene diphosphonate. *Invest Ophthalmol Vis Sci.* 1994;35:3505–3515.
28. Kaufmann A, Salentin R, Gemsa D, Sprenger H. Increase of CCR1 and CCR5 expression and enhanced functional response to MIP-1α during differentiation of human monocytes to macrophages. *J Leukoc Biol.* 2001;69:248–252.
29. Fantuzzi L, Borghi P, Ciolli V, Pavlakis G, Belardelli F, Gessani S. Loss of CCR2 expression and functional response to monocyte chemotactic protein (MCP-1) during the differentiation of human monocytes: role of secreted MCP-1 in the regulation of the chemotactic response. *Blood.* 1999;94:875–883.
30. Tumpey TM, Cheng H, Yan XT, et al. Chemokine synthesis in the HSV-1-infected cornea. *J Leukoc Biol.* 1998;63:486–492.
31. Sosne G, Szliter EA, Barrett R, et al. Thymosin beta 4 promotes corneal wound healing and decreases inflammation in vivo following alkali injury. *Exp Eye Res.* 2002;74:293–299.
32. Kernacki KA, Barrett RP, McClellan S, et al. MIP-1alpha regulates CD4+ T cell chemotaxis and indirectly enhances PMN persistence in Pseudomonas aeruginosa corneal infection. *J Leukoc Biol.* 2001;70:911–919.
33. Hall LR, Diaconu E, Patel R, et al. CXC chemokine receptor 2 but not C-C chemokine receptor 1 expression is essential for neutrophil recruitment to the cornea in helminth-mediated keratitis (river blindness). *J Immunol.* 2001;166:4035–4041.
34. Klotz O, Park JK, Pleyer U, et al. Inhibition of corneal neovascularization by alpha(v)-integrin antagonists in the rat. *Graefes Arch Clin Exp Ophthalmol.* 2000;238:88–93.